BIOMATERIALS FOR BRAIN THERAPY AND REPAIR

EDITED BY: Sara Pedron and Brendan A. C. Harley
PUBLISHED IN: Frontiers in Materials and Frontiers in Bioengineering and Biotechnology

frontiers Research Topics

ISSN 1664-8714
ISBN 978-2-88945-747-2
DOI 10.3389/978-2-88945-747-2

About Frontiers

Frontiers is more than just an open-access publisher of scholarly articles: it is a pioneering approach to the world of academia, radically improving the way scholarly research is managed. The grand vision of Frontiers is a world where all people have an equal opportunity to seek, share and generate knowledge. Frontiers provides immediate and permanent online open access to all its publications, but this alone is not enough to realize our grand goals.

Frontiers Journal Series

The Frontiers Journal Series is a multi-tier and interdisciplinary set of open-access, online journals, promising a paradigm shift from the current review, selection and dissemination processes in academic publishing. All Frontiers journals are driven by researchers for researchers; therefore, they constitute a service to the scholarly community. At the same time, the Frontiers Journal Series operates on a revolutionary invention, the tiered publishing system, initially addressing specific communities of scholars, and gradually climbing up to broader public understanding, thus serving the interests of the lay society, too.

Dedication to Quality

Each Frontiers article is a landmark of the highest quality, thanks to genuinely collaborative interactions between authors and review editors, who include some of the world's best academicians. Research must be certified by peers before entering a stream of knowledge that may eventually reach the public - and shape society; therefore, Frontiers only applies the most rigorous and unbiased reviews.
Frontiers revolutionizes research publishing by freely delivering the most outstanding research, evaluated with no bias from both the academic and social point of view. By applying the most advanced information technologies, Frontiers is catapulting scholarly publishing into a new generation.

What are Frontiers Research Topics?

Frontiers Research Topics are very popular trademarks of the Frontiers Journals Series: they are collections of at least ten articles, all centered on a particular subject. With their unique mix of varied contributions from Original Research to Review Articles, Frontiers Research Topics unify the most influential researchers, the latest key findings and historical advances in a hot research area! Find out more on how to host your own Frontiers Research Topic or contribute to one as an author by contacting the Frontiers Editorial Office: researchtopics@frontiersin.org

BIOMATERIALS FOR BRAIN THERAPY AND REPAIR

Topic Editors:
Sara Pedron, University of Illinois at Urbana-Champaign, United States
Brendan A. C. Harley, University of Illinois at Urbana-Champaign, United States

Photo credit: iStock.com/wildpixel

Prevalence of brain related diseases is expected to increase significantly in the next decades. Therefore, there is a vital need to develop effective, personalized models of human brain that can provide information about brain development, and the unique neurobiology of brain disorders. The use of biomaterials can play a strategic role for the future understanding and treatment of complex CNS diseases. Three-dimensional brain cultures have shown promise in disease modelling, cell transplantation and modulation of tissue repair.

Citation: Pedron, S., Harley, B. A. C., eds. (2019). Biomaterials for Brain Therapy and Repair. Lausanne: Frontiers Media. doi: 10.3389/978-2-88945-747-2

Table of Contents

frontiers in Materials

EDITORIAL
published: 15 November 2018
doi: 10.3389/fmats.2018.00067

Editorial: Biomaterials for Brain Therapy and Repair

Sara Pedron[1]* *and Brendan A. C. Harley*[1,2]*

[1] Carl R. Woese Institute for Genomic Biology, University of Illinois at Urbana-Champaign, Champaign, IL, United States, [2] Department of Chemical and Biomolecular Engineering, University of Illinois at Urbana-Champaign, Champaign, IL, United States

Keywords: 3D cell culture, biomaterial disease models, neurodegeneration, tumor, blood brain barrier (BBB), brain disorders, iPSC = induced pluripotent stem cell, bioprinting

Editorial on the Research Topic

Biomaterials for Brain Therapy and Repair

Acute or chronic alterations of brain function, either in the form of brain disorders, including developmental, psychiatric, neurodegenerative, and autoimmune diseases, cancer or injury represent a tremendous social and economic burden that has increased considerably over the last 20 years (Feigin et al., 2017). Technologies to repair or induce regeneration of brain tissue are still in early stages of development, but the use of induced pluripotent stem cells (iPSCs) have opened the possibility of modeling and reconstructing brain circuits (Barker et al., 2018). Recent efforts have begun to consider the explicit development of tools to analyze brain composition and function as a means to better diagnose, prevent, or treat brain diseases. Artificial models of healthy and diseased brain tissue may eventually help decipher patterns of regional cell diversity and connectivity and allow the precise manipulation of cells and extracellular conditions to mimic neural microenvironments. In this context, biomaterials can act as a dynamic stimulatory platform that can recreate the native cerebral tissue, deliver growth factors or immune-modulating components to support neural growth and allow detailed analysis of therapeutic outcomes.

Over the last 30 years we have witnessed advances in biomaterials technologies supporting regeneration of a range of tissues, from skin to heart valves, urinary bladder and cartilage (Langer and Vacanti, 2016). However, central nervous tissues such as the brain remains a challenge due to their native complexity. Recently, increasingly interdisciplinary efforts are combining fields such as chemical and functional imaging, developmental biology, animal models and behavioral studies, and tissue engineering to develop new understanding regarding mechanisms of homeostasis and disease progression in the brain, as well as to discover and validate new therapeutic strategies.

This collection of research articles highlights recent biomaterials-centric approaches to study and treat disorders, diseases, and injuries to the brain. Topics span diverse areas of interest, such as tissue engineering, targeted drug delivery, *ex vivo* disease models, dynamic biomaterials, neurovascular diseases, molecular imaging, neurobiology, proteomics, systems biology, protein biosensors, and biomimetic scaffold design.

One area of significant effort is the development of biomaterials to examine the progression and treatment of brain cancer. Efforts highlighted here seek to model influential regulators of the glioblastoma tumor microenvironment (Cha and Kim) that may yield clinically-actionable data (Cornelison and Munson), including using cytokines to direct angiogenesis, improving drug delivery and increasing the circulation of immune cells at the tumor site, as well as manipulating biophysical properties to control cell phenotype and migration. Such platforms also facilitate study of cellular level heterogeneity associated with brain cancer, such as the role played by

OPEN ACCESS

Edited and reviewed by:
Hasan Uludag,
University of Alberta, Canada

***Correspondence:**
Sara Pedron
spedron@illinois.edu
Brendan A. C. Harley
bharley@illinois.edu

Specialty section:
This article was submitted to Biomaterials, a section of the journal Frontiers in Materials

Received: *08 October 2018*
Accepted: *25 October 2018*
Published: *15 November 2018*

Citation:
Pedron S and Harley BAC (2018) Editorial: Biomaterials for Brain Therapy and Repair. Front. Mater. 5:67. doi: 10.3389/fmats.2018.00067

a subpopulation of glioblastoma stem-like cells (Heffernan and Sirianni) and heterogeneity of tyrosine kinase receptor density (Chen et al.) on tumor recurrence and therapeutic resistance. They also examine the role of matrix composition, such as the molecular weight of hyaluronic acid, on glioblastoma cell invasion capacity (Chen et al.).

This virtual issue also includes an exciting compilation of research describing biomaterials to recapitulate native neural behavior *in vitro*. Biomaterial environments can guide controlled differentiation of neural cells and support neuronal processes (Farrukh et al.) and may serve as a platform to culture embryonic neuronal cells in a brain-mimetic hydrogel matrix (Magariños et al.). The microscale architecture of biomaterial culture platforms can directly affect the efficacy of neural cell transplants (Meco and Lampe), while the precise manipulation of topographical, chemical, electrical, and mechanical cues enhance control over directionality of regenerating neurites (Cangellaris and Gillette). Recent advances in 3D bioprinting may ultimately provide the resolution necessary to replicate the native complexity of the neural environment tissue (Thomas and Willerth). Precisely embedded bioactive signals may alternatively provide a pathway to direct migration and differentiation of neural stem cells (Matta and Gonzalez) as a means to regenerate the subventricular zone following stroke. This issue also provides an overview of delivery systems that support the repair of the stroke-damaged tissue (Tuladhar et al.).

Changes in the neural vascular environment play a critical role in acute brain damage and chronic neurodegenerative disorders. Such injuries are characterized by inflammatory reactions that include possible alterations of the extracellular matrix and modifications of the blood-brain barrier (BBB) (Nih et al., 2018). Here, a review article compiles efforts employing iPSCs in biomaterial models of the BBB to analyze mechanisms of neurovascular diseases (Bosworth et al.), while a research article examines the role of BBB integrity on the functional behavior of intracortical electrodes (Falcone et al.).

Together, this Research Topic illustrates the current state-of-the-art and future opportunities for the development of biomaterials to sustain and support differentiation of cells involved in neurological conditions. Due to the complexity of the brain, further progress in this area will presumably be related to technological advances at multiple scales and from multiple disciplines. However, it is clear that biomaterial platforms will play an essential role in these ongoing and future efforts. They may: aid the development of models to study the dysregulation and degradation of neuronal architectures; act as templates to promote neural regeneration; facilitate study of the progression of a wide range of brain related diseases including trauma and cancer; and play a central role in the optimization and delivery of therapeutic strategies. As a result, we have been excited to help organize this Research Topic *Biomaterials for Brain Therapy and Repair* and hope it serves as a relevant and useful resource to our colleagues.

AUTHOR CONTRIBUTIONS

All authors listed have made a substantial, direct and intellectual contribution to the work, and approved it for publication.

ACKNOWLEDGMENTS

The authors gratefully acknowledge support from the Scott H. Fisher IGB Graduate Student Research Fund.

REFERENCES

Barker, R. A., Götz, M., and Parmar, M. (2018). New approaches for brain repair—from rescue to reprogramming. *Nature* 557, 329–334. doi: 10.1038/s41586-018-0087-1

Feigin, V. L., Abajobir, A. A., Abate, K. H., Abd-Allah, F., Abdulle, A. M., Abera, S. F., et al. (2017). Global, regional, and national burden of neurological disorders during 1990–2015: a systematic analysis for the Global Burden of Disease Study 2015. *Lancet Neurol.* 16, 877–897. doi: 10.1016/S1474-4422(17)30299-5

Langer, R., and Vacanti, J. (2016). Advances in tissue engineering. *J. Pediatr. Surg.* 51, 8–12. doi: 10.1016/j.jpedsurg.2015.10.022

Nih, L. R., Gojgini, S., Carmichael, S. T., and Segura, T. (2018). Dual-function injectable angiogenic biomaterial for the repair of brain tissue following stroke. *Nat. Mater.* 17, 642–651. doi: 10.1038/s41563-018-0083-8

Conflict of Interest Statement: The authors declare that the research was conducted in the absence of any commercial or financial relationships that could be construed as a potential conflict of interest.

frontiers in Materials

REVIEW
published: 02 November 2018
doi: 10.3389/fmats.2018.00062

Microenvironments Designed to Support Growth and Function of Neuronal Cells

Aleeza Farrukh[1], *Shifang Zhao*[1,2] *and Aránzazu del Campo*[1,2]*

[1] INM – Leibniz Institute for New Materials, Saarbrücken, Germany, [2] Chemistry Department, Saarland University, Saarbrücken, Germany

Strategies for neural tissue repair heavily depend on our ability to temporally reconstruct the natural cellular microenvironment of neural cells. Biomaterials play a fundamental role in this context, as they provide the mechanical support for cells to attach and migrate to the injury site, as well as fundamental signals for differentiation. This review describes how different cellular processes (attachment, proliferation, and (directional) migration and differentiation) have been supported by different material parameters, *in vitro* and *in vivo*. Although incipient guidelines for biomaterial design become visible, literature in the field remains rather phenomenological. As in other fields of tissue regeneration, progress will depend on more systematic studies on cell-materials response, better understanding on how cells behave and understand signals in their natural milieu from neurobiology studies, and the translation of this knowledge into engineered microenvironments for clinical use.

Keywords: biomaterials, neuroregeneration, axon growth, neurite guidance, nerve repair

OPEN ACCESS

Edited by:
Sara Pedron,
University of Illinois at Urbana-Champaign, United States

Reviewed by:
Kirsten Haastert-Talini,
Hannover Medical School, Germany
Bin Duan,
University of Nebraska Medical Center, United States

***Correspondence:**
Aránzazu del Campo
aranzazu.delcampo@leibniz-inm.de

Specialty section:
This article was submitted to Biomaterials, a section of the journal Frontiers in Materials

Received: *22 February 2018*
Accepted: *05 October 2018*
Published: *02 November 2018*

Citation:
Farrukh A, Zhao S and del Campo A (2018) Microenvironments Designed to Support Growth and Function of Neuronal Cells. Front. Mater. 5:62. doi: 10.3389/fmats.2018.00062

INTRODUCTION

Disfunction in the nervous system due to aging, trauma or neurodegeneration leads to severe disabilities and is a major concern in an aging society. Regeneration of nerve functions involves migration and generation of new born cells at the damage site, the oriented growth and branching of axons to reform nerves, and the formation of functional synapses between adjacent neurons (Liu et al., 2011; Lee et al., 2014). Over the last two decades neural tissue regenerative therapies based on stem cell transplantation to the injury site have been explored (Lunn et al., 2011; Gage and Temple, 2013; Casarosa et al., 2014). Different biomaterials have been used as carriers for stem cell delivery in order to improve the viability and to guide differentiation of implanted cells (Roach et al., 2010). These biomaterials are conceived, in part, to reproduce the mechanical properties, morphology and composition of the extracellular matrix (ECM) around neuronal cells.

The next sections present relevant examples of biomaterial designs that support different neuronal processes (adhesion, proliferation, migration or (directional) differentiation) in 2D or 3D formats *in vitro*, and also nerve tissue regeneration *in vivo*. The sections in this review are organized attending to the biomaterial-elicited cellular response. Inside each section, the literature is structured along specific material properties exploited to support such response, i.e., (i) biofunctionalization with adhesive proteins, mimetic peptides and growth factors used to mediate specific interactions with cells, (ii) mechanical properties, and (iii) dimensionality and topographical features for guiding axon extension and directional growth. Within each section the response from different cell types is presented. At the end of this article the overall progress and remaining challenges for the future of this field are critically discussed.

BIOMATERIALS THAT SUPPORT NEURONAL CELL ADHESION

The most basic requirement for a synthetic biomaterial scaffold for cell growth and tissue regeneration (beyond toxicity) is its ability to support cell attachment (Cooke et al., 2010). For this purpose, synthetic biomaterials for neuronal regeneration are typically coated or functionalized with either (a) polymers which are able to interact with the negatively charged cell membrane, (b) reactive layers that can (covalently) bind to the cell surface, or (c) specific cell adhesive molecules able to interact with adhesive receptors at the cell membrane (i.e., integrins) (Berns et al., 2014; Lu et al., 2014; Akizawa et al., 2016; Hamsici et al., 2017). Positively charged polymers like polylysine (PL), poly(ornithine) (PO), poly(ethyleneimine) (PEI), poly(propyleneimine) (PPI) or poly(allylamine hydrochloride) are traditionally used in neuronal cell cultures (Roach et al., 2010). These positively charged layers interact with the negatively charged cellular membrane and allow cell attachment. Reactive polycatechol coatings like poly(dopamine) or poly(norepinephrine) (pNE) have also been used to immobilize neurons (Park et al., 2014; Kim et al., 2015). Such coatings can form on almost any kind of material. The polycatechol layer can covalently react with proteins from serum forming a protein layer onto the biomaterial that supports fast adhesion of human neural stem cells (hNSCs) (**Figure 1A**), or bind secreted adhesive proteins from the cells, or directly bind to the surface of the cells (Park et al., 2014).

Alternatively to positively charged or reactive coatings, biomaterials can be functionalized with cell adhesive ECM proteins, such as laminin (LN), collagen (CO) or fibronectin (FN) (Yamada, 1989; Belkin and Stepp, 2000; Guarnieri et al., 2007; Durbeej, 2010; Lei et al., 2012; Lee et al., 2014). These proteins offer specific binding sites for adhesion receptors at the cell membrane (i.e., integrins) that mediate cell adhesion. For example, poly(L-lactic acid) (PLLA) nanofibers coated with LN enhanced the attachment and proliferation of PC12 cells vs. unmodified fibers (**Figure 1B**) (Koh et al., 2008). In some cases, protein fragments containing the binding domains or peptidomimetica are used for surface functionalization instead of the whole protein (Mizuno et al., 2017). Short peptidomimetics are easier to control and manipulate in comparison to the full protein for biomaterial applications. Typical sequences used in neuronal cell cultures are IKVAV, RKRLQVQLSIRT or YIGSR peptides derived from LN, or the RGD binding site from FN (Frith et al., 2012; Kharkar et al., 2013). The YIGSR and RKRLQVQLSIRT peptides support neural cells adhesion, while IKVAV sequence is stated to support differentiation, migration and neurite extension of neural cells (Freitas et al., 2007; Mochizuki et al., 2007; Thid et al., 2007; Frith et al., 2012; Yamada et al., 2012). Functionalized PAs with IKVAV enhanced adhesion by two-folds and aligned neurite extension of hippocampal neurons in comparison to unmodified fibers (**Figure 1C**) (Berns et al., 2014). Neurotrophic factors (NF) and glial cell line-derived neurotrophic factor (GDNF) have also been combined with adhesion peptides to promote attachment of hNSCs (Kang et al., 2011; Yang et al., 2012; Taylor et al., 2017).

In many cases the nonspecific (electrostatic) and specific (receptor-mediated) functionalization approaches are used together to improve neural adhesion to surfaces. Poly(acrylamide) P(AAm) gels covalently derivatized with IKVAV and PL mixture through orthogonal thiol and amine coupling chemistries enhanced neuronal maturation of mouse embryonic neural progenitor cells (NPCs) by 3-fold in comparison to hydrogels modified only with IKVAV or PL (**Figure 1D**) (Farrukh et al., 2017b). Neuronal cells behaved differently when seeded on laminin micropatterns on glass or on PEI coated surfaces. Cells on glass/laminin surface extended neurites only on micropatterned laminin lines, while on PEI/laminin surface neurites grew randomly and did not follow the laminin pattern (Liu et al., 2006).

The attachment of the adhesive proteins or ligands to the biomaterial can be performed either by physical adsorption, or by covalent reaction of the adhesive molecule with reactive groups on the materials surface. Physical adsorption is the simplest method, which only requires incubation of the surface with a concentrated protein solution. However, physical interactions are reversible and this might limit the stability of the coating during cell culture time. In addition, immobilization by physical interactions lacks spatial orientation of the absorbed protein and can lead to loss of protein function in the immobilized state. Covalent binding of the adhesive molecules is expected to lead to more homogenous and stable coatings, and eventually allow specific orientation of ligands and more effective binding (Ho et al., 2006). Amines and thiols are the most common reactive groups present in peptides or proteins used for derivatization of functional surfaces. Typically glycidyl, carboxyl or maleimide groups are the reactive functionalities at the surface (Taylor et al., 2017). The performance of covalent vs. physical immobilization strategies for neuronal cell attachment has been addressed in some reports. NSCs seeded on soft chitosan hydrogels (0.5–0.7 kPa) covalently functionalized with LN showed enhanced cell spreading *vs*. hydrogels with physically adsorbed LN (Wilkinson et al., 2014). In a different study, adult hippocampal NSCs

Abbreviations: 3D-GFs, 3D porous graphene foam; AFG, Aligned fibrillar fibrin hydrogel; aNSCs, Adult neural stem cells; BDNF, Brain-derived neurotrophic factor; BMHP, Bone marrow homing peptide; BMP, Bone morphogenetic protein; BMSCs, Bone marrow stromal cells; CNGs, Chitosan nerve guides; CNS, Central nervous system; CO, Collagen; DRGs, Dorsal root ganglion; ECM, Extracellular matrix; EGF, Epidermal growth factor; ELP, Elastin-like proteins; EPO, Erythropoietin; ESMN, Embryonic stem cell-derived motor neurons; FGF-2, Fibroblast growth factor 2; FN, Fibronectin; GDNF, Glial cell line-derived neurotrophic factor; GO, Graphene oxide; h-iN, Human induced neuronal cells; hiPSCs, human induced pluripotent stem cells; HNPCs, Hippocampal neural progenitor cells; hNSCs, Human neural stem cells; hUMSCs, human umbilical cord mesenchymal stem cells; LN, Laminin; MAC, Methacrylamide chitosans; MaSp1, Major ampullate spidroin 1; mNSCs, Mouse neural stem cells; MSCs, Mesenchymal stem cells; NCAM, Neural cell adhesion molecule; NF, Neurotrophic factors; NGCs, Nerve guidance channels; NGF, Nerve growth factor; NPCs, Neural progenitor cells; NSCs, Neural stem cells; NSPCs, Neural stem progenitor cells; P(AAm), Poly(Acrylamide); PAN-MA, Poly(Acrylonitrile-co-Methylacrylate); PAs, Peptide amphiphiles; PCL, Poly(ε-Caprolactone); PDMS, Poly(Dimethylsiloxane); PEG, Poly(Ethyleneglycol); PEI, Poly(Ethyleneimine); PL, Poly(Lysine); PLGA, Poly(L-lactide-co-glycolide); PLLA, Poly(L-lactic acid); pNE, Poly(Norepinephrine); PNS, Peripheral nervous system; PO, Poly(Ornithine); PPI, Poly(Propyleneimine); PVC, Poly(Vinyl chloride); RFG, Random fibrin hydrogel; SAPs, Self-assembling peptides; SF, Silk fibroin; SGN, Spiral ganglion neurons; TCP, Tissue culture plate.

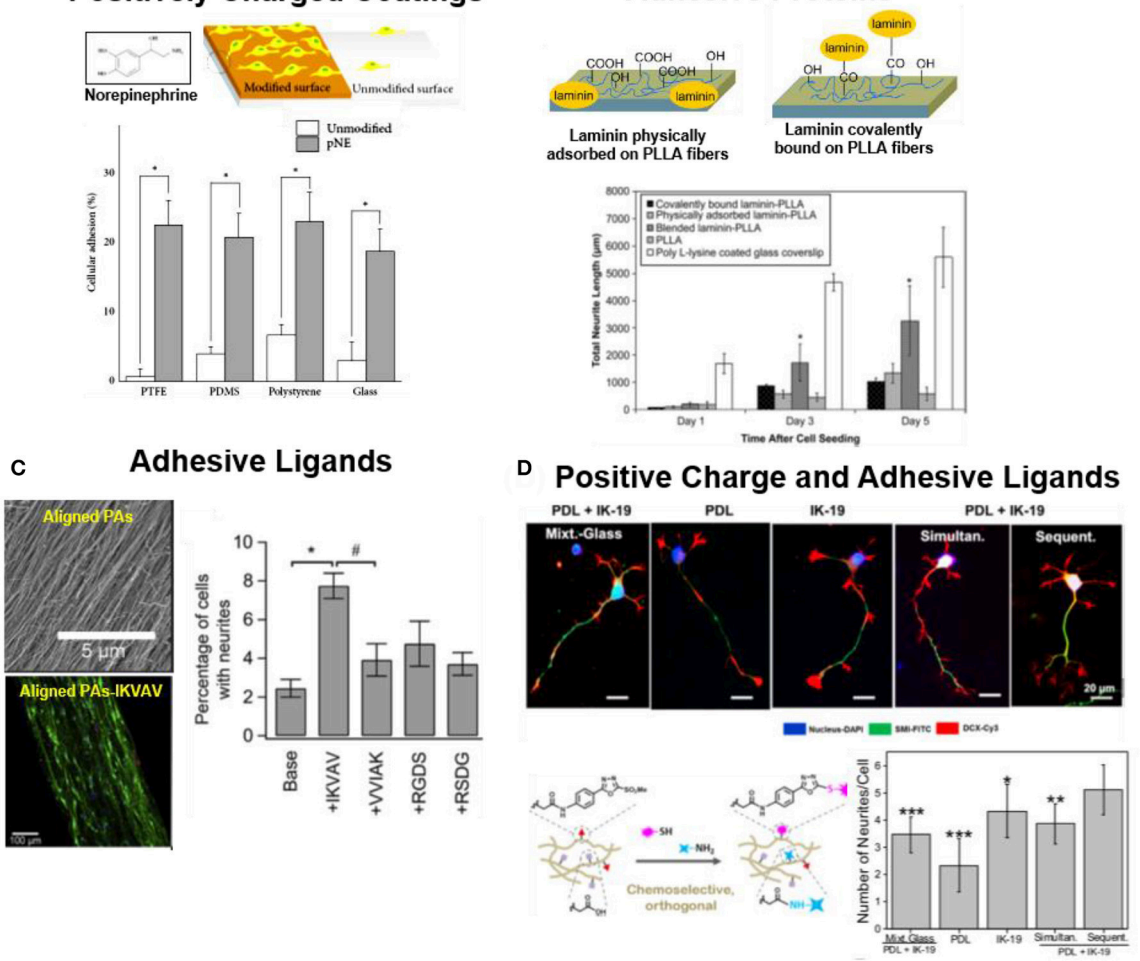

FIGURE 1 | Strategies to support adhesion of neuronal cells to biomaterials **(A)** hNSCs on pNE coated and uncoated substrates. pNE coating after 2 h of cell seeding significantly enhance cell adhesion (Park et al., 2014) Copyright 2014, Minah Park et al.; **(B)** PLLA nanofibers coated or covalently functionalized with LN. LN coated substrates support adhesion and neurite extension of PC12 cells (Koh et al., 2008) Copyright 2008, Elsevier; **(C)** PAs (Palmitoyl-VVAAEE-NH_2) functionalized with adhesive epitope to support adhesion of hippocampal neurons. Aligned PA-IKVAV significantly enhance cell adhesion and directional neurite extension during 2 days of culture (Berns et al., 2014) Copyright 2014, Elsevier; **(D)** IKVAV (IK-19) and PL functionalized polyacrylamide hydrogels either by mixed (simultaneous binding) or by orthogonal coupling chemistries (sequential binding). Sequential binding of PL/IKVAV enhance the cell neurite extension of NPCs, during 5 days of culture in comparison to simultaneous binding (Farrukh et al., 2017b) Copyright 2017, American Chemical Society.

were cultured on phospholipid bilayers supported on glass functionalized with different RGD-containing peptides. NSCs attached to RGD functionalized bilayers in a similar way to glass substrates coated with LN, and underwent differentiation into neurons and astrocytes (Ananthanarayanan et al., 2010).

Typically, neural cells are attached to flat plastic/glass coated surfaces or thin hydrogel coatings for 2D culture. Alternative, more complex or conductive materials can be used in order to implement additional functions to the interface. For example, LN coated graphene films support adhesion of hNSCs during long term cell culture (3–4 weeks) and promote neuronal differentiation (**Figure 2A**) (Park et al., 2011). Such 2D cell culture environments are attractive due to their simple preparation and facile imaging. Eventually a topology, i.e., a patterned distribution of adhesive molecules, can be superposed on the substrate using established micropatterning methods (typically microcontactprinting), in order to provide directionality or site-specificity to neuronal attachment (Mammadov et al., 2013). For example, polydimethylsiloxane (PDMS) substrates were microcontactprinted with FN, N-cadherin, and Jagged1 proteins to promote spatially resolved adhesion of NSCs (**Figure 2B**) (Wang et al., 2014). In contrast to *in vivo* cellular environment where cells can adopt a 3D body shape by attaching to the 3D space, cells in 2D adhere within a single plane and develop an apical-basal polarization that might not be representative for the *in vivo* case (Caliari and Burdick, 2016). Therefore, 3D culture models of neuronal cells have developed in recent years. Different biomaterials

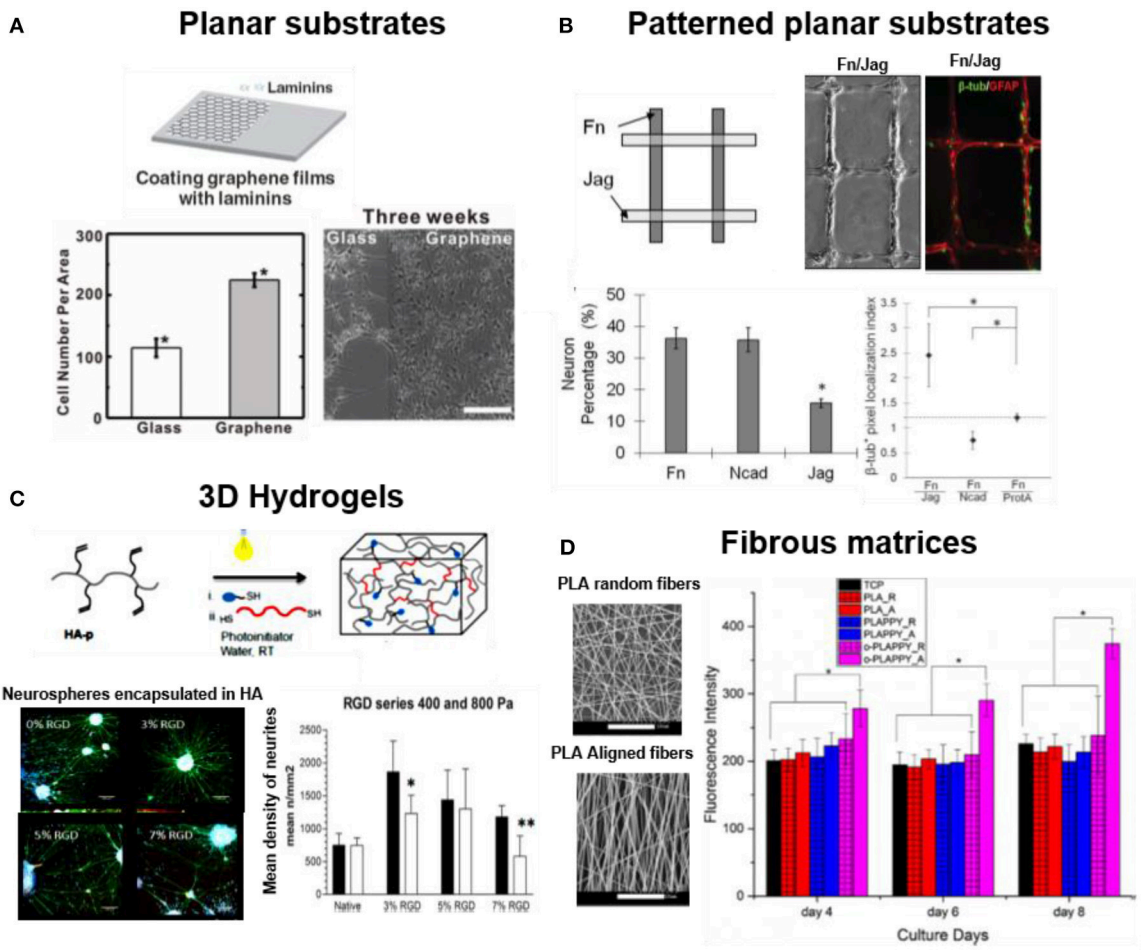

FIGURE 2 | Dimensionality in neuronal cell cultures. Examples of 2D and 3D substrates supporting attachment of neuronal cells **(A)** hNSCs cultured on laminin coated glass and on graphene film (Park et al., 2011) Copyright 2011, John Wiley and Sons; **(B)** NSCs cultured on micro-contact printed patterns of FN, Jag or N-cadherin adhesive proteins on PDMS films. FN support higher neuronal cell adhesion while combination of FN/Jag support neuronal differentiation (Wang et al., 2014) Copyright 2014, John Wiley and Sons; **(C)** Neural cultures in 3D gels of soft (Young's Modulus = 0.4 kPa) photopolymerized hyaluronic acid functionalized with RGD. The soft hydrogel facilitated neurite extension from encapsulated neurospheres during 17 days of culture (Tarus et al., 2016) Copyright 2016, American Chemical Society; **(D)** Neural cultures on 3D fibrous matrices of aligned (-A) and random PLA fibers (-R), modified with polypyrrole (PLAPPY) and poly-ornithine (o-PLAPPY) (Tian et al., 2016) Copyright 2016, Elsevier.

have been used as scaffolds: carbohydrates (alginate, dextran or hyaluronic acid), synthetic hydrogels (poly(ethyleneglycol) (PEG), fibrous matrices of peptide amphiphiles (PAs) nanofibers, or electrospun membranes from degradable polymers, i.e., PLLA, poly(L-lactide-*co*-glycolide) (PLGA) or silk. These materials are also coated with adhesive proteins, or modified with adhesive bioactive peptide for supporting cell attachment (Cooke et al., 2010). Embryonic stem cell-derived motor neurons (ESMN) encapsulated in PEG hydrogel showed outgrowth of neurites only when the gel was functionalized with KGRGDS sequence (McKinnon et al., 2014). Mouse embryonic stem cells (ESCs) encapsulated into 3D alginate beads modified with FN or hyaluronic acid supported adhesion and differentiation of ESCs into neuronal lineage (Bozza et al., 2014). PEG hydrogel functionalized with IKVAV derived peptide sequence (CCRRIKVAVWLC) supported adhesion and proliferation of hNSCs (Li X. et al., 2014). RGD functionalized hyaluronic acid based 3D hydrogel enhanced 2 folds adhesion and neurite outgrowth of hippocampal NPCs (**Figure 2C**) (Tarus et al., 2016). Hydrogels formed by nanofibers of peptide amphiphiles (PAs) containing the repeating RADA sequence and different peptidomimetica (RGD for cell adhesion, PFSSTKT for signal transduction and SKPPGTSS for apoptosis inhibition) allowed attachment, survival and proliferation of NSCs into NPCs, neurons, astrocytes and oligodendrocytes during 5 months of cell culture (Koutsopoulos and Zhang, 2013; Zweckberger et al., 2016). The enhanced cell survival on hydrogels of PAs modified with SKPPGTSS (69%), RGD (58%), and PFSSTKT (56%) was significantly higher than on matrigel (37%) or collagen-1 (25%) gels (Koutsopoulos and Zhang, 2013). PA hydrogels containing RGD and IKVAV motif showed enhanced adhesion and proliferation of embedded NSCs in comparison to unmodified fibers (Sun et al., 2016). Spider silk based 3D scaffold has also been used for neural cell culture due to biocompatibility, tunable

surface charge and mechanical properties. Primary cortical neurons showed growth, extension and higher expression of neural cell adhesion molecule (NCAM) on recombinant major ampullate spidroin 1 (MaSp1) spider silk. The modification of MaSp1 with GRGGL adhesive sequence (N-cadherin binding site) lead to a significant improvement in neuronal growth (An et al., 2015). The Self-assembling peptides (SAPs) nanofiber scaffolds from $K_2(QL)_6K_2(QL_6)$-IKVAV and $RADA_{16}$-I-BMHP-1 were tested for spinal cord injury (SCI) model. These peptides increased the stem cell viability and facilitated differentiation into neurons (Zweckberger et al., 2016). A hybrid nanofiber scaffold based on PLGA and $RADA_{16}$ and modified with bone marrow homing peptide-1 (BMHP-1) supported adhesion and proliferation of rat Schwann cells for application in peripheral nervous system (PNS) repair (Nune et al., 2016).

Topological and topographical features at micro- and nanoscale influence the behavior of neurons in multiple ways, not yet well understood (Micholt et al., 2013; Kulangara et al., 2014; Yang et al., 2014; Nagamine et al., 2015). Line micropatterns with 1–10 μm width and several mm length are the preferred geometrical designs to meet the characteristic elongated morphology of neurons. Either adhesive protein micropatterns on planar substrates (**Figure 2**) or microchannels have been used for this purpose. Different examples demonstrate positive effect of topographical features in supporting neuronal adhesion. hNSCs showed a two folds enhanced adhesion to LN coated graphene films *vs.* glass, presumably due to the surface roughness (Park et al., 2011). A micro-grated PDMS substrate coated with PO/LN were designed with dimensions of different heights (0.35–4 μm), width (2 μm), and spacing (2 μm). Higher cell adhesion, alignment (10–50 %), and neuronal differentiation (∼10–20%) of murine NPCs was reported in deeper (2 and 4 μm) PDMS channels *vs.* shallow channels (Chua et al., 2014). Electrospun PLGA nanofibers with smooth and nanorough surfaces (∼100–400 nm) were used to culture A-172 cell line derived from human brain. The PLGA fibers with rough surface enhanced the adhesion and up to 50% increase in viability of cells (Zamani et al., 2013). A scaffold of aligned electrospun PLLA nanofibers coated with PO enhanced adhesion and proliferation of PC-12 cells by two-fold in comparison to randomly oriented PLLA-PO fibers (**Figure 2D**) (Tian et al., 2016). In some cases microtopographies are used to define the direction for neurons to attach and grow. Alginate hydrogels containing microchannels functionalized with RGD supported adhesion and differentiation of bone marrow stromal cells (Lee et al., 2015). Electrospun PLLA fibers coated with graphene oxide (GO) supported adhesion of Schwann cells and PC12. The surface roughness was introduced by coating of GO nanosheets (Zhang et al., 2016).

BIOMATERIALS THAT SUPPORT PROLIFERATION OF NEURONAL CELLS

Low cell proliferation ratio is a major barrier in the clinical success of cell therapies (Karow et al., 2012; Ortega et al., 2013). Similar to adhesive behavior, proliferation varies with material parameters such as coating chemistry, mechanics, dimensionality or morphology.

Functionalization of biodegradable polyesters with hydrophilic and charged functional groups has a positive effect in proliferation ratios. Hydrophilic O_2 plasma treated PCL fiber meshes enhanced by ∼2 folds the viability and proliferation of mouse ESCs after 3 days of cell culture (Abbasi et al., 2014). Schwann cells showed doubled proliferation ratio on PCL surfaces treated with hexamethylenediamine than on non-functionalized ones during 5 days of cell culture (Luca et al., 2014). Electrospun PLLA-*co*-PCL/silk fibers loaded with vitamin B5 supported 20% higher proliferation of Schwann cells due to increased surface hydrophilicity (Bhutto et al., 2016).

Several reports demonstrate the positive effect of surface anchored adhesive proteins and peptidomimetics in proliferation. Matrigel functionalized PCL nanofibers enhanced ∼2.5 times proliferation of nerve precursor cells during 4 days of cell culture compared to bare PCL (Hiraoka et al., 2009; Ghasemi-Mobarakeh et al., 2010). Laminin peptides from α1 (LP3) or γ1 (LP) chains improved cell survival in *in vivo* collagen implants. Implanted NSCs encapsulated in the functionalized collagen at striatum of healthy rats showed enhanced cell viability (Nakaji-Hirabayashi et al., 2013). GRGDS modified gellan gum used to culture neural stem progenitor cells (NSPCs) showed 3-fold increase in proliferation than unmodified gellan gum (Silva et al., 2012). Collagen hydrogels functionalized with peptide sequence PPFLMLLKGSTR from LN α3 chain enhanced the viability and proliferation (∼4 folds) of neurosphere isolated from striatum of embryonic rat. Schwann cells cultured on core-shell electrospun PLLA-*co*-PCL nanofibers (316 ± 110 nm) coated with LN showed a 78% enhanced proliferation after 7 days of culture (Kijenska et al., 2014). Hydrogels formed by PA nanofibers functionalized with IKVAV and RGD promoted ∼1 fold higher proliferation ratios of Schwann cells after 7–14 days of cell culture. The RGD-PA hydrogels were slightly (∼20%) more effective in supporting cell proliferation and maintaining cell viability than IKVAV during 21 days of culture (Li A. et al., 2014). IKVAV functionalized poly(ester carbonate) fibers enhanced cell proliferation (20%) and neurite outgrowth (∼5 folds) of PC12 cells compared to unmodified fibers (Xing et al., 2014).

Improvement in cell proliferation was also reported on natural matrices modified with adhesive peptides in combination with NGFs. The fibroblast growth factor-2 (FGF2) embedded in a collagen sponge enhanced the viability and proliferation of NSCs (Ma et al., 2014). Slow release of NGFs (10 ng/mL) from collagen gel enhanced the viability and decreased apoptosis of PC12 cell during 4 days of cell culture more effectively than NGFs directly added to medium (Bhang et al., 2009).

It is now well accepted that the mechanical properties of the natural cellular microenvironment influence the behavior of embedded cells. In a similar manner, the mechanical properties of the culture substrate in 2D or 3D impact cellular processes (Laura et al., 2008; Norman and Aranda-Espinoza, 2010; Hanein et al., 2011). In general culture conditions tend to match the properties of the natural environment. In the case of brain tissue, which belongs to the softest in the body, biomaterials with stiffness 0.1–20 kPa are preferred. For the retina tissue,

the stiffness with 1–20 kPa is the preferred mechanical designs for biomaterials. Several reports show how the stiffness of the biomaterial influences proliferation of neuronal cells. Soft P(AAm) hydrogels (2 kPa) functionalized with PL/IKVAV enhance proliferation (11–24%) of NSCs during 4 days of culture vs. glass or stiff gel (20 kPa) (**Figure 3A**) (Farrukh et al., 2017a). A soft N-carboxyethyl chitosan/oxidized sodium alginate hydrogel with Young's Modulus between 0.1 and 1 kPa was demonstrated to support proliferation and differentiation of NSCs. Enhanced cell proliferation (∼1 fold) and a 38% increase in neuronal differentiation was observed in the hydrogel with Young's Modulus 0.5 kPa. This hydrogel is also injectable and, therefore, it could be a suitable carrier for NSCs based regeneration (Wei et al., 2016). A study of NSCs proliferation in materials with different stiffness was reported using thermo-responsive polyurethane hydrogels with varying compositional ranges with Young's Modulus between 0.68 and 2.4 kPa. NSCs on 0.68 kPa gels proliferated 30% faster than cells on 2.4 kPa hydrogels (**Figure 3B**). Low stiffness facilitated NSCs survival and growth (Hsieh et al., 2015). Electrospun blends of silk fibroin (SF) and poly(L-lactic acid-*co*-ε-caprolactone) (PLLA-*co*-PCL) with Young's Modulus between 13 and 120 MPa supported adhesion, proliferation and preferential differentiation of retinal progenitor cells (RPCs) into retinal neurons. The cells show highest proliferation on 105 MPa SF:PLCL (1:1) substrates (Zhang et al., 2015).

Topography and alignment also influence neuronal cell proliferation. Electrospun gelatin nanofiber meshes with randomly oriented nanofibers showed enhanced adhesion (20%) and proliferation of Schwann (RT4-D6P2T) (30%) and sensory neuron-like (50B11) (40%) cell lines, while aligned fibers enhanced the differentiation (Gnavi et al., 2015). Similarly stimuli responsive biomaterials also influence cell proliferation. Electrically conducting aligned PLLA and polypyrrole electrospun nanofibers coated with PO support proliferation (40%) and differentiation of PC-12 cells while on electric stimulation it improves the neurite out growth (Tian et al., 2016). **Table 1** presents an overview of biomaterials reported to support cell proliferation.

BIOMATERIAL DESIGNS TO SUPPORT DIFFERENTIATION OF STEM CELLS INTO NEURONAL CELL LINEAGES

The success of nerve regeneration therapies is based on optimized differentiation of stem cells into different nerve cell lineage. The undifferentiated multipotent NSCs can differentiate into unipotent neurons, astrocytes, and oligodendrocytes lineage. The following section describes biomaterials to guide differentiation of stem cells into neural cells.

Several adhesive proteins and peptidomimetics have been reported to support neuronal differentiation on different biomaterials. Micropatterned FN/N-cadherin on PDMS substrates allows formation of cell-cell and cell-matrix contacts and stimulate differentiation of NSCs into neural linage (Wang et al., 2014). LN coated graphene films preferential enhance neuronal differentiation of hNSCs during 2–4 weeks culture (Park et al., 2011). Bioactive IKVAV peptide functionalized phospholipid bilayers supported differentiation of embryonic NSCs into neuronal lineage over the glial phenotype (Thid et al., 2008). YIGSR modified aligned PLLA-DIBO nanofibers prepared by metal-free click chemistry promoted neurogenic differentiation of mouse ESCs (Callahan et al., 2013). Gelatin coated PCL electrospun fibers in combination with retinoic acid were reported to trigger differentiation of embryonic stem cells (ESCs) into neural progenitors (Xie et al., 2009). Hybrid scaffolds such as silk-carbon nanotube scaffold coated with PO promoted ∼1 fold increase in neuronal differentiation of human ESCs compared to bare silk fibers (Chen et al., 2012). Similarly, silk fibroin films decorated with integrin-binding LN peptide motifs (YIGSR and GYIGSR) triggered differentiation of human Mesenchymal stem cells (MSCs) into neurogenic cells (Manchineella et al., 2016). Growth factors such as ciliary neurotrophic factor (CNTF) pattern printed on P(AAm) hydrogels promoted astrogenic differentiation of MSCs at the printed areas, while cells remained undifferentiated on fibroblast growth factor-2 (FGF2) printed area (Ilkhanizadeh et al., 2007). MSCs cultured on gold surfaces modified with FN, RGD (cyclic and linear form), or KRDGVC ligands developed into different phenotypes. Neurogenesis was observed at low surface concentration of linear RGD ligand, and myogenesis when cultured on high concentrations of linear RGD. The rest of adhesive ligands promoted osteogenesis (Kilian and Mrksich, 2012).

Biofunctionalization of biomaterials for 3D cultures with adhesive ligands also influences neural differentiation. Aligned electrospun cyclodextrin nanofibers conjugated with admantane-IKVAV increased neuronal differentiation (∼1 fold) and oriented neurite extension (Hamsici et al., 2017). IKVAV modified hyaluronic acid–PEG hydrogel supported neural differentiation, neurite outgrowth and growth of long axons (Xing et al., 2017). Recombinant 3D spider silk (4RepCT) matrices enhance differentiation of NSCs isolated from the cerebral cortices into neurons (Lewicka et al., 2012). Electrospun PLC fibers coated with GO result in PCL-GO hybrid nanofibers. NSCs undergo differentiation into neuronal lineage at low GO concentration, while into oligodendrocyte lineage at high GO concentration. The authors predict that differentiation is based on interaction of cells with material, influenced by high elasticity and flexibility of GO (Shah et al., 2014). Soft 3D hydrogels formed by self-assembling of $RADA_{16}$ sequence containing RGD support differentiation of adult mouse NSCs into neurons (Gelain et al., 2006). $RADA_{16}$ based SAPs functionalized with RGD or LN derived BMHP-1 and BMHP-2 were used for 3D cell culture of adult mouse NSCs. The $RADA_{16}$-RGD promoted cell differentiation while $RADA_{16}$-BMHP supported proliferation (Cunha et al., 2011). DNA nanotubes functionalized with RGD also supported differentiation of NSCs into neurons (Stephanopoulos et al., 2014). NSCs cultured on 3D porous graphene foam (3D-GFs) functionalized with LN supported cell differentiation into neurons and astrocytes (Nasir et al., 2013). Super porous 2-hydroxyethyl methacrylate with 2-aminoethyl methacrylate

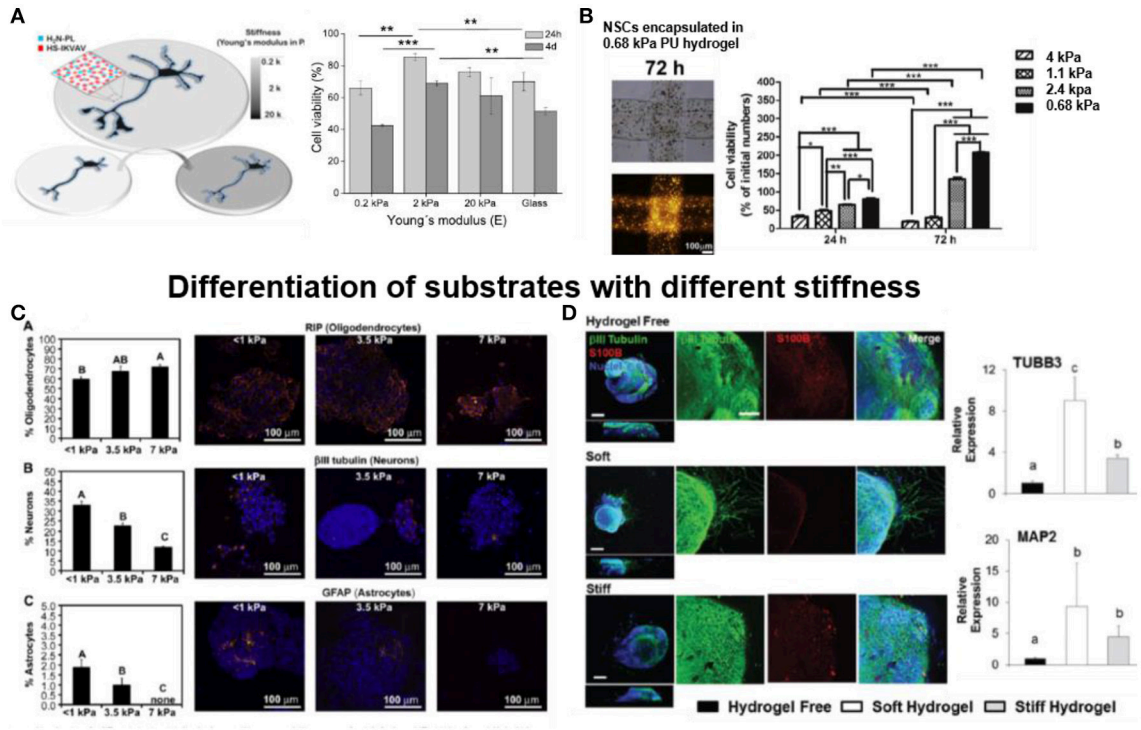

FIGURE 3 | Influence of the stiffness of the biomaterial in cell proliferation and differentiation **(A)** Soft (2 kPa) 2D polyacrylamide hydrogels functionalized with PL and IKVAV support proliferation of NSCs during 4 days of culture (Farrukh et al., 2017a) Copyright 2017, The Authors; **(B)** Soft (0.68 kPa) 3D polyurethane hydrogel encapsulating NSCs enhance proliferation of encapsulated cells (Hsieh et al., 2015) Copyright 2015, Elsevier; **(C)** Soft (<1 kPa) 2D methacrylamide chitosan hydrogel on glass, preferentially support neuronal differentiation of NSPCs during 8 days of culture (Leipzig and Shoichet, 2009) Copyright 2009, Elsevier; **(D)** Soft (0.5 kPa) 3D hyaluronic acid hydrogels trigger neurite extension from hiPSC-NPC spheroids, while stiff (1.4 kPa) hydrogel failed to support neurite extension, after 28 days of culture (Wu et al., 2017) Copyright 2017, Royal Society of Chemistry.

scaffolds modified with IKVAV support cell adhesion and the differentiation of human fetal NSCs into neurons (Kubinová et al., 2010). IKVAV grafted 3D silk fibroin-based hydrogel promote differentiation of progenitor cells into neuronal cells (Sun et al., 2017). Alginate hydrogels biochemically conjugated with Fc-tagged recombinant N-cadherin (N-Cad-Fc) protein promoted a ∼80% increased neurogenic differentiation of neural cortical cells of rat embryo (E18) compared to unmodified hydrogel (Lee et al., 2016). IKVAV modified self-assembled 3D PAs nanofibers, preferentially promotes neuronal cell growth over glial cells (Silva et al., 2004). Rat embryonic NPCs embedded in 3D graphene oxide (GO) scaffold coated with PL developed interconnected synapsis and differentiated into neurons (∼62%) and astrocytes (∼41%) during 14 days of cell culture (Serrano et al., 2014). The differentiation of neural precursor cells in 3D collagen gels modified with PO/LN, growth factor-reduced matrigel (gfrMG) or PuraMatrix® gels depicted enhanced (∼2 folds) neurogenic differentiation in gfrMG modified matrices (Uemura et al., 2010). IKVAV functionalized 3D collagen hydrogels enhanced (∼5 folds) differentiation of dorsal root ganglions (DRGs) into neuronal phenotype in comparison to unmodified collagen matrix (Hosseinkhani et al., 2013). Hybrid 3D matrices formed by collagen and PAs nanofibers modified with IKVAV were reported to support survival and dendritic growth of purkinje neurons (PC) (Sur et al., 2014). High PA-IKVAV to collagen ratio (1:0.45) promoted dendritic growth (∼4 folds) and axonal guidance of PC neurons (Sur et al., 2014). Gradient of IKVAV on photochemically modified PCL fibers supports neuronal differentiation and expression of β-III-tubulin in PC12 cells, and neurite growth in the direction of increasing peptide concentration (Kim et al., 2015).

The stiffness of the biomaterial also plays an important role in defining cell phenotype. MSCs cultured on soft P(AAm) gels (i.e., Young's Modulus of 0.1- 1 kPa, mimicking the stiffness of brain tissue) developed into neurogenic cells, while the culture conditions rendered myocytes or osteogenic phenotypes when harder gels were used for culture (8–17 or 25–40 kPa respectively).(Engler et al., 2006) These findings have been supported by other reports as well (Wen et al., 2014). ESCs differentiation was studied on covalently crosslinked gelatin gels with Young's Modulus ranging from 2 to 35 kPa. Soft 2 kPa substrate preferentially supported differentiation of ESCs into mature neurons, while a 83% decrease in neuronal differentiation was reported on gelatin of higher (35 kPa) stiffness (Ali et al., 2015). Neuronal differentiation of mouse embryonic NPCs

TABLE 1 | Biomaterial scaffold for neural cell proliferation.

Biomaterial	Functionalization	Cells	References
Polydopamine coating	YIGSR and RGD	NSCs	Taylor et al., 2017
PEG hydrogel	CCRRIKVAVWLC	NSCs	Li et al., 2015
$RADA_{16}$ SAPs	RGD, PFSSTKT, SKPPGTSS	NSCs	Koutsopoulos and Zhang, 2013
$RADA_{16}$ SAPs	RGD and IKVAV	NSCs	Sun et al., 2016
$RADA_{16}$ SAPs	BMHP-1	Schwann cells	Nune et al., 2016
PLCL fibers	LN	Schwann cells	Kijenska et al., 2014
PLLA nanofibers	LN	PC 12	Koh et al., 2008
PLLA fibers	GO	Schwann cells, PC12	Zhang et al., 2016
Gellan gum	GRGDS	NSPCs	Silva et al., 2012
PLCL nanofibers	LN	Schwann cells	Kijenska et al., 2014
PCL	Matrigel	NPCs	Ghasemi-Mobarakeh et al., 2010
Collagen gel	NGFs	PC 12	Bhang et al., 2009
Gelatin fibers	Gelatin	Schwann Cells	Gnavi et al., 2015
Pas	RGD and IKVAV	Schwann cells	Li A. et al., 2014

on P(AAm) hydrogels (0.2–20 kPa) covalently functionalized with IKVAV and PL showed a 6 folds enhancement of NPCs neuronal maturation on 2 kPa gels *vs.* IKVAV/PL coated glass, while the 20 kPa hydrogel enhanced (30% increase) neuronal differentiation of adult neural stem cells (aNSCs) (Farrukh et al., 2017a). Methacrylamide chitosan (MAC) hydrogels (1–10 kPA) functionalized with LN showed the highest neuronal differentiation of NSPCs at <1 kPa (30%), low density of astrocytes (2%) between 1 and 3.5 kPa, and oligodendrocyte differentiation (70%) on stiff 7 kPa hydrogel (**Figure 3C**) (Leipzig and Shoichet, 2009).

3D cultures of hyaluronic acid hydrogels with tunable stiffness (1.5–7 kPa) coated with PL showed differentiation of NPCs into neurons at low stiffness (1.5 kPa) and into astrocytes at higher stiffness (7 kPa) (Seidlits et al., 2010). mNSCs encapsulated in soft elastin-like proteins (ELP) hydrogel modified with RGD ($G' = 0.36$ kPa) showed enhanced viability ∼97% and differentiation into neurons (Madl et al., 2016). ELPs without RGD sequence or scramble RDG sequence failed to support cell survival or differentiation. RGD functionalized 3D hyaluronic acid hydrogel with different stiffness (G' 400 and 800 Pa) is reported for culture of hippocampal NPCs. Neurite extend through the hydrogel with enhanced neurite outgrowth and branching on soft hydrogel (G' 400 Pa) (Tarus et al., 2016). Hydrogel films of 3-hydroxybutyrate and 3-hydroxyhexanoate copolymers promoted neuronal differentiation of NSCs during 2D cell culture. The same polymers used as 3D matrices supported attachment, synaptic outgrowth and synaptogenesis (Xu et al., 2010). Chitosan 2D films promoted astrocytic differentiation of NSCs, while chitosan porous scaffolds and chitosan multimicrotubule conduits supported neuronal differentiation (Wang et al., 2010a). Methacrylated hyaluronic acid (0.5–1.5 kPa) 3D hydrogels promoted differentiation of human induced pluripotent stem (hiPSCs) derived NPCs and Down syndrome patient-specific hiPSCs derived NPCs spheroids into neurons (**Figure 3D**). Soft (0.5 kPa) hydrogels enhanced neuronal phenotype (∼1 fold), suppressed (∼40%) astrocytic differentiation and triggered neurite outgrowth (Wu et al., 2017). RGD functionalized 3D ELP based polymeric hydrogels (0.5–2.1 kPa) enhanced DRGs neuronal viability and promote neurite outgrowth from DRGs explant. Soft 0.5 kPa ELPs-RGD promoted neurite extension up to ∼1,800 μm from DRS during 7 days of cell culture, in contrast to ∼500 μm neurite extension on 2.1 kPa hydrogel (Lampe et al., 2013). Gelatin-hydroxyphenylpropionic acid hydrogels with tunable stiffness (G' 0.28–0.84 kPa) modulated differentiation of hMSCs. Low stiffness (0.28 kPa) hydrogels promoted neurogenesis, while high stiffness (0.84 kPa) increased cell proliferation (Wang et al., 2010b). Thixotropic 3D PEG-silica hydrogel with 7, 25, and 75 Pa stiffness functionalized with RGD promoted neuronal differentiation of MSCs only above 75 Pa. Very soft hydrogels failed to support cell viability, proliferation and differentiation of cells (Pek et al., 2010).

Several reports demonstrate the effect of geometry and topography of substrates on cell differentiation. Rat hippocampus-derived adult NSCs on laminin-coated electrospun polyethersulfone fiber with different fiber diameter (∼ 250–1,500 nm) showed a 40% increase in oligodendrocyte differentiate on small diameter mesh (280 nm), while a 20% increase in neuronal differentiation was observed on meshes with diameter 750 nm. Authors attribute this effect to random spreading of cells on densely packed small fiber mesh vs. aligned extension of cell along single fiber of large diameter (Christopherson et al., 2009). PCL loop mesh, bimodal, and biaxially aligned electrospun scaffold (fiber diameter ∼40–85 μm) promoted neuronal differentiation and guided the neurite outgrowth of human iPSCs along the fiber, as depicted in **Figure 4A**. Biaxial aligned scaffolds promoted the highest viability (95%) and neurite extension along the fibers (Mohtaram et al., 2015). Micro-patterned PDMS with PL and LN stripes directed differentiation and guidance of adult human stem cells. Microstripes significantly wider than the cell soma (3 μm) promoted neural differentiation, while stripes narrower than 10 μm hindered differentiation (**Figure 4B**) (Béduer et al., 2012). LN functionalized P(AAm) hydrogels (0.6 kPa) with un-patterned or with circular (50 μm) geometrical patterns, trigger preferential differentiation of MSCs into neurogenic cells (90%) on un-patterned substrate while adipogenic cells (60%) on circular geometry (Lee et al., 2013).

BIOMATERIALS SUPPORTING NEURONAL MIGRATION

Regenerative strategies for neural tissue involve the recruitment and instruction of endogenous neural stem cells or Schwann cells by using scaffolds containing relevant features of the migratory environment in brain tissue and assist cells to

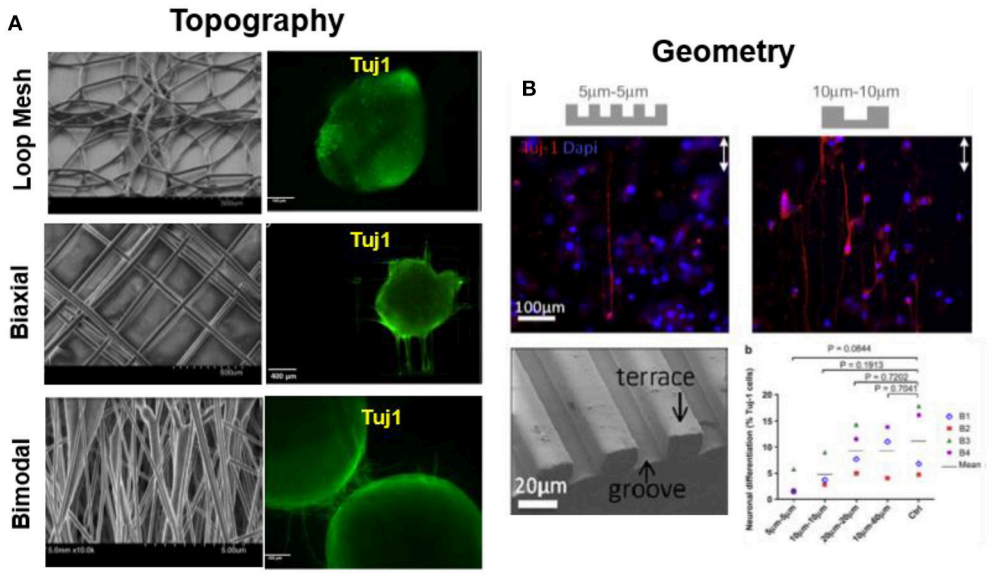

FIGURE 4 | Substrate topography modulates cell differentiation. **(A)** PCL loop mesh, bimodal and biaxially aligned electrospun scaffold (fiber diameter ∼40–85 µm) influence on differentiation of iPSCs. Biaxially aligned fibers preferentially promoted the highest neurite extension as labeled by Tuj1 immunostaining (Mohtaram et al., 2015) Copyright 2015, John Wiley and Sons; **(B)** Micro-patterned PDMS with PL and LN stripes directed differentiation and guidance of adult hNSCs. Microstripes >10 µm promote neuronal differentiation, while < 10 µm hinder differentiation, during 7 days of culture (B1-B4 represents individuals with 4 different biopsies) (Béduer et al., 2012) Copyright 2012, Elsevier.

organize and relocate at appropriate positions. Similar to neural attachment, neural migration is influenced by biochemical (adhesive ligands, growth factors), mechanical factors and topographical of the extracellular matrix, and also by adhesive contacts to neighboring cells. Examples of reported migratory responses of neural cells to these material parameters are detailed below.

The type and concentration of adhesive ligand on a biomaterial influences migration of neural cells by stabilizing the attachment of the growth cone of neurites. LN, for example, has been demonstrated to stimulate and guide migration of olfactory epithelial neurons *in vitro* (Calof and Lander, 1991). Depending on the cell type, different responses to the same adhesive coating can be expected. For example, aNSCs and astrocytes migrated on PL surfaces and became less migratory on PL/LN mixtures, while neuron preferred to spread and not move on PL (Joo et al., 2015a,b). A recent article describes morphological features on the migration of neuronal cells on different protein coatings FN, LN, LN mimetic peptides, reelin etc. Using micropatterned substrates with contrasting regions with different proteins, the role of specific adhesive cues in triggering, guide or stop migration of Early postmitotic cortical neurons on a biomaterial surface was explored (Zhao et al., 2017). In particular the role of adhesion for terminal somal translocation, i.e., the specific migratory behavior of cortical neurons when they position in the cortex layers, was studied. Somal translocation could be efficiently triggered when the growth cone of a neurite spread and stabilized on an area of stronger adhesive interactions, for example with a higher concentration of adhesive molecules (**Figure 5A**). *In vivo*, LN coated scaffolds promote migration of neuroblasts to injured brain tissue, contributing to neuronal regeneration after stroke in mice (**Figure 5B**) (Fujioka et al., 2017).

Gradients of soluble neurotrophic factors and neurotransmitters influence neuronal migration (Li Jeon et al., 2002). These molecules can be added to cell cultures, or secreted by other co-cultured cells like astrocytes (Mason et al., 2001). Glial and neural migration through hydrogels was demonstrated to be enhanced through delivery of soluble growth factors such as nerve growth factor (NGF) from fibrin in *in vitro* cultures (Wood and Sakiyama-Elbert, 2008). *In vivo*, the delivery of stimulating molecules to the CNS represents a clinical challenge because the blood–brain barrier limits the diffusion of molecules into the brain by traditional oral or intravenous routes. Injectable hydrogels have the capacity to overcome the challenges associated with drug delivery to the CNS (Pakulska et al., 2012). Intraventricular sequential delivery of epidermal growth factor (EGF) and erythropoietin (EPO) into a stroke injured rat brain showed enhanced migration of endogenous NSPCs to the injury site, resulting in neurogenesis and improved functional recovery (Kolb et al., 2007).

During growth and migration cells sense and can be guided by the variation of mechanical properties of their microenvironment. The relevance of mechanical signaling in different contexts of cell function is a current vivid area of research, also related to neural tissue. Stiffness gradients have been reported in CNS tissue (Franze, 2011, 2013; Wrobel and Sundararaghavan, 2013). LN-coated P(AAm) hydrogel with high stiffness (20 kPa) greatly promoted the migration of Schwann cells progenitors from embryonic DRGs compared to low stiffness hydrogel (1 kPa)(Rosso et al., 2017).

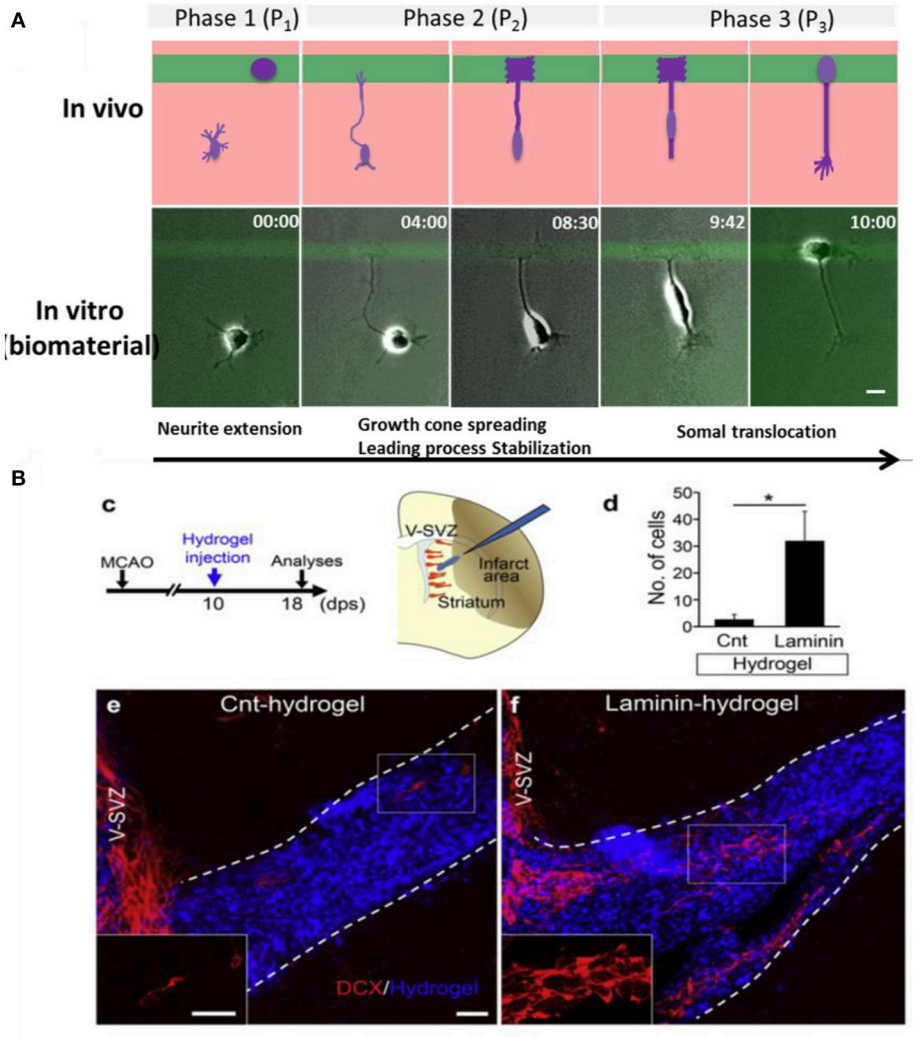

FIGURE 5 | Neuronal migration on biomaterials. **(A)** Hydrogel coated glass slides modified with mircopatterens of PL/IKVAV to trigger neuronal migration and somal translocation of cortical neurons *in vitro* (Zhao et al., 2017) Copyright 2017, Elsevier; **(B)** Migration of neuroblasts along a LN coated hydrogels toward the injured area *in vivo* (Fujioka et al., 2017) Copyright 2017, Elsevier.

During development, migration of neuronal cells often occurs in a directional way. Neurons attach and migrate along fibers of the ECM or along glial cell tracts (Malatesta et al., 2008). The sensitivity of neurons to topographical features has been exploited *in vitro* and *in vivo* (Hoffman-Kim et al., 2010; Gumera et al., 2011). Oligodendrocytes (Webb et al., 1995) and neurons (Gomez et al., 2007), have been shown to migrate along grooved topographies. The average migration speed of cells was higher on microgrooved substrates than on flat surfaces (Nikkhah et al., 2012). In 3D environments, DRGs cells exhibited unidirectional migration into micro-channels of the PEGylated fibrinogen hydrogel (Sarig-Nadir et al., 2009).

Neuronal migration has been also modulated *via* cell-cell contacts, specifically involving glial cells in cocultures. The membrane proteins connexin 46 and 23 expressed by radial glia (Valiente and Marín, 2010) and the cell adhesive proteins L1-CAM and neural cell adhesion molecule (NCAM) (Schmid and Maness, 2008) seem to play a relevant role in neuronal migration.

BIOMATERIALS FOR DIRECTIONAL NEURITE EXTENSION

In order to achieve successful regeneration of nerve tissue, sprouting axons from the proximal stump of one neuron need to grow and establish a new connection with the distal stump of the next neuron (Shin et al., 2003). Following injury, the remaining functional neurons will try to grow processes and reestablish connections with neighboring partners, but they often meet an impenetrable scar tissue composed of myelin, cellular debris, and other cells (astrocytes, oligodendrocytes, microglia) at the injury

site. The scar tissue blocks existing neurons from reaching their synaptic target and hinder the regeneration process (Schmidt and Leach, 2003). Guidance in neurite growth plays a vital role in nerve repair. Many approaches to support nerve regeneration, therefore, have focused on the development of biomaterials that provide guidance cues for directional neurite growth.

Topographical Cues for Guiding Neurite Extension

The topography of the neuronal microenvironment, including fibrillar ECM proteins and elongated glial cells, plays a major role for the directional growth of neurites. In the biomaterials field nerve guidance channels, surface topographies and 3D fibrillar meshworks have been used as supportive scaffolds for directional neural regeneration.

Nerve Guidance Channels (NGCs) for Peripheral Nerve Regeneration

Nerve guidance channels (NGCs) are tubular constructs with a hollow lumen through which the neuron axon should grow. This geometry has several advantages for spatial guidance of peripheral nerve regeneration: protection of the regenerating nerve against compression by the surrounding tissue, isolation of the regenerating axons from surrounding tissue, and longitudinal directional guidance of the regenerating neurites toward target tissue. Hollow nerve conduits have been widely used in research and clinical applications. Porous and not porous NGCs providing longitudinally oriented grooves in their lumen surface, (Göpferich, 1996) and eventually functionalized with cell adhesive ligands (e.g., LN-derived peptides YIGSR and IKVAV (Chiono et al., 2009) or controlled released growth factor (neurotrophic factors (Pfister et al., 2007) promote directional axon growth *in vivo* in small animals test. However, in some cases dispersion of the regenerating axons through the comparatively large lumen of the NGCs leads to inappropriate target reinnervation or polyinnervation of different targets by the axonal branches of the same neuron. Single hollow lumen NGCs are thus only recommended for small lesions (<30 mm) in the sensory nerves (Weber et al., 2000). *In vitro* neuronal, Schwann and DRGs culture were used to test the NGCs and *in vivo* a thy-1-YFP-H mouse common fibular nerve injury model or a nerve gap in the rat sciatic nerve were normally used. Generally, typical NGCs dimensions for experimental use in small animals are inner diameters of 1–2 mm and lengths of several millimeters, depending on the experimental gap.

Considerable effort has been focused on the development of more effective NGCs, in which a microstructured lumen of the NGC provides higher directionality. Structured lumens including multichannels, porous matrices or oriented fibrous conduits have been proposed (**Figure 6**). Multichannel NGCs mimic the natural compartment structure of nerves (He et al., 2009; Chiono and Tonda-Turo, 2015). They reduce axon dispersion, offer higher surface area for functionalization, cell adhesion and migration as compared to single lumen NGCs. The disadvantages of the multichannel NGC design reduced permeability and mechanical flexibility. In fact, multichannel NGCs did not lead to significant functional improvement in the repair of a 1-cm nerve gap in the rat sciatic nerve compared to single lumen nerve tubes (de Ruiter et al., 2008). NGCs might also incorporate fillers to form an internal porous or aligned 3D matrix. Fillers may include longitudinally aligned fibers (Matsumoto et al., 2000; Wang et al., 2005), porous sponges (Tonda-Turo et al., 2011) or gels (Ceballos et al., 1999; Nakayama et al., 2007). Fillers can also be functionalized with specific peptides/proteins or growth factors, as described in recent reviews (Pfister et al., 2007; Gu et al., 2011). Filling of the lumen of silicon NGCs with longitudinally oriented polyamide filaments lead to improved nerve regeneration by bridging a 15-mm sciatic nerve gap in rats (Lundborg et al., 1997). The ability of tubular channels mininally supplemented with aligned nanofiber-based thin-films to promote regeneration across a 14 mm tibial nerve gap was studied(Clements et al., 2009). They evaluated two different channels: a 1-film guidance channel–containing a single continuous thin-film of aligned fibers, and a 3-film channel. Interestingly, they found that the 1-film channels supported enhanced regeneration compared to the 3-film channels, because the two additional thin-film reduced permeability. Recently, the hollow chitosan nerve guides (CNGs) enhanced by introduction of a longitudinal chitosan film to reconstruct critical length 15 mm sciatic nerve defects in rats(Meyer et al., 2016). Compare to simple hollow CNGs, the CNGs with the introduced chitosan film significantly improved nerve regeneration, almost reached the regeneration outcome after autologous nerve grafting.

An alternative strategy to guide neurites growth within the luminal cavity of the NGC involves the use of electrospun tube walls. The use of tubes with walls consisting of oriented fibers has a number of advantages over the filled lumen strategy. (i) The materials are highly flexible and porous, well adapted for use within biological systems; (ii) nano- and micro-scale fibers have a high surface area-to-volume ratio increasing the area available for protein absorption, neural cells migration and regeneration of axons; (iii) fibers that can be preferentially aligned resulting in increased promotion of guided axonal growth (Daly et al., 2012).

Scaffolds for Guided Central Nerve Regeneration

Although regeneration of the mammalian CNS was thought to be impossible, studies have shown that axonal growth after spinal cord injury can occur when neurons are provided with the suitable substrata that support directional growth (Fawcett, 1998, 2002). Natural, ECM-derived biomaterials and also synthetic polymers processed in different ways to generate microtopographies have been used as matrices for supporting spinal nerve regeneration.

The relationship between microscale topography and neuronal development has been recently investigated *in vitro* in a high-throughput screening assay (Li et al., 2015). Primary neurons were presented to patterned substrates with a large library of topographical features including isotropic (e.g., dots, grids, squares) and anisotropic pattern designs (e.g., gratings) with lateral width between 5 and 15 μm and 1 μm depth. Anisotropic topographies enhanced axonal and in some cases dendritic extension *vs.* isotropic ones. However, dendritic branching occurred preferentially on planar substrates. The depth of the topographical features also influences the growth

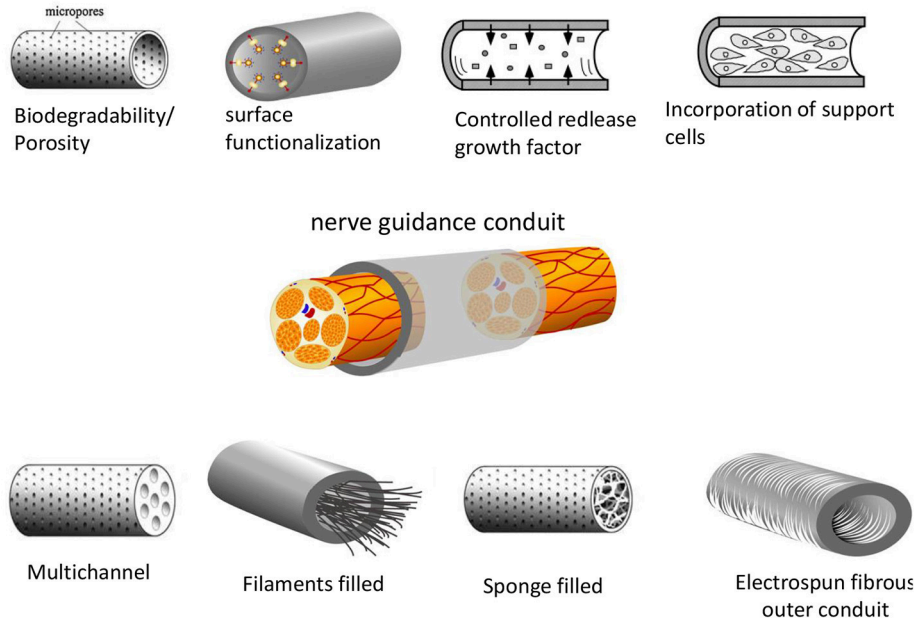

FIGURE 6 | Different designs of nerve guidance conduits (NGCs). The basic design parameters include: a biodegradable and porous channel wall, a biofunctionalized wall surface including adhesive and growth factors, intraluminal structures to mimic the structure of nerve fascicles, intraluminal guidance structures (filaments, sponge or hydrogel-like) or wall microstructures to support cell migration and axonal growth. Support cells can also be incorporated to the NGCs (Daly et al., 2012) Copyright 2012, The Royal Society.

of processes. Murine NPCs sensed the depth of micro-gratings and neurite elongation, alignment and neuronal differentiation increased with grating depth (Chua et al., 2014).

In vivo studies using poly(2-hydroxyethyl methacrylate-*co*-methylmethacrylate) hydrogel channels demonstrated improved tissue regeneration of transected rat spinal cords (Tsai et al., 2004). The hydrogel guidance channels were designed to match the dimensions and modulus of the rat spinal cord; the outside diameter of the channels was approximately 4.2 mm, the inside diameter was 3.6 mm, giving a wall thickness of 0.3 mm and the length was 6 mm. By inserting the transected cord stumps into the hydrogel nerve guidance channels, alignment of the cord stumps occurs, and cells were able to migrate along them. Axonal regeneration was enabled, and no significant scar formation appears.

Guided Neurite Extension on 3D Fibrillar Meshworks

Fibrillar 3D matrices can serve as substrates for neuronal growth. The fibrils provide spatial guidance to the extension of processes, while retaining an open matrix structure to be repopulated by the growing cells (Lietz et al., 2006; Schnell et al., 2007). This is of particular interest in the development of biomaterial-based scaffolds intended to promote the repair of highly organized nerve tissues, such as the retina or white matter tracts of the spinal cord.

Protein based and synthetic polymer fibers have been used to form fibrillar matrices and guide axonal growth. Fibers can be processed by different technologies, like electrospinning, bioprinting or self-assembly. Among these methods, electrospinning offers an uncomplicated and low-cost method for processing and applicable to different kinds of materials. Electrospun membranes with randomly or aligned fibers can be produced, and neuronal growth along the fibers has been demonstrated (Sell et al., 2007). NPCs and DRGs cells grew preferentially along aligned PLLA electrospun scaffolds with fiber diameters between 150 to 3,000 nm independently of the adhesive coating (Yang et al., 2005; Corey et al., 2007). NSCs elongated and outgrew neurites along aligned fiber scaffolds without adhesive coating (**Figure 7A**) (Yang et al., 2005). Authors could not establish a significant effect of the fiber diameter (between 300 and 1,500 nm) on the cell orientation. NSCs differentiation rate was found to be higher on PLLA nanofibers (diameter 300 nm) than that of micro fibers (diameter 1,500 nm), independently of alignment. Aligned nanofibers significantly improved neurite outgrowth compared to not aligned ones. On thicker fibers and fibers coated with adhesive factors, however, different tendencies were observed. Fibers of 35 μm coated with PL and LN promoted directional neurite outgrowth and promoted greater oriented process growth than large-caliber fibers (500 μm) (Smeal et al., 2005; Smeal and Tresco, 2008). Many studies have demonstrated that the aligned nanofibers, pattern nanofibers (half random and half aligned) and also cross-patterned nanofiber can guide the neurites to extend along the nanostructure. However, the contact cues provided by the nanofibers can be far more complicated than just guiding the neurites to extend along them. Xie et al. demonstrated that the neurites could not only project along the nanofibers, but also be directed to grow along a direction

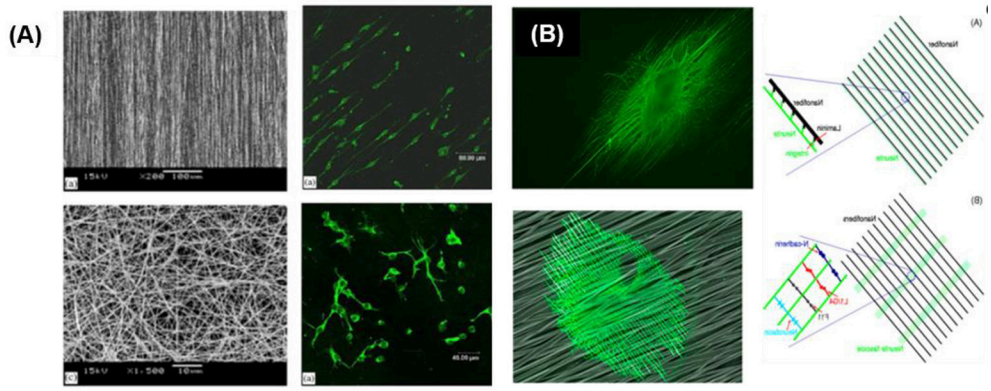

FIGURE 7 | Guided neurite extension on fibrillar networks **(A)** Neuron cells cultured on random and aligned fibers (Yang et al., 2005) Copyright 2005, Elsevier; **(B)** Neurites oriented along the nanofibers previously coated with laminin and perpendicularly to the nanofibers without adhesive coating (Xie et al., 2014) Copyright 2014, American Chemical Society.

perpendicular to the aligned nanofibers. The DRGs neurites grew perpendicularly to the alignment direction of electrospun PCL fibers (**Figure 7B**) (Xie et al., 2014). The growing direction of neurite on fibers was dependent on the adhesive interaction between neurites and nanofibers and on the dimensions and separation between fibers. A strong interaction leads to parallel growth of neurites along the fibers (e.g., low density fiber and fiber with LN coating), while a weak interaction (i.e., fibers without adhesive proteins) lead to perpendicular growth while high density mesh works lead also to perpendicular growth.

In vivo, aligned oriented fibers elicit regeneration, while randomly distributed fibers do not, demonstrating how topographical cues can influence endogenous nerve repair mechanisms in the absence of exogenous growth promoting proteins (Kim et al., 2008). Using electrospinning method, poly(acrylonitrile-*co*-methylacrylate) (PAN-MA) fibrillar constructs (19 mm long and 1.5 mm inner diameter) were produced. Axons regenerated across a 17 mm nerve gap, re-innervated muscles, and reformed neuromuscular junctions. Electrophysiological and behavioral analyses revealed that aligned but not randomly oriented constructs facilitated both sensory and motor nerve regeneration, improving significantly functional outcomes.

Fibers have been also integrated within hydrogel materials to provide hybrid three-dimensional construct for neuronal guidance within a growth promoting environment (Newman et al., 2006; Novikova et al., 2008). Studies showed that magnetic collagen fibers in collagen gels, aligned using magnetic fields, provide an improved template for neurite extension compared to randomly oriented collagen fibers (Ceballos et al., 1999; Dubey et al., 1999). Recently, magnetoresponsive PEG based microgel are reported by incorporation of iron oxide nanoparticles for directional growth of DRGs (Rose et al., 2017). Natural protein based hydrogels also provide adhesive factors to support attachment and neurite grown. Yao et al. developed a hierarchically aligned fibrillar fibrin hydrogel (AFG) with low rigidity and aligned topography to mimics both the soft and oriented features of nerve tissue. They found that the AFG exhibit co-effects on promoting the neurogenic differentiation of human umbilical cord mesenchymal stem cells (hUMSCs) in comparison to random fibrin hydrogel (RFG) and tissue culture plate (TCP). Also, AFG induces DRGs neurons to rapidly project numerous long neurite outgrowths longitudinally along the AFG fibers (Yao et al., 2016).

Recently, Johnson et al. have developed a novel 3D printing approach for manufacturing of a custom nerve repair technology which is personalized to anatomical geometries, and augmented with physical (microgrooves) and biochemical cues (multicomponent diffusive biomolecular gradients) to promote the regeneration of multiple nerve pathways (Johnson et al., 2015). The custom scaffolds are prepared via a 3D printing using 3D models, which are reverse engineered from patient anatomies by 3D scanning. The bifurcating pathways (sensory and motor path) are augmented with microgrooves and path-specific biochemical cues for the regeneration of complex mixed nerve injuries (**Figure 8**). This 3D printed scaffold provides axonal guidance *in vitro* and achieved successful regeneration of bifurcated injuries across a 10 mm complex nerve gap in rats *in vivo*.

Synthetic hydrogels formed by self-assembling PAs show also a nanofibrilar structure that has been used in nerve regeneration. Encapsulated NPCs were observed to differentiate into neurons with extensive neurite outgrowth within nanofibrillar hydrogels (Silva et al., 2004).

Guided Neurite Growth by Rigidity Patterns

The rigidity of the biomaterial contributes to the oriented growth of neurites in spiral ganglion neurons (SGN) on micropatterns. Alignment was significantly enhanced when the material stiffness increased from 650 to 2,000 MPa (Tuft et al., 2014). Increasing substrate stiffness of a LN-coated P(AAm) hydrogel also promoted directional neurite outgrowth from embryonic DRGs (Rosso et al., 2017). The neurite in low stiffness substrate (1 kPa) show relax and less aligned morphology, whereas the neurite display stretch, more aligned morphology in high stiffness (20 kPa). Interestingly, the opposite observation

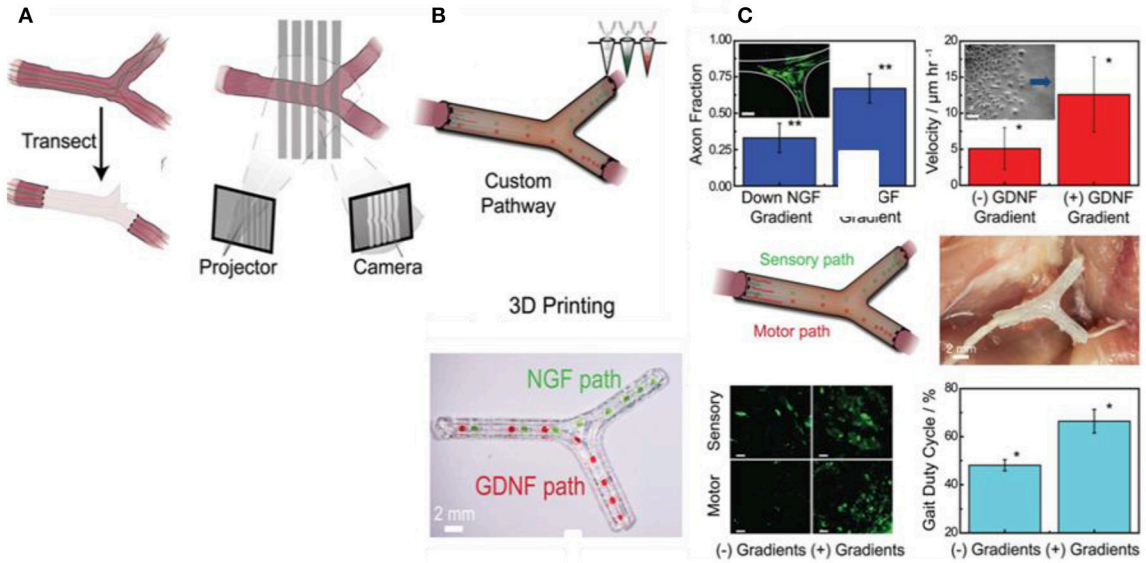

FIGURE 8 | Guided neurite extension in 3D printed scaffold; **(A)** Nerve regeneration pathways enabled by 3D scanning and printing, **(B)** The 3D printing process provided the ability to introduce advantageous physical and biochemical cues in the form of microgrooves and multicomponent diffusive biomolecular gradients, **(C)** *In vitro* and *in vivo* characterization of regeneration with 3D printed nerve pathways (Johnson et al., 2015), Copyright 2015, John Wiley and Sons.

was made in 3D cultures. A hyaluronic acid (HA) hydrogel with tunable Young's Modulus between 400 and 800 Pa was used to culture hippocampal neural progenitor cells (HNPCs) (Tarus et al., 2016). Neurites of HNPCs grew into the soft HA hydrogel at increased outgrowth and density. The growth of neurites (in quantity and length) from DRGs was also promoted in softer (0.5 kPa) elastin-like hydrogels (Lampe et al., 2013). Authors hypothesize that on 2D environments the stiffer substrates provide more stable anchoring to facilitate the outgrowth of neurite. In contrast, stiffer 3D matrices (i.e., higher crosslinking degree) hinder the outgrowth of neurites due to the small pore sizes.

Neural Growth on Patterns of Cell Adhesive Ligands

Patterns of adhesive ligands (full proteins or peptidomimetics) on non-adhesive backgrounds (typically PEG) can be used to selectively promote neuronal attachment and guided outgrowth on the adhesive regions of the pattern (Zhang et al., 2005; Straley et al., 2010; Joo et al., 2015a). Recent studies demonstrate that responsive biomaterials can be used to *in situ* guide axonal growth. *In vivo*, poly(vinyl chloride) (PVC) channels filled with different adhesive matrices (a YIGSR peptide containing agarose gel, a plain gel, and PBS solution) have been applied to fill a 4 mm segment of dissected dorsal root. A significant increase of myelinated axons was shown in the peptide modified agarose gel (Borkenhagen et al., 1998).

In addition to promoting cell growth, the presentation of neurotrophic factors in a gradient distribution within scaffold has also been studied for guidance of regenerating neurons. Several *in vitro* studies have demonstrated that neuronal cells are guided by immobilized gradients of nerve growth factors or neurotrophic factors on scaffolds (Moore et al., 2006; Dodla and Bellamkonda, 2008). The presence of LN and NGF gradients in agarose scaffolds has also shown better functional recovery of long peripheral nerve gaps than uniform concentration scaffolds (Dodla and Bellamkonda, 2008).

Directed Growth on "Living Scaffolds"

During neural morphogenesis and development, directed axon growth and cell migration typically occurs along pathways formed by other cells. This concept has long been appreciated in developmental neurobiology as crucial to the proper formation of the nervous system, including necessary axonal connectivity and localization of cellular constituents. This idea has also been embraced by the tissue regeneration community and lead to the concept of "living scaffolds" for regeneration. These are tissue engineered constructs containing supporting guiding material and cells from the neural environment, typically glial cells and astrocytes (**Figure 9**). These follow the haptotactic cues of the scaffold and arrange in oriented dispositions. These cells secrete neural growth factor and combine haptotactic and chemotactig signals to neuronal cells to grow along them (Struzyna et al., 2014).

In vitro, higher order structures can be formed by first culturing and aligning support cells on microgrooves, followed by seeding of neurons (Nikkhah et al., 2012). Micropatterned PLLA substrates containing grooves selectively coated with LN were used to culture rat Schwann cells to support neurites outgrowth (Miller et al., 2001). Neurons cultured on those substrates displayed accelerated outgrowth of nerve fibers and 98% alignment of neurites along the microgrooves. In a different study, micropatterned Schwann cells controlled by

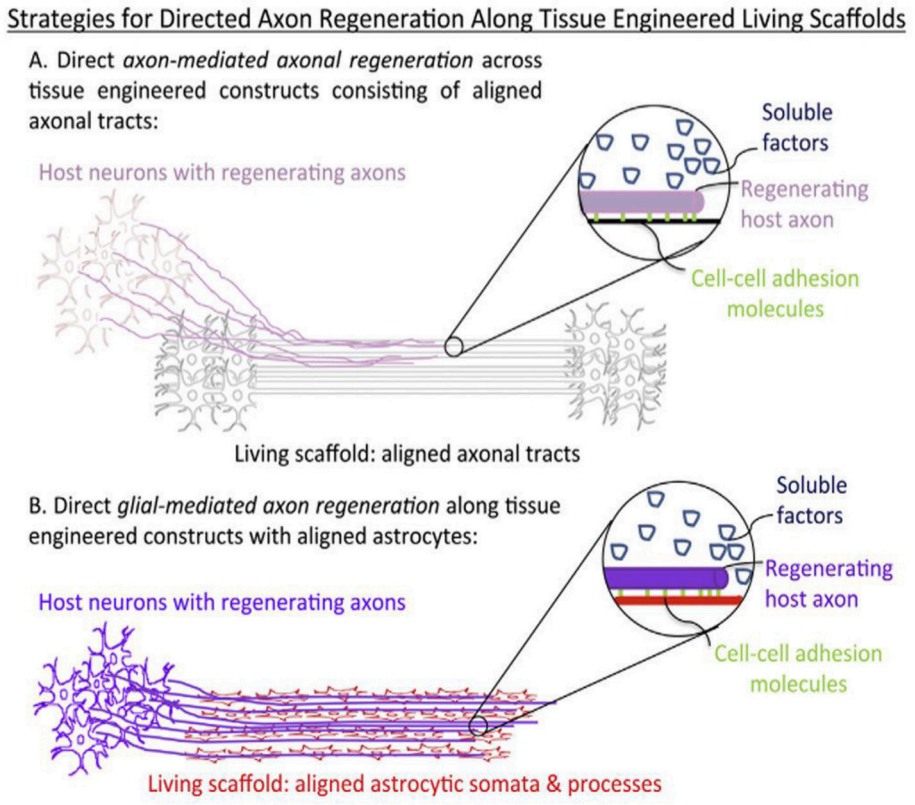

FIGURE 9 | Structural and soluble cues directing axonal outgrowth along "living scaffolds" (Struzyna et al., 2014) Copyright 2014, Elsevier.

micropatterned LN stipes on glass substrates were used to direct neuronal regeneration (Thompson and Buettner, 2004; Schmalenberg and Uhrich, 2005).

Winter et al. have developed a living scaffold that structurally mimicked the glial tube. It consisted of aligned astrocytes that guided the migration of NPCs and facilitated directed axonal regeneration for CNS repair. The networks of longitudinally aligned astrocytes on patterned hydrogels, supported seeded neurons to extend neurites along the aligned astrocytes bundles (Winter et al., 2016). In a different approach, collagen sheets supported alignment of astrocytes in the presence of transforming growth factor (East et al., 2010). The collagen sheets were then rolled to create cylindrical constructs. Dissociated DRGs neurons and astrocytes were seeded together on the scaffolds. Neurites preferentially grew along the aligned astrocytes.

In vivo, living scaffolds consisting of neurons and stretch-grown axonal tracts were grown to 10 mm in length, encapsulated in collagenous matrices, and transplanted to repair equally sized lateral hemisection spinal cord lesions in rats for spinal cord repair (Iwata et al., 2006). At 1 month post-surgery, the constructs had integrated with the host by extending axons into the spinal cord. Similar constructs containing "stretch-grown" axonal tracts were also used for peripheral nerve repair (East et al., 2010).

BIOMATERIALS SUPPORTING NEURAL GROWTH *IN-VIVO*

Central nervous system (CNS) injuries emerge from accidents or trauma affecting brain and spinal cord or by neurodegenerative disorders such as Parkinson's or Alzheimer's disease (Daly et al., 2012). Peripheral nervous system (PNS) disorders occurred through cut or injury to nerve cord, effecting autonomic motor and sensory functions resulting in impairment of body performance (Kabu et al., 2015). The common strategies to repair CNS injuries involves grafting of stem cells at injured site, while PNS system repair is frequently based on autograft or hollow nerve guidance conduits. However, after implantation the grafted cells fails to survive, remain undifferentiated or chiefly differentiate into to glial cell forming glial scar and fail to develop oriented nerves. In addition, the rejection of implant due to inflammation and infection at surgery site also affect success of transplant. Biomaterials for neural regeneration are designed to resemble the properties of the natural cellular niche (stiffness, topography), accompanied with tunable release of growth factors and availability of ECM bioactive motifs. This section presents a brief overview of new advances in biomaterial based implants for nervous system regeneration.

Inert biocompatible scaffolds functionalized with bioactive sequences in combination with addition or immobilization

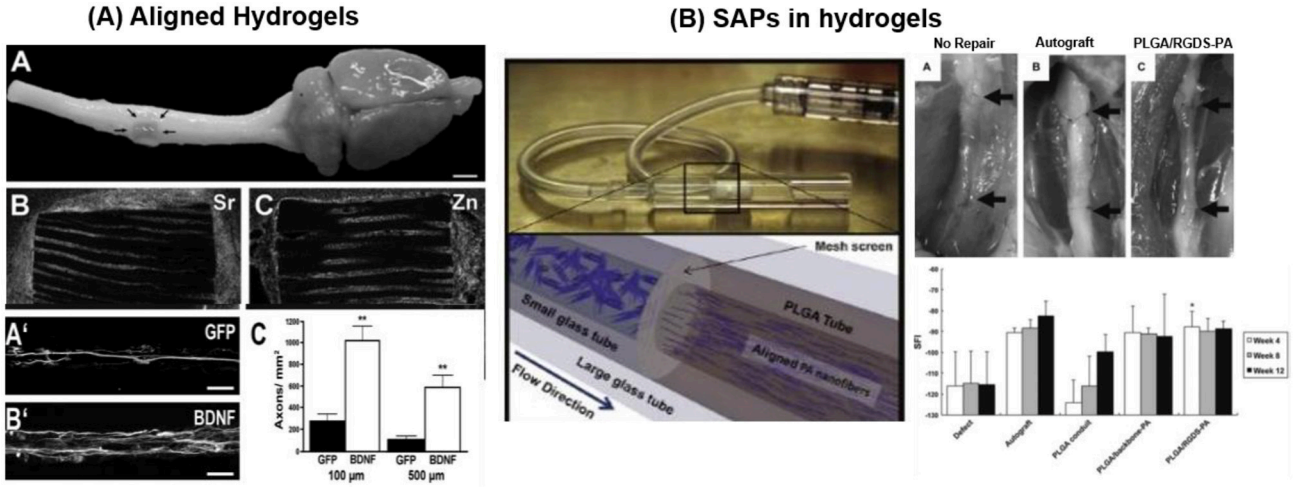

FIGURE 10 | Biomaterials applied for regeneration therapies **(A)** Alginate hydrogel scaffolds encapsulating BMSC (expressing GFP or BDNF) to promote directed linear axonal regeneration in the injured rat spinal cord model. Cell-filled alginate scaffold implanted at injured area with Sr^{2+} and Zn^{2+} ions staining demonstrates numerous cells within the channels. BMSC expressing BDNF cell preferentially promote axonal growth (Günther et al., 2015) Copyright 2015, Elsevier; **(B)** PLGA based peripheral nerve construct filled with aligned PAs (PAs-RGD and PAs-IKVAV) for recovery of peripheral nerve injury. PAs solution, filled inside PLGA tubes was crosslinked by $CaCl_2$. PAs-RGD filled PLGA construct provide faster recovery than bare PAs and comparable with autograft (Li A. et al., 2014) Copyright 2014, Elsevier.

of nerve growth factors have been tested for regeneration therapies. Injectable 3D IKVAV containing SAPs ($RADA_{16}$-IKVAV) hydrogel (G' 300 Pa) was reported for recovery of cerebral neocortex injury in rat brain surgery model. *In-situ* self-assembly of $RADA_{16}$-IKVAV hydrogel fill the injury gap, enhanced cell survival and reduced the glial astrocytes differentiation in comparison to bare $RADA_{16}$ during 6 weeks after post-implantation (Cheng et al., 2013). MAC scaffold functionalized with growth factors and LN modulated the differentiation of subcutaneously implanted NPCs into different lineages. MAC was functionalized with interferon-γ (IFN-γ) for neurons, platelet derived growth factor-AA (PDGF-AA) for oligodendrocytes, or Bone morphogenetic protein-2 (BMP-2) for astrocytes differentiation. Cells differentiation was more effective when the growth factors were conjugated with the scaffold and not added freely to the medium. Differentiation into neuron was significant and rosette like neurons were reported after 28 days of implantation (Li H. et al., 2014). A 3D scaffold of poly(desaminotyrosyl tyrosine ethyl ester carbonate) electrospun fibers with 1.25–3.23 µm diameters was implanted at mouse brain striatum to enhance the cell viability and neuronal differentiation at implantation site. Human induced neuronal cells (h-iN), dispersed in fiber suspension were injected at the site of injury forming a gel *in-situ*. h-iN inside the hydrogel showed ∼38-fold enhanced *in vivo* cell viability and 3.5-folds improvement in neurite outgrowth in comparison to isolated h-iN (Carlson et al., 2016). Cell viability and outgrowth of spiral ganglion neurites has reported to be enhanced by coupling of IKVAV peptide (∼100%) on PuraMatrix® hydrogel in comparison to unmodified hydrogel (∼40%) (Frick et al., 2017). IKVAV containing PAs nanofibers employed in *in vivo* mouse spinal cord injury model enhanced cell viability (∼2 folds) at the site of injury and promoted development of motor neurons (Tysseling-Mattiace et al., 2008; Cui et al., 2010; Sun et al., 2017). Alginate-based capillary hydrogels seeded with brain-derived neurotrophic factor (BDNF) expressing bone marrow stromal cells (BMSCs) guided axon extension on lesion site. A 3–4 folds increase in the axon length along the rostro-caudal direction, extending through the whole implant in rat spinal cord was achieved (**Figure 10A**) (Günther et al., 2015).

PLGA conduits filled with aligned PAs (palmitoyl-$VVAAEENH_2$) with and without bioactive RGD or IKVAV epitope were reported to repair rat sciatic nerve injury. Agarose hydrogel loaded with concentration gradient of LN and NGF, promote sciatic nerve repair covering the gap of 20 mm (Dodla and Bellamkonda, 2008). PLGA implant containing bioactive (IKVAV or RGD) PAs grafted at injury site of peripheral nerve critical sized defect model enhanced Schwann cells (∼20–40% increase) and axonal growth (∼20% increase) during 21 days of implant in comparison to bare PLGA-PAs (**Figure 10B**). Bioactive PLGA-PAs support recovery of motor and sensory activity after 12 weeks of implantation comparable to autograft (positive control) (Li A. et al., 2014). Commercially available inert PuraMatrix® hydrogel functionalized with IKVAV is applied for cochlear implants (CI). **Table 2** entailed biomaterials relevant for neural tissue engineering.

CRITICAL OVERVIEW

Strategies for brain repair heavily depend on our ability to temporally reconstruct the natural cellular microenvironment of neural cells. Biomaterials play a fundamental role in this context, as they provide the mechanical support for cells to attach and migrate to the injury site, as well as fundamental signals for differentiation. The increasing evidence that (neural) cells sense and specifically respond to biochemical and physical material parameters like stiffness or morphology opens

TABLE 2 | Biomaterial scaffold applied for neural tissue engineering.

Biomaterial	Modification	Application	Outcome	References
PAs	IKVAV	mouse spinal cord injury (SCI)	Reduced astrogliosis and apoptosis, increase oligodendroglia	Tysseling-Mattiace et al., 2008
Collagen hydrogel	LN polypeptide	Rat striatum	Viability of NSCs	Nakaji-Hirabayashi et al., 2013
PLGA microspheres in chitosan channels	Dibutyryl cyclic-AMP (dbcAMP) in PLGA microspheres	Rat SCI	Viability and differentiation of NSPCs	Kim et al., 2011
Hyaluronan hydrogel	Rat platelet derived growth factor-A (rPDGF-A)	Rat SCI	Viability and oligodendrocytic of NSPCs	Mothe et al., 2013

enormous possibilities for material-supported cell therapies for brain repair. However, reported work up to now, as described in this article, is mostly phenomenological and limits attempts to extract generic material properties-cellular response relationships out of our analysis. The still phenomenological character of most publications does not allow scientifically grounded statements that could lead biomaterials design for nervous tissue regeneration.

Break-through approaches in the field will depend on several factors. From the materials side, the analysis and quantification of the material properties to which cells are exposed is a fundamental requirement. The density of protein or peptide of an adhesive coating depends on the chemistry of the surface and the coating strategy. Same incubation conditions lead to different surface densities on different materials, and this will influence the biological response. No comparison between biological readouts from different articles is possible if there is no quantitative information about the surface composition with which the neuronal cell interacts. The stiffness of a material is typically analyzed as a macroscopic parameter, whereas the cell senses stiffness at a molecular lengthscale. Fibrous or continuous matrices can appear very different to a neuron from a mechanical perspective. Moreover, the Young's Modulus of a material describes only part of the mechanical response, and not necessarily the one a cell might feel long-term. Viscous components might play a role, as demonstrated for other cell types. All these factors have to be properly described in order to make meaningful interpretation of cell responses to biomaterials, and to extract useful information for advanced materials design.

Novel strategies for brain repair will also depend on the ability of biomaterials developers to assimilate and translate increasing knowledge from cell and matrix biology of neural tissue into artificial models. The regenerative biomaterials community is traditionally dominated by material scientists cooperating with surgeons in best case, and it has little interaction with neurobiology or neuronal development community. All these fields have a lot to share with each other, though the languages and experimental methods are very different. Approximation between the different communities is starting and will profoundly impact development in biomaterials for brain tissue repair, as it is impacting in other tissue types. We face a challenging and exciting era.

Experimental work with neuronal cells is challenging. Neurons are difficult to culture and the access to primary cells is more complicated than in other tissue types. The analysis of the existing literature evidences that biomaterials development for brain repair lies behind other tissue types. However, knowledge transfer will occur and will accelerate development in the coming years. There is a long way to go until break-through approaches in brain repair will translate into revolutionary therapies, but there is hope to get there in the next decade.

AUTHOR CONTRIBUTIONS

All authors listed have made a substantial, direct and intellectual contribution to the work, and approved it for publication.

FUNDING

SZ acknowledges funding from China Scholarship Council. AdC acknowledges funding from Deutsche Forschungsgemeinschaft (SFB1027).

REFERENCES

Abbasi, N., Soudi, S., Hayati-Roodbari, N., Dodel, M., and Soleimani, M. (2014). The effects of plasma treated electrospun nanofibrous poly (ε-caprolactone) scaffolds with different orientations on mouse embryonic stem cell proliferation. *Cell J.* 16, 245–254. Available online at: http://celljournal.org/journal/article/abstract/275

Akizawa, Y., Morita, Y., Hsu, Y., Yamaoka, T., and Nakamachi, E. (2016). "Development of IKVAV Modified PLLA Guide Tube Having Unidirectional Fibers on Inner Surface to Enhance Axonal Extension," in: *ASME 2016 International Mechanical Engineering Congress and Exposition* (American Society of Mechanical Engineers), V003T004A073-V003T004A073.

Ali, S., Wall, I. B., Mason, C., Pelling, A. E., and Veraitch, F. S. (2015). The effect of Young's modulus on the neuronal differentiation of mouse embryonic stem cells. *Acta Biomater.* 25, 253–267. doi: 10.1016/j.actbio.2015.07.008

An, B., Tang-Schomer, M. D., Huang, W., He, J., Jones, J. A., Lewis, R. V., et al. (2015). Physical and biological regulation of neuron regenerative growth and network formation on recombinant dragline silks. *Biomaterials* 48, 137–146. doi: 10.1016/j.biomaterials.2015.01.044

Ananthanarayanan, B., Little, L., Schaffer, D. V., Healy, K. E., and Tirrell, M. (2010). Neural stem cell adhesion and proliferation on phospholipid bilayers functionalized with RGD peptides. *Biomaterials* 31, 8706–8715. doi: 10.1016/j.biomaterials.2010.07.104

Béduer, A., Vieu, C., Arnauduc, F., Sol, J.-C., Loubinoux, I., and Vaysse, L. (2012). Engineering of adult human neural stem cells

differentiation through surface micropatterning. *Biomaterials* 33, 504–514. doi: 10.1016/j.biomaterials.2011.09.073

Belkin, A. M., and Stepp, M. A. (2000). Integrins as receptors for laminins. *Micro. Res. Tech.* 51, 280–301. doi: 10.1002/1097-0029(20001101)51:3<280::AID-JEMT7>3.0.CO;2-O

Berns, E. J., Sur, S., Pan, L., Goldberger, J. E., Suresh, S., Zhang, S., et al. (2014). Aligned neurite outgrowth and directed cell migration in self-assembled monodomain gels. *Biomaterials* 35, 185–195. doi: 10.1016/j.biomaterials.2013.09.077

Bhang, S. H., Lee, T. J., Lim, J. M., Lim, J. S., Han, A. M., Choi, C. Y., et al. (2009). The effect of the controlled release of nerve growth factor from collagen gel on the efficiency of neural cell culture. *Biomaterials* 30, 126–132. doi: 10.1016/j.biomaterials.2008.09.021

Bhutto, M. A., Wu, T., Sun, B., Hany, E. H., Al-Deyab, S. S., and Mo, X. (2016). Fabrication and characterization of vitamin B5 loaded poly (l-lactide-co-caprolactone)/silk fiber aligned electrospun nanofibers for schwann cell proliferation. *Coll. Surf. B Biointerf.* 144, 108–117. doi: 10.1016/j.colsurfb.2016.04.013

Borkenhagen, M., Clémence, J. F., Sigrist, H., and Aebischer, P. (1998). Three-dimensional extracellular matrix engineering in the nervous system. *J. Biomed. Mater. Res. A* 40, 392–400.

Bozza, A., Coates, E. E., Incitti, T., Ferlin, K. M., Messina, A., Menna, E., et al. (2014). Neural differentiation of pluripotent cells in 3D alginate-based cultures. *Biomaterials* 35, 4636–4645. doi: 10.1016/j.biomaterials.2014.02.039

Caliari, S. R., and Burdick, J. A. (2016). A practical guide to hydrogels for cell culture. *Nat. Methods* 13, 405–414. doi: 10.1038/nmeth.3839

Callahan, L. A. S., Xie, S., Barker, I. A., Zheng, J., Reneker, D. H., Dove, A. P., et al. (2013). Directed differentiation and neurite extension of mouse embryonic stem cell on aligned poly (lactide) nanofibers functionalized with YIGSR peptide. *Biomaterials* 34, 9089–9095. doi: 10.1016/j.biomaterials.2013.08.028

Calof, A. L., and Lander, A. D. (1991). Relationship between neuronal migration and cell-substratum adhesion: laminin and merosin promote olfactory neuronal migration but are anti-adhesive. *J. Cell Biol.* 115, 779–794. doi: 10.1083/jcb.115.3.779

Carlson, A. L., Bennett, N. K., Francis, N. L., Halikere, A., Clarke, S., Moore, J. C., et al. (2016). Generation and transplantation of reprogrammed human neurons in the brain using 3D microtopographic scaffolds. *Nat. Commun.* 7:10862. doi: 10.1038/ncomms10862

Casarosa, S., Bozzi, Y., and Conti, L. (2014). Neural stem cells: ready for therapeutic applications? *Mol. Cell. Ther.* 2:31. doi: 10.1186/2052-8426-2-31

Ceballos, D., Navarro, X., Dubey, N., Wendelschafer-Crabb, G., Kennedy, W. R., and Tranquillo, R. T. (1999). Magnetically aligned collagen gel filling a collagen nerve guide improves peripheral nerve regeneration. *Exp. Neurol.* 158, 290–300. doi: 10.1006/exnr.1999.7111

Chen, C.-S., Soni, S., Le, C., Biasca, M., Farr, E., Chen, E. Y., et al. (2012). Human stem cell neuronal differentiation on silk-carbon nanotube composite. *Nanoscale Res. Lett.* 7:126. doi: 10.1186/1556-276X-7-126

Cheng, T. Y., Chen, M. H., Chang, W. H., Huang, M. Y., and Wang, T. W. (2013). Neural stem cells encapsulated in a functionalized self-assembling peptide hydrogel for brain tissue engineering. *Biomaterials* 34, 2005–2016. doi: 10.1016/j.biomaterials.2012.11.043

Chiono, V., and Tonda-Turo, C. (2015). Trends in the design of nerve guidance channels in peripheral nerve tissue engineering. *Prog. Neurobiol.* 131, 87–104. doi: 10.1016/j.pneurobio.2015.06.001

Chiono, V., Tonda-Turo, C., and Ciardelli, G. (2009). "Chapter 9: Artificial scaffolds for peripheral nerve reconstruction," in *International Review of Neurobiology*, eds S. Geuna, P. Tos, and B. Battiston (Academic Press), 173–198.

Christopherson, G. T., Song, H., and Mao, H.-Q. (2009). The influence of fiber diameter of electrospun substrates on neural stem cell differentiation and proliferation. *Biomaterials* 30, 556–564. doi: 10.1016/j.biomaterials.2008.10.004

Chua, J. S., Chng, C.-P., Moe, A. A. K., Tann, J. Y., Goh, E. L., Chiam, K.-H., et al. (2014). Extending neurites sense the depth of the underlying topography during neuronal differentiation and contact guidance. *Biomaterials* 35, 7750–7761. doi: 10.1016/j.biomaterials.2014.06.008

Clements, I. P., Kim, Y.-,t., English, A. W., Lu, X., Chung, A., and Bellamkonda, R. V. (2009). Thin-film enhanced nerve guidance channels for peripheral nerve repair. *Biomaterials* 30, 3834–3846. doi: 10.1016/j.biomaterials.2009.04.022

Cooke, M., Vulic, K., and Shoichet, M. (2010). Design of biomaterials to enhance stem cell survival when transplanted into the damaged central nervous system. *Soft Matter* 6, 4988–4998. doi: 10.1039/c0sm00448k

Corey, J. M., Lin, D. Y., Mycek, K. B., Chen, Q., Samuel, S., Feldman, E. L., et al. (2007). Aligned electrospun nanofibers specify the direction of dorsal root ganglia neurite growth. *J. Biomed. Mater. Res. A* 83, 636–645. doi: 10.1002/jbm.a.31285

Cui, H., Webber, M. J., and Stupp, S. I. (2010). Self-assembly of peptide amphiphiles: from molecules to nanostructures to biomaterials. *Peptide Sci.* 94, 1–18. doi: 10.1002/bip.21328

Cunha, C., Panseri, S., Villa, O., Silva, D., and Gelain, F. (2011). 3D culture of adult mouse neural stem cells within functionalized self-assembling peptide scaffolds. *Int. J. Nanomed.* 6:943. doi: 10.2147/IJN.S17292

Daly, W., Yao, L., Zeugolis, D., Windebank, A., and Pandit, A. (2012). A biomaterials approach to peripheral nerve regeneration: bridging the peripheral nerve gap and enhancing functional recovery. *J. R. Soc. Interf.* 9, 202–221. doi: 10.1098/rsif.2011.0438

de Ruiter, G. C., Spinner, R. J., Malessy, M. J. A., Moore, M. J., Sorenson, E. J., Currier, B. L., et al. (2008). Accuracy of motor axon regeneration across autograft, single-lumen, and multichannel poly(lactic-co-glycolic acid) nerve tubes. *Neurosurgery* 63, 144–153. doi: 10.1227/01.NEU.0000335081.47352.78

Dodla, M. C., and Bellamkonda, R. V. (2008). Differences between the effect of anisotropic and isotropic laminin and nerve growth factor presenting scaffolds on nerve regeneration across long peripheral nerve gaps. *Biomaterials* 29, 33–46. doi: 10.1016/j.biomaterials.2007.08.045

Dubey, N., Letourneau, P., and Tranquillo, R. (1999). Guided neurite elongation and Schwann cell invasion into magnetically aligned collagen in simulated peripheral nerve regeneration. *Exp. Neurol.* 158, 338–350. doi: 10.1006/exnr.1999.7095

Durbeej, M. (2010). Laminins. *Cell Tissue Res.* 339:259. doi: 10.1007/s00441-009-0838-2

East, E., de Oliveira, D. B., Golding, J. P., and Phillips, J. B. (2010). Alignment of astrocytes increases neuronal growth in three-dimensional collagen gels and is maintained following plastic compression to form a spinal cord repair conduit. *Tissue Eng. A* 16, 3173–3184. doi: 10.1089/ten.tea.2010.0017

Engler, A. J., Sen, S., Sweeney, H. L., and Discher, D. E. (2006). Matrix elasticity directs stem cell lineage specification. *Cell* 126, 677–689. doi: 10.1016/j.cell.2006.06.044

Farrukh, A., Ortega, F., Fan, W., Marichal, N., Paez, J. I., Berninger, B., et al. (2017a). Bifunctional hydrogels containing the laminin motif IKVAV promote neurogenesis. *Stem Cell Rep.* 9, 1432–1440 doi: 10.1016/j.stemcr.2017.09.002

Farrukh, A., Paez, J. I., Salierno, M., Fan, W., Berninger, B., and del Campo, A. (2017b). Bifunctional poly (acrylamide) hydrogels through orthogonal coupling chemistries. *Biomacromolecules* 18, 906–913. doi: 10.1021/acs.biomac.6b01784

Fawcett, J. (2002). Repair of spinal cord injuries: where are we, where are we going? *Spinal Cord* 40:615. doi: 10.1038/sj.sc.3101328

Fawcett, J. W. (1998). Spinal cord repair: from experimental models to human application. *Spinal Cord* 36, 811–817. doi: 10.1038/sj.sc.3100769

Franze, K. (2011). Atomic force microscopy and its contribution to understanding the development of the nervous system. *Curr. Opin. Genet. Dev.* 21, 530–537. doi: 10.1016/j.gde.2011.07.001

Franze, K. (2013). The mechanical control of nervous system development. *Development* 140, 3069–3077. doi: 10.1242/dev.079145

Freitas, V. M., Vilas-Boas, V. F., Pimenta, D. C., Loureiro, V., Juliano, M. A., Carvalho, M. R., et al. (2007). SIKVAV, a laminin α1-derived peptide, interacts with integrins and increases protease activity of a human salivary gland adenoid cystic carcinoma cell line through the ERK 1/2 signaling pathway. *Am. J. Pathol.* 171, 124–138. doi: 10.2353/ajpath.2007.051264

Frick, C., Müller, M., Wank, U., Tropitzsch, A., Kramer, B., Senn, P., et al. (2017). Biofunctionalized peptide-based hydrogels provide permissive scaffolds to attract neurite outgrowth from spiral ganglion neurons. *Coll. Surf. B Biointerf.* 149, 105–114. doi: 10.1016/j.colsurfb.2016.10.003

Frith, J. E., Mills, R. J., Hudson, J. E., and Cooper-White, J. J. (2012). Tailored integrin–extracellular matrix interactions to direct human mesenchymal stem cell differentiation. *Stem Cells Dev.* 21, 2442–2456. doi: 10.1089/scd.2011.0615

Fujioka, T., Kaneko, N., Ajioka, I., Nakaguchi, K., Omata, T., Ohba, H., et al. (2017). β1 integrin signaling promotes neuronal migration along vascular scaffolds in the post-stroke brain. *EBioMed.* 16(Suppl. C), 195–203. doi: 10.1016/j.ebiom.2017.01.005

Gage, F. H., and Temple, S. (2013). Neural stem cells: generating and regenerating the brain. *Neuron* 80, 588–601. doi: 10.1016/j.neuron.2013.10.037

Gelain, F., Bottai, D., Vescovi, A., and Zhang, S. (2006). Designer self-assembling peptide nanofiber scaffolds for adult mouse neural stem cell 3-dimensional cultures. *PLoS ONE* 1:e119. doi: 10.1371/journal.pone.0000119

Ghasemi-Mobarakeh, L., Prabhakaran, M. P., Morshed, M., Nasr-Esfahani, M. H., and Ramakrishna, S. (2010). Bio-functionalized PCL nanofibrous scaffolds for nerve tissue engineering. *Mater. Sci. Eng. C* 30, 1129–1136. doi: 10.1016/j.msec.2010.06.004

Gnavi, S., Fornasari, B. E., Tonda-Turo, C., Laurano, R., Zanetti, M., Ciardelli, G., et al. (2015). The effect of electrospun gelatin fibers alignment on Schwann cell and axon behavior and organization in the perspective of artificial nerve design. *Int. J. Mol. Sci.* 16, 12925–12942. doi: 10.3390/ijms160612925

Gomez, N., Chen, S., and Schmidt, C. E. (2007). Polarization of hippocampal neurons with competitive surface stimuli: contact guidance cues are preferred over chemical ligands. *J. R. Soc. Interf.* 4, 223–233. doi: 10.1098/rsif.2006.0171

Göpferich, A. (1996). Mechanisms of polymer degradation and erosion. *Biomaterials* 17, 103–114. doi: 10.1016/0142-9612(96)85755-3

Gu, X. S., Ding, F., Yang, Y. M., and Liu, J. (2011). Construction of tissue engineered nerve grafts and their application in peripheral nerve regeneration. *Prog. Neurobiol.* 93, 204–230. doi: 10.1016/j.pneurobio.2010.11.002

Guarnieri, D., Battista, S., Borzacchiello, A., Mayol, L., De Rosa, E., Keene, D., et al. (2007). Effects of fibronectin and laminin on structural, mechanical and transport properties of 3D collageneous network. *J. Mater. Sci. Mater. Med.* 18, 245–253. doi: 10.1007/s10856-006-0686-5

Gumera, C., Rauck, B., and Wang, Y. (2011). Materials for central nervous system regeneration: bioactive cues. *J. Mater. Chem.* 21, 7033–7051. doi: 10.1039/c0jm04335d

Günther, M. I., Weidner, N., Müller, R., and Blesch, A. (2015). Cell-seeded alginate hydrogel scaffolds promote directed linear axonal regeneration in the injured rat spinal cord. *Acta Biomater.* 27, 140–150. doi: 10.1016/j.actbio.2015.09.001

Hamsici, S., Cinar, G., Celebioglu, A., Uyar, T., Tekinay, A. B., and Guler, M. O. (2017). Bioactive peptide functionalized aligned cyclodextrin nanofibers for neurite outgrowth. *J. Mater. Chem. B* 5, 517–524. doi: 10.1039/C6TB02441F

Hanein, Y., Tadmor, O., Anava, S., and Ayali, A. (2011). Neuronal soma migration is determined by neurite tension. *Neuroscience* 172, 572–579. doi: 10.1016/j.neuroscience.2010.10.022

He, L., Zhang, Y., Zeng, C., Ngiam, M., Liao, S., Quan, D., et al. (2009). Manufacture of PLGA multiple-channel conduits with precise hierarchical pore architectures and *in vitro/vivo* evaluation for spinal cord injury. *Tissue Eng. C Methods* 15, 243–255. doi: 10.1089/ten.tec.2008.0255

Hiraoka, M., Kato, K., Nakaji-Hirabayashi, T., and Iwata, H. (2009). Enhanced survival of neural cells embedded in hydrogels composed of collagen and laminin-derived cell adhesive peptide. *Bioconjug. Chem.* 20, 976–983. doi: 10.1021/bc9000068

Ho, M., Yu, D., Davidsion, M. C., and Silva, G. A. (2006). Comparison of standard surface chemistries for culturing mesenchymal stem cells prior to neural differentiation. *Biomaterials* 27, 4333–4339. doi: 10.1016/j.biomaterials.2006.03.037

Hoffman-Kim, D., Mitchel, J. A., and Bellamkonda, R. V. (2010). Topography, cell response, and nerve regeneration. *Annu. Rev. Biomed. Eng.* 12, 203–231. doi: 10.1146/annurev-bioeng-070909-105351

Hosseinkhani, H., Hiraoka, Y., Li, C.-H., Chen, Y.-R., Yu, D.-S., Hong, P.-D., et al. (2013). Engineering three-dimensional collagen-IKVAV matrix to mimic neural microenvironment. *ACS Chem. Neurosci.* 4, 1229–1235. doi: 10.1021/cn400075h

Hsieh, F.-Y., Lin, H.-H., and Hsu, S.-,h. (2015). 3D bioprinting of neural stem cell-laden thermoresponsive biodegradable polyurethane hydrogel and potential in central nervous system repair. *Biomaterials* 71, 48–57. doi: 10.1016/j.biomaterials.2015.08.028

Ilkhanizadeh, S., Teixeira, A. I., and Hermanson, O. (2007). Inkjet printing of macromolecules on hydrogels to steer neural stem cell differentiation. *Biomaterials* 28, 3936–3943. doi: 10.1016/j.biomaterials.2007.05.018

Iwata, A., Browne, K. D., Pfister, B. J., Gruner, J. A., and Smith, D. H. (2006). Long-term survival and outgrowth of mechanically engineered nervous tissue constructs implanted into spinal cord lesions. *Tissue Eng.* 12, 101–110. doi: 10.1089/ten.2006.12.101

Johnson, B. N., Lancaster, K. Z., Zhen, G., He, J., Gupta, M. K., Kong, Y. L., et al. (2015). 3D printed anatomical nerve regeneration pathways. *Adv. Funct. Mater.* 25, 6205–6217. doi: 10.1002/adfm.201501760

Joo, S., Kang, K., and Nam, Y. (2015a). *In vitro* neurite guidance effects induced by polylysine pinstripe micropatterns with polylysine background. *J. Biomed. Mater. Res. A* 103, 2731–2739. doi: 10.1002/jbm.a.35405

Joo, S., Kim, J. Y., Lee, E., Hong, N., Sun, W., and Nam, Y. (2015b). Effects of ECM protein micropatterns on the migration and differentiation of adult neural stem cells. *Sci. Rep.* 5:13043. doi: 10.1038/srep13043

Kabu, S., Gao, Y., Kwon, B. K., and Labhasetwar, V. (2015). Drug delivery, cell-based therapies, and tissue engineering approaches for spinal cord injury. *J. Control. Release* 219, 141–154. doi: 10.1016/j.jconrel.2015.08.060

Kang, K., Choi, I. S., and Nam, Y. (2011). A biofunctionalization scheme for neural interfaces using polydopamine polymer. *Biomaterials* 32, 6374–6380. doi: 10.1016/j.biomaterials.2011.05.028

Karow, M., Sánchez, R., Schichor, C., Masserdotti, G., Ortega, F., Heinrich, C., et al. (2012). Reprogramming of pericyte-derived cells of the adult human brain into induced neuronal cells. *Cell Stem Cell* 11, 471–476. doi: 10.1016/j.stem.2012.07.007

Kharkar, P. M., Kiick, K. L., and Kloxin, A. M. (2013). Designing degradable hydrogels for orthogonal control of cell microenvironments. *Chem. Soc. Rev.* 42, 7335–7372. doi: 10.1039/C3CS60040H

Kijenska, E., Prabhakaran, M. P., Swieszkowski, W., Kurzydlowski, K. J., and Ramakrishna, S. (2014). Interaction of Schwann cells with laminin encapsulated PLCL core–shell nanofibers for nerve tissue engineering. *Eur. Polym. J.* 50, 30–38. doi: 10.1016/j.eurpolymj.2013.10.021

Kilian, K. A., and Mrksich, M. (2012). Directing stem cell fate by controlling the affinity and density of ligand–receptor interactions at the biomaterials interface. *Angew. Chem. Int. Ed.* 51, 4891–4895. doi: 10.1002/anie.201108746

Kim, H., Zahir, T., Tator, C. H., and Shoichet, M. S. (2011). Effects of dibutyryl cyclic-AMP on survival and neuronal differentiation of neural stem/progenitor cells transplanted into spinal cord injured rats. *PLoS ONE* 6:e21744. doi: 10.1371/journal.pone.0021744

Kim, S.-E., Harker, E. C., De Leon, A. C., Advincula, R. C., and Pokorski, J. K. (2015). Coextruded, aligned, and gradient-modified poly (ε-caprolactone) fibers as platforms for neural growth. *Biomacromolecules* 16, 860–867. doi: 10.1021/bm501767x

Kim, Y.-,t., Haftel, V. K., Kumar, S., and Bellamkonda, R. V. (2008). The role of aligned polymer fiber-based constructs in the bridging of long peripheral nerve gaps. *Biomaterials* 29, 3117–3127. doi: 10.1016/j.biomaterials.2008.03.042

Koh, H., Yong, T., Chan, C., and Ramakrishna, S. (2008). Enhancement of neurite outgrowth using nano-structured scaffolds coupled with laminin. *Biomaterials* 29, 3574–3582. doi: 10.1016/j.biomaterials.2008.05.014

Kolb, B., Morshead, C., Gonzalez, C., Kim, M., Gregg, C., Shingo, T., et al. (2007). Growth factor-stimulated generation of new cortical tissue and functional recovery after stroke damage to the motor cortex of rats. *J. Cereb. Blood Flow Metabol.* 27, 983–997. doi: 10.1038/sj.jcbfm.9600402

Koutsopoulos, S., and Zhang, S. (2013). Long-term three-dimensional neural tissue cultures in functionalized self-assembling peptide hydrogels, matrigel and collagen I. *Acta Biomater.* 9, 5162–5169. doi: 10.1016/j.actbio.2012.09.010

Kubinová, Š., Horák, D., Kozubenko, N., Vaněček, V., Proks, V., Price, J., et al. (2010). The use of superporous Ac-CGGASIKVAVS-OH-modified PHEMA scaffolds to promote cell adhesion and the differentiation of human fetal neural precursors. *Biomaterials* 31, 5966–5975. doi: 10.1016/j.biomaterials.2010.04.040

Kulangara, K., Adler, A. F., Wang, H., Chellappan, M., Hammett, E., Yasuda, R., et al. (2014). The effect of substrate topography on direct reprogramming of fibroblasts to induced neurons. *Biomaterials* 35, 5327–5336. doi: 10.1016/j.biomaterials.2014.03.034

Lampe, K. J., Antaris, A. L., and Heilshorn, S. C. (2013). Design of three-dimensional engineered protein hydrogels for tailored control of neurite growth. *Acta Biomater.* 9, 5590–5599. doi: 10.1016/j.actbio.2012.10.033

Laura, M., Leipzig, N. D., and Shoichet, M. S. (2008). Promoting neuron adhesion and growth. *Mater. Today* 11, 36–43. doi: 10.1016/S1369-7021(08)70088-9

Lee, J., Abdeen, A. A., Zhang, D., and Kilian, K. A. (2013). Directing stem cell fate on hydrogel substrates by controlling cell geometry, matrix mechanics and adhesion ligand composition. *Biomaterials* 34, 8140–8148. doi: 10.1016/j.biomaterials.2013.07.074

Lee, M. K., Qin, E. C., Rich, M., Lee, K. Y., Kim, D. H., Chung, H. J., et al. (2016). Three dimensional conjugation of recombinant N-cadherin to a hydrogel

for *in vitro* anisotropic neural growth. *J. Mater. Chem. B* 4, 6803–6811. doi: 10.1039/C6TB01814A

Lee, M. K., Rich, M. H., Lee, J., and Kong, H. (2015). A bio-inspired, microchanneled hydrogel with controlled spacing of cell adhesion ligands regulates 3D spatial organization of cells and tissue. *Biomaterials* 58, 26–34. doi: 10.1016/j.biomaterials.2015.04.014

Lee, W., Frank, C. W., and Park, J. (2014). Directed axonal outgrowth using a propagating gradient of IGF-1. *Adv. Mater.* 26, 4936–4940. doi: 10.1002/adma.201305995

Lei, W. L., Xing, S. G., Deng, C. Y., Ju, X. C., Jiang, X. Y., and Luo, Z. G. (2012). Laminin/β1 integrin signal triggers axon formation by promoting microtubule assembly and stabilization. *Cell Res.* 22, 954–972. doi: 10.1038/cr.2012.40

Leipzig, N. D., and Shoichet, M. S. (2009). The effect of substrate stiffness on adult neural stem cell behavior. *Biomaterials* 30, 6867–6878. doi: 10.1016/j.biomaterials.2009.09.002

Lewicka, M., Hermanson, O., and Rising, A. U. (2012). Recombinant spider silk matrices for neural stem cell cultures. *Biomaterials* 33, 7712–7717. doi: 10.1016/j.biomaterials.2012.07.021

Li Jeon L., Baskaran, H., Dertinger, S. K., Whitesides, G. M., Van De Water, L., and Toner, M. (2002). Neutrophil chemotaxis in linear and complex gradients of interleukin-8 formed in a microfabricated device. *Nat. Biotechnol.* 20, 826–830. doi: 10.1038/nbt712

Li, A., Hokugo, A., Yalom, A., Berns, E. J., Stephanopoulos, N., McClendon, M. T., et al. (2014). A bioengineered peripheral nerve construct using aligned peptide amphiphile nanofibers. *Biomaterials* 35, 8780–8790. doi: 10.1016/j.biomaterials.2014.06.049

Li, H., Koenig, A. M., Sloan, P., and Leipzig, N. D. (2014). *In vivo* assessment of guided neural stem cell differentiation in growth factor immobilized chitosan-based hydrogel scaffolds. *Biomaterials* 35, 9049–9057. doi: 10.1016/j.biomaterials.2014.07.038

Li, W., Tang, Q. Y., Jadhav, A. D., Narang, A., Qian, W. X., Shi, P., et al. (2015). Large-scale topographical screen for investigation of physical neural-guidance cues. *Sci. Rep.* 5:8664. doi: 10.1038/srep08644

Li, X., Liu, X., Josey, B., Chou, C. J., Tan, Y., Zhang, N., et al. (2014). Short laminin peptide for improved neural stem cell growth. *Stem Cells Transl. Med.* 3, 662–670. doi: 10.5966/sctm.2013-0015

Lietz, M., Dreesmann, L., Hoss, M., Oberhoffner, S., and Schlosshauer, B. (2006). Neuro tissue engineering of glial nerve guides and the impact of different cell types. *Biomaterials* 27, 1425–1436. doi: 10.1016/j.biomaterials.2005.08.007

Liu, B., Ma, J., Xu, Q., and Cui, F. (2006). Regulation of charged groups and laminin patterns for selective neuronal adhesion. *Coll. Surf. B Biointerf.* 53, 175–178. doi: 10.1016/j.colsurfb.2006.08.018

Liu, K., Tedeschi, A., Park, K. K., and He, Z. (2011). Neuronal intrinsic mechanisms of axon regeneration. *Annu. Rev. Neurosci.* 34, 131–152. doi: 10.1146/annurev-neuro-061010-113723

Lu, Y. P., Yang, C. H., Yeh, J. A., Ho, F. H., Ou, Y. C., Chen, C. H., et al. (2014). Guidance of neural regeneration on the biomimetic nanostructured matrix. *Int. J. Pharm.* 463, 177–183. doi: 10.1016/j.ijpharm.2013.08.006

Luca, A. C., Terenghi, G., and Downes, S. (2014). Chemical surface modification of poly-ε-caprolactone improves Schwann cell proliferation for peripheral nerve repair. *J. Tissue Eng. Regen. Med.* 8, 153–163. doi: 10.1002/term.1509

Lundborg, G., Dahlin, L., Dohi, D., Kanje, M., and Terada, N. (1997). A new type of "bioartificial" nerve graft for bridging extended defects in nerves. *J. Hand Surg. Br Eur. Vol.* 22, 299–303.

Lunn, J. S., Sakowski, S. A., Hur, J., and Feldman, E. L. (2011). Stem cell technology for neurodegenerative diseases. *Ann. Neurol.* 70, 353–361. doi: 10.1002/ana.22487

Ma, F., Xiao, Z., Chen, B., Hou, X., Han, J., Zhao, Y., et al. (2014). Accelerating proliferation of neural stem/progenitor cells in collagen sponges immobilized with engineered basic fibroblast growth factor for nervous system tissue engineering. *Biomacromolecules* 15, 1062–1068. doi: 10.1021/bm500062n

Madl, C. M., Katz, L. M., and Heilshorn, S. C. (2016). Bio-orthogonally crosslinked, engineered protein hydrogels with tunable mechanics and biochemistry for cell encapsulation. *Adv. Funct. Mater.* 26, 3612–3620. doi: 10.1002/adfm.201505329

Malatesta, P., Appolloni, I., and Calzolari, F. (2008). Radial glia and neural stem cells. *Cell Tissue Res.* 331, 165–178. doi: 10.1007/s00441-007-0481-8

Mammadov, B., Sever, M., Guler, M. O., and Tekinay, A. B. (2013). Neural differentiation on synthetic scaffold materials. *Biomater. Sci.* 1, 1119–1137. doi: 10.1039/c3bm60150a

Manchineella, S., Thrivikraman, G., Basu, B., and Govindaraju, T. (2016). Surface-functionalized silk fibroin films as a platform to guide neuron-like differentiation of human mesenchymal stem cells. *ACS Appl. Mater. Interf.* 8, 22849–22859. doi: 10.1021/acsami.6b06403

Mason, H. A., Ito, S., and Corfas, G. (2001). Extracellular signals that regulate the tangential migration of olfactory bulb neuronal precursors: inducers, inhibitors, and repellents. *J. Neurosci.* 21, 7654–7663. doi: 10.1523/JNEUROSCI.21-19-07654.2001

Matsumoto, K., Ohnishi, K., Kiyotani, T., Sekine, T., Ueda, H., Nakamura, T., et al. (2000). Peripheral nerve regeneration across an 80-mm gap bridged by a polyglycolic acid (PGA)-collagen tube filled with laminin-coated collagen fibers: a histological and electrophysiological evaluation of regenerated nerves. *Brain Res.* 868, 315–328. doi: 10.1016/S0006-8993(00)02207-1

McKinnon, D., Domaille, D., Brown, T., Kyburz, K., Kiyotake, E., Cha, J., et al. (2014). Measuring cellular forces using bis-aliphatic hydrazone crosslinked stress-relaxing hydrogels. *Soft Matter* 10, 9230–9236. doi: 10.1039/C4SM01365D

Meyer, C., Stenberg, L., Gonzalez-Perez, F., Wrobel, S., Ronchi, G., Udina, E., et al. (2016). Chitosan-film enhanced chitosan nerve guides for long-distance regeneration of peripheral nerves. *Biomaterials* 76, 33–51. doi: 10.1016/j.biomaterials.2015.10.040

Micholt, L., Gärtner, A., Prodanov, D., Braeken, D., Dotti, C. G., and Bartic, C. (2013). Substrate topography determines neuronal polarization and growth *in vitro*. *PLoS ONE* 8:e66170. doi: 10.1371/journal.pone.0066170

Miller, C., Jeftinija, S., and Mallapragada, S. (2001). Micropatterned Schwann cell–seeded biodegradable polymer substrates significantly enhance neurite alignment and outgrowth. *Tissue Eng.* 7, 705–715. doi: 10.1089/107632701753337663

Mizuno, A., Matsuda, K., and Shuto, S. (2017). Peptides to peptidomimetics: a strategy based on the structural features of cyclopropane. *Chemistry* 23, 14394–14409. doi: 10.1002/chem.201702119

Mochizuki, M., Philp, D., Hozumi, K., Suzuki, N., Yamada, Y., Kleinman, H. K., et al. (2007). Angiogenic activitiy of syndecan-binding laminin peptide AG73 (RKRLQVQLSIRT). *Arch. Biochem. Biophys.* 459, 249–255. doi: 10.1016/j.abb.2006.12.026

Mohtaram, N. K., Ko, J., King, C., Sun, L., Muller, N., Jun, M. B. G., et al. (2015). Electrospun biomaterial scaffolds with varied topographies for neuronal differentiation of human-induced pluripotent stem cells. *J. Biomed. Mater. Res. A* 103, 2591–2601. doi: 10.1002/jbm.a.35392

Moore, K., Macsween, M., and Shoichet, M. (2006). Immobilized concentration gradients of neurotrophic factors guide neurite outgrowth of primary neurons in macroporous scaffolds. *Tissue Eng.* 12, 267–278. doi: 10.1089/ten.2006.12.267

Mothe, A. J., Tam, R. Y., Zahir, T., Tator, C. H., and Shoichet, M. S. (2013). Repair of the injured spinal cord by transplantation of neural stem cells in a hyaluronan-based hydrogel. *Biomaterials* 34, 3775–3783. doi: 10.1016/j.biomaterials.2013.02.002

Nagamine, K., Hirata, T., Okamoto, K., Abe, Y., Kaji, H., and Nishizawa, M. (2015). Portable micropatterns of neuronal cells supported by thin hydrogel films. *ACS Biomater. Sci. Eng.* 1, 329–334. doi: 10.1021/acsbiomaterials.5b00020

Nakaji-Hirabayashi, T., Kato, K., and Iwata, H. (2013). *In vivo* study on the survival of neural stem cells transplanted into the rat brain with a collagen hydrogel that incorporates laminin-derived polypeptides. *Bioconjug. Chem.* 24, 1798–1804. doi: 10.1021/bc400005m

Nakayama, K., Takakuda, K., Koyama, Y., Itoh, S., Wang, W., Mukai, T., et al. (2007). Enhancement of peripheral nerve regeneration using bioabsorbable polymer tubes packed with fibrin gel. *Artificial Organs* 31, 500–508. doi: 10.1111/j.1525-1594.2007.00418.x

Nasir, S., Ramirez, P., Ali, M., Ahmed, I., Fruk, L., Mafe, S., et al. (2013). Nernst-Planck model of photo-triggered, p H–tunable ionic transport through nanopores functionalized with "caged" lysine chains. *J. Chem. Phys.* 138:034709. doi: 10.1063/1.4775811

Newman, K., McLaughlin, C., Carlsson, D., Li, F., Liu, Y., and Griffith, M. (2006). Bioactive hydrogel-filament scaffolds for nerve repair and regeneration. *Int. J. Artif. Organs* 29, 1082–1091. doi: 10.1177/039139880602901109

Nikkhah, M., Edalat, F., Manoucheri, S., and Khademhosseini, A. (2012). Engineering microscale topographies to control the cell-substrate interface. *Biomaterials* 33, 5230–5246. doi: 10.1016/j.biomaterials.2012.03.079

Norman, L. L., and Aranda-Espinoza, H. (2010). Cortical neuron outgrowth is insensitive to substrate stiffness. *Cell. Mol. Bioeng.* 3, 398–414. doi: 10.1007/s12195-010-0137-8

Novikova, L. N., Pettersson, J., Brohlin, M., Wiberg, M., and Novikov, L. N. (2008). Biodegradable poly-β-hydroxybutyrate scaffold seeded with Schwann cells to promote spinal cord repair. *Biomaterials* 29, 1198–1206. doi: 10.1016/j.biomaterials.2007.11.033

Nune, M., Krishnan, U. M., and Sethuraman, S. (2016). PLGA nanofibers blended with designer self-assembling peptides for peripheral neural regeneration. *Mater. Sci. Eng. C* 62, 329–337. doi: 10.1016/j.msec.2016.01.057

Ortega, F., Gascon, S., Masserdotti, G., Deshpande, A., Simon, C., Fischer, J., et al. (2013). Oligodendrogliogenic and neurogenic adult subependymal zone neural stem cells constitute distinct lineages and exhibit differential responsiveness to Wnt signalling. *Nat. Cell Biol.* 15:602. doi: 10.1038/ncb2736

Pakulska, M. M., Ballios, B. G., and Shoichet, M. S. (2012). Injectable hydrogels for central nervous system therapy. *Biomed. Mater.* 7:024101. doi: 10.1088/1748-6041/7/2/024101

Park, M., Shin, M., Kim, E., Lee, S., Park, K. I., Lee, H., et al. (2014). The promotion of human neural stem cells adhesion using bioinspired poly (norepinephrine) nanoscale coating. *J. Nanomater.* 2014:2. doi: 10.1155/2014/793052

Park, S. Y., Park, J., Sim, S. H., Sung, M. G., Kim, K. S., Hong, B. H., et al. (2011). Enhanced differentiation of human neural stem cells into neurons on graphene. *Adv. Mater.* 23:H263–7. doi: 10.1002/adma.201101503

Pek, Y. S., Wan, A. C., and Ying, J. Y. (2010). The effect of matrix stiffness on mesenchymal stem cell differentiation in a 3D thixotropic gel. *Biomaterials* 31, 385–391. doi: 10.1016/j.biomaterials.2009.09.057

Pfister, L. A., Papaloïzos, M., Merkle, H. P., and Gander, B. (2007). Nerve conduits and growth factor delivery in peripheral nerve repair. *J. Peripher. Nerv. Syst.* 12, 65–82. doi: 10.1111/j.1529-8027.2007.00125.x

Roach, P., Parker, T., Gadegaard, N., and Alexander, M. (2010). Surface strategies for control of neuronal cell adhesion: a review. *Surf. Sci. Rep.* 65, 145–173. doi: 10.1016/j.surfrep.2010.07.001

Rose, J. C., Cámara-Torres, M., Rahimi, K., Köhler, J., Möller, M., and De Laporte, L. (2017). Nerve cells decide to orient inside an injectable hydrogel with minimal structural guidance. *Nano Lett.* 17, 3782–3791. doi: 10.1021/acs.nanolett.7b01123

Rosso, G., Young, P., and Shahin, V. (2017). Mechanosensitivity of embryonic neurites promotes their directional extension and schwann cells progenitors migration. *Cell Physiol. Biochem.* 44, 1263–1270. doi: 10.1159/000485485

Sarig-Nadir, O., Livnat, N., Zajdman, R., Shoham, S., and Seliktar, D. (2009). Laser photoablation of guidance microchannels into hydrogels directs cell growth in three dimensions. *Biophys. J.* 96, 4743–4752. doi: 10.1016/j.bpj.2009.03.019

Schmalenberg, K. E., and Uhrich, K. E. (2005). Micropatterned polymer substrates control alignment of proliferating Schwann cells to direct neuronal regeneration. *Biomaterials* 26, 1423–1430. doi: 10.1016/j.biomaterials.2004.04.046

Schmid, R. S., and Maness, P. F. (2008). L1 and NCAM adhesion molecules as signaling coreceptors in neuronal migration and process outgrowth. *Curr. Opin. Neurobiol.* 18, 245–250. doi: 10.1016/j.conb.2008.07.015

Schmidt, C. E., and Leach, J. B. (2003). Neural tissue engineering: Strategies for repair and regeneration. *Ann. Rev. Biomed. Eng.* 5, 293–347. doi: 10.1146/annurev.bioeng.5.011303.120731

Schnell, E., Klinkhammer, K., Balzer, S., Brook, G., Klee, D., Dalton, P., et al. (2007). Guidance of glial cell migration and axonal growth on electrospun nanofibers of poly-ε-caprolactone and a collagen/poly-ε-caprolactone blend. *Biomaterials* 28, 3012–3025. doi: 10.1016/j.biomaterials.2007.03.009

Seidlits, S. K., Khaing, Z. Z., Petersen, R. R., Nickels, J. D., Vanscoy, J. E., Shear, J. B., et al. (2010). The effects of hyaluronic acid hydrogels with tunable mechanical properties on neural progenitor cell differentiation. *Biomaterials* 31, 3930–3940. doi: 10.1016/j.biomaterials.2010.01.125

Sell, S., Barnes, C., Smith, M., McClure, M., Madurantakam, P., Grant, J., et al. (2007). Extracellular matrix regenerated: tissue engineering via electrospun biomimetic nanofibers. *Polym. Int.* 56, 1349–1360. doi: 10.1002/pi.2344

Serrano, M., Patiño, J., García-Rama, C., Ferrer, M., Fierro, J., Tamayo, A., et al. (2014). 3D free-standing porous scaffolds made of graphene oxide as substrates for neural cell growth. *J. Mater. Chem. B* 2, 5698–5706. doi: 10.1039/C4TB00652F

Shah, S., Yin, P. T., Uehara, T. M., Chueng, S. T. D., Yang, L., and Lee, K. B. (2014). Guiding stem cell differentiation into oligodendrocytes using graphene-nanofiber hybrid scaffolds. *Adv. Mater.* 26, 3673–3680. doi: 10.1002/adma.201400523

Shin, H., Jo, S., and Mikos, A. G. (2003). Biomimetic materials for tissue engineering. *Biomaterials* 24, 4353–4364. doi: 10.1016/S0142-9612(03)00339-9

Silva, G. A., Czeisler, C., Niece, K. L., Beniash, E., Harrington, D. A., Kessler, J. A., et al. (2004). Selective differentiation of neural progenitor cells by high-epitope density nanofibers. *Science* 303, 1352–1355. doi: 10.1126/science.1093783

Silva, N. A., Cooke, M. J., Tam, R. Y., Sousa, N., Salgado, A. J., Reis, R. L., et al. (2012). The effects of peptide modified gellan gum and olfactory ensheathing glia cells on neural stem/progenitor cell fate. *Biomaterials* 33, 6345–6354. doi: 10.1016/j.biomaterials.2012.05.050

Smeal, R. M., Rabbitt, R., Biran, R., and Tresco, P. A. (2005). Substrate curvature influences the direction of nerve outgrowth. *Ann. Biomed. Eng.* 33, 376–382. doi: 10.1007/s10439-005-1740-z

Smeal, R. M., and Tresco, P. A. (2008). The influence of substrate curvature on neurite outgrowth is cell type dependent. *Exp. Neurol.* 213, 281–292. doi: 10.1016/j.expneurol.2008.05.026

Stephanopoulos, N., Freeman, R., North, H. A., Sur, S., Jeong, S. J., Tantakitti, F., et al. (2014). Bioactive DNA-peptide nanotubes enhance the differentiation of neural stem cells into neurons. *Nano Lett.* 15, 603–609. doi: 10.1021/nl504079q

Straley, K. S., Foo, C. W., and Heilshorn, S. C. (2010). Biomaterial design strategies for the treatment of spinal cord injuries. *J. Neurotrauma* 27, 1–19. doi: 10.1089/neu.2009.0948

Struzyna, L. A., Katiyar, K., and Cullen, D. K. (2014). Living scaffolds for neuroregeneration. *Curr. Opin. Solid State Mater. Sci.* 18, 308–318. doi: 10.1016/j.cossms.2014.07.004

Sun, W., Incitti, T., Migliaresi, C., Quattrone, A., Casarosa, S., and Motta, A. (2017). Viability and neuronal differentiation of neural stem cells encapsulated in silk fibroin hydrogel functionalized with an IKVAV peptide. *J. Tissue Eng. Regener. Med.* 11, 1532–1541. doi: 10.1002/term.2053

Sun, Y., Li, W., Wu, X., Zhang, N., Zhang, Y., Ouyang, S., et al. (2016). Functional self-assembling peptide nanofiber hydrogels designed for nerve degeneration. *ACS Appl. Mater. Interf.* 8, 2348–2359. doi: 10.1021/acsami.5b11473

Sur, S., Guler, M. O., Webber, M. J., Pashuck, E. T., Ito, M., Stupp, S. I., et al. (2014). Synergistic regulation of cerebellar Purkinje neuron development by laminin epitopes and collagen on an artificial hybrid matrix construct. *Biomater. Sci.* 2, 903–914. doi: 10.1039/C3BM60228A

Tarus, D., Hamard, L., Caraguel, F., Wion, D., Szarpak-Jankowska, A., van der Sanden, B., et al. (2016). Design of hyaluronic acid hydrogels to promote neurite outgrowth in three dimensions. *ACS Appl. Mater. Interf.* 8, 25051–25059. doi: 10.1021/acsami.6b06446

Taylor, A. C., González, C. H., Miller, B. S., Edgington, R. J., Ferretti, P., and Jackman, R. B. (2017). Surface functionalisation of nanodiamonds for human neural stem cell adhesion and proliferation. *Sci. Rep.* 7:7307. doi: 10.1038/s41598-017-07361-y

Thid, D., Bally, M., Holm, K., Chessari, S., Tosatti, S., Textor, M., et al. (2007). Issues of ligand accessibility and mobility in initial cell attachment. *Langmuir* 23, 11693–11704. doi: 10.1021/la701159u

Thid, D., Holm, K., Eriksson, P. S., Ekeroth, J., Kasemo, B., and Gold, J. (2008). Supported phospholipid bilayers as a platform for neural progenitor cell culture. *J. Biomed. Mater. Res. A* 84, 940–953. doi: 10.1002/jbm.a.31358

Thompson, D. M., and Buettner, H. M. (2004). Oriented Schwann cell monolayers for directed neurite outgrowth. *Ann. Biomed. Eng.* 32, 1121–1131. doi: 10.1114/B:ABME.0000036648.68804.e7

Tian, L., Prabhakaran, M. P., Hu, J., Chen, M., Besenbacher, F., and Ramakrishna, S. (2016). Synergistic effect of topography, surface chemistry and conductivity of the electrospun nanofibrous scaffold on cellular response of PC12 cells. *Coll. Surf. B Biointerf.* 145, 420–429. doi: 10.1016/j.colsurfb.2016.05.032

Tonda-Turo, C., Audisio, C., Gnavi, S., Chiono, V., Gentile, P., Raimondo, S., et al. (2011). Porous poly (ε-caprolactone) nerve guide filled with porous gelatin matrix for nerve tissue engineering. *Adv. Eng. Mater.* 13, B151–B164. doi: 10.1002/adem.201080099

Tsai, E. C., Dalton, P. D., Shoichet, M. S., and Tator, C. H. (2004). Synthetic hydrogel guidance channels facilitate regeneration of adult rat brainstem motor

axons after complete spinal cord transection. *J. Neurotrauma* 21, 789–804. doi: 10.1089/0897715041269687

Tuft, B. W., Zhang, L., Xu, L., Hangartner, A., Leigh, B., Hansen, M. R., et al. (2014). Material stiffness effects on neurite alignment to photopolymerized micropatterns. *Biomacromolecules* 15, 3717–3727. doi: 10.1021/bm501019s

Tysseling-Mattiace, V. M., Sahni, V., Niece, K. L., Birch, D., Czeisler, C., Fehlings, M. G., et al. (2008). Self-assembling nanofibers inhibit glial scar formation and promote axon elongation after spinal cord injury. *J. Neurosci.* 28, 3814–3823. doi: 10.1523/JNEUROSCI.0143-08.2008

Uemura, M., Refaat, M. M., Shinoyama, M., Hayashi, H., Hashimoto, N., and Takahashi, J. (2010). Matrigel supports survival and neuronal differentiation of grafted embryonic stem cell-derived neural precursor cells. *J. Neurosci. Res.* 88, 542–551. doi: 10.1002/jnr.22223

Valiente, M., and Marín, O. (2010). Neuronal migration mechanisms in development and disease. *Curr. Opin. Neurobiol.* 20, 68–78. doi: 10.1016/j.conb.2009.12.003

Wang, G., Ao, Q., Gong, K., Wang, A., Zheng, L., Gong, Y., et al. (2010a). The effect of topology of chitosan biomaterials on the differentiation and proliferation of neural stem cells. *Acta Biomater.* 6, 3630–3639. doi: 10.1016/j.actbio.2010.03.039

Wang, L. S., Chung, J. E., Chan, P. P. Y., and Kurisawa, M. (2010b). Injectable biodegradable hydrogels with tunable mechanical properties for the stimulation of neurogenesic differentiation of human mesenchymal stem cells in 3D culture. *Biomaterials* 31, 1148–1157. doi: 10.1016/j.biomaterials.2009.10.042

Wang, X., Hu, W., Cao, Y., Yao, J., Wu, J., and Gu, X. (2005). Dog sciatic nerve regeneration across a 30-mm defect bridged by a chitosan/PGA artificial nerve graft. *Brain* 128, 1897–1910. doi: 10.1093/brain/awh517

Wang, Y., Xu, Z., Kam, L. C., and Shi, P. (2014). Site-specific differentiation of neural stem cell regulated by micropatterned multicomponent interfaces. *Adv. Healthcare Mater.* 3, 214–220. doi: 10.1002/adhm.201300082

Webb, A., Clark, P., Skepper, J., Compston, A., and Wood, A. (1995). Guidance of oligodendrocytes and their progenitors by substratum topography. *J. Cell Sci.* 108, 2747–2760.

Weber, R. A., Breidenbach, W. C., Brown, R. E., Jabaley, M. E., and Mass, D. P. (2000). A randomized prospective study of polyglycolic acid conduits for digital nerve reconstruction in humans. *Plastic Reconstruc. Surg.* 106, 1036–1045. doi: 10.1097/00006534-200010000-00013

Wei, Z., Zhao, J., Chen, Y. M., Zhang, P., and Zhang, Q. (2016). Self-healing polysaccharide-based hydrogels as injectable carriers for neural stem cells. *Sci. Rep.* 6:37841. doi: 10.1038/srep37841

Wen, J. H., Vincent, L. G., Fuhrmann, A., Choi, Y. S., Hribar, K. C., Taylor-Weiner, H., et al. (2014). Interplay of matrix stiffness and protein tethering in stem cell differentiation. *Nat. Mater.* 13, 979–987. doi: 10.1038/nmat4051

Wilkinson, A. E., Kobelt, L. J., and Leipzig, N. D. (2014). Immobilized ECM molecules and the effects of concentration and surface type on the control of NSC differentiation. *J. Biomed. Mater. Res. A* 102, 3419–3428. doi: 10.1002/jbm.a.35001

Winter, C. C., Katiyar, K. S., Hernandez, N. S., Song, Y. J., Struzyna, L. A., Harris, J. P., et al. (2016). Transplantable living scaffolds comprised of micro-tissue engineered aligned astrocyte networks to facilitate central nervous system regeneration. *Acta Biomater.* 38, 44–58. doi: 10.1016/j.actbio.2016.04.021

Wood, M. D., and Sakiyama-Elbert, S. E. (2008). Release rate controls biological activity of nerve growth factor released from fibrin matrices containing affinity-based delivery systems. *J. Biomed. Mater. Res. A* 84, 300–312. doi: 10.1002/jbm.a.31269

Wrobel, M. R., and Sundararaghavan, H. G. (2013). Directed migration in neural tissue engineering. *Tissue Eng. B Rev.* 20, 93–105. doi: 10.1089/ten.teb.2013.0233

Wu, S., Xu, R., Duan, B., and Jiang, P. (2017). Three-dimensional hyaluronic acid hydrogel-based models for *in vitro* human iPSC-derived NPC culture and differentiation. *J. Mater. Chem. B.* 5, 3870–3878. doi: 10.1039/C7TB00721C

Xie, J., Liu, W., MacEwan, M. R., Bridgman, P. C., and Xia, Y. (2014). Neurite outgrowth on electrospun nanofibers with uniaxial alignment: the effects of fiber density, surface coating, and supporting substrate. *ACS nano* 8, 1878–1885. doi: 10.1021/nn406363j

Xie, J., Willerth, S. M., Li, X., Macewan, M. R., Rader, A., Sakiyama-Elbert, S. E., et al. (2009). The differentiation of embryonic stem cells seeded on electrospun nanofibers into neural lineages. *Biomaterials* 30, 354–362. doi: 10.1016/j.biomaterials.2008.09.046

Xing, D., Ma, L., and Gao, C. (2014). Synthesis of functionalized poly (ester carbonate) with laminin-derived peptide for promoting neurite outgrowth of PC12 cells. *Macromol. Biosci.* 14, 1429–1436. doi: 10.1002/mabi.201400186

Xing, D., Ma, L., and Gao, C. (2017). A bioactive hyaluronic acid–based hydrogel cross-linked by Diels–Alder reaction for promoting neurite outgrowth of PC12 cells. *J. Bioact. Compat. Polym.* 32:0883911516684654. doi: 10.1177/0883911516684654

Xu, X.-Y., Li, X.-T., Peng, S.-W., Xiao, J.-F., Liu, C., Fang, G., et al. (2010). The behaviour of neural stem cells on polyhydroxyalkanoate nanofiber scaffolds. *Biomaterials* 31, 3967–3975. doi: 10.1016/j.biomaterials.2010.01.132

Yamada, K. M. (1989). "Fibronectin domains and receptors," in *Fibronectin*, ed D. Mosher (New York, NY: Academic Press), 47–121.

Yamada, Y., Hozumi, K., Aso, A., Hotta, A., Toma, K., Katagiri, F., et al. (2012). Laminin active peptide/agarose matrices as multifunctional biomaterials for tissue engineering. *Biomaterials* 33, 4118–4125. doi: 10.1016/j.biomaterials.2012.02.044

Yang, F., Murugan, R., Wang, S., and Ramakrishna, S. (2005). Electrospinning of nano/micro scale poly(l-lactic acid) aligned fibers and their potential in neural tissue engineering. *Biomaterials* 26, 2603–2610. doi: 10.1016/j.biomaterials.2004.06.051

Yang, K., Jung, H., Lee, H.-R., Lee, J. S., Kim, S. R., Song, K. Y., et al. (2014). Multiscale, hierarchically patterned topography for directing human neural stem cells into functional neurons. *ACS Nano* 8, 7809–7822. doi: 10.1021/nn501182f

Yang, K., Lee, J. S., Kim, J., Lee, Y. B., Shin, H., Um, S. H., et al. (2012). Polydopamine-mediated surface modification of scaffold materials for human neural stem cell engineering. *Biomaterials* 33, 6952–6964. doi: 10.1016/j.biomaterials.2012.06.067

Yao, S. L., Liu, X., Yu, S. K., Wang, X. M., Zhang, S. M., Wu, Q., et al. (2016). Co-effects of matrix low elasticity and aligned topography on stem cell neurogenic differentiation and rapid neurite outgrowth. *Nanoscale* 8, 10252–10265. doi: 10.1039/C6NR01169A

Zamani, F., Amani-Tehran, M., Latifi, M., and Shokrgozar, M. A. (2013). The influence of surface nanoroughness of electrospun PLGA nanofibrous scaffold on nerve cell adhesion and proliferation. *J. Mater. Sci. Mater. Med.* 24, 1551–1560. doi: 10.1007/s10856-013-4905-6

Zhang, D., Ni, N., Chen, J., Yao, Q., Shen, B., Zhang, Y., et al. (2015). Electrospun SF/PLCL nanofibrous membrane: a potential scaffold for retinal progenitor cell proliferation and differentiation. *Sci. Rep.* 5:14326. doi: 10.1038/srep14326

Zhang, K., Zheng, H., Liang, S., and Gao, C. (2016). Aligned PLLA nanofibrous scaffolds coated with graphene oxide for promoting neural cell growth. *Acta Biomater.* 37, 131–142. doi: 10.1016/j.actbio.2016.04.008

Zhang, Z., Yoo, R., Wells, M., Beebe, T. P., Biran, R., and Tresco, P. (2005). Neurite outgrowth on well-characterized surfaces: preparation and characterization of chemically and spatially controlled fibronectin and RGD substrates with good bioactivity. *Biomaterials* 26, 47–61. doi: 10.1016/j.biomaterials.2004.02.004

Zhao, S., Fan, W., Guo, X., Xue, L., Berninger, B., Salierno, M. J., et al. (2017). Microenvironments to study migration and somal translocation in cortical neurons. *Biomaterials* 156, 238–247. doi: 10.1016/j.biomaterials.2017.11.042

Zweckberger, K., Ahuja, C. S., Liu, Y., Wang, J., and Fehlings, M. G. (2016). Self-assembling peptides optimize the post-traumatic milieu and synergistically enhance the effects of neural stem cell therapy after cervical spinal cord injury. *Acta Biomater.* 42, 77–89. doi: 10.1016/j.actbio.2016.06.016

Conflict of Interest Statement: The authors declare that the research was conducted in the absence of any commercial or financial relationships that could be construed as a potential conflict of interest.

frontiers in Materials

MINI REVIEW
published: 10 April 2018
doi: 10.3389/fmats.2018.00021

Biomaterials for Enhancing Neuronal Repair

Olivia V. Cangellaris [1,2,3,4] *and Martha U. Gillette* [1,3,4,5,6*]

[1] Department of Bioengineering, University of Illinois at Urbana-Champaign, Urbana, IL, United States, [2] Medical Scholars Program, College of Medicine, University of Illinois at Urbana-Champaign, Urbana, IL, United States, [3] Micro and Nanotechnology Laboratory, University of Illinois at Urbana-Champaign, Urbana, IL, United States, [4] Beckman Institute for Advanced Science and Technology, University of Illinois at Urbana-Champaign, Urbana, IL, United States, [5] Department of Cell and Developmental Biology, University of Illinois at Urbana-Champaign, Urbana, IL, United States, [6] Neuroscience Program, University of Illinois at Urbana-Champaign, Urbana, IL, United States

As they differentiate from neuroblasts, nascent neurons become highly polarized and elongate. Neurons extend and elaborate fine and fragile cellular extensions that form circuits enabling long-distance communication and signal integration within the body. While other organ systems are developing, projections of differentiating neurons find paths to distant targets. Subsequent post-developmental neuronal damage is catastrophic because the cues for reinnervation are no longer active. Advances in biomaterials are enabling fabrication of micro-environments that encourage neuronal regrowth and restoration of function by recreating these developmental cues. This mini-review considers new materials that employ topographical, chemical, electrical, and/or mechanical cues for use in neuronal repair. Manipulating and integrating these elements in different combinations will generate new technologies to enhance neural repair.

Keywords: neuroregenerative therapy, neural scaffolds, topography, electrical stimulation, hydrogels, self-rolled-up membranes, nerve-guide-conduits, flexible electronics

OPEN ACCESS

Edited by:
Brendan Harley, University of Illinois at Urbana-Champaign, United States

Reviewed by:
Stephanie Michelle Willerth, University of Victoria, Canada
Marcelo Salierno, Johannes Gutenberg-Universität Mainz, Germany

***Correspondence:**
Martha U. Gillette
mgillett@illinois.edu

Specialty section:
This article was submitted to Biomaterials, a section of the journal Frontiers in Materials

Received: *13 December 2017*
Accepted: *26 March 2018*
Published: *10 April 2018*

Citation:
Cangellaris OV and Gillette MU (2018) Biomaterials for Enhancing Neuronal Repair. Front. Mater. 5:21. doi: 10.3389/fmats.2018.00021

INTRODUCTION

Neurons are characterized by dendrites, multiple slender filamentous protrusions that receive and integrate incoming information, and a single axon, which transmits integrated signals downstream in a multicellular network. These cellular extensions are typically several times longer than the relatively small cell body and form a myriad of interconnections that enable humans to sense, integrate, remember, and respond to the world. Unlike other systems in the human body, cues for growth and repair in the nervous system are no longer active post-developmentally and, consequently, structural and functional losses following disease or damage are catastrophic. Neurological deficits contribute to over 600 classified neurological disorders and affect ∼50 million people in the United States alone (Brown et al., 2005). Neurological disorders often result in debilitation rather than immediate death, and the personal and financial costs become staggering. The global burden of neurological afflictions, measured in disability-adjusted life years (DALYs), exceeds that of other diseases including heart disease and cancer (WHO, 2006). Therefore, new methods of treatment that ameliorate or resolve neurological disorders are necessary.

Innovative therapies for neurodegeneration and traumatic injury are emerging from novel biomaterials. Development of materials that support and nurture growth without introducing trauma while facilitating neural repair have the potential to alleviate peripheral neuropathies; diabetic sensory neuropathy or spinal cord trauma would benefit (Teng et al., 2002; Gu et al., 2014). New techniques and advances in material design, such as pore-enhanced hydrogels to promote

neuronal alignment (Lee et al., 2015b), are facilitating targeted neuronal growth and repair. Innovations in neural monitoring through flexible, biodegradable electronics provide a means to understand these processes at a more fundamental level, as well as track and monitor repair *in vivo* (Viventi et al., 2011; Kang et al., 2016). These engineered interfaces address specific challenges inherent to damaged neural tissue by reducing glial scarring and overcoming limited distances of regeneration (Orive et al., 2009; Tam et al., 2014).

Unmodified planar substrates inadequately capitalize on endogenous factors that could enhance the efficacy of the substrate to promote targeted cellular development and growth. Modifying the substrate to better approximate the native developmental environment of neurons encourages the extension of neurites and repair of lesions. This review explores recent advances in the manipulation of topography, electric cues, and stiffness in biomaterials to enhance neuronal dynamics (e.g., neuritogenesis), improve growth, and allow monitoring of neural systems. Cues or properties are compared for relative impact on neuronal behavior and development (**Table 1**). While the integration of chemical cues into materials has been widely employed in other neuronal studies (Moore et al., 2006; Patel et al., 2007; Millet et al., 2010), the influence of chemical signals is intertwined in the discussion of the aforementioned parameters. This review focuses on neurons, while discussion of neural repair of all major cell populations within the nervous system, including glia, has been considered elsewhere (Schmidt and Leach, 2003; Tian et al., 2015).

TOPOGRAPHICAL CUES DRIVE ALIGNMENT AND DIRECTIONALITY

Cellular dynamics are strongly influenced by substrate topography (Bettinger et al., 2009; Ventre et al., 2012). Throughout the body, the extracellular matrix (ECM), with its fibers of collagen, fibronectin, and/or laminin, provides scaffolding that cells can adhere to and climb on, over, and through to travel to their terminal point. Neurons themselves can provide critical topography. An example is during formation of laminar brain structures, where new daughter cells use the scaffold provided by radial glial cells to migrate outward and form successive cortical layers (Rakic, 1972; Edmondson and Hatten, 1987; Kriegstein, 2005; Barros et al., 2011).

When designing customized materials and substrates for use in neural repair, the relationship between neuronal cells and native *in vivo* topography informs the relation to the desired functional outcome. Neuronal migration and neurite extension or directionality can be guided by the addition of topographical cues to a substrate, which enhances control by providing a recognizable path (Jang et al., 2010; Baranes et al., 2012). In the case of damaged spinal neurons, a 3D scaffold can provide a sturdy framework to support directional neurite regrowth. A tubular design allows for directed tunneling of the neurite to the distal region needing reinnervation. Nanotopography is also important for cell adhesion and plays a critical role in material design (Yu et al., 2008; Khan and Newaz, 2010). Cellular adhesion depends on surface properties such as wettability and charge. These elements can be modified during fabrication and functionalization through protein deposition to the substrate surface (Subramanian et al., 2009). Furthermore, cells can respond to nanoscale features in ways that change morphology, attachment, proliferation, and even gene expression in response to nano-gratings, posts, and pits (Bettinger et al., 2009).

Polymer nanofibers are used to build scaffolds that support and direct neurite extension of neuron cultures *in vitro*. These scaffolds are fabricated using electrospinning, a technique that allows for accumulation of nanofibers in specific orientations. The process is highly customizable and the fibers can be spun in nm or μm scales (Pettikiriarachchi et al., 2010). Polylactic acid (PLLA) fibers of large diameter (>1,000 nm) have been shown to enhance neurite extension in dissociated chick dorsal root ganglia (DRG) cultures (Wang et al., 2010). Functionalizing PLLA fibers with fibronectin or laminin further improves neurite interaction by replicating these endogenous chemical cues (Koppes et al., 2014). Other electrospun nanofiber scaffolds improve DRG neurite extension, promote differentiation of mouse embryonic stem cells (ESCs) into neural progenitors, and enhance outgrowth of neurites on the scaffolds with aligned fibers. Neural crest stem cells differentiated from iPSCs cultured within nanofiber-modified conduits enhanced sciatic nerve regeneration (Xie et al., 2009; Schaub and Gilbert, 2011; Wong et al., 2011). Nanofibers can be spun from a variety of biocompatible materials, including natural proteins such as collagen. However, there are several limitations to these scaffolds. It is difficult to create an environment mimicking the endogenous ECM, because its components are smaller than what is currently achievable when fabricating nanofibers (∼100 nm thick). Additionally, nanofiber scaffolds cannot support embedded cells without compromising the structural integrity of the scaffold (Liu et al., 2012).

Hydrogels, networks of polymers that have been swollen with water, are attractive materials for cellular applications due to their biocompatibility, ease of fabrication, and capacity for customization (Caliari and Burdick, 2016). One advantage of hydrogels is that their porosity is not detrimental to their structure and can allow for migration of cells within the hydrogel scaffold. Hydrogels fabricated with an additional internal topography promote alignment or directionality of hippocampal and DRG neurons (Liu et al., 2015), and differentiation of stem cells into a neuronal cell-type (Lee et al., 2015b). When human bone marrow stromal cells (hBMSCs) were cultured in hydrogels with both aligned microchannels (**Figure 1A**) and stochastically formed micropores (**Figure 1B**), hBMSCs differentiated into neuronal cells and elongated to grow within the microchannels (**Figure 1C**). Differentiation was attributed to the topography facilitating binding between cellular integrins and ligands, which

Abbreviations: DALYs, Disability-adjusted life years; ECM, Extracellular matrix; PLLA, Polylactic acid; DRG, Dorsal root ganglia; ESCs, Embryonic stem cells; iPSCs, Induced pluripotent stem cells; hBMSCs, Human bone marrow stromal cells; S-RuMs, Self-rolled-up membranes; NGCs, Nerve-guide-conduits or nerve-guidance-channels; PHB-HV, Poly(3-hydroxybutyrate-co-3-hydroxyvalerate); EFs, Electric fields; DC, Direct current; AC, Alternating current; PPy, Polypyrrole; E, Elastic modulus; NPCs, Neural progenitor cells; CSF, Cerebral spinal fluid.

TABLE 1 | Impact of various material properties on neuronal behavior and development.

Material property	Neurites	Directionality	Cell fate
Topographical[a]	• Increased neurite length	Neurite direction guided by • Tubular structures • Microchannels • Confined spaces	iPSCs, ESCs, hBMSCs differentiate to neural cell type
Electrical[b]	• Increased neurite length • Enhanced neuritogenesis	• Neurites grow/extend in direction of EF • Neurite growth rate increased • Neurons migrate in EF direction • Polarization of neurons	• Direct neural tube formation • Direct cell migration and organization • Influence neuronal differentiation
Mechanical Stiffness[c]	Decreased stiffness supports increased neurite length Increased stiffness results in: • Improved network connectivity • Improved signal transduction	No effect	Decreased stiffness directs stem cell differentiation toward the neural lineage

[a] *Topographical References: (Xie et al., 2009; Schaub and Gilbert, 2011; Wong et al., 2011; Froeter et al., 2014; Koppes et al., 2014; Lee et al., 2015b).*
[b] *Electrical References: (Jaffe and Stern, 1979; Patel and Poo, 1982; Hotary and Robinson, 1991; Davenport and McCaig, 1993; Metcalf and Borgens, 1994; Yao et al., 2008, 2009, 2011; Graves et al., 2011; Koppes et al., 2014; Kim et al., 2016; Ma et al., 2016).*
[c] *Mechanical Stiffness References: (Balgude et al., 2001; Discher et al., 2005; Jiang et al., 2010; Keung et al., 2012; Lee et al., 2013; Zhang et al., 2014; Mosley et al., 2017).*

is important for stem cell differentiation to neurons. The stochastic micropore gels could not support this binding, leading to mostly undifferentiated hBMSCs (Lee et al., 2015b). Hydrogels can also be used for cell encapsulation or fabricated with particles bearing trophic factors to enhance cellular interactions on and within the gel (Carballo-Molina and Velasco, 2015).

A semiconductor-based microtube substrate, composed of a thin nanomembrane of oppositely strained layers of silicon nitride that can self-roll, significantly enhances neurite alignment (**Figure 1D**). These self-rolled-up membranes (S-RuMs) have a unique combination of features that make them attractive for manipulating topography. S-RuMs are optically transparent under most conventional microscopy techniques, including phase-contrast and fluorescence imaging, which makes them ideal for use with cultured cells. Since they are manufactured using a scalable semiconductor process (Li, 2008; Huang et al., 2012), they are highly customizable and versatile, which facilitates many different designs (Froeter et al., 2013). They also are biocompatible, an essential characteristic for cell and tissue interfaces (Froeter et al., 2014). The S-RuMs can be tuned to a range of diameters and lengths, can be rolled into a single or binocular tube, and can be incorporated with pores to allow for nutrient and gas exchange across the tube membrane. By restricting the diameter of the S-RuM to the 5-μm range, a single neurite can be captured within each tube. By altering the fabrication process to widen the diameter, a bundle of neurites can traverse a single tube. Additionally, a thin deposition of metal can be added during the fabrication process to create an electrode that is rolled within the S-RuM (**Figure 1E**). This characteristic will enable selective and targeted stimulation and recording of a neurite contained on a single substrate and continuous tracking of functional neurite dynamics under electrical stimulation. Scanning electron microscopy (SEM) of rat hippocampal neurons in culture reveal the S-RuMs provide adequate space for neurites to extend, turn, and extend through the lumen (**Figure 1F**).

Nerve-guide-conduits or nerve-guidance-channels (NGCs) are 3D constructs for whole nerve therapies *in vivo* (Anderson et al., 2017; Lackington et al., 2017). They are currently used as implants for neural repair in humans. Commercially available NGCs are primarily single-lumen tubes, with no added topographical features, through which the two ends of a severed nerve are inserted and left to grow together (de Ruiter et al., 2009). There are limitations to these models, most notably in the injury gap distance over which they are effective. Functionalization to improve rate of regrowth, limit scarring, and improve permeability for nutrient transfer has yet to be integrated into these devices.

Techniques that have proven successful during *in vitro* neuroregenerative studies are currently being applied and evaluated in NGCs in animal models. An experimental NGC, composed of poly(3-hydroxybutyrate-co-3-hydroxyvalerate) (PHB-HV) and enhanced with a conductive polypyrrole co-polymer coating along the inner diameter of the NGC, has been implanted in Sprague-Dawley rats with severed sciatic nerves. When the conduits were harvested at 8 weeks and analyzed for neuronal markers, nerve tissue was found throughout the conduit with no evidence of inflammation. Thus, the NGC supports and promotes regeneration of damaged nerves (Durgam et al., 2010). A more recent study in rats demonstrated nerve regeneration *in vivo* that utilized NGCs made of zein, a corn-derived polymer. NGCs were fabricated in three configurations: non-porous NGCs, porous NGCs, and porous NGCs that contained smaller zein microtubes. A 10-mm section of the sciatic nerve was removed and replaced with the NGCs, and recovery was tracked over a 4-month period. The rats showed improved gait 2 months after implantation. The porous zein conduit showed significantly increased density of myelinated nerve fibers and increased myelin sheath thickness at 2- and 4-months post-implantation (Wang et al., 2017). The porous nature of these zein NGCs enabled nutrient diffusion and facilitated eventual degradation of the scaffold over the

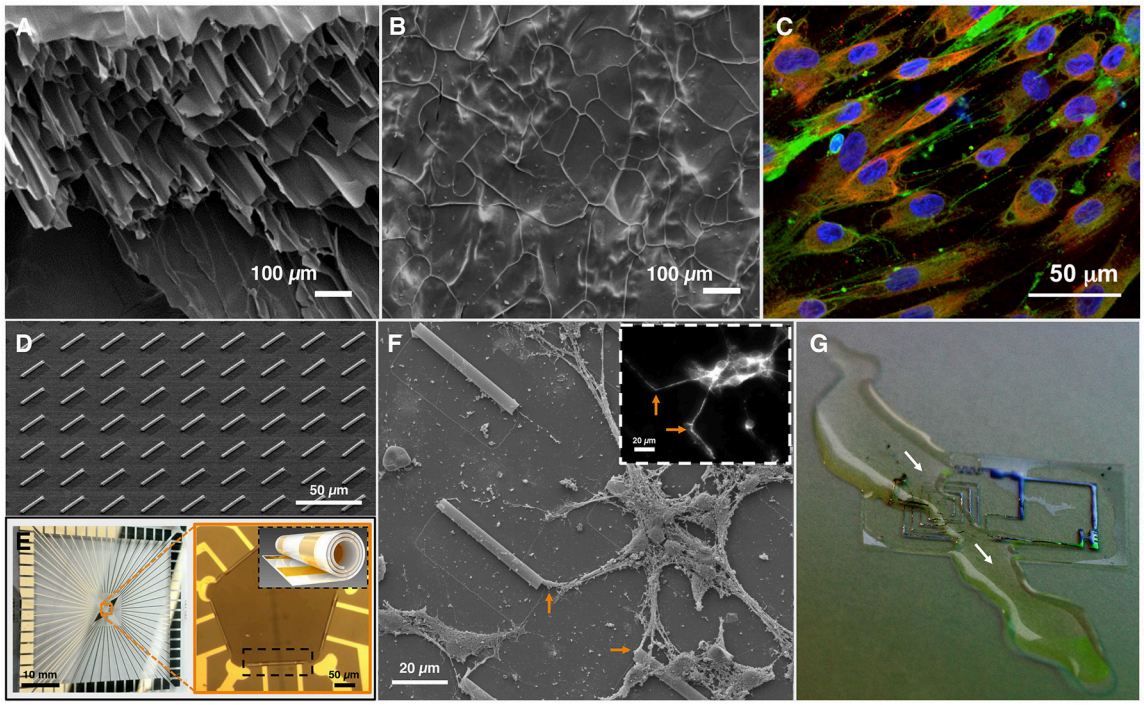

FIGURE 1 | Material applications of topography, electrical stimulation, and stiffness. **(A)** Scanning electron micrograph (SEM) of fractured hydrogels reveals the internal structure of the hydrogel with microchannels, or **(B)** micropores (images **A,B** adapted from Lee et al., 2015a). **(C)** Human bone marrow stromal cells (hBMSCs) cultured on hydrogel with aligned microchannels differentiate into a neuronal phenotype. Fluorescence imaging reveals MAP2 (neuronal marker, green), GFAP (glial marker, red), and DAPI (nuclear marker, blue) immunoreactivity, demonstrating differentiation of hBMSCs into cells expressing neuronal or glial markers, and elongating in the microchanneled hydrogel (image contributed by H. J. Kong, University of Illinois at Urbana-Champaign). **(D)** SEM of array of self-rolled-up membranes (S-RuMs) composed of thin-film silicon nitride bilayers. **(E)** A multi-electrode array chip (left) with S-RuMs patterned in a pentagon formation (orange box, right). Black inset shows schematic of single S-RuM with gold electrodes rolled inside (images **D,E** contributed by X. Li, University of Illinois at Urbana-Champaign). **(F)** SEM of rat hippocampal neurons cultured on S-RuM substrate (3 days *in vitro*). Inset: Fluorescence imaging reveals MAP2 (neuronal marker, white) immunoreactivity, confirming neuronal cell type. Orange arrows correspond to entry of neurites into S-RuMs. **(G)** An example of flexible, biocompatible, dissolvable electronics: an electronic circuit dissolving in a stream of water. White arrows indicate the path of the water and the region of the circuit that is dissolving (image contributed by J.A. Rogers, Northwestern University).

course of 4 months, when nerve regeneration in the conduit with microtubes was comparable to the regeneration observed in autograft controls (Wang et al., 2017). Collectively, these results highlight how topography can positively promote neurite outgrowth and enhance regeneration.

APPLICATION OF ELECTRIC FIELDS TO MANIPULATE NEURITE EXTENSION

The nervous system relies on electrical signals for development and communication. In early development, electric potentials define migration paths of the cells and differentiation, driving the formation of the neural tube (Hotary and Robinson, 1990, 1991; Metcalf and Borgens, 1994; Yao et al., 2008; Ma et al., 2016). Signal transmission in neurons is mediated by ion fluxes across the cell membrane. In instances of traumatic injury, ion flux establishes an electric potential gradient that promotes repair (Reid et al., 2007; McCaig et al., 2009). Numerous studies support the positive effect of electric fields (EFs) on neurite extension, growth-rate, and neuron polarization and migration (Jaffe and Stern, 1979; Patel and Poo, 1982; McCaig, 1990; Davenport and McCaig, 1993; Yao et al., 2009, 2011; Graves et al., 2011; Kim et al., 2016). Consequently, electrical cues can be utilized to positively regulate, facilitate, and enhance neuroregeneration.

Nanofiber scaffolds can be augmented to enhance neurite outgrowth by providing both electrical stimulation and topographical cues. An external EF was introduced in parallel or perpendicular orientation to planar PLLA fiber scaffolds using an agar salt-bridge and platinum reference electrode. When rat DRG cultured on each of these scaffolds were stimulated with an applied direct current (DC) EF for 8 h, neurite outgrowths on the electrically stimulated scaffolds were significantly longer compared to controls. Neurite outgrowth increased by 74% on the PLLA fibers (topography alone), 32% on the PLLA planar films (electrical stimulation alone), and by 126% on the PLLA fibers aligned to the direction of the DC EF (Koppes et al., 2014). Therefore, the combination of topographical and electrical cues greatly improves length of neurite extension. Electrical stimulation can be further integrated into the scaffold

by choosing a conductive base material. Polypyrrole (PPy) is biocompatible, biodegradable, as well as electrically conductive, so NGCs augmented with PPy can support electrical stimulation (Nguyen et al., 2014). When DRGs on PPy-modified flat scaffolds were stimulated with an electric field, neurite extension was enhanced by 13% in a DC EF, and 21% in an alternating current (AC) EF. PPy-modified NGCs without electrical stimulation were shown to support regrowth of severed sciatic nerves in rats *in vivo* (Durgam et al., 2010). To translate this technology to *in vivo* models, electrical stimulation needs to be introduced to a PPy-modified NGC. Electric stimulation is a native signal that strongly impacts neurons and can be further manipulated to direct neuritogenesis in strategies for neuroregenerative therapy.

MANIPULATION OF SUBSTRATE STIFFNESS

The intrinsic mechanical properties of the body determine neuronal differentiation, dynamics, behavior, and organization (Hynes, 2009; Janmey and Miller, 2011; Koser et al., 2016). The importance of substrate mechanics as a cue is evident during differentiation of stem cells in environments of controlled stiffness. Increasingly higher stiffness encourages their differentiation into muscle [elastic modulus (E) ∼10 kPa] or bone ($E > 30$ kPa), whereas a lower stiffness on the order of hundreds of Pa encourages differentiation into neurons (Lee et al., 2013). This is consistent with the elastic modulus within the central and peripheral nervous systems, which ranges between 0.5 and 1 kPa, and the shear stiffness of human brain tissue *in vivo*, which has been measured between 2 and 3 kPa (Lee et al., 2013; Bai et al., 2014; Hiscox et al., 2016). Such measurements of human brain tissue are highly dependent on frequency and region, and therefore variable. Additional studies have demonstrated that timing and duration of exposure to stiffness cues impacts stem cell differentiation to neural cell types, and that while neuritogenesis may be enhanced on soft substrates, network connectivity and signal transduction are enhanced by stiffer substrates (Balgude et al., 2001; Jiang et al., 2010; Keung et al., 2012; Zhang et al., 2014; Mosley et al., 2017). These findings emphasize that stiffness cues should be adjusted depending on the desired outcome, with close attention to the region of interest in the human body.

Hydrogels are a compelling choice for neuronal scaffolds because their elastic modulus is easily tuned during fabrication, although dependent upon the monomer/material used. Polyacrylamide can be used to create hydrogels with gradient stiffness ranging from ∼1 to 240 kPa. Polyacrylamide can act as a strong analog to the endogenous ECM when invested with proteins and chemical signals specific to the cell of interest (Sunyer et al., 2012; Lee et al., 2015b). Hydrogels can be constructed in planar or 3D configurations maintaining precise control over the elastic modulus (Chatterjee et al., 2011; Wylie et al., 2011). They facilitate nutrient exchange and diffusion of gasses through their natural pores. This exchange contributes to healthier cells within the deepest parts of the scaffold. In designing scaffolds for use in repair of nervous tissue, manipulating the base material to more closely resemble the endogenous elastic modulus can facilitate more natural integration with the existing cellular structure.

INNOVATIVE SUBSTRATES FOR EFFECTIVE REPAIR

An ideal substrate for effective repair should take into account a combination of topographical, chemical, electrical, and mechanical properties of the substrate. The parameters must be carefully tailored to address the site of application, as biocompatibility with surrounding tissue will differ, and the time course for repair, which will influence the duration of the implant. For an acute spinal cord injury, the ideal substrate should facilitate the initial regrowth, and protect against glial scarring while nurturing the damaged axons during the healing process via embedded trophic factors. Once the lesion has healed and the scaffold has served its purpose, the scaffold can either be resorbed or fully integrated into the recovered tissue. Such a substrate must be flexible with an elastic modulus matching the native spinal column for an environment that closely resembles the endogenous condition. The scaffold can be enriched with microchannels, which attract the regenerating neurites given their affinity for edges and enclosed spaces (Millet et al., 2007; Froeter et al., 2014; Li et al., 2015). To enhance regrowth and influence its directionality, electronics that support electrical stimuli can be embedded in the scaffold. These electronics can also support recording capabilities to assess neuronal activity. Impregnating the scaffold with stem cells could enhance this therapy even more.

A recent study demonstrated how grafted human spinal cord-derived neural progenitor cells (NPCs) restore functionality to primates with lesioned spinal cords. The NPCs survived in the graft 9 months following injury and enabled recovered functionality in the primate forelimbs. Two notable challenges were encountered before a successful grafting method was developed: (1) in initial grafts, the NPCs were washed away by the native cerebral spinal fluid (CSF) that refilled the lesion site, and (2) the initial immunosuppressive regimen was not robust enough to enable the graft to survive the host immune response, leading to poor filling of the lesion with the NPCs. These two challenges were resolved by draining the CSF in the region of the lesion prior to grafting, increasing the grafting mixture to hasten the rate of gelling, subjecting the primates to higher initial doses of the immunosuppressants, and monitoring the subjects more frequently (Rosenzweig et al., 2018). The success of this study could be improved by loading the NPCs on an idealized scaffold as described above, which would protect the NPCs and allow for active monitoring of the regeneration.

With advancements in materials engineering, a new wave of flexible and biodegradable electronics has been introduced (**Figure 1G**). Applications for their use in the nervous system are especially promising. Flexible, transient, silicon-based, biocompatible, implantable biosensors are being developed that allow for wireless monitoring capability. They have been used successfully on skin, cardiac tissue, muscle, and the brain (Viventi et al., 2010, 2011; Hwang et al., 2012; Kang et al., 2016). A wireless communication device composed of bioresorbable

materials has been successfully implanted and used in rats for monitoring intracranial pressure and temperature (Kang et al., 2016). Another flexible, non-penetrating multi-electrode array with embedded ultrathin silicon transistors was used for *in vivo* neural recording and monitoring of electrical brain activity in feline models. The electrode array was applied to the visual cortex, or folded and inserted into the interhemispheric fissure, and electrical signals corresponding to visual stimuli were recorded (Viventi et al., 2011). The connection between these technologies and solutions for neuronal repair lies in three major advantages of these devices: (1) the flexible nature of the material allows for intimate contact between the biosensor and the neural tissue, minimizing current-loss (Viventi et al., 2010, 2011), (2) the materials are biocompatible and do not trigger an inflammatory response (Kang et al., 2016), and (3) the devices are bioresorbable. Each of these elements addresses requirements of an ideal substrate for neural repair. While long-term clinical translation of these devices must ensure longevity of the materials and sustained biocompatibility, progress in flexible electronics development is promising.

CONCLUSION

Recovering function following damage to neuronal systems is challenging due to loss of native cues, inflammation, and scarring. Solutions to this problem lie in clever development and functionalization of new scaffolds on which neurons can regenerate complex, 3D circuits. Important advances are being made in development of biomaterials for neuronal repair, including: (1) the development of new polymer/co-polymer substrates to enhance scaffolds for better integration with neural tissue, (2) new topographical structures to heighten neurite capture, support, and growth, and (3) novel manipulations of silicon-based electronics to design and implement flexible substrates for stimulation and recording. New materials enabling manipulation of substrate topography, such as hydrogels, mimic similar *in vivo* structures and enhance control over directionality in regenerating neurites. Introduction of electrical stimulation will amplify growth rate and length of regeneration, and influence orientation. Embedded wireless sensors will enable real-time monitoring of regenerating nerves *in situ*. Substrates can be manipulated to further emulate the endogenous neural environment by tuning the elastic modulus to better match the range of local stiffnesses *in vivo* and provide transitions between native tissue and supportive scaffold. By developing scaffolds and devices that dissolve away after fulfilling their purpose, the need for an additional surgery for removal is eliminated, thereby reducing the risks of added surgical complications, such as infection, as well as additional medical costs. For the brain and the nervous system, the future is pliable and electronic.

AUTHOR CONTRIBUTIONS

The manuscript was conceived and prepared by OVC. OVC and MUG revised the manuscript.

FUNDING

The authors acknowledge funding from the Medical Scholars Program at the University of Illinois and Christie Foundation Award (OVC), and the National Science Foundation STC Emergent Behaviors of Integrated Cellular Systems CBET 0939511 (MUG).

ACKNOWLEDGMENTS

The authors thank Guillermo L. Monroy for contributions to revising the manuscript, Jennifer W. Mitchell for insights in figure preparation, and Ann C. Benefiel for facilitating manuscript submission. The authors thank Xiuling Li, Paul Froeter, and Hyun Joon Kong (University of Illinois at Urbana-Champaign), and John A. Rogers (Northwestern University) for providing images.

REFERENCES

Anderson, M., Shelke, N. B., Manoukian, O. S., Yu, X., McCullough, L. D., and Kumbar, S. G. (2017). Peripheral nerve regeneration strategies: electrically stimulating polymer based nerve growth conduits. *Crit. Rev. Biomed. Eng.* 43, 131–159. doi: 10.1615/CritRevBiomedEng.2015014015

Bai, S., Zhang, W., Lu, Q., Ma, Q., Kaplan, D. L., and Zhu, H. (2014). Silk nanofiber hydrogels with tunable modulus to regulate nerve stem cell fate. *J. Mater. Chem. B. Mater. Biol. Med.* 2, 6590–6600. doi: 10.1039/C4TB00878B

Balgude, A. P., Yu, X., Szymanski, A., and Bellamkonda, R. V. (2001). Agarose gel stiffness determines rate of DRG neurite extension in 3D cultures. *Biomaterials* 22, 1077–1084. doi: 10.1016/S0142-9612(00)00350-1

Baranes, K., Chejanovsky, N., Alon, N., Sharoni, A., and Shefi, O. (2012). Topographic cues of nano-scale height direct neuronal growth pattern. *Biotechnol. Bioeng.* 109, 1791–1797. doi: 10.1002/bit.24444

Barros, C. S., Franco, S. J., and Müller, U. (2011). Extracellular matrix: functions in the nervous system. *Cold Spring Harb. Perspect. Biol.* 3:a005108. doi: 10.1101/cshperspect.a005108

Bettinger, C. J., Langer, R., and Borenstein, J. T. (2009). Engineering substrate topography at the micro- and nanoscale to control cell function. *Angew. Chemie Int. Ed.* 48, 5406–5415. doi: 10.1002/anie.200805179

Brown, R. C., Lockwood, A. H., and Sonawane, B. R. (2005). Neurodegenerative diseases: an overview of environmental risk factors. *Environ. Health Perspect.* 113, 1250–1256. doi: 10.1289/ehp.7567

Caliari, S. R., and Burdick, J. A. (2016). A practical guide to hydrogels for cell culture. *Nat. Methods* 13, 405–414. doi: 10.1038/nmeth.3839

Carballo-Molina, O. A., and Velasco, I. (2015). Hydrogels as scaffolds and delivery systems to enhance axonal regeneration after injuries. *Front. Cell. Neurosci.* 9:13. doi: 10.3389/fncel.2015.00013

Chatterjee, K., Young, M. F., and Simon, C. G. Jr. (2011). Fabricating gradient hydrogel scaffolds for 3D cell culture. *Comb. Chem. High Throughput Screen.* 14, 227–236. doi: 10.2174/138620711795222455

Davenport, R. W., and McCaig, C. D. (1993). Hippocampal growth cone responses to focally applied electric fields. *J. Neurobiol.* 24, 89–100. doi: 10.1002/neu.480240108

de Ruiter, G. C., Malessy, M. J., Yaszemski, M. J., Winderbank, A. J., and Spinner, R. J. (2009). Designing ideal conduits for peripheral nerve repair. *Neurosurg. Focus* 26:E5. doi: 10.3171/FOC.2009.26.2.E5

Discher, D., Janmey, P., and Wang, Y. (2005). Tissue cells feel and respond to the stiffness of their substrate. *Science* 310, 1139–1143. doi: 10.1126/science.1116995

Durgam, H., Sapp, S., Deister, C., Khaing, Z., Chang, E., Luebben, S., et al. (2010). Novel degradable co-polymers of polypyrrole support cell proliferation and enhance neurite outgrowth with electrical stimulation. *J. Biomater. Sci. Polym. Ed.* 21, 1265–1282. doi: 10.1163/092050609X12481751806330

Edmondson, J. C., and Hatten, M. E. (1987). Glial-guided granule neuron migration *in vitro*: a high-resolution time-lapse video microscopic study. *J. Neurosci.* 7, 1928–1934.

Froeter, P., Huang, Y., Cangellaris, O. V., Huang, W., Dent, E. W., Gillette, M. U., et al. (2014). Toward intelligent synthetic neural circuits: directing and accelerating neuron cell growth by self-rolled-up silicon nitride microtube array. *ACS Nano* 8, 11108–11117. doi: 10.1021/nn504876y

Froeter, P., Yu, X., Huang, W., Du, F., Li, M., Chun, I., et al. (2013). 3D hierarchical architectures based on self-rolled-up silicon nitride membranes. *Nanotechnology* 24:475301. doi: 10.1088/0957-4484/24/47/475301

Graves, M. S., Hassell, T., Beier, B. L., Albors, G. O., and Irazoqui, P. P. (2011). Electrically mediated neuronal guidance with applied alternating current electric fields. *Ann. Biomed. Eng.* 39, 1759–1767. doi: 10.1007/s10439-011-0259-8

Gu, X., Ding, F., and Williams, D. F. (2014). Neural tissue engineering options for peripheral nerve regeneration. *Biomaterials* 35, 6143–6156. doi: 10.1016/j.biomaterials.2014.04.064

Hiscox, L. V., Johnson, C. L., Barnhill, E., McGarry, M. D., Huston, J., van Beek, E. J., et al. (2016). Magnetic resonance elastography (MRE) of the human brain: technique, findings and clinical applications. *Phys. Med. Biol.* 61, R401–R437. doi: 10.1088/0031-9155/61/24/R401

Hotary, K. B., and Robinson, K. R. (1990). Endogenous electrical currents and the resultant voltage gradients in the chick embryo. *Dev. Biol.* 140, 149–160. doi: 10.1016/0012-1606(90)90062-N

Hotary, K. B., and Robinson, K. R. (1991). The neural tube of the Xenopus embryo maintains a potential difference across itself. *Dev. Brain Res.* 59, 65–73. doi: 10.1016/0165-3806(91)90030-M

Huang, W., Yu, X., Froeter, P., Xu, R., Ferreira, P., and Li, X. (2012). On-chip inductors with self-rolled-up SiNx nanomembrane tubes: a novel design platform for extreme miniaturization. *Nano Lett.* 12, 6283–6288. doi: 10.1021/nl303395d

Hwang, S. W., Tao, H., Kim, D.-H., Cheng, H., Song, J.-K., Rill, E., et al. (2012). A physically transient form of silicon electronics, with integrated sensors, actuators and power supply. *Science* 337, 1640–1644. doi: 10.1126/science.1226325

Hynes, R. O. (2009). Extracellular matrix: not just pretty fibrils. *Science* 326, 1216–1219. doi: 10.1126/science.1176009

Jaffe, L. F., and Stern, C. D. (1979). Strong electrical currents leave the primitive streak of chick embryos. *Science* 206, 569–571. doi: 10.1126/science.573921

Jang, K. J., Kim, M. S., Feltrin, D., Jeon, N. L., Suh, K. Y., and Pertz, O. (2010). Two distinct filopodia populations at the growth cone allow to sense nanotopographical extracellular matrix cues to guide neurite outgrowth. *PLoS ONE* 5:e15966. doi: 10.1371/journal.pone.0015966

Janmey, P. A., and Miller, R. T. (2011). Mechanisms of mechanical signaling in development and disease. *J. Cell Sci.* 124, 9–18. doi: 10.1242/jcs.071001

Jiang, F. X., Yurke, B., Schloss, R. S., Firestein, B. L., and Langrana, N. A. (2010). Effect of dynamic stiffness of the substrates on neurite outgrowth by using a DNA-crosslinked hydrogel. *Tissue Eng. A* 16, 1873–1889. doi: 10.1089/ten.tea.2009.0574

Kang, S. K., Murphy, R. K., Hwang, S. W., Lee, S. M., Harburg, D. V., Krueger, N. A., et al. (2016). Bioresorbable silicon electronic sensors for the brain. *Nature* 530, 71–76. doi: 10.1038/nature16492

Keung, A. J., Asuri, P., Kumar, S., and Schaffer, D. V. (2012). Soft microenvironments promote the early neurogenic differentiation but not self-renewal of human pluripotent stem cells. *Integr. Biol.* 4, 1049–1058. doi: 10.1039/c2ib20083j

Khan, S., and Newaz, G. (2010). A comprehensive review of surface modification for neural cell adhesion and patterning. *J. Biomed. Mater. Res. Part A* 93, 1209–1224. doi: 10.1002/jbm.a.32698

Kim, K. M., Kim, S. Y., and Palmore, G. T. (2016). Axon outgrowth of rat embryonic hippocampal neurons in the presence of an electric field. *ACS Chem. Neurosci.* 7, 1325–1330. doi: 10.1021/acschemneuro.6b00191

Koppes, A. N., Zaccor, N. W., Rivet, C. J., Williams, L. A., Piselli, J. M., Gilbert, R. J., et al. (2014). Neurite outgrowth on electrospun PLLA fibers is enhanced by exogenous electrical stimulation. *J. Neural Eng.* 11:46002. doi: 10.1088/1741-2560/11/4/046002

Koser, D. E., Thompson, A. J., Foster, S. K., Dwivedy, A., Pillai, E. K., Sheridan, G. K., et al. (2016). Mechanosensing is critical for axon growth in the developing brain. *Nat. Neurosci.* 19, 1592–1598. doi: 10.1038/nn.4394

Kriegstein, A. R. (2005). Constructing circuits: neurogenesis and migration in the developing neocortex. *Epilepsia* 46, 15–21. doi: 10.1111/j.1528-1167.2005.00304.x

Lackington, W. A., Ryan, A. J., and O'Brien, F. J. (2017). Advances in nerve guidance conduit-based therapeutics for peripheral nerve repair. *ACS Biomater. Sci. Eng.* 3, 1221–1235. doi: 10.1021/acsbiomaterials.6b00500

Lee, J., Abdeen, A. A., Zhang, D., and Kilian, K. A. (2013). Directing stem cell fate on hydrogel substrates by controlling cell geometry, matrix mechanics and adhesion ligand composition. *Biomaterials* 34, 8140–8148. doi: 10.1016/j.biomaterials.2013.07.074

Lee, M. K., Rich, M. H., Baek, K., Lee, J., and Kong, H. (2015a). Bioinspired tuning of hydrogel permeability-rigidity dependency for 3D cell culture. *Sci. Rep.* 5:8948. doi: 10.1038/srep0894

Lee, M. K., Rich, M. H., Lee, J., and Kong, H. (2015b). A bio-inspired, microchanneled hydrogel with controlled spacing of cell adhesion ligands regulates 3D spatial organization of cells and tissue. *Biomaterials* 58, 26–34. doi: 10.1016/j.biomaterials.2015.04.014

Li, W., Tang, Q. Y., Jadhav, A. D., Narang, A., Qian, W. X., Shi, P., et al. (2015). Large-scale topographical screen for investigation of physical neural-guidance cues. *Sci. Rep.* 5:8644. doi: 10.1038/srep08644

Li, X. (2008). Strain induced semiconductor nanotubes: from formation process to device applications. *J. Phys. D. Appl. Phys.* 41:193001. doi: 10.1088/0022-3727/41/19/193001

Liu, S. C., Lee, M. K., Slater, B. J., Kouzehgarani, G. N., Yu, M., Cangellaris, O. V., et al. (2015). "Engineering a 3D platform to mimic *in vivo* neural network morphology and activity," in *Program No. P030. 2015 Neuroscience Meeting Planner* (Chicago, IL: Society for Neuroscience).

Liu, W., Thomopoulos, S., and Xia, Y. (2012). Electrospun nanofibers for regenerative medicine. *Adv. Healthc. Mater.* 1, 10–25. doi: 10.1002/adhm.201100021

Ma, Q., Chen, C., Deng, P., Zhu, G., Lin, M., Zhang, L., et al. (2016). Extremely low-frequency electromagnetic fields promote *in vitro* neuronal differentiation and neurite outgrowth of embryonic neural stem cells via up-regulating TRPC1. *PLoS ONE* 11:e0150923. doi: 10.1371/journal.pone.0150923

McCaig, C. D. (1990). Nerve branching is induced and oriented by a small applied electric field. *J. Cell Sci.* 95(Pt 4), 605–615.

McCaig, C. D., Song, B., and Rajnicek, A. M. (2009). Electrical dimensions in cell science. *J. Cell Sci.* 122, 4267–4276. doi: 10.1242/jcs.023564

Metcalf, M. E. M., and Borgens, R. B. (1994). Weak applied voltages interfere with amphibian morphogenesis and pattern. *J. Exp. Zool.* 268, 323–338. doi: 10.1002/jez.1402680408

Millet, L. J., Stewart, M. E., Nuzzo, R. G., and Gillette, M. U. (2010). Guiding neuron development with planar surface gradients of substrate cues deposited using microfluidic devices. *Lab Chip* 10, 1525–1535. doi: 10.1039/c001552k

Millet, L. J., Stewart, M. E., Sweedler, J. V., Nuzzo, R. G., and Gillette, M. U. (2007). Microfluidic devices for culturing primary mammalian neurons at low densities. *Lab Chip* 7, 987–994. doi: 10.1039/b705266a

Moore, K., Macsween, M., and Shoichet, M. (2006). Immobilized concentration gradients of neurotrophic factors guide neurite outgrowth of primary neurons in macroporous scaffolds. *Tissue Eng.* 12, 267–278. doi: 10.1089/ten.2006.12.267

Mosley, M. C., Lim, H. J., Chen, J., Yang, Y. H., Li, S., Liu, Y., et al. (2017). Neurite extension and neuronal differentiation of human induced pluripotent stem cell derived neural stem cells on polyethylene glycol hydrogels containing a continuous Young's Modulus gradient. *J. Biomed. Mater. Res. Part A* 105, 824–833. doi: 10.1002/jbm.a.35955

Nguyen, H. T., Sapp, S., Wei, C., Chow, J. K., Nguyen, A., Coursen, J., et al. (2014). Electric field stimulation through a biodegradable polypyrrole-co-polycaprolactone substrate enhances neural cell growth. *J. Biomed. Mater. Res. Part A* 102, 2554–2564. doi: 10.1002/jbm.a.34925

Orive, G., Anitua, E., Pedraz, J. L., and Emerich, D. F. (2009). Biomaterials for promoting brain protection, repair and regeneration. *Nat. Rev. Neurosci.* 10, 682–692. doi: 10.1038/nrn2685

Patel, N., and Poo, M. M. (1982). Orientation of neurite growth by extracellular electric fields. *J. Neurosci.* 2, 483–496.

Patel, S., Kurpinski, K., Quigley, R., Gao, H., Hsiao, B. S., Poo, M. M., et al. (2007). Bioactive nanofibers: synergistic effects of nanotopography and chemical signaling on cell guidance. *Nano Lett.* 7, 2122–2128. doi: 10.1021/nl071182z

Pettikiriarachchi, J. T. S., Parish, C. L., Shoichet, M. S., Forsythe, J. S., and Nisbet, D. R. (2010). Biomaterials for brain tissue engineering. *Aust. J. Chem.* 63, 1143–1154. doi: 10.1071/CH10159

Rakic, P. (1972). Mode of cell migration to the superficial layers of fetal monkey neocortex. *J. Comp. Neurol.* 145, 61–83. doi: 10.1002/cne.901450105

Reid, B., Nuccitelli, R., and Zhao, M. (2007). Non-invasive measurement of bioelectric currents with a vibrating probe. *Nat. Protoc.* 2, 661–669. doi: 10.1038/nprot.2007.91

Rosenzweig, E. S., Brock, J. H., Lu, P., Kumamaru, H., Salegio, E. A., Kadoya, K., et al. (2018). Restorative effects of human neural stem cell grafts on the primate spinal cord. *Nat. Med.* doi: 10.1038/nm.4502. [Epub ahead of print].

Schaub, N. J., and Gilbert, R. J. (2011). Controlled release of 6-aminonicotinamide from aligned, electrospun fibers alters astrocyte metabolism and dorsal root ganglia neurite outgrowth. *J. Neural Eng.* 8:046026. doi: 10.1088/1741-2560/8/4/046026

Schmidt, C. E., and Leach, J. B. (2003). Neural tissue engineering: strategies for repair and regeneration. *Annu. Rev. Biomed. Eng.* 5, 293–347. doi: 10.1146/annurev.bioeng.5.011303.120731

Subramanian, A., Krishnan, U. M., and Sethuraman, S. (2009). Development of biomaterial scaffold for nerve tissue engineering: biomaterial mediated neural regeneration. *J. Biomed. Sci.* 16:108. doi: 10.1186/1423-0127-16-108

Sunyer, R., Jin, A. J., Nossal, R., and Sackett, D. L. (2012). Fabrication of hydrogels with steep stiffness gradients for studying cell mechanical response. *PLoS ONE* 7:e46107. doi: 10.1371/journal.pone.0046107

Tam, R. Y., Fuehrmann, T., Mitrousis, N., and Shoichet, M. S. (2014). Regenerative therapies for central nervous system diseases: a biomaterials approach. *Neuropsychopharmacology* 39, 169–188. doi: 10.1038/npp.2013.237

Teng, Y. D., Lavik, E. B., Qu, X., Park, K. I., Ourednik, J., Zurakowski, D., et al. (2002). Functional recovery following traumatic spinal cord injury mediated by a unique polymer scaffold seeded with neural stem cells. *Proc. Natl. Acad. Sci. U.S.A.* 99, 3024–3029. doi: 10.1073/pnas.052678899

Tian, L., Prabhakaran, M. P., and Ramakrishna, S. (2015). Strategies for regeneration of components of nervous system: scaffolds, cells and biomolecules. *Regen. Biomater.* 2, 31–45. doi: 10.1093/rb/rbu017

Ventre, M., Causa, F., and Netti, P. A. (2012). Determinants of cell-material crosstalk at the interface: towards engineering of cell instructive materials. *J. R. Soc. Interface* 9, 2017–2032. doi: 10.1098/rsif.2012.0308

Viventi, J., Kim, D. H., Moss, J. D., Kim, Y. S., Blanco, J. A., Annetta, N., et al. (2010). A conformal, bio-interfaced class of silicon electronics for mapping cardiac electrophysiology. *Sci. Transl. Med.* 2:24ra22. doi: 10.1126/scitranslmed.3000738

Viventi, J., Kim, D. H., Vigeland, L., Frechette, E. S., Blanco, J. A., Kim, Y. S., et al. (2011). Flexible, foldable, actively multiplexed, high-density electrode array for mapping brain activity *in vivo*. *Nat. Neurosci.* 14, 1599–1605. doi: 10.1038/nn.2973

Wang, G. W., Yang, H., Wu, W. F., Zhang, P., and Wang, J. Y. (2017). Design and optimization of a biodegradable porous zein conduit using microtubes as a guide for rat sciatic nerve defect repair. *Biomaterials* 131, 145–159. doi: 10.1016/j.biomaterials.2017.03.038

Wang, H. B., Mullins, M. E., Cregg, J. M., Mccarthy, C. W., and Gilbert, R. J. (2010). Varying the diameter of aligned electrospun fibers alters neurite outgrowth and Schwann cell migration. *Acta Biomater.* 6, 2970–2978. doi: 10.1016/j.actbio.2010.02.020

WHO. (2006). "Neurological disorders: a public health approach," in *Neurological Disorders: Public Health Challenges*, eds J. A. Aarli, G. Avanzini, J. M. Bertolote, H. de Boer, H. Breivik, T. Dua, N. Graham, A. Janca, J. Kesselring, C. Mathers, A. Muscetta, L. Prilipko, B. Saraceno, S. Saxena, and T. J. Steiner (Geneva), 41–176.

Wong, A., Tang, Z., Park, I. H., Zhu, Y., Patel, S., Daley, G. Q., et al. (2011). Induced pluripotent stem cells for neural tissue engineering. *Biomaterials* 32, 5023–5032. doi: 10.1016/j.biomaterials.2011.03.070

Wylie, R. G., Ahsan, S., Aizawa, Y., Maxwell, K. L., Morshead, C. M., and Shoichet, M. S. (2011). Spatially controlled simultaneous patterning of multiple growth factors in three-dimensional hydrogels. *Nat. Mater.* 10, 799–806. doi: 10.1038/nmat3101

Xie, J., Willerth, S. M., Li, X., Macewan, M. R., Rader, A. and Sakiyama-Elbert S. E. (2009). The differentiation of embryonic stem cells seeded on electrospun nanofibers into neural lineages. *Biomaterials* 30, 354–362. doi: 10.1016/j.biomaterials.2008.09.046

Yao, L., McCaig, C. D., and Zhao, M. (2009). Electrical signals polarize neuronal organelles, direct neuron migration, and orient cell division. *Hippocampus* 19, 855–868. doi: 10.1002/hipo.20569

Yao, L., Pandit, A., Yao, S., and McCaig, C. D. (2011). Electric field-guided neuron migration: a novel approach in neurogenesis. *Tissue Eng. B. Rev.* 17, 143–153. doi: 10.1089/ten.teb.2010.0561

Yao, L., Shanley, L., McCaig, C., and Zhao, M. (2008). Small applied electric fields guide migration of hippocampal neurons. *J. Cell. Physiol.* 216, 527–535. doi: 10.1002/jcp.21431

Yu, L. M. Y., Leipzig, N. D., and Shoichet, M. S. (2008). Promoting neuron adhesion and growth. *Mater. Today* 11, 36–43. doi: 10.1016/S1369-7021(08)70088-9

Zhang, Q. Y., Zhang, Y. Y., Xie, J., Li, C. X., Chen, W. Y., Liu, B. L., et al. (2014). Stiff substrates enhance cultured neuronal network activity. *Sci. Rep.* 4:6215. doi: 10.1038/srep06215

Conflict of Interest Statement: The authors declare that the manuscript was developed in the absence of any commercial or financial relationships that could be construed as a potential conflict of interest.

The handling Editor declared a shared affiliation, though no other collaboration, with the authors.

frontiers in Materials

REVIEW
published: 01 February 2018
doi: 10.3389/fmats.2018.00002

Microscale Architecture in Biomaterial Scaffolds for Spatial Control of Neural Cell Behavior

Edi Meco and Kyle J. Lampe**

Department of Chemical Engineering, University of Virginia, Charlottesville, VA, United States

Biomaterial scaffolds mimic aspects of the native central nervous system (CNS) extracellular matrix (ECM) and have been extensively utilized to influence neural cell (NC) behavior in *in vitro* and *in vivo* settings. These biomimetic scaffolds support NC cultures, can direct the differentiation of NCs, and have recapitulated some native NC behavior in an *in vitro* setting. However, NC transplant therapies and treatments used in animal models of CNS disease and injury have not fully restored functionality. The observed lack of functional recovery occurs despite improvements in transplanted NC viability when incorporating biomaterial scaffolds and the potential of NC to replace damaged native cells. The behavior of NCs within biomaterial scaffolds must be directed in order to improve the efficacy of transplant therapies and treatments. Biomaterial scaffold topography and imbedded bioactive cues, designed at the microscale level, can alter NC phenotype, direct migration, and differentiation. Microscale patterning in biomaterial scaffolds for spatial control of NC behavior has enhanced the capabilities of *in vitro* models to capture properties of the native CNS tissue ECM. Patterning techniques such as lithography, electrospinning and three-dimensional (3D) bioprinting can be employed to design the microscale architecture of biomaterial scaffolds. Here, the progress and challenges of the prevalent biomaterial patterning techniques of lithography, electrospinning, and 3D bioprinting are reported. This review analyzes NC behavioral response to specific microscale topographical patterns and spatially organized bioactive cues.

Keywords: lithography, three-dimensional bioprinting, electrospinning, biomaterials, neural stem cells

OPEN ACCESS

Edited by:
Sara Pedron, University of Illinois at Urbana–Champaign, United States

Reviewed by:
Stephanie Michelle Willerth, University of Victoria, Canada
Stephanie K. Seidlits, University of California, Los Angeles, United States
Francesca Taraballi, Houston Methodist Research Institute, United States

****Correspondence:***
Edi Meco
em4zv@virginia.edu;
Kyle J. Lampe
lampe@virginia.edu

Specialty section:
This article was submitted to Biomaterials, a section of the journal Frontiers in Materials

Received: *28 October 2017*
Accepted: *10 January 2018*
Published: *01 February 2018*

Citation:
Meco E and Lampe KJ (2018) Microscale Architecture in Biomaterial Scaffolds for Spatial Control of Neural Cell Behavior. Front. Mater. 5:2. doi: 10.3389/fmats.2018.00002

INTRODUCTION

Tissue Damage in the Central Nervous System (CNS)

Tissue damage in the CNS caused by injury and disease cannot be fully repaired through endogenous healing mechanisms. For therapeutic treatments of CNS injury and disease to be successful they need to address a variety of challenges that are specific to the individual injury or disease, but can be broadly defined as replacing dead neural cells (NCs), remodeling the extracellular matrix (ECM) to a healthy state, and restoring nervous system functionality. In the autoimmune disease multiple sclerosis (MS), for instance, immune cells infiltrate the CNS and cause demyelination of neuronal axons (Correale et al., 2015). In the aftermath of this demyelination, the axons deteriorate and neuronal death occurs, leading to reactive astrogliosis (Correale et al., 2015). During reactive astrogliosis astrocytes form inhibitory glial scars around the demyelinated lesion and prevent both remyelination

of damaged axons and axonal regeneration (Correale et al., 2015). The therapeutic needs for successful tissue regeneration of this particular disease are to replace dead neurons and oligodendrocytes, remodel the inhibitory scar tissue to allow for infiltration of endogenous cells, and prevent further immune cell infiltration into the CNS. A related sequence of events occurs in ischemic stroke, where the blood supply to the CNS is blocked, leading to hypoxia. Unlike MS, where preventative medicine is used to inhibit immune cell infiltration and mitigate tissue damage, tissue damage in ischemic stroke is difficult to prevent because it only takes approximately 4 min for the adenosine triphosphate (ATP) concentration to be fully depleted (Krause et al., 1988). Most of the cell death occurs during reperfusion, when blood flow returns to the CNS and the oxygen concentration suddenly elevates (White et al., 2000). Re-established metabolism of oxygen causes the overproduction of reactive oxygen species (ROS), leading to lipid peroxidation of unsaturated fatty acids on the cell membranes, increasing their permeability, and causing apoptosis (White et al., 2000; Lipinski, 2011). This is followed by reactive astrogliosis and formation of a glial scar around the original oxygen deficient region (Huang et al., 2014). Successful therapeutic treatment of damaged tissue after ischemic strike would replace dead NCs and remodel the inhibitory scar tissue to allow for infiltration of endogenous cells. There is a significant difference in the types of cells that need to be replaced when comparing ischemic stroke, which indiscriminately leads to NC death within a region, to diseases like MS which targets specific cell types. Unlike MS and ischemic stroke, tissue damage in the form of cell necrosis occurs immediately after a mechanical insult in spinal cord (SC) contusion injury (Yuan and He, 2013). Cell debris and ROS cause cytotoxicity in the microenvironment, and subsequently apoptosis of surrounding cells (Macaya and Spector, 2012). Over the course of several days to months after the initial injury, reactive astrocytes, in conjunction with infiltrating periphery cells in some instances, form glial scar tissue in the area of the mechanical insult (White et al., 2000; Macaya and Spector, 2012). Treatment of CNS tissue damaged by SC contusion injury requires ECM remodeling to remove the cytotoxic cell debris and excess ROS before cells in the injury lesion can be replaced. The mechanisms of NC death are different in each case, but the requirements for effective treatments can be broadly defined as remodeling the ECM to remove cytotoxic and inhibitory aspects, replacing damaged cells, and recovering functionality.

Reparative Effects of Endogenous NCs

Interest in developing NC transplant therapies to treat tissue damage caused by CNS injury and disease is derived from evidence that endogenous NCs have reparative effects on damaged tissue (Cooke et al., 2010). After ischemic stroke in the rat stratium *via* middle cerebral artery occlusion (MCAO), new neurons derived from proliferating neural precursor cells (NPCs) in the subventricular zone (SVZ) were observed (Arvidsson et al., 2002). Similar results occurred in mice with an ipsilateral cerebral cortex infarction induced by MCAO, where the number of Nestin-positive cells in the ischemic region increased (Nakagomi et al., 2009). When extracted and cultured, the Nestin-positive cells from the ischemic region displayed neural stem cell (NSC) properties *in vitro* (Nakagomi et al., 2009). NSC populations, derived from ependymal cells, were also discovered in mouse SC after a transverse dorsal funiculus incision (Barnabé-Heider et al., 2010). These findings have led researchers to transplant NCs as therapies to heal CNS tissue damage in both the brain and SC. However, most of the NCs transplanted to the injury environment do not survive and cells that do survive do not display integrative behavior. Only 2–4.5% of mouse NPCs transplanted into rats after traumatic brain injury survived 24 h after the transplant (Bakshi et al., 2005). In addition, the caspase activity of transplanted NPCs that survived was higher in injured rats than sham surgery controls, indicating that the population of cells that survived was apoptotic in the CNS injury environment (Bakshi et al., 2005). While transplanted cell viability is higher if the transplant is performed 1 week postinjury (Hill et al., 2006; Walker et al., 2015), NCs alone do not restore functionality to preinjury baselines.

It is important to highlight distinctions between NC populations used to research *in vitro* and *in vivo* models because there is a wide range of capabilities of each cell line. Mature NCs such as neurons do not contain the capacity to self-renew or further differentiate and are typically not used because *in vitro* cell cultures cannot be maintained. NSCs can self-renew indefinitely and exhibit multipotent differentiation, while NPCs and neural progenitor cells have a limited capacity to self-renew and have a restricted capacity to differentiate (Seaberg and Van Der Kooy, 2003). Typically NPCs display unipotent differentiation behavior while neural progenitor cells maintain multipotent differentiation, but these descriptions are not rigid rules so overlap between NPCs and neural progenitor cells does exist in literature. Neural precursor and progenitor cells are preferred over NSCs for transplant therapies because their differentiation is more controlled, resulting in less heterogeneous cell cultures. Many NC lines are derived from neuronal tumors because these cell lines are immortalized and are relatively easy to grow and maintain in *in vitro* cell cultures (Gordon et al., 2013). The capabilities and limitations of NC lines are discussed by other reviews (Seaberg and Van Der Kooy, 2003; Dell'Albani, 2008; Murry and Keller, 2008; Politis and Lindvall, 2012; Gordon et al., 2013). Here, we will focus on the microscale architecture design of biomaterial scaffolds and how NCs respond to that architecture.

Bulk Biomaterials for Tissue Repair

Biomaterial scaffolds are designed to be biocompatible and influence cell behavior, making them promising tools for developing CNS tissue treatment therapies. Implantation of biomaterials into CNS injury lesions has helped improve cell infiltration and functional recovery (Shrestha et al., 2014). A collagen and PuraMatrix hydrogel transplanted into a 5-mm gap thoracic (T9–T11) rat SC transection increased animal Basso, Beattie, and Bresnahan (BBB) scores over phosphate-buffered saline (PBS) controls 4 months postsurgery (Kaneko et al., 2015). Neuronal and astrocyte infiltration into the injury lesion increased in animals with the collagen and PuraMatrix biomaterial scaffold. A similar endogenous cell response occurred when implanting a fibronectin-based scaffold into 2-mm gap thoracic (T7–T9) rat SC transection (King et al.,

2003, 2006). Axons infiltrated the fibronectin scaffold and were myelinated by Schwann cells 4 weeks postinjury (King et al., 2003). Animals with the fibronectin scaffold also had early and aggressive macrophage infiltration into the lesion site, which was speculated to provide trophic support for axon infiltration (King et al., 2006). Biomaterial scaffolds have also been utilized to transplant NCs into damaged CNS tissue. NCs transplanted with biomaterial scaffolds have improved posttransplant viability and improve functional recovery over the standalone scaffold and NC transplantations. Improved functional recovery from a 10-mm gap thoracic (T9–T10) SC hemisection injury on African green monkeys was observed when implanting human NSCs seeded on a poly(lactide-co-glycolide) (PLGA) scaffold (Pritchard et al., 2010). Implanting the PLGA scaffold improved the left hindlimb neuromotor score 44 days postinjury over no-treatment controls, and incorporating human NSCs into the PLGA scaffold led to further improvement. Similar results were found when human NSCs in a fibrin scaffold were transplanted into a complete 2-mm long thoracic (T3) rat SC transection, where the inclusion of human NSCs with the fibrin scaffold improved hindlimb locomotion BBB scores 8 weeks postinjury over untreated controls (Lu et al., 2012b). While implanting NCs with biomaterial scaffolds has been shown to promote CNS tissue recovery in animal models, regeneration is still limited and functionality cannot be restored to the preinjury state. Biomaterial scaffolds need to be designed with greater control over NC behavior to improve the efficacy of transplant therapies.

Microscale Architecture in Biomaterials

Current biomaterial design strategies are focused on controlling NC behavior at the microscale level (less than 1 mm in size). The goals for controlling microscale architecture within biomaterial scaffolds are to direct NC behavior toward clinical therapy needs and to investigate how NCs interact with the ECM. The microscale architecture within biomaterials has a significant impact on cell behavior and differentiation (Gunther et al., 2015; Lynam et al., 2015; Dye et al., 2016). Chitosan-based hydrogels were fragmented into varying microscale sizes (**Figure 1A**) and incorporated into thoracic (T8–T9) rat SC bilateral dorsal hemisection injury model (Chedly et al., 2017). The hydrogel transplants improved endogenous cell infiltration into the injury lesion (**Figures 1B–D**) and the degree of cell infiltration depended largely on the chitosan fragment size. Hydrogels with 20-μm chitosan fragments (**Figure 1D**) led to robust endogenous cell infiltration while hydrogels with 150-μm chitosan fragments (**Figure 1C**) had limited cell infiltration 4 weeks postinjury. In addition, scaffolds with 150-μm fragments did not have infiltration of axons and few glial cells, while scaffolds with 20-μm fragments had robust infiltration of both. While the microstructure alterations were not designed to direct endogenous NC behavior in a specific way, these results illustrate the significance scaffold microstructure on NC behavior for clinical applications. For SC injury, a clinical goal is to guide axons through the injury lesion, which was only achieved by the hydrogel with 20-μm fragments. These results provide motivation for exploring techniques that allow greater control over material architecture and cell positioning to guide tissue growth. The prevailing techniques used to design microscale architecture in biomaterial scaffolds for influence over NC behavior are lithography, electrospinning, and three-dimensional (3D) bioprinting (**Figure 2**).

LITHOGRAPHY

Lithographic Techniques

Several lithographic techniques are used to pattern biomaterial scaffolds: photolithography, soft lithography, stereolithography, and two-photon lithography (sometimes referred to by the more general term multiphoton lithography in literature). Photolithography refers to techniques that pattern a photoresist onto a substrate using a photomask and a light source, usually in the ultraviolet (UV) wavelength range (Jang et al., 2016). The substrate is the biomaterial housing and the photoresist is a material that is chemically responsive to the presence of light within a specific wavelength range. A photomask is used to create a pattern by shielding parts of the photoresist material from the light source. The process can be repeated to create multiple layers with differing patterns. Since most of the processing is cytotoxic, for biological research the photoresist is patterned, washed, and cells are seeded on top of the material afterward. Stereolithography is similar to photolithography except the photoresist material is replaced with a photocurable polymer resin or solution (Wang et al., 2017). The polymer resin or solution is solidified in the presence of a light source. Patterns are made either by using a photomask or a mobile laser light source. Soft lithography is a technique used in conjunction with photolithography. First a patterned stamp or mold is made from materials such as polydimethylsiloxane (PDMS) using photolithography (Turunen et al., 2013). The patterned stamp is then placed on the substrate and the voids created by the stamp's pattern are filled with a biomaterial of interest, called ink. The benefits of patterning using soft lithography are that the ink solidification chemistry does not need to be light based and the processing can be biocompatible. Two-photon lithography is an extension of photolithography and stereolithography because it is used to pattern the same materials, either a photoresist or photocurable polymer, with a different light source. The UV light source is replaced with a femtosecond pulsed infrared (IR) laser, such as titanium:sapphire lasers, going through an objective lens to focus the beam. The laser wavelength is twice that of the maximum absorbance wavelength of UV light-based chemistry; therefore, two of these lower energy photons are required to generate the same free radical (Ciuciu and Cywiński, 2014). Since the process of absorbing two photons requires a high light intensity, absorbance only occurs at the objective lens focal point, allowing for patterning in the *z*-direction of a UV light responsive material. The advantage of two-photon lithography is the increased resolution in the *z*-direction, which allows for patterning in three dimensions. In contrast, photo- and stereolithography techniques require repeating the processing to create multiple layers for design of 3D structures. Lithography-based techniques have been successfully used to organize biomaterial topography and spatially immobilized ECM materials.

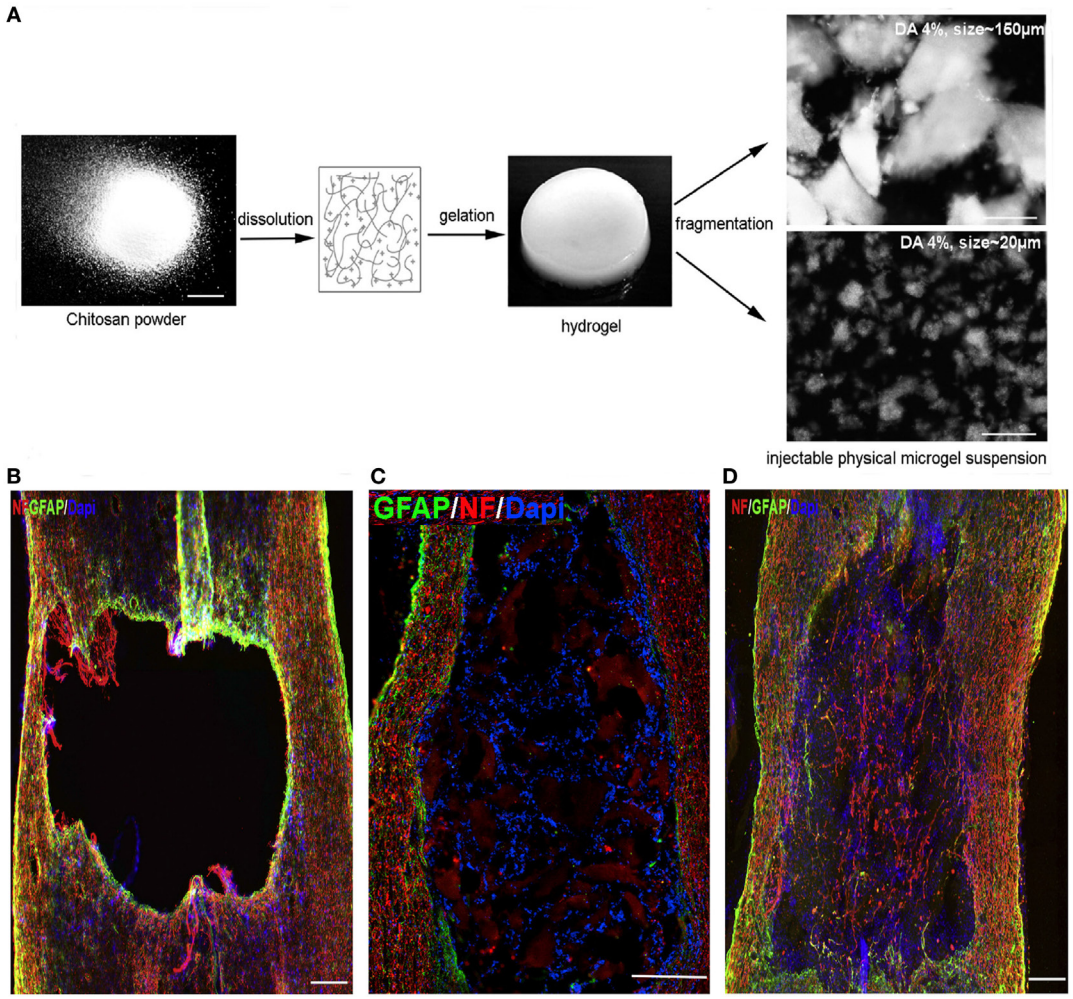

FIGURE 1 | **(A)** Chitosan solution gelled by contacting with ammonia vapors and then fragmented mechanically into differing average microscale architecture. **(B–D)** Immunostaining of spinal cord lesion site 4 weeks postinjury/injection for neurofilament (NF), astrocytes (GFAP), and cell nuclei (DAPI). **(B)** Lesion only, **(C)** lesion with chitosan-FPHS hydrogel implant with 150-μm average fragment size, and **(D)** lesion with chitosan-FPHS 20-μm average fragment size. Smaller fragments result in greater presence of NF in the lesion site. **(B,D)** Scale bar = 240 μm and **(C)** Scale bar = 300 μm. Reproduced with permission of Chedly et al. (2017), Copyright 2017, Elsevier.

Grooves on Scaffold Surfaces

Lithographic patterning of grooves into biomaterial surfaces has been extensively shown to direct NC alignment, migration, and differentiation (Dos Reis et al., 2010; Haring et al., 2017). Astrocytes seeded onto a polystyrene mold patterned with channels that were 10-μm wide and 3-μm deep using photolithography, and subsequently coated with laminin, had elongated process extensions that aligned with the grooves (Recknor et al., 2004). In the non-patterned surface astrocytes had rounded cell bodies and process extensions were not oriented toward a particular direction. Adult hippocampal progenitor cells behaved in a similar manner by aligning processes with patterned channels on a laminin-coated polystyrene scaffold (Oh et al., 2009). In addition, cells seeded onto the patterned scaffold had longer process extensions than those on the non-patterned surface. Differentiation down the neuronal, oligodendrocyte, and astrocyte pathways was similar for cells seeded on both the patterned and non-patterned polystyrene surfaces, indicating that this effect was not caused by a difference in the cell differentiation. The dimensions of the grooves are important for being able to control both differentiation and alignment. Dorsal root ganglion (DRG) cells seeded onto the surface of a coumarin-based biomaterial scaffold that was patterned into square pillars using a modified stereolithography technique did not show robust alignment with the grooves (McCormick et al., 2014). This could be because the grooves were very shallow, with 20 nm being the largest depth tested. Other studies have investigated the effects of groove width on NC behavior. Adult human NSCs aligned better on smaller, 5-μm wide, channels than on larger, 60-μm wide, channels when seeded onto patterned PDMS channels coated with poly-L-lysine (Béduer et al., 2012). However, more cells seeded on the PDMS scaffold with larger channels differentiated down the neuronal lineage, and had more neurites per cell. Similar results were found when radial glia cells were seeded on polymethylmethacrylate

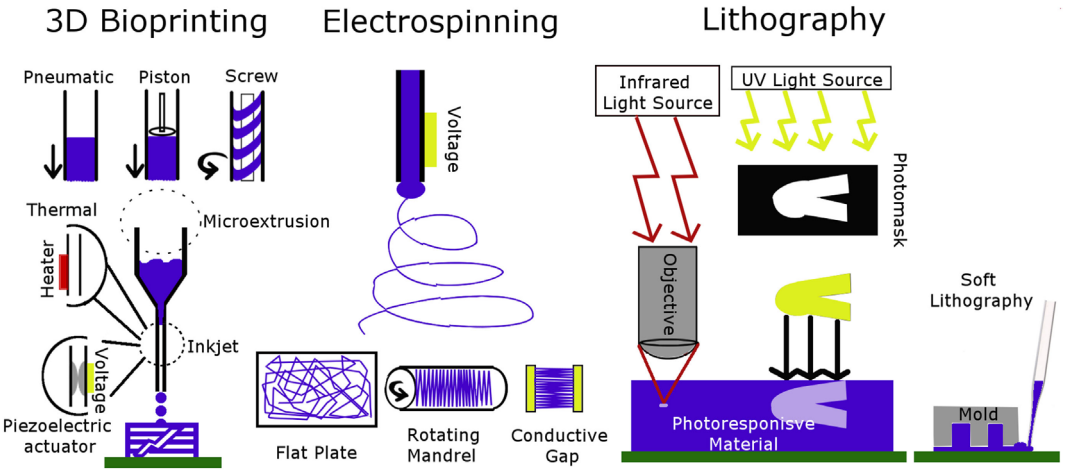

FIGURE 2 | Schematic of 3D bioprinting, electrospinning, and lithography techniques. The type of 3D bioprinter is chosen based on biomaterial rheological properties. Electrospun fibers are patterned by changing the collector. Lithography patterning is done by adjusting light-based techniques or using a mold.

(PMMA) scaffolds patterned with 2- and 10-μm wide channels, where cells aligned with the grooves and migrated along the channels (**Figure 3**) (Mattotti et al., 2012). Patterning channels on the scaffold surface can also affect the behavior of NCs encapsulated within the biomaterial scaffold. Bone marrow-derived stem cells encapsulated in alginate gels with 500-μm wide surface microchannels had a fourfold decrease in the glial cell to neuron differentiation ratio when compared to non-patterned hydrogels (Lee et al., 2015). Simulations of oxygen and water transport into the alginate hydrogels indicated that the surface microchannels improved oxygen and water diffusion into the scaffolds. The decrease in the glial cell to neuron differentiation ratio was attributed to better nutrient transport in hydrogels with the surface microchannels. Lithographic patterning can also be used to spatially orient bioactive motifs to direct NC behavior.

Immobilization of Bioactive Motifs

Lithographic techniques have been developed that can spatially immobilize proteins and ECM molecules onto the polymer network of biomaterial scaffolds. A prevalent theme in the literature is the microscale attachment of adhesive ECM proteins and peptide sequences, such as arginine-glycine-aspartic acid (RGD), which can be used to direct cell migration and the extension of processes (Hahn et al., 2005; Huval et al., 2015). DRG cells seeded on the surface of an agarose scaffold migrated and extended processes into the interior of the scaffold when RGD was immobilized within the agarose scaffold (Luo and Shoichet, 2004a,b). The RGD polypeptide was incorporated into the agarose hydrogel by first functionalizing agarose with 2-nitrobenzyl-protected cysteine. The nitrobenzyl group was cleaved to expose a free thiol group when UV light was shined onto the agarose scaffold. The free thiol group subsequently reacted with a maleimide-modified RGD polypeptide dissolved in the scaffold encompassing solution. RGD attachment onto the agarose scaffold was constrained to cylindrical sections down the *z*-axis by using a photomask with open circles. The versatility of this method was demonstrated by achieving the similar results on a hyaluronic acid (HA)-based scaffold (Musoke-Zawedde and Shoichet, 2006). Adhesive motifs can also be used to direct where NCs attach on biomaterial surfaces. LRM55 astroglioma and primary rat hippocampal neurons seeded onto an acrylamide-based substrate with immobilized fibronectin, laminin, and the IKVAV polypeptide sequence (separately) only attached to the fibronectin, laminin or IKVAV portion of the scaffold (Hynd et al., 2006, 2009). Soft lithography was used to immobilize the adhesive motifs into a crosshatch pattern. Primary rat hippocampal neurons extended processes preferentially along the grid pattern and were found to have functional synapses 10 days post seeding. Similar results were achieved when hybrid mouse neuroblastoma and rat glioma cell cultures were seeded onto a bovine serum albumen (BSA)-modified collagen scaffold surface with immobilized matrigel (Nagamine et al., 2015). Matrigel was immobilized into a crosshatch pattern and cells migrated to the nodes of the matrigel pattern, extended processes along the matrigel grid 15 h after seeding. Although most research has focused patterning motifs that promote adhesion, the techniques described here are versatile and can be expanded to immobilize other proteins.

The biological activity of immobilized proteins depends on the immobilization process and the specific protein tolerances to the processing environment(s). Photolithography was used to test if the activity of two known axon inhibitor proteins, semaphorin 6A and ephrin-B3, was affected by immobilizing them onto an agarose-based hydrogel (Curley et al., 2014; Horn-ranney et al., 2014). The technique involved creating a mold from poly(ethylene glycol) (PEG) designed in the shape of a well attached to a channel that splits into two separate channels. The mold was then filled with 2-nitrobenzyl-protected cysteine-modified-agarose solution, similar to the chemistry described above. Semaphorin 6A or ephrin-B3 were immobilized onto one of the two channels by exposing the scaffold to UV light and using a photomask. The second channel did not contain immobilized protein and was

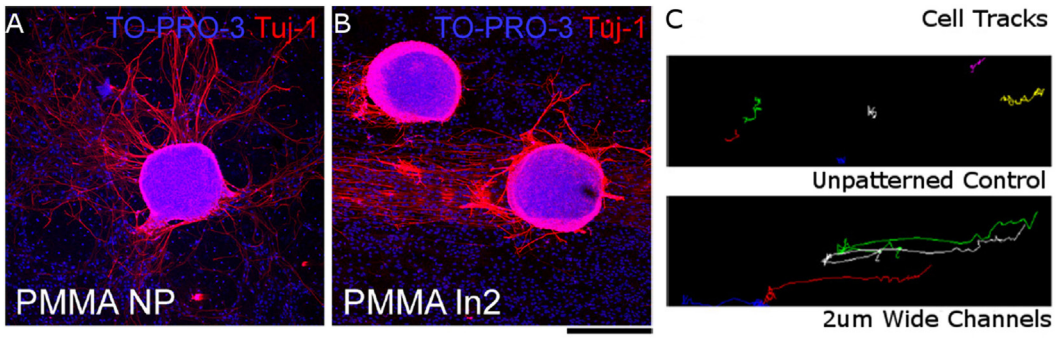

FIGURE 3 | Radial glial cells seeded on **(A)** unpatterned PMMA surface and **(B)** PMMA surface with 2-μm wide channels. Cell nuclei stained with TO-PRO-S (blue) and neurons stained with beta tubulin III (red). **(C)** Particle tracks of neuronal trajectories over 3 h in unpatterned PMMA (top) and PMMA with 2-μm wide channels (bottom). Scale bar = 200 μm. Reproduced with permission of Mattotti et al. (2012), Copyright 2012, Elsevier.

used as a control. DRG explants from the lumbosacral, thoracic, and cervicothoracic regions were placed inside the well and the direction of their process extensions was used to determine if the immobilized proteins maintained biological activity. DRG explants from the lumbosacral region did not extend processes into the channel with immobilized semaphorin 6A, indicating that the immobilized protein was still biologically active. However, processes from thoracic and cervicothoracic DRG explants were not inhibited by semaphorin 6A. In addition, Ephrin-B3 did not inhibit the process extensions from any of the DRG explants. These results demonstrate one of the weaknesses of photolithography, where the process of immobilizing proteins can denature them. However, it is unclear what part of the immobilization process (exposure to UV light or the chemical reaction) had deleterious effects. Another chemical reaction scheme available to immobilize proteins onto biomaterial scaffolds uses UV light to cleave a nitrobenzyl ester bond and expose an alkoxyamine that can react with aldehyde groups on proteins in the encompassing solution (DeForest and Anseth, 2011, 2012; DeForest and Tirrell, 2015). This scheme was used to immobilize collagenase to a PEG-based scaffold and the immobilized collagenase activity was quantified to be 24% of the soluble enzyme. In addition, immobilized mouse anti-6xHis monoclonal antibody attached to the PEG scaffold retained sufficient bioactivity to recognize a secondary antibody. Finally, vitronectin was immobilized in the PEG scaffolds and encapsulated human mesenchymal stem cells only differentiated in regions where the protein was attached. These studies demonstrate that proteins can be spatially immobilized onto biomaterial scaffolds, but the process does affect biological activity.

Microscale Design in 3D Space

While most lithographic processes are used for surface-based patterning and protein immobilization on biomaterial scaffolds, there have been several advances that have allowed for patterning in three dimensions. The design of biocompatible materials that are sensitive to UV light has allowed for encapsulating NCs inside biomaterial scaffolds using stereolithography. PC12 cells encapsulated in methacrylate-modified gelatin hydrogels patterned as a crosshatch survived the gelation process and could differentiate 14 days post encapsulation (Zhu et al., 2016). A similar process was used to encapsulate PC12 cells in an acrylate-modified PEG (PEGDA) hydrogel, where cells could differentiate 3 days post encapsulation (Jhaveri et al., 2006). Combining cytocompatible materials with two-photon lithography has allowed for the design of biomaterials with sophisticated 3D architecture (Maruo et al., 1997). Channels with a denser concentration of PEG were created by first crosslinking a large molecular weight PEGDA to form a bulk hydrogel, then leaching in a small molecular weight PEGDA into the scaffold, and finally exposing specific regions in the bulk hydrogel to a two-photon laser for a second round of crosslinking (Hahn et al., 2006). Fluorescent BSA was then leached into the PEG scaffold to demonstrate that regions exposed to the two-photon laser did not allow for BSA diffusion because of the denser network created by crosslinking the small molecular weight PEGDA. The same technique was used to add adhesive domains to the scaffold in various 3D spatial patterns by attaching the RGD polypeptide to the small molecular weight PEGDA before leaching it into the scaffold (Hahn et al., 2006). Two-photon lithography was also used to create a PEG-based scaffold patterned with tunnels inside the scaffold (Livnat et al., 2007). Encapsulated DRG preferentially migrated through the tunnels over 4 days. Two-photon lithography has been combined with other chemical processes to spatially orient bioactive motifs. BSA was immobilized into an HA-based hydrogel in the shape of a spiral using two-photon lithography (Seidlits et al., 2009). The adhesive IKVAV polypeptide was then linked to the immobilized BSA using an avidin-biotin complex. DRG encapsulated in the scaffold and near the immobilized IKVAV polypeptide extended processes toward the IKVAV protein and followed designed spiral pattern. Proteins have been immobilized onto biomaterial scaffolds with a 3D resolution of a couple of microns, which allows for influencing single cell behavior. BSA was immobilized to a PEG-based scaffold with a resolution of 1 μm × 1 μm in the *xy*-plane and 3–5 μm down the *z*-axis (DeForest and Tirrell, 2015). A similar resolution of 0.5 μm radially and 1–2 μm down the *z*-axis was achieved for the immobilization of the IKVAV polypeptide (Seidlits et al., 2009). Biomaterial scaffold architecture can be designed at the microscale level by utilizing a combination of lithographic techniques with cytocompatible materials.

ELECTROSPINNING

Electrospinning Techniques

The electrospinning process involves pumping a polymer solution through a charged needle (Pham et al., 2006; Kishan and Cosgriff-Hernandez, 2017). Enough voltage is applied to the needle tip to cause droplets of the polymer solution to overcome the surface tension and emerge from the needle tip in the form of a liquid jet. The liquid jet then undergoes bending instability and rapidly whips into multiple expanding loops. During this whipping process the polymer solution stretches and thins into micrometer and nanometer fibers, and solvents evaporate. The jet is ultimately collected on a grounded or oppositely charged plate that is a variable distance away from the needle tip. The distance of the collector from the needle tip is selected to allow enough time for solvents to evaporate fully and to control the diameter of the fibers. There are several parameters that require careful tuning in order to electrospin a polymer solution into fibers: polymer solution viscosity, conductivity, and flow rate, applied voltage to the needle, and the temperature and humidity of the environment.

Electrospun fibers are patterned by changing the collector used to gather the polymer (**Figure 2**). A flat plate collector produces fibers with a random orientation. A rotating mandrel is used to align fibers in a singular direction (Matthews et al., 2002). Increasing the speed of the mandrel improves fiber alignment but also affects the mechanical properties of the bulk scaffold formed. Another way to align fibers is to collect them using two conducting electrodes separated by an insulating gap (Li et al., 2004). The gap causes the electrostatic forces to become directional and the fibers align in-between the two electrodes. This method of fiber alignment is limited to thin fiber scaffolds because the fibers carry a charge. As more fiber layers are added the collector starts to behave like a flat plate and subsequent fiber layers become randomly oriented. There are workarounds to this limitation that involve gathering the fibers layer-by-layer and combining them into a single-scaffold post electrospinning (Orr et al., 2015). Electrospun fibers can also be aligned by using two parallel magnets as a collector (Yang et al., 2007). This method is not limited to thin layered scaffolds but does require magnetizing the polymer solution. More sophisticated patterns can be created by adjusting the topography of the collector. Researchers have gathered polyurethane-based fibers on a PDMS collector with a square grid pattern etched onto the surface (Dempsey et al., 2010). The resulting scaffold had aligned fibers along the grid lines and random fibers in the square sections.

NCs on Aligned Fibers

The alignment of electrospun fibers has a robust effect on NC behavior. Researchers seeded human neural progenitor-derived astrocytes (hNP-AC), human astrocytoma cell line U373, and human neuroblastoma cell line SH-SY5Y on aligned polycaprolactone (PCL) and PCL/collagen-blended fibers (Gerardo-Nava et al., 2009). All three cell types had elongated cell bodies in alignment with fiber direction, extended processes in that direction, and migrated preferentially in parallel with the aligned. These findings were consistent on both PCL and PCL/collagen-blended fiber scaffolds. Human umbilical mesenchymal stem cells (hUMSCs) displayed similar behavior when seeded onto aligned fibrin fibers by orienting actin filaments with the fiber orientation (**Figure 4E**) (Yao et al., 2016). When hUMSCs were seeded on randomly aligned fibrin fibers they expressed actin filaments in a random orientation, but their morphology did differ from cells cultured on tissue culture plastic controls (**Figures 4C,D**) (Yao et al., 2016). Alignment of electrospun fibers influences both the direction of NC process extensions and promotes longer processes. DRG seeded on randomly oriented polypyrrole tube fibers extended neurites radially (Xie et al., 2009). By comparison, DRG seeded on aligned polypyrrole tube fibers extended neurites in the directions of the fibers, and displayed a longer maximum neurite length. The effects of aligned fibers are robust and can be repeated across many NC lines.

Fiber Material Composition

Most biocompatible materials are difficult to electrospin into fibrous scaffolds and some cell lines do not adhere to commonly electrospun polymers like PCL. As a result, many electrospun fiber scaffolds used to seed NCs are either blended with native ECM proteins and polymers or coated with a bioactive material. The effects of material composition on NC behavior are cell line dependent. The adhesion and migration rate of hNP-AC was improved on the PCL/collagen-blended fibers when compared to the PCL fibers (Gerardo-Nava et al., 2009). In contrast, U373 cells did not display a difference in migration rate or adhesion behavior when seeded on PCL/collagen-blended and PCL fiber scaffolds. SH-SY5Y neuroblastoma cells had an increased metabolic activity when seeded on PCL/hyaluronan-blended fibers over PCL fibers (Entekhabi et al., 2016). Electrospun fibers made from PCL blended with gelatin increased C17.2 NSC neurite length over PCL fiber scaffold controls (Ghasemi-Mobarakeh et al., 2008). Fibers made from conductive biomaterials, such as polypyrrole, have gained interest because electrical stimulation also promotes process extensions. Applying an electrical stimulation to randomly oriented and aligned polypyrrole nanotubes increased the DRG maximum neurite length over unstimulated controls (Xie et al., 2009). Electrical stimulation can also increase the number of processes NSCs extend. The percentage of PC12 cells seeded on silk fibroin fibers coated with reduced graphene oxide that extended neurites increased after applying electrical stimulation (Aznar-Cervantes et al., 2017). The increase was comparable to the increase in number of cells with neurites observed when adding soluble nerve growth factor to the media. In addition, multiple rounds of electrical stimulation did not further promote more PC12 cells to extend neurites. NC behavior can also be directed by controlling the electrospun fiber diameter.

Fiber Diameter

The distance between the charged needle tip and the fiber collector can be adjusted to control fiber diameter. Several 2D studies have investigated the impact of fiber diameter on NC behavior. Hippocampus-derived adult rat NSCs were seeded on laminin-coated poly(ethersulfone) fibers with 0.283-, 0.749-,

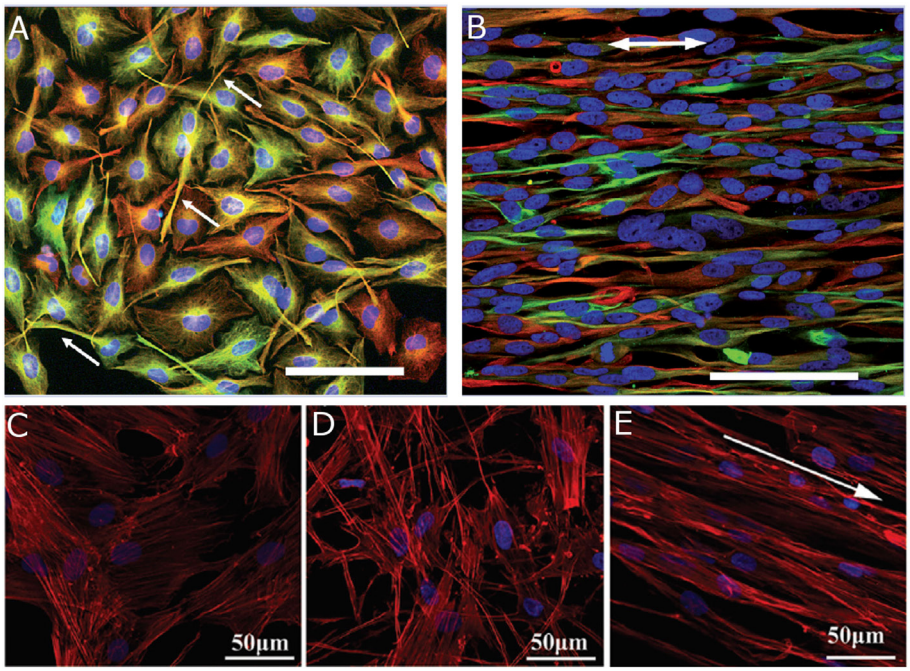

FIGURE 4 | Human astrocytoma cell line U373 cultured on **(A)** poly-L-lysine substrate for 4 days and **(B)** aligned PCL fibers for 7 days. Arrows indicate **(A)** process extensions and **(B)** fiber orientation. Reproduced with permission of Gerardo-Nava et al. (2009), Copyright 2009, Future Medicine Ltd. Human umbilical cord mesenchymal stem cells cultured on **(C)** tissue culture plastic, **(D)** randomly oriented fibrin fibers, and **(E)** aligned fibrin fibers for 1 day. Arrow indicates fiber orientation. Reproduced with permission of Yao et al. (2016), Copyright 2016, Royal Society of Chemistry. **(A,B)** Cell nuclei (blue), GFAP (green), vimentin (red), and scale bars = 100 μm. **(C–E)** Cell nuclei (blue) and F-actin (red).

and 1.452-μm diameters (Christopherson et al., 2009). In proliferation media conditions, an increase in fiber diameter led to reduced NSC migration, spreading, and proliferation. Under differentiation media conditions, NSCs on 0.283-μm diameter fibers preferentially differentiated into oligodendrocytes, while NSCs on 0.749- and 1.452-μm diameter fibers preferentially differentiated down a neuronal lineage. Differences in electrospun fiber diameter have also been utilized to elucidate oligodendrocyte myelination behavior. Researchers seeded oligodendrocyte precursor cells on poly(L-lysine)-coated polystyrene fibers with diameter ranges of 0.2–0.4 and 2–4 μm (Lee et al., 2012). In part, fibers served as artificial axons, and a higher percentage of the cells cultured on the larger diameter fibers wrapped myelin around the fibers than cells cultured on the smaller diameter fibers. This suggests that axon diameter is an influencing factor in determining which axons are myelinated by oligodendrocytes and which axons are not in the CNS. While electrospinning has been successfully utilized to direct NC behavior on biomaterial scaffolds in 2D culture systems, it has been difficult to translate those results to three dimensions.

Fibers in 3D Scaffolds

The effects of electrospun fibers have also been investigated in 3D biomaterial scaffolds. Fibers produced by the electrospinning process do not fully mimic the 3D nature of native tissue. Electrospun fibers are too densely packed to allow for cell infiltration into the biomaterial scaffold. The effects of fiber topography, material composition, and orientation on NCs are limited to surface effects. However, researchers have developed several techniques to incorporate electrospun fibers in 3D biomaterial scaffolds. A simple way to do this is to gel a hydrogel scaffold on top of the fibers. Researchers gelled a Puramatrix-based hydrogel on top of aligned PCL fibers and investigated if human pluripotent stem cell-derived neuron (hPSC) could sense the presence of the fibers (Hyysalo et al., 2017). hPSCs seeded on top of a 15-μm thick Puramatrix hydrogel could not sense the aligned PCL fibers at the bottom and extended processes with random orientation. hPSCs encapsulated inside the Puramatrix hydrogel and within 10 μm of the fibers did align processes along the PCL fiber axis. Cells further away from the PCL fibers, yet still inside the gel, extended processes with a random orientation. A similar study was conducted using stereolithography to gel a square grid patterned PEGDA hydrogel on top of aligned PCL and PCL/gelatin fibers (Lee et al., 2017). Primary cortical neurons and NSCs seeded on top the PEGDA hydrogel did orient process extensions with PCL/gelatin fiber alignment. Although there was no mention of how thick the PEGDA hydrogel was, it suggests that NCs do not need to be in direct contact with aligned fibers to direct behavior. Similar results were obtained by placing PCL, PCL/gelatin, and laminin-coated PCL aligned fibers in the center of HA-based hydrogels using soft lithography (McMurtrey, 2014). Encapsulated SH-5Y5Y neuronal cells grew

into large spherical clusters away from the fiber layer and had an elongated phenotype at the fiber layer. NCs at the fiber layer extended processes in the direction of the fiber orientation. The average neurite length was quantified and shown to be highest in HA hydrogels with laminin-coated PCL fibers, indicating that cell adhesion to fibers plays a critical role in their behavior. In order get a more uniform cell response across the *z*-axis of 3D biomaterial scaffolds, researchers have stacked multiple fiber layers in-between hydrogel layers. A single-scaffold layer consisted of aligned poly-L,D-lactic acid fibers placed on top of a thin collagen gel with cells seeded on top of the fibers (Weightman et al., 2014). Astrocytes, oligodendrocytes, and oligodendrocyte precursor cells had elongated cell bodies in alignment with fiber direction and extended processes in that direction. It is unclear if this stacking method truly represents a 3D culture system because cells cannot migrate through the individual fiber layers. The effects of electrospun fibers on directing NSC behavior have been consistent across the *in vitro* literature, and researchers have begun incorporating them into animal studies.

Fiber Scaffolds *In Vivo*

The implementation of electrospun fiber-based biomaterial scaffolds into animal models has not yielded similar results to *in vitro* experiments. Poly(ε-caprolactone-co-ethyl ethylene phosphate)-aligned fibers were incorporated into a collagen hydrogel and implanted into a C5 rat SC incision injury (Milbreta et al., 2016). Endogenous cell response to a collagen scaffold without fibers, a collagen scaffold with fibers in parallel with the SC longitudinal axis, and a collagen scaffold with fibers at an angle to the SC longitudinal axis was analyzed. Collagen scaffolds with fibers had more neurite infiltration and longer neurites 12 weeks post implantation when compared to the collagen scaffold without fibers. However, aligning the fibers in parallel to the SC longitudinal axis did not further improve endogenous cell response. Similar results were found with the implantation of aligned and randomly oriented fibrin fibers into a 4-mm gap thoracic (T9–T10) SC hemisection injury (Yao et al., 2016). Endogenous cell infiltration into the aligned fibers did follow the fiber orientation 4 weeks post implant, but total cell infiltration was similar into both randomly oriented and aligned fibrin scaffolds. From these animal studies, it is unclear as to whether or not fiber alignment is important *in vivo*. Researchers have also investigated the effects of fiber surface charge on endogenous cell infiltration. Polyurethane fibers were plasma coated with films of positive, negative and neural relative surface charge and implanted into rat dorsum for 5 weeks (Sanders et al., 2005). Cell infiltrations into the implants were similar for all conditions, and the study did not investigate infiltrating cell morphology. NCs have also been incorporated with electropun fiber-based scaffolds *in vivo*. Dopaminergic neurons encapsulated in a xyloglucan hydrogel with short poly(L-lactic acid) fibers were injected into the ventral midbrain of Parkinsonian mice (Wang et al., 2016). There was no difference in transplanted cell viability between xyluglucan scaffolds with and without fibers. Taken together, these findings indicate that the incorporation of scaffolds made from electrospun fibers into animal models have not confirmed *in vitro* findings and more investigation is necessary.

3D BIOPRINTING

Bioprinting Techniques

Three-dimensional bioprinting is defined as the layer-by-layer positioning of biomaterials, biochemicals, and cells with spatial control to build a bulk 3D structure. Computer-aided design software is used to control the placement of materials in a syringe, or print head, onto a substrate in the *x*-, *y*-, and *z*-directions. 3D bioprinting techniques have the potential to mimic the complex micro-architecture of tissue because the biomaterial scaffolds are built using an additive approach and multiple print heads with different biomaterials can be combined to create a single construct (**Figure 5**). The vast majority of printed biomaterial scaffolds are patterned using the inkjet and microextrusion printing techniques (Murphy and Atala, 2014; Johnson et al., 2016; Ratheesh et al., 2017). Inkjet bioprinting is used to print controlled volumes and works best when printing low-viscosity materials or cells. There are two types of inkjet 3D printing heads, thermal and piezoelectric actuated, that provide similar benefits. Thermal inkjet printing is done by electrically heating the print head to produce a pulse of pressure. Although the localized heat generates temperatures in the range of 200–300°C, the short time frame of heating (~2 μs) only results in a material temperature increase of 4–10°C (Cui et al., 2010). While cells can survive the thermal stress, the technique may be incompatible with biomaterials, such as agarose, that undergo a thermal transition to gel or solidify. Piezoelectric actuator inkjet printing is done by applying a voltage to change the actuator shape and produce a droplet of controlled volume. This printing technique does not alter the printed material properties but the mechanical stress produced by the actuator change in shape can induce some cell membrane damage (Chang et al., 2008). Microextrusion 3D printing is used for higher viscosity biomaterials or high cell density applications because inkjet printers are prone to clogging under those conditions. Instead of printing controlled volumes, microextrusion 3D printing applies a force to break the material up into beads in the print head. The force is applied either pneumatically or mechanically with a piston or screw assembly. While there are advantages and disadvantages to each print head set up, they are not limiting for printing biomaterial scaffolds. Microextrusion printers do not

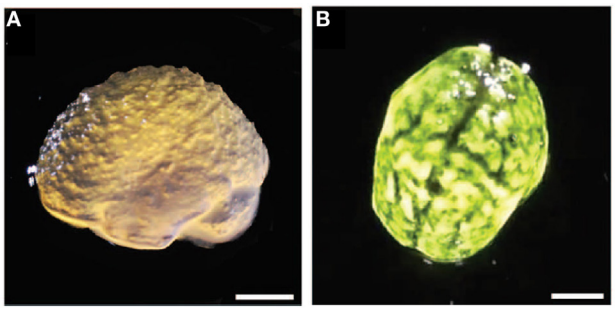

FIGURE 5 | **(A)** Lateral view of 3D printed alginate gel matching anatomical features of the cortex and cerebellum with microscale resolution. **(B)** Top view with black dye dripped on alginate gels. Scale bars = 1 cm. Reproduced with permission of Hinton et al. (2015), Creative Commons Copyright (CC-BY).

have the resolution of inkjet printers and cell viability is lower in some cases (Smith et al., 2004; Cui et al., 2012), but the technique is usable with a larger variety of biomaterials. Ultimately, the print head is selected based on the biomaterial physical properties because scaffold resolution is currently limited by how well biomaterials maintain the printed structure and not the print head capabilities.

For biomaterial applications, the 3D printing process works best with materials that exhibit yield stress and shear thinning rheological properties (Truby and Lewis, 2016). Materials going through the printing process undergo three stress profiles: low stress while the material is inside the syringe, high stress when the material flows through the print head, and low stress when the printed material is on the stage. Yield-stress materials exhibit two types of responses to stress: when a small stress is applied they deform elastically, maintaining their structure, and when a high stress is applied they deform plastically, causing the material to flow. The transition between the two responses, called the yield point, is material dependent. Any viscous material can be pushed through a print head, but only materials with yield-stress rheological properties will maintain the printed structure on the stage (Malek et al., 2017; Siqueira et al., 2017). Most yield-stress materials also exhibit shear thinning behavior, which helps shield cells from the high shear forces caused by traveling through the print head (Thakur et al., 2016).

Strategies for Biomaterial Printing

Bioinks are materials that can be 3D printed, maintain their structure, and are cytocompatible. Most biomaterials do not exhibit favorable rheological properties for 3D printing so bioinks are developed by simple mixing of existing materials that individually exhibit desired properties, or through chemical modification of existing biomaterials (Lee et al., 2009; Shim et al., 2011; Diamantides et al., 2017). Cortical human NSCs were encapsulated in 3D printed blend of alginate, carboxymethyl-chitosan, and agarose (Gu et al., 2016). The bioink maintained the printed crosshatch structure initially through the cooling of agarose and was subsequently soaked in a calcium chloride solution to crosslink the alginate component. Encapsulated NSCs had an initial cell viability of ~75% and were able to differentiate into neurons and glial cells. Similar results were found with a bioink of sodium alginate, fibrinogen, and gelatin (Dai et al., 2016). The bioink was soaked in calcium chloride and thrombin solutions after printing to crosslink the sodium alginate and fibrinogen components, respectively. Glioma stem cells encapsulated in the bioink had an initial cell viability of ~85% and could differentiate into glial and NCs. Cells encapsulated in the printed bioink had a higher resistance to the cancer drug temozolomide than two dimensional controls, highlighting that cells in native 3D tissue do not behave similar to cell cultures on surfaces. This study also demonstrated the potential of 3D printing to form hierarchical structures because the crosshatch structure at the microscale level was used to form a bulk scaffold in the shape of a tube. Materials can also be mixed during the printing process. Alginate, matrigel, and human NSCs were printed through a coaxial syringe with three chambers (Alessandri et al., 2016). Human NSCs and matrigel were surrounded by alginate to form capsules and were printed into a calcium chloride bath for crosslinking. Cells extended neurites within the capsules indicating that they were still functional. Ideally, this system would not require alginate to hold the capsule structure of the NSCs in matrigel, but matrigel does not have favorable physical properties for 3D printing. In addition, the chemical structure of matrigel is not well defined so it would be difficult to chemically modify the structure reliably for 3D printing applications. Biomaterials with well-defined chemical structures do not have this limitation and have been chemically modified to alter their rheological properties for 3D printing.

Most biomaterials do not exhibit favorable rheological properties for 3D printing so researchers have transformed the rheological properties of biomaterials by functionalizing them with moieties that form physical crosslinks (Lu et al., 2012a; Shepherd et al., 2012; Ouyang et al., 2016). An example of this involves supramolecular bonding of adamantane and β-cyclodextrin moieties, which assemble into a complex at low stress and disassemble when exposed to high stress (Ouyang et al., 2016). HA scaffolds were formed using supramolecular bonds by modifying the HA macromer with adamantine and β-cyclodextrin separately, and mixing of the two modified HA solutions together to form the scaffold (Ouyang et al., 2016). Modified HA was successfully printed into a crosshatch pattern, but the scaffold could only maintain the crosshatch structure when few layers were printed. In order to prevent the scaffold from collapsing from the stress caused by overlaying layers and maintain the crosshatch pattern at higher printing heights, HA was further modified with methacrylate groups. HA hydrogels crosslinked with both the supramolecular assembly and chemical methacrylate bonds, after being exposed to UV light, maintained their printed structure for up to one month with as many as 16 printed layers. This study also highlights the importance of gelation kinetics for maintaining printed structure integrity. Only the scaffolds that were exposed to additional UV light in the presence of a photoinitiator after the printing process was complete maintained their structure for 1 month. This indicated that UV exposure during the printing process did not fully crosslink methacrylate groups. Crosslinking kinetics are important considerations for 3D printing biomaterials.

Researchers have investigated inducing fast gelation kinetics in biomaterials to avoid requiring yield-stress rheological properties to maintain the printed structure. Gellan gum was printed using a coaxial syringe needle set up, with the gellan gum solution in the inner syringe ring and a crosslinking solution on the outer ring (Lozano et al., 2015). The material was not printed into a pattern, instead layers with and without encapsulated primary cortical neurons were alternately printed on top of each other. Encapsulated primary cortical neurons had a viability of 70–80%, differentiated into neurons and glia, and extended processes into up to 100 μm into layers without cells 5 days after printing. Waterborne polyurethane, which undergoes gelation through a temperature transition at 37°C, was successfully 3D printed by mixing with soy protein isolate to reduce the gelation time and printing onto a heated stage (Hsieh et al., 2015; Lin et al., 2016). Up to eight layers were printed into a crosshatch pattern, and encapsulated murine NSCs had high viability 3 days after printing. However, cell metabolic activity was lower than tissue

culture polystyrene controls, indicating that the printing process had a negative impact on the murine NSCs.

Bioprinting Bioactive Molecules

The 3D bioprinting technique is not limited to printing bioinks with cells, proteins, and other bioactive molecules can also be incorporated. Growth factors incorporated with bioinks maintain protein bioactivity after being printed. Fibroblast growth factor-2 (FGF2) and ciliary neurotrophic factor (CNTF) were printed onto polyacrylamide hydrogels, and primary fetal NSCs were subsequently seeded onto the hydrogels to demonstrate that the growth factors remained biologically active after printing (Ilkhanizadeh et al., 2007). Soluble FGF2 promotes proliferation and NSCs seeded on portions of the gel with FGF2 did not differentiate into glial cells. Soluble CNTF promotes differentiation and NSCs did differentiate into glial cells when seeded on portions of the hydrogel with CNTF. The amount of NSC differentiation into glial cells could be spatially controlled by printing a concentration gradient of CNTF across the polyacrylamide scaffold. 3D bioprinting has the potential to be utilized as a local drug delivery mechanism because the printed pattern affects cumulative drug release. The chemotherapeutic drug 5-fluorouracil was printed with a bioink composed of PLGA and PCL (Yi et al., 2016). The cumulative release of the drug from the printed scaffold depended on both the printed pore structure and the number of printed layers in the *z*-direction. Combinations of bioinks with growth factors have directed NSC behavior. A fibrin hydrogel was printed with vascular endothelial growth factor (VEGF) and placed next to a collagen gel with murine NSCs encapsulated (Lee et al., 2010). The NSCs migrated and proliferated toward the fibrin hydrogel when VEGF was incorporated and did not do so when fibrin was printed without VEGF.

FUTURE PERSPECTIVES

Advances in microscale patterning of biomaterial scaffolds have allowed researchers to investigate NC behavior in response to both physical and biochemical environmental cues. Topographical cues such as grooves and aligned fibers can direct NSC differentiation and neural process extensions. Similar effects can also be biochemically induced by spatially patterning adhesive motifs. Microscale patterning of biomaterial scaffolds has been performed predominantly by the use of lithography, electrospinning, and 3D bioprinting techniques. The final goal remains to develop microarchitecture to direct NC behavior for *in vivo* therapeutic treatments and tissue regeneration, and the immediate challenges for further developing each technique vary significantly.

Lithography has been successfully implemented to pattern grooves on surfaces, channels within biomaterial scaffolds, and spatially immobilize proteins to scaffolds. It has proved to be a powerful tool for developing *in vitro* models to mimic some aspects of native tissue at the microscale level. However, it will be challenging to translate the techniques developed for *in vitro* models to *in vivo* applications. The use of light as a source for patterning at the microscale level is inherently limited to thin or transparent scaffolds. Optically transparent materials, such as PEG, can be patterned well using light but scaffolds made from proteins, such as collagen, are optically dense and cannot be patterned deep within the scaffold. This limitation will be significant when attempting to translate these scaffolds to large animal studies and clinical trials because the biomaterial scaffolds will need to be scaled to appropriate sizes. In addition, current protein immobilization techniques require incubating the biomaterial scaffold in the protein of interest and then using a light source to initiate the immobilization reaction. This has limited application *in vivo* because it takes hours for large proteins, such as growth factors, to diffuse into the scaffold and the process requires several rinse steps. For this technique to be used in a transplant *in vivo* the scaffold must be designed *in vitro* and then transplanted. While applicable for acellular "device" implants, this method has several drawbacks when incorporating NC into the scaffolds. For example, encapsulated NCs may uptake the protein during the incubation step and not allow for the protein to be dispersed throughout the scaffold as desired for immobilization. These issues do not limit investigating the effects of microscale architecture on NC behavior in *in vitro* models but do hamper translation into *in vivo* studies.

Electrospinning of fibers into an aligned orientation affects a wide range of cell lines in a similar fashion in a 2D setting. NCs elongate cell bodies, extend processes, and migrate preferentially in alignment with fiber scaffold orientation. However, electrospun fibers have not yet been translated into homogeneous 3D biomaterial scaffolds, and differences in NC behavior have been observed when moving from 2D culture systems to 3D culture systems (Lampe et al., 2010; Bozza et al., 2014; Park et al., 2014; Shin et al., 2014). Current attempts at creating 3D biomaterial scaffolds from electrospun fiber are limited to layering a fiber mesh sandwiched between gels or in-between another biomaterial and NCs. While the bulk material is 3D, this method does not allow for cells to readily embed past a single layer in the *z*-direction because electrospun fiber meshes are generally too dense for deep cell infiltration. Cell infiltration into the fiber mesh can be improved by electrospinning sacrificial fibers alongside the main fiber material (Baker et al., 2008). The sacrificial fibers are dissolved in solution after electrospinning, leaving behind a more porous fiber mesh. Attempts at incorporating electrospun fibers into animal studies have not induced similar NC behavior as observed *in vitro* (Sanders et al., 2005; Milbreta et al., 2016; Wang et al., 2016; Yao et al., 2016). The challenge for the field is to recapitulate the desired NC behavior observed on 2D fiber meshes into 3D biomaterial scaffolds. Collector topography has been used to pattern fiber scaffolds into more sophisticated patterns than simply aligning fibers (Dempsey et al., 2010; Kishan et al., 2017), and may become a useful tool in creating a porous 3D fiber mesh. The alignment of fibers has the potential to direct NC process extensions *in vivo*, which has many applications like aligning neural synapses along a damaged SC. However, this potential using electrospun materials has yet to be realized in a 3D culture system. The problem can be tackled by either improving the porosity of the electrospun fibers, incorporating cells in the electrospinning process (Stankus et al., 2006; Zanatta et al., 2012), or by combining electrospinning with another technique such as 3D bioprinting.

Three-dimensional bioprinting has the most potential for developing tissue-like biomaterial scaffolds because it is an additive process. However, 3D bioprinting of scaffolds is currently limited by the available biomaterials. The printing process requires cytocompatible materials that exhibit yield stress and shear thinning rheological properties. Research has focused on blending biomaterials with materials that exhibit the desired rheological properties, or modifying biomaterials chemically. However, simple blending of materials and chemical modifications have many limitations. For example, the blend ratios have a drastic impact on the rheological properties of bioinks created by simply mixing materials. Adding a new protein or bioactive cue to the mixture may alter the rheological properties of the bioink enough to where it is no longer printable (Shim et al., 2011). Chemical modifications are limited to materials that have a well-defined chemical structure and materials such as collagen are challenging to modify reliably and repeatable. The current challenge is developing biomaterials with favorable properties for 3D printing. A universal way to tackle these issues is to use a sacrificial material to act as a mold to contain the biomaterial scaffold until it is solidified through crosslinking (Hinton et al., 2015). Using sacrificial materials allows for 3D printing a plethora of biomaterials with differing crosslinking kinetics but also slows down the printing process since the sacrificial material needs to be printed in conjunction to the desired biomaterial. The development of suitable biomaterials for 3D bioprinting will remain a challenge in the field for the foreseeable future.

A major challenge in tissue engineering is to develop microscale architectures that will lead to therapeutic treatments of CNS injury and disease. Microscale architecture can be used to spatially direct NC differentiation, process extensions, and migration. However, the field is uncertain as to how NC behavior should be directed and which NC line should be used for therapeutic treatments. For example, for repair of SC contusion injury it is important to replace damaged neurons, but that is not the only cell type required to restore functionality. When designing a biomaterial scaffold, should NSC be directed solely toward a neuronal pathway or are other cell types, such as oligodendrocytes and/or astrocytes, also required? In addition, are NSC the best cell type to transplant or would a scaffold with several encapsulated NPC lines be more effective? Encapsulating NCs in biomaterial scaffolds with microscale architecture in an *in vitro* setting may help answer some of these questions. For example, in order to determine how NSC differentiation should be directed for transplant therapies it is important to investigate how each cell line remodels the ECM. However, the CNS ECM is complex, difficult to isolate intact and challenging to characterize. By immobilizing individual proteins onto a scaffold NC behavior can be investigated on an individual protein basis. Spatial control of NCs and proteins within biomaterial scaffolds will help create reductionist *in vitro* models of *in vivo* features such as the glial scar which may help elucidate the importance of specific interactions. A common challenge shared by research using all three techniques discussed here is the development of relevant microscale patterns. For example, can astrocytes, neurons and proteins be organized at the microscale level to mimic glial scar behavior *in vitro*? Currently there are few patterns that accomplish this because most research has focused on developing the capability to control microscale architecture and refining the resolution. Finding a clear link between microscale patterning techniques and physiological relevance remains a challenge for the neural tissue engineering field to meet. As the technical challenges of patterning biomaterial scaffolds at the microscale level are now being overcome, meaningful designs and patterns must be achieved that replicate the complicated architecture of native tissue in order to improve NC treatment therapies.

AUTHOR CONTRIBUTIONS

EM and KL wrote and edited the manuscript.

FUNDING

This work was supported by the University of Virginia, and the School of Engineering and Applied Science Research Innovation Award.

REFERENCES

Alessandri, K., Feyeux, M., Gurchenkov, B., Delgado, C., Trushko, A., Krause, K.-H., et al. (2016). A 3D printed microfluidic device for production of functionalized hydrogel microcapsules for culture and differentiation of human neuronal stem cells (hNSC). *Lab. Chip* 16, 1593–1604. doi:10.1039/C6LC00133E

Arvidsson, A., Collin, T., Kirik, D., Kokala, Z., and Lindvall, O. (2002). Neuronal replacement from endogenous precursors in the adult brain after stroke. *Nat. Med.* 8, 963–970. doi:10.1038/nm

Aznar-Cervantes, S., Pagán, A., Martínez, J. G., Bernabeu-Esclapez, A., Otero, T. F., Meseguer-Olmo, L., et al. (2017). Electrospun silk fibroin scaffolds coated with reduced graphene promote neurite outgrowth of PC-12 cells under electrical stimulation. *Mater. Sci. Eng. C* 79, 315–325. doi:10.1016/j.msec.2017.05.055

Baker, B. M., Gee, A. O., Metter, R. B., Nathan, A. S., Marklein, R. A., Burdick, J. A., et al. (2008). The potential to improve cell infiltration in composite fiber-aligned electrospun scaffolds by the selective removal of sacrificial fibers. *Biomaterials* 29, 2348–2358. doi:10.1016/j.biomaterials.2008.01.032

Bakshi, A., Keck, C. A., Koshkin, V. S., Lebold, D. G., Siman, R., Snyder, E. Y., et al. (2005). Caspase-mediated cell death predominates following engraftment of neural progenitor cells into traumatically injured rat brain. *Brain Res.* 1065, 8–19. doi:10.1016/j.brainres.2005.09.059

Barnabé-Heider, F., Göritz, C., Sabelström, H., Takebayashi, H., Pfrieger, F. W., Meletis, K., et al. (2010). Origin of new glial cells in intact and injured adult spinal cord. *Cell Stem Cell* 7, 470–482. doi:10.1016/j.stem.2010.07.014

Béduer, A., Vieu, C., Arnauduc, F., Sol, J. C., Loubinoux, I., and Vaysse, L. (2012). Engineering of adult human neural stem cells differentiation through surface micropatterning. *Biomaterials* 33, 504–514. doi:10.1016/j.biomaterials.2011.09.073

Bozza, A., Coates, E. E., Incitti, T., Ferlin, K. M., Messina, A., Menna, E., et al. (2014). Neural differentiation of pluripotent cells in 3D alginate-based cultures. *Biomaterials* 35, 4636–4645. doi:10.1016/j.biomaterials.2014.02.039

Chang, R., Nam, J., and Sun, W. (2008). Effects of dispensing pressure and nozzle diameter on cell survival from solid freeform fabrication-based direct cell writing. *Tissue Eng. Part A* 14, 41–48. doi:10.1089/ten.a.2007.0004

Chedly, J., Soares, S., Montembault, A., von Boxberg, Y., Veron-Ravaille, M., Mouffle, C., et al. (2017). Physical chitosan microhydrogels as scaffolds for spinal cord injury restoration and axon regeneration. *Biomaterials* 138, 91–107. doi:10.1016/j.biomaterials.2017.05.024

Christopherson, G. T., Song, H., and Mao, H. Q. (2009). The influence of fiber diameter of electrospun substrates on neural stem cell differentiation and proliferation. *Biomaterials* 30, 556–564. doi:10.1016/j.biomaterials.2008.10.004

Ciuciu, A. I., and Cywiński, P. J. (2014). Two-photon polymerization of hydrogels-versatile solutions to fabricate well-defined 3D structures. *RSC Adv.* 4, 45504–45516. doi:10.1039/c4ra06892k

Cooke, M. J., Vulic, K., and Shoichet, M. S. (2010). Design of biomaterials to enhance stem cell survival when transplanted into the damaged central nervous system. *Soft Matter* 6, 4988. doi:10.1039/c0sm00448k

Correale, J., Farez, M. F., and Cardona, A. E. (2015). The role of astrocytes in multiple sclerosis progression. *Front. Neurol.* 6:1–12. doi:10.3389/fneur.2015.00180

Cui, X., Boland, T., D'Lima, D. D., and Lotz, M. K. (2012). Thermal inkjet printing in tissue engineering and regenerative medicine. *Recent Pat. Drug Deliv. Formul.* 6, 149–155. doi:10.1086/498510.Parasitic

Cui, X., Dean, D., Ruggeri, Z. M., and Boland, T. (2010). Cell damage evaluation of thermal inkjet printed Chinese hamster ovary cells. *Biotechnol. Bioeng.* 106, 963–969. doi:10.1002/bit.22762

Curley, J. L., Catig, G. C., Horn-Ranney, E. L., and Moore, M. J. (2014). Sensory axon guidance with semaphorin 6A and nerve growth factor in a biomimetic choice point model. *Biofabrication* 6, 35026. doi:10.1088/1758-5082/6/3/035026

Dai, X., Ma, C., Lan, Q., and Xu, T. (2016). 3D bioprinted glioma stem cells for brain tumor model and applications of drug susceptibility. *Biofabrication* 8, 45005. doi:10.1088/1758-5090/8/4/045005

DeForest, C. A., and Anseth, K. S. (2011). Cytocompatible click-based hydrogels with dynamically tunable properties through orthogonal photoconjugation and photocleavage reactions. *Nat. Chem.* 3, 925–931. doi:10.1038/nchem.1174

DeForest, C. A., and Anseth, K. S. (2012). Photoreversible patterning of biomolecules within click-based hydrogels. *Angew. Chem. Int. Ed.* 51, 1816–1819. doi:10.1002/anie.201106463

DeForest, C. A., and Tirrell, D. A. (2015). A photoreversible protein-patterning approach for guiding stem cell fate in three-dimensional gels. *Nat. Mater.* 14, 523–531. doi:10.1038/nmat4219

Dell'Albani, P. (2008). Stem cell markers in gliomas. *Neurochem. Res.* 33, 2407–2415. doi:10.1007/s11064-008-9723-8

Dempsey, D. K., Schwartz, C. J., Ward, R. S., Iyer, A. V., Parakka, J. P., and Cosgriff-Hernandez, E. M. (2010). Micropatterning of electrospun polyurethane fibers through control of surface topography. *Macromol. Mater. Eng.* 295, 990–994. doi:10.1002/mame.201000152

Diamantides, N., Wang, L., Pruiksma, T., Siemiatkoski, J., Dugopolski, C., Shortkroff, S., et al. (2017). Correlating rheological properties and printability of collagen bioinks: the effects of riboflavin photocrosslinking and pH. *Biofabrication* 9, 34102. doi:10.1088/1758-5090/aa780f

Dos Reis, G., Fenili, F., Gianfelice, A., Bongiorno, G., Marchesi, D., Scopelliti, P. E., et al. (2010). Direct microfabrication of topographical and chemical cues for the guided growth of neural cell networks on polyamidoamine hydrogels. *Macromol. Biosci.* 10, 842–852. doi:10.1002/mabi.200900410

Dye, B. R., Dedhia, P. H., Miller, A. J., Nagy, M. S., White, E. S., Shea, L. D., et al. (2016). A bioengineered niche promotes in vivo engraftment and maturation of pluripotent stem cell derived human lung organoids. *Elife* 5, 1–18. doi:10.7554/eLife.19732

Entekhabi, E., Haghbin Nazarpak, M., Moztarzadeh, F., and Sadeghi, A. (2016). Design and manufacture of neural tissue engineering scaffolds using hyaluronic acid and polycaprolactone nanofibers with controlled porosity. *Mater. Sci. Eng. C* 69, 380–387. doi:10.1016/j.msec.2016.06.078

Gerardo-Nava, J., Führmann, T., Klinkhammer, K., Seiler, N., Mey, J., Klee, D., et al. (2009). Human neural cell interactions with orientated electrospun nanofibers in vitro. *Nanomedicine* 4, 11–30. doi:10.2217/17435889.4.1.11

Ghasemi-Mobarakeh, L., Prabhakaran, M. P., Morshed, M., Nasr-Esfahani, M. H., and Ramakrishna, S. (2008). Electrospun poly(ε-caprolactone)/gelatin nanofibrous scaffolds for nerve tissue engineering. *Biomaterials* 29, 4532–4539. doi:10.1016/j.biomaterials.2008.08.007

Gordon, J., Amini, S., and White, M. K. (2013). General overview of neuronal cell culture. *Methods Mol. Biol.* 1078, 1–6. doi:10.1007/978-1-62703-640-5

Gu, Q., Tomaskovic-Crook, E., Lozano, R., Chen, Y., Kapsa, R. M., Zhou, Q., et al. (2016). Functional 3D neural mini-tissues from printed gel-based bioink and human neural stem cells. *Adv. Healthc. Mater.* 5, 1429–1438. doi:10.1002/adhm.201600095

Gunther, M. I., Weidner, N., Muller, R., and Blesch, A. (2015). Cell-seeded alginate hydrogel scaffolds promote directed linear axonal regeneration in the injured rat spinal cord. *Acta Biomater.* 27, 140–150. doi:10.1016/j.actbio.2015.09.001

Hahn, M. S., Miller, J. S., and West, J. L. (2006). Three-dimensional biochemical and biomechanical patterning of hydrogels for guiding cell behavior. *Adv. Mater. Weinheim* 18, 2679–2684. doi:10.1002/adma.200600647

Hahn, M. S., Taite, L. J., Moon, J. J., Rowland, M. C., Ruffino, K. A., and West, J. L. (2006). Photolithographic patterning of polyethylene glycol hydrogels. *Biomaterials* 27, 2519–2524. doi:10.1016/j.biomaterials.2005.11.045

Haring, A. P., Sontheimer, H., and Johnson, B. N. (2017). Microphysiological human brain and neural systems-on-a-chip: potential alternatives to small animal models and emerging platforms for drug discovery and personalized medicine. *Stem Cell Rev. Rep.* 13, 381–406. doi:10.1007/s12015-017-9738-0

Hill, C. E., Moon, L. D. F., Wood, P. M., and Bunge, M. B. (2006). Labeled Schwann cell transplantation: cell loss, host Schwann cell replacement, and strategies to enhance survival. *Glia* 53, 338–343. doi:10.1002/glia.20287

Hinton, T. J., Jallerat, Q., Palchesko, R. N., Park, J. H., Grodzicki, M. S., Shue, H.-J., et al. (2015). Three-dimensional printing of complex biological structures by freeform reversible embedding of suspended hydrogels. *Sci. Adv.* 1, e1500758. doi:10.1126/sciadv.1500758

Horn-ranney, E. L., Curley, J. L., Catig, G. C., Huval, R. M., and Michael, J. (2014). Structural and molecular micropatterning of dual hydrogel constructs for neural growth models using photochemical strategies. *Biomed. Microdevices* 15, 49–61. doi:10.1007/s10544-012-9687-y

Hsieh, F. Y., Lin, H. H., and Hsu, S. H. (2015). 3D bioprinting of neural stem cell-laden thermoresponsive biodegradable polyurethane hydrogel and potential in central nervous system repair. *Biomaterials* 71, 48–57. doi:10.1016/j.biomaterials.2015.08.028

Huang, L., Wu, Z., Zhuge, Q., Zheng, W., Shao, B., Wang, B., et al. (2014). Glial scar formation occurs in the human brain after ischemic stroke. *Int. J. Med. Sci.* 11, 344–348. doi:10.7150/ijms.8140

Huval, R. M., Miller, O. H., Curley, J. L., Fan, Y., Hall, B. J., and Moore, M. J. (2015). Microengineered peripheral nerve-on-a-chip for preclinical physiological testing. *Lab. Chip* 15, 2221–2232. doi:10.1039/C4LC01513D

Hynd, M. R., Frampton, J. P., Burnham, M.-R., Martin, D. L., Dowell-mesfin, N., Turner, J. N., et al. (2006). Functionalized hydrogel surfaces for the patterning of multiple biomolecules. *J. Biomed. Mater. Res. A* 81, 347–354. doi:10.1002/jbm.a.31002

Hynd, M. R., Frampton, J. P., Dowell-mesfin, N., Turner, J. N., and Shain, W. (2009). Directed cell growth on protein functionalized hydrogel surfaces. *J. Neurosci. Methods* 162, 255–263. doi:10.1016/j.jneumeth.2007.01.024

Hyysalo, A., Ristola, M., Joki, T., Honkanen, M., Vippola, M., and Narkilahti, S. (2017). Aligned poly(ε-caprolactone) nanofibers guide the orientation and migration of human pluripotent stem cell-derived neurons, astrocytes, and oligodendrocyte precursor cells in vitro. *Macromol. Biosci.* 17, 1–8. doi:10.1002/mabi.201600517

Ilkhanizadeh, S., Teixeira, A. I., and Hermanson, O. (2007). Inkjet printing of macromolecules on hydrogels to steer neural stem cell differentiation. *Biomaterials* 28, 3936–3943. doi:10.1016/j.biomaterials.2007.05.018

Jang, J., Song, Y., Yoo, D., Ober, C. K., Lee, J., and Lee, T. (2016). The development of fluorous photolithographic materials and their applications to achieve flexible organic electronic devices. *Flexible Printed Electron.* 1, 1–16. doi:10.1088/2058-8585/1/2/023001

Jhaveri, S. J., Senaratne, W., Hynd, M. R., Turner, J. N., Sengupta, P., Shain, W., et al. (2006). Defining the biology-materials interface using both 2D and 3D lithography. *J. Photopolym. Sci. Technol.* 19, 435–440. doi:10.2494/photopolymer.19.435

Johnson, B. N., Lancaster, K. Z., Hogue, I. B., Meng, F., Kong, Y. L., Enquist, L. W., et al. (2016). 3D printed nervous system on a chip. *Lab. Chip* 16, 1393–1400. doi:10.1039/C5LC01270H

Kaneko, A., Matsushita, A., and Sankai, Y. (2015). A 3D nanofibrous hydrogel and collagen sponge scaffold promotes locomotor functional recovery, spinal repair, and neuronal regeneration after complete transection of the spinal cord in adult rats. *Biomed. Mater.* 10, 15008. doi:10.1088/1748-6041/10/1/015008

King, V. R., Henseler, M., Brown, R. A., and Priestley, J. V. (2003). Mats made from fibronectin support oriented growth of axons in the damaged spinal cord of the adult rat. *Exp. Neurol.* 182, 383–398. doi:10.1016/S0014-4886(03)00033-5

King, V. R., Phillips, J. B., Hunt-Grubbe, H., Brown, R., and Priestley, J. V. (2006). Characterization of non-neuronal elements within fibronectin mats implanted into the damaged adult rat spinal cord. *Biomaterials* 27, 485–496. doi:10.1016/j.biomaterials.2005.06.033

Kishan, A. P., and Cosgriff-Hernandez, E. M. (2017). Recent advancements in electrospinning design for tissue engineering applications: a review. *J. Biomed. Mater. Res. A* 105, 2892–2905. doi:10.1002/jbm.a.36124

Kishan, A. P., Robbins, A. B., Mohiuddin, S. F., Jiang, M., Moreno, M. R., and Cosgriff-Hernandez, E. M. (2017). Fabrication of macromolecular gradients in aligned fiber scaffolds using a combination of in-line blending and air-gap electrospinning. *Acta Biomater.* 56, 118–128. doi:10.1016/j.actbio.2016.12.041

Krause, G. S., White, B. C., Aust, S. D., Nayini, N. R., and Kumar, K. (1988). Brian cell death following ischemia and reperfusion: a proposed biochemical sequence. *Crit. Care Med.* 16, 714–726. doi:10.1097/00003246-198807000-00015

Lampe, K. J., Bjugstad, K. B., and Mahoney, M. J. (2010). Impact of degradable macromer content in a poly (ethylene glycol) hydrogel on neural cell metabolic acitvity, redox state, proliferation, and differentiation. *Tissue Eng. Part A* 16, 1857–1866. doi:10.1089/ten.tea.2009.0509

Lee, M. K., Rich, M. H., Baek, K., Lee, J., and Kong, H. (2015). Bioinspired tuning of hydrogel permeability-rigidity dependency for 3D cell culture. *Sci. Rep.* 5, 8948. doi:10.1038/srep08948

Lee, S., Leach, M. K., Redmond, S. A., Chong, S. Y. C., Mellon, S. H., Tuck, S. J., et al. (2012). A culture system to study oligodendrocyte myelination processes using engineered nanofibers. *Nat. Methods* 9, 917–922. doi:10.1038/nmeth.2105

Lee, S., Nowicki, M., Harris, B., and Zhang, L. G. (2017). Fabrication of a highly aligned neural scaffold via a table top stereolithography 3D printing and electrospinning. *Tissue Eng. Part A* 23, 491–502. doi:10.1089/ten.tea.2016.0353

Lee, W., Pinckney, J., Lee, V., Lee, J., Fischer, K., Polio, S., et al. (2009). Three-dimensional bioprinting of rat embryonic neural cells. *Neuroreport* 20, 798–803. doi:10.1097/WNR.0b013e32832b8be4

Lee, Y. B., Polio, S., Lee, W., Dai, G., Menon, L., Carroll, R. S., et al. (2010). Bio-printing of collagen and VEGF-releasing fibrin gel scaffolds for neural stem cell culture. *Exp. Neurol.* 223, 645–652. doi:10.1016/j.expneurol.2010.02.014

Li, D., Wang, Y., and Xia, Y. (2004). Electrospinning nanofibers as uniaxially aligned arrays and layer-by-layer stacked films. *Adv. Mater. Weinheim* 16, 361–366. doi:10.1002/adma.200306226

Lin, H., Hsieh, F., Tseng, C., and Hsu, S. (2016). Preparation and characterization of a biodegradable polyurethane hydrogel and the hybrid gel with soy protein for 3D cell-laden bioprinting. *J. Mater. Chem. B* 4, 6694–6705. doi:10.1039/C6TB01501H

Lipinski, B. (2011). Hydroxyl radical and its scavengers in health and disease. *Oxid. Med. Cell. Longev.* 2011, 8089696. doi:10.1155/2011/809696

Livnat, N., Sarig-Nadir, O., Zajdman, R., Seliktar, D., and Shoham, S. (2007). "A hydrogel-based nerve regeneration conduit with sub-micrometer feature control," in *Proceedings of the 3rd International IEEE EMBS Conference on Neural Engineering*. Kohala Coast, HI, 101–103.

Lozano, R., Stevens, L., Thompson, B. C., Gilmore, K. J., Gorkin, R., Stewart, E. M., et al. (2015). 3D printing of layered brain-like structures using peptide modified gellan gum substrates. *Biomaterials* 67, 264–273. doi:10.1016/j.biomaterials.2015.07.022

Lu, H. D., Charati, M. B., Kim, I. L., and Burdick, J. A. (2012a). Injectable shear-thinning hydrogels engineered with a self-assembling dock-and-lock mechanism. *Biomaterials* 33, 2145–2153. doi:10.1016/j.biomaterials.2011.11.076

Lu, P., Wang, Y., Graham, L., McHale, K., Gao, M., Wu, D., et al. (2012b). Long-distance growth and connectivity of neural stem cells after severe spinal cord injury. *Cell* 150, 1264–1273. doi:10.1016/j.cell.2012.08.020

Luo, Y., and Shoichet, M. S. (2004a). A photolabile hydrogel for guided three-dimensional cell growth and migration. *Nat. Mater.* 3, 249–253. doi:10.1038/nmat1092

Luo, Y., and Shoichet, M. S. (2004b). Light-activated immobilization of biomolecules to agarose hydrogels for controlled cellular response. *Biomacromolecules* 5, 2315–2323. doi:10.1021/bm0495811

Lynam, D. A., Shahriari, D., Wolf, K. J., Angart, P. A., Koffler, J., Tuszynski, M. H., et al. (2015). Brain derived neurotrophic factor release from layer-by-layer coated agarose nerve guidance scaffolds. *Acta Biomater.* 18, 128–131. doi:10.1016/j.actbio.2015.02.014

Macaya, D., and Spector, M. (2012). Injectable hydrogel materials for spinal cord regeneration: a review. *Biomed. Mater.* 7, 12001. doi:10.1088/1748-6041/7/1/012001

Malek, S., Raney, J. R., Lewis, J. A., and Gibson, L. J. (2017). Lightweight 3D cellular composites inspired by balsa. *Bioinspir. Biomim.* 12, 26014. doi:10.1088/1748-3190/aa6028

Maruo, S., Nakamura, O., and Kawata, S. (1997). Three-dimensional microfabrication with two-photon-absorbed photopolymerization. *Opt. Lett.* 22, 132–134. doi:10.1364/OL.22.000132

Matthews, J. A., Wnek, G. E., Simpson, D. G., and Bowlin, G. L. (2002). Electrospinning of collagen nanofibers. *Biomacromolecules* 3, 232–238. doi:10.1021/bm015533u

Mattotti, M., Alvarez, Z., Ortega, J. A., Planell, J. A., Engel, E., and Alcántara, S. (2012). Inducing functional radial glia-like progenitors from cortical astrocyte cultures using micropatterned PMMA. *Biomaterials* 33, 1759–1770. doi:10.1016/j.biomaterials.2011.10.086

McCormick, A. M., Maddipatla, M. V. S. N., Shi, S., Chamsaz, E. A., Yokoyama, H., Joy, A., et al. (2014). Micropatterned coumarin polyester thin films direct neurite orientation. *ACS Appl. Mater. Interfaces* 6, 19655–19667. doi:10.1021/am5044328

McMurtrey, R. J. (2014). Patterned and functionalized nanofiber scaffolds in three-dimensional hydrogel constructs enhance neurite outgrowth and directional control. *J. Neural Eng.* 11, 66009. doi:10.1088/1741-2560/11/6/066009

Milbreta, U., Nguyen, L. H., Diao, H., Lin, J., Wu, W., Sun, C. Y., et al. (2016). Three-dimensional nanofiber hybrid scaffold directs and enhances axonal regeneration after spinal cord injury. *ACS Biomater. Sci. Eng.* 2, 1319–1329. doi:10.1021/acsbiomaterials.6b00248

Murphy, S. V., and Atala, A. (2014). 3D bioprinting of tissues and organs. *Nat. Biotechnol.* 32, 773–785. doi:10.1038/nbt.2958

Murry, C. E., and Keller, G. (2008). Differentiation of embryonic stem cells to clinically relevant populations: lessons from embryonic development. *Cell* 132, 661–680. doi:10.1016/j.cell.2008.02.008

Musoke-Zawedde, P., and Shoichet, M. S. (2006). Anisotropic three-dimensional peptide channels guide neurite outgrowth within a biodegradable hydrogel matrix. *Biomed. Mater.* 1, 162–169. doi:10.1088/1748-6041/1/3/011

Nagamine, K., Hirata, T., Okamoto, K., Abe, Y., Kaji, H., and Nishizawa, M. (2015). Portable micropatterns of neuronal cells supported by thin hydrogel films. *ACS Biomater. Sci. Eng.* 1, 329–334. doi:10.1021/acsbiomaterials.5b00020

Nakagomi, T., Taguchi, A., Fujimori, Y., Saino, O., Nakano-Doi, A., Kubo, S., et al. (2009). Isolation and characterization of neural stem/progenitor cells from post-stroke cerebral cortex in mice. *Eur. J. Neurosci.* 29, 1842–1852. doi:10.1111/j.1460-9568.2009.06732.x

Oh, J., Recknor, J. B., Recknor, J. C., Mallapragada, S. K., and Sakaguchi, D. S. (2009). Soluble factors from neocortical astrocytes enhance neuronal differentiation of neural progenitor cells from adult rat hippocampus on micropatterned polymer substrates. *J. Biomed. Mater. Res. A* 91, 575–585. doi:10.1002/jbm.a.32242

Orr, S. B., Chainani, A., Hippensteel, K. J., Kishan, A., Gilchrist, C., Garrigues, N. W., et al. (2015). Aligned multilayered electrospun scaffolds for rotator cuff tendon tissue engineering. *Acta Biomater.* 24, 117–126. doi:10.1016/j.actbio.2015.06.010

Ouyang, L., Highley, C. B., Rodell, C. B., Sun, W., and Burdick, J. A. (2016). 3D printing of shear-thinning hyaluronic acid hydrogels with secondary cross-linking. *ACS Biomater. Sci. Eng.* 2, 1743–1751. doi:10.1021/acsbiomaterials.6b00158

Park, J. W., Kang, Y. D., Kim, J. S., Lee, J. H., and Kim, H. W. (2014). 3D microenvironment of collagen hydrogel enhances the release of neurotrophic factors from human umbilical cord blood cells and stimulates the neurite outgrowth of human neural precursor cells. *Biochem. Biophys. Res. Commun.* 447, 400–406. doi:10.1016/j.bbrc.2014.03.145

Pham, Q. P., Sharma, U., and Mikos, A. G. (2006). Electrospinning of polymeric nanofibers for tissue engineering applications: a review. *Tissue Eng.* 12, 1197–1211. doi:10.1089/ten.2006.12.1197

Politis, M., and Lindvall, O. (2012). Clinical application of stem cell therapy in Parkinson's disease. *BMC Med.* 10:1. doi:10.1186/1741-7015-10-1

Pritchard, C. D., Slotkin, J. R., Yu, D., Dai, H., Lawrence, M. S., Bronson, R. T., et al. (2010). Establishing a model spinal cord injury in the African green monkey for the preclinical evaluation of biodegradable polymer scaffolds seeded with human neural stem cells. *J. Neurosci. Methods* 188, 258–269. doi:10.1016/j.jneumeth.2010.02.019

Ratheesh, G., Venugopal, J. R., Chinappan, A., Ezhilarasu, H., Sadiq, A., and Ramakrishna, S. (2017). 3D fabrication of polymeric scaffolds for regenerative therapy. *ACS Biomater. Sci. Eng.* 3, 1175–1194. doi:10.1021/acsbiomaterials.6b00370

Recknor, J. B., Recknor, J. C., Sakaguchi, D. S., and Mallapragada, S. K. (2004). Oriented astroglial cell growth on micropatterned polystyrene substrates. *Biomaterials* 25, 2753–2767. doi:10.1016/j.biomaterials.2003.11.045

Sanders, J. E., Lamont, S. E., Karchin, A., Golledge, S. L., and Ratner, B. D. (2005). Fibro-porous meshes made from polyurethane micro-fibers: effects of surface charge on tissue response. *Biomaterials* 26, 813–818. doi:10.1016/j.biomaterials.2004.03.030

Seaberg, R. M., and Van Der Kooy, D. (2003). Stem and progenitor cells: the premature desertion of rigorous definitions. *Trends Neurosci.* 26, 125–131. doi:10.1016/S0166-2236(03)00031-6

Seidlits, S. K., Schmidt, C. E., and Shear, J. B. (2009). High-resolution patterning of hydrogels in three dimensions using direct-write photofabrication for cell guidance. *Adv. Funct. Mater.* 19, 3543–3551. doi:10.1002/adfm.200901115

Shepherd, J. N. H., Parker, S. T., Shepherd, R. F., Gillette, M. U., Lewis, J. A., and Nuzzo, R. G. (2012). 3D microperiodic hydrogel scaffolds for robust neuronal cultures. *Adv. Funct. Mater.* 61, 47–54. doi:10.1002/adfm.201001746.3D

Shim, J. H., Kim, J. Y., Park, M., Park, J., and Cho, D. W. (2011). Development of a hybrid scaffold with synthetic biomaterials and hydrogel using solid freeform fabrication technology. *Biofabrication* 3, 034102. doi:10.1088/1758-5082/3/3/034102

Shin, Y., Yang, K., Han, S., Park, H. J., Heo, Y. S., Cho, S. W., et al. (2014). Reconstituting vascular microenvironment of neural stem cell niche in three-dimensional extracellular matrix. *Adv. Healthc. Mater.* 3, 1457–1464. doi:10.1002/adhm.201300569

Shrestha, B., Coykendall, K., Li, Y., Moon, A., Priyadarshani, P., and Yao, L. (2014). Repair of injured spinal cord using biomaterial scaffolds and stem cells. *Stem Cell Res. Ther.* 5, 91. doi:10.1186/scrt480

Siqueira, G., Kokkinis, D., Libanori, R., Hausmann, M. K., Gladman, A. S., Neels, A., et al. (2017). Cellulose nanocrystal inks for 3D printing of textured cellular architectures. *Adv. Funct. Mater.* 27:1604619. doi:10.1002/adfm.201604619

Smith, C. M., Stone, A. L., Parkhill, R. L., Stewart, R. L., Simpkins, M. W., Kachurin, A. M., et al. (2004). Three-dimensional bioassembly tool for generating viable tissue-engineered constructs. *Tissue Eng.* 10, 1566–1576. doi:10.1089/ten.2004.10.1566

Stankus, J. J., Guan, J., Fujimoto, K., and Wagner, W. R. (2006). Microintegrating smooth muscle cells into a biodegradable elastomeric fiber matrix. *Biomaterials* 27, 735–744. doi:10.1002/nbm.3066

Thakur, A., Jaiswal, M. K., Peak, C. W., Carrow, J. K., Gentry, J., Dolatshahi-Pirouz, A., et al. (2016). Injectable shear-thinning nanoengineered hydrogels for stem cell delivery. *Nanoscale* 8, 12362–12372. doi:10.1039/C6NR02299E

Truby, R. L., and Lewis, J. A. (2016). Printing soft matter in three dimensions. *Nature* 540, 371–378. doi:10.1038/nature21003

Turunen, S., Haaparanta, A., Äänismaa, R., and Kellomäki, M. (2013). Chemical and topographical patterning of hydrogels for neural cell guidance in vitro. *J. Tissue Eng. Regener. Med.* 7, 253–270. doi:10.1002/term

Walker, C. L., Wang, X., Bullis, C., Liu, N.-K., Lu, Q., Fry, C., et al. (2015). Biphasic bisperoxovanadium administration and Schwann cell transplantation for repair after cervical contusive spinal cord injury. *Exp. Neurol.* 264, 163–172. doi:10.1016/j.expneurol.2014.12.002

Wang, T. Y., Bruggeman, K. F., Kauhausen, J. A., Rodriguez, A. L., Nisbet, D. R., and Parish, C. L. (2016). Functionalized composite scaffolds improve the engraftment of transplanted dopaminergic progenitors in a mouse model of Parkinson's disease. *Biomaterials* 74, 89–98. doi:10.1016/j.biomaterials.2015.09.039

Wang, X., Jiang, M., Zhou, Z., Gou, J., and Hui, D. (2017). 3D printing of polymer matrix composites: a review and prospective. *Compos. Part B Eng.* 110, 442–458. doi:10.1016/j.compositesb.2016.11.034

Weightman, A., Jenkins, S., Pickard, M., Chari, D., and Yang, Y. (2014). Alignment of multiple glial cell populations in 3D nanofiber scaffolds: toward the development of multicellular implantable scaffolds for repair of neural injury. *Nanomedicine* 10, 291–295. doi:10.1016/j.nano.2013.09.001

White, B. C., Sullivan, J. M., DeGracia, D. J., O'Neil, B. J., Neumar, R. W., Grossman, L. I., et al. (2000). Brain ischemia and reperfusion: molecular mechanisms of neuronal injury. *J. Neurol. Sci.* 179, 1–33. doi:10.1016/S0022-510X(00)00386-5

Xie, J., MacEwan, M. R., Willerth, S. M., Li, X., Moran, D. W., Sakiyama-Elbert, S. E., et al. (2009). Conductive core-sheath nanofibers and their potential application in neural tissue engineering. *Adv. Funct. Mater.* 19, 2312–2318. doi:10.1002/adfm.200801904

Yang, D., Lu, B., Zhao, Y., and Jiang, X. (2007). Fabrication of aligned fibrous arrays by magnetic electrospinning. *Adv. Mater. Weinheim* 19, 3702–3706. doi:10.1002/adma.200700171

Yao, S., Liu, X., Yu, S., Wang, X., Zhang, S., Wu, Q., et al. (2016). Co-effects of matrix low elasticity and aligned topography on stem cell neurogenic differentiation and rapid neurite outgrowth. *Nanoscale* 8, 10252–10265. doi:10.1039/C6NR01169A

Yi, H., Choi, Y., Kang, K. S., Hong, J. M., Pati, R. G., Park, M. N., et al. (2016). A 3D-printed local drug delivery patch for pancreatic cancer growth suppression. *J. Control. Release* 238, 231–241. doi:10.1016/j.jconrel.2016.06.015

Yuan, Y.-M., and He, C. (2013). The glial scar in spinal cord injury and repair. *Neurosci. Bull.* 29, 421–435. doi:10.1007/s12264-013-1358-3

Zanatta, G., Steffens, D., Braghirolli, D. I., Fernandes, R. A., Netto, C. A., and Pranke, P. (2012). Viability of mesenchymal stem cells during electrospinning. *Braz. J. Med. Biol. Res.* 45, 125–130. doi:10.1590/S0100-879X2011007500163

Zhu, W., Harris, B. T., and Zhang, L. G. (2016). Gelatin methacrylamide hydrogel with graphene nanoplatelets for neural cell-laden 3D bioprinting. *Conf. Proc. IEEE Eng. Med. Biol. Soc.* 2016, 4185–4188. doi:10.1109/EMBC.2016.7591649

Conflict of Interest Statement: The authors declare that the research was conducted in the absence of any commercial or financial relationships that could be construed as a potential conflict of interest.

frontiers in Bioengineering and Biotechnology

REVIEW
published: 17 November 2017
doi: 10.3389/fbioe.2017.00069

3-D Bioprinting of Neural Tissue for Applications in Cell Therapy and Drug Screening

Michaela Thomas[1] *and Stephanie M. Willerth*[1,2,3,4]*

[1] Department of Mechanical Engineering, University of Victoria, Victoria, BC, Canada, [2] Division of Medical Sciences, University of Victoria, Victoria, BC, Canada, [3] Centre for Biomedical Research, University of Victoria, Victoria, BC, Canada, [4] International Collaboration on Repair Discoveries (ICORD), Vancouver, BC, Canada

Neurodegenerative diseases affect millions of individuals in North America and cost the health-care industry billions of dollars for treatment. Current treatment options for degenerative diseases focus on physical rehabilitation or drug therapies, which temporarily mask the effects of cell damage, but quickly lose their efficacy. Cell therapies for the central nervous system remain an untapped market due to the complexity involved in growing neural tissues, controlling their differentiation, and protecting them from the hostile environment they meet upon implantation. Designing tissue constructs for the discovery of better drug treatments are also limited due to the resolution needed for an accurate cellular representation of the brain, in addition to being expensive and difficult to translate to biocompatible materials. 3-D printing offers a streamlined solution for engineering brain tissue for drug discovery or, in the future, for implantation. New microfluidic and bioplotting devices offer increased resolution, little impact on cell viability and have been tested with several bioink materials including fibrin, collagen, hyaluronic acid, poly(caprolactone), and poly(ethylene glycol). This review details current efforts at bioprinting neural tissue and highlights promising avenues for future work.

Keywords: neural tissue engineering, 3-D bioprinting, biomaterials, stem cells, neurodegenerative diseases, drug discovery

OPEN ACCESS

Edited by:
Sara Pedron, University of Illinois at Urbana–Champaign, United States

Reviewed by:
Soneela Ankam, Mayo Clinic Minnesota, United States
Diego Mantovani, Laval University, Canada

***Correspondence:**
Stephanie M. Willerth
willerth@uvic.ca

Specialty section:
This article was submitted to Biomaterials, a section of the journal Frontiers in Bioengineering and Biotechnology

Received: *19 August 2017*
Accepted: *19 October 2017*
Published: *17 November 2017*

Citation:
Thomas M and Willerth SM (2017) 3-D Bioprinting of Neural Tissue for Applications in Cell Therapy and Drug Screening. Front. Bioeng. Biotechnol. 5:69. doi: 10.3389/fbioe.2017.00069

INTRODUCTION

Neurodegenerative diseases affect over 55 million individuals annually in North America, creating a multi-billion dollar burden on the health-care industry due to the costs associated with treatment, and rehabilitation therapy (Institute for Neurodegenerative Diseases, 2017). Often selective cell loss in the central nervous system (CNS) leads to these neurodegenerative diseases. Cell therapy can potentially treat neurodegenerative disease by replacing damaged tissues or augmenting remaining cell function (Levy et al., 2016). The basis of cell therapy is that living human cells can be injected into a damaged region of the body to instigate healing (Dove, 2002). Neurodegenerative diseases, such as Alzheimer's disease, Parkinson's disease, Huntington's disease, multiple sclerosis, and amyotrophic lateral sclerosis, as well as neurodegenerative disorders, such as traumatic brain injury, serve as potential candidates for cell therapy as they result in neuronal death in targeted areas of the brain (Vila and Przedborksi, 2003). Neuronal cells possess a low regenerative capacity as they do not proliferate after maturation (Tam et al., 2014). Thus, cell therapy can replace damaged neuronal and

support cells, or work indirectly by secreting soluble factors to facilitate the repair process (Tsintou et al., 2015).

While current treatments for these diseases mainly focus on alleviating symptoms and physical rehabilitation, cell therapy can potentially promote cellular repair and remodeling, resulting in improved function. Several issues must be addressed before cell therapy can be widely implemented. These issues include ensuring that the proper number and type of cell are being generated, especially when using stem cells as they can become multiple types of cells. Large quantities of cells are often required for cell therapies to treat neurodegenerative disorders and thus, high-throughput methods for generating these cells must be developed (Rossi and Cattaneo, 2002; Cooke et al., 2010). Direct transplantation of cells in the damaged CNS is possible, but often these cells fail to properly integrate into the brain (Rossi and Cattaneo, 2002). Bioprinting, the use of 3-D printing technology with biocompatible materials that can be seeded with living cells to create tissue constructs, can potentially produce carefully controlled human neural tissue in a consistent rapid manner. The biomaterial scaffolds used in the 3-D printing process are often referred to as bioinks (Skardal and Atala, 2015). Engineered biomaterial microenvironments can help overcome low cell survival rates after transplantation in the damaged CNS and limit migration of cells away from the implantation site while providing a controlled environment for cell growth and differentiation (Cooke et al., 2010; Struzyna et al., 2014). These printable cell scaffolds degrade as the cells develop, either through hydrolysis, or through enzymatic degradation by byproduct proteases, leaving a biologically accurate tissue construct as the result (Freed et al., 1994).

Different types of stem cells have been evaluated *in vitro* and *in vivo* for neural regeneration. These cells include human embryonic stem cells (hESCs), which are pluripotent stem cells derived from a human embryo; mesenchymal stem cells (MSCs), which are multipotent stromal cells that can differentiate into osteoblasts, chondrocytes, myocytes, and adipocytes; neural stem/progenitor stem cells, which are multipotent and can differentiate into neurons, astrocytes, and oligodendrocytes; and human induced pluripotent stem cells (hiPSCs), which are adult cells taken back to a pluripotent state (Mothe and Tator, 2012). Both hESCs and hiPSCs are pluripotent, meaning they can differentiate into any cell type in the body (Itskovitz-Eldor et al., 2000). However, hESCs pose the risk of immune rejection after transplantation and remain ethically controversial because the blastocyst from which they are isolated does not survive the derivation process (Bobbert, 2006). hiPSCs are adult somatic cells reprogrammed into a pluripotent state using transcription factors (Takahashi et al., 2007). They offer the opportunity to replace cells lost while minimizing the risk of immune rejection as these cells lines can be derived directly from a patient's own cells (Kamao et al., 2014). Neurodegenerative diseases can be modeled using hiPSCs by reprogramming adult cells taken from patients into neural cells, which then display disease hallmarks (Durnaoglu et al., 2011).

Any cell line chosen for bioprinting must have the ability to expand to sufficient numbers to be printable (Murphy and Atala, 2014). Many primary cell types cannot self-renew while being difficult to isolate, making pluripotent stem cells a more attractive option when bioprinting (Murphy and Atala, 2014). Recent advancements such as clustered regularly interspaced short palindromic repeats (CRISPER/Cas9) make it possible to correct gene mutations found in cell lines, enhancing the potential of hiPSCs for use in cell replacement therapies for treatment of neurodegenerative disease (McMahon et al., 2012). Scaffold-based strategies provide an attractive approach for culturing, expanding, and delivering cells because they offer structural support for growing cells and axons and can be loaded with chemical factors to encourage differentiation and integration with existing cell culture. 3-D bioprinting can control the spatial distribution of these factors to control cell differentiation. Biomaterial scaffolds that have supported neural cell scaffolds culture *in vitro* in mouse and rat trials include polyethylene glycol (PEG) (Freudenberg et al., 2008), modified peptide gels such as RADA16-YIGSR (Cui et al., 2016), hyaluronan (Gardin et al., 2011), fibrin (Gardin et al., 2011), and alginate (Perez et al., 2016). Many studies use extracellular matrix molecules to provide structural support such as collagen, fibrin, fibronectin, and laminin (Itosaka et al., 2009; Tate et al., 2009; Johnson et al., 2010; Elias and Spector, 2012; Lu et al., 2012; Wilems et al., 2015) and polymers such as poly(lactic-co-glycolic acid), *N*-(2-Hydroxypropyl) methacrylamide, and poly(a-hydroxy-acids) (Sykova et al., 2006).

In addition to cell therapy applications, 3-D bioprinted neural tissues can be used to model diseases and for drug discovery. Several groups have grown functional neural tissue in small tissue constructs, but these methods require long and labor-intensive culture protocols (Hopkins et al., 2015). Often the function of the resulting tissues is not fully developed, lacking fully mature neural cells and their associated function as assessed by electrophysiology (Hopkins et al., 2015). Bioprinting could create accurate, reproducible tissue constructs in a high-throughput manner, allowing for large sample sizes for evaluating electrophysiological function over time.

Cell therapy can repair damaged tissues by supplying growth factors to the injury site (Kim, 2004). To produce brain tissue constructs for drug screening, or disease modeling, the current bioprinting technologies must be changed to incorporate nutrient flow throughout the cell construct. Replacing brain tissue remains a futuristic goal, but finding a way to accurately produce neural tissue that mimics the mechanical and biochemical conditions found *in vivo*. These properties include reproducing the calcium and potassium gated voltage response for neuronal signaling (Kohler et al., 1996), displaying an elastic modulus of less than 1,000 Pa, similar to brain tissue (Georges et al., 2006), and supporting a mixed cell population to better represent the native population of neuronal and support cells. Such properties must be achieved without inducing inflammation or unexpected cellular responses. Engineering biologically accurate neural tissue requires a platform with complex controls with regards to sterilization and culture conditions as well as cell and scaffold placement.

CULTURING NEURAL CELLS *IN VITRO*

2-Dimensional Cell Culture

2-D culture platforms are effective in inducing early neuronal developmental structures (such as neural rosettes) from hESCs

and hiPSCs, but they impose unnatural geometric constraints on the cells (Shao et al., 2015). Deriving neuroepithelial cells from hESCs and hiPSCs requires a lengthy differentiation protocol. The most common method requires the formation of embryonic bodies (EBs) followed by manual isolation of neural rosettes or adherent differentiation in combination with small molecule inhibitors that promote differentiation (Chambers et al., 2009). This process takes 17–19 days and requires several replating steps (Chambers et al., 2009). Similar conversion rates can be obtained in approximately 6 days by culturing human pluripotent stem cells on laminin coated plates in the presence of E6 media (Lippmann et al., 2014). NSCs are cultured in a similar manner either as adherent or suspension cultures but face the same geometric and morphological constraints as hESCs and hiPSCs. 2-D cultures do not exhibit the same morphology as neurons in the body because they cannot grow in 3-D. Thus, many researchers have transitioned into culturing cell lines in 3-D systems.

3-Dimensional Cell Culture of Neural Cells Using Biomaterials

3-D cell culture requires suspending cells within a permeable scaffold matrix, resulting in a more physiologically relevant cell microenvironment (Shao et al., 2015). NPCs derived from hiPSCs cultured in 3-D produce more neuronal cells and less astrocytes compared with cells cultured in 2-D (Edgar et al., 2017). The 3-D structure of EBs in a scaffold allows intricate cell to cell and cell to scaffold interactions not possible in 2-D culture, enabling patterned and structured cell differentiation and morphogenesis (Shao et al., 2015). Neural differentiation of stem cells has been evaluated in a number of biomaterial scaffolds, including fibrin (Robinson et al., 2015), laminin (Edgar et al., 2017), alginate (Gu et al., 2016), and PEG (Schwartz et al., 2015).

Fibrin scaffolds promote neural adhesion, proliferation, and differentiation likely because low-concentration fibrin gels possess biochemical and mechanical cues similar to those of soft tissue (Willerth et al., 2006, 2007a,b, 2008; Kolehmainen and Willerth, 2012; Montgomery et al., 2015; Robinson et al., 2015). Fibrin polymerizes under mild conditions with the addition of thrombin, but this slow process is unsuitable for extrusion bioprinting. Thus, it is often mixed with polysaccharides, such as alginate, to produce a printable bioink (Gu et al., 2016). Alginate, one of the most widely employed bioinks, polymerizes quickly with the addition of a divalent cation (Skardal and Atala, 2015). Other polysaccharides, such as gellan gum, have similar rates of polymerization (Lozano et al., 2015). However, these polysaccharides are mostly inert, resulting in limited cell adhesion (Skardal and Atala, 2015).

Laminin stimulates axonal outgrowth when added to 3-D biomaterial scaffolds, likely because it plays a role in axonal guidance and cell migration in the developing CNS (Edgar et al., 2017). Fibrin functionalized with laminin elicits higher neurite outgrowth than unmodified fibrin scaffolds (Pittier et al., 2005). PEG gels functionalized with peptides and seeded with ESC-derived NPCs, endothelial cells, MSCs, and microglia/macrophage precursors showed 3-D constructs with diverse neuronal and glial populations including vascular networks (Schwartz et al., 2015). The addition of small molecules, such as retinoic acid and purmorphamine, into 3-D culture promotes more efficient differentiation, of hiPSCs into spinal motor neurons (Edgar et al., 2017). While natural hydrogels can retain the biological activities of native ECM molecules, they suffer from batch-to-batch variability and limited possibilities for biochemical modification (Caliari and Burdick, 2016). In addition, natural hydrogels pose a risk of immunogenicity and disease transfer for clinical applications (Caliari and Burdick, 2016). By contrast, synthetic hydrogels can be more amenable for biochemical functionalization, such as growth factors, ECM adhesive motifs, and specific molecules agonistic or antagonistic to cell surface receptors, biophysical modulations, including mechanical stiffness, pore size, and 3-D architecture, and mimicking key degradation characteristics. Synthetic hydrogels also have a lower risk for immunogenic reactions as their monomers are produced using chemically defined reactions (Shao et al., 2015).

In terms of comparable technology to 3-D printing, Lancaster et al. cultured brain-like organoids, mini organs that possess similar characteristics to their human counterparts, inside of Matrigel droplets using a spinning bioreactor (Lancaster et al., 2013). After 30 days, a continuous neuroepithelium had formed surrounding a fluid-filled cavity with defined brain regions similar to the cerebral cortex, choroid plexus, retina, and meninges. Achieving a nanoscale resolution to ensure directed differentiation into unique brain areas presents one of the greatest challenges when engineering tissues (Rafat et al., 2017). The organoids reached a maximum size of approximately 4 mm after 2 months in culture. They survived up to 10 months when maintained in the bioreactor. The researchers surmised that the lack of the vascular network resulted in limited size, causing cells toward the center of the mass to die due to lack of oxygen (Lancaster et al., 2013). Bioprinting can address this important limitation of organoid formation as cell placement and their associated function could be more closely controlled by specific mechanical cues from the surrounding scaffold. Large hollow structures have already been bioprinted, but being able to incorporate blood vessels into such tissues would allow for natural vascularization (Hoch et al., 2014).

Printed scaffolds display similar degradation timelines and kinetics to their unprinted counterparts. Biomaterials for neural tissue engineering must consider that they are meant to be directly implanted or mimic natural brain tissue. Any degradation products can impact the developing or existing tissues (Wang et al., 2003). The chemical kinetics surrounding the degradation of the chosen scaffold material must be well understood to ensure the materials being released are not biologically active, or are active to a very low degree. This will depend both on scaffold composition and rate of degradation. In general, neural scaffold materials degrade via hydrolysis, ion exchange or through enzymatic reactions over a period of 2–8 weeks (Wang et al., 2003). Common degradation products include salts like calcium, protein fragments or weak acids such as lactic acid (Anderson et al., 2008). All mid- and end-point degradation products must be thoroughly investigated for possible immunogenic reactions. Possible host reactions to the biomaterial include injury, blood-material interactions, inflammation, and development of a fibrous capsule to isolate the foreign material (Anderson and Jones, 2007).

EARLY BIOPRINTING

Bioprinting enables significant control over the arrangement of cells and bioactive nanomaterials in defined-scaffold geometries in comparison with other tissue-engineering techniques (O'Brien et al., 2015). Printing cell scaffolds means more effective composition with less effort, achieving biomimetic constructs with ECM feature size and composition, chemical gradients, varied mechanical properties, and specific morphologies that were not previously accessible (Chia and Wu, 2015). 3-D printing has been widely investigated for industrial rapid prototyping and additive manufacturing protocols (Gross et al., 2014). 3-D printing neural tissue requires creating a computer-aided design (CAD) model of the desired tissue structure including cell type and elastic moduli, input your starting materials, and letting the program associated with the 3-D printer run. The program parses the solid object into a stack of cross-sections and then prints the desired structure upwards from the bottom along the *Z*-axis (O'Brien et al., 2015).

Fabricating tissues in a controlled environment outside of a living organism requires reproducing the chemical, mechanical, and morphological properties found *in vivo* (Ahmad and Makoto, 2017). Several key components when bioprinting must be optimized to achieve *in vivo* mimicry, including the most important component—the bioink. Many natural polymers, such as fibrin, laminin, gelatin, and collagen, can be crosslinked under mild conditions into a cytocompatible hydrogel scaffold suitable for 3-D bioprinting (O'Brien et al., 2015). Many synthetic scaffold materials require complex reactions for functionalization, which hinders their ability to be bioprinted (Carrow et al., 2015). Mechanical restrictions also influence the choice of bioink when 3-D printing. Inkjet and laser-based bioprinting methods require a low-viscosity liquid, while extrusion printing requires a higher viscosity, indicating that different formulations are necessary depending on the printing method (Ahmad and Makoto, 2017). Supplements such as alginate are often added to the bioink to improve gelation speed and mechanical strength and maintain a good printing environment (Ahmad and Makoto, 2017). Another important consideration for bioink preparation is the printability, which depends on several rheological factors, including viscosity, surface tension, and thixotropy (O'Brien et al., 2015). Bioprinting requires the ability to eject the bioink, deposit, and solidify the bioink while retaining spatial resolution of the material to control and generate desired high-quality 3-D construct with accurate geometry. Thus, bioink viscosity plays a vital role in determining the flexibility of freestanding constructs and preserving their structural integrity during and after the printing process. Cells and biomolecules experience shear stress, local rheologic forces, or other external physical forces during printing process, which influences cell response (O'Brien et al., 2015). Thus, understanding how the parameters of bioprinting affect cellular processes throughout the printing process ensures the ability to obtain a viable construct (Ahmad and Makoto, 2017). Physiochemical properties (such as viscosity, elastic moduli, yield strength, reactivity, and degradation products) and cytocompatibility for the chosen cell line for printing serve as the two most important factors when designing a bioink (Ahmad and Makoto, 2017). Neuronal lineage cells derived from any source tend to be delicate and easily disrupted, presenting a major challenge when bioprinting (Potter and DeMarse, 2001). Controlling neural cell differentiation often uses defined culture conditions to ensure lineage (Ahmad and Makoto, 2017). The cell scaffold introduces a new set of proteins and biomolecules which cells will encounter during growth. The scaffold presents a 3-D microenvironment for controlling cell behavior through biophysical and biochemical cues (Ahmad and Makoto, 2017).

The following sections introduce several methods of bioprinting (**Figure 1**). These printing technologies can be improved by developing more sophisticated nozzles, cartridges that allow for automated loading, and speed and accuracy of the printing process. High resolution cell distribution remains an issue despite being improved in the last decade (Ahmad and Makoto, 2017).

Fused-Deposition Modeling

Fused-deposition modeling (FDS) uses a melted thermoplastic which is deposited layer-by-layer onto a flat substrate to build a 3-D construct (O'Brien et al., 2015). While FDS is extremely inexpensive, it has a low accuracy (±127 μm) and height resolution (50–762 μm). The thermoplastic cannot support itself immediately when deposited, limiting potential geometries. Cells can either be encapsulated in the material prior to extruding or seeded on top of the construct. Most FDS trials have been with cells seeded on top of the scaffold for musculoskeletal applications (since the materials are harder and more compatible with bone or dense muscle tissue), but some success has been had with encapsulated cells for neural tissue engineering (O'Brien et al., 2015).

Selective Laser Sintering (SLS)

Selective laser sintering uses a similar process as FDM, but SLS has a higher resolution (O'Brien et al., 2015). A long wavelength laser fuses beads of premade material together one layer at a time. Common materials include polycaprolactone (PCL) (Tan et al., 2005; Partee et al., 2006), polyvinyl alcohol (Chua et al., 2004; Tan et al., 2005), hydroxyapatite (Chua et al., 2004; Tan et al., 2005), and poly(L-lactic acid) (Tan et al., 2005). A layer of powder or beads is deposited, heated, and fused and then another layer deposited building up a 3-D construct. This process is both costly and slow with limited ability to remove non-sintered material. Very few materials are compatible with SLS and biocompatible. SLS, such as FDS, has largely generated scaffolds for bone tissue or other support structures for tissues (O'Brien et al., 2015).

Stereolithography

Stereolithography is the highest resolution option for bioprinting (O'Brien et al., 2015). It can print light-sensitive polymeric materials, which often polymerize to soft substrate materials with similar mechanical cues to that of neural tissue, which helps differentiate seeded cells into neuronal subtypes (Edgar et al., 2017). In stereolithography a laser and directed mirror array project patterned light onto the surface of a resin-containing vat, curing the resin. A fresh layer of resin is added with the process being repeated to generate the desired structure. Uncured resin remains liquid, making for easy removal. This process can be used to incorporate nanomaterials, as well as growth factors

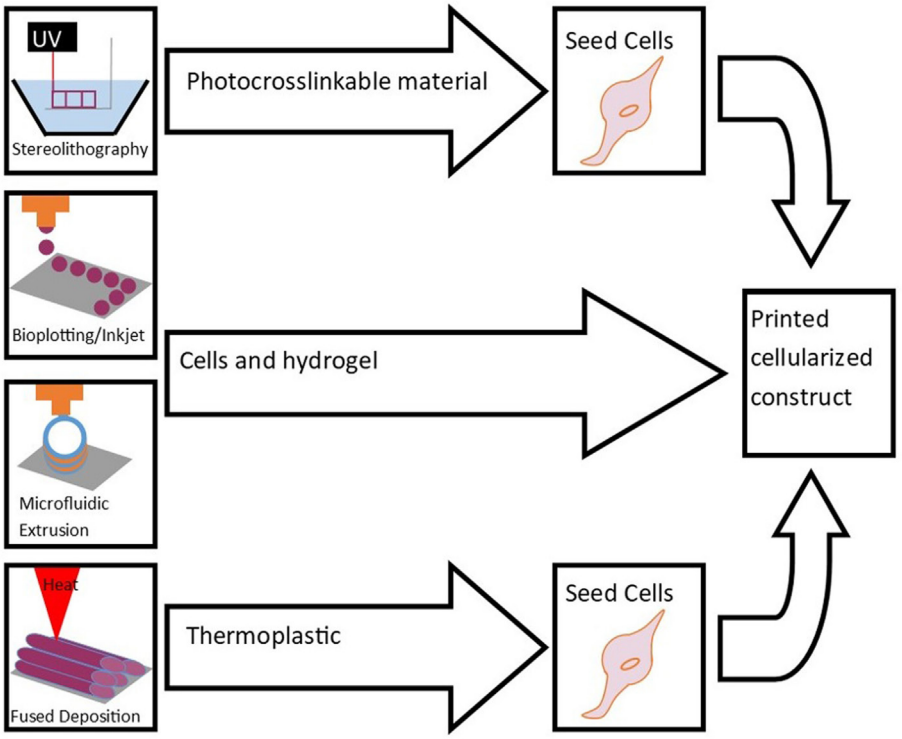

FIGURE 1 | Bioprinting methods include stereolithography, bioplotting, inkjet printing, microfluidic extrusion, and fused-deposition modeling. These techniques are used to print scaffolds for cell seeding and culture to engineer tissue.

and other additives without additional processes if they are not light-sensitive. Commercial systems for stereolithography use propriety nonbiomimetic inks, and the printing process can take long periods of time for printing (O'Brien et al., 2015). Stereolithography remains an understudied area with respect to applications in neural tissue engineering.

Inkjet Bioprinting

Inkjet bioprinting uses a modified inkjet printer to deposit cells encapsulated in a bioink onto a chosen substrate (O'Brien et al., 2015). The bioink cannot have a high viscosity, often resulting in constructs with poor mechanical properties. In addition, the small nozzle size damages the cells being printed as they become deformed when passing through the nozzle. The nozzle size and flow rate also restrict the volume deposited per drop (<10 pL), meaning high concentrations of cells (greater than 5 million cells/mL) must be seeded to maximize the possibility that each drop of bioink contains one cell. However, inkjet bioprinting offers a simple process to print multiple cell types, making it useful for printing thin tissue constructs like brain slices (O'Brien et al., 2015).

Bioplotting

Bioplotting using syringes to print tubes or spheroids layered on top of each other (O'Brien et al., 2015). Radiation, chemical reaction, or solidification then cures the material after printing. Bioprinting requires viscous bioinks as they need to hold their shape after extrusion from the needle. These bioinks tend to either be too hard or possess a low elastic modulus unsuitable for neural tissue-engineering applications. Several syringes can be used over the same substrate when placing different cell types in a desired format, but resolution is lower than microfluidic extrusion. It can print cocultured scaffolds and tissue constructions (O'Brien et al., 2015).

Microfluidic Extrusion

Microfluidic extrusion represents an extension of bioplotting (Pfister et al., 2004). This process continuously extrudes a cell-seeded bioink-precursor in tandem with a crosslinking agent. The mixture meets in a chamber, before being extruded at the desired flow rate. The mixing initiates polymerization before deposition, allowing for easy flow through the nozzle and a defined structure after printing. Multiple valves and chambers can control of the cell type and mechanical properties of the construct. The computer-guided deposition process is hands off, allowing for aseptic conditions during printing. This method requires hydrogel precursors that polymerize into semisolid hydrogels (O'Brien et al., 2015).

BIOPRINTING NEURAL TISSUE

Several groups have bioprinted neural tissue using various cell types with varying levels of success (**Table 1**). In 2006, Xu et al. inkjet printed primary embryonic hippocampal and cortical neurons suspended in phosphate-buffered saline onto collagen-based

TABLE 1 | Bioprinting neural tissue by various printing methods using different cell types and bioinks.

Bioink	Cell type	Cell source	Printing method	*In vivo/ in vitro*	Outcome	Reference
Cell suspension in DPBS printed on collagen biopaper	Primary embryonic hippocampal and cortical neurons	Day-18 fetal tissue from pregnant Sprague-Dawley rats	Inkjet bioprinting of NT2 cells	*In vitro*	Immunostaining and whole-cell patch clamp showed healthy neuronal phenotypes with electrophysiological activity	Xu et al., 2006
Fibrin hydrogel	Primary embryonic hippocampal and cortical neurons	Day-18 fetal tissue from pregnant Sprague-Dawley rats	Inkjet bioprinting alternating layers of fibrin hydrogel and NT2 cells	*In vitro*	Cells stained positive for DAPI and spread over the fibrin. Some cells exhibited neurite growth	Xu et al., 2006
Hyaluronic acid hydrogels grafted with laminin	Schwann cells seeded on surface	Day 15 embryonic rats	Photopatterned layer by layer	*In vitro*	Cells retained viability for 36 h, but did not adhere to scaffolds without laminin	Suri et al., 2011
Puramatrix/agarose	Dorsal root ganglia	E-15 rat pups	Digital micromirror device to crosslink polyethylene glycol, then cell material injected into the voids	*In vitro*	Cell migration and neurite extension limited to cell permissive regions	Curley et al., 2011
Polycaprolactone (PCL) microfibers and PCL with gelatin	Neural stem cells	Mouse NSC line C17.2	Stereolithography and electrospinning	*In vitro*	Fibers improved cell adhesion, aligned fibers enhanced cell proliferation, increased neurite length and directed neurite extension of primary cortical neurons along the fiber	Lee et al., 2017
Alginate, carboxymethyl chitosan, and agarose	Cortical neural stem cells encapsulated in the scaffold	Human	Microextrusion bioprinting	*In vitro*	Proliferated for 10 days with spontaneous activity and a bicuculline-induced increase calcium response, predominantly expressing gamma-aminobutyric acid	Gu et al., 2016
Polyurethane	Neural stem cells encapsulated in scaffold	Adult mouse brain	Fused-deposition manufacturing	*In vitro*	Remained viable and stained positive for β-tubulin (neuronal marker) at 7 days	Hsieh et al., 2015
				In vivo (zebrafish)	Implanted scaffold improved in-chorion coiling contraction (motor function) and hatching rate [central nervous system (CNS) function] in embryonic CNS-deficit zebrafish, and improved motor function and survival rate in adult zebrafish with induced TBI	Hsieh et al., 2015
Suspension in B27 Neurobasal-A medium	Retinal ganglion cells (RGCs) and glia encapsulated in scaffold	Adult male Sprague-Dawley rats	Piezoelectric inkjet printer	*In vitro*	No significant difference in survival and neurite outgrowth between printed RGCs and glia and plated cells	Lorber et al., 2014
Media with brain derived neurotrophic factor and ciliary neurotrophic factor	RGCs	Postnatal Sprague-Dawley rats	Inkjet printing onto electrospun scaffolds	*In vitro*	RGCs maintained survival and normal electrophysiological function, and displayed radial axon outgrowth	Kador et al., 2016
Collagen and fibrin, fibrin loaded with VEGF	Neural stem cells	Mouse NSC line C17.2	Microfluidic pneumatic based bioprinting	*In vitro*	Greater than 90% cell viability was observed with cells migrating toward the fibrin	Lee et al., 2010
Gellan gum modified with RGD peptide	Primary neural stem cells encapsulated in the scaffold	E18 embryos of BALB/cArcAusb mice	Handheld microfluidic device	*In vitro*	Cells remained viable at 5 days, forming neuronal networks with glial cells	Lozano et al., 2015
GelMA and PEGDA in PBS with a photo initiator and low-level light therapy	Neural stem cells seeded on top of scaffold	Mouse	Stereolithography	*In vitro*	Light stimulation promoted NSC neuronal differentiation and inhibited generation of glial cells	Zhu et al., 2017

biopaper (Xu et al., 2006). Circular single-layer constructs were printed and maintained in Dulbecco's Modified Eagle Media with 10% fetal bovine serum and 5% retinoic acid. After 8 days, cell viability was 74.2 ± 6.3%, and after 15 days, cells stained positive for the neuronal marker MAP2. Electrophysiological measurements at 15 days indicated neurons had developed voltage-gated potassium and sodium channels. The same study alternating printing a layer of cells with a layer of fibrin hydrogels (Xu et al., 2006). Initially, fibrinogen was printed in a thin layer and then thrombin was printed on top. The addition of thrombin polymerized the scaffold. A single layer or neurons was then printed on top using direct cell printing. Constructs were printed 50–70 μm thick resulting in a 3-D neural sheet 25 mm × 5 mm × 1 mm. The resulting samples stained positive for DAPI, and the cells spread and exhibited neurite outgrowth after 12 days in culture.

In 2014, Lorber et al. inkjet printed retinal glial cells and disassociated retinal cells, resulting in 57% cell death in glial cells and 33% cell death in retinal cells compared with controls of unprinted cells grown on tissue culture plates (Lorber et al., 2014). No differences in neurite outgrowth or survival were observed after 5 days compared with control cultures. The high levels of cell death suggest the need for optimization of nozzle technology to reduce cell stress and deformation to improve viability post-printing.

Suri et al. (2011) photopatterned glycidyl methacrylate modified hyaluronic acid containing laminin using a digital micromirror device before seeding Schwann cells upon the resulting construct. Scaffolds were printed in various geometries including circles, hexagons, and squares with different pore characteristics (**Figure 2**). Adhered cells maintained viability

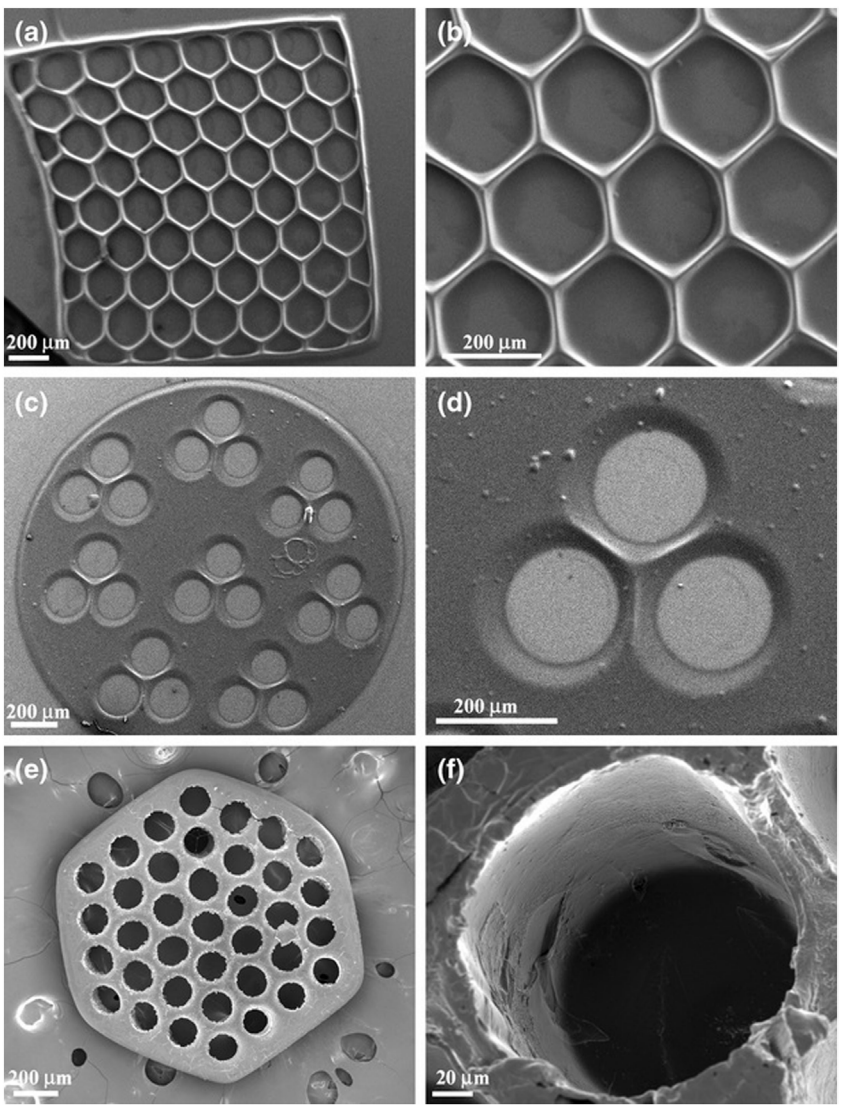

FIGURE 2 | SEM micrographs of single-layered scaffolds made up of photopatterned glycidyl methacrylate and hyaluronic acid with intricate pore geometries, **(A,B)** hexagonal patterns, **(C,D)** circular patterns with three channels, and **(E,F)** circular patterns with more than 30 channels created using a digital micromirror fabrication system. Reprinted with permission from Suri et al. (2011).

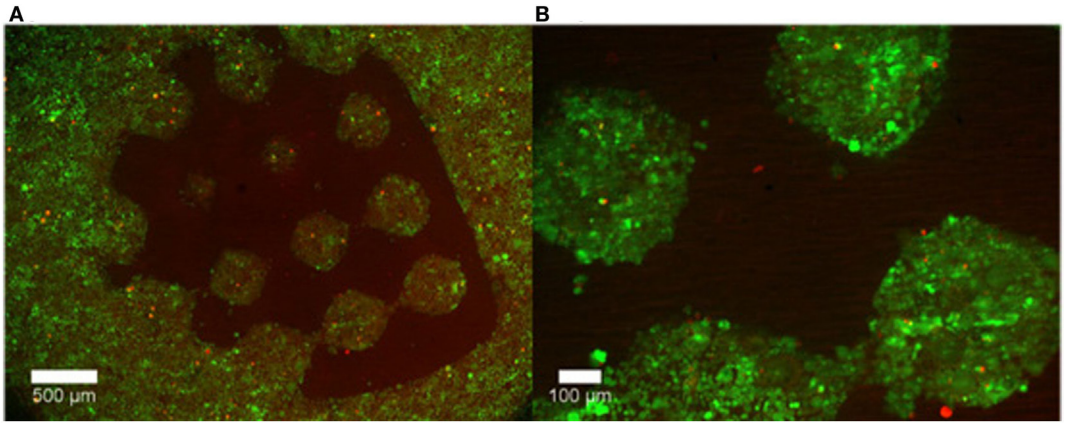

FIGURE 3 | Representative images of cell growth in **(A)** the permissive region (puramatrix/agarose) versus **(B)** PEG after 48 hours. Live cells are labelled with calcein (green) while dead cells are labeled with ethidium homodimer-1 (red). Reprinted from Curley et al. (2011) under a Creative Commons License 3.0.

after 36 h. The researchers also showed this method could be used to create gradients of fluorescent microparticles as a model for growth factor gradients, which have been shown to guide developing neurites.

Curley et al. (2011) also used a micromirror array to polymerize PEG into various geometries. The voids in the PEG gel were then filled with a puramatrix/agarose cell suspension. It was shown that cells retained their viability and grew only in the cell permissive (puramatrix or agarose) region of the scaffold (**Figure 3**).

Lee et al. (2017) combined stereolithography and electrospinning techniques to create PCL microfibers. Scaffolds with fibers improved neural stem cell adhesion, increased neurite length, and directed neurite extensions along the length of the fiber. Zhu et al. (2017) used stereolithography to cure GelMA and PEGDA and then seeded NSCs on top of the scaffold. These constructs showed comparable viability to plated cells. Low-level light stimulation increased cell proliferation and expression of the neural marker TUJ1 (Zhu et al., 2017).

Gu et al. (2016) extruded a bioink made up of alginate, carboxymethyl chitosan (CMC) and agarose seeded with frontal cortical human NSCs. The CMC concentration influenced the cell viability. Immediately after printing 25% of seeded cells died, and cell proliferation peaked on day 11. After 3 weeks, samples stained positive for DAPI and vimentin, but had little SOX2 expression, indicating mature neurons (**Figure 4**).

Similarly, Lozano et al. (2015) extruded a peptide modified gellan gum seeded with primary cortical neurons. Cells remained viable and exhibited neuronal cell morphology after 5 days of culture and stained positive for the neuronal marker TUJ1 (**Figure 5**). A comparable study using FDM to print polyurethane seeded with murine NSCs by Hsieh et al. (2015) observed cell proliferation 72 h after printing. After 3 days, printed NSCs expressed more neurotrophic factor genes than NSCs cultured on tissue culture plates. The corresponding *in vivo* study implanted 3-D printed constructs into cerebellum-lesioned zebrafish. Treated fish showed increased spontaneous coiling contraction and increased hatching rate compared with lesioned untreated fish, indicating cellular restoration.

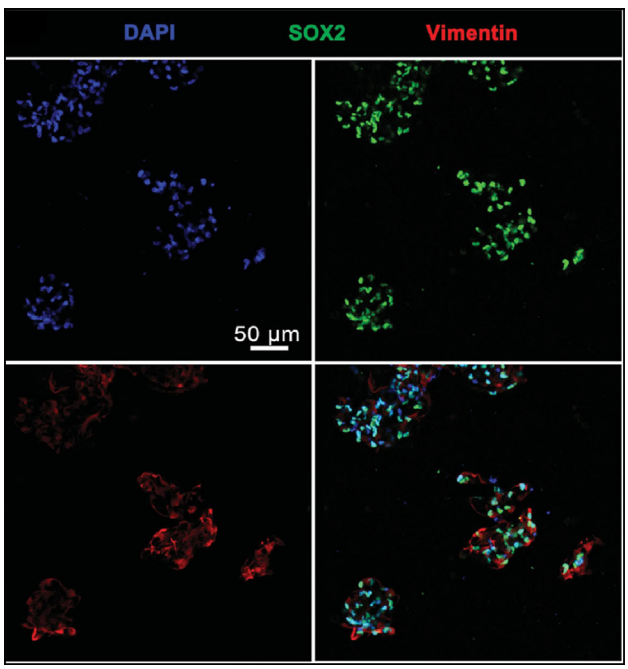

FIGURE 4 | Cells Cells stained with DAPI, vimentin, and SOX2 24 days after printing. Cells largely expressed both DAPI and vimentin, indicating mature neurons. Reprinted with permission from Gu et al. (2016).

Lee et al. (2010) used microextrusion to print collagen and fibrin as well as fibrin loaded with VEGF seeded with murine neural stem cells. Constructs were printed layer-by-layer into a cylindrical shape on a tissue culture dish. Printed cells showed no difference in viability compared with manually plating cells. Cells located up to 1 mm from the fibrin border migrated toward the VEGF-containing fibrin gel, indicating that cells will migrate toward a more permissive region.

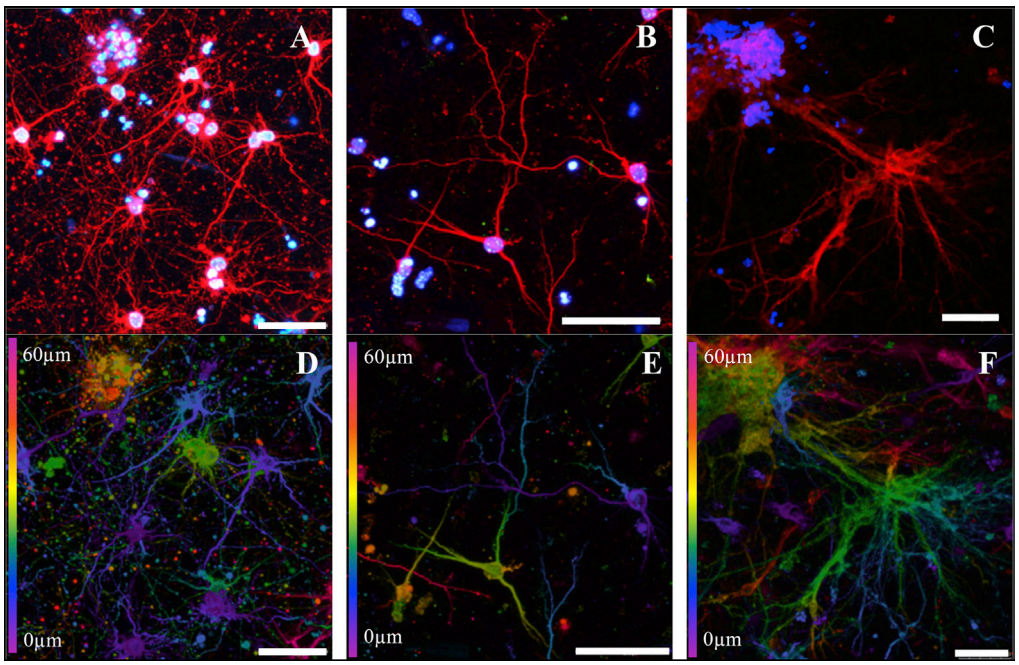

FIGURE 5 | Cortical neurons encapsulated in a peptide modified gellan gum at different gel concentrations (0.075, 0.15, and 0.5% w/v, respectively) after 5 days of culture. **(A–C)** Cells stained with β-III tubulin (red) for cortical neurons and DAPI (blue) for nuclei. **(D–F)** Confocal microscope images (depth decoding) of neuronal 3-D culture models after 5 days of culture. Color decoding for the depth of the cells in the RGD-GG gel along the *Z*-axis is given (0–60 µm). Different colors represent the different planes along the *Z*-axis as shown on the sides of the images. Scale bars represent 50 µm. Reprinted with permission from Lozano et al. (2015).

These studies differ greatly in the number of cells lost due to the stress of the printing process. Cell viability allows the user to seed at the correct cell density. However, some studies do not report cell death while others report up to 57% cell death during the printing (Lorber et al., 2014). Cell death during printing can be due to small nozzle size, polymerization or solidification reactions, or bioink composition (Zhu et al., 2017). Optimizing the bioink makeup is key to reducing the immediate loss of cell viability post-printing.

Current work indicates that a wide variety of bioink materials may be suitable for 3-D printing neural tissue. However, more research needs to be done comparing the printability of each of these materials in terms of efficiency and ease-of-use, both which become important when scaling up production. This review has covered multiple methods of 3-D printing neural constructs. Inkjet bioprinting is the most well documented but is limited in both bioink material and geometries. Microfluidic extrusion has recently seen success in printing complex shapes with various neural cell types and remains an option of interest that needs further research in creating ideal bioink compositions. Other possibilities, such as stereolithography and SLS, remain underused for neural tissue applications.

What remains to be done is finding a cohesive unit of bioink and bioprinting method which results in a high cell viability post-printing and is adaptable enough to print multiple different neural cell types with a bioink which has controllable elastic properties and porosity and can be loaded with factors to further control differentiation.

In addition, most studies lack a hands-off manner of controlling bioprinting. Incorporating CAD and microtechnology into printing projects would help fully realize the high-throughput nature of 3-D bioprinting tissue, as the field is still largely limited by human-controlled systems. The use of CAD would further assist in increasing cell resolution within printed constructs. Advancing the resolution of bioprinting could also allow the printing of vascular networks within a designed tissue, something which would allow neural models to be scaled-up beyond a maximum achieved size of mm. This development would allow more physiologically relevant constructs to be printed for disease modeling and drug discovery.

CONCLUSION

Bioprinting can change how neural tissue are engineered, moving it from a time consuming, hands-on process that can vary from lab-to-lab to a sterile, high-throughput process that can rapidly produce physiologically accurate brain constructs for applications in cell therapy and drug screening. The low throughout methods for engineering brain tissue limit their applicability for drug screening. Cell therapy has had limited success for the same reason: the number of cells required for injection requires lengthy culture time in addition to the difficulty controlling cell diffusion and differentiation. For bioprinting to succeed as the new standard for engineering neural tissue more bioinks must be done to accurately control brain region development, and the issue of vascularization

must be solved to print accurate constructs suitable for long-term culture. However, such bioprinted neural tissues hold great promise for applications in both cell therapy and for drug screening.

AUTHOR CONTRIBUTIONS

MT and SW both contributed to the authorship. SW proposed the topic and provided feedback through the writing process. MT wrote the initial draft and completed revisions based on feedback provided.

FUNDING

This work was supported by the Stem Cell Network Commercialization Impact Grant program along with funding the Natural Science and Engineering Research Council Discovery Grants program and the Canada Research Chair program.

REFERENCES

Ahmad, M. T., and Makoto, N. (2017). Three-dimensional bioprinting: toward the era of manufacturing human organs as spare parts for healthcare and medicine. *Tissue Eng. Part B Rev.* 23, 245–256. doi:10.1089/ten.TEB.2016.0398

Anderson, J. M., and Jones, J. A. (2007). Phenotypic dichotomies in the foreign body reaction. *Biomaterials.* 28, 5114–5120. doi:10.1016/j.biomaterials.2007.07.010

Anderson, J. M., Rodriguez, A., and Chang, D. T. (2008). Foreign body reaction to biomaterials. *Semin. Immunol.* 20, 86–100. doi:10.1016/j.smim.2007.11.004

Bobbert, M. (2006). Ethical questions concerning research on human embryos, embryonic stem cells and chimeras. *Biotechnol. J.* 1, 1352–1369. doi:10.1002/biot.200600179

Caliari, S. R., and Burdick, J. A. (2016). A practical guide to hydrogels for cell culture. *Nat. Methods* 13, 405–414. doi:10.1038/nmeth.3839

Carrow, J. K., Kerativitayanan, P., Jaiswal, M. K., Lokhande, G., and Caharwar, A. (2015). "Polymers for bioprinting," in *Essentials of 3D Biofabrication and Translation*, eds A. Atala and J. J. Yoo (Cambridge, MA: Elsevier Inc), 229–248.

Chambers, S. M., Fasano, C. A., Papapetrou, E. P., Tomishima, M., Sadelain, M., and Studer, L. (2009). Highly efficient neural conversion of human ES and iPS cells by dual inhibition of SMAD signaling. *Nat. Biotechnol.* 27, 275–280. doi:10.1038/nbt.1529

Chia, H. N., and Wu, B. M. (2015). Recent advances in 3D printing of biomaterials. *J. Biol. Eng.* 9, 1–14. doi:10.1186/s13036-015-0001-4

Cooke, M., Vulic, K., and Shoichet, M. (2010). Design of biomaterials to enhance stem cell survival when transplanted into the damaged central nervous system. *Soft Matter* 20, 4988–4998. doi:10.1039/C0SM00448K

Chua, C. K., Leong, K. F., Tan, K. H., Wiria, F. E., and Cheah, C. M. (2004). Development of tissue scaffolds using selective laser sintering of polyvinyl alcohol/hydroxyapatite biocomposite for craniofacial and joint defects. *J. Mater. Sci. Mater. Med.* 15, 1113–1121. doi:10.1023/B:JMSM.0000046393.81449.a5

Cui, G.-H., Shao, S.-J., Yang, J.-J., Liu, J.-R., and Guo, H.-D. (2016). Designer self-assemble peptides maximize the therapeutic benefits of neural stem cell transplantation for Alzheimer's disease via enhancing neuron differentiation and paracrine action. *Mol. Neurobiol.* 53, 1108–1123. doi:10.1007/s12035-014-9069-y

Curley, J., Jennings, S., and Moore, M. (2011). Fabrication of micropatterned hydrogels for neural culture systems using dynamic mask projection photolithography. *J. Vis. Exp.* 48, 2636. doi:10.3791/2636

Dove, A. (2002). Cell-based therapies go live. *Nat. Biotechnol.* 20, 339–343. doi:10.1038/nbt0402-339

Durnaoglu, S., Genc, S., and Genc, K. (2011). Patient-specific pluripotent stem cells in neurological diseases. *Stem Cells Int.* 3, 19–29. doi:10.4061/2011/212487

Edgar, J., Robinson, M., and Willerth, S. (2017). Fibrin hydrogels induce mixed dorsal/ventral spinal neuron identities during differentiation of human induced pluripotent stem cells. *Acta Biomater.* 51, 237–245. doi:10.1016/j.actbio.2017.01.040

Elias, P., and Spector, M. (2012). Implantation of a collagen scaffold seeded with adult rat hippocampal progenitors in a rat model of penetrating brain injury. *J. Neurosci. Methods* 209, 199–211. doi:10.1016/j.jneumeth.2012.06.003

Freed, L. E., Vunjak-Novakovic, G., Biron, R. J., Eagles, D. B., Lesnoy, D. C., Barlow, S. K., et al. (1994). Biodegradable polymer scaffolds for tissue engineering. *Nat. Biotechnol.* 12, 689–693. doi:10.1038/nbt0794-689

Freudenberg, U., Hermann, A., Welzel, P. B., Stirl, K., Schwarz, C., Grimmer, M., et al. (2008). A star-PEG-heparin hydrogel platform to aid cell replacement therapies for neurodegenerative diseases. *Biomaterials* 30, 5049–5060. doi:10.1016/j.biomaterials.2009.06.002

Gardin, C., Vindigni, V., Bressan, E., Ferroni, L., Nalesso, E., Puppa, A. D., et al. (2011). Hyaluronan and fibrin biomaterials as scaffolds for neuronal differentiation of adult stem cells derived from adipose tissue and skin. *Int. J. Mol. Sci.* 12, 6749–6764. doi:10.3390/ijms12106749

Georges, P. C., Miller, W. J., Meaney, D. F., Sawyer, E. S., and Janmey, P. A. (2006). Matrices with compliance comparable to that of brain tissue select neuronal over glial growth in mixed cortical cultures. *Biophys. J.* 90, 3012–3018. doi:10.1529/biophysj.105.073114

Gross, B. C., Erkal, J. L., Lockwood, S. Y., Chen, C., and Spence, D. M. (2014). Evaluation of 3D printing and its potential impact on biotechnology and the chemical sciences. *Anal. Chem.* 86, 3240–3253. doi:10.1021/ac403397r

Gu, Q., Tomaskovic-Crook, E., Lazano, R., Chen, Y., Kapsa, R. M., Zhou, Q., et al. (2016). Functional 3D neural mini-tissues from printed gel-based bioink and human neural stem cells. *Adv. Healthc. Mater.* 5, 1429–1438. doi:10.1002/adhm.201600095

Hoch, E., Tovar, G. E., and Borchers, K. (2014). Bioprinting of artificial blood vessels: current approaches towards a demanding goal. *Eur. J. Cardiothorac. Surg.* 46, 767–778. doi:10.1093/ejcts/ezu242

Hopkins, A. M., DeSimone, E., Chwalek, K., and Kaplan, D. L. (2015). 3D in vitro modeling of the central nervous system. *Prog. Neurobiol.* 125, 1–25. doi:10.1016/j.pneurobio.2014.11.003

Hsieh, F.-Y., Lin, H.-H., and Hsu, S.-H. (2015). 3D bioprinting of neural stem cell-laden thermoresponsive biodegradable polyurethane hydrogel and potential in central nervous system repair. *Biomaterials* 71, 48–57. doi:10.1016/j.biomaterials.2015.08.028

Institute for Neurodegenerative Diseases. (2017). *The Cost of Dementia*. Institute for Neurodegenerative Diseases. Available at: https://ind.ucsf.edu/supporting-our-work/cost-dementia

Itosaka, H., Kuroda, S., Shichinohe, H., Yasuda, H., Yano, S., Kamei, S., et al. (2009). Fibrin matrix provides a suitable scaffold for bone marrow stromal cells transplanted into injured spinal cord: a novel material for CNS tissue engineering. *Neuropathology* 29, 248–257. doi:10.1111/j.1440-1789.2008.00971.x

Itskovitz-Eldor, J., Schuldiner, M., Karsenti, D., Eden, A., Yanuka, O., Amit, M., et al. (2000). Differentiation of human embryonic stem cells into embryoid bodies comprising the three embryonic germ layers. *Mol. Med.* 6, 88–95.

Johnson, P. J., Tatara, A., Shiu, A., and Sakiyama-Elbert, S. E. (2010). Controlled release of neurotrophin-3 and platelet-derived growth factor from fibrin scaffolds containing neural progenitor cells enhances survival and differentiation into neurons in a subacute model of SCI. *Cell Transplant.* 19, 89–101. doi:10.3727/096368909X477273

Kador, K. E., Grogan, S. P., Dorthe, E. W., Veugopalan, P., Malek, M. F., Goldberg, J. L., et al. (2016). Control of retinal ganglion cell positioning and neurite growth: combining 3D printing with radial electrospun scaffolds. *Tissue Eng. Part A* 22, 286–294. doi:10.1089/ten.TEA.2015.0373

Kamao, H., Mandai, M., Wakamiya, S., Ishida, J., Goto, K., Ono, T., et al. (2014). Objective evaluation of the degree of pigmentation in human induced pluripotent stem cell-derived RPE. *Invest. Ophthalmol. Vis. Sci.* 55, 8309–8318. doi:10.1167/iovs.14-14694

Kim, S. U. (2004). Human neural stem cells genetically modified for brain repair in neurological disorders. *Neuropathology* 24, 159–171. doi:10.1111/j.1440-1789.2004.00552.x

Kohler, M., Hirshberg, B., Bond, C. T., Kinzie, J. M., Marrion, N. V., Maylie, J., et al. (1996). Small-conductance, calcium-activated potassium channels from mammalian brain. *Science* 273, 1709–1714. doi:10.1126/science.273.5282.1709

Kolehmainen, K., and Willerth, S. M. (2012). Preparation of 3D fibrin scaffolds for stem cell culture applications. *J. Vis. Exp.* e3641. doi:10.3791/3641

Lancaster, M. A., Renner, M., Martin, C.-A., Wenzel, D., Bicknell, L. S., Hurles, M. E., et al. (2013). Cerebral organoids model human brain development and microcephaly. *Nature* 501, 373–379. doi:10.1038/nature12517

Lee, S.-J., Nowicki, M., Harris, B., and Zhang, L. G. (2017). Fabrication of a highly aligned neural scaffold via a table top stereolithography 3D printing and electrospinning. *Tissue Eng. Part A* 23, 491–502. doi:10.1089/ten.TEA.2016.0353

Lee, Y.-B., Polio, S., Lee, W., Dai, G., Menon, L., Carroll, R. S., et al. (2010). Bio-printing of collagen and VEGF-releasing fibrin gel scaffolds for neural stem cell culture. *Exp. Neurol.* 223, 645–652. doi:10.1016/j.expneurol.2010.02.014

Levy, M., Boulis, N., Rao, M., and Svendsen, C. N. (2016). Regenerative cellular therapies for neurologic diseases. *Brain Res.* 1638, 88–96. doi:10.1016/j.brainres.2015.06.053

Lippmann, E., Estevez-Silva, M., and Ashton, R. (2014). Defined human pluripotent stem cell culture enables highly efficient neuroepithelium derivation without small molecule inhibitors. *Stem Cells* 32, 1032–1042. doi:10.1002/stem.1622

Lorber, B., Hsiao, W.-K., Hutchings, I. M., and Martin, K. R. (2014). Adult rat retinal ganglion cells and glia can be printed by piezoelectric inkjet printing. *Biofabrication* 6, 015001. doi:10.1088/1758-5082/6/1/015001

Lozano, R., Stevens, L., Thompson, B. C., Gilmore, K. J., Gorkin, R., Stewart, E. M., et al. (2015). 3D printing of layered brain-like structures using peptide modified gellan gum substrates. *Biomaterials* 67, 264–273. doi:10.1016/j.biomaterials.2015.07.022

Lu, P., Wang, Y., Graham, L., McHale, K., Gao, M., Wu, D., et al. (2012). Long-distance growth and connectivity of neural stem cells after severe spinal cord injury. *Cell* 150, 1264–1273. doi:10.1016/j.cell.2012.08.020

McMahon, M. A., Rahdar, M., and Porteus, M. (2012). Gene editing: not just for translation anymore. *Nat. Methods* 9, 28–31. doi:10.1038/nmeth.1811

Montgomery, A., Wong, A., Gabers, N., and Willerth, S. (2015). Engineering personalized neural tissue by combining induced pluripotent stem cells with fibrin scaffolds. *Biomater. Sci.* 3, 401–403. doi:10.1039/c4bm00299g

Mothe, A. J., and Tator, C. H. (2012). Advances in stem cell therapy for spinal cord injury. *J. Clin. Invest.* 122, 3824–3834. doi:10.1172/JCI64124

Murphy, S. V., and Atala, A. (2014). 3D bioprinting of tissues and organs. *Nat. Biotechnol.* 32, 773–785. doi:10.1038/nbt.2958

O'Brien, C., Holmes, B., Faucett, S., and Zhang, L. (2015). Three-dimensional printing of nanomaterial scaffolds for complex tissue regeneration. *Tissue Eng. Part B* 21, 103–114. doi:10.1089/ten.TEB.2014.0168

Partee, B., Hollister, S. J., and Das, S. (2006). Selective laser sintering process optimization for layered manufacturing of CAPA® 6501 polycaprolactone bone tissue engineering scaffolds. *J. Manuf. Sci. Eng.* 128, 531–540. doi:10.1115/1.2162589

Perez, R. A., Choi, S.-J., Han, C.-M., Kim, J.-J., Shim, H., Leong, K. W., et al. (2016). Biomaterials control of pluripotent stem cell fate for regenerative therapy. *Prog. Mater. Sci.* 82, 234–293. doi:10.1016/j.pmatsci.2016.05.003

Pfister, A., Landers, R., Laib, A., Hubner, U., Schmelzeisen, R., and Mulhaupt, R. (2004). Biofunctional rapid prototyping for tissue-engineering applications: 3D bioplotting versus 3D printing. *J. Polym. Sci. Part A* 42, 624–638. doi:10.1002/pola.10807

Pittier, R., Sauthier, F., Hubbell, J., and Hall, H. (2005). Neurite extension and in vitro myelination within three-dimensional modified fibrin matrices. *J. Neurobiol.* 63, 1–14. doi:10.1002/neu.20116

Potter, S. M., and DeMarse, T. B. (2001). A new approach to neural cell culture for long-term studies. *J. Neurosci. Methods* 110, 17–24. doi:10.1016/S0165-0270(01)00412-5

Rafat, H. S., Yoshikazu, O., and Puri, R. K. (2017). Current status and challenges of three-dimensional modeling and printing of tissues and organs. *Tissue Eng. Part A* 23, 471–473. doi:10.1089/ten.tea.2017.29000.srh

Robinson, M., Yau, S.-Y., Sun, L., Gabers, N., Bibault, E., Christie, B. R., et al. (2015). Optimizing differentiation protocols for producing dopaminergic neurons from human induced pluripotent stem cells for tissue engineering applications. *Biomarkers Insight* (Suppl. 1), 61–70. doi:10.4137/BMI.S20064

Rossi, F., and Cattaneo, E. (2002). Opinion: neural stem cell therapy for neurological diseases: dreams and reality. *Nat. Rev. Neurosci.* 3, 401–409. doi:10.1038/nrn809

Schwartz, M. P., Hou, Z., Propson, N. E., Zhang, J., Engstrom, C. J., Santos Costa, V., et al. (2015). Human pluripotent stem cell-derived neural constructs for predicting neural toxicity. *Proc. Natl. Acad. Sci. U.S.A.* 112, 12516–12521. doi:10.1073/pnas.1516645112

Shao, Y., Sang, J., and Fu, J. (2015). On human pluripotent stem cell control: the rise of 3D bioengineering and mechanobiology. *Biomaterials* 52, 26–43. doi:10.1016/j.biomaterials.2015.01.078

Skardal, A., and Atala, A. (2015). Biomaterials for integration with 3-D bioprinting. *Ann. Biomed. Eng.* 43, 730–746. doi:10.1007/s10439-014-1207-1

Struzyna, L. A., Katiyar, K., and Cullen, D. K. (2014). Living scaffolds for neuroregeneration. *Curr. Opin. Solid State Mater. Sci.* 18, 308–318. doi:10.1016/j.cossms.2014.07.004

Suri, S., Han, L.-H., Zhang, W., Singh, A., Chen, S., and Schmidt, C. E. (2011). Solid freeform fabrication of designer scaffold of hyaluronic acid for nerve tissue engineering. *Biomed. Microdevices* 13, 983–993. doi:10.1007/s10544-011-9568-9

Sykova, E., Jendelova, P., and Urdzikova, L. (2006). Bone marrow stem cells and polymer hydrogels – two strategies for spinal cord injury repair. *Cell. Mol. Neurobiol.* 26, 111–127. doi:10.1007/s10571-006-9007-2

Takahashi, K., Tanabe, K., Ohnuki, M., Narita, M., Ichisaka, T., Tomoda, K., et al. (2007). Induction of pluripotent stem cells from adult human fibroblasts by defined factors. *Cell* 131, 861–872. doi:10.1016/j.cell.2007.11.019

Tam, R. Y., Fuehrmann, T., Mitrousis, N., and Shoichet, M. S. (2014). Regenerative therapies for central nervous system diseases: a biomaterials approach. *Neuropsychopharmacology* 39, 169–188. doi:10.1038/npp.2013.237

Tan, K. H., Chua, C. K., Leong, K. F., Cheah, C. M., Gui, W. S., Tan, W. S., et al. (2005). Selective laser sintering of biocompatible polymers for applications in tissue engineering. *Biomed. Mater. Eng.* 15, 113–124.

Tate, C. C., Shear, D. A., Tate, M. C., Archer, D. R., Stein, D. G., and LaPlaca, M. C. (2009). Laminin and fibronectin scaffolds enhance neural stem cell transplantation into the injured brain. *J. Tissue Eng. Regen. Med.* 3, 208–217. doi:10.1002/term.154

Tsintou, M., Dalamagkas, K., and Seifalian, A. (2015). Advances in regenerative therapies for spinal cord injury: a biomaterials approach. *Neural Regen. Res.* 10, 726–742. doi:10.4103/1673-5374.156966

Vila, M., and Przedborksi, S. (2003). Targeting programmed cell death in neurodegenerative diseases. *Nat. Rev. Neurosci.* 4, 365–375. doi:10.1038/nrn1100

Wang, Y., Kim, Y. M., and Langer, R. (2003). *In vivo* degradation characteristics of poly(glycerol sebacate). *J. Biomed. Mater. Res. A.* 66A, 192–197. doi:10.1002/jbm.a.10534/

Wilems, T. S., Pardieck, J., Iyer, N., and Sakiyama-Elbert, S. E. (2015). Combination therapy of stem cell derived neural progenitors and drug delivery of anti-inhibitory molecules for spinal cord injury. *Acta Biomater.* 28, 23–32. doi:10.1016/j.actbio.2015.09.018

Willerth, S., Arendas, K., Gottlieb, D., and Sakiyama-Elbert, S. (2006). Optimization of fibrin scaffolds for differentiation of murine embryonic stem cells into neural lineage cells. *Biomaterials* 27, 5990–6003. doi:10.1016/j.biomaterials.2006.07.036

Willerth, S., Faxel, T., Gottlieb, D., and Sakiyama-Elbert, S. (2007a). The effects of soluble growth factors on embryonic stem cell differentiation inside of fibrin scaffolds. *Stem Cells* 25, 2235–2244. doi:10.1634/stemcells.2007-0111

Willerth, S., Johnson, P., Maxwell, D., Parsons, S., Doukas, M., and Sakiyama-Elbert, S. (2007b). Rationally designed peptides for controlled release of nerve growth factor from fibrin matrices. *J. Biomed. Mater. Res. A.* 80, 13–23. doi:10.1002/jbm.a.30844

Willerth, S., Rader, A., and Sakiyama-Elbert, S. (2008). The effects of controlled growth factor release on embryonic stem cell differentiation inside of fibrin scaffolds. *Stem Cell Res.* 2, 205–218. doi:10.1016/j.scr.2008.05.006

Xu, T., Gregory, C. A., Molnar, P., Cui, X., Jalota, S., Bhaduri, S. B., et al. (2006). Viability and electrophysiology of neural cell structures generated by the inkjet printing method. *Biomaterials* 27, 3580–3588. doi:10.1016/j.biomaterials.2006.01.048

Zhu, W., George, J. K., Sorger, V. J., and Zhang, L. G. (2017). 3D printing scaffold coupled with low level light therapy for neural tissue regeneration. *Biofabrication* 9, 025002. doi:10.1088/1758-5090/aa6999

Conflict of Interest Statement: The authors declare that the research was conducted in the absence of any commercial or financial relationships that could be construed as a potential conflict of interest.

frontiers in Materials

ORIGINAL RESEARCH
published: 28 June 2018
doi: 10.3389/fmats.2018.00040

The Feasibility of Encapsulated Embryonic Medullary Reticular Cells to Grow and Differentiate Into Neurons in Functionalized Gelatin-Based Hydrogels

Ana M. Magariños[1]*, *Sara Pedron*[2], *Marc Creixell*[1], *Murat Kilinc*[1], *Inna Tabansky*[1], *Donald W. Pfaff*[1] and *Brendan A. C. Harley*[2,3]*

[1] Laboratory of Neurobiology and Behavior, The Rockefeller University, New York, NY, United States, [2] Carl R. Woese Institute for Genomic Biology, University of Illinois at Urbana-Champaign, Urbana, IL, United States, [3] Department of Chemical and Biomolecular Engineering, University of Illinois at Urbana-Champaign, Urbana, IL, United States

OPEN ACCESS

Edited by:
Evelyn K. F. Yim,
University of Waterloo, Canada

Reviewed by:
Lohitash Karumbaiah,
University of Georgia, United States
Silviya Petrova Zustiak,
Saint Louis University, United States

***Correspondence:**
Ana M. Magariños
amagarinos@rockefeller.edu
Brendan A. C. Harley
bharley@illinois.edu

Specialty section:
This article was submitted to Biomaterials, a section of the journal Frontiers in Materials

Received: 31 January 2018
Accepted: 08 June 2018
Published: 28 June 2018

Citation:
Magariños AM, Pedron S, Creixell M, Kilinc M, Tabansky I, Pfaff DW and Harley BAC (2018) The Feasibility of Encapsulated Embryonic Medullary Reticular Cells to Grow and Differentiate Into Neurons in Functionalized Gelatin-Based Hydrogels. Front. Mater. 5:40. doi: 10.3389/fmats.2018.00040

The study of the behavior of embryonic neurons in controlled *in vitro* conditions require methodologies that take advantage of advanced tissue engineering approaches to replicate elements of the developing brain extracellular matrix. We report here a series of experiments that explore the potential of photo-polymerized gelatin hydrogels to culture primary embryonic neurons. We employed large medullary reticular neurons whose activity is essential for brain arousal as well as a library of gelatin hydrogels that span a range of mechanical properties, inclusion of brain-mimetic hyaluronic acid, and adhesion peptides. These hydrogel platforms showed inherent capabilities to sustain neuronal viability and were permissive for neuronal differentiation, resulting in the development of neurite outgrowth under specific conditions. The maturation of embryonic medullary reticular cells took place in the absence of growth factors or other exogenous bioactive molecules. Immunocytochemistry labeling of neuron-specific tubulin confirmed the initiation of neural differentiation. Thus, this methodology provides an important validation for future studies of nerve cell growth and maintenance.

Keywords: 3D cell culture, hyaluronic acid, neurons, nucleus gigantocellularis, brain development, biomaterial models, gelatin hydrogels

INTRODUCTION

Large reticular formation neurons in the medulla, neurons in the nucleus gigantocellularis (NGC), have recently been identified as master cells responsible for the arousal of the mammalian brain (Calderon et al., 2016). NGC neurons are located just above the spinal cord and are essential for supporting generalized CNS arousal (Pfaff, 2006), responsible for facilitating the initiation and vigor of all motivated behaviors. They may have evolved from the large Mauthner cells similarly placed in the fish hindbrain and similarly responsible for the rapid initiation of behavior (Pfaff et al., 2014). These nerve cells have extremely wide dendritic arbors and are able to respond to stimuli in all sensory modalities tested (Martin et al., 2010, 2011). Their axonal distribution encompasses ascending projections to the thalamus

and hypothalamus and descending projections to all levels of the spinal cord, bilaterally (Jones and Yang, 1985). Their increase in excitability activates the electroencephalogram in a deeply anesthetized animal (Wu et al., 2007) and their growing ability to fire trains of action potentials as a mouse pup grows from postnatal day 3 to postnatal day 6 is correlated with the increased behavioral arousal of the mouse pup during those 4 days (Liu et al., 2016). As a result, increasingly detailed studies of these neurons under controlled conditions may yield significant new information to help understand their roles in brain function and response to injury. However, such studies are difficult in traditional *in vivo* settings.

It is generally acknowledged that standard 2D *in vitro* systems lack important architectural features of native tissues. Tissue engineering approaches have increasingly been used to recreate a myriad of tissue microenvironments in the context of tissue regeneration or for the development of *in vitro* model systems for the study of biological processes, personalized medicine, and pharmacological testing (Neves et al., 2016; Pradhan et al., 2016; Caballero et al., 2017). However, fabrication of *ex vivo* cerebral tissue has been elusive, due to the high complexity, including multiple hierarchical levels of interconnected neuronal networks. Tumor models have been described within hydrogel matrices (Xiao et al., 2017) and neural cells have been encapsulated successfully within synthetic (Mckinnon et al., 2013), natural (Palazzolo et al., 2015; Alessandri et al., 2016), and protein (Lampe et al., 2013) hydrogels. Besides the use of bulk hydrogels, more sophisticated fabrication techniques have been used such as three-dimensional printing (Gu et al., 2016), lithography (Gurkan et al., 2013), and compartmentalized scaffolds (Tang-Schomer et al., 2014). Organoids of certain regions of the brain have been described (Di Lullo and Kriegstein, 2017) but they lack the oxygen and nutrient diffusion provided by biocompatible hydrogel matrices. In order to study the development of these NGC neurons, complementary to *in vivo* studies, 3-dimensional growth platforms may be an ideal framework that could mimic features of the brain's unique extracellular matrix.

Hydrogel technologies have become increasingly well developed, with recent efforts beginning to utilize a series of hydrogel platforms to study features of brain tumor such as primary glioblastoma (GBM) or tumor metastasis to the brain (Rape et al., 2014; Heffernan et al., 2015; Kingsmore et al., 2016; Chung et al., 2017; Pedron et al., 2017a,b). Recent efforts in our lab have focused on the development of a class of photopolymerizable gelatin hydrogels. Gelatin is a natural polymer that provides cell binding sites (e.g., RGD) and degradation moieties (e.g., MMP sensitive). The functionalization with methacrylamide groups allows for the formation of a covalently crosslinked gel (Pedron and Harley, 2013). Hyaluronic acid (HA) is the major component in the fetal mammalian brain ECM (Baier et al., 2007) and it has been used to culture neuronal cells (Seidlits et al., 2010). Efforts in our lab have demonstrated covalent incorporation of methacrylated hyaluronic acid into a methacrylamide functionalized gelatin hydrogel, yielding the capacity to orthogonally manipulate hydrogel stiffness and HA content within the hydrogel. In addition to providing a platform to explore the effect of matrix-immobilized HA on GBM cell expansion, invasion, and response to therapeutic inhibitors (Chen et al., 2017; Pedron et al., 2017a), we recently demonstrated it was possible to incorporate vascular cells into the hydrogel, yielding complex vascular networks that remodeled over time (Ngo and Harley, 2017). While 3D organoid-type cultures have fostered the production of "human brain-like tissue" (Sasai, 2013; Lancaster and Knoblich, 2014), so far attention has focused primarily on forebrain cell groups (Birey et al., 2017; Quadrato et al., 2017) or traumatic brain injury (Tang-Schomer et al., 2014), yielding opportunities to explore.

This project set out to examine the translation of a HA-modified gelatin hydrogel for the *in vitro* culture of NGC neurons. To date, these neural cells have not been studied *ex vivo*, and given their relevance in linking brain development to behavior, a permissive culture system will allow neuroscientists systematically to sort out the separate contributions of extracellular matrix components and growth factors to their survival, growth and development. Here we report examination of the ability to grow NGC neurons *in vitro* in such hydrogels without the assistance of growth factors.

MATERIALS AND METHODS

Hydrogel Preparation and Characterization

Gelatin methacrylamide (GelMA) and HA methacrylate (HAMA) were synthesized as described previously (Pedron et al., 2015). The degree of functionalization (%DOF) was established by NMR as the ratio of methacrylamide groups (5.5 ppm) to aromatic groups (7.3 ppm). Freeze dried GelMA (3.5 wt%) was mixed with HAMA (0.5 wt%) into PBS containing 0.02% (w/v) lithium phenyl-2,4,6-trimethyl benzoyl phosphinate (LAP) as a photoinitiator until fully dissolved. Prepolymer solution was pipetted into Teflon molds 1.5 mm deep and 5 mm in diameter, and exposed to 10 mW/cm^2 UV light (365 nm, LED AccuCure Spot) for 20 s.

Mechanical analyses were performed on fully swollen disks as described previously (Pedron et al., 2013). Specimens were tested in compression at room temperature via an Instron 5493 (100 N load cell) mechanical testing apparatus (20% strain/min). The compressive modulus was determined from the linear region corresponding to ∼0–5% strain. Full laminin protein was replaced by CYIGSR sequence (generated at the Rockefeller University Proteomics Resource Center) previously described in the literature to support neuronal adhesion and growth (Mckinnon et al., 2013).

Experimental Animals

C57BL/6/J mice (Jackson Laboratories) were maintained on a 12/12 light dark cycle with lights on at 7 a.m. and free access to water and food. Adult male and female animals were paired in the late afternoon to obtain timed pregnant dams and the morning when the formation of a vaginal plug was observed was counted as embryonic day 0. All experimental procedures were performed in accordance with the NIH guide for care and use of animals and approved by the Animal Care and Use Committee

at The Rockefeller University. Pregnant females at 12 days post conception (E12) were sacrificed by cervical dislocation. After cleaning the abdomen with an excess of 70% ethanol, a V-shape cut was performed onto the abdomen through the skin and muscle layers to expose the peritoneum. The uterine horns were removed and transferred into a clean plastic dish containing ice-cold dissection buffer (DB) consisting of Hanks balanced salt solution, HBSS, Ca^{2+}, Mg^{2+} free (Gibco), 20 mM D-Glucose (Sigma Aldrich) and 1% penicillin/streptomycin (Gibco). The average number of embryos per pregnant female was 6–8.

Hindbrain Dissection and Primary E12 Hindbrain Cell Cultures

Under a dissecting stereomicroscope (Zeiss, model 10298), each embryo sac was separated from the intact uterine horns. The embryos were transferred to a clean plastic dish containing fresh ice-cold DB. The embryonic hindbrains were dissected according to Fantin et al. (2013) and the hindbrain dissociations were performed immediately after (see below). On average, the timing of dissection was 5 min per hindbrain.

Hindbrain Dissociation

The collected hindbrains in DB were transferred to the tissue culture hood, and they were transferred to one of the wells of a 24-multiwell plate containing fresh DB. The dissection buffer was then replaced with 500 µl of the pre-warmed enzymatic cell dissociation reagent (StemPro® Accutase, Thermo Fisher Scientific) and incubated at 37°C for 5 min with gentle shaking. The hindbrains were then mechanically dissociated pipetting up and down 12 times using a 1,000 µl tip and 12 more times using a 200 µl tip. Great care was taken in avoiding the formation of air bubbles during this step to maximize cell viability. The overall enzymatic and mechanical hindbrain dissociation step never exceeded 7 min. The enzymatic digestion was stopped by adding 3 ml of standard medium containing Dulbecco's Modified Eagle's Medium, DMEM (Gibco) supplemented with 10% fetal bovine serum (Gibco) and 1% penicillin/streptomycin (Gibco). The resulting cell suspension was filtered through a tube fitted with a cell strainer snap cap (35 µm nylon mesh, Falcon), transfer to a 15 ml Falcon tube and further diluted with standard media to a final volume of 10 ml. After gentle inversion, an aliquot of the suspension was mixed with an equal volume of trypan blue and the viable cell yield (cells/ml) was estimated using a Neubauer chamber. Immediately after, the volume of the suspension was adjusted with media to the desired cell concentration per gel and the samples were centrifuged at 200 g for 4 min at room temperature. After discarding the supernatant, the resulting cell pellet was immediately resuspended on the prepolymer hydrogel mixture (see section below).

Encapsulation of Dissociated Embryonic Hindbrain Cells

We examined a library of hydrogel prepolymer solutions that varied by the overall total polymer concentration (5 or 4 wt%), the degree of methacrylamide functionalization of the gelatin macromer (DOF: 85, 60, or 55%), the fraction of HAMA (0.5 or 1 wt%) added to the GelMA solution, or the amount of LAP photoinitiator (0.05, 0.02 wt%) used to polymerize the hydrogel (**Table 1**). To promote the attachment of the embryonic hindbrain dissociated cells, a subset of hydrogels were functionalized with 800 µg/ml of a laminin peptide mimic (CYIGSR). The hydrogel components were dissolved in warm (45°C) neurobasal serum-free medium consisting of neurobasal medium, 2% B27 Supplement, 1% Glutamax, 1% penicillin/streptomycin. In one experiment, the components were dissolved in phosphate buffer saline as a control. All reagents were purchased from Gibco. The solution was kept at 37°C until the cell pellet was ready to be resuspended. After gently mixing, either 30 µl (10 million cells per ml) of the embryonic hindbrain cell suspension was pipetted onto Teflon molds anchored on top of a glass slide and secured with binder clips (Pedron et al., 2013, 2017a). Hydrogels were subsequently created: disks of 5 mm diameter; the height of the gels was 1.5 mm. The cell-laden prepolymer suspension was photopolymerized by exposure to 10 mW/cm^2 UV light (365 nm) for 20 or 30 s (**Table 1**). Neurobasal medium was added to the gels immediately after polymerization to prevent dehydration. Each cell-seeded hydrogel was then transferred to a well of a 24-multiwell plate (Corning) containing neurobasal media and incubated at 37°C, 5% CO_2 on top of the plate of an orbital shaker (lowest speed setting) inside a cell culture incubator. Neurobasal medium was exchanged every 3 days over the course of all experiments.

Live/Dead Cell Viability Assay

The evaluation of cell viability was performed at 7 and 14 days *in vitro* (DIV) using the Live/Dead assay (Molecular Probes). After rinsing hydrogels with PBS (3X for 5 min each) they were incubated at room temperature with PBS containing 2 µM Calcein-AM (stains the cytoplasm of viable cells green) and 4 µM ethidium homodimer-1 (stains the nuclei of dead cells red). After 40 min, the cell-laden hydrogels were rinsed in PBS and immediately imaged using a confocal microscope (Zeiss LSM 880 inverted confocal laser scanning microscope). Because the hydrogel area exceeded an individual confocal image field we acquired the complete hydrogel image using the tile module

TABLE 1 | The composition (overall hydrogel wt %; GelMA/HAMA ratio; degree of methacrylamide functionalization of the gelatin macromer; inclusion of CYIGSR peptide), fabrication conditions (photoinitiator wt%; UV exposure time), and resulting elastic modulus ($n = 4$) of the family of hydrogel samples used in the encapsulation of NGC cells.

Total wt%	GelMA/HAMA %wt	DOF %	CYIGSR µg/ml	PI wt%	Time (s)	Modulus kPa
5	4.5/0.5	85	0	0.05	30	8.7 ± 0.8
4	3/1	60	0	0.02	20	5.0 ± 0.3
4	3/1	55	0	0.02	20	5.0 ± 0.3
4	3/1	55	800	0.02	20	
4	3.5/0.5	55	0	0.02	20	1.1 ± 0.2
4	3.5/0.5	55	800	0.02	20	

included in the Zen confocal software (Zeiss). Starting at the surface and imaging down toward the center of the hydrogel, the first and last z positions for each z-stack/tile were defined for a total thickness of 100 or 200 μm. The acquired image tiles were then combined into one final output by a stitching process using a 10% tile overlap. For automated cell counts, and estimation of cell viability, the stitched output images were imported to the 3D rendering software Imaris (Bitplane). We used the spot detection module, and spots were defined using cell count parameters for size and fluorescence strength of voxels to represent each cell soma. Parameters were then subjected to multiple image tests between manually counted and automated cell counts in multiple regions of interest of the imported tiled images to ensure accuracy. Because the quantification of spots using 200 and 100 μm thick tiled z-stacks did not differ statistically within hydrogels, we did the analysis using the thinner tiled z-stacks images. After validation, parameters were saved and then applied through the entire 100 μm z-stacks and overall cell count data was obtained for each image. Cell viability was calculated as (number of green stained cells/number of total cells) X 100%.

Immunocytochemistry

After 7 days *in vitro*, cell-laden hydrogels were rinsed 3X in PBS for 5 min per rinse and then fixed in 4% paraformaldehyde (Sigma Aldrich) for 5 min at room temperature. After rinsing with PBS, the gels were permeabilized with 0.5% Triton X-100 (Sigma Aldrich), blocked with 5% donkey serum (Invitrogen) and incubated overnight at 4°C with anti-TUJ1 mouse IgG primary antibody (1:1,000, Biolegend). Hydrogels were rinsed in PBS and then incubated for 2 h at room temperature with donkey anti-mouse IgG secondary antibody conjugated to Alexa Fluor 488 (Life Technologies, 1:1,000). Cellular nuclei were counter stained with 0.4 μl/ml DAPI in PBS for 5 min. The labeled hydrogels were examined and imaged using a Zeiss LSM 880 inverted confocal laser scanning microscope.

Statistics

Statistical analysis was performed via one-way analysis of variance (ANOVA) tests after which a Tukey-HSD *post-hoc* test was used. Analysis of hydrogel mechanical properties used $n = 5$ constructs per group. Significance was set at $p < 0.05$. Error bars are reported as standard error of the mean unless otherwise noted.

RESULTS

Gelatin-Based Hydrogel Fabrication

Both the biomechanical and cell-adhesive properties of 3D hydrogel matrices are critical for the viability and behavior of encapsulated cultured cells. Initially, the conditions used for the encapsulation of E12.5 hindbrain cells comprised the use of 5 wt% total polymer concentration with an 85% degree of functionalization and 0.05 wt% photoinitiator. These conditions resulted in highly crosslinked polymer network that led to stiff hydrogels (8.7 ± 0.8 kPa) and proved to be highly detrimental to the survival and differentiation of the embryonic cells (data not shown). With the aim of designing a more compliant hydrogel, in subsequent experiments, we resorted to a hydrogel containing a lower total polymer concentration (4 wt%), lower degrees of functionalization of GelMA (60 or 55%), and photoinitiator concentration of 0.02 wt%. The more permissive conditions (1.1 ± 0.2 kPa) for cell viability resulted from platforms containing 55% DOF GelMA and 0.02 wt% concentration of photoinitiator. Interestingly, the addition of matrix immobilized HA to the GelMA hydrogel proved to be beneficial to sustain cell viability and differentiation, in some cases, of neuritic processes. The hydrogel composition employed

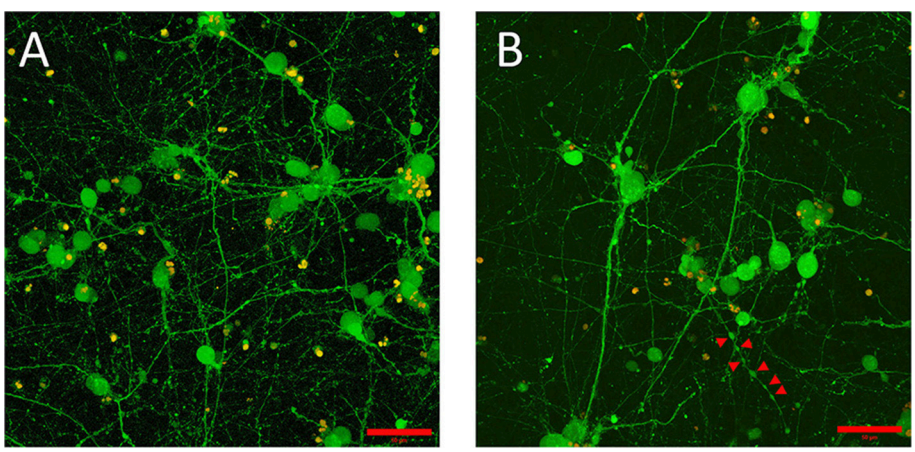

FIGURE 1 | Embryonic 12.5 (E12.5) hindbrain cells encapsulated in 3D hydrogel scaffolds (GelMA/HAMA: 3.5/0.5 wt%, no laminin added) remained viable after 10 days *in vitro* (10DIV). **(A)** Maximum intensity projection depicts cell bodies projecting extensive processes adopting elaborated arborization patterns. Viable cells, shown in green, were labeled with calcein-AM (see Materials and Methods section for details). Scale bar: 50 μm. **(B)** Some encapsulated E12.5 hindbrain cells [same conditions as **(A)**] showed varicose neurites. Red arrows indicate the putative boutons along the neurite outgrowth. Scale bar: 50 μm.

in the present report consisted of GelMA/HAMA 3.5/0.5% and 0.02% photoinitiator.

Survival and Growth of Nucleus Gigantocellularis (NGC) Neurons

The initial, pre-gel viability of these NGC neurons measured by dye exclusion was in the range of 60–85%. Cells encapsulated within the GelMA/HAMA (3.5/0.5 wt%) hydrogels and their associated neurite processes remained viable for up to 2 weeks *in vitro*. Cell viability at the termination of experiments was found to be between 30 and 60% as measured by the Live/Dead assay. Viable neurons usually sent out neurite processes, in some cases with the primary neurite branching and producing second-level or even third-level neurite segments (**Figure 1A**). This phenomenon was highly variable, both within and between gels. In some cases, neurites displayed ovoid varicosities along their length, with complex neuronal processes observed after 2 weeks *in vitro* (**Figure 1B**). Importantly, neurons were distributed three-dimensionally throughout the hydrogel, with **Figure 2** depicting NGC cells extending processes (color coded by depth of penetration) into the hydrogel scaffolding.

Experiments did not include a systematic comparison of results with and without laminin. Instead, it must be said that, while it was possible to see robust neuronal network formation in hydrogels containing the laminin peptide (800 μg/ml) (**Figure 3**), morphologically similar results could be observed in the absence of laminin (**Figure 4**).

Neuronal Differentiation of NGC Cells

We subsequently explored the initial stages of neuronal differentiation of NGC cells maintained within the HA-modified

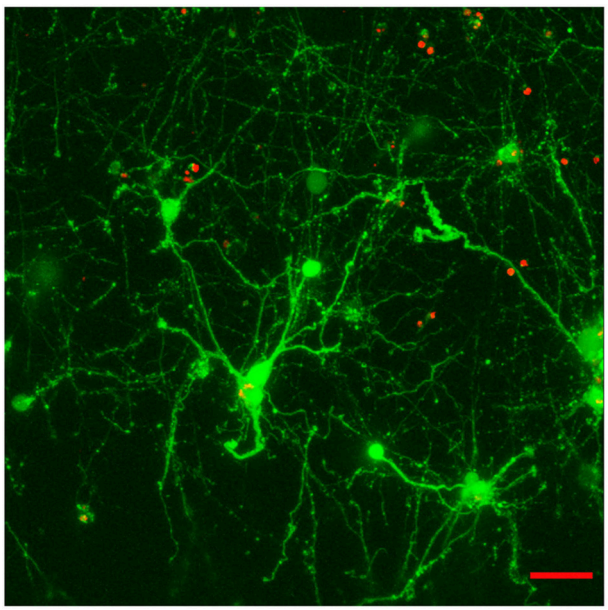

FIGURE 3 | Effect of the incorporation of a cell-adhesive laminin peptide mimic into E12.5 hindbrain cell-laden hydrogels (GelMA/HAMA: 3.5/0.5 wt% plus 800 μg/ml CYIGSR) after 15DIV. Maximum projection of a 70 μm z-stack showing that encapsulated cells mature and give out neurites in the presence of laminin mimic. Scale bar: 50 μm.

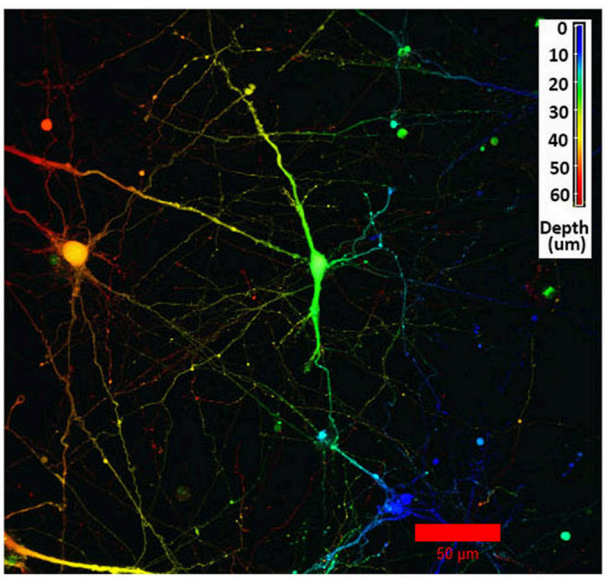

FIGURE 2 | Confocal microscopy image using depth decoding of an E12.5 hindbrain cell hydrogel culture (GelMA/HAMA: 3.5/0.5 wt%, no laminin added) after 15DIV. Color decoding for the depth of the cells in the hydrogel along the z-axis is given. The difference in colors indicate the different planes along the z-axes. Scale bar: 50 μm.

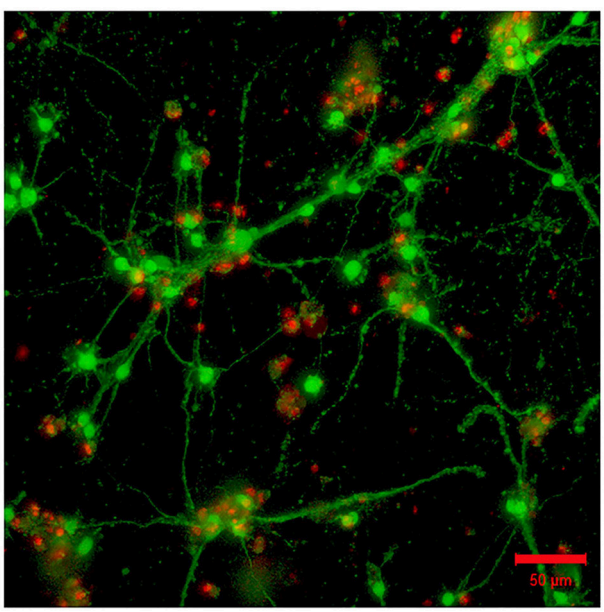

FIGURE 4 | Absence of laminin in the 3D hydrogel (GelMA/HAMA: 3.5/0.5 wt%) is permissive for the outgrowth of neurites from encapsulated embryonic hindbrain cells after 15DIV. Scale bar: 50 μm.

GelMA hydrogel. Excitingly, viable NGC cells adopted a neuronal morphology. Immunocytochemistry using an antibody against neuron-specific class III-beta-tubulin, a microtubule component used as a neuronal marker, confirmed that the cells encapsulated within the GelMA hydrogels displayed a neuronal phenotype (**Figure 5**). Further, after 7 days of culture in the hydrogels *in vitro*, cellular processes exhibited morphologies suggesting that they could form more complex neuronal networks.

DISCUSSION

This work shows that it is possible to grow embryonic reticular formation neurons in 3D hydrogels in the absence of growth factors or nerve cell adhesion molecules. The neurons used, from the medial medullary reticular formation, which would include the large cells of nucleus gigantocellularis, are crucial for CNS arousal and the initiation of a wide range of behaviors. It remains to be seen whether optimum conditions for such neurons differ from those, for example, in the forebrain (Birey et al., 2017).

We selected gelatin-HA hydrogel as the base material for the fabrication of culture platforms for NGC neurons due to their success in hosting mammalian cells (Du et al., 2017), and our previous experience with cancerous glial cells (Chen et al., 2017; Pedron et al., 2017a,b). Biophysical properties of gelatin hydrogels can be easily manipulated by dialing concentration, degree of functionalization and photoreaction conditions (Pedron and Harley, 2013; Pedron et al., 2013, 2015, 2017a). Primary neural cells are very vulnerable to *in vitro* culture conditions and need very specific environmental conditions (e.g., mechanical stress, porosity, degradability, attachment sites) to keep them viable and functional. Very mild conditions of polymerization, low polymer concentration, and compliant resulting gels (Palazzolo et al., 2015) are known to be necessary for achieving a high initial cell viability, very important in the case of neurons that do not proliferate. In this case, the most permissive gels presented an elastic modulus around 1.1 kPa, and cells show long interconnected processes with the appearance of varicosities (**Figure 1**). In photo-initiated reactions, for instance, time, and intensity of exposure to UV light is a critical variable that needs to be considered during cell encapsulation that also engages material mechanical compliance. Ongoing work focuses on developing more compliant hydrogel constructs to ensure greater and more stable neuronal outgrowth. Indeed, matrix architecture is highly important in 3D microenvironments to allow for neurite extension at the same time as nutrients and oxygen flow. Current advancements in formation of endothelial networks within these constructs (Chen et al., 2017) could demonstrate as a prospective solution for the alteration of oxygen and biomolecule transport within the hydrogel network. Future directions aim to achieve a broader array of matrix architectures in order to optimize cell culture conditions: alternative crosslinking chemistries and simplification of sample fabrication by using spatially graded hydrogels (Pedron et al., 2017b) using microfluidics.

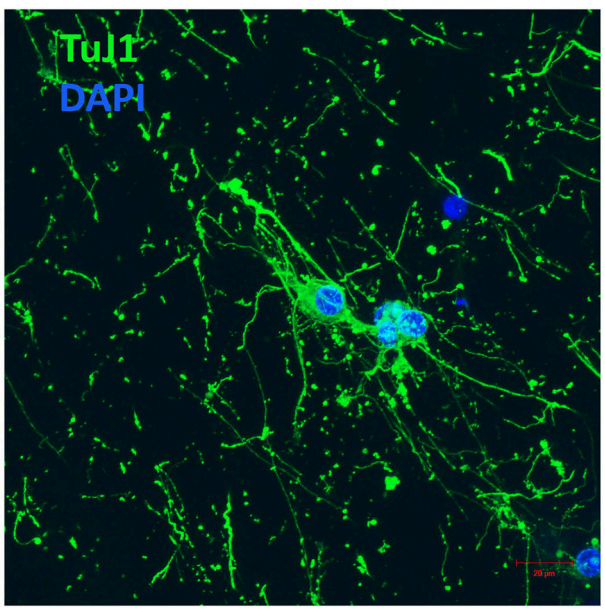

FIGURE 5 | E12 hindbrain cells encapsulated in GelMA/HAMA: 3.5/0.5 wt% plus 800 μg/ml CYIGSR display a neuronal phenotype after 7DIV. Hydrogels were immunostained with Tuj-1, an antibody against neuron-specific class III-beta tubulin (see Materials and Methods section for details). Scale bar: 20 μm.

Despite our success in growing these neurons that are crucial for the initiation of behavior, several aspects of the work indicated that this methodology deserves further development. First, our 3D gels should in principle be amenable for electrophysiological recording. We note that it is harder to visualize the surfaces of target neurons through the gel than in a simple bath; and with the micropipette entering the gel from the right, advancing in the gel toward the target neuron pushes the gel (and the neuron) to the left even to the point where the neuron would be deformed. Second, despite exquisite attention to methodological detail, we noted variability in neuron viability and the consistency of neuron processes. In particular, we observed in some cases neurites presenting non uniform widths suggestive of varicosities or putative boutons. Although signs of axonal degeneration cannot be ruled out, future studies should address the latter possibility exploring the presence of vesicle associated proteins such as synapsin (Neto et al., 2014). In trying to explain the variability in neuron viability, one possibility lies with the method of neuronal concentration in the pellet of tissue immediately before adding the pre-polymer solution. Another possible cause of variability could stem from the crosslinking reaction and the hydrogel network formed thereof. Moreover, although adding laminin-derived adhesion peptide to the gel preparation did not systematically improve results, we had a small number of experiments in which the presence of the peptide mimic did improve viability and neuronal network formation, opening the door to exploring alternative methods to present adhesion moieties to NGC cells. One possible strategy to explore a wider range of combinations of adhesion molecules or a wider range of activity inducing factors would be the use of microfluidic patterning tools that we have previously described to create

gelatin hydrogels containing embossed patterns of biomolecules (Pedron et al., 2013; Mahadik et al., 2015). Such tools can build on the observations here to test a wider range of concentrations, create patterns employing either or both soluble vs. hydrogel-immobilized signals, and would be ideally suited to examine a wider range of bioactive factors that might enhance neuron outgrowth that have been previously identified in the literature such as EGF and bFGF (Rao, 1999; Maric et al., 2003).

CONCLUSION

For the first time, we report the successful *in vitro* culture and growth of primary NGC neurons, crucial for the initiation of behavior, within gelatin-based biomaterial platforms. HA-functionalized GelMA hydrogels, previously identified for the growth and expansion of glioblastoma cells, provides a 3D-hydrogel environment in which NGC viability, neuronal process extension, and the expression of markers of neuronal differentiation could be observed. Ongoing efforts are exploring modifications to the gelatin-based hydrogel biophysical properties to achieve a robust growth and stable neural differentiation for prolonged periods of time.

AUTHOR CONTRIBUTIONS

AM and SP designed experiments, modified and adapted 2D cell culture for 3D hydrogel cultures, performed results interpretation and wrote the manuscript. AM and MC performed data analysis. MK and IT worked out conditions for 2D embryonic hindbrain primary cell cultures, BH and DP designed experiments, performed results interpretation, and manuscript writing.

ACKNOWLEDGMENTS

Research reported in this publication was supported by the National Cancer Institute of the National Institutes of Health under Award Number R01 CA197488. The content is solely the responsibility of the authors and does not necessarily represent the official views of the NIH. This material is based upon work supported by the National Science Foundation under Grant No. 1254738 (BH). The authors are also grateful for additional funding provided by the New York Neuroscience Foundation (DP), the Department of Chemical & Biomolecular Engineering and the Carl R. Woese Institute for Genomic Biology at the University of Illinois at Urbana-Champaign.

REFERENCES

Alessandri, K., Feyeux, M., Gurchenkov, B., Delgado, C., Trushko, A., Krause, K. H., et al. (2016). A 3D printed microfluidic device for production of functionalized hydrogel microcapsules for culture and differentiation of human Neuronal Stem Cells (hNSC). *Lab Chip* 16, 1593–1604. doi: 10.1039/C6LC00133E

Baier, C., Baader, S. L., Jankowski, J., Gieselmann, V., Schilling, K., Rauch, U., et al. (2007). Hyaluronan is organized into fiber-like structures along migratory pathways in the developing mouse cerebellum. *Matrix Biol.* 26, 348–358. doi: 10.1016/j.matbio.2007.02.002

Birey, F., Andersen, J., Makinson, C. D., Islam, S., Wei, W., Huber, N., et al. (2017). Assembly of functionally integrated human forebrain spheroids. *Nature* 545, 54–59. doi: 10.1038/nature22330

Caballero, D., Kaushik, S., Correlo, V. M., Oliveira, J. M., Reis, R. L., and Kundu, S. C. (2017). Organ-on-chip models of cancer metastasis for future personalized medicine: from chip to the patient. *Biomaterials* 149, 98–115. doi: 10.1016/j.biomaterials.2017.10.005

Calderon, D. P., Kilinc, M., Maritan, A., Banavar, J. R., and Pfaff, D. (2016). Generalized CNS arousal: an elementary force within the vertebrate nervous system. *Neurosci. Biobehav. Rev.* 68, 167–176. doi: 10.1016/j.neubiorev.2016.05.014

Chen, J. W. E., Pedron, S., and Harley, B. A. C. (2017). The combined influence of hydrogel stiffness and matrix-bound hyaluronic acid content on glioblastoma invasion. *Macromol. Biosci.* 17:1700018-n/a. doi: 10.1002/mabi.201700018

Chung, B., Esmaeili, A. A., Gopalakrishna-Pillai, S., Murad, J. P., Andersen, E. S., Kumar Reddy, N., et al. (2017). Human brain metastatic stroma attracts breast cancer cells via chemokines CXCL16 and CXCL12. *npj Breast Cancer* 3:6. doi: 10.1038/s41523-017-0008-8

Di Lullo, E., and Kriegstein, A. R. (2017). The use of brain organoids to investigate neural development and disease. *Nat. Rev. Neurosci.* 18:573. doi: 10.1038/nrn.2017.107

Du, C., Collins, W., Cantley, W., Sood, D., and Kaplan, D. L. (2017). Tutorials for electrophysiological recordings in neuronal tissue engineering. *ACS Biomater. Sci. Eng.* 3, 2235–2246. doi: 10.1021/acsbiomaterials.7b00318

Fantin, A., Vieira, J. M., Plein, A., Maden, C. H., and Ruhrberg, C. (2013). The embryonic mouse hindbrain as a qualitative and quantitative model to study the molecular and cellular mechanisms of angiogenesis. *Nat. Protoc.* 8, 418–429. doi: 10.1038/nprot.2013.015

Gu, Q., Tomaskovic-Crook, E., Lozano, R., Chen, Y., Kapsa, R. M., Zhou, Q., et al. (2016). Functional 3D neural mini-tissues from printed gel-based bioink and human neural stem cells. *Adv. Healthcare Mater.* 5, 1429–1438. doi: 10.1002/adhm.201600095

Gurkan, U. A., Fan, Y., Xu, F., Erkmen, B., Urkac, E. S., Parlakgul, G., et al. (2013). Simple precision creation of digitally specified, spatially heterogeneous, engineered tissue architectures. *Adv. Mater.* 25, 1192–1198. doi: 10.1002/adma.201203261

Heffernan, J. M., Overstreet, D. J., Le, L. D., Vernon, B. L., and Sirianni, R. W. (2015). Bioengineered scaffolds for 3D analysis of glioblastoma proliferation and invasion. *Ann. Biomed. Eng.* 43, 1965–1977. doi: 10.1007/s10439-014-1223-1

Jones, B. E., and Yang, T. Z. (1985). The efferent projections from the reticular formation and the locus coeruleus studied by anterograde and retrograde axonal transport in the rat. *J. Comp. Neurol.* 242, 56–92. doi: 10.1002/cne.902420105

Kingsmore, K. M., Logsdon, D. K., Floyd, D. H., Peirce, S. M., Purow, B. W., and Munson, J. M. (2016). Interstitial flow differentially increases patient-derived glioblastoma stem cell invasion via CXCR4, CXCL12, and CD44-mediated mechanisms. *Integr. Biol.* 8, 1246–1260. doi: 10.1039/C6IB00167J

Lampe, K. J., Antaris, A. L., and Heilshorn, S. C. (2013). Design of three-dimensional engineered protein hydrogels for tailored control of neurite growth. *Acta Biomater.* 9, 5590–5599. doi: 10.1016/j.actbio.2012.10.033

Lancaster, M. A., and Knoblich, J. A. (2014). Organogenesis in a dish: modeling development and disease using organoid technologies. *Science* 345:1247125. doi: 10.1126/science.1247125

Liu, X., Pfaff, D. W., Calderon, D. P., Tabansky, I., Wang, X., Wang, Y., et al. (2016). Development of electrophysiological properties of nucleus gigantocellularis neurons correlated with increased CNS arousal. *Dev. Neurosci.* 38, 295–310. doi: 10.1159/000449035

Mahadik, B. P., Pedron Haba, S., Skertich, L. J., and Harley, B. A. (2015). The use of covalently immobilized stem cell factor to selectively affect

hematopoietic stem cell activity within a gelatin hydrogel. *Biomaterials* 67, 297–307. doi: 10.1016/j.biomaterials.2015.07.042

Maric, D., Maric, I., Chang, Y. H., and Barker, J. L. (2003). Prospective cell sorting of embryonic rat neural stem cells and neuronal and glial progenitors reveals selective effects of basic fibroblast growth factor and epidermal growth factor on self-renewal and differentiation. *J. Neurosci.* 23:240. doi: 10.1523/JNEUROSCI.23-01-00240.2003

Martin, E. M., Devidze, N., Shelley, D. N., Westberg, L., Fontaine, C., and Pfaff, D. W. (2011). Molecular and neuroanatomical characterization of single neurons in the mouse medullary gigantocellular reticular nucleus. *J. Comp. Neurol.* 519, 2574–2593. doi: 10.1002/cne.22639

Martin, E. M., Pavlides, C., and Pfaff, D. (2010). Multimodal sensory responses of nucleus reticularis gigantocellularis and the responses' relation to cortical and motor activation. *J. Neurophysiol.* 103:2326. doi: 10.1152/jn.01122.2009

Mckinnon, D. D., Kloxin, A. M., and Anseth, K. S. (2013). Synthetic hydrogel platform for three-dimensional culture of embryonic stem cell-derived motor neurons. *Biomater. Sci.* 1, 460–469. doi: 10.1039/c3bm00166k

Neto, E., Alves, C. J., Sousa, D. M., Alencastre, I. S., Lourenço, A. H., Leitão, L., et al. (2014). Sensory neurons and osteoblasts: close partners in a microfluidic platform. *Integr. Biol.* 6, 586–595. doi: 10.1039/C4IB00035H

Neves, L. S., Rodrigues, M. T., Reis, R. L., and Gomes, M. E. (2016). Current approaches and future perspectives on strategies for the development of personalized tissue engineering therapies. *Expert Rev. Precision Med. Drug Dev.* 1, 93–108. doi: 10.1080/23808993.2016.1140004

Ngo, M. T., and Harley, B. A. (2017). The influence of hyaluronic acid and glioblastoma cell coculture on the formation of endothelial cell networks in gelatin hydrogels. *Adv. Healthcare Mater.* 6:1700687-n/a. doi: 10.1002/adhm.201700687

Palazzolo, G., Broguiere, N., Cenciarelli, O., Dermutz, H., and Zenobi-Wong, M. (2015). Ultrasoft alginate hydrogels support long-term three-dimensional functional neuronal networks. *Tissue Eng. Part A* 21, 2177–2185. doi: 10.1089/ten.tea.2014.0518

Pedron, S., and Harley, B., A. (2013). Impact of the biophysical features of a 3D gelatin microenvironment on glioblastoma malignancy. *J. Biomed. Mater. Res. Part A* 101, 3404–3415. doi: 10.1002/jbm.a.34637

Pedron, S., Becka, E., and Harley, B. A. (2015). Spatially gradated hydrogel platform as a 3D engineered tumor microenvironment. *Adv. Mater.* 27, 1567–1572. doi: 10.1002/adma.201404896

Pedron, S., Becka, E., and Harley, B. A.(2013). Regulation of glioma cell phenotype in 3D matrices by hyaluronic acid. *Biomaterials* 34, 7408–7417. doi: 10.1016/j.biomaterials.2013.06.024

Pedron, S., Hanselman, J. S., Schroeder, M. A., Sarkaria, J. N., and Harley, B. A. C. (2017a). Extracellular hyaluronic acid influences the efficacy of egfr tyrosine kinase inhibitors in a biomaterial model of glioblastoma. *Adv. Healthcare Mater.* 6:1700529. doi: 10.1002/adhm.201700529

Pedron, S., Polishetty, H., Pritchard, A. M., Mahadik, B. P., Sarkaria, J. N., and Harley, B. A. C. (2017b). Spatially graded hydrogels for preclinical testing of glioblastoma anticancer therapeutics. *MRS Commun.* 7, 442–449. doi: 10.1557/mrc.2017.85

Pfaff, D. W. (2006). *Brain Arousal and Information Theory: Neural and Genetic Mechanisms*. Cambridge, MA: Harvard University Press.

Pfaff, D. W., Martin, E. M., and Faber, D. (2014). Origins of arousal: roles for medullary reticular neurons. *Trends Neurosci.* 35, 468–476. doi: 10.1016/j.tins.2012.04.008

Pradhan, S., Hassani, I., Clary, J. M., and Lipke, E. A. (2016). Polymeric biomaterials for *in vitro* cancer tissue engineering and drug testing applications. *Tissue Eng. Part B Rev.* 22, 470–484. doi: 10.1089/ten.teb.2015.0567

Quadrato, G., Nguyen, T., Macosko, E. Z., Sherwood, J. L., Min Yang, S., Berger, D. R., et al. (2017). Cell diversity and network dynamics in photosensitive human brain organoids. *Nature* 545, 48–53. doi: 10.1038/nature22047

Rao, M. S. (1999). Multipotent and restricted precursors in the central nervous system. *Anatomical Record* 257, 137–148.

Rape, A., Ananthanarayanan, B., and Kumar, S. (2014). Engineering strategies to mimic the glioblastoma microenvironment. *Adv. Drug Delivery Rev.* 79–80, 172–183. doi: 10.1016/j.addr.2014.08.012

Sasai, Y. (2013). Cytosystems dynamics in self-organization of tissue architecture. *Nature* 493, 318–326. doi: 10.1038/nature11859

Seidlits, S. K., Khaing, Z. Z., Petersen, R. R., Nickels, J. D., Vanscoy, J. E., Shear, J. B., et al. (2010). The effects of hyaluronic acid hydrogels with tunable mechanical properties on neural progenitor cell differentiation. *Biomaterials* 31, 3930–3940. doi: 10.1016/j.biomaterials.2010.01.125

Tang-Schomer, M. D., White, J. D., Tien, L. W., Schmitt, L. I., Valentin, T. M., Graziano, D. J., et al. (2014). Bioengineered functional brain-like cortical tissue. *Proc. Natl. Acad. Sci. U. S. A.* 111, 13811–13816. doi: 10.1073/pnas.1324214111

Wu, H. B., Stavarache, M., Pfaff, D. W., and Kow, L. M. (2007). Arousal of cerebral cortex electroencephalogram consequent to high-frequency stimulation of ventral medullary reticular formation. *Proc. Natl. Acad. Sci. U. S. A.* 104, 18292–18296. doi: 10.1073/pnas.0708620104

Xiao, W., Sohrabi, A., and Seidlits, S. K. (2017). Integrating the glioblastoma microenvironment into engineered experimental models. *Future Sci. OA* 3:FSO189. doi: 10.4155/fsoa-2016-0094

Conflict of Interest Statement: The authors declare that the research was conducted in the absence of any commercial or financial relationships that could be construed as a potential conflict of interest.

frontiers in Bioengineering and Biotechnology

REVIEW
published: 30 January 2018
doi: 10.3389/fbioe.2017.00087

Modeling Neurovascular Disorders and Therapeutic Outcomes with Human-Induced Pluripotent Stem Cells

*Allison M. Bosworth[1], Shannon L. Faley[2], Leon M. Bellan[2,3] and Ethan S. Lippmann[1,3]**

[1] Department of Biomedical Engineering, Vanderbilt University, Nashville, TN, United States, [2] Department of Mechanical Engineering, Vanderbilt University, Nashville, TN, United States, [3] Department of Chemical and Biomolecular Engineering, Vanderbilt University, Nashville, TN, United States

The neurovascular unit (NVU) is composed of neurons, astrocytes, pericytes, and endothelial cells that form the blood–brain barrier (BBB). The NVU regulates material exchange between the bloodstream and the brain parenchyma, and its dysfunction is a primary or secondary cause of many cerebrovascular and neurodegenerative disorders. As such, there are substantial research thrusts in academia and industry toward building NVU models that mimic endogenous organization and function, which could be used to better understand disease mechanisms and assess drug efficacy. Human pluripotent stem cells, which can self-renew indefinitely and differentiate to almost any cell type in the body, are attractive for these models because they can provide a limitless source of individual cells from the NVU. In addition, human-induced pluripotent stem cells (iPSCs) offer the opportunity to build NVU models with an explicit genetic background and in the context of disease susceptibility. Herein, we review how iPSCs are being used to model neurovascular and neurodegenerative diseases, with particular focus on contributions of the BBB, and discuss existing technologies and emerging opportunities to merge these iPSC progenies with biomaterials platforms to create complex NVU systems that recreate the *in vivo* microenvironment.

Keywords: induced pluripotent stem cell, blood–brain barrier, neurovascular unit, disease modeling, tissue engineering

OPEN ACCESS

Edited by:
Sara Pedron, University of Illinois at Urbana–Champaign, United States

Reviewed by:
Mark Andrew Skylar-Scott, Harvard University, United States
Stephanie Michelle Willerth, University of Victoria, Canada

****Correspondence:***
Ethan S. Lippmann
ethan.s.lippmann@vanderbilt.edu

Specialty section:
This article was submitted to Biomaterials, a section of the journal Frontiers in Bioengineering and Biotechnology

Received: *27 October 2017*
Accepted: *26 December 2017*
Published: *30 January 2018*

Citation:
Bosworth AM, Faley SL, Bellan LM and Lippmann ES (2018) Modeling Neurovascular Disorders and Therapeutic Outcomes with Human-Induced Pluripotent Stem Cells. Front. Bioeng. Biotechnol. 5:87. doi: 10.3389/fbioe.2017.00087

INTRODUCTION

The blood–brain barrier (BBB) maintains central nervous system (CNS) homeostasis by strictly regulating transport of ions, small molecules, proteins, and cells between the bloodstream and CNS (Obermeier et al., 2013). The BBB is formed by a monolayer of brain microvascular endothelial cells (BMECs), which express intercellular tight junctions that limit paracellular transport. Owing to the fidelity of these intercellular contacts, the BBB exhibits high transendothelial electrical resistance (TEER), a quantitative measure of barrier integrity performed by applying a voltage across the cell monolayer, measuring resulting current, and calculating resistance using Ohm's Law. The BBB also expresses molecular transporters (e.g., GLUT-1, LAT-1) that shuttle nutrients and waste products and expresses efflux transporters that restrict the diffusion of lipophilic substances. These properties allow the BBB to protect the CNS neurons from harmful toxins and pathogens in the bloodstream, as well as regulate CNS homeostasis (Obermeier et al., 2013). Unfortunately, in aging and the progression of various disease states, such as Alzheimer's disease (AD), multiple sclerosis, and traumatic

brain injury, many of these BBB-specific properties are disrupted or lost (Korn et al., 2005; Marques et al., 2013; Friese et al., 2014). As such, improved understanding of BBB function and its alterations in disease may lead to new strategies for therapeutic intervention in neurological and neurodegenerative disorders.

In vitro models of the BBB are useful for understanding proper endothelial cell functionality and gaining insight into disease mechanisms. Primary mouse, rat, bovine, and porcine BBB endothelium have been often used for constructing various *in vitro* models (Helms et al., 2016), but it has been recognized that non-human cell sources are often insufficient for modeling human mechanisms because of species' differences in receptor and transporter expression levels and homology (Syvänen et al., 2009; Helms et al., 2016). Therefore, human cell sources would be preferred in many cases. However, primary human BBB endothelial cells exhibit only moderate barrier functionality *in vitro* are usually very difficult and time consuming to isolate and can only be obtained in low yield (approximately 1 million cells per 5–10 mm^3 tissue) (Bernas et al., 2010). Patient heterogeneity also provides an additional obstacle to the reproducibility of primary human cells. Immortalized BBB endothelial cell lines have been tested as an alternative to primary cells because they bypass the process of isolation from tissue and are derived from a clonal source (Weksler et al., 2005), but the immortalization process typically yields poor barrier functionality.

These issues with primary cells and immortalized cell lines have led to the exploration of human-induced pluripotent stem cells (iPSCs) as a new cell source for modeling BBB. iPSCs are characterized by their ability to proliferate indefinitely and differentiate into any cell type of the human body (Takahashi et al., 2007; Yu et al., 2007). Recent work has shown that iPSCs can be differentiated into BBB endothelial cells (Lippmann et al., 2012), and follow-up studies have improved on this differentiation process to produce cells that have properties approaching *in vivo* characteristics (Lippmann et al., 2014). In addition, the presence of astrocytes and pericytes, which reside in the neurovascular unit (NVU) and further support BBB function *in vivo*, can similarly enhance the BBB phenotype *in vitro* (Hollmann et al., 2017). Finally, the use of biomaterials such as hydrogels has facilitated the development of three-dimensional models that can prospectively mimic NVU architecture. **Figure 1** illustrates the general process by which patient-derived cells can be incorporated into such models. In this review, we summarize these advancements in BBB modeling with iPSCs, discuss how iPSC-derived BBB endothelium could be used to enhance neurodegenerative disease mechanistic interrogations and drug screening campaigns, and outline engineering and fabrication approaches that may be used in future studies to produce NVU models with more predictive power.

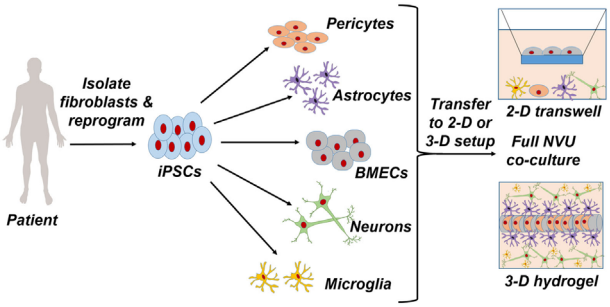

FIGURE 1 | Patient-specific fibroblasts are isolated and reprogrammed to a pluripotent state, from which pericytes, astrocytes, brain microvascular endothelial cells, neurons, and microglia are differentiated. Full coculture models of the neurovascular unit are achieved through a two-dimensional Transwell setup or a three-dimensional hydrogel setup.

MODELING THE BBB WITH iPSCs

As described above, the BBB is characterized by specialized properties such as high TEER, low passive permeability to both hydrophilic and hydrophobic substances, and expression of a bevy of molecular transporters. The differentiation of iPSCs to endothelial cells with these properties was first described in the seminal work (Lippmann et al., 2012). This procedure begins with a codifferentiation process that generates both neural and endothelial cells to mimic endogenous neurovascular development, whereby neural progenitors impart BBB identity onto endothelial cells. Wnt/β-catenin signaling plays a key role in this process *in vivo* (Stenman et al., 2008; Daneman et al., 2009) and was therefore assayed in the iPSC system; it was determined that several key WNTs were expressed during differentiation, and localization of β-catenin to the nucleus of PECAM-1^+ endothelial cells was found to increase throughout the differentiation process, indicating that Wnt/β-catenin signaling was activated. Endothelial cells were then purified from the heterogeneous mixture by selective adhesion to collagen IV and fibronectin. Expression of endothelial and tight junction markers, as well as active efflux transporter expression and representative permeability to a panel of small molecules, confirmed BBB-like identity. Finally, TEER was measured at ~800 $\Omega \times cm^2$ after coculture with astrocytes; although this level of barrier fidelity was higher than any previous human model, it still decreased well below measured values in rats (up to 5,900 $\Omega \times cm^2$) (Butt et al., 1990) and theoretical maximums calculated by radioactive ion permeability (~8,000 $\Omega \times cm^2$) (Smith and Rapoport, 1986).

Animal and human models of the developing brain have shown that radial glial cell-secreted retinoic acid (RA) helps induce BBB properties (Mizee et al., 2013). For this reason, follow-up work to optimize BMEC differentiation methods used media supplemented with RA to boost barrier properties in iPSC-derived BBB endothelial cells. RA treatment during the differentiation process yielded cells with increased expression of VE-cadherin and occludin and drastically elevated TEER values to ~3,000 $\Omega \times cm^2$ (Lippmann et al., 2014). Further optimization of seeding density (Wilson et al., 2015) and defined medium composition (Hollmann et al., 2017) have shortened the differentiation time from 13 to 8 days, with the final BBB population still exhibiting excellent barrier properties (TEER > 6,000 $\Omega \times cm^2$ upon coculture with astrocytes and pericytes). The reproducibility of the differentiation procedure has been subsequently confirmed in several publications all demonstrating BBB identity through elevated TEER and other molecular

characterizations (Katt et al., 2016; Appelt-Menzel et al., 2017; Kokubu et al., 2017; Lim et al., 2017; Wang et al., 2017b). While initial protocols yielded stable TEER measurements (≥1,000 $\Omega \times cm^2$) for approximately 4 days (Lippmann et al., 2014), more recent protocols have yielded stable measurements for up to 14 days (Hollmann et al., 2017). As these protocols advance and more closely resemble *in vivo* conditions, it is expected that TEER measurements will stabilize even further and extend over longer periods of time.

The availability of these high-quality human BMECs has spurred numerous advancements in disease modeling. Other than their excellent barrier properties relative to other sources of human BMECs (Helms et al., 2016), the core utility of iPSC-derived BMECs is their derivation from a specific genetic background, which permits explicit studies of genotype/phenotype linkages. This powerful approach was applied in two recent studies. First, iPSCs from patients with Allan–Herndon–Dudley syndrome (AHDS; characterized by severe neuropsychomotor impairments) were used to study BBB transport properties (Vatine et al., 2017). AHDS is caused by inactivating mutations in monocarboxylate transporter 8, which is a thyroid hormone transporter, but the mechanism of the disease has been unclear. Although iPSC-derived neurons developed normally in the presence of thyroid hormone, BBB endothelial cells derived from AHDS iPSCs were deficient at transporting thyroid hormone in an apical-to-basolateral direction ("blood" to "brain"). These results imply that AHDS could potentially be corrected if this delivery problem were overcome. Moreover, this study in iPSCs was particularly crucial because rodents express a separate transporter (Oatp1c1) at the BBB that can transport thyroid hormone, which is absent at the human BBB; thus, to accurately mimic the disease, it was particularly crucial to work with human cells. The second study to explore the contribution of human genetics to BBB disease utilized Huntington's disease (HD) iPSCs (Lim et al., 2017). BBB deficits have been observed in live measurements in HD patients and within postmortem tissue analyses, but it was unclear if these phenotypes were cell autonomous or due to secondary damage incurred by neural inflammation and death. Thus, using the standard iPSC-to-BMEC differentiation procedure (Lippmann et al., 2014), it was observed that BMECs differentiated from HD-iPSCs had defects in barrier formation, including diminished TEER and increased transcytosis. Further analyses suggested that these malfunctioning barrier properties may be related to an increased proliferative/angiogenic capacity. Intriguingly, the severity of most BBB defects increased with the number of CAG repeats in the huntingtin protein, which also correlates with the severity of the disease *in vivo*. These results suggest that defects in the BBB could potentially contribute to HD onset and progression.

In the future, we hypothesize that other diseases with explicit changes or deficits in BBB function will be modeled with iPSCs. For example, cerebral cavernous malformations (CCMs), which are vascular malformations found predominantly in the CNS that cause hemorrhagic stroke, are caused by the loss of function mutations in three genes that form an intracellular adaptor protein complex (Cavalcanti et al., 2011). However, the clinical course of the familial form of the disease is highly variable, suggesting additional genetic modifiers could play a role in disease progression. For example, a recent study demonstrated that polymorphisms in the innate immunity gene *TLR4* are associated with higher disease burden in humans (Tang et al., 2017a). iPSCs from CCM patients could be a powerful tool for interrogating the genetic and environmental factors that exacerbate this disease. Another disease that may benefit from iPSC modeling is drug-resistant epilepsy. Nearly one-third of epilepsy patients are refractory to pharmacotherapy, and the mechanism of this drug resistance is hotly debated (Tang et al., 2017b). Much of the clinical data in drug-resistant epilepsy has focused on polymorphisms and expression changes in efflux transporters at the BBB. iPSCs would again represent an excellent tool for studying the influence of transporter gene polymorphisms on protein expression levels and drug pharmacology. Overall, iPSCs do not even need to be derived from specific patient populations to be useful for these applications. Several studies have assayed the responses of iPSC-derived BMECs to hypoxia and glucose deprivation in an effort to mimic ischemia (Page et al., 2016; Kokubu et al., 2017), and these types of mechanistic analyses into basic BBB function under disease-like conditions can be conducted with generic iPSCs. Moreover, cutting-edged genome engineering techniques [e.g. CRISPR/Cas (Cong et al., 2013; Mali et al., 2013)] now allow researchers to remove genes or introduce specific mutations into iPSCs (González et al., 2014; Mandegar et al., 2016). As such, the ability to make isogenic pairs of iPSCs will most likely be leveraged in the future to shed light on the genetics of BBB dysfunction.

HOW iPSC-DERIVED BBB ENDOTHELIUM CAN PROVIDE INSIGHT INTO NEUROVASCULAR DISEASE MECHANISMS AND TREATMENT STRATEGIES

In the previous section, we described current and theoretical examples for how iPSCs can be used to study diseases that directly influence BBB function. However, BBB dysfunction has been observed in many neurodegenerative diseases, including AD, Parkinson's disease (PD), and amyotrophic lateral sclerosis (ALS); whether this dysfunction causes the degeneration or is secondary to the diseases and simply exacerbates their progression remains to be determined. iPSCs represent a potential route for deconstructing neurovascular changes in these disorders, especially given the progress in differentiating other NVU cell types including neurons, microglia, pericytes, and astrocytes (Chambers et al., 2009; Orlova et al., 2014; Chandrasekaran et al., 2016; Pandya et al., 2017). Below we describe some of these disorders and current routes for modeling them with iPSCs, as well as advancements that could be realized by incorporating iPSC-derived BBB endothelium into existing model systems. This list is by no means all encompassing and is intended to mainly provide the readers with intriguing research avenues and questions.

Alzheimer's Disease

Hallmarks of AD pathology include the deposition of amyloid-β (A-β) in the extracellular space and buildup of

hyperphosphorylated tau fibers in the cytoplasm of neurons (Selkoe, 2001). Genetic mutations in the β-amyloid precursor protein (APP) and presenilin genes have been linked to cases of familial AD. Israel et al. (2012) were the first to use iPSC-derived neurons from patients with APP genetic duplications and patients with sporadic AD to assess disease mechanisms *in vitro*. They reported that the APP genetic mutation led to increased levels of pathological markers A-β and phosphor-tau. Other studies have shown that familial AD-derived iPSCs produce neurons with altered Aβ42/Aβ40 ratios (Mertens et al., 2013; Muratore et al., 2014), which recapitulates a key phenotype observed in the CSF of AD patients (Borchelt et al., 1996; Kumar-Singh et al., 2006). Given these findings, how then could iPSC-derived BMECs be incorporated with these defective neurons and other neurovascular cell types to model disease progression? For one, both soluble Aβ1–40 (Hartz et al., 2016) and Aβ1–42 (Park et al., 2014) have been shown to reduce p-glycoprotein expression at the BBB in animal models; as such, loss of p-glycoprotein in human neurovascular models may be a point of interest. Second, human ApoE4, but not ApoE2 or ApoE3, has been implicated in neurovascular breakdown (Bell et al., 2012); ApoE4 is a major genetic risk factor in AD, and iPSC-derived neurovascular models represent an excellent system to study its effects in a human genetic background. Third, PICALM, another genetic risk factor for AD, is expressed at the BBB and involved in amyloid clearance *via* transcytosis; iPSC-derived endothelial cells (albeit not BBB-specific) carrying a protective PICALM allele exhibit increased amyloid transport (Zhao et al., 2015). Ostensibly, the regulation of PICALM expression and prospective drugs that increase its expression or activity could be screened in iPSC-derived brain endothelium. More broadly, because amyloid clearance occurs at least in part through the vasculature and is implicated in AD progression (Sagare et al., 2012), its incorporation into human neurovascular models is vital for understanding plaque and tangle accumulation and removal.

Parkinson's Disease

Parkinson's disease features the main clinical symptom of bradykinesia resulting from the loss of dopaminergic neurons in the substantia nigra (Lees et al., 2009). Familial versions of this disease can be traced to mutations in the Parkin, LRRK2, and α-synuclein proteins, which lead to phenotypes such as compromised mitochondrial functionality and aggregation of α-synuclein to form Lewy bodies. iPSCs derived from patients with Parkin mutations can recapitulate PD phenotype *in vitro* (Imaizumi et al., 2012), including impaired mitochondrial function, accumulation of α-synuclein in differentiated neurons, and formation of Lewy bodies that corresponded to the structures found in the patient's postmortem brain tissue. Meanwhile, neurons derived from the iPSCs of patients with LRRK2 mutations are more susceptible to stress activators, leading to caspase activation and cell death (Nguyen et al., 2011). Neurons derived from the iPSCs of patients with triplication of the *SNCA* gene (which encodes α-synuclein) exhibit elevated α-synuclein protein expression, thus recapitulating the *in vivo* phenotype (Devine et al., 2011). More recently, iPSC-derived neurons from patients with a different *SNCA* mutation were shown to exhibit protein aggregation and fragment axons, which could be rescued through small molecule treatment (Kouroupi et al., 2017). Intriguingly, preformed α-synuclein fibrils can influence tight junction expression in a human *in vitro* BBB model (Kuan et al., 2016); however, the model used in this case (hCMEC/D3 immortalized cells) is notably not very tight (TEER less than 20 $\Omega \times cm^2$). Given the more significant tightness of iPSC-derived BMECs, accumulation and/or transport of α-synuclein, and its influence on barrier function, could be examined in a more physiologically relevant model system. This is particularly relevant given recent findings that α-synuclein assemblies can cross the BBB *in vivo* (Sui et al., 2014; Peelaerts et al., 2015) and that iPSC-derived BMECs derived from a patient with *PARK2* mutations may have defective or altered p-glycoprotein expression (Hollmann et al., 2017).

Amyotrophic Lateral Sclerosis

Amyotrophic lateral sclerosis is characterized by axonal degeneration and ultimately death of the neuronal cell body in CNS motor neurons. While it has been shown that this neurodegeneration is correlated with protein accumulation in motor neurons (Hirano et al., 1984), the underlying mechanisms of protein accumulation and how it leads to selective degradation of motor neurons is still largely unknown. To study this disease using iPSCs, many have chosen to look at the superoxide dismutase (SOD1) gene mutation since it is responsible for approximately 20% of all cases of familial ALS (Sau et al., 2007). Although familial cases account for only 5–10% of total ALS cases, many phenotypic similarities occur among sporadic and familial types, so it is still viewed as informative to study the disease using SOD1 mutations. Chen et al. (2014) used this approach to assess neurofilament aggregation and neurite degeneration in iPSC-derived motor neurons containing the SOD1 gene. They found that mutant SOD1 binds the mRNA of NF-L, a neurofilament subunit, leading to an overall reduction in NF-L levels and altered neurofilament subunit ratios in ALS motor neurons. This was predicted to be an early event in ALS onset, later leading to neurite degeneration. Meanwhile, Kiskinis et al. (2014) used isogenic pairs of iPSCs (wild-type and mutant SOD1) to show that the SOD1 mutation alters a variety of transcriptional signatures in motor neurons, including upregulation of stress pathways. Others have used iPSC-derived motor neurons to reveal a hyperexcitability phenotype that is broadly applicable to many ALS gene mutations, including variants of SOD1, C9ORF72, and TARDBP (Wainger et al., 2014; Devlin et al., 2015). These particular findings have led to an ALS clinical trial using ezogabine, an approved antiepileptic and Kv7.2/3 potassium channel agonist (McNeish et al., 2015), which presumably crosses the BBB in rodents (Large et al., 2012). Ideally, the permeation of this compound through the human BBB, as well as other variants and classes of potassium channel agonists, could be tested within the iPSC model. However, correcting aberrant phenotypes solely in motor neurons may not cure ALS, as mutant astrocytes are also selectively toxic to motor neurons (Di Giorgio et al., 2007, 2008; Nagai et al., 2007; Marchetto et al., 2008). It is intriguing to further note that vascular disruption has been noted in ALS using cell culture models (Meister et al., 2015), animal models (Zhong et al., 2008; Winkler et al., 2014), and postmortem human tissue (Garbuzova-Davis et al., 2012; Winkler et al., 2013).

Of particular interest, in the animal models, BBB disruption precedes motor neuron death. Whether this vascular degeneration is a direct cause of the ALS-causing mutations or due to altered crosstalk with astrocytes (which clearly have toxic capacity) or another NVU cell type remains to be determined, but the iPSC model represents a possible route for deconstructing these disease mechanisms and ultimately elucidating the role of BBB dysfunction in disease progression.

In addition to improving the accuracy of disease modeling applications, inclusion of a BBB component in these models also facilitates a more accurate prediction of drug outcomes (as alluded to in reference to the ezogabine clinical trial). Academia has made significant strides in screening both existing and newly developed drugs within iPSC-derived neurological models (Avior et al., 2016), including models of complex behavioral disorders such as autism (Shcheglovitov et al., 2013; Griesi-Oliveira et al., 2015; Mariani et al., 2015; Forrest et al., 2017) and schizophrenia (Brennand et al., 2011; Hook et al., 2014; Wen et al., 2014; Yoon et al., 2014). These models report drug efficacy among human diseased and control lines and provide perspectives on how they may be implemented clinically. However, as mentioned previously, the BBB blocks transport of ions, small molecules, and proteins between the bloodstream and the CNS. As such, an estimated 98% of all small molecules do not cross the BBB in appreciable amounts (Pardridge, 2005). Therefore, if a drug that exhibits effectiveness against neural cultures is not BBB penetrant, it will likely be ineffective in treating diseased CNS tissue, which represents a major constraint within the drug development process. Given the overall difficulties in CNS drug discovery (Choi et al., 2014), we believe that the addition of a BBB component is vital toward modeling complex CNS disorders and accurately predicting drug delivery and responses.

ROUTES FOR ENGINEERING COMPLEX *IN VITRO* NEUROVASCULAR MODELS USING iPSCs

Much of the discussion in the above section focused on the prospective interplay between BMECs and other resident cell types in the NVU. Historically, such crosstalk has been explored primarily in planar cultures or Transwell setups. However, 2D cell culture platforms overall are often inadequate as model tissue systems due to their inability to support truly biomimetic cell–cell and cell–matrix interactions and thus are unable to fully integrate the complex biochemical and mechanical cues affecting cell homeostasis and responses to environmental perturbations (Pampaloni et al., 2007; Edmondson et al., 2014; Banerjee et al., 2016; Helms et al., 2016). For this reason, there is a need to adopt 3D models that better recapitulate the native cellular environment to achieve *in vitro* model systems capable of yielding accurate predictions regarding factors that influence both disease progression and useful clinical interventions. This need has driven efforts in biomaterials patterning and microfluidic fabrication methods that enable the production of 3D cell culture systems with cellular constituents adopting behavior that more closely mimics that observed *in vivo* (Huh et al., 2011; Wikswo, 2014; Ravi et al., 2015). For the purposes of this review, we discuss a range of techniques that could be used to derive 3D neurovascular models, many of which were initially validated using non-stem cell sources, but nonetheless reflect significant advances in tissue engineering with the potential to provide insights into BBB and NVU function not currently obtainable in 2D formats (Cucullo et al., 2008). To develop truly biomimetic tissue models, however, researchers must still overcome several challenges, one of which is the need to develop approaches that incorporate iPSC-derived cells in these complex platforms.

Microfluidic fabrication techniques provide a powerful method for constructing NVU models in a highly controlled, perfused environment. Microfluidic BBB models, some commercially available (Prabhakarpandian et al., 2013; Lamberti et al., 2014), have proven useful for examining the impact of shear stress and scaffold geometry on brain endothelium function and morphology, as well as for drug screening applications (Cucullo et al., 2008; Booth and Kim, 2012; Yeon et al., 2012; Griep et al., 2013; Ye et al., 2014; Sellgren et al., 2015). While most of these platforms were developed using non-stem cell sources, a recent report of iPSC-derived BMECs cocultured with astrocytes on opposite sides of a porous membrane housed within a microfluidic channel indicated that these cells maintained a robust, *in vivo*-like barrier in the presence of continuous fluid flow for up to 12 days (Wang et al., 2017b).

Microfluidic BBB models are particularly well-suited to high-throughput, massively parallel drug screening efforts. Typically, microfluidic platforms are based on polydimethylsiloxane (PDMS) or glass substrates, which, while conducive to long-term cell culture, fail to recapitulate the complex 3D microenvironment of natural tissue. Scaffolds fabricated from hydrogel matrices are appealing for modeling the NVU, in that they offer a more physiologically representative platform in terms of stiffness, architecture, degradability, and a means by which to allow more natural interactions with surrounding cell populations (Tibbitt and Anseth, 2009). Hybrid platforms have emerged that incorporate hydrogel-filled channels or compartments to provide tissue-specific biological cues within a microfluidic format. This approach facilitates the use of fragile hydrogels composed of natural matrix proteins such as collagen, fibronectin, and hyaluronic acid that, depending on the concentration, often lack the structural integrity to support integrated fluidic channels in 3D as a free-standing unit. Such microfluidic compartments, filled with hydrogels containing endothelial cells, have been shown to be conducive to "bottom-up" formation of vascularized constructs through cell-driven angiogenic processes (Phan et al., 2017; Wang et al., 2017a). These methods have also been used in highly complex, organ-on-a-chip platforms. Composed of modular components of cells grown in hydrogel matrices as well as those cultured on porous membranes connected by microfluidic channels, organ-on-a-chip systems provide a potentially powerful method for gaining critical insights into population-specific responses to environmental perturbations with multiple readout mechanisms (Markov et al., 2012; Brown et al., 2015; Herland et al., 2016; Adriani et al., 2017). As illustrated by the experimental setup in **Figure 2**, the compartmentalized aspect of organ-on-a-chip

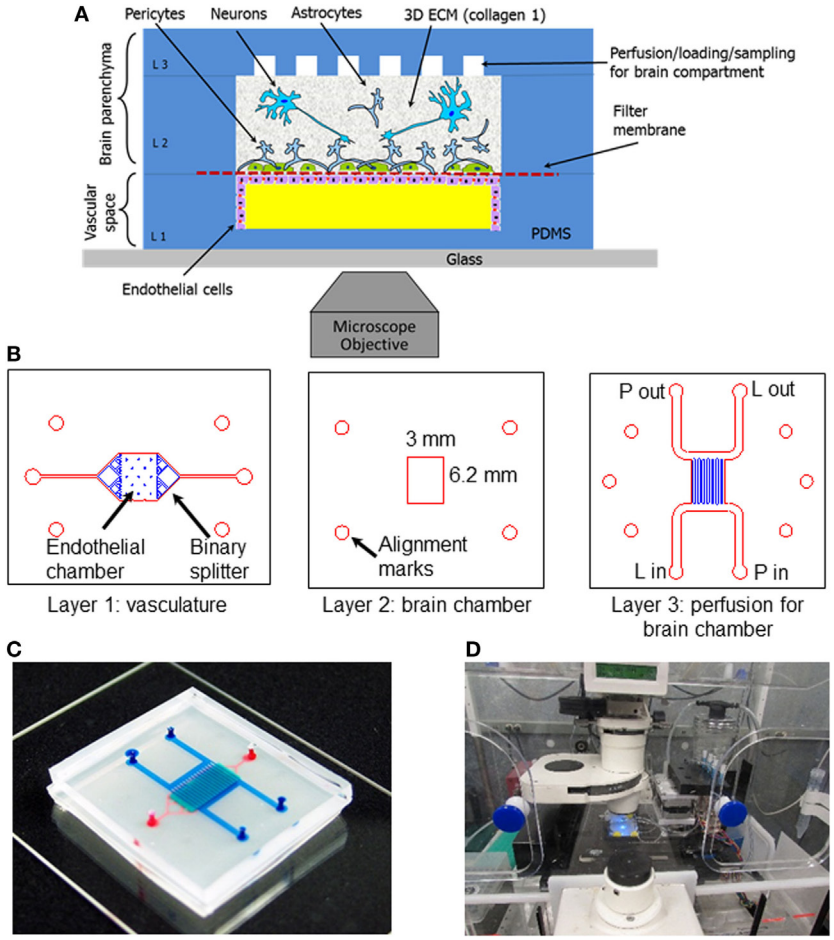

FIGURE 2 | Schematic and experimental setup of the neurovascular unit (NVU)-on-a-chip. **(A)** Schematic view of the neurovascular unit (NVU) indicating major components, cell types, and their spatial arrangement. **(B)** Photolithographic masks used to fabricate the three-layered NVU. **(C)** A photograph of the assembled NVU loaded with colored dyes indicating different compartments: red = vasculature; semi-transparent white = filter membrane; turquoise = brain compartment; and blue = brain perfusion. **(D)** NVU device on an incubated microscope stage. Reproduced from Brown et al. (2015), with the permission of AIP Publishing.

systems provide a novel mechanism for intrapopulation and interpopulation soluble communication that is incredibly useful in determining specific response profiles of individual cell population to toxic/therapeutic compounds in combination with downstream impacts on neighboring cell compartments. As such, these platforms are ideal for analyzing both drug permeability and drug metabolism for pharmacokinetic and pharmacodynamic modeling. However, scaffolds designed to identify critical biological mechanisms underlying pathological conditions should ideally be more biomimetic, such that the scale, biological matrix, cellular components, and organization better approximate physiological processes, including both soluble and contact-based cellular interactions. Furthermore, none of these platforms have yet to incorporate matched cells derived from stem cell sources, which would further enhance the ability to represent native physiological systems.

Microfluidic fabrication methods often require highly specialized equipment and training that are typically outside the scope of standard biological laboratory facilities and staff experience. In contrast, incorporation of hydrogel matrices into standard culture platforms is generally simpler and more scalable; although microfluidic NVU devices are generally fabricated to be less than 1 mm in thickness, hydrogel platforms are only limited by the size of the culture vessel as long as the construct can be appropriately perfused. 3D NVU models created based on the hydrogel scaffolds have thus far yielded promising results. Cells cultured on the surface of chemically defined synthetic PEG hydrogels have been shown to self-assemble into biomimetic NVU constructs have been used for high-throughput toxicity screening (Murphy et al., 2010; Pellett et al., 2015; Schwartz et al., 2015; Zanotelli et al., 2016; Barry et al., 2017). Others have shown that embedding neural cells in alginate hydrogels promotes self-assembly of "BBB spheroids," composed of an astrocytic core sheathed in layers of pericytes and brain endothelial cells, which may be useful for drug screening applications (Nguyen et al., 2013; Cho et al., 2017). Non-differentiated cells encapsulated in hydrogel matrices and directed through combined mechanical cues and growth factors offer an attractive method for yielding complex multicellular constructs that mimic *in vivo* cellular organization (Bozza et al.,

2014; Cho et al., 2017). However, these all lack the integrated, perfused vasculature necessary for a truly biomimetic model.

Like the aforementioned PDMS microfluidic platforms, hydrogels can also be patterned as free-standing constructs with perfusable internal channel networks (Faley et al., 2015). In fact, initial efforts in generating vascular models in biomimetic hydrogels scaffolds utilized lithographic and soft templating techniques adopted from traditional microfluidic fabrication methods (Cabodi et al., 2005; Golden and Tien, 2007; Zheng et al., 2012). These approaches are extremely good at producing micron and submicron patterns, but scaling the resulting devices to achieve tissue-scale constructs often requires cumbersome sequential assembly that is not particularly well suited to cell-laden scaffolds. Recent advances in 3D printing allow large-scale patterning with cell-laden bioinks in combination with sacrificial templates to yield integrated channel networks (Miller et al., 2012; Bertassoni et al., 2014; Kolesky et al., 2014). Currently, however, printer resolution limitations generally make fabricating channels in 3D printed scaffolds below 100 μm in diameter impractical. Still, these platforms allow modeling of arteriole (and larger) sized structures in an immediately perfusable format that is easily tailored to accommodate variations in shear, mechanical forces, cellular organization, and soluble signaling factors, thereby mimicking natural tissue in structure and scale. Only a few studies have used these techniques to examine brain endothelial dynamics using differentiated stem cells in fluidic hydrogel scaffolds (Jiménez-Torres et al., 2016; Ingram et al., 2017), but none have yielded endothelial lumens with appreciable barrier strength.

The next step in the fabrication of a biomimetic *in vitro* neurovascular model involves integrating the latest advances in iPSC derivation methods along with tissue engineering approaches for generating capillary-sized vascular structures. As opposed to extrusion-based 3D printing, projection stereolithographic printing techniques can produce 3D scaffolds with complex integrated fluidic channels (diameters as small as 20 μm) through spatially controlled cross-linkage of photosensitive prepolymer solution by targeted light exposure, delivered by computer-controlled digital micro-mirror assemblies or through a 2D "mask" in a layer-by layer fashion (Hribar et al., 2015; Wang et al., 2015; Raman et al., 2016; Valentin et al., 2017). Laser-assisted printing operates in a similar fashion, except that the laser focus is traditionally "patterned" by CAD file and, in the case of two-photon systems utilizing pulsed femtosecond laser sources, has achieved pattering of hydrogel features as small as 10 μm (Hoffmann and West, 2013). In addition, a novel hybrid approach recently demonstrated the ability to generate 20-μm channels using multiphoton stereolithography to photobleach biotin-4-fluorescein in unpolymerized collagen (Skylar-Scott et al., 2016). This particular method is capable of achieving down to 1-μm resolution for patterning much smaller structures, but at the expense of scalability with overall scaffold thicknesses limited to 1 mm. While lithographic methods such as these allow for reproducible fabrication of complex fluidic architecture of capillary scale within hydrogel scaffolds, the toxic and/or mutagenic effects of high-intensity laser exposure, photoinitiating components, and radicals/harmful byproducts produced during fabrication remain a significant concern, especially when applied to highly sensitive stem cell-derived populations. Laser ablation lithography attempts to circumvent the concerns associated with photo-initiated hydrogel polymerization by sculpting channels in blocks of hydrogels after polymerization by more cell-friendly processes (Brandenberg and Lutolf, 2016). However, the specialized equipment and necessary skills to implement most of these lithographic fabrication methods comprise the greatest obstacle to becoming a technique widely accessible to the broader neurovascular modeling community.

In contrast, a technologically straightforward approach to fabricating capillary-sized channels is to simply embed a sacrificial mesh of microscale fibers within the hydrogel matrix that, after polymerization, is washed away. The utility of this approach for developing biomimetic tissue constructs is entirely contingent upon identifying a sacrificial material that is non-cytotoxic, easily spun into microfibers, insoluble in water at 37°C, and can be removed from the crosslinked hydrogel using non-cytotoxic methods. A recent report demonstrating the ability to generate capillary-like channels from thermoresponsive poly-NIPAM fibers. The unique LCST properties of P-NIPAM result in shift from water-insoluble to water-soluble when temperatures fall below 32°C, enabling facile fiber removal at room temperature yielding immediately perfusable microscale channels that are promising for modeling brain microvasculature networks (Lee et al., 2016).

Other than fabrication, another hurdle for modeling complex neurovascular assemblies is the incompatibility of a traditional biological readout for validating the integrity and the functionality of brain endothelium. Measuring the resistance of the endothelial barrier (TEER) is the most common method for assessing barrier strength in 2D cultures, but obtaining reliable resistance measurements from endothelial lumens lining perfused channel networks within 3D hydrogel scaffolds is not realistic (Srinivasan et al., 2015). For this reason, the permeability of endothelial layers in hydrogel channels is typically evaluated by monitoring tracer diffusion across cell barriers using compound such as radiolabeled or fluorescently conjugated compounds (Bowman et al., 1983; Franke et al., 1999; Lippmann et al., 2013; Hollmann et al., 2017). Calculating the permeability coefficients from these observations is straightforward for non-intersecting channels in 2D arrays (Zheng et al., 2012). However, randomly intersecting channels in 3D matrices that mimic physiological architecture introduce a significant degree of complexity for establishing quantitative values of lumen permeability. Furthermore, tracers can perturb cellular activity and consequently effect barrier integrity. Thus, alternative methods, ideally those that are non-invasive and allow continuous monitoring of barrier integrity, are needed to realize the full potential of these newly emerging biomimetic neurovascular models. One solution may be to leverage advances in CRISPR technologies to produce iPSC lines that include reporters of cell function, including barrier integrity. Overall, recent innovations in 3D cell scaffold fabrication techniques, iPSC derivation methods, and genome editing have facilitated this exciting juncture in the field of tissue engineering; these progressive resources should ultimately facilitate the development of complex, truly biomimetic *in vitro* models of the NVU.

DISCUSSION

Major strides have been made toward building BBB models that take advantage of human iPSC technology. In addition,

ever-better microfluidics platforms and perfusable hydrogels are being developed to provide three-dimensional architectures that better mimic *in vivo* vessel structures. Valuable insights into neurological diseases have already been reported using iPSC-based model systems, and it is expected that these models will improve further when combined with novel biomaterial scaffolds into full NVU constructs. Once built, these complex *in vitro* models are poised to provide relevant clinical knowledge regarding debilitating cerebrovascular diseases and ultimately facilitate the next generation of therapeutic interventions.

AUTHOR CONTRIBUTIONS

All authors contributed to the preparation of this review.

FUNDING

Research related to the topics in this review is supported in our laboratories by the NIH grant 4R00EB013630 (LB), the NSF grant BMAT 1506717 (LB), and a NARSAD Young Investigator Award from the Brain and Behavior Research Foundation (EL).

REFERENCES

Adriani, G., Ma, D., Pavesi, A., Kamm, R. D., and Goh, E. L. K. (2017). A 3D neurovascular microfluidic model consisting of neurons, astrocytes and cerebral endothelial cells as a blood–brain barrier. *Lab. Chip* 17, 448–459. doi:10.1039/C6LC00638H

Appelt-Menzel, A., Cubukova, A., Günther, K., Edenhofer, F., Piontek, J., Krause, G., et al. (2017). Establishment of a human blood-brain barrier co-culture model mimicking the neurovascular unit using induced pluri- and multi-potent stem cells. *Stem Cell Rep.* 8, 894–906. doi:10.1016/j.stemcr.2017.02.021

Avior, Y., Sagi, I., and Benvenisty, N. (2016). Pluripotent stem cells in disease modelling and drug discovery. *Nat. Rev. Mol. Cell Biol.* 17, 170–182. doi:10.1038/nrm.2015.27

Banerjee, J., Shi, Y., and Azevedo, H. S. (2016). In vitro blood–brain barrier models for drug research: state-of-the-art and new perspectives on reconstituting these models on artificial basement membrane platforms. *Drug Discov. Today* 21, 1367–1386. doi:10.1016/j.drudis.2016.05.020

Barry, C., Schmitz, M. T., Propson, N. E., Hou, Z., Zhang, J., Nguyen, B. K., et al. (2017). Uniform neural tissue models produced on synthetic hydrogels using standard culture techniques. *Exp. Biol. Med. (Maywood)* 242, 1679–1689. doi:10.1177/1535370217715028

Bell, R. D., Winkler, E. A., Singh, I., Sagare, A. P., Deane, R., Wu, Z., et al. (2012). Apolipoprotein E controls cerebrovascular integrity via cyclophilin A. *Nature* 485, 512–516. doi:10.1038/nature11087

Bernas, M. J., Cardoso, F. L., Daley, S. K., Weinand, M. E., Campos, A. R., Ferreira, A. J. G., et al. (2010). Establishment of primary cultures of human brain microvascular endothelial cells to provide an in vitro cellular model of the blood-brain barrier. *Nat. Protoc.* 5, 1265–1272. doi:10.1038/nprot.2010.76

Bertassoni, L. E., Cecconi, M., Manoharan, V., Nikkhah, M., Hjortnaes, J., Cristino, A. L., et al. (2014). Hydrogel bioprinted microchannel networks for vascularization of tissue engineering constructs. *Lab. Chip* 14, 2202–2211. doi:10.1039/c4lc00030g

Booth, R., and Kim, H. (2012). Characterization of a microfluidic in vitro model of the blood-brain barrier (μBBB). *Lab. Chip* 12, 1784–1792. doi:10.1039/C2LC40094D

Borchelt, D. R., Thinakaran, G., Eckman, C. B., Lee, M. K., Davenport, F., Ratovitsky, T., et al. (1996). Familial Alzheimer's disease–linked presenilin 1 variants elevate Aβ1–42/1–40 ratio in vitro and in vivo. *Neuron* 17, 1005–1013. doi:10.1016/S0896-6273(00)80230-5

Bowman, P. D., Ennis, S. R., Rarey, K. E., Betz, A. L., and Goldstein, G. W. (1983). Brain microvessel endothelial cells in tissue culture: a model for study of blood-brain barrier permeability. *Ann. Neurol.* 14, 396–402. doi:10.1002/ana.410140403

Bozza, A., Coates, E. E., Incitti, T., Ferlin, K. M., Messina, A., Menna, E., et al. (2014). Neural differentiation of pluripotent cells in 3D alginate-based cultures. *Biomaterials* 35, 4636–4645. doi:10.1016/j.biomaterials.2014.02.039

Brandenberg, N., and Lutolf, M. P. (2016). In situ patterning of microfluidic networks in 3D cell-laden hydrogels. *Adv. Mater.* 28, 7450–7456. doi:10.1002/adma.201601099

Brennand, K. J., Simone, A., Jou, J., Gelboin-Burkhart, C., Tran, N., Sangar, S., et al. (2011). Modelling schizophrenia using human induced pluripotent stem cells. *Nature* 473, 221–225. doi:10.1038/nature09915

Brown, J. A., Pensabene, V., Markov, D. A., Allwardt, V., Neely, M. D., Shi, M., et al. (2015). Recreating blood-brain barrier physiology and structure on chip: a novel neurovascular microfluidic bioreactor. *Biomicrofluidics* 9, 054124. doi:10.1063/1.4934713

Butt, A. M., Jones, H. C., and Abbott, N. J. (1990). Electrical resistance across the blood-brain barrier in anaesthetized rats: a developmental study. *J. Physiol.* 429, 47–62. doi:10.1113/jphysiol.1990.sp018243

Cabodi, M., Choi, N. W., Gleghorn, J. P., Lee, C. S. D., Bonassar, L. J., and Stroock, A. D. (2005). A microfluidic biomaterial. *J. Am. Chem. Soc.* 127, 13788–13789. doi:10.1021/ja054820t

Cavalcanti, D. D., Kalani, M. Y. S., Martirosyan, N. L., Eales, J., Spetzler, R. F., and Preul, M. C. (2011). Cerebral cavernous malformations: from genes to proteins to disease. *J. Neurosurg.* 116, 122–132. doi:10.3171/2011.8.JNS101241

Chambers, S. M., Fasano, C. A., Papapetrou, E. P., Tomishima, M., Sadelain, M., and Studer, L. (2009). Highly efficient neural conversion of human ES and iPS cells by dual inhibition of SMAD signaling. *Nat. Biotechnol.* 27, 275. doi:10.1038/nbt.1529

Chandrasekaran, A., Avci, H. X., Leist, M., Kobolák, J., and Dinnyés, A. (2016). Astrocyte differentiation of human pluripotent stem cells: new tools for neurological disorder research. *Front. Cell. Neurosci.* 10:215. doi:10.3389/fncel.2016.00215

Chen, H., Qian, K., Du, Z., Cao, J., Petersen, A., Liu, H., et al. (2014). Modeling ALS with iPSCs reveals that mutant SOD1 misregulates neurofilament balance in motor neurons. *Cell Stem Cell* 14, 796–809. doi:10.1016/j.stem.2014.02.004

Cho, C.-F., Wolfe, J. M., Fadzen, C. M., Calligaris, D., Hornburg, K., Chiocca, E. A., et al. (2017). Blood-brain-barrier spheroids as an in vitro screening platform for brain-penetrating agents. *Nat. Commun.* 8, 15623. doi:10.1038/ncomms15623

Choi, D. W., Armitage, R., Brady, L. S., Coetzee, T., Fisher, W., Hyman, S., et al. (2014). Medicines for the mind: policy-based "Pull" incentives for creating breakthrough CNS drugs. *Neuron* 84, 554–563. doi:10.1016/j.neuron.2014.10.027

Cong, L., Ran, F. A., Cox, D., Lin, S., Barretto, R., Habib, N., et al. (2013). Multiplex genome engineering using CRISPR/Cas systems. *Science* 339, 819–823. doi:10.1126/science.1231143

Cucullo, L., Couraud, P.-O., Weksler, B., Romero, I.-A., Hossain, M., Rapp, E., et al. (2008). Immortalized human brain endothelial cells and flow-based vascular modeling: a marriage of convenience for rational neurovascular studies. *J. Cereb. Blood Flow Metab.* 28, 312–328. doi:10.1038/sj.jcbfm.9600525

Daneman, R., Agalliu, D., Zhou, L., Kuhnert, F., Kuo, C. J., and Barres, B. A. (2009). Wnt/β-catenin signaling is required for CNS, but not non-CNS, angiogenesis. *Proc. Natl. Acad. Sci. U.S.A.* 106, 641–646. doi:10.1073/pnas.0805165106

Devine, M. J., Ryten, M., Vodicka, P., Thomson, A. J., Burdon, T., Houlden, H., et al. (2011). Parkinson's disease induced pluripotent stem cells with triplication of the α-synuclein locus. *Nat. Commun.* 2, ncomms1453. doi:10.1038/ncomms1453

Devlin, A.-C., Burr, K., Borooah, S., Foster, J. D., Cleary, E. M., Geti, I., et al. (2015). Human iPSC-derived motoneurons harbouring *TARDBP* or *C9ORF72* ALS mutations are dysfunctional despite maintaining viability. *Nat. Commun.* 6, ncomms6999. doi:10.1038/ncomms6999

Di Giorgio, F. P., Boulting, G. L., Bobrowicz, S., and Eggan, K. C. (2008). Human embryonic stem cell-derived motor neurons are sensitive to the toxic effect of glial cells carrying an ALS-causing mutation. *Cell Stem Cell* 3, 637–648. doi:10.1016/j.stem.2008.09.017

Di Giorgio, F. P., Carrasco, M. A., Siao, M. C., Maniatis, T., and Eggan, K. (2007). Non-cell autonomous effect of glia on motor neurons in an embryonic stem cell-based ALS model. *Nat. Neurosci.* 10, 608–614. doi:10.1038/nn1885

Edmondson, R., Broglie, J. J., Adcock, A. F., and Yang, L. (2014). Three-dimensional cell culture systems and their applications in drug discovery and cell-based biosensors. *Assay Drug Dev. Technol.* 12, 207–218. doi:10.1089/adt.2014.573

Faley, S. L., Baer, B. B., Larsen, T. S. H., and Bellan, L. M. (2015). Robust fluidic connections to freestanding microfluidic hydrogels. *Biomicrofluidics* 9, 036501. doi:10.1063/1.4921453

Forrest, M. P., Zhang, H., Moy, W., McGowan, H., Leites, C., Dionisio, L. E., et al. (2017). Open chromatin profiling in hiPSC-derived neurons prioritizes functional noncoding psychiatric risk variants and highlights neurodevelopmental loci. *Cell Stem Cell* 21, 305.e–318.e. doi:10.1016/j.stem.2017.07.008

Franke, H., Galla, H. J., and Beuckmann, C. T. (1999). An improved low-permeability in vitro-model of the blood–brain barrier: transport studies on retinoids, sucrose, haloperidol, caffeine and mannitol. *Brain Res.* 818, 65–71. doi:10.1016/S0006-8993(98)01282-7

Friese, M. A., Schattling, B., and Fugger, L. (2014). Mechanisms of neurodegeneration and axonal dysfunction in multiple sclerosis. *Nat. Rev. Neurol.* 10, 225–238. doi:10.1038/nrneurol.2014.37

Garbuzova-Davis, S., Hernandez-Ontiveros, D. G., Rodrigues, M. C. O., Haller, E., Frisina-Deyo, A., Mirtyl, S., et al. (2012). Impaired blood-brain/spinal cord barrier in ALS patients. *Brain Res.* 1469, 114–128. doi:10.1016/j.brainres.2012.05.056

Golden, A. P., and Tien, J. (2007). Fabrication of microfluidic hydrogels using molded gelatin as a sacrificial element. *Lab. Chip* 7, 720–725. doi:10.1039/b618409j

González, F., Zhu, Z., Shi, Z.-D., Lelli, K., Verma, N., Li, Q. V., et al. (2014). An iCRISPR platform for rapid, multiplexable, and inducible genome editing in human pluripotent stem cells. *Cell Stem Cell* 15, 215–226. doi:10.1016/j.stem.2014.05.018

Griep, L. M., Wolbers, F., de Wagenaar, B., ter Braak, P. M., Weksler, B. B., Romero, I. A., et al. (2013). BBB on chip: microfluidic platform to mechanically and biochemically modulate blood-brain barrier function. *Biomed. Microdevices* 15, 145–150. doi:10.1007/s10544-012-9699-7

Griesi-Oliveira, K., Acab, A., Gupta, A. R., Sunaga, D. Y., Chailangkarn, T., Nicol, X., et al. (2015). Modeling non-syndromic autism and the impact of TRPC6 disruption in human neurons. *Mol. Psychiatry* 20, 1350–1365. doi:10.1038/mp.2014.141

Hartz, A. M. S., Zhong, Y., Wolf, A., LeVine, H., Miller, D. S., and Bauer, B. (2016). Aβ40 reduces P-glycoprotein at the blood–brain barrier through the ubiquitin–proteasome pathway. *J. Neurosci.* 36, 1930–1941. doi:10.1523/JNEUROSCI.0350-15.2016

Helms, H. C., Abbott, N. J., Burek, M., Cecchelli, R., Couraud, P.-O., Deli, M. A., et al. (2016). In vitro models of the blood-brain barrier: an overview of commonly used brain endothelial cell culture models and guidelines for their use. *J. Cereb. Blood Flow Metab.* 36, 862–890. doi:10.1177/0271678X16630991

Herland, A., van der Meer, A. D., FitzGerald, E. A., Park, T.-E., Sleeboom, J. J. F., and Ingber, D. E. (2016). Distinct contributions of astrocytes and pericytes to neuroinflammation identified in a 3D human blood-brain barrier on a chip. *PLoS ONE* 11:e0150360. doi:10.1371/journal.pone.0150360

Hirano, A., Nakano, I., Kurland, L. T., Mulder, D. W., Holley, P. W., and Saccomanno, G. (1984). Fine structural study of neurofibrillary changes in a family with amyotrophic lateral sclerosis. *J. Neuropathol. Exp. Neurol.* 43, 471–480. doi:10.1097/00005072-198409000-00002

Hoffmann, J. C., and West, J. L. (2013). Three-dimensional photolithographic micropatterning: a novel tool to probe the complexities of cell migration. *Integr. Biol.* 5, 817–827. doi:10.1039/C3IB20280A

Hollmann, E. K., Bailey, A. K., Potharazu, A. V., Neely, M. D., Bowman, A. B., and Lippmann, E. S. (2017). Accelerated differentiation of human induced pluripotent stem cells to blood–brain barrier endothelial cells. *Fluids Barriers CNS* 14, 9. doi:10.1186/s12987-017-0059-0

Hook, V., Brennand, K. J., Kim, Y., Toneff, T., Funkelstein, L., Lee, K. C., et al. (2014). Human iPSC neurons display activity-dependent neurotransmitter secretion: aberrant catecholamine levels in schizophrenia neurons. *Stem Cell Rep.* 3, 531–538. doi:10.1016/j.stemcr.2014.08.001

Hribar, K. C., Meggs, K., Liu, J., Zhu, W., Qu, X., and Chen, S. (2015). Three-dimensional direct cell patterning in collagen hydrogels with near-infrared femtosecond laser. *Sci. Rep.* 5, 17203. doi:10.1038/srep17203

Huh, D., Hamilton, G. A., and Ingber, D. E. (2011). From 3D cell culture to organs-on-chips. *Trends Cell Biol.* 21, 745–754. doi:10.1016/j.tcb.2011.09.005

Imaizumi, Y., Okada, Y., Akamatsu, W., Koike, M., Kuzumaki, N., Hayakawa, H., et al. (2012). Mitochondrial dysfunction associated with increased oxidative stress and α-synuclein accumulation in PARK2 iPSC-derived neurons and postmortem brain tissue. *Mol. Brain* 5, 35. doi:10.1186/1756-6606-5-35

Ingram, P. N., Hind, L. E., Jiminez-Torres, J. A., Huttenlocher, A., and Beebe, D. J. (2017). An accessible organotypic microvessel model using iPSC-derived endothelium. *Adv. Healthc. Mater.* doi:10.1002/adhm.201700497

Israel, M. A., Yuan, S. H., Bardy, C., Reyna, S. M., Mu, Y., Herrera, C., et al. (2012). Probing sporadic and familial Alzheimer's disease using induced pluripotent stem cells. *Nature* 482, 216–220. doi:10.1038/nature10821

Jiménez-Torres, J. A., Peery, S. L., Sung, K. E., and Beebe, D. J. (2016). LumeNEXT: a practical method to pattern luminal structures in ECM gels. *Adv. Healthc. Mater.* 5, 198–204. doi:10.1002/adhm.201500608

Katt, M. E., Xu, Z. S., Gerecht, S., and Searson, P. C. (2016). Human brain microvascular endothelial cells derived from the BC1 iPS cell line exhibit a blood-brain barrier phenotype. *PLoS ONE* 11:e0152105. doi:10.1371/journal.pone.0152105

Kiskinis, E., Sandoe, J., Williams, L. A., Boulting, G. L., Moccia, R., Wainger, B. J., et al. (2014). Pathways disrupted in human ALS motor neurons identified through genetic correction of mutant SOD1. *Cell Stem Cell* 14, 781–795. doi:10.1016/j.stem.2014.03.004

Kokubu, Y., Yamaguchi, T., and Kawabata, K. (2017). In vitro model of cerebral ischemia by using brain microvascular endothelial cells derived from human induced pluripotent stem cells. *Biochem. Biophys. Res. Commun.* 486, 577–583. doi:10.1016/j.bbrc.2017.03.092

Kolesky, D. B., Truby, R. L., Gladman, A. S., Busbee, T. A., Homan, K. A., and Lewis, J. A. (2014). 3D bioprinting of vascularized, heterogeneous cell-laden tissue constructs. *Adv. Mater.* 26, 3124–3130. doi:10.1002/adma.201305506

Korn, A., Golan, H., Melamed, I., Pascual-Marqui, R., and Friedman, A. (2005). Focal cortical dysfunction and blood–brain barrier disruption in patients with postconcussion syndrome. *J. Clin. Neurophysiol.* 22, 1–9. doi:10.1097/01.WNP.0000150973.24324.A7

Kouroupi, G., Taoufik, E., Vlachos, I. S., Tsioras, K., Antoniou, N., Papastefanaki, F., et al. (2017). Defective synaptic connectivity and axonal neuropathology in a human iPSC-based model of familial Parkinson's disease. *Proc. Natl. Acad. Sci. U.S.A.* 114, E3679–E3688. doi:10.1073/pnas.1617259114

Kuan, W.-L., Bennett, N., He, X., Skepper, J. N., Martynyuk, N., Wijeyekoon, R., et al. (2016). α-Synuclein pre-formed fibrils impair tight junction protein expression without affecting cerebral endothelial cell function. *Exp. Neurol.* 285(Part A), 72–81. doi:10.1016/j.expneurol.2016.09.003

Kumar-Singh, S., Theuns, J., Van Broeck, B., Pirici, D., Vennekens, K., Corsmit, E., et al. (2006). Mean age-of-onset of familial alzheimer disease caused by presenilin mutations correlates with both increased Aβ42 and decreased Aβ40. *Hum. Mutat.* 27, 686–695. doi:10.1002/humu.20336

Lamberti, G., Prabhakarpandian, B., Garson, C., Smith, A., Pant, K., Wang, B., et al. (2014). Bioinspired microfluidic assay for in vitro modeling of leukocyte-endothelium interactions. *Anal. Chem.* 86, 8344–8351. doi:10.1021/ac5018716

Large, C. H., Sokal, D. M., Nehlig, A., Gunthorpe, M. J., Sankar, R., Crean, C. S., et al. (2012). The spectrum of anticonvulsant efficacy of retigabine (ezogabine) in animal models: implications for clinical use. *Epilepsia* 53, 425–436. doi:10.1111/j.1528-1167.2011.03364.x

Lee, J. B., Wang, X., Faley, S., Baer, B., Balikov, D. A., Sung, H.-J., et al. (2016). Development of 3D microvascular networks within gelatin hydrogels using thermoresponsive sacrificial microfibers. *Adv. Healthc. Mater.* 5, 781–785. doi:10.1002/adhm.201500792

Lees, A. J., Hardy, J., and Revesz, T. (2009). Parkinson's disease. *Lancet* 373, 2055–2066. doi:10.1016/S0140-6736(09)60492-X

Lim, R. G., Quan, C., Reyes-Ortiz, A. M., Lutz, S. E., Kedaigle, A. J., Gipson, T. A., et al. (2017). Huntington's disease iPSC-derived brain microvascular endothelial cells reveal WNT-mediated angiogenic and blood-brain barrier deficits. *Cell Rep.* 19, 1365–1377. doi:10.1016/j.celrep.2017.04.021

Lippmann, E. S., Al-Ahmad, A., Azarin, S. M., Palecek, S. P., and Shusta, E. V. (2014). A retinoic acid-enhanced, multicellular human blood-brain barrier model derived from stem cell sources. *Sci. Rep.* 4, 4160. doi:10.1038/srep04160

Lippmann, E. S., Al-Ahmad, A., Palecek, S. P., and Shusta, E. V. (2013). Modeling the blood-brain barrier using stem cell sources. *Fluids Barriers CNS* 10, 2. doi:10.1186/2045-8118-10-2

Lippmann, E. S., Azarin, S. M., Kay, J. E., Nessler, R. A., Wilson, H. K., Al-Ahmad, A., et al. (2012). Derivation of blood-brain barrier endothelial cells from human pluripotent stem cells. *Nat. Biotechnol.* 30, 783–791. doi:10.1038/nbt.2247

Mali, P., Yang, L., Esvelt, K. M., Aach, J., Guell, M., DiCarlo, J. E., et al. (2013). RNA-guided human genome engineering via Cas9. *Science* 339, 823–826. doi:10.1126/science.1232033

Mandegar, M. A., Huebsch, N., Frolov, E. B., Shin, E., Truong, A., Olvera, M. P., et al. (2016). CRISPR interference efficiently induces specific and reversible gene silencing in human iPSCs. *Cell Stem Cell* 18, 541–553. doi:10.1016/j.stem.2016.01.022

Marchetto, M. C. N., Muotri, A. R., Mu, Y., Smith, A. M., Cezar, G. G., and Gage, F. H. (2008). Non-cell-autonomous effect of human SOD1 G37R astrocytes on motor neurons derived from human embryonic stem cells. *Cell Stem Cell* 3, 649–657. doi:10.1016/j.stem.2008.10.001

Mariani, J., Coppola, G., Zhang, P., Abyzov, A., Provini, L., Tomasini, L., et al. (2015). FOXG1-dependent dysregulation of GABA/glutamate neuron differentiation in autism spectrum disorders. *Cell* 162, 375–390. doi:10.1016/j.cell.2015.06.034

Markov, D. A., Lu, J. Q., Samson, P. C., Wikswo, J. P., and McCawley, L. J. (2012). Thick-tissue bioreactor as a platform for long-term organotypic culture and drug delivery. *Lab. Chip* 12, 4560–4568. doi:10.1039/c2lc40304h

Marques, F., Sousa, J. C., Sousa, N., and Palha, J. A. (2013). Blood–brain-barriers in aging and in Alzheimer's disease. *Mol. Neurodegener.* 8, 38. doi:10.1186/1750-1326-8-38

McNeish, J., Gardner, J. P., Wainger, B. J., Woolf, C. J., and Eggan, K. (2015). From dish to bedside: lessons learned while translating findings from a stem cell model of disease to a clinical trial. *Cell Stem Cell* 17, 8–10. doi:10.1016/j.stem.2015.06.013

Meister, S., Storck, S. E., Hameister, E., Behl, C., Weggen, S., Clement, A. M., et al. (2015). Expression of the ALS-causing variant hSOD1(G93A) leads to an impaired integrity and altered regulation of claudin-5 expression in an in vitro blood-spinal cord barrier model. *J. Cereb. Blood Flow Metab.* 35, 1112–1121. doi:10.1038/jcbfm.2015.57

Mertens, J., Stüber, K., Wunderlich, P., Ladewig, J., Kesavan, J. C., Vandenberghe, R., et al. (2013). APP processing in human pluripotent stem cell-derived neurons is resistant to NSAID-based γ-secretase modulation. *Stem Cell Rep.* 1, 491–498. doi:10.1016/j.stemcr.2013.10.011

Miller, J. S., Stevens, K. R., Yang, M. T., Baker, B. M., Nguyen, D.-H. T., Cohen, D. M., et al. (2012). Rapid casting of patterned vascular networks for perfusable engineered three-dimensional tissues. *Nat. Mater.* 11, 768–774. doi:10.1038/nmat3357

Mizee, M. R., Wooldrik, D., Lakeman, K. A. M., Hof, B., van het, Drexhage, J. A. R., Geerts, D., et al. (2013). Retinoic acid induces blood–brain barrier development. *J. Neurosci.* 33, 1660–1671. doi:10.1523/JNEUROSCI.1338-12.2013

Muratore, C. R., Rice, H. C., Srikanth, P., Callahan, D. G., Shin, T., Benjamin, L. N. P., et al. (2014). The familial Alzheimer's disease APPV717I mutation alters APP processing and Tau expression in iPSC-derived neurons. *Hum. Mol. Genet.* 23, 3523–3536. doi:10.1093/hmg/ddu064

Murphy, J. L., Vollenweider, L., Xu, F., and Lee, B. P. (2010). Adhesive performance of biomimetic adhesive-coated biologic scaffolds. *Biomacromolecules* 11, 2976–2984. doi:10.1021/bm1007794

Nagai, M., Re, D. B., Nagata, T., Chalazonitis, A., Jessell, T. M., Wichterle, H., et al. (2007). Astrocytes expressing ALS-linked mutated SOD1 release factors selectively toxic to motor neurons. *Nat. Neurosci.* 10, 615–622. doi:10.1038/nn1876

Nguyen, D. H. T., Stapleton, S. C., Yang, M. T., Cha, S. S., Choi, C. K., Galie, P. A., et al. (2013). Biomimetic model to reconstitute angiogenic sprouting morphogenesis in vitro. *Proc. Natl. Acad. Sci. U.S.A.* 110, 6712–6717. doi:10.1073/pnas.1221526110

Nguyen, H. N., Byers, B., Cord, B., Shcheglovitov, A., Byrne, J., Gujar, P., et al. (2011). LRRK2 mutant iPSC-derived DA neurons demonstrate increased susceptibility to oxidative stress. *Cell Stem Cell* 8, 267–280. doi:10.1016/j.stem.2011.01.013

Obermeier, B., Daneman, R., and Ransohoff, R. M. (2013). Development, maintenance and disruption of the blood-brain barrier. *Nat. Med.* 19, 1584–1596. doi:10.1038/nm.3407

Orlova, V. V., Drabsch, Y., Freund, C., Petrus-Reurer, S., van den Hil, F. E., Muenthaisong, S., et al. (2014). Functionality of endothelial cells and pericytes from human pluripotent stem cells demonstrated in cultured vascular plexus and zebrafish xenografts significance. *Arterioscler. Thromb. Vasc. Biol.* 34, 177–186. doi:10.1161/ATVBAHA.113.302598

Page, S., Munsell, A., and Al-Ahmad, A. J. (2016). Cerebral hypoxia/ischemia selectively disrupts tight junctions complexes in stem cell-derived human brain microvascular endothelial cells. *Fluids Barriers CNS* 13, 16. doi:10.1186/s12987-016-0042-1

Pampaloni, F., Reynaud, E. G., and Stelzer, E. H. K. (2007). The third dimension bridges the gap between cell culture and live tissue. *Nat. Rev. Mol. Cell Biol.* 8, 839–845. doi:10.1038/nrm2236

Pandya, H., Shen, M. J., Ichikawa, D. M., Sedlock, A. B., Choi, Y., Johnson, K. R., et al. (2017). Differentiation of human and murine induced pluripotent stem cells to microglia-like cells. *Nat. Neurosci.* 20, 753. doi:10.1038/nn.4534

Pardridge, W. M. (2005). The blood-brain barrier: bottleneck in brain drug development. *NeuroRx* 2, 3–14. doi:10.1602/neurorx.2.1.3

Park, R., Kook, S.-Y., Park, J.-C., and Mook-Jung, I. (2014). Aβ1–42 reduces P-glycoprotein in the blood–brain barrier through RAGE–NF-κB signaling. *Cell Death Dis.* 5, e1299. doi:10.1038/cddis.2014.258

Peelaerts, W., Bousset, L., Van der Perren, A., Moskalyuk, A., Pulizzi, R., Giugliano, M., et al. (2015). α-Synuclein strains cause distinct synucleinopathies after local and systemic administration. *Nature* 522, 340–344. doi:10.1038/nature14547

Pellett, S., Schwartz, M. P., Tepp, W. H., Josephson, R., Scherf, J. M., Pier, C. L., et al. (2015). Human induced pluripotent stem cell derived neuronal cells cultured on chemically-defined hydrogels for sensitive in vitro detection of botulinum neurotoxin. *Sci. Rep.* 5, 14566. doi:10.1038/srep14566

Phan, D. T. T., Wang, X., Craver, B. M., Sobrino, A., Zhao, D., Chen, J. C., et al. (2017). A vascularized and perfused organ-on-a-chip platform for large-scale drug screening applications. *Lab. Chip* 17, 511–520. doi:10.1039/c6lc01422d

Prabhakarpandian, B., Shen, M.-C., Nichols, J. B., Mills, I. R., Sidoryk-Wegrzynowicz, M., Aschner, M., et al. (2013). SyM-BBB: a microfluidic blood brain barrier model. *Lab. Chip* 13, 1093–1101. doi:10.1039/C2LC41208J

Raman, R., Bhaduri, B., Mir, M., Shkumatov, A., Lee, M. K., Popescu, G., et al. (2016). High-resolution projection microstereolithography for patterning of neovasculature. *Adv. Healthc. Mater.* 5, 610–619. doi:10.1002/adhm.201500721

Ravi, M., Paramesh, V., Kaviya, S. R., Anuradha, E., and Solomon, F. D. P. (2015). 3D cell culture systems: advantages and applications. *J. Cell. Physiol.* 230, 16–26. doi:10.1002/jcp.24683

Sagare, A. P., Bell, R. D., and Zlokovic, B. V. (2012). Neurovascular dysfunction and faulty amyloid β-peptide clearance in Alzheimer disease. *Cold Spring Harb. Perspect. Med.* 2, a011452. doi:10.1101/cshperspect.a011452

Sau, D., De Biasi, S., Vitellaro-Zuccarello, L., Riso, P., Guarnieri, S., Porrini, M., et al. (2007). Mutation of SOD1 in ALS: a gain of a loss of function. *Hum. Mol. Genet.* 16, 1604–1618. doi:10.1093/hmg/ddm110

Schwartz, M. P., Hou, Z., Propson, N. E., Zhang, J., Engstrom, C. J., Costa, V. S., et al. (2015). Human pluripotent stem cell-derived neural constructs for predicting neural toxicity. *Proc. Natl. Acad. Sci. U.S.A.* 112, 12516–12521. doi:10.1073/pnas.1516645112

Selkoe, D. J. (2001). Alzheimer's disease: genes, proteins, and therapy. *Physiol. Rev.* 81, 741–766. doi:10.1152/physrev.2001.81.2.741

Sellgren, K. L., Hawkins, B. T., and Grego, S. (2015). An optically transparent membrane supports shear stress studies in a three-dimensional microfluidic neurovascular unit model. *Biomicrofluidics* 9, 061102. doi:10.1063/1.4935594

Shcheglovitov, A., Shcheglovitova, O., Yazawa, M., Portmann, T., Shu, R., Sebastiano, V., et al. (2013). SHANK3 and IGF1 restore synaptic deficits in neurons from 22q13 deletion syndrome patients. *Nature* 503, 267–271. doi:10.1038/nature12618

Skylar-Scott, M. A., Liu, M.-C., Wu, Y., Dixit, A., and Yanik, M. F. (2016). Guided homing of cells in multi-photon microfabricated bioscaffolds. *Adv. Healthc. Mater.* 5, 1233–1243. doi:10.1002/adhm.201600082

Smith, Q. R., and Rapoport, S. I. (1986). Cerebrovascular permeability coefficients to sodium, potassium, and chloride. *J. Neurochem.* 46, 1732–1742. doi:10.1111/j.1471-4159.1986.tb08491.x

Srinivasan, B., Kolli, A. R., Esch, M. B., Abaci, H. E., Shuler, M. L., and Hickman, J. J. (2015). TEER measurement techniques for in vitro barrier model systems. *J. Lab. Autom.* 20, 107–126. doi:10.1177/2211068214561025

Stenman, J. M., Rajagopal, J., Carroll, T. J., Ishibashi, M., McMahon, J., and McMahon, A. P. (2008). Canonical Wnt signaling regulates organ-specific assembly and differentiation of CNS vasculature. *Science* 322, 1247–1250. doi:10.1126/science.1164594

Sui, Y.-T., Bullock, K. M., Erickson, M. A., Zhang, J., and Banks, W. A. (2014). Alpha synuclein is transported into and out of the brain by the blood–brain barrier. *Peptides* 62, 197–202. doi:10.1016/j.peptides.2014.09.018

Syvänen, S., Lindhe, Ö, Palner, M., Kornum, B. R., Rahman, O., Långström, B. (2009). Species differences in blood-brain barrier transport of three positron emission tomography radioligands with emphasis on P-glycoprotein transport. *Drug Metab. Dispos.* 37, 635–643. doi:10.1124/dmd.108.024745

Takahashi, K., Tanabe, K., Ohnuki, M., Narita, M., Ichisaka, T., Tomoda, K., et al. (2007). Induction of pluripotent stem cells from adult human fibroblasts by defined factors. *Cell* 131, 861–872. doi:10.1016/j.cell.2007.11.019

Tang, A. T., Choi, J. P., Kotzin, J. J., Yang, Y., Hong, C. C., Hobson, N., et al. (2017a). Endothelial TLR4 and the microbiome drive cerebral cavernous malformations. *Nature* 545, 305–310. doi:10.1038/nature22075

Tang, Y., Xia, W., Yu, X., Zhou, B., Luo, C., Huang, X., et al. (2017b). Short-term cerebral activity alterations after surgery in patients with unilateral mesial temporal lobe epilepsy associated with hippocampal sclerosis: a longitudinal resting-state fMRI study. *Seizure* 46, 43–49. doi:10.1016/j.seizure.2016.12.021

Tibbitt, M. W., and Anseth, K. S. (2009). Hydrogels as extracellular matrix mimics for 3D cell culture. *Biotechnol. Bioeng.* 103, 655–663. doi:10.1002/bit.22361

Valentin, T. M., Leggett, S. E., Chen, P.-Y., Sodhi, J. K., Stephens, L. H., McClintock, H. D., et al. (2017). Stereolithographic printing of ionically-crosslinked alginate hydrogels for degradable biomaterials and microfluidics. *Lab. Chip* 17, 3474–3488. doi:10.1039/C7LC00694B

Vatine, G. D., Al-Ahmad, A., Barriga, B. K., Svendsen, S., Salim, A., Garcia, L., et al. (2017). Modeling psychomotor retardation using iPSCs from MCT8-deficient patients indicates a prominent role for the blood-brain barrier. *Cell Stem* 20, 831.e–843.e. doi:10.1016/j.stem.2017.04.002

Wainger, B. J., Kiskinis, E., Mellin, C., Wiskow, O., Han, S. S. W., Sandoe, J., et al. (2014). Intrinsic membrane hyperexcitability of amyotrophic lateral sclerosis patient-derived motor neurons. *Cell Rep.* 7, 1–11. doi:10.1016/j.celrep.2014.03.019

Wang, X., Phan, D. T. T., George, S. C., Hughes, C. C. W., and Lee, A. P. (2017a). 3D anastomosed microvascular network model with living capillary networks and endothelial cell-lined microfluidic channels. *Methods Mol. Biol* 1612, 325–344. doi:10.1007/978-1-4939-7021-6_24

Wang, Y. I., Abaci, H. E., and Shuler, M. L. (2017b). Microfluidic blood–brain barrier model provides in vivo-like barrier properties for drug permeability screening. *Biotechnol. Bioeng.* 114, 184–194. doi:10.1002/bit.26045

Wang, Z., Abdulla, R., Parker, B., Samanipour, R., Ghosh, S., Kim, K., et al. (2015). A simple and high-resolution stereolithography-based 3D bioprinting system using visible light crosslinkable bioinks. *Biofabrication* 7, 045009. doi:10.1088/1758-5090/7/4/045009

Weksler, B. B., Subileau, E. A., Perrière, N., Charneau, P., Holloway, K., Leveque, M., et al. (2005). Blood-brain barrier-specific properties of a human adult brain endothelial cell line. *FASEB J.* 19, 1872–1874. doi:10.1096/fj.04-3458fje

Wen, Z., Nguyen, H. N., Guo, Z., Lalli, M. A., Wang, X., Su, Y., et al. (2014). Synaptic dysregulation in a human iPS cell model of mental disorders. *Nature* 515, 414–418. doi:10.1038/nature13716

Wikswo, J. P. (2014). The relevance and potential roles of microphysiological systems in biology and medicine. *Exp. Biol. Med. (Maywood)* 239, 1061–1072. doi:10.1177/1535370214542068

Wilson, H. K., Canfield, S. G., Hjortness, M. K., Palecek, S. P., Shusta, E. V., et al. (2015). Exploring the effects of cell seeding density on the differentiation of human pluripotent stem cells to brain microvascular endothelial cells. *Fluids Barriers CNS* 12, 13. doi:10.1186/s12987-015-0007-9

Winkler, E. A., Sengillo, J. D., Sagare, A. P., Zhao, Z., Ma, Q., Zuniga, E., et al. (2014). Blood-spinal cord barrier disruption contributes to early motor-neuron degeneration in ALS-model mice. *Proc. Natl. Acad. Sci. U.S.A.* 111, E1035–E1042. doi:10.1073/pnas.1401595111

Winkler, E. A., Sengillo, J. D., Sullivan, J. S., Henkel, J. S., Appel, S. H., Zlokovic, B. V., et al. (2013). Blood-spinal cord barrier breakdown and pericyte reductions in amyotrophic lateral sclerosis. *Acta Neuropathol.* 125, 111–120. doi:10.1007/s00401-012-1039-8

Ye, M., Sanchez, H. M., Hultz, M., Yang, Z., Bogorad, M., Wong, A. D., et al. (2014). Brain microvascular endothelial cells resist elongation due to curvature and shear stress. *Sci. Rep.* 4, sre04681. doi:10.1038/srep04681

Yeon, J. H., Na, D., Choi, K., Ryu, S.-W., Choi, C., and Park, J.-K., et al. (2012). Reliable permeability assay system in a microfluidic device mimicking cerebral vasculatures. *Biomed. Microdevices* 14, 1141–1148. doi:10.1007/s10544-012-9680-5

Yoon, K.-J., Nguyen, H. N., Ursini, G., Zhang, F., Kim, N.-S., Wen, Z., et al. (2014). Modeling a genetic risk for schizophrenia in iPSCs and mice reveals neural stem cell deficits associated with adherens junctions and polarity. *Cell Stem Cell* 15, 79–91. doi:10.1016/j.stem.2014.05.003

Yu, J., Vodyanik, M. A., Smuga-Otto, K., Antosiewicz-Bourget, J., Frane, J. L., Tian, S., et al. (2007). Induced pluripotent stem cell lines derived from human somatic cells. *Science* 318, 1917–1920. doi:10.1126/science.1151526

Zanotelli, M. R., Ardalani, H., Zhang, J., Hou, Z., Nguyen, E. H., Swanson, S., et al. (2016). Stable engineered vascular networks from human induced pluripotent stem cell-derived endothelial cells cultured in synthetic hydrogels. *Acta Biomater.* 35, 32–41. doi:10.1016/j.actbio.2016.03.001

Zhao, Z., Sagare, A. P., Ma, Q., Halliday, M. R., Kong, P., Kisler, K., et al. (2015). Central role for PICALM in amyloid-β blood-brain barrier transcytosis and clearance. *Nat. Neurosci.* 18, 978–987. doi:10.1038/nn.4025

Zheng, Y., Chen, J., Craven, M., Choi, N. W., Totorica, S., Diaz-Santana, A., et al. (2012). In vitro microvessels for the study of angiogenesis and thrombosis. *Proc. Natl. Acad. Sci. U.S.A.* 109, 9342–9347. doi:10.1073/pnas.1201240109

Zhong, Z., Deane, R., Ali, Z., Parisi, M., Shapovalov, Y., O'Banion, M. K., et al. (2008). ALS-causing SOD1 mutants generate vascular changes prior to motor neuron degeneration. *Nat. Neurosci.* 11, 420–422. doi:10.1038/nn2073

Conflict of Interest Statement: The authors declare that the research was conducted in the absence of any commercial or financial relationships that could be construed as a potential conflict of interest.

frontiers in Bioengineering and Biotechnology

ORIGINAL RESEARCH
published: 27 March 2018
doi: 10.3389/fbioe.2018.00026

Correlation of mRNA Expression and Signal Variability in Chronic Intracortical Electrodes

*Jessica D. Falcone[1], Sheridan L. Carroll[2], Tarun Saxena[2], Dev Mandavia[3], Alexus Clark[3], Varun Yarabarla[3] and Ravi V. Bellamkonda[2]**

[1] School of Electrical and Computer Engineering, Georgia Institute of Technology, Atlanta, GA, United States,
[2] Department of Biomedical Engineering, Pratt School of Engineering, Duke University, Durham, NC, United States,
[3] Wallace H. Coulter Department of Biomedical Engineering, Georgia Institute of Technology and Emory University School of Medicine, Atlanta, GA, United States

Objective: The goal for this research was to identify molecular mechanisms that explain animal-to-animal variability in chronic intracortical recordings.

Approach: Microwire electrodes were implanted into Sprague Dawley rats at an acute (1 week) and a chronic (14 weeks) time point. Weekly recordings were conducted, and action potentials were evoked in the barrel cortex by deflecting the rat's whiskers. At 1 and 14 weeks, tissue was collected, and mRNA was extracted. mRNA expression was compared between 1 and 14 weeks using a high throughput multiplexed qRT-PCR. Pearson correlation coefficients were calculated between mRNA expression and signal-to-noise ratios at 14 weeks.

Main results: At 14 weeks, a positive correlation between signal-to-noise ratio (SNR) and NeuN and GFAP mRNA expression was observed, indicating a relationship between recording strength and neuronal population, as well as reactive astrocyte activity. The inflammatory state around the electrode interface was evaluated using M1-like and M2-like markers. Expression for both M1-like and M2-like mRNA markers remained steady from 1 to 14 weeks. Anti-inflammatory markers, CD206 and CD163, however, demonstrated a significant positive correlation with SNR quality at 14 weeks. VE-cadherin, a marker for adherens junctions, and PDGFR-β, a marker for pericytes, both partial representatives of blood–brain barrier health, had a positive correlation with SNR at 14 weeks. Endothelial adhesion markers revealed a significant increase in expression at 14 weeks, while CD45, a pan-leukocyte marker, significantly decreased at 14 weeks. No significant correlation was found for either the endothelial adhesion or pan-leukocyte markers.

Significance: A positive correlation between anti-inflammatory and blood–brain barrier health mRNA markers with electrophysiological efficacy of implanted intracortical electrodes has been demonstrated. These data reveal potential mechanisms for further evaluation to determine potential target mechanisms to improve consistency of intracortical electrodes recordings and reduce animal-to-animal/implant-to-implant variability.

Keywords: intracortical microelectrodes, blood–brain barrier, neuro-inflammatory response, chronic recordings, signal-to-noise ratio, correlation analysis

OPEN ACCESS

Edited by:
Sara Pedron, University of Illinois at Urbana–Champaign, United States

Reviewed by:
Jeffrey R. Capadona, Case Western Reserve University, United States
Mahdis Shayan, Yale University, United States

****Correspondence:***
Ravi V. Bellamkonda
ravi@duke.edu

Specialty section:
This article was submitted to Biomaterials, a section of the journal Frontiers in Bioengineering and Biotechnology

Received: *22 December 2017*
Accepted: *06 March 2018*
Published: *27 March 2018*

Citation:
Falcone JD, Carroll SL, Saxena T, Mandavia D, Clark A, Yarabarla V and Bellamkonda RV (2018) Correlation of mRNA Expression and Signal Variability in Chronic Intracortical Electrodes. Front. Bioeng. Biotechnol. 6:26. doi: 10.3389/fbioe.2018.00026

INTRODUCTION

Brain machine interfaces (BMIs) using intracortical electrodes are promising to restore virtual and physical functionality to paralysis patients (Simeral et al., 2011; Collinger et al., 2013; Perge et al., 2014; Bouton et al., 2016; Downey et al., 2016; Ajiboye et al., 2017). However, reduction in amplitude and number of recorded spikes directly impacts the accuracy of machine control (Perge et al., 2014). Signal loss in both clinical (Simeral et al., 2011; Collinger et al., 2013; Perge et al., 2014; Bouton et al., 2016; Downey et al., 2016; Ajiboye et al., 2017) and preclinical (Karumbaiah et al., 2013; Saxena et al., 2013; Kozai et al., 2015; Nolta et al., 2015; Sharma et al., 2015; McCreery et al., 2016) intracortical electrode models have been well documented. A potential biological cause is chronic neurodegeneration, which has been characterized at the electrode–tissue interface (McConnell et al., 2009; Potter-Baker et al., 2015). Additionally, histology of neuronal nuclei density has been significantly correlated with signal-to-noise ratio (SNR) at the time of sacrifice (~300 days) (McCreery et al., 2016).

Previous work has suggested that the severity and duration of chronic blood–brain barrier (BBB) breach may influence chronic recordings (Potter et al., 2012; Saxena et al., 2013; Nolta et al., 2015; Kozai et al., 2016). The results have shown a negative correlation between IgG localization (a circulatory macromolecule) at the electrode interface and SNR (Karumbaiah et al., 2013; Saxena et al., 2013; Nolta et al., 2015). IgG accumulation has also shown to significantly and inversely correlate with impacts on behavioral motor function following electrode implantation in the motor cortex (Goss-Varley et al., 2017). While IgG localization demonstrates BBB leakage, it provides no information on how the BBB has been breached. Here, we investigate the molecular sequelae to implanted intracortical electrodes in the context of SNR to identify possible contributors to recording success.

For this study, key markers of BBB dysregulation, macrophage phenotype, and neuronal health at the mRNA level were quantified following electrode implantation. Animal-to-animal recording variability was leveraged to analyze correlations with mRNA expression at a chronic (14 week) time point to better elucidate potential mechanisms associated with electrode failure. To achieve this objective, functional microwire electrodes were implanted into the rat barrel cortex acutely (for 1 week) and chronically (for 14 weeks). At each endpoint, mRNA was extracted for Fluidigm multiplex qRT-PCR analysis. The calculated fold changes for each animal were compared to its functional recordings *via* a Pearson coefficient correlation. Primers for neuroinflammation, BBB integrity, innate inflammation, and leukocyte infiltration were investigated (see **Table 1**).

TABLE 1 | Overview of significant Pearson correlation at 14 weeks for (A) neuroinflammation markers, (B) blood–brain barrier (BBB) markers, (C) leukocyte infiltration markers, and (D) inflammation markers.

Groups	Primers	Pearson correlation ($p < 0.05$)
Neuro-inflammtion	CD68	No
	GFAP	Yes
	NeuN	Yes
BBB	claudin-5	No
	occludin	No
	zona-occludens-1	No
	cdh5	Yes
	PDGFR-β	Yes
	AQP-4	No
Leukocyte adhesion	CD45	No
	ACAM	No
	ICAM1	No
	ICAM2	No
	sel-e	No
	sel-p	No
	VCAM1	No
Inflammation M1-like	CCR7	No
	CD32	No
	CD64	No
	CD80	No
	CD86	No
Inflammation M2-like	Arg-1	No
	CD163	Yes
	CD206	Yes

MATERIALS AND METHODS

Surgical Preparation and Electrode Implantation

This study was carried out in accordance with the recommendations of the Institutional Animal Care and Use Committee (IACUC) at the Georgia Institute of Technology. The protocol was approved by the Georgia Institute of Technology. Adult male Sprague Dawley rats (250–300 g) were implanted for 1 week ($n = 5$) or 14 weeks ($n = 6$). The implanted electrodes were polyimide coated tungsten microwires (Tucker-Davis Technologies, FL, USA). The array had 16 electrodes arranged in a 2 × 8 pattern spaced 300 μm apart in the x-direction and 500 μm apart in the y-direction (see **Figure 1A**). The electrodes were 50 μm in diameter and 5 mm in length. All microwires were sterilized by ethylene oxide and degassed for 12 h. Each rat was anesthetized with 2% isoflurane, and their head was shaved and sterilized with chlorohexidine and isopropanol. Each rat's head was stereotaxtically positioned and a subcutaneous injection of lidocaine (Henry Schein, NY, USA) was administered locally prior to incision. Following a midline incision, the periosteum was scraped away and etch gel (Henry Schein, NY, USA) was applied to the skull. Holes for the anchoring screws were then drilled (2 anterior to bregma, 2 posterior to lambda, and 1 opposite the craniotomy), and five screws were inserted (see **Figure 1B**). A 3 mm × 5 mm craniotomy was drilled at 1.5 mm posterior from bregma and 4 mm lateral from the midline (see **Figure 1B**). The dura was retracted using a bent 25-gage needle and bleeding was controlled using gel foam (Pfizer, NY, USA) soaked with sterile saline. Grounding wires were wrapped around the anchoring screws prior to insertion. Each array was implanted at a 15° angle to a depth of 1,200 μm, targeting the IV cortical layer of the barrel cortex. Sterile 1.5% SeaKem agarose (Lonza, NJ, USA) was applied above the craniotomy and UV curing dental cement (Henry Schein, NY, USA) was used to secure the electrodes to the anchor screws and the skull. The incision was wound clipped and animals were injected intramuscularly with buprenorphine.

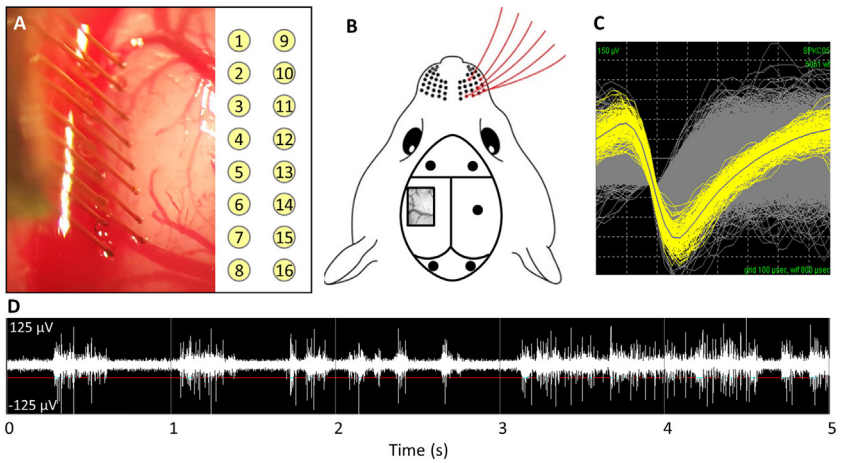

FIGURE 1 | **(A)** Implantation of microwire array and electrode site map. **(B)** Representative image of barrel cortex craniotomy and anchoring/grounding screws. **(C)** Average waveforms for a single unit. **(D)** Acquired raw waveforms from recording system with example threshold setting.

Animals received daily subcutaneous injections of antibiotic, Baytril (Bayer, PA, USA), for 2 weeks.

Electrophysiology and Analysis

Weekly recordings were collected with a 32-channel data-acquisition system (Plexon, TX, USA). Signals were amplified at 1,000 × gain, band-pass filtered at 500–5,000 Hz and sampled at 40 kHz. Animals were anesthetized with ketamine/xylazine/acepromazine cocktail as isoflurane suppresses cortical firing in the barrel cortex. For each recording session, two files where recorded: (1) an evoked file in which the rat's whiskers were deflected for ~1 min, generating action potentials (see **Figures 1C,D**) and (2) a noise file in which no signals were evoked for 10 s. In Offline Sorter (Plexon, TX, USA), the channels in the evoked files were thresholded at −4σ (standard orders of deviation), and units were sorted using K means cluster cutting. To verify units, the interspike interval histogram was analyzed and the presence of a clear refractory period was observed for a unit to be declared. Units that had fewer than 100 action potentials were excluded. Spontaneous action potentials were removed from the noise file. Sorted files were then exported into Matlab and custom code was used to calculate the SNR by dividing the peak-to-peak voltage ($V_{p\text{-}p}$) by two times the SD of noise (Eq. 1) (Nordhausen et al., 1996; Srinivasan et al., 2016).

$$\mathrm{SNR} = \frac{v_{p-p}}{2^{*}\mathrm{Std}_{\mathrm{noise}}} = \frac{(V_{\max} - V_{\min})}{2^{*}\sqrt{\frac{\sum(\mathrm{noise}_j - \mu_{\mathrm{noise}})^2}{(n-1)}}} \quad (1)$$

qRT-PCR and Analysis

At the designated time point, animals were transcardially perfused with sterile PBS (200 mL). The electrodes and headcap were removed and the brain was extracted. A 4-mm biopsy punch was taken at a depth of 2 mm around the electrode implant site. The biopsy punch was immediately frozen in liquid nitrogen and stored at −80°C. Age-matched naïve animals were sacrificed in the same manner as well and the 4-mm biopsy punch was removed from a depth of 2 mm at the same location in the brain. Total RNA was extracted using the RNeasy Plus Universal Kit (Qiagen, CA, USA). RNA integrity was assessed with the Agilent Bioanalyzer using Agilent RNA 6000 Nano Kit (Agilent Technologies, CA, USA), and purity was assessed with the Nanodrop 8000 Spectrophotometer (Thermo Fisher Scientific, MA, USA). For all samples, RNA integrity numbers were above 7, 260/280 were above 1.8, and 260/230 were above 1.0. cDNA was synthesized using the Fluidigm Reverse Transcription kit (#100-6298) (Fluidigm, CA, USA). A 96 qRT-PCR assay using the Fluidigm Biomark HD (Fluidigm, CA, USA) was run in triplicate for each sample using the Duke Center for Genomic and Computational Biology. The Delta Gene Assays (Fluidigm, CA, USA) were designed using the D3 Assay Design (Fluidigm, CA, USA). CT values were averaged together across triplicates. ΔCT values were calculated by subtracting the geometric mean of four housekeeping genes (GAPDH, HRPT, SDHA, RPL13A) from each CT value. ΔΔCT values were calculated by subtracting the arithmetic average of the naïve samples from the ΔCT values. All statistics were performed in the ΔΔCT space. Fold change was then calculated by taking the base 2 exponent of—ΔΔCT. A Bonferroni sequential correction (Benjamini and Hochberg, 1995) was applied to a Student's *t*-test to determine significance between 1- and 14-week microwire animals.

Correlation Analysis

To correlate the relation between average SNR and mRNA fold change, a Pearson correlation coefficient (*r*) with a *p*-value was calculated in Matlab. The electrode SNRs for each animal were averaged at each timepoint. The 14-week SNRs were compared with the mRNA extracted at 14 weeks for each animal.

Immunohistochemistry

At 1 week, rats implanted with microwires were transcardially perfused with PBS, 4% paraformaldehyde, and 20% sucrose. Following decapitation, the skulls were exposed and placed in 4% paraformaldehyde overnight at 4°C and then 30% sucrose overnight at 4°C. The brains were then extracted and stored in 30% sucrose at 4°C overnight or until the brains sunk to the bottom of the container. Brains were frozen at −20°C and cryosectioned transversely onto charged glass slides (VWR, PA, USA). Slides were thawed to room temperature and washed with PBS. The slides were incubated at room temperature in blocking solution (0.4% Triton-X, 4% goat serum in PBS) for 1 h. The following primary antibodies were used: rabbit anti-GFAP (1:1,000, DAKO, CA, USA), mouse IgG1 anti-NeuN (1:500, Millipore, CA, USA), and mouse anti-CD68 (1:500, Millipore, CA, USA). Primary antibodies were diluted in blocking solution and incubated overnight at 4°C. Slides were then washed in PBS and washing solution (0.4% Triton-X in PBS). The appropriate secondary antibody was applied for 1 h at room temperature, followed by DAPI for 15 min. Slides were washed again in PBS and washing solution, dried, and coverslipped with Fluoromount-G (Southern Biotech, AL, USA). Stained slides were imaged at 10× on a Zeiss Axiovert 200 M (Carl Zeiss, NY, USA).

RESULTS

Animal-to-Animal Variability in Electrophysiology

Weekly recordings were conducted in the barrel cortex. Rats were anesthetized and whiskers were deflected to generate evoked potentials. SNRs were calculated for each electrode within each time point within each animal. Eight rats were implanted for the chronic time point, but two were removed from the study due to headcap failure (C3 and C6). **Figure 2A** demonstrates the animal-to-animal variability present at 14 weeks for both SNR and percentage of active electrodes. **Figures 2B,C** shows the average SNR and percentage of active electrodes plots, subsequently, for each individual animal over time. A three-way nested ANOVA was run in Matlab on the SNR and electrode percentage data. Over time, no significant change was observed for either metric ($p > 0.05$). However, animal variability in SNR and percentage of active electrodes was significant. This variability was used to investigate possible correlations with underlying molecular differences through mRNA expression. Briefly, Pearson correlation coefficients and p-values were calculated for each mRNA primer and the corresponding animal's SNR. Pearson correlation coefficients were considered significant when the p-value ≤ 0.05. Additionally, mRNA expression was compared between 1 and 14 weeks using a Bonferroni sequential corrected Student's t-test in which significance was determined when the p-value was ≤ 0.05.

Neuroinflammation

At the conclusion of each time point, mRNA was extracted from biopsied brain tissue and mRNA expression was calculated. Neuroinflammation markers, classically found in the intracortical electrode implant literature, were analyzed. This included CD68 for activated microglia/macrophages, GFAP for astrocytes, and NeuN for neuronal nuclei (Polikov et al., 2005; Potter et al., 2012; Saxena et al., 2013; Sawyer et al., 2014; Nolta et al., 2015).

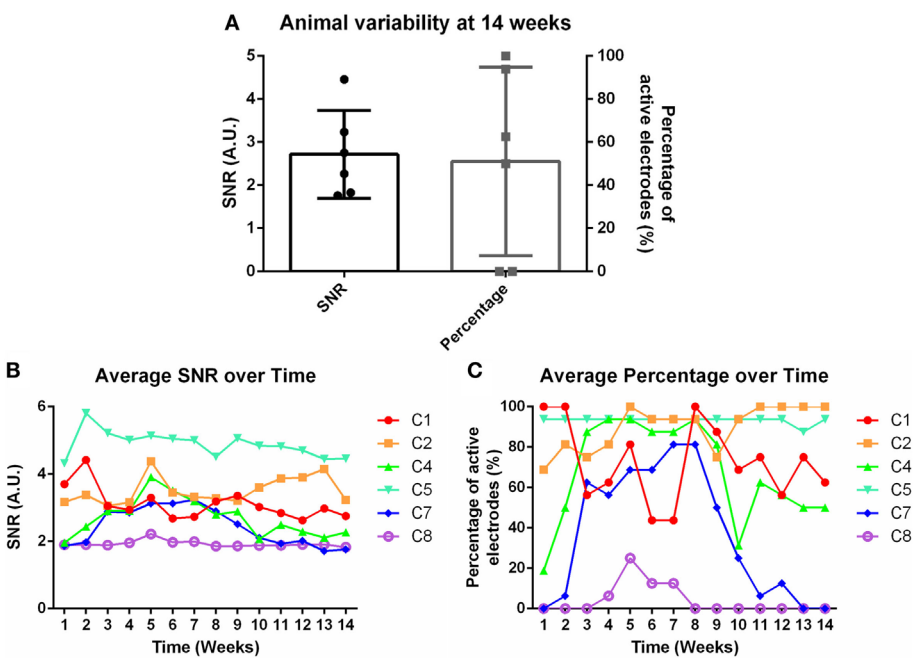

FIGURE 2 | **(A)** Animal variability at 14 weeks demonstrated through signal-to-noise ratio (SNR) and percentage of active electrodes. **(B)** Average SNR and **(C)** average percentage of active electrodes over time for individual animals.

Representative immunohistochemistry images of CD68, GFAP, and NeuN at the microwire interface are shown in **Figures 3A–C** at 1 week. There was a significant reduction of CD68 expression from 1 to 14 weeks, and a significant increase of GFAP from 1 to 14 weeks ($p < 0.05$) (**Figures 3E,F**). No change was observed for NeuN expression (**Figure 3D**). At 14 weeks, the Pearson correlation coefficient was positively significant for both NeuN and GFAP ($r = 0.85$, $p < 0.05$, and $r = 0.85$, $p < 0.05$, **Figure 3G**; Figures S1A,B in Supplementary Material). As NeuN marks neuronal nuclei, the positive correlation with SNR is suggestive that SNR represents neuronal population at the electrode interface.

Inflammation Milieu

Macrophages are a strong part of the wound healing and neuroinflammatory response (Strauss-Ayali et al., 2007; Kigerl et al., 2009; David and Kroner, 2011; Mokarram et al., 2017). Markers for M1-like or pro-inflammatory response were analyzed and were upregulated at both 1 and 14 weeks (**Figures 4A–E**). However, there was no significant change over time. No significance was found for Pearson correlation coefficients for pro-inflammatory markers at 14 weeks (**Figure 4I**; Figure S1C in Supplementary Material). For M2-like markers or anti-inflammatory response (**Figures 4F–H**), CD206 and CD163 had a significant positive Pearson correlation coefficient at 14 weeks ($r = 0.84$, $r = 0.89$, $p < 0.05$, **Figure 4J**; Figure S1D in Supplementary Material).

Vascular Integrity/BBB Breach Status

Previous research has demonstrated the importance of BBB and vasculature to neuronal health (Abbott et al., 2006; Ivens et al., 2007; Stolp and Dziegielewska, 2009; Zlokovic, 2011; Obermeier et al., 2013; Ryu et al., 2015). Here, tight junction proteins and additional BBB markers were observed. First, common tight junction proteins, zona-occludens-1 (ZO-1), claudin-5 (cldn5), and occludin (ocln) were evaluated to assess BBB fidelity. ZO-1 had a significant upregulation at 14 weeks compared to 1 week (**Figure 5C**). No other significant changes from 1 to 14 weeks were observed for cldn5 or ocln (**Figures 5A,B**). No significant Pearson coefficient correlation was found for cldn5, ocln, or ZO-1 at 14 weeks (**Figure 5D**; Figure S1E in Supplementary Material). With no significant correlations with tight junction proteins, additional BBB markers were next evaluated. These included cell-to-cell junctions, VE-cadherin (cdh-5), pericytes (PDGFR-β), and astrocyte end-feet (Aqp-4). Aqp-4 was significantly upregulated at 14 weeks compared to 1 week (**Figure 5G**). Expression levels remained the same for cdh-5 and PDGFR-β (**Figures 5E,F**). There was a significant positive Pearson correlation coefficient at 14 weeks for cdh-5 and PDGFR-β ($r = 0.85$, $r = 0.89$, $p < 0.05$, **Figure 5H**; Figure S1F in Supplementary Material). However, no significant correlation was observed for Aqp-4.

Leukocyte Recruitment and Adhesion

A detrimental outcome of BBB leakage is the infiltration of leukocytes (Greenwood et al., 2011; Obermeier et al., 2013). This can be monitored by leukocyte cell markers and endothelial cell adhesion markers. The fold change for the pan-leukocyte marker (CD45) was analyzed and expression significantly decreased at 14 weeks compared to 1 week ($p < 0.05$, **Figure 6G**). However, no significant Pearson correlation was observed with SNR (**Figure 6H**). A variety of adhesion markers were analyzed (ACAM, ICAM1, ICAM2, sel-e, sel-p, VCAM1, **Figures 6A–F**). All were significantly upregulated at 14 weeks (except for ICAM2), suggesting increased leukocyte extravasation, but again, no significant Pearson correlation was found (**Figure 6H**; Figure S1G in Supplementary Material).

DISCUSSION

If BMIs are to be successful, the signal from the intracortical electrode (i.e., the input) must be able to reliably and robustly record for long durations (on the order of years). Previously, a

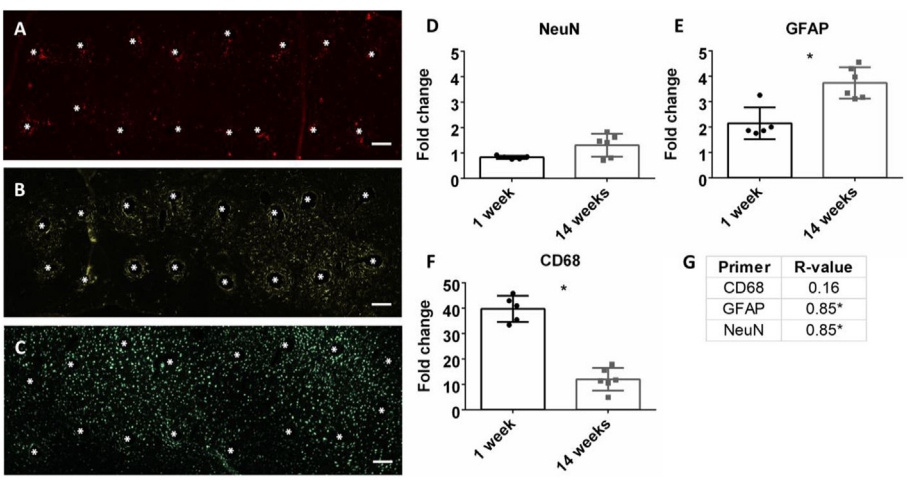

FIGURE 3 | Representative images of 16 electrode microwire arrays at 1 week with * representing electrode location for **(A)** CD68, **(B)** GFAP, and **(C)** NeuN antibody staining (scale bar = 100 μm). Fold change comparison between 1 and 14 weeks for **(D)** NeuN, **(E)** GFAP, and **(F)** CD68 (*$p < 0.05$, Student's *t*-test, Bonferroni corrected). Each time point was compared to age-matched naïve controls to calculate fold change. **(G)** Pearson correlation values for CD68, GFAP, and CD68 (*$p < 0.05$).

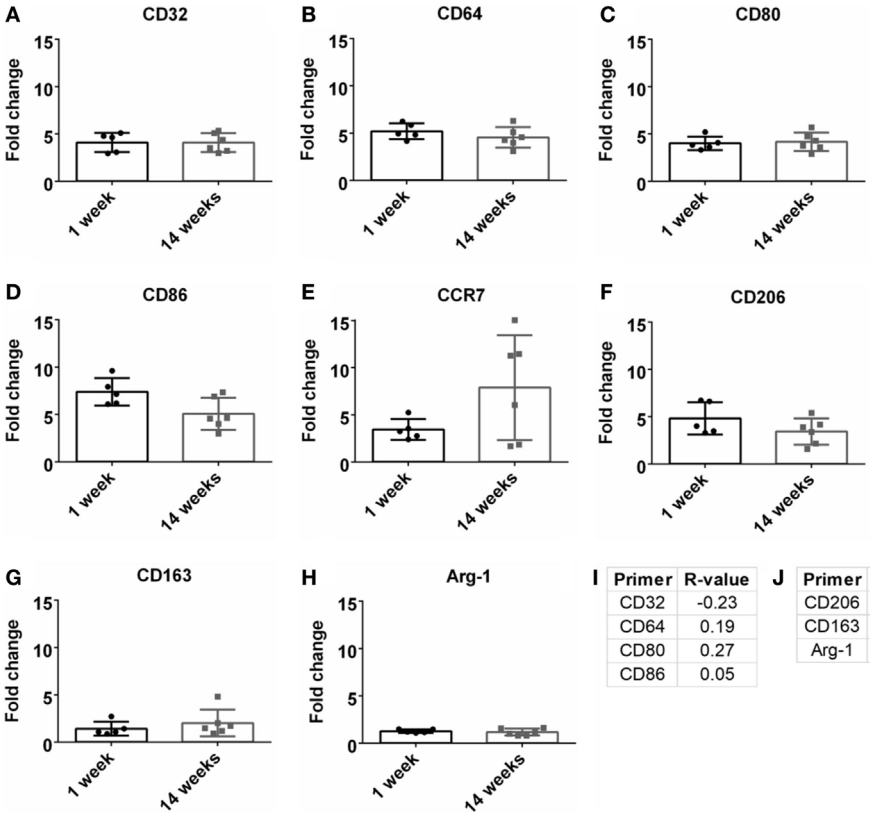

I Primer	R-value
CD32	-0.23
CD64	0.19
CD80	0.27
CD86	0.05

J Primer	R-value
CD206	0.84*
CD163	0.89*
Arg-1	0.43

FIGURE 4 | Fold change comparisons between 1 and 14 weeks for M1-like pro-inflammatory markers **(A)** CD32, **(B)** CD64, **(C)** CD80, **(D)** CD86, and **(E)** CCR7, and M2-like anti-inflammatory markers **(F)** CD206, **(G)** CD163, and **(H)** Arg-1 (*$p < 0.05$, Student's *t*-test, Bonferroni corrected). Each time point was compared to age-matched naïve controls to calculate fold change. Pearson correlations for **(I)** M1-like and **(J)** M2-like markers (*$p < 0.05$).

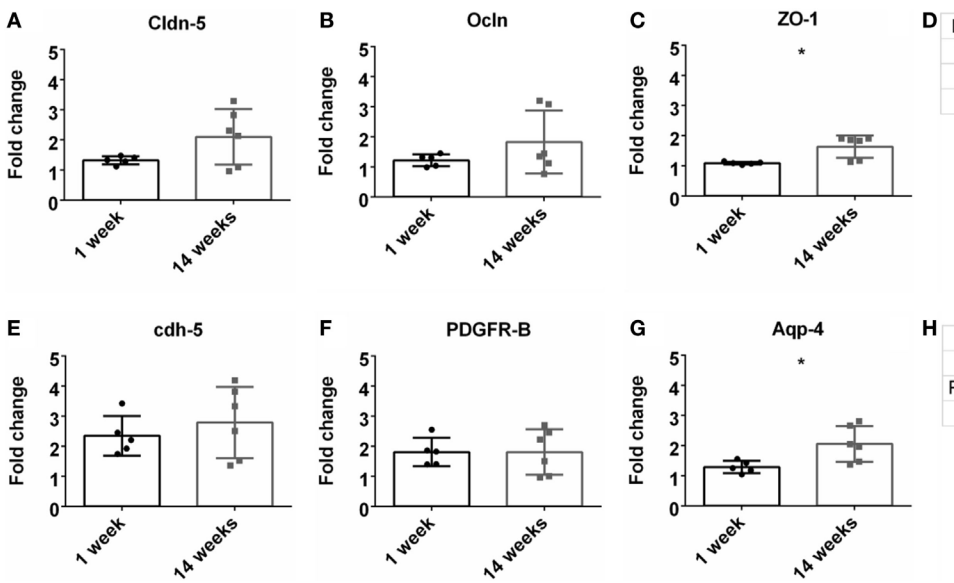

D Primer	R-value
Cldn-5	0.5
ocln	0.19
ZO-1	0.73

H Primer	R-value
cdh-5	0.85*
PDGFR-B	0.89*
AQP-4	0.72

FIGURE 5 | Fold change comparisons between 1 and 14 weeks for tight junction proteins **(A)** Cldn-5, **(B)** occluding (Ocln), and **(C)** zona-occludens-1 (ZO-1) and other blood–brain barrier (BBB) markers, **(E)** cdh-5, **(F)** PDGFR-β, and **(G)** AQP-4 (*$p < 0.05$, Student's *t*-test, Bonferroni corrected). Each time point was compared to age-matched naïve controls to calculate fold change. Pearson correlations for **(D)** tight junction protein markers and **(H)** other BBB markers (*$p < 0.05$).

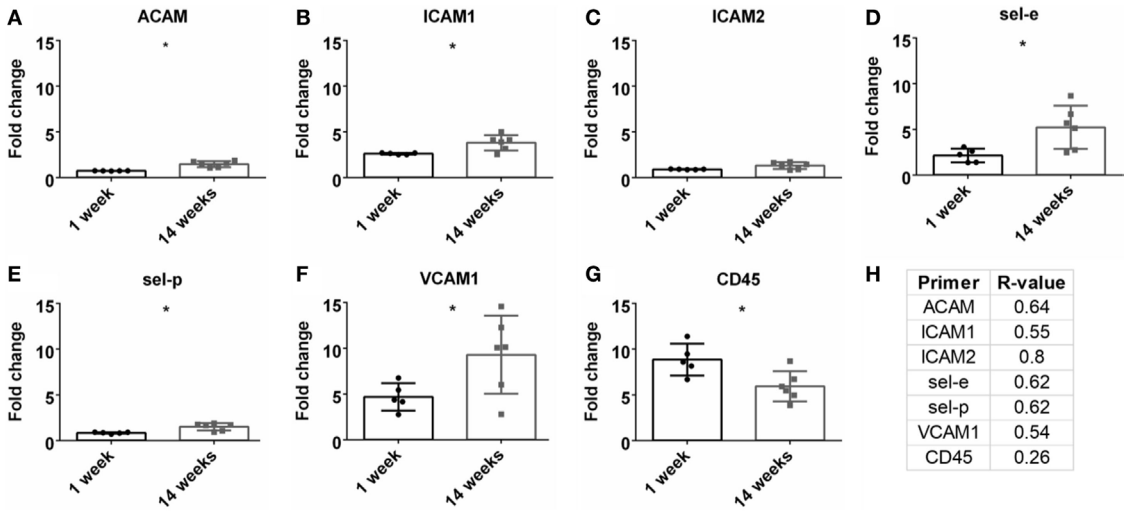

FIGURE 6 | Fold change comparisons between 1 and 14 weeks for endothelial adhesion markers **(A)** ACAM, **(B)** ICAM1, **(C)** ICAM2, **(D)** sel-e, **(E)** sel-p, **(F)** VCAM1 and pan-leukocyte marker, **(G)** CD45 (*$p < 0.05$, Student's *t*-test, Bonferroni corrected). Each time point was compared to age-matched naïve controls to calculate fold change. **(H)** Pearson correlation for endothelial adhesion and pan-leukocyte markers (*$p < 0.05$).

relation between BBB integrity and electrode performance has been demonstrated (Saxena et al., 2013), and here, these findings have been extended *via* an investigation of the underlying molecular mechanisms. Penetration and destruction of vessels during implantation may explain electrode recording variability per animal, and the importance of vascular integrity has been implicated in several studies in regards to neural health and electrodes (Kozai et al., 2010; Shih et al., 2012; Saxena et al., 2013; Nolta et al., 2015). However, the direct mechanisms driving BBB dysregulation and electrode failure are not well understood. These data have shown a positive correlation between SNR and different molecular targets, and this information could be further investigated to evaluate the importance in relation to electrode failure.

Expression levels for common neuroinflammation markers were evaluated. As seen in **Table 1** and **Figures 3D,E**, significant positive correlation was observed for NeuN and GFAP, but not for CD68. Previous electrode literature has suggested that the development of the astroglial scar at the electrode tissue interface is the primary cause for signal degeneration (Polikov et al., 2005). This attitude was pervasive through other neurodegenerative fields; however, this view has begun to change. The Sofroniew lab has demonstrated the importance of astrocyte support in a spinal cord injury model and through knock-out models, when the astrocytic scar is ablated, axonal regeneration is in fact impaired (Anderson et al., 2016). McCreery et al. (2016) conducted an analysis with Utah electrodes implanted in the cat sensorimotor cortex for almost a year. Histology was correlated with electrophysiology using the Pearson correlation, and a significant positive correlation was found for both NeuN and GFAP within 80 μm of the electrode for signal amplitudes at the experiment endpoint. Our data corroborate McCreery's findings, suggesting that presence of GFAP+ astrocytes is positively correlated with increased SNR. Therefore, developing treatment strategies to improve astrocyte recruitment (as opposed to inhibiting astrocytes) may prove beneficial for chronic intracortical implants.

The influence of M1-like and M2-like environments on neural health has been an area of study within the central and peripheral nervous systems (Kigerl et al., 2009; David and Kroner, 2011; Mikita et al., 2011; Mokarram et al., 2012; Vogel et al., 2013; Cherry et al., 2014; Sawyer et al., 2014; Kim et al., 2016; Tang and Le, 2016). With BBB breach following disease or injury, the influx of innate monocytes and macrophages can influence the neurological outcomes (Kigerl et al., 2009; Mikita et al., 2011). Common M1-like (CCR7, CD32, CD64, CD80, CD86) and M2-like (Arg-1, CD163, CD206) markers were evaluated to determine the relation between inflammation and SNR (**Table 1**; **Figure 4**). At 14 weeks, M2-like CD163 and CD206 were significantly positively correlated with SNR. CD163 is a general receptor found on all subsets M2-like macrophages, while CD206 is specific for M2a and M2c, which is responsible for tissue repair and pro-healing functions (David and Kroner, 2011; Mokarram et al., 2012). Research from the spinal cord (Kigerl et al., 2009) and the peripheral nerve (Mokarram et al., 2017) have demonstrated the benefits of a M2-like macrophage environment for neural health and repair. Additionally, non-functional electrodes implanted in a bone marrow chimera mouse model showed blood-borne macrophage accumulation at 16 weeks (Ravikumar et al., 2014). It would be beneficial to investigate if the M2 macrophage theory also holds true for functional recordings from the cortex.

To investigate the status of the BBB, tight junction protein expression was analyzed (**Table 1**; **Figures 5A,B**). Tight junctions are crucial to maintaining a healthy, intact BBB, and loss can lead to neurodegeneration (Kanda et al., 2004; Abbott et al., 2006; Zhong et al., 2008; Argaw et al., 2009; Henkel et al., 2009; Liu et al., 2012; Paul et al., 2013). Interestingly, no significant correlations were observed for these tight junction expressions.

Additional components of the BBB were then investigated, including AQP-4, cdh5, and PDGFR-β (**Table 1**; **Figures 5C,D**). While there was a significant correlation with GFAP expression, there was no correlation with AQP-4, which is a common marker on astrocyte end-feet interacting with the BBB. VE-cadherin (cdh5) had a significant positive correlation with the SNR. VE-cadherin is a cell-to-cell junction for endothelial cells, and the removal of VE-cadherin severely weakens the BBB (Wallez and Huber, 2008; Giannotta et al., 2013; Tietz and Engelhardt, 2015). Thus far, no work has been done confirming the impact of VE-cadherin loss on neurodegeneration. Further work exploring the potential connection between VE-cadherin loss and its impact on neurodegeneration could be of interest.

The data also show a significant positive correlation between PDGFR-β, a common pericyte receptor, and SNR (see **Table 1**; **Figures 5C,D**). Evaluation of PDGFR-β knockout mice demonstrated that vascular integrity in the brain was significantly compromised and became more susceptible to macromolecule leakage (Armulik et al., 2010). The Zlokovic lab built upon this work with the PDGFR-β knockout model showing that pericyte loss reduced cerebral blood flow and degraded BBB tight junction proteins. This resulted in neurodegeneration, and pericyte loss exacerbated amyloid-β clearance in Alzheimer's disease models (Bell et al., 2010; Sagare et al., 2013; Halliday et al., 2016). The results from this study thus corroborate previously published data describing the importance of pericytes in the neurovascular unit and might suggest the importance of maintaining pericyte health to improve performance for intracortical electrodes.

A common cause/impact of BBB leakage is the increased expression of adhesion markers and leukocytes (Greenwood et al., 2011; de Vries et al., 2012; Obermeier et al., 2013; Shechter et al., 2013). Therefore, these markers were investigated in correlation with SNR (**Table 1**; **Figures 6C,D**). No significant correlation was found for leukocytes (CD45) or adhesion markers (ACAM, ICAM1, ICAM2, sel-e, sel-p, VCAM1). Elahy et al. (2015) demonstrated that loss of BBB integrity and inflammation does occur in an aging model, but no leukocytes were recruited. Others have shown that while leukocytes are recruited in different BBB leakage models, this cellular presence does not lead to neurodegeneration (Boztug et al., 2002; Shaftel et al., 2007). Our data may suggest that leukocyte infiltration is not a primary cause for neurodegeneration in an electrode implant model.

Overall, these data showed significant positive correlation between SNR and GFAP, VE-cadherin, and PDGFR-β. No significant correlations for leukocyte extravasation, inflammatory phenotypes, or tight junction expression were observed. This would suggest the importance of astrocytes (GFAP), adherens junctions (VE-cadherin), and pericytes (PDGFR- β) for maintaining strong SNR at chronic time points. These data offer insight into potential molecular mechanisms to explore for improving chronic intracortical recordings.

CONCLUSION

The objective of this work was to better understand the molecular mechanisms influencing recording fidelity in electrode implant models. Previous work has suggested that BBB breach can influence chronic recordings. mRNA expression was correlated with SNR at a chronic (14 week) time point. Astrocytes, pericytes, and adherens junctions were identified as potential therapeutic targets to improve chronic intracortical recordings. Additional work with knock-out models and histological analysis is necessary to further validate the effect of these pathways. It is also important to remember that microwires were used for this study, and comparison to commonly used Michigan (research) and Utah (clinical) electrodes would be beneficial. This work provides direction for future studies and identification of BBB integrity markers that may influence and benefit chronic recordings in intracortical electrodes.

ETHICS STATEMENT

This study was carried out in accordance with the recommendations of the Institutional Animal Care and Use Committee (IACUC) at the Georgia Institute of Technology. The protocol was approved by the Georgia Institute of Technology.

AUTHOR CONTRIBUTIONS

JF designed experiments, performed animal work, electrophysiology, data analysis, results interpretation, and wrote the manuscript. SC performed qRT-PCR and assisted with manuscript writing. TS assisted with experiment design, results interpretation, and manuscript writing. DM, AC, and VY assisted with animal work and data analysis. RB is the principal investigator.

FUNDING

The authors would like to thank Dr. Harbi Sohal and Dr. Nassir Mokarram for constructive scientific guidance and editorial discussions. The authors would also like to thank Dr. Brani Vidakovic for his guidance in statistics. Supported by the National Center for Advancing Translational Sciences of the National Institutes of Health under Award Number UL1TR000454. The content is solely the responsibility of the authors and does not necessarily represent the official views of the National Institutes of Health. The authors would like to thank the Duke Sequencing and Genomic Technologies Shared Resource (Duke Cancer Institute and a Duke Genomic and Computational Biology shared resource facility) who performed the Fluidigm Biomark HD RTPCR assays and RNA QC. This work was funded by the Defense Advanced Research Projects Agency (DARPA) MTO under the auspices of Dr. Jack Judy through the Space and NavalWarfare Systems Center, Pacific Grant/Contract No. N66001-11-1-4014.

SUPPLEMENTARY MATERIAL

The Supplementary Material for this article can be found online at https://www.frontiersin.org/articles/10.3389/fbioe.2018.00026/full#supplementary-material.

REFERENCES

Abbott, N. J., Rönnbäck, L., and Hansson, E. (2006). Astrocyte-endothelial interactions at the blood-brain barrier. *Nat. Rev. Neurosci.* 7, 41–53. doi:10.1038/nrn1824

Ajiboye, A. B., Willett, F. R., Young, D. R., Memberg, W. D., Walters, B. C., Sweet, J. A., et al. (2017). Restoration of reaching and grasping in a person with tetraplegia through brain-controlled muscle stimulation: a proof-of-concept demonstration. *Lancet* 6736, 1821–1830. doi:10.1016/S0140-6736(17)30601-3

Anderson, M. A., Burda, J. E., Ren, Y., Ao, Y., O'Shea, T. M., Kawaguchi, R., et al. (2016). Astrocyte scar formation aids central nervous system axon regeneration. *Nature* 532, 195–200. doi:10.1038/nature17623

Argaw, A. T., Gurfein, B. T., Zhang, Y., Zameer, A., and John, G. R. (2009). VEGF-mediated disruption of endothelial CLN-5 promotes blood-brain barrier breakdown. *Proc. Natl. Acad. Sci. U.S.A* 106, 1977–1982. doi:10.1073/pnas.0808698106

Armulik, A., Genové, G., Mäe, M., Nisancioglu, M. H., Wallgard, E., Niaudet, C., et al. (2010). Pericytes regulate the blood-brain barrier. *Nature* 468, 557–561. doi:10.1038/nature09522

Bell, R. D., Winkler, E. A., Sagare, A. P., Singh, I., LaRue, B., Deane, R., et al. (2010). Pericytes control key neurovascular functions and neuronal phenotype in the adult brain and during brain aging. *Neuron* 68, 409–427. doi:10.1016/j.neuron.2010.09.043

Benjamini, Y., and Hochberg, Y. (1995). Controlling the false discovery rate: a practical and powerful approach to multiple testing. *J. R. Stat. Soc. B.* 57, 289–300.

Bouton, C. E., Shaikhouni, A., Annetta, N. V., Bockbrader, M. A., Friedenberg, D. A., Nielson, D. M., et al. (2016). Restoring cortical control of functional movement in a human with quadriplegia. *Nature* 533, 247–250. doi:10.1038/nature17435

Boztug, K., Carson, M. J., Pham-Mitchell, N., Asensio, V. C., DeMartino, J., and Campbell, I. L. (2002). Leukocyte infiltration, but not neurodegeneration, in the CNS of transgenic mice with astrocyte production of the CXC chemokine ligand 10. *J. Immunol.* 169, 1505–1515. doi:10.4049/jimmunol.169.3.1505

Cherry, J. D., Olschowka, J. A., and O'Banion, M. K. (2014). Neuroinflammation and M2 microglia: the good, the bad, and the inflamed. *J. Neuroinflammation* 11, 98. doi:10.1186/1742-2094-11-98

Collinger, J. L., Wodlinger, B., Downey, J. E., Wang, W., Tyler-Kabara, E. C., Weber, D. J., et al. (2013). High-performance neuroprosthetic control by an individual with tetraplegia. *Lancet* 381, 557–564. doi:10.1016/S0140-6736(12)61816-9

David, S., and Kroner, A. (2011). Repertoire of microglial and macrophage responses after spinal cord injury. *Nat. Rev. Neurosci.* 12, 388–399. doi:10.1038/nrn3053

de Vries, H. E., Kooij, G., Frenkel, D., Georgopoulos, S., Monsonego, A., and Janigro, D. (2012). Inflammatory events at blood-brain barrier in neuroinflammatory and neurodegenerative disorders: implications for clinical disease. *Epilepsia* 53, 45–52. doi:10.1111/j.1528-1167.2012.03702.x

Downey, J. E., Weiss, J. M., Muelling, K., Venkatraman, A., Valois, J. S., Hebert, M., et al. (2016). Blending of brain-machine interface and vision-guided autonomous robotics improves neuroprosthetic arm performance during grasping. *J. Neuro Eng. Rehabil.* 13, 28. doi:10.1186/s12984-016-0134-9

Elahy, M., Jackaman, C., Mamo, J. C., Lam, V., Dhaliwal, S. S., Giles, C., et al. (2015). Blood-brain barrier dysfunction developed during normal aging is associated with inflammation and loss of tight junctions but not with leukocyte recruitment. *Immunity Ageing* 12, 2. doi:10.1186/s12979-015-0029-9

Giannotta, M., Trani, M., and Dejana, E. (2013). VE-cadherin and endothelial adherens junctions: active guardians of vascular integrity. *Dev. Cell* 26, 441–454. doi:10.1016/j.devcel.2013.08.020

Goss-Varley, M., Dona, K. R., McMahon, J. A., Shoffstall, A. J., Ereifej, E. S., Lindner, S. C., et al. (2017). Microelectrode implantation in motor cortex causes fine motor deficit: implications on potential considerations to brain computer interfacing and human augmentation. *Sci. Rep.* 7, 1–12. doi:10.1038/s41598-017-15623-y

Greenwood, J., Heasman, S. J., Alvarez, J. I., Prat, A., Lyck, R., and Engelhardt, B. (2011). Review: leucocyte-endothelial cell crosstalk at the blood-brain barrier: a prerequisite for successful immune cell entry to the brain. *Neuropathol. Appl. Neurobiol.* 37, 24–39. doi:10.1111/j.1365-2990.2010.01140.x

Halliday, M. R., Rege, S. V., Ma, Q., Zhao, Z., Miller, C. A., Winkler, E. A., et al. (2016). Accelerated pericyte degeneration and blood–brain barrier breakdown in apolipoprotein E4 carriers with Alzheimer's disease. *J. Cereb. Blood Flow Metab.* 36, 216–227. doi:10.1038/jcbfm.2015.44

Henkel, J. S., Beers, D. R., Wen, S., Bowser, R., and Appel, S. H. (2009). Decreased mRNA expression of tight junction proteins in lumbar spinal cords of patients with ALS. *Neurology* 72, 1614–1616. doi:10.1212/WNL.0b013e3181a41228

Ivens, S., Kaufer, D., Flores, L. P., Bechmann, I., Zumsteg, D., Tomkins, O., et al. (2007). TGF-beta receptor-mediated albumin uptake into astrocytes is involved in neocortical epileptogenesis. *Brain* 130(Pt 2), 535–547. doi:10.1093/brain/awl317

Kanda, T., Numata, Y., and Mizusawa, H. (2004). Chronic inflammatory demyelinating polyneuropathy: decreased claudin-5 and Relocated ZO-1. *J. Neurol. Neurosurg. Psychiatry* 75, 765–769. doi:10.1136/jnnp.2003.025692

Karumbaiah, L., Saxena, T., Carlson, D., Patil, K., Patkar, R., Gaupp, E. A., et al. (2013). Relationship between intracortical electrode design and chronic recording function. *Biomaterials* 34, 8061–8074. doi:10.1016/j.biomaterials.2013.07.016

Kigerl, K. A., Gensel, J. C., Ankeny, D. P., Alexander, J. K., Donnelly, D. J., and Popovich, P. G. (2009). Identification of two distinct macrophage subsets with divergent effects causing either neurotoxicity or regeneration in the injured mouse spinal cord. *J. Neurosci.* 29, 13435–13444. doi:10.1523/JNEUROSCI.3257-09.2009

Kim, Y. K., Na, K. S., Myint, A. M., and Leonard, B. E. (2016). The role of pro-inflammatory cytokines in neuroinflammation, neurogenesis and the neuroendocrine system in major depression. *Prog. Neuro Psychopharmacol. Biol. Psychiatry* 64, 277–284. doi:10.1016/j.pnpbp.2015.06.008

Kozai, T. D., Du, Z., Gugel, Z. V., Smith, M. A., Chase, S. M., Bodily, L. M., et al. (2015). Comprehensive chronic laminar single-unit, multi-unit, and local field potential recording performance with planar single shank electrode arrays. *J. Neurosci. Methods* 242, 15–40. doi:10.1016/j.jneumeth.2014.12.010

Kozai, T. D., Eles, J. R., Vazquez, A. L., and Cui, X. T. (2016). Two-photon imaging of chronically implanted neural electrodes: sealing methods and new insights. *J. Neurosci. Methods* 258, 46–55. doi:10.1016/j.jneumeth.2015.10.007

Kozai, T. D., Marzullo, T. C., Hooi, F., Langhals, N. B., Majewska, A. K., Brown, E. B., et al. (2010). Reduction of neurovascular damage resulting from microelectrode insertion into the cerebral cortex using in vivo two-photon mapping. *J. Neural Eng.* 7, 1–12. doi:10.1088/1741-2560/7/4/046011

Liu, J., Jin, X., Liu, K. J., and Liu, W. (2012). Matrix metalloproteinase-2-mediated occludin degradation and caveolin-1-mediated claudin-5 redistribution contribute to blood-brain barrier damage in early ischemic stroke stage. *J. Neurosci.* 32, 3044–3057. doi:10.1523/JNEUROSCI.6409-11.2012

McConnell, G. C., Rees, H. D., Levey, A. I., Gutekunst, C. A., Gross, R. E., and Bellamkonda, R. V. (2009). Implanted neural electrodes cause chronic, local inflammation that is correlated with local neurodegeneration. *J. Neural Eng.* 6, 1–12. doi:10.1088/1741-2560/6/5/056003

McCreery, D., Cogan, S., Kane, S., and Pikov, V. (2016). Correlations between histology and neuronal activity recorded by microelectrodes implanted chronically in the cerebral cortex. *J. Neural Eng.* 13, 1–17. doi:10.1088/1741-2560/13/3/036012

Mikita, J., Dubourdieu-Cassagno, N., Deloire, M. S., Vekris, A., Biran, M., Raffard, G., et al. (2011). Altered M1/M2 activation patterns of monocytes in severe relapsing experimental rat model of multiple sclerosis. amelioration of clinical status by M2 activated monocyte administration. *Mult. Scler.* 17, 2–15. doi:10.1177/1352458510379243

Mokarram, N., Dymanus, K., Srinivasan, A., Lyon, J. G., Tipton, J., Chu, J., et al. (2017). Immunoengineering nerve repair. *Proc. Natl. Acad. Sci. U.S.A* 114, E5077–E5084. doi:10.1073/pnas.1705757114

Mokarram, N., Merchant, A., Mukhatyar, V., Patel, G., and Bellamkonda, R. V. (2012). Effect of modulating macrophage phenotype on peripheral nerve repair. *Biomaterials* 33, 8793–8801. doi:10.1016/j.biomaterials.2012.08.050

Nolta, N. F., Christensen, M. B., Crane, P. D., Skousen, J. L., and Tresco, P. A. (2015). BBB leakage, astrogliosis, and tissue loss correlate with silicon microelectrode array recording performance. *Biomaterials* 53, 753–762. doi:10.1016/j.biomaterials.2015.02.081

Nordhausen, C. T., Maynard, E. M., and Normann, R. A. (1996). Single unit recording capabilities of a 100 microelectrode array. *Brain Res.* 726, 129–140. doi:10.1016/0006-8993(96)00321-6

Obermeier, B., Daneman, R., and Ransohoff, R. M. (2013). Development, maintenance and disruption of the blood-brain barrier. *Nat. Med.* 19, 1584–1596. doi:10.1038/nm.3407

Paul, D., Cowan, A. E., Ge, S., and Pachter, J. S. (2013). Novel 3D analysis of claudin-5 reveals significant endothelial heterogeneity among CNS microvessels. *Microvasc. Res.* 86, 1–10. doi:10.1016/j.mvr.2012.12.001

Perge, J. A., Zhang, S., Malik, W. Q., Homer, M. L., Cash, S., Friehs, G., et al. (2014). Reliability of directional information in unsorted spikes and local field potentials recorded in human motor cortex. *J. Neural Eng.* 11, 1–14. doi:10.1088/1741-2560/11/4/046007

Polikov, V. S., Tresco, P. A., and Reichert, W. M. (2005). Response of brain tissue to chronically implanted neural electrodes. *J. Neurosci. Methods* 148, 1–18. doi:10.1016/j.jneumeth.2005.08.015

Potter, K. A., Buck, A. C., Self, W. K., and Capadona, J. R. (2012). Stab injury and device implantation within the brain results in inversely multiphasic neuroinflammatory and neurodegenerative responses. *J. Neural Eng.* 9, 1–14. doi:10.1088/1741-2560/9/4/046020

Potter-Baker, K. A., Stewart, W. G., Tomaszewski, W. H., Wong, C. T., Meador, W. D., Ziats, N. P., et al. (2015). Implications of chronic daily anti-oxidant administration on the inflammatory response to intracortical microelectrodes. *J. Neural Eng.* 12, 1–15. doi:10.1088/1741-2560/12/4/046002

Ravikumar, M., Sunil, S., Black, J., Barkauskas, D. S., Haung, A. Y., Miller, R. H., et al. (2014). The roles of blood-derived macrophages and resident microglia in the neuroinflammatory response to implanted intracortical microelectrodes. *Antivir. Chem. Chemother. Biomater.* 35, 8049–8064. doi:10.1016/j.biomaterials.2014.05.084

Ryu, J. K., Petersen, M. A., Murray, S. G., Baeten, K. M., Meyer-Franke, A., Chan, J. P., et al. (2015). Blood coagulation protein fibrinogen promotes autoimmunity and demyelination via chemokine release and antigen presentation. *Nat. Commun.* 6, 8164. doi:10.1038/ncomms9164

Sagare, A. P., Bell, R. D., Zhao, Z., Ma, Q., Winkler, E. A., Ramanathan, A., et al. (2013). Pericyte loss influences Alzheimer-like neurodegeneration in mice. *Nat. Commun.* 4, 1–14. doi:10.1038/ncomms3932

Sawyer, A. J., Tian, W., Saucier-Sawyer, J. K., Rizk, P. J., Saltzman, W. M., Bellamkonda, R. V., et al. (2014). The effect of inflammatory cell-derived MCP-1 loss on neuronal survival during chronic neuroinflammation. *Biomaterials* 35, 6698–6706. doi:10.1016/j.biomaterials.2014.05.008

Saxena, T., Karumbaiah, L., Gaupp, E. A., Patkar, R., Patil, K., Betancur, M., et al. (2013). The impact of chronic blood-brain barrier breach on intracortical electrode function. *Biomaterials* 34, 4703–4713. doi:10.1016/j.biomaterials.2013.03.007

Shaftel, S. S., Carlson, T. J., Olschowka, J. A., Kyrkanides, S., Matousek, S. B., and O'Banion, M. K. (2007). Chronic interleukin-1β expression in mouse brain leads to leukocyte infiltration and neutrophil-independent blood–brain barrier permeability without overt neurodegeneration. *J. Neurosci.* 27, 9301–9309. doi:10.1523/JNEUROSCI.1418-07.2007

Sharma, G., Annetta, N., Friedenberg, D., Blanco, T., Vasconcelos, D., Shaikhouni, A., et al. (2015). Time stability and coherence analysis of multiunit, single-unit and local field potential neuronal signals in chronically implanted brain electrodes. *Bioelectronic Med.* 2, 63–71. doi:10.15424/bioelectronmed.2015.00010

Shechter, R., London, A., and Schwartz, M. (2013). Orchestrated leukocyte recruitment to immune-privileged sites: absolute barriers versus educational gates. *Nat. Rev. Immunol.* 13, 206–218. doi:10.1038/nri3391

Shih, A. Y., Blinder, P., Tsai, P. S., Friedman, B., Stanley, G., Lyden, P. D., et al. (2012). The smallest stroke: occlusion of one penetrating vessel leads to infarction and a cognitive deficit. *Nat. Neurosci.* 16, 55–63. doi:10.1038/nn.3278

Simeral, J. D., Kim, S. P., Black, M. J., Donoghue, J. P., and Hochberg, L. R. (2011). Neural control of cursor trajectory and click by a human with tetraplegia 1000 days after implant of an intracortical microelectrode array. *J. Neural Eng.* 8, 1–24. doi:10.1088/1741-2560/8/2/025027

Srinivasan, A., Tipton, J., Tahilramani, M., Kharbouch, A., Gaupp, E., Song, C., et al. (2016). A regenerative microchannel device for recording multiple single-unit action potentials in awake, ambulatory animals. *Eur. J. Neurosci.* 43, 474–485. doi:10.1111/ejn.13080

Stolp, H. B., and Dziegielewska, K. M. (2009). Review: role of developmental inflammation and blood-brain barrier dysfunction in neurodevelopmental and neurodegenerative diseases. *Neuropathol. Appl. Neurobiol.* 35, 132–146. doi:10.1111/j.1365-2990.2008.01005.x

Strauss-Ayali, D., Conrad, S. M., and Mosser, D. M. (2007). Monocyte subpopulations and their differentiation patterns during infection. *J. Leukoc. Biol.* 82, 244–252. doi:10.1189/jlb.0307191

Tang, Y., and Le, W. (2016). Differential roles of M1 and M2 microglia in neurodegenerative diseases. *Mol. Neurobiol.* 53, 1181–1194. doi:10.1007/s12035-014-9070-5

Tietz, S., and Engelhardt, B. (2015). Brain barriers: crosstalk between complex tight junctions and adherens junctions. *J. Cell Biol.* 209, 493–506. doi:10.1083/jcb.201412147

Vogel, D. Y., Vereyken, E. J., Glim, J. E., Heijnen, P. D., Moeton, M., van der Valk, P., et al. (2013). Macrophages in inflammatory multiple sclerosis lesions have an intermediate activation status. *J. Neuroinflammation* 10, 35. doi:10.1186/1742-2094-10-35

Wallez, Y., and Huber, P. (2008). Endothelial adherens and tight junctions in vascular homeostasis, inflammation and angiogenesis. *Biochim Biophys Acta* 1778, 794–809. doi:10.1016/j.bbamem.2007.09.003

Zhong, Z., Deane, R., Ali, Z., Parisi, M., Shapovalov, Y., O'Banion, M. K., et al. (2008). ALS-causing SOD1 mutants generate vascular changes prior to motor neuron degeneration. *Nat. Neurosci.* 11, 420–422. doi:10.1038/nn2073

Zlokovic, B. V. (2011). Neurovascular pathways to neurodegeneration in Alzheimer's disease and other disorders. *Nat. Rev. Neurosci.* 12, 723–738. doi:10.1038/nrn3114

Conflict of Interest Statement: The authors declare that the research was conducted in the absence of any commercial or financial relationships that could be construed as a potential conflict of interest.

frontiers in Materials

REVIEW
published: 12 March 2018
doi: 10.3389/fmats.2018.00014

Harnessing the Potential of Biomaterials for Brain Repair after Stroke

*Anup Tuladhar[1†], Samantha L. Payne[1,2†] and Molly S. Shoichet[1,2,3]**

[1] Institute of Biomaterials and Biomedical Engineering, University of Toronto, Toronto, ON, Canada, [2] Department of Chemical Engineering and Applied Chemistry, University of Toronto, Toronto, ON, Canada, [3] Department of Chemistry, University of Toronto, Toronto, ON, Canada

Stroke is a devastating disease for which no clinical treatment exists to regenerate lost tissue. Strategies for brain repair in animal models of stroke include the delivery of drug or cell-based therapeutics; however, the complex anatomy and functional organization of the brain presents many challenges. Biomaterials may alleviate some of these challenges by providing a scaffold, localizing the therapy to the site of action, and/or modulating cues to brain cells. Here, the challenges associated with delivery of therapeutics to the brain and the biomaterial strategies used to overcome these challenges are described. For example, innovative hydrogel delivery systems have been designed to provide sustained trophic factor delivery for endogenous repair and to support transplanted cell survival and integration. Novel treatments, such as electrical stimulation of transplanted cells and the delivery of factors for the direct reprogramming of astrocytes into neurons, may be further enhanced by biomaterial delivery systems. Ultimately, improved clinical translation will be achieved by combining clinically relevant therapies with biomaterials strategies.

Keywords: stroke, regeneration, biomaterials, drug delivery, cell delivery

OPEN ACCESS

Edited by:
Sara Pedron, University of Illinois at Urbana–Champaign, United States

Reviewed by:
Mark William Tibbitt, ETH Zurich, Switzerland
Jennifer Patterson, KU Leuven, Belgium
April Kloxin, University of Delaware, United States

****Correspondence:***
Molly S. Shoichet
molly.shoichet@utoronto.ca

[†]Co-first authors.

Specialty section:
This article was submitted to Biomaterials, a section of the journal Frontiers in Materials

Received: *15 December 2017*
Accepted: *22 February 2018*
Published: *12 March 2018*

Citation:
Tuladhar A, Payne SL and Shoichet MS (2018) Harnessing the Potential of Biomaterials for Brain Repair after Stroke. Front. Mater. 5:14. doi: 10.3389/fmats.2018.00014

ISCHEMIC STROKE

Physiology and Pathology

Brain injury, unlike degenerative conditions that manifest as a gradual decline in tissue function, is a sudden event resulting in a permanent loss of tissue and functional deficits. The brain is a particularly challenging organ to develop therapeutics for due to its limited capacity for self-repair, the presence of the blood–brain barrier (BBB), as well as its inherently complex cellular and functional composition. A stroke is caused by local oxygen deprivation in the brain due to either hemorrhaged or occluded blood vessels, accounting for 13 and 87% of strokes, respectively (Mozaffarian et al., 2016). Within

Abbreviations: BBB, blood–brain barrier; BDNF, brain-derived neurotrophic factor; BMP4, bone morphogenic protein 4; ChABC, chondroitinase ABC; CSPG, chondroitin sulfate proteoglycan; ECM, extracellular matrix; EGF, epidermal growth factor; EPO, erythropoietin; ESC, embryonic stem cell; FGF2, fibroblast growth factor 2; GDNF, glial-derived neurotrophic factor; GFAP, glial fibrillary acidic protein; HA, hyaluronan; HAMC, hyaluronan methylcellulose; hCG, human chorionic gonadotrophin; HGF, hepatocyte growth factor; IGF, insulin growth factor; iPSC, induced pluripotent stem cell; MC, methylcellulose; MMP, matrix metalloproteinase; MRI, magnetic resonance imaging; MSC, mesenchymal stromal cell; NPC, neural progenitor cell; NSC, neural stem cell; NSPC, neural stem/progenitor cell; NT-3, neurotrophin-3; PCL, polycaprolactone; PDMS, polydimethylsilosane; PEG, polyethylene glycol; PGA, polyglycolic acid; PLGA, poly(D,L-lactic acid co-glycolic acid); PSA, poly(sebacic acid); SAP, self-assembling peptide; CSF, cerebrospinal fluid; SDF-1α, stromal-derived factor-1α; SGZ, subgranular zone; STAiRS, Stroke Therapy Academic Industry Round Table; SVZ, subventricular zone; TBI, traumatic brain injury; TMS, transcranial magnetic stimulation; tPA, tissue plasminogen activator; VEGF, vascular endothelial growth factor.

minutes following the depletion of blood flow, neurons and glial cells undergo apoptosis and necrosis, resulting in the formation of a cavity or infarct (Barkho and Zhao, 2011). The cellular and tissue events that follow the onset of a stroke can be categorized into three phases: acute, subacute, and chronic (Heiss, 2012).

The acute phase of stroke is characterized by rapid cell death, breakdown of the BBB, and infiltration of immune cells into the infarct. Hypoxia and the resulting energy deficit triggers a cascade of cell necrosis to form a infarct (Heiss, 2012; Xing et al., 2012). Cellular excitotoxicity occurs as glutamate is released by dying neurons into the extracellular matrix (ECM) and reuptake is inhibited, resulting in high intracellular calcium concentrations. By 6 h poststroke, the majority of cell death has occurred (Heiss, 2012; Hossmann, 2012). However, in the hours and days after a stroke there is continued cell death and impaired function in the area surrounding the infarct core, known as the peri-infarct. The peri-infarct contains cells that are impaired but can be potentially restored using therapeutic strategies (Touzani et al., 2001; Brouns and De Deyn, 2009).

In the subacute phase, waves of neuronal depolarization trigger further cell injury, caspase-mediated cell apoptosis and cell necrosis, which propagate from the ischemic core into the peri-infarct (Velier et al., 1999). Several molecular cascades contributing to cell death are initiated at this time, including free radical production, excitotoxicity, release of cytokines, and infiltration of macrophages and microglia causing inflammation and gliosis (Besancon et al., 2008; Barkho and Zhao, 2011).

The last phase of a stroke is the delayed injury or chronic phase, occurring in the weeks following the initial occlusion (Heiss, 2012; Kanekar et al., 2012). In this phase, there is widespread edema and activation of proteases and cytokines. Oxidative stress activates matrix metalloproteinases (MMPs), which disrupt tight junctions between cells and the basal lamina, and lead to a secondary breakdown of the BBB. Breakdown of the BBB in turn causes leakage of plasma, red blood cells, and infiltration of immune cells into the brain parenchyma (Brouns and De Deyn, 2009; Heiss, 2012). Once in the brain, neutrophils and other leukocytes release proinflammatory factors, initiating a secondary wave of inflammation (Doyle et al., 2008; Brouns and De Deyn, 2009). There are also changes to the brain ECM that occur over time following stroke. As the basement membrane around blood vessels is degraded, collagen IV and laminin are reduced, and fibrinogen is deposited and converted to fibrin (Baeten and Akassoglou, 2011). High-molecular-weight hyaluronan (HA) is deposited in the interstitial ECM and contributes to chondroitin sulfate proteoglycan (CSPG)-mediated restriction in plasticity and regrowth of axons (Lau et al., 2013). These changes can persist in the stroke infarct, and although the majority of tissue loss occurs early in the injury process, it has been shown in humans that gradual tissue loss can continue years after the initial stroke (Seghier et al., 2014).

Current Clinical Treatments

Despite the high prevalence of stroke in North America, clinical therapies remain limited. The only FDA-approved treatment for ischemic stroke is tissue plasminogen activator (tPA), which activates plasminogen by catalyzing its conversion into plasmin, improving the outcome in ischemic stroke when administered up to 4.5 h following stroke (Stemer and Lyden, 2010). Due to the narrow therapeutic window and risk of bleeding associated with tPA, only 3–6% of stroke patients are eligible for tPA administration (de Los Ríos la Rosa et al., 2012). An endovascular thrombectomy can be performed as a complement to tPA for larger vessel occlusions, but this strategy is also time-dependent (Meretoja et al., 2017). Rehabilitation to regain function and encourage remodeling of the neural circuitry is also utilized following a stroke. Low-intensity training begins around 72 h after a stroke, followed by additional rehabilitation programs for up to 2 months poststroke (Winstein et al., 2016). While many of the aforementioned therapies are successful, they do not promote sufficient regeneration of brain tissue to completely restore function to the brain.

Barriers to Regeneration

Blood–Brain Barrier

The BBB serves as a gatekeeper between the brain and circulating blood. The three main components of the BBB (endothelial cells, astrocytic end-feet, and pericytes) interact to form and maintain the tight junctions between endothelial cells which permit the diffusion of dissolved gases such as O_2 but limit the transport of large molecules (Ballabh et al., 2004). Following a stroke there is breakdown of the BBB leading to a lack of vascular support, infiltration of immune cells, and ultimately the formation of a cavity (Brouns and De Deyn, 2009). The loss of BBB integrity also limits the use of tPA due to the risk of causing a lethal hemorrhage in a blood vessel (Cheng et al., 2014). After two waves of hyperpermeability, the first at 4–6 h and a second delayed permeability at 24–72 h (Kuroiwa et al., 1985; Krueger et al., 2013), the BBB is gradually reestablished.

Reactive Astrocytes

Injury to the central nervous system (CNS) activates quiescent astrocytes, which undergo morphological changes to become reactive in the peri-infarct region as early as one day after stroke (Duggan et al., 2009; Barreto et al., 2011), forming a physical and chemical barrier, known as the glial scar (Yasuda et al., 2004). Reactive astrocytes and pericytes secrete proteoglycans, such as CSPGs, that inhibit axonal outgrowth, making their degradation a target for regenerative strategies (Fawcett and Asher, 1999; Zhang and Chopp, 2009). Perineuronal nets, a normal component of the brain ECM, also inhibit axon regeneration (Liu et al., 2006). However, reactive astrocytes can also play a positive role following stroke, isolating the injury site to prevent the spread of degeneration into healthy tissue, and secreting many growth-promoting proteins that can stimulate axonal sprouting (Lu et al., 2003; Liu et al., 2014). Since the sequence of release of both growth inhibiting and growth promoting molecules by endogenous reactive astrocytes is spatiotemporally coordinated, designing a strategy that targets astrocytes at the optimal time for therapeutic results is challenging.

Endogenous Response

Following a stroke, a considerable amount of circuit remapping takes place in both animal models (Winship and Murphy, 2008)

and humans (Dancause et al., 2005). This includes local axonal sprouting and remodeling in areas adjacent to the injury, as well as larger-scale hyperactivation of contralateral motor pathways (Tombari et al., 2004; Dancause et al., 2005). This rewiring can serve as a compensatory mechanism to redirect functional pathways of the brain but is often insufficient to induce meaningful recovery (Winhuisen et al., 2005).

It has been demonstrated in both rodents and humans that the brain attempts to replace lost cells through the stimulation of endogenous neural stem and progenitor cells (NSPCs) found in the subventricular zone (SVZ) of the lateral ventricles and the subgranular zone (SGZ) of the dentate gyrus (Morshead et al., 1994; Chiasson et al., 1999; Arvidsson et al., 2002; Yamashita et al., 2006; Minger et al., 2007). The cells of the SVZ normally function to continually replace neurons of the olfactory bulb by migrating along the rostral migratory stream, but newly-born neuroblasts will be redirected to areas of ischemia in the striatum and cortex following injury (Pencea et al., 2001; Bedard and Parent, 2004; Kernie and Parent, 2010). In animal models, the time of NSPC activation will vary depending on the type and size of injury, from 5 to 7 days posthypoxic/ischemic injury (Ikeda et al., 2005) and 2 and 6 weeks after middle cerebral artery occlusion injury (Li et al., 2010). Due to the presence of cytotoxic factors and a lack of supportive ECM, the majority of NSPCs from the SVZ do not survive past 2 weeks (Arvidsson et al., 2002; Parent et al., 2002; Guerra-Crespo et al., 2012) and their ultimate contribution to regeneration is suggested to be minimal (Wernig et al., 2004; Bithell and Williams, 2005; Bliss et al., 2010; Kernie and Parent, 2010). The cells of the SGZ, thought to be primarily neural progenitor cells (NPCs) (Nakatomi et al., 2002), actively regenerate neurons in the granular layer of the adult hippocampus and are activated following an ischemic insult (Lindvall and Kokaia, 2010). While there is evidence of neurogenesis in the hippocampus after global ischemia, the cells in the SGZ do not change their normal migratory pathway following injury (Wiltrout et al., 2007), limiting their therapeutic potential beyond hippocampal injury.

Biomaterials for Brain Repair

The goal of regenerative medicine therapies after stroke is to increase the amount of functional tissue available for recovery of lost neurological function. This is achievable by: (1) protecting degenerating neural cells in the peri-infarct region, (2) regenerating new tissue to replace lost neural cells using endogenous or exogenous stem cells, and (3) creating a growth-permissive environment for new neural cells and circuitry to survive and integrate into the host tissue.

Strategies for promoting repair have revolved around delivery of drugs (proteins, antibodies, and small molecules) and cells. While promising, progress has been hindered by multiple challenges. Drug therapies are severely impeded by the restriction of drug diffusion into the brain parenchyma by the BBB, rendering most systemically administered therapies ineffective. Cell transplantation is limited by poor survival after delivery, a loss of supportive ECM and vasculature in the injured brain, and difficulty achieving maturity and integration into host tissue.

Biomaterials refer to a class of materials that are tailored to provide a beneficial effect in the targeted biological system. They can be utilized in the brain as scaffolds to provide mechanical stability to the injured brain, to provide a substrate for endogenous repair, and to address challenges in drug and cell therapies. Namely, they can be used to: bypass the BBB, provide temporal control over drug delivery, localize drug and cell therapies to targeted sites, reduce the negative effects of the hostile microenvironment, increase drug stability and cell survival, provide modulatory cues to the brain, serve as scaffolds to endogenous and exogenous stem cells, and provide guidance cues for the creation of new neural circuits.

Material Properties of the Brain

The brain is one of the softest tissues in the body, with an elastic modulus reported in the range of 0.1–500 Pa in rodents (Christ et al., 2010) and 1–14 kPa in humans (Hiscox et al., 2016). The brain has a structurally heterogeneous anisotropy with distinct regions that vary in cellular composition and stiffness. Differences in stiffness are most pronounced between the cell-body containing gray matter and axon-dense white matter (~500 Pa in the gray matter of the rat brain versus ~300 Pa in the white matter; Kruse et al., 2008; Christ et al., 2010), but substantial variation exists even within the same anatomical structure (Elkin et al., 2007). The anisotropy of the brain is also reflected in the inhomogeneous diffusion parameters; for example, diffusion in the corpus callosum occurs more readily in parallel with the axon bundle than perpendicular to it (Syková and Nicholson, 2008). The structural integrity of the brain is mediated by the ECM, which consists primarily of collagen type IV, HA, fibronectin, laminin, and proteoglycans such as CSPGs (Lau et al., 2013; Medberry et al., 2013). These molecules may be subdivided into three compartments with differing function: (1) the basement membrane that binds the CNS parenchyma and the vasculature, composed of collagen, laminin, fibronectin, and proteoglycans; (2) perineuronal nets that surround neuronal cell bodies, dendrites, and synapses, made primarily of CSPGs; and (3) the interstitial matrix that contains a network of molecules loosely bound to the basement membrane or perineuronal nets, consisting of proteoglycans, HA, and small amounts of collagen, elastin, laminin, and fibronectin (Lau et al., 2013). The composition of the brain ECM is important in the injury response; whilst scar tissue in most regions of the body (i.e., skin, heart, muscle) is typically stiffer than the surrounding healthy tissue, the glial scar is actually softer than healthy tissue. This may be partly due to the lack of fibrous collagen type I in the brain (Moeendarbary et al., 2017).

Design Criteria for Brain Biomaterials

The delicate nature of brain tissue and the confined space of the skull imposes a unique set of design criteria for biomaterial use in the brain. The criteria for the material depend on the type of therapy but some common features emerge. The material should be biocompatible with brain tissue, which is more sensitive to mechanical and environmental stresses than other tissues (Saxena and Caroni, 2011). For maximum biocompatibility, the mechanical properties of the material should be similar to those of brain tissue, as stiffer materials lead to increased gliosis and worsened outcomes, whereas materials softer than the host tissue lead to poor material stability at the implant site (Moshayedi

et al., 2016; Spencer et al., 2017). Due to the confined space of the skull the material must also be minimally swelling to avoid compressing the brain tissue and increasing intracranial pressure. Injectable and shape-adaptable materials are favored over stiff implants because they require less invasive surgical procedures and can conform to heterogeneous spaces. The material must be degradable and resorbable as it has been demonstrated that long-term or non-biodegradable implants, such as those made from silicone, leads to chronic inflammation, scarring, and neuron death (Biran et al., 2005). Additionally, the degradation products must also be non-cytotoxic. The immunogenicity of the material has a significant impact on its biocompatibility. Although some inflammation is inevitable, this response can be reduced by choices in material design, such as having physical properties similar to native brain tissue (i.e., low modulus and elastic in nature) and low interfacial tension with biological fluids to minimize immune cell adhesion.

The intended use of the material will determine the importance of its properties. For drug delivery, the ability to control drug release is important for regenerative therapies and is largely dependent on material stability, drug solubility, and tissue penetration. For protein therapeutics the ability to shield against enzymatic degradation, especially in the acutely injured brain, is crucial. Yet, some materials or chemistries necessary for controlled drug release are incompatible with cell delivery due to degradation by-products or harsh fabrication conditions (Bible et al., 2012; Pakulska et al., 2013). For cell delivery, the material must be cytocompatible, able to promote cell adhesion to prevent anoikis, able to provide good cell distribution in order to prevent cell aggregation (often observed with transplants in saline; Ballios et al., 2015), and degradable. Topographical features, bioactive ligands, or drugs incorporated into the material can be used to guide cell behavior and fate. Finding a material with all the desired properties is challenging, thus requiring the mechanical and chemical properties to be tuned.

Types of Biomaterials Used in the Brain

Biomaterials can be produced from both natural and synthetic materials. Natural materials are derived from ECM components (e.g., HA, collagen, fibrin, laminin, heparin, peptides, and proteins) or from xenobiotic sources [e.g., alginate, chitosan, Matrigel™, silk, methylcellulose (MC)]. Naturally derived polymers are advantageous over synthetic polymers because they are made of components of the ECM or have properties similar to the ECM and are therefore less likely to stimulate an immune response (Nair and Laurencin, 2007). Synthetic biomaterials for the brain are commonly made of polyethylene glycol (PEG), poly(D,L-lactic acid), polyglycolic acid (PGA), poly(D,L-lactic acid co-glycolic acid) (PLGA), poly(D-lysine), poly(sebacic acid) (PSA), and polycaprolactone (PCL) (Drury and Mooney, 2003; Hoffman, 2012). Synthetic polymers are easier to tune and possess superior *in vivo* stability. Though they lack innate ECM components necessary for cell survival (such as adhesive ligands to prevent anoikis), they can be functionalized with bioactive ligands (Hoffman, 2012). Biomaterials used in the brain can take on the form of injectable hydrogels, nano- and microparticles, and electrospun fibers.

Hydrogels are of particular interest as scaffolds for tissue engineering and drug delivery because they are able to form ECM-mimetic architectures. They are polymer networks crosslinked *via* chemical bonds or physical interactions and are primarily composed of water. Their porous and shape adaptable nature is effective for filling the stroke cavity and allows diffusion of oxygen, nutrients, and drugs required by transplanted and host cells (Drury and Mooney, 2003). They can often be tuned to match the mechanical properties of the brain (Tyler, 2012). Hydrogel stability is dependent, in part, on the number of the crosslinks formed; generally, physically crosslinked gels are less stable than chemically crosslinked gels, but the chemistry required for crosslinking can be detrimental to encapsulated proteins and cells, and, in some cases, the host tissue (Lee and Mooney, 2001). The crosslinking method also affects the rheological properties of the gel; *in situ* crosslinking is preferred as it allows the gel to be injected and conform to the space (Stabenfeldt et al., 2006). Ultraviolet crosslinking can be used to chemically crosslink gels *in situ*, but this method has not been extensively used in the brain due to limited UV light penetration. In addition to taking advantage of their innate properties, hydrogels can be modified with customizable factors such as proteins or peptides using a number of methods, including: blending, adsorption, electrostatic interaction, chemical modification such as Schiff base reaction (Stabenfeldt et al., 2006), Diels-Alder click chemistry (Nimmo and Shoichet, 2011), covalent modifications (Tam et al., 2012), and/or affinity-based binding (Vulic and Shoichet, 2014). These modifications promote host interactions, support cell transplantation and control drug release.

Other polymeric biomaterials have been used extensively in drug delivery and tissue engineering as well; namely, particles and electrospun fibers. Particles are typically used for drug delivery and range in size from hundreds of nanometers to hundreds of micrometers (Soppimath et al., 2001; Taluja et al., 2007). Synthetic polymers are the most widely used material for forming particles. Block copolymers of PLGA are widely used in the field of controlled drug delivery because they are one of the few biodegradable polymers approved for clinical use by the FDA (Langer, 1990; Cohen-Sela et al., 2009). The degradation rate of polymeric particles is typically tuned by varying the particle size and composition. A common concern with PLGA is acidification of the local environment due to its acidic degradation products, potentially causing further cellular and tissue damage; however, this is a concern mostly for larger polymeric implants vs. nano/micro-particles where the acidic products can diffuse away. Particles made of natural materials, such as heparin (Hettiaratchi et al., 2014) and chitosan (Mo et al., 2010), avoid this issue but are less commonly used, in part due to their limited tunability. Synthetic material-derived electrospun scaffolds are attractive because their nanofibrous structure can recapitulate the microstructure of neural networks and can guide axons and neurites topographically (Schnell et al., 2007; Nisbet et al., 2009). Cell migration into these scaffolds is limited, but may be enhanced by inclusion of electrospun fibers in hydrogels, resulting in a cell-permissive scaffold that retains the biomimetic microstructure (Bosworth et al., 2013).

DRUG DELIVERY

Goals of Drug Therapy

Drug therapy utilizes endogenous repair mechanisms for protecting neural cells, creating a growth permissive environment, stimulating endogenous neural stem cells (NSCs), and promoting brain rewiring and plasticity. The therapeutics may take the form of small molecules, peptides or proteins. However, the BBB limits tissue penetration of systemically-administered therapeutics, rendering conventional systemic delivery strategies (intravenous and oral) ineffective (Pardridge, 2012). The small fraction of drugs that cross the BBB are often exported by surface transporters on the BBB, such as G-protein–coupled receptors (Misra et al., 2003). Large systemic doses can increase drug diffusion across the BBB but many compounds carry risks of systemic toxicity. Modifications to drugs and carrier-mediated transport across the BBB (Pardridge, 2003) may improve delivery but still expose the body to non-specific effects of the drug and require large doses due to systemic dilution. BBB breakdown after stroke does increase diffusion into the brain parenchyma, but is limited to the infarcted tissue and a narrow window of opportunity for administration; with reestablishment of the BBB, systemic delivery of therapeutics is again limited (Pardridge, 2012). Similarly, methods to disrupt the BBB, such as hypotonic solutions or focused ultrasound (Vykhodtseva et al., 2008), are non-specific and render the CNS vulnerable to circulating pathogens, making them unsuitable for sustained drug therapies.

Circumventing the BBB with local drug delivery increases the amount of drug at the target site, reducing systemic exposure and the risk of systemic toxicity. Clinical methods administer drugs by intracerebroventricular or intracortical infusion through a catheter (the Ommaya reservoir; Mead et al., 2014). These routes are fraught with issues, as fluid injection into the small ventricular spaces increases intracranial pressure and has been associated with hemorrhage, leakage of cerebrospinal fluid (CSF), and infection (Misra et al., 2003; Mead et al., 2014). Additionally, there is evidence that administration of drug into the CSF does not necessarily increase drug transport into the brain parenchyma (Pardridge, 2011). Convection enhanced delivery has been tested as a solution to increase drug distribution into the brain parenchyma by using a pressure gradient to drive convective transport through the interstitial spaces in the brain, achieving tissue penetration up to several centimeters vs. the millimeter range observed with diffusive transport (Mehta et al., 2017). However, this method is only conducive to bolus injections and cannot provide sustained delivery. Additionally, problems of increased intracranial pressure, damage to the infusion site, and damage due to needle insertion into brain tissue are still present.

Biomaterials that can be used for sustained local drug delivery to the brain in a minimally invasive manner have become important for drug therapy because they address many of the challenges surrounding delivery. Here, we discuss the use of biomaterials to improve local drug delivery and control drug release. We focus on the advances that have been made using biomaterials and drugs to: (1) protect cells, (2) stimulate regeneration, and (3) promote plasticity (**Table 1**). The therapeutic effects of biomaterials on host tissue will also be discussed.

Local Drug Delivery to the Brain

Biomaterial-based local drug delivery systems can overcome the limitations of traditional catheter-based systems. Drug diffusion in the brain is affected by the size (38–64 nm between cells) and tortuosity (λ = ~1.7 in uninjured brain, ~2.1 in injured brain) of the extracellular space, interactions with cellular receptors, and affinities for charged moieties in the ECM (Thorne et al., 2008). Brain injury will change these parameters and reduce the effective diffusivity, thereby making it difficult to achieve therapeutic concentrations at distances greater than several centimeters. Tissue penetration—the distance the drug is found from the source at detectable concentrations—can be enhanced by increasing the drug concentration at the source, reducing binding to the ECM, or decreasing elimination and degradation. Providing a sustained source of drugs would maintain a higher driving force for diffusion and increase penetration. Shielding the protein from extracellular degradation can increase effective diffusion, as was shown by the threefold increased tissue penetration after PEGylating epidermal growth factor (EGF) (Wang et al., 2011b). In some cases, it is important to control the spatial distribution of the molecule, not just the tissue penetration, as this can profoundly affect physiological response. For example, mice expressing vascular endothelial growth factor-A (VEGF-A) isoforms with high ECM binding affinity, with steep concentration gradients and low tissue penetration, exhibited thin, highly branched blood vessels while non-ECM binding VEGF isoforms, with shallow concentration gradients and higher concentrations further away from the source, exhibited wide, leaky vessels (Ruhrberg et al., 2002).

Delivery can take two forms: intracranial delivery and epi-cortical delivery (**Figure 1**). Intracranial delivery into the stroke infarct limits damage to healthy tissue. As the peri-infarct region is often the site of many protective and regenerative therapies (Carmichael et al., 2005), this also positions the drug closer to the site of action and reduces the diffusion distance, ensuring therapeutically relevant concentrations are reached. One limitation of intracranial delivery is the limited range of drug transport by diffusion (in the range of millimeters) that is adequate for animal models but may not scale to the larger human brain. However, postinjury plasticity is often mediated by the peri-infarct tissue located millimeters to tens of millimeters from the infarct boundary zone (Nudo et al., 1996; Luft et al., 2004; Carmichael et al., 2005; Brown et al., 2009). Thus, in most cases, the diffusive range seen in animal models may be translatable to humans.

Epi-cortical delivery has been explored as a minimally invasive method of drug delivery to the brain (Cooke et al., 2011; Tuladhar et al., 2015). With this method a drug-loaded scaffold is implanted onto the surface of the brain, thus avoiding tissue damage caused by needle insertion as is seen with intracranial and convection-enhanced delivery. In the mouse and rat, proteins and drugs delivered epi-cortically can diffuse through the cortex and reach the subcortical NSPCs located in the lateral ventricles. A drawback of this approach is the larger diffusion distance required to reach the site of action. Although this method may not be amenable to targeting the subcortical ventricles in the larger human brain due to limits of diffusive transport, treatments targeting the thin (1–5 mm) cortical regions of the human brain (Fischl and Dale, 2000) may be amenable to epi-cortical delivery.

TABLE 1 | Biomaterials for local drug delivery to the brain.

Therapeutic	Material description	Outcome	Reference
CsA	CsA-loaded PLGA microparticles inside HAMC hydrogel implanted epi-cortically in Et-1 stroke-injured mouse and rat	Controlled local delivery for 2–3 weeks, reduced stroke infarct volume, proliferation increased in rat NSPC niche with CsA, reduced infarct volume with HAMC	Caicco et al. (2013) and Tuladhar et al. (2015)
EGF	EGF-loaded HAMC hydrogel implanted epi-cortically in Et-1 stroke-injured mouse	PEG-modified EGF increased diffusion distance during 2-d release, increased proliferation of neuroblasts in SVZ	Cooke et al. (2011) and Wang et al. (2011b)
EPO	EPO HAMC hydrogel implanted epi-cortically in Et-1 stroke-injured mouse	EPO released to brain for 2 days, stroke cavity volume decreased with HAMC; further decreased with EPO. Reduced astrogliosis and microglia response with HAMC, increased number of proliferating neuroblasts in SVZ, reduced cell death in SVZ and more neurons	Wang et al. (2012b)
EGF + EPO	EGF loaded PLGA nanoparticles and EPO loaded PLGA/PSA microparticles inside HAMC hydrogel implanted epi-cortically at 4 days poststroke in Et-1-injured mouse	Sequential and sustained release of PEG-EGF followed by EPO. Increased number of NSPCs in SVZ niche and increased proliferation. Reduced cavity size with EGF + EPO vs. vehicle and more neurons	Wang et al. (2013)
VEGF	Alginate hydrogel loaded with $VEGF_{165}$ by premixing alginate solution with lyophilized VEGF and crosslink at RT for 30 min, kept on ice until injected into striatum 15 min before MCAO in young adult male SD rats	$VEGF_{165}$ released from hydrogel found in brain for 1 week compared to <10 h from bolus injection, resulting in reduced infarct volume and reduced neurological deficit	Emerich et al. (2010)
	VEGF encapsulated in poly(dimethylsiloxane-tetraethoxysilane) and injected into injury cavity	Increased number of astrocytes and endothelial cells with VEGF release. The PDMS-TEOS material helped restore/preserve brain shape, serving as a structural support	Zhang et al. (2007)
VEGF + Ang1 + Anti-NOGOa	HA hydrogel chemically crosslinked with reversibly conjugated anti-NOGOa, loaded with VEGF and Ang1 PLGA particles and implanted into MCAO-injured mice	Increased angiogenesis with VEGF and Ang1, reduced astrogliosis and microglial response and significant recovery with Ang1 and VEGF treatment	Ju et al. (2014)
Anti-NOGOa	HA hydrogel chemically crosslinked with reversibly conjugated anti-NOGOa	Moderate behavioral recovery in a reaching task and increased nerve fiber growth	Ma et al. (2007)
BDNF	HA hydrogel with collagen-binding domains to control BDNF release, tested in mice and non-human primate	Sustained BDNF release, over 3 weeks in mouse. Increased axonal sprouting in contralateral striatum, following existing axon patterns, concomitant with behavioral recovery. Increased neurogenesis (DCX and NeuN + BrdU)	Cook et al. (2017)
BDNF + AMPAkine	HA hydrogel with collagen-binding domains to control BDNF release, injected into infarct with AMPAkine administered systemically in aged mice	Recovery seen with both BDNF and AMPAkine alone, further increased with combination. Increased expression of proplasticity signaling (e.g., p-CREB, p-AKT) with BDNF, AMPAkine, increased further in some cases by combination	Clarkson et al. (2015)
BDNF + GDNF	BDNF and GDNF were separately encapsulated in PLGA particles to achieve different release rates and loaded into a biodegradable PEG hydrogel strand, injected into the substantia nigra and striatum of uninjured female SD rats	Achieved slow and long-term release of BDNF for over 8 weeks, and faster release of GDNF over 28 days. Swelling was minimal. Slightly elevated astrogliosis but reduced microgliosis	Lampe et al. (2011)
NT-3	Chitosan microparticles loaded with NT-3 by adsorption onto particle surface and suspended in a collagen-1 solution, injected into infarct in hippocampal TBI model	Chitosan carrier reduced gliosis and slightly increased axon regeneration. NT-3 increased axon regeneration into the injury site. Recovery in water maze task with chitosan carrier group; no further recovery with NT-3	Mo et al. (2010)
HGF or IGF1	HGF or IGF1 absorbed to gelatin hydrogel microspheres by incubation for 1 h. Injection into striatum of uninjured and MCAO-injured mice. Drugs were tested independently	Increased number of neuroblasts with IGF1 or HGF only when delivered in hydrogel carrier. No behavior tested	Nakaguchi et al. (2012)

Controlling Drug Release

Protective and regenerative therapies require sustained drug exposure to be efficacious (Wieloch and Nikolich, 2006). In the absence of control mechanisms, drugs given by bolus injection are cleared in several hours and drug release from a hydrogel depot is typically complete within 2–4 days. The release window may be extended to several weeks or months by retarding diffusion out of the depot through encapsulation or immobilization in the matrix (Soppimath et al., 2001) or by affinity interactions with the matrix (Vulic and Shoichet, 2014).

Polymeric micro- and nano-particle systems control release by encapsulating drugs within a biodegradable polymer matrix. Drug release from bulk-degrading polymers, such as PLGA, involves multiple mechanisms (Han et al., 2016). The initial release,

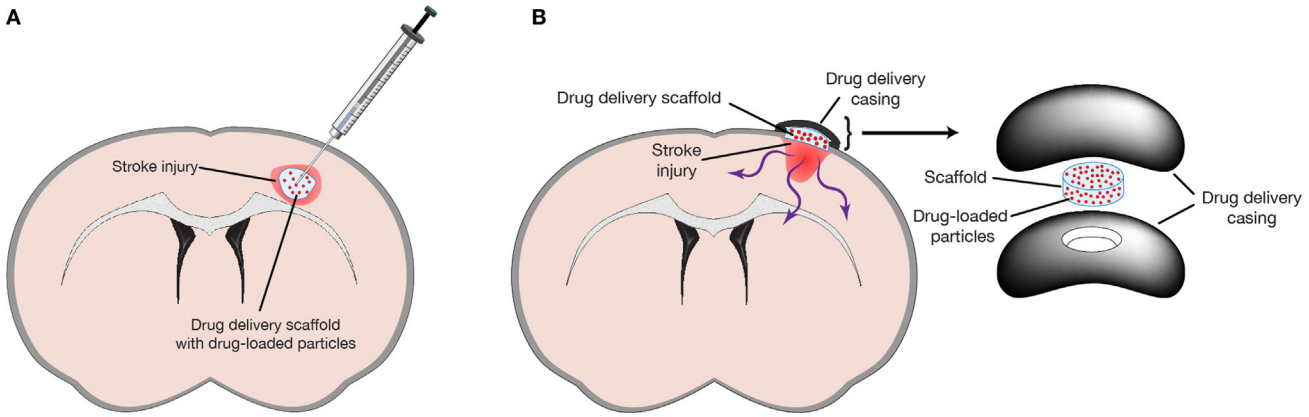

FIGURE 1 | Biomaterials can be used to delivery drugs by either **(A)** intracranial injection into space provided by the stroke injury or **(B)** epi-cortical implant on the surface of the brain to prevent any further damage due to injection. Reprinted from Tuladhar et al. (2015) with permission from Elsevier.

termed the burst phase, occurs from the surface bound drug and usually takes place within hours barring any interactions between drug and material. The next release phase occurs by diffusion of the drug through pores formed in the particle as the polymer degrades or swells. Finally, bulk degradation and polymer erosion results in the release of any remaining drug. Polymeric particles for drug release can range from several hundred nanometers to approximately 100 μm (Soppimath et al., 2001; Taluja et al., 2007). Microparticles made from natural or ECM components, such as heparin and chitosan (Agnihotri et al., 2004; Lin et al., 2009), have been used but they lack the tunability of common synthetic materials such as poly(esters) (e.g., PLGA; Mohammadi-Samani and Taghipour, 2015) and poly(anhydrides) (e.g., PSA) (Kumar et al., 2002). The release period from PLGA particles can be tuned from 1 to 2 weeks to several months by varying the relative ratios of lactic acid and glycolic acid monomers, the copolymer chain length, the molecular weight of PLGA, or the terminal functional groups (Pollauf et al., 2005). Multiple drugs can be incorporated into the same particle and the use of slow and fast degrading PLGA variants allows for precise temporal release that better mimics signaling patterns found *in vivo* (Richardson et al., 2001; Lampe et al., 2011; Brudno et al., 2013). In addition, double-walled particles can be made using a mix of two polymers (Pekarek et al., 1994). Here, a drug-loaded core is coated with a drug-free shell; using a polyanhydride for the shell will result in a delayed release, where the surface eroding shell degrades before the drug is released from the core. Combining a classical PLGA particle with this double-walled particle allowed the sequential release of EGF followed a week later by erythropoietin (EPO) (Wang et al., 2013), mimicking the release paradigm of more invasive osmotic mini-pumps and cannulas used to stimulate endogenous brain NSPCs (Kolb et al., 2007) but in a minimally invasive manner.

Drugs can also be covalently immobilized within hydrogel matrices. The drug can act on cells at the hydrogel–tissue interface and on infiltrating cells. Immobilized proteins can cause a drastically different tissue response compared to soluble protein by inducing differential changes in receptor internalization and trafficking (Clegg and Mac Gabhann, 2015) and in downstream signaling pathways (Chen et al., 2010b). Proteins can be immobilized in a hydrogel using chemical conjugation (Ehrbar et al., 2007). Drug release is dictated by the rate of hydrogel degradation, which can be tuned to be environmentally responsive to enzymes [e.g., MMPs (Purcell et al., 2014)] secreted by, for example, NSPCs (Barkho et al., 2008) or endothelial cells (Rundhaug, 2005).

Naturally occurring affinity interactions between proteins and the ECM have been employed in biomaterials through natural or functionalized binding sites that control release through transient hydrophobic and electrostatic interactions. A key advantage of these systems is that the harsh encapsulation process necessary for particle systems is avoided, preserving protein function and stability. Release can be tuned by modifying the strength of the affinity interaction, the concentration of binding ligand, and the rate of dissociation (Vulic and Shoichet, 2014). Heparin is the most popular platform for affinity release because it has a natural affinity for a number of heparin binding proteins relevant for regeneration [e.g., fibroblast growth factor (FGF), VEGF, insulin growth factor (IGF), platelet-derived growth factor, stromal-derived factor (SDF), and bone morphogenic proteins (BMPs); Capila and Linhardt, 2002]. It has been used to form hydrogels and particles or to functionalize other materials (Sakiyama-Elbert, 2014). To overcome the lack of specificity of heparin interactions, which is problematic in the heparin binding protein rich environment found *in vivo*, a variety of solutions have been pursued and include: heparan sulfate variants, selectively desulfated heparin, and heparin fractions with protein-specific affinity (Wang et al., 2014). A drawback to this approach is the limited ability to tune the strength of the heparin–protein interaction and the inherent limitation to heparin-binding proteins. The creation of fusion proteins with SH3-domains that interact with SH3-binding peptides bound to a gel enables specific affinity release strategies for a wider range of proteins (Vulic and Shoichet, 2012). This strategy allows for the controlled release of many proteins, including those too delicate for encapsulation and lacking affinity for heparin, as was demonstrated with the

enzyme chondroitinase ABC (ChABC) (Pakulska et al., 2013). Multiple drugs can be released from the same vehicle with this system using the same material; however, the release rate of two or more drugs cannot be independently tuned. If the system is reversed whereby SH3-binding peptides are coexpressed with proteins and SH3 covalently bound to the hydrogel, controlled release of multiple proteins with independent release rates will be dictated by the unique SH3-binding peptide on each fusion protein (Delplace et al., 2016). Advances in computational design of protein–protein interactions and phage display libraries will increase the variety of binding interactions available for affinity release strategies, increasing their utility (Pakulska et al., 2016b). Recently, innovative work has used electrostatic interactions to control drug release from PLGA particles without the need for encapsulation (Pakulska et al., 2016a). The key advantage to this approach is the ability to control release of many relevant molecules [e.g., SDF, neurotrophin-3 (NT-3), and brain-derived neurotrophic factor (BDNF)] using the same nanoparticle, avoiding the harsh encapsulation process that often denatures proteins and reduces drug loading. Release can be tuned simply by varying nanoparticle size, concentration, and degradation rate. One limitation to the system is that the anionic particle can only interact with positively charged proteins. Modifying the particle with a positively charged component, such as chitosan, may allow electrostatic control of negatively charged proteins (Kumar et al., 2004). Laponite, derived from clay, can electrostatically control release of negatively charged proteins (Koshy et al., 2018), but the non-biodegradable silica degradation products make the platform incompatible with the brain.

Protecting Neural Cells

Neuroprotective strategies for stroke have been investigated to save existing cells and neural circuits by either (a) directly reducing cell death, demyelination, and axon death in the stroke peri-infarct or (b) mitigating secondary damage caused by excitotoxicity, inflammation, and oxidative stress. However, the utility of this approach was brought into question when it was noted, in 2006, that although 1,026 neuroprotective agents had been identified and tested in preclinical studies (O'Collins et al., 2006) and almost 200 had reached various stages of clinical trial, nearly all had failed to demonstrate clinical efficacy. tPa, first tested in 1988, was the only exception (Stroke trials registry page, http://www.strokecenter.org/trials) (Minnerup et al., 2012). Discrepancies between preclinical and clinical studies (e.g., population age, scope of injury, and primary endpoint) likely contribute to the clinical failures (Sutherland et al., 2012). Despite the lack of clinical translation, neuroprotective strategies are still actively being investigated and evaluated using more targeted approaches based on mechanistic studies (Rajah and Ding, 2017).

The advent of biomaterials may give new life to neuroprotective molecules that have previously failed due to poor BBB penetration and low concentrations in poorly perfused ischemic regions. VEGF released from an alginate hydrogel provided exposure for 1 week, compared to <10 h from a bolus injection, resulting in reduced stroke infarct size and neurological deficit (Emerich et al., 2010). The materials themselves offer some neuroprotection by providing structural support, attenuating gliosis and inflammation, and reducing cavitation. Bioactive materials, like HA, reduce inflammation through the CD44 receptor by inhibiting leukocyte migration and inflammation (Forrester and Wilkinson, 1981; Cooper et al., 2008), resulting in reduced microglial activation (Wang et al., 2012b) and stroke infarct volume (Hou et al., 2005; Austin et al., 2012; Wang et al., 2013; Tuladhar et al., 2015).

Recently, the effect of hydrogel structure alone on tissue repair was investigated by comparing a micro-porous HA hydrogel, synthesized by crosslinking HA-RGD microbeads *in situ*, to a nano-porous hydrogel while keeping the bulk moduli and biochemical signaling the same (**Figures 2A–E**) (Nih et al., 2017). Both structures reduced the thickness of the glial scar and degree of macrophage activation in the peri-infarct region; however, the magnitude of this effect was greatly increased in the microporous gel. Additionally, the microporous gel reduced macrophage activity within the stroke infarct. To have even greater benefit, neuroprotective drugs may be delivered from a microporous gel, as has been shown with gelatin microspheres to deliver anti-inflammatory (Jin et al., 2011b) or proregenerative molecules.

Stimulating Endogenous Stem Cells

Stimulating endogenous NSPC populations in the brain requires therapeutics to influence their proliferation, survival, migration, and differentiation (Wiltrout et al., 2007; Hunt and Morshead, 2010; Guerra-Crespo et al., 2012; Wang et al., 2012a). An array of growth factors and cytokines has been found to be important in endogenous NSPC signaling. Often, these factors have multiple and overlapping effects on the NSPCs. Many of the factors investigated for endogenous NSPC stimulation are naturally upregulated within hours to days after stroke as part of the injury response, but this is transient and in the majority of cases returns to basal levels within a week. These molecules include growth factors and cytokines to stimulate: proliferation [e.g., EGF, FGF2, VEGF, human chorionic gonadotrophin (hCG), hepatocyte growth factor (HGF), BDNF, IGF1], survival [e.g., VEGF, EGF, BDNF, glial-derived neurotrophic factor (GDNF)], migration (e.g., SDF1a, VEGF, BDNF), and differentiation (e.g., BDNF, EPO, GDNF, BMP4, HGF). The only drugs that have been tested clinically are hCG and EPO, and while preclinical results demonstrated increased endogenous NSPC mobilization and neuronal differentiation (Belayev et al., 2009), the clinical trial was inconclusive (Cramer et al., 2010). Although the clinical trial failed to demonstrate a benefit compared to saline controls, and was thus prematurely terminated, it was found in *post hoc* analysis that the subgroup of patients also receiving occupational therapy benefited from hCG and EPO treatment. Small molecule drugs clinically used for other therapeutic purposes have been found to stimulate NSPCs and promote recovery. Cyclosporine (CsA), a common immunosuppressant, is found to increase NSPC survival *in vitro* and *in vivo,* and to reduce stroke infarct volume (Hunt et al., 2010; Erlandsson et al., 2011; Sachewsky et al., 2014). Metformin, a drug for diabetes, stimulates neurogenesis in the hippocampus, improving memory in injured mice (Wang et al., 2012a); a clinical trial is underway to evaluate its potential in treating brain injury in children (NCT02040376).

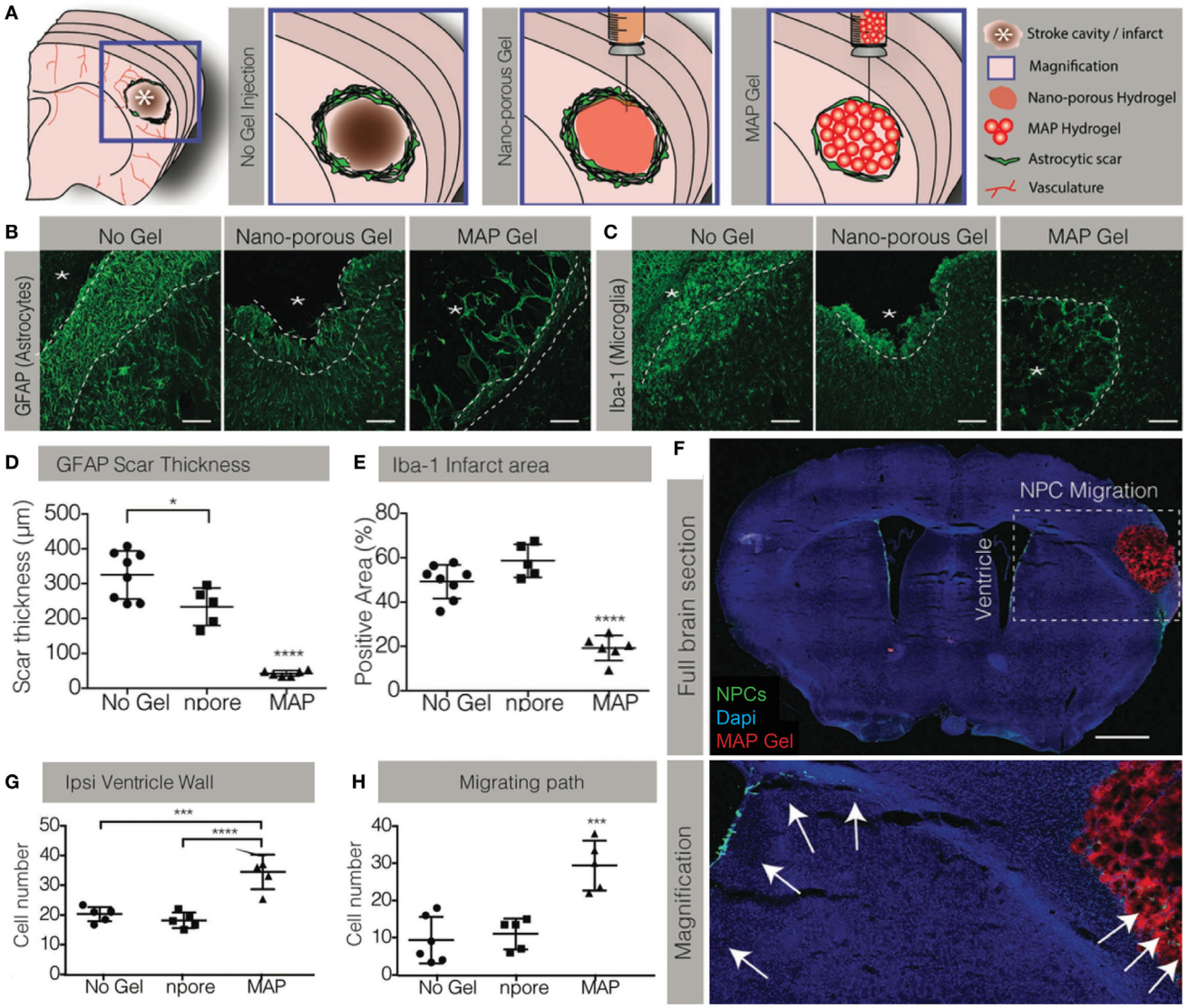

FIGURE 2 | Manipulating the biomaterial structure can drastically change the host response. **(A)** A microporous (MAP) hydrogel was synthesized using HA-RGD microbeads. The gel had the same bulk modulus and chemical structure as a nanoporous hydrogel. Representative images of the **(B)** astrocytic and **(C)** microglial responses in the stroke cavity with no gel, nanoporous gel and MAP gel. **(D)** The MAP hydrogel significantly reduced the glial scar thickness compared to the nanoporous hydrogel. **(E)** The microglial response was only reduced by the microporous MAP hydrogel; despite possessing the same modulus and biochemical signaling, the nanoporous hydrogel did not affect the response. **(F)** Representative images of endogenous neural progenitor cells (NPCs) stimulated by the MAP hydrogel. **(G)** Only the microporous MAP hydrogel increased the number of NPCs in the subventricular zone and **(H)** migrating into the infarct. Reproduced with permission from Nih et al. (2017).

Many studies have demonstrated improved outcomes when combining regenerative strategies with biomaterial delivery systems for controlled release of drugs. Controlled release of HGF and IGF1 from gelatin microspheres increased the number of neuronal progenitors while bolus IGF1 or HGF injections failed to stimulate the NSPCs (Nakaguchi et al., 2012). Although controlled release may be achieved through infusion strategies, this method is deleterious to the NSPC niche and may negate any beneficial effects of delivered factors (Wang et al., 2013). Intracortical BDNF injections can stimulate NSPCs but requires extended exposure (Schabitz et al., 1997). BDNF modified with a collagen binding domain increased retention in the tissue by binding to collagen in the ventricular NSPC niche, significantly stimulating NSPC proliferation and neurogenesis compared to unmodified BDNF that lacks the ability to bind to the niche (Guan et al., 2012). Incorporating the collagen binding domain in a HA hydrogel results in drug release over multiple weeks (Cook et al., 2017). Stroke-injured animals receiving BDNF from this hydrogel recovered motor function accompanied by NSPC proliferation and neurogenesis. However, because BDNF can exert recovery through a variety of mechanisms (e.g., synaptogenesis and angiogenesis) it is unclear how recovery was mediated.

Epi-cortical EGF and EPO delivery with HAMC, a hydrogel blend of HA and methycellulose, increased NSPC proliferation and neurogenesis, but the short release window (2 days) may be insufficient for substantial regeneration and long-term recovery (Cooke et al., 2011; Wang et al., 2012b). Previous work with EGF and EPO demonstrated that sequential delivery of the two compounds into the ventricle with a cannula, for 7 days each, produced significant tissue regeneration and motor recovery (Kolb et al., 2007). Therefore, to mimic this release profile a composite delivery system using HAMC, PLGA nanoparticles, and double-walled PLGA/polyanhydride microparticles was used to achieve sequential and extended release of EGF and EPO (Wang et al., 2013). This bioengineered strategy increased NSPC proliferation and survival compared to cannula delivery in a mouse model of stroke. This appears to be partly caused by reduced glial scarring and microglial activation by the vehicle, likely mediated by the HA component, and increased cell death in the SVZ due to cannula insertion. Controlled release of individual drugs was not tested, so it is unclear whether a synergistic effect of EGF and EPO was necessary for the effects reported. While a clear tissue benefit was seen, it is unknown whether this was accompanied by behavioral recovery. Epi-cortical delivery has also been tested in the larger rat model with cyclosporine, demonstrating sufficient tissue penetration to stimulate proliferating endogenous NSPCs (Tuladhar et al., 2015).

In a few cases, the material alone has had an impact on host NSPCs. The aforementioned micro-porous HA-RGD hydrogels stimulated NSPC proliferation in the SVZ—an effect not seen with nanoporous gels (**Figures 2A,F–H**) (Nih et al., 2017). While neuroblasts were reported to have migrated into the gels, it is unclear how the material stimulated NSPC proliferation. Aligned PCL nanofibers were used to promote NSPC migration into the injury site; however, long-term neuroblast survival required inclusion of a BDNF-mimetic peptide (Fon et al., 2014).

Promoting Plasticity

Neuroplasticity is defined as the brain's ability to modify its neural circuitry and is necessary to restore function (Dimyan and Cohen, 2011). Spared or newly generated tissue must be integrated into the uninjured neural network and adapt to functional demands. This requires the creation of new connections, modification of existing neural circuitry, and removal of plasticity inhibiting elements. Agonists of Trk receptors are involved in neuronal plasticity (Thoenen, 1995) and the two factors most investigated for stimulating this mechanism are NT-3 and BDNF. NT-3 has a key role in the development and repair of motor circuits (Patel et al., 2003; Chen et al., 2006) and delivery to stroke-injured animals increases axonal sprouting (Duricki et al., 2016). Chitosan particles suspended in a collagen 1 solution have been used to deliver NT-3 to the hippocampus in a traumatic brain injury (TBI) model (Mo et al., 2010). Interestingly, the chitosan particles alone resulted in increased axonal sprouting compared to injury-only groups, while NT-3 further increased the amount of axon regeneration. However, behavioral recovery was significant with the chitosan vehicle alone and, surprisingly, the addition of NT-3 did not increase this recovery. This lack of additional recovery with NT-3 may not necessarily indicate that NT-3 is ineffective; rather, the axonal sprouting seen with chitosan may be sufficient for behavioral recovery and any additional improvement requires other mechanisms. In contrast, in a rat spinal cord injury model, a HAMC and PLGA-based NT-3 delivery system induced both axonal sprouting and motor recovery (Elliott Donaghue et al., 2015). The difference in outcomes may be due to differing etiologies in the two CNS compartments and different requirements for recovery.

Modifying existing neural circuits requires synaptic plasticity at axon-dendrite terminals to strengthen or weaken existing connections and appears to be mediated by BDNF. Delivering BDNF improves motor recovery (Müller et al., 2008) while blocking BDNF signaling reduces any recovery seen with plasticity-dependent rehabilitative training (Ploughman et al., 2009). Although BDNF expression is upregulated after stroke injury this effect is transient and is reduced with age, making plasticity-based recovery paradigms difficult in chronic stroke and aged populations. While systemically delivered AMPAkine stimulated recovery in young animals, by inducing BDNF release (Clarkson et al., 2011), recovery was dampened in aged animals (Clarkson et al., 2015) due to reduced BDNF expression in this population. Interestingly, combining the systemically administered AMPAkine with local BDNF delivery through a HA-based hydrogel modified with collagen-binding domains improved recovery in aged animals to levels comparable to young animals (Clarkson et al., 2015). This is one of the few studies involving biomaterials that investigated mechanistic pathways mediating this process, demonstrating that BDNF delivered from the hydrogel upregulates canonical BDNF signaling pathways. The delivery system uses the affinity of BDNF for collagen to control release and increased local BDNF concentrations for at least 3 weeks postimplant (Cook et al., 2017). Additionally, intracranial delivery of the gel to a non-human primate stroke model resulted in sufficient BDNF accumulation in the peri-infarct area (within 1–2 cm), a distance relevant for recovery in humans (Nudo et al., 1996; Luft et al., 2004). Interestingly, the drug concentration around the implant varied depending on the direction measured, highlighting the anisotropy of the brain and its effect on diffusion. Importantly, the authors highlight that BDNF only increases the strength of existing connections and cannot overcome growth inhibitors. Thus, BDNF treatment alone may be in insufficient in cases where new connections need to be made, such as when existing connections are insufficient to support adaptive plasticity, or in chronic stroke, where glial inhibition is a significant barrier.

The adult brain ECM and glial cells express many growth inhibitory molecules that limit synaptogenesis and axonogenesis, such as the neurite outgrowth inhibitor (Nogo) (Schwab and Strittmatter, 2014). Inhibiting the activity of these molecules, such as with an anti-NogoA antibody, enhances regeneration, plasticity, and recovery (Buchli and Schwab, 2005). A HA hydrogel was used to deliver a Nogo66 receptor antibody in stroke-injured rats; although increased nerve fiber growth was seen, it was insufficient to produce any significant behavioral recovery (Ma et al., 2007). Combining NogoA inhibition with a growth stimulatory molecule may produce a synergistic effect on axon growth. Controlling the release of anti-NogoA and codelivering it with NT-3 was investigated using a blend of HAMC and PLGA

particles; increased axon density and improved motor function were achieved in a rat spinal cord injury model (Elliott Donaghue et al., 2016). Perineuronal nets are ECM structures surrounding axon terminals that stabilize synapses in the healthy brain but inhibit new connections in the injured and adult brain (Wang and Fawcett, 2012). ChABC has been found to increase synaptic plasticity by transiently destabilizing these perineuronal nets (Massey et al., 2006). Biomaterial delivery systems have been developed for ChABC (Pakulska et al., 2013), to stimulate recovery in spinal cord injury (Pakulska et al., 2017), and can be applied to existing delivery paradigms in the brain.

CELL DELIVERY

Goals of Cell Therapy

As an alternative to drug delivery, many strategies focus on the delivery of an exogenous source of cells to treat stroke. The aim of cell transplantation is to increase the survival of endogenous cells as well as to directly replace damaged tissue to promote regeneration. Cell types used for transplantation to the brain include adult NSCs, mesenchymal stromal cells (MSCs), embryonic stem cell (ESC)- or induced pluripotent stem cell (iPSC)-derived NPCs, and directly reprogrammed induced neural stem cells (Yamashita et al., 2017). Early research also included undifferentiated pluripotent stem cells, however, their use has become limited due to the risk of teratoma and tumor formation (Kawai et al., 2010; Yamashita et al., 2011). Transplanted cells have been demonstrated to promote stroke recovery in animal models through a variety of mechanisms: stimulating both endogenous NPCs and endothelial progenitor cells to migrate to ischemic sites (Bliss et al., 2010; Lindvall and Kokaia, 2011; Dailey et al., 2013), stimulating the proliferation of neuroblasts in the SVZ (Chen et al., 2003; Jin et al., 2011a; Zhang et al., 2011), promoting angiogenesis in the peri-infarct zone (Horie et al., 2011; Zhang et al., 2011; Oki et al., 2012), and decreasing infarct size (Chen et al., 2010a; Gomi et al., 2012; Oki et al., 2012). In addition to the effects on endogenous tissue, transplanted cells can integrate into the existing neural circuitry, reestablishing connections with host cells (Niclis et al., 2017); however, it remains unclear if these new connections contribute directly to recovery.

Although cell transplantation can stimulate stroke recovery in animal models, appreciable long-term survival of cells continues to remain elusive, with an estimated survival of only 2–8% of the initial transplant population (Nakagomi et al., 2009). This poor survival is attributed to cell death during the transplantation process, lack of endogenous ECM and vasculature in the stroke cavity, lack of prosurvival signals, and low rates of cell differentiation and integration (Modo et al., 2002; Kelly et al., 2004; Hicks et al., 2009). Biomaterials are becoming an important part of the cell delivery paradigm, enhancing the success of cell transplantation through four main strategies, discussed herein, by providing: (1) a platform for *in vitro* predifferentiation of cells prior to transplantation; (2) a delivery vehicle to reduce acute cell death during the delivery process; (3) a scaffold for cell adhesion and survival after delivery; and (4) a platform for the codelivery of cells and factors to promote cell differentiation and integration (**Figure 3**). Most biomaterials used for cell transplantation to the brain are hydrogels, and thus will be the focus of this discussion. It is also important to note that many strategies are multifaceted, involving ECM components and proteins that will enhance cell survival, direct differentiation, and/or recruit endogenous cells.

Biomaterials for Cell Therapy

Early studies of biomaterials for cell transplantation focused on the use of synthetic polymers such as PEG, a highly hydrophilic polymer that is biocompatible and non-immunogenic (Bjugstad et al., 2008; Bhattarai et al., 2010). PEG can be combined with other synthetic polymers, such as PLGA, or with natural polymers. PEG has been used to design hydrogels for cell culture, incorporating FGF2 and type I collagen (Mahoney and Anseth, 2007), or heparin and RGD (Freudenberg et al., 2009) to culture embryonic NSCs, which were both found to increase cell viability. Other synthetic polymers [PGA, PLGA, poly(d-lysine), PCL] are used for a range of applications including: *in vitro* coating of polycarbonate or plastics [e.g., poly(L-lysine); Jongpaiboonkit et al., 2008], scaffold particles for structural support for cell transplantation (e.g., PLGA; Bible et al., 2009), electrospun nanoparticles (e.g., PCL; Horne et al., 2010), and 3D scaffolds (e.g., PGA; Park et al., 2002). For example, when a PGA 3D scaffold was used to

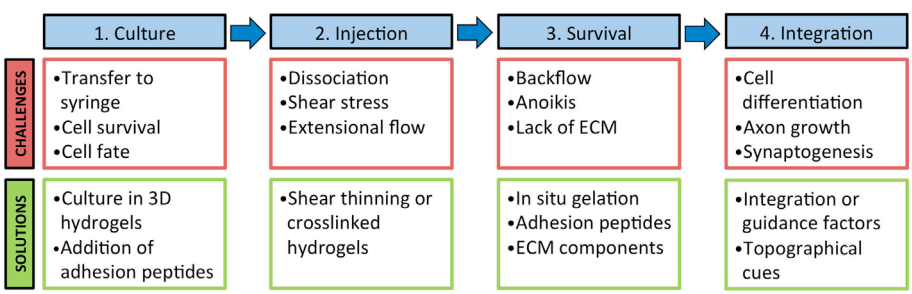

FIGURE 3 | Biomaterials can be used to address challenges at multiple stages of the cell transplantation paradigm. 1. Biomaterials can be used to prime cells in culture prior to injection to guide cell fate and limit death during transfer to a syringe. 2. The use of a shear thinning or crosslinked hydrogel can decrease mechanical stress that cells undergo during processing and injection. 3. Biomaterials can aid in cell retention at the injection site and increase cell survival with the addition of adhesion peptides and ECM components. 4. Long-term cell integration can be supported with a biomaterial with factors and topographical cues for cell differentiation, axon guidance, and synapse formation.

deliver NSCs into the stroke-injured neonatal mouse brain and compared to cell delivery in saline, the scaffold attenuated the immune response, reduced glial scarring, allowed penetration of blood vessels, and promoted differentiation of delivered cells into neurons and glia (Park et al., 2002). While there are advantages to synthetic biomaterials, there are also drawbacks such as biocompatibility issues with many of their acidic degradation products and their inability to interface with native cells and enzymes (Hoffman, 2012).

Natural hydrogels are favored for cell transplantation after stroke due to the similarity in mechanical properties with native brain tissue (i.e., soft consistency and elastic nature) (**Table 2**). One natural hydrogel used for cell delivery is Matrigel™, a material derived from a mouse sarcoma cell line primarily composed of laminin-1 and collagen IV and containing many adhesive molecules and growth factors that promote cell viability. Transplantation of mouse ESC-derived NPCs in Matrigel™ into the striatum resulted in a larger graft volume and increased the number of tyrosine hydroxylase-positive dopaminergic neurons (Uemura et al., 2010). Unfortunately, as Matrigel™ is derived from a xenobiotic source, it has high batch-to-batch variability and is unsuitable for clinical use (Jin et al., 2010). In addition, Matrigel™ gels at room temperature through hydrophobic interactions between the components, causing it to be technically challenging for cell injection. To retain the desirable properties of Matrigel™ without its drawbacks, other strategies have favored the use of ECM-based hydrogels such as HA, fibrin, and collagen as they are well-defined and tunable (Nair and Laurencin, 2007; Nih et al., 2016).

As an alternative to isolating one individual component of the ECM to create a hydrogel, researchers have also derived a multicomponent hydrogel from decellularized natural ECM. Porcine bladder-derived ECM hydrogels promote *in vitro* 3D neurite extension (Medberry et al., 2013), and when injected into the cavity of stroke-injured rat brain led to infiltration of neural progenitors and oligodendrocytes into the gel-filled space (Massensini et al., 2015; Ghuman et al., 2016). Natural ECM hydrogels have also been derived from brain and spinal cord, and some have been electrospun with other components for *in vitro* culture to demonstrate neurite extension (Baiguera et al., 2014; De Waele et al., 2015). One study comparing bladder, spinal cord, and brain ECM reported that there were differences in the chemical composition and mechanical properties between them, and that while all three were able to promote neurite formation, brain ECM promoted the longest and most numerous neurites in a neuroblastoma cell line (Medberry et al., 2013) indicating the superiority of brain-derived ECM for neuronal culture.

TABLE 2 | Naturally-derived biomaterials for cell delivery to the brain.

Biomaterial	Cell type	Modifications	Outcome	Reference
Physical blend of hyaluronan/ methyl cellulose (HAMC)	Adult neural stem/progenitor cells	None	Behavioral recovery, better cell distribution within brain compared to saline	Ballios et al. (2015)
	IPSC-derived neural progenitor cells		Cell survival to 7 days; improved sensorimotor performance	Payne et al. (2017)
Matrigel™	ESC-derived progenitor cells	None	Reduction in cavity volume; improved sensorimotor and cognitive performance	Jin et al. (2010)
Hyaluronan (HA)	IPSC-derived progenitor cells	MMP-degradable or non-degradable crosslinker	Increased DCX, better cell distribution with hydrogel; adding MMP-degradable crosslinker reduced microglial response	Lam et al. (2014)
		BDNF, BMP4, laminin, and/or fibronectin	Growth factors promoted astrocytic differentiation; adhesion proteins promoted neuronal differentiation	Moshayedi et al. (2016)
	Primary rodent NPCs	Crosslinked with heparin	Increased cell survival; decreased microglial response compared to cells alone	Zhong et al. (2010)
Collagen	ESC-derived neural stem cells	Laminin or fibronectin	Collagen I gel with laminin improved cell survival a behavioral recovery over untreated group	Tate et al. (2009)
Fibrin	iPSC-derived NPCs	None	Fibrin glue + cells reduced infarct volume, promoted functional recovery	Chen et al. (2010a)
			Reduced infarct volume, inflammation and gliosis; increased recovery, angiogenesis and white matter tract integrity	Lee et al. (2017)
Self-assembling peptides	Primary rodent NSCs	IKVAV peptide	RADA peptide hydrogel with and without IKVAV; enhanced cell survival and neuronal marker expression	Cheng et al. (2013)
	Human iPSC-derived NPCs	IKVAV peptide	Reduced brain atrophy, long-term functional recovery, and neuronal differentiation	Somaa et al. (2017)

In Vitro Cell Priming

Biomaterials can be used to culture cells prior to transplantation, enhancing the success of cell therapies. It has been demonstrated that priming cells *in vitro* through a variety of mechanisms—guiding differentiation, stimulating the secretion of factors, or exposing cells to stressful conditions—can increase their therapeutic efficacy once delivered to the brain (Rosenblum et al., 2015; Lee et al., 2017). It has also been suggested that predifferentiating pluripotent or multipotent cells toward a neuronal lineage prior to transplantation can increase tissue and behavioral recovery (Fricker-Gates et al., 2002; Tornero et al., 2013). Culturing adult and embryonic NPCs in 3D HA hydrogels can promote differentiation and enhance neurite outgrowth and synapse formation (Ma et al., 2004; Hou et al., 2005; Khaing and Seidlits, 2015). The addition of factors into HA hydrogels can enhance the desired priming effects. For example, a design of experiment approach was used by Lam et al. to optimize the concentration of adhesive peptides—RGD, IKVAV, and YIGSR—on HA hydrogels for 3D NPC survival and differentiation (Lam et al., 2015). The authors determined that the optimal concentration of each peptide was not the often used 1:1:1 ratio, and that strategic optimization of each factor concentration can lead to enhanced survival and neurite length. Another study combined both RGD and heparin components within a HA hydrogel using click chemistry to culture hPSC-derived NPCs and differentiate them into midbrain dopaminergic neurons for transplantation (Adil et al., 2017). The use of both factors increased cell differentiation, neurite extension, and resulted in functional neurons that could fire action potentials *in vitro*. When transplanted into the rat striatum these cells showed a fivefold increase in cell number compared to unencapsulated controls. Lastly, in an approach targeting cell migration, Addington et al. (2015) aimed to enhance the NSC response to *in vivo* SDF-1α gradients by priming the cells in culture with HA-laminin hydrogels. The authors reported that culturing NSPCs in these gels resulted in an increased response to SDF-1α gradients *in vitro*, with increased CXCR4 receptor expression after 48 h of culture that was dependent on the concentration of HA and laminin used. In a follow-up study, the researchers transplanted HA-laminin-primed NSPCs into intact mouse brains and reported an increase in cell migration out of the transplantation site that was dependent on the SDF-1α/CXCR4 interaction (Addington et al., 2017).

Improving Cell Delivery

The majority of intracerebral cell delivery strategies are syringe-based. Necessary steps in the transplantation paradigm, such as preparation of cells for transfer from culture into a syringe, and injection of cells into the brain, can result in a substantial amount of cell death (Rossetti et al., 2016; Payne et al., 2017). Small-bore needles are favored for cell delivery as they are minimally-invasive for the host tissue; however, they increase the mechanical disruption and shear stress that cells experience during injection (Rossetti et al., 2016). Other variables such as time between preparation and implantation of cells, concentration of cells, needle length, rate of injection, and suspension medium all impact the survival of cells (Heng et al., 2009; Amer et al., 2015; Rossetti et al., 2016). Although not often reported, this acute loss of cells can impact the therapeutic success of cell transplantation at the onset of delivery.

The ability of biomaterials to reduce acute cell death has been tested using several hydrogel systems. The extensional shear stress that cells experience as they pass through the comparatively large diameter syringe into the smaller diameter needle can be reduced by encapsulation in a biomaterial. Amer et al. (2015) investigated the effect of the vehicle during injection on fibroblast viability using crosslinked or non-crosslinked alginate gels, as well as a high viscosity carboxymethylcellulose solution, and determined that only the crosslinked alginate hydrogel significantly increased acute viability of cells. It has been suggested that crosslinked hydrogels can undergo plug flow where the hydrogel at the interface of the syringe and needle will undergo shear thinning and this acts as a lubricant to the inner core of the gel, thus reducing the shear stress and extensional forces experienced by the cells. A crosslinked alginate hydrogel also increased viability of human umbilical vein endothelial cells and mouse NPCs immediately after injection, from 59% survival in saline to 89% in the hydrogel (Aguado et al., 2011); however, the authors did not test the hydrogel for long-term cell culture or *in vivo* viability, which could be impacted by the hydrogel crosslinking, which determines the elastic modulus and the gel stiffness (Banerjee et al., 2009). HA also promotes iPSC-NPC viability when high concentrations of cells (i.e., 60–90k cells/μL) were injected through a needle of 28-gage or higher compared to a buffer solution (Lam et al., 2014). Interestingly, viability can vary depending on the susceptibility of the specific cell type to damage. For example, a mature neuronal phenotype experiences more cell death with the use of a HA-MC gel than less-differentiated NPCs (Payne et al., 2017).

A single scaffold can be used to first culture and then deliver cells into the brain, avoiding cell death due to dissociation and supporting cell survival and function both pre- and postinjection. Electrospun synthetic poly(desaminotyrosyl tyrosine ethyl ester carbonate) microfibers were used to accelerate the differentiation of human iPSCs into induced neuronal cells *in vitro* (Carlson et al., 2016). Cells grown and differentiated on these fibers and transplanted into the mouse striatum survived better than dissociated cells alone. In an interesting approach, the Cullen lab devised micro-tissue engineered neural networks (micro-TENNs) to deliver preformed networks of axonal tracts both with and without astrocyte support (Struzyna et al., 2015; Winter et al., 2016). These constructs consist of an outer columnar agarose shell that is filled with an ECM hydrogel, such as collagen or laminin. Cells are then either seeded at one end of the tube where they extend neurites through the construct, or are dispersed along the length of the construct and cultured to create a neural network that can then be transplanted directly into the brain. In addition, once formed, the neural network can be removed still intact from the construct for further culture or immunochemical analysis. Micro-TENNS can be inserted directly without the use of a needle into the brain and, in naïve rats, resulted in cell survival for up to 1 month, maintenance of an axonal network, and short-distance integration into the host tissue (Struzyna et al., 2015). Coculturing neurons along astrocyte networks within collagen hydrogel micro-columns resulted in neurites that extended along the astrocytic bundles, mimicking the glial tube of the rostral

migratory stream that guides neuroblasts *in vivo* (Winter et al., 2016). Although promising, one potential issue with these constructs is scaling up for humans; it is unclear how much larger the scaffolds would need to be to traverse damaged areas in the human brain, and whether this would affect insertability and cell viability. In addition, material degradation and cytocompatibility of bioresorption products require further investigation.

Increasing Cell Retention and Survival

Cell Retention

Although cell delivery can be achieved *via* intravascular or intracerebroventricular delivery, the preferred route is directly into the stroke site (Jin et al., 2005; Bliss et al., 2010). The infarct provides a convenient space for delivery of a relatively large volume of cells, avoiding damage to nearby intact tissue while also localizing cells to the potentially salvageable tissue in the peri-infarct (Zhong et al., 2010; Willing and Shahaduzzaman, 2013; Ballios et al., 2015). Smith et al. compared cell transplantation to the intracerebroventricular or intraparenchymal peri-infarct locations and after 14 weeks only found surviving cells when delivered into the intraparenchymal peri-infarct (Smith et al., 2012). However, the advantages of injection into the infarct also come with obstacles: there is a lack of ECM and vasculature to retain cells at the site of injection and support survival, the presence of proapoptotic signals from surrounding cells, and immune cell infiltration (Modo et al., 2002; Kelly et al., 2004; Hicks et al., 2009). Biomaterials can provide a scaffold to fill the stroke cavity, providing a substrate for cell adhesion and aiding in cell distribution and retention at the injection site to prevent washout into the CSF.

Cell retention immediately after injection into the brain is important for long-term cell survival and functional recovery. If injected in a saline solution, cells can backflow out of the brain tissue through the needle tract made by the injection (Ballios et al., 2015). A hydrogel system that can gel *in situ* is ideal as it provides an injectable material that becomes more viscous once in the brain and retains cells at the infarct site. Studies directly comparing cell transplantation with and without a hydrogel carrier have reported a higher number of cells in the brain immediately following injection with the use of a hydrogel (Ballios et al., 2015; Cai et al., 2015), which is attributed to increased cell retention. HAMC, which is shear-thinning and inverse-thermal gelling, allows cells to be injected through a fine-gage needle into the brain where it will gel to localize cells to the injury site (Ballios et al., 2015; Payne et al., 2017). HAMC provides superior cell distribution and larger maximal depth in the infarct area, which correlates to improved functional recovery compared to saline (Ballios et al., 2015). In a different approach, Cai et al. developed a dual crosslinking hydrogel system, termed SHIELD, composed of a star-PEG copolymer and a recombinant peptide sequence (Cai et al., 2015). The components of SHIELD form a weak physical network prior to delivery in order to protect cells as they pass through the syringe, then undergoes a second crosslinking *in situ* by thermal phase transition of the recombinant protein to increase the percentage of cells retained postinjection. While only tested with adipose-derived stem cells transplanted subcutaneously, this biomaterial system may enhance cell survival and retention in other tissues.

Cell Survival

Transplantation of cells directly into the stroke cavity often leads to widespread cell death, attributable in part to anoikis (i.e., lack of adhesion cues) (Jen et al., 1996; Hersel et al., 2003). The addition of ECM components to a cell delivery vehicle can mimic the native ECM, providing adhesion cues to transplanted cells and increasing the success of transplantation. An alternative to full-length protein immobilization is the use of short synthetic peptide sequences, which are advantageous because they are more stable than proteins and thus less susceptible to degradation, are easier and less costly to synthesize, and can target one particular molecular pathway in the cell, unlike proteins that often have different functional domains that may elicit unwanted responses (Hersel et al., 2003; Cooke et al., 2010). NSCs express many integrins that allow them to interact with ECM proteins, such as β1-integrin, which binds to the IKVAV sequence of laminin and promotes neuronal differentiation (Pan et al., 2014). During development many integrins are expressed on NSCs in a temporal fashion as they differentiate, which should be taken into account when designing a hydrogel with adhesion molecules (Milner and Campbell, 2002; Wojcik-Stanaszek et al., 2011). The developmental stage from which NSCs are derived can also determine which integrins are expressed, affecting the binding ability of cells to ECM ligands. For example, of mouse NSPCs derived from embryonic, early postnatal or adult SVZ, only postnatal-derived NSPCs adhered to a collagen I hydrogel (Bergström et al., 2014).

Notwithstanding other common adhesive ligands, laminin and the laminin-derived peptide IKVAV have been used successfully for cell delivery to the brain (Stabenfeldt et al., 2006; Cheng et al., 2013; Somaa et al., 2017). NPCs express the major integrin for laminin, α6β1, which promotes differentiation of hESCs to neurons *in vitro* (Ma et al., 2008; Stabenfeldt et al., 2010). When collagen I hydrogels containing fibronectin or laminin were compared for delivery of fetal-derived NSCs, laminin-containing gels resulted in increased cell survival 8 weeks posttransplantation compared to those with fibronectin (Tate et al., 2009). The authors do not offer a mechanism for the superior performance of laminin over fibronectin, but laminin may promote neuronal differentiation and neurite extension (Ma et al., 2008; Li et al., 2014). Another study which used a self-assembling peptide (SAP) hydrogel of repeating RADA amino acid units with IKVAV enhanced survival of rat NSCs *in vitro* compared to an SAP hydrogel without IKVAV, and improved survival of NSCs and expression of neuronal markers 6 weeks after transplantation into a rat TBI model (Cheng et al., 2013). Using a similar SAP IKVAV hydrogel, human NPCs transplanted into a rat stroke model reduced brain atrophy and improved recovery of motor function up to 9 months posttransplantation while enhancing neuronal differentiation (Somaa et al., 2017) (**Figure 4**).

Promoting Cell Differentiation and Integration

Once cells are delivered to the site of injury, they must not only survive long enough to be therapeutically efficacious, but also differentiate and integrate into the host tissue to promote sustained functional recovery. It has been reported that when

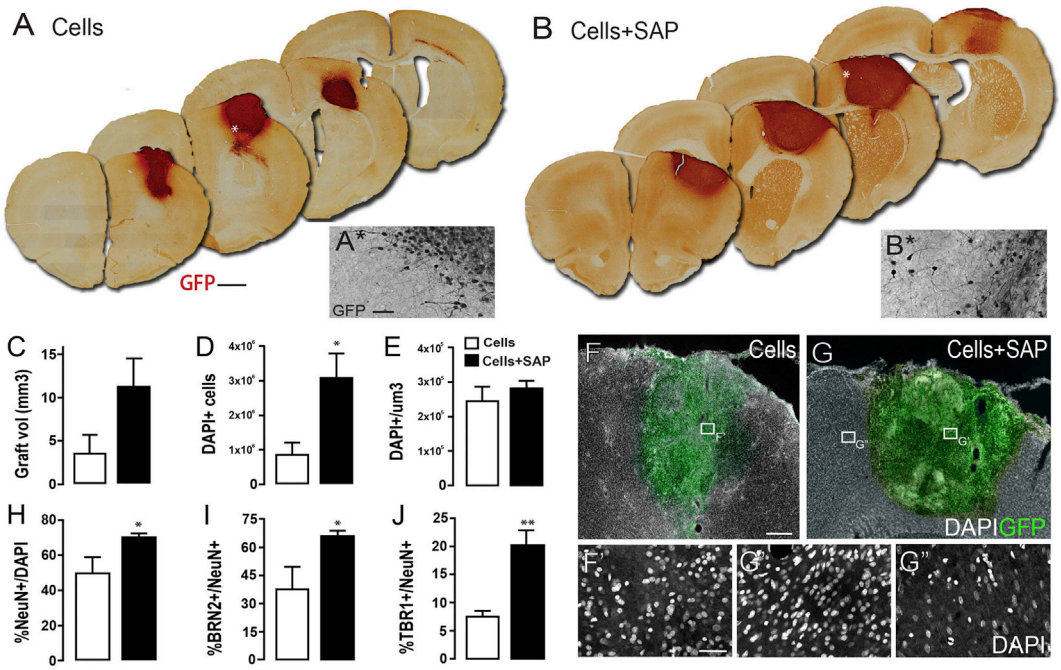

FIGURE 4 | Human neural progenitor cells (hNPCs) encapsulated in a self-assembling peptide (SAP) hydrogel and delivered into a stroke-injured rat brain demonstrate increased cell survival and differentiation into neurons. Representative coronal brain sections containing **(A)** cells or **(B)** cells + SAP. **(C)** Graft volume. **(D)** Number and **(E)** density of hNPCs detected in each group. **(F–G)** Representative images of **(F)** transplanted cells alone or **(G)** in combination with SAP hydrogel. **(H–J)** Percentage of hNPCs expressing neuronal markers. Reproduced with permission from Somaa et al. (2017).

undifferentiated NSCs are transplanted into the stroke-injured brain, they often differentiate into astrocytes over neurons (Dziewczapolski et al., 2003; Abeysinghe et al., 2015; Ballios et al., 2015), which may contribute to the glial scar. Therefore, if the goal is neuronal replacement, it is desirable to control the cell fate after injection with the delivery system.

The properties of the biomaterial alone can influence neural cell fate. For example, ventral midbrain-derived NPCs will differentiate into neurons when the mechanical properties of an HA hydrogel match that of the neonatal brain (Seidlits et al., 2010). Proliferation of NSCs can be controlled by changing the modulus of 3D alginate hydrogels, with stiffer gels causing a reduction in proliferation and βIII-tubulin expression (Banerjee et al., 2009). The differentiation of cells cultured on fibrous scaffolds can be controlled by tuning the thickness of the fibers; rat NSCs cultured on polyethersulfone fiber meshes differentiate preferentially into oligodendrocytes on smaller diameter fibers and into neurons on wider diameter fibers (Christopherson et al., 2009). Others have seen an increase in NSC differentiation *in vivo* with the use of HA hydrogels (Lam et al., 2014; Führmann et al., 2016; Moshayedi et al., 2016).

Differentiation of Transplanted Cells

In addition to acting as a physical scaffold, biomaterials can be combined with factors to help promote the integration of transplanted cells by guiding axon growth and synapse formation, and/or stimulating the differentiation of delivered cells into the desired phenotype. As biomaterials allow the controlled release of factors for sustained availability to transplanted cells, they can be used to deliver cells concurrently with factors to both support initial survival of cells and promote later differentiation. Many factors can control cell fate, yet few have been tested in combination with cell delivery in a hydrogel delivery system for stroke. Moshayedi et al. (2016) encapsulated hiPSC-derived NPCs in HA gels modified with MMP-cleavable sequences for degradation in the brain, as well as soluble factors, BDNF and BMP4, and adhesive laminin peptides, YIGSR and IKVAV (Moshayedi et al., 2016). The authors found that after injection of the hydrogel with cells into the stroke-injured mouse brain, BDNF and BMP4 promoted astrocytic differentiation whereas the laminin sequences promoted neuronal differentiation. Other studies have used synthetic microparticles to release growth factors in conjunction with cell delivery, albeit with mixed results. One study used PLGA microparticles coated with laminin and containing encapsulated VEGF to deliver MSCs that were adhered to the particle surface (Quittet et al., 2015). The authors reported that MSC transdifferentiated into neurons due to the presence of laminin, recruited blood vessels to the site, and increased the number of endogenous DCX-positive cells in the infarct. Despite the beneficial tissue effects, the authors did not report functional recovery in a battery of behavioral tests and suggested that this could have been the result of an unanticipated delay in VEGF release *in vivo*, such that an insufficient amount of VEGF was released during the therapeutic window. Another study combined BDNF-releasing PLGA microparticles, coated with fibronectin, seeded with MSC-like cells on the surface, and all blended into

a silanized-hydroxypropyl MC hydrogel (Kandalam et al., 2017). The authors found that this combination promoted neural differentiation of the cells as well as upregulated the secretion of beneficial growth factors and chemokines, but did not test cell viability. A study which implanted VEGF-releasing PLGA microparticles with human NSCs into the brain saw neovascularization within the infarct site, but also a large amount of immune cell infiltration and decreased transplanted cell viability over time (Bible et al., 2012). The authors suggested that the increased cell death may have been a result of the degradation of the PLGA into acidic byproducts. Indeed, a significantly higher concentration of PLGA was used in their formulation compared to the previously described studies, as well as a different cell type (NSC vs. MSC), suggesting that the concentration of PLGA requires optimization for cell viability. Although multicomponent strategies such as these can target multiple repair pathways, it remains a challenge to gain mechanistic insight into recovery without the many required controls. In many cases, although the effect of a factor alone is known, the synergistic interactions between two or more factors are not. Further work needs to be done to identify promising combinations to augment cell delivery while elucidating the mechanism behind recovery.

Axon Guidance and Synapse Formation

The ability of delivered cells to form connections with the host neurons, functionally integrating into the established circuitry, is a crucial step for successful cell replacement therapy (Ishibashi et al., 2004; Tornero et al., 2017). Without the appropriate stimuli, such as topographical or chemical cues, transplanted cells may not form these functional connections. Biomaterials have been used extensively to provide topographical cues to cells *in vitro* and in spinal cord injury models, but this is a newly emerging strategy for *in vivo* stroke models (Béduer et al., 2012; Nih et al., 2016; Tarus et al., 2016). A pioneering study engineered a micropatterned solid polydimethylsilosane (PDMS) scaffold containing microchannels and seeded with neurons for implantation into the rat brain. The authors reported significant motor recovery and increased cell survival 3 weeks after implantation compared to the sham animals (Vaysse et al., 2015). In a follow-up publication, the host response to the scaffold was analyzed: there was no significant increase in activated ED1-positive microglia at the implant site and surprisingly a decrease in the astrogliosis response compared to the sham (Davoust et al., 2017), suggesting that the implant is well tolerated long-term. Future studies could also focus on combining topographical cues with some of the factors discussed in previous sections known to promote connectivity and plasticity in the brain (Wei et al., 2007; Bliss et al., 2010).

OUTLOOK

Improving Biomaterial Design

Biomaterials have been successfully used as delivery vehicles for drug and cell therapeutics to the brain. Many of the materials discussed meet necessary design criteria (biocompatibility, minimally swelling, injectable, shape adaptable, and biodegradable/bioresorbable). However, there has been limited exploration of the material itself as a therapeutic. Advances in material design that have been implemented in other tissue systems, such as modifications to material porosity, topography and mechanical cues to control the cellular response to the biomaterial, can be adapted for brain repair. Only recently has porosity been explored in the context of brain repair; a micro-porous HA hydrogel, injected into the stroke cavity, demonstrated that porosity can be used to achieve superior cellular infiltration and attenuation of the inflammatory response compared to non-porous hydrogels (Nih et al., 2017). Future work may include optimizing the pore size of a material for the desired cellular response, such as for neurogenesis, axonogenesis or vasculogenesis. In addition, surface functionalization, such as peptide modification, can be combined with a porous hydrogel to mimic cell–cell interactions at the biomaterial–cell interface, which has been demonstrated to control stem cell differentiation (Stabenfeldt et al., 2006; Tate et al., 2009; Li et al., 2014). While the mechanical and chemical properties of a biomaterial are typically linked, new synthetic strategies will allow the ECM ligand concentration to be decoupled from the hydrogel crosslink density, thereby resulting in materials with independently tunable mechanical and chemical properties (Fisher et al., 2015). Computational advancements and machine learning will allow us to use predictive modeling to explore and optimize multiple biomaterial parameters (e.g., elasticity, porosity, composition) simultaneously, enabling improvements in existing materials and the development of novel materials (Vasilevich et al., 2017).

Biomaterials in Novel Treatments

Biomaterials will enable sustained delivery of novel treatments. The direct reprogramming of astrocytes in the glial scar into proliferative neuroblasts has been proposed as a feasible method of reducing the glial scar, and generating neuron and oligodendrocyte precursors at the site of injury and repair, even in aged brains (Niu et al., 2013; Guo et al., 2014b). This can be achieved through retroviral or lentiviral transfection of $GFAP^+$ astrocytes to express reprogramming factors NeuroD1 or Sox2. However, low transfection efficiency and concerns of diffuse non-specific targeting hinder this approach (Li et al., 2016). Biomaterials can be used to address these concerns by sequestering viral particles, increasing local concentrations of the vector and extending the length of virus activity to increase transfection efficiency of infiltrating cells. Retaining the viral particles within the gel limits transfection to cells at the boundary and to infiltrating cells, controlling reprogramming to cells solely within the glial scar-bounded infarct and reducing diffuse non-specific exposure (Shin and Shea, 2010; Seidlits et al., 2013). Recent developments have found that cocktails of small molecules can achieve the same reprogramming as viral vectors, without xenobiotic concerns, in astroglial cells (Zhang et al., 2015) and fibroblasts (Hu et al., 2015; Li et al., 2015). Indeed, a few innovative researchers have begun incorporating these factors into nanoparticles to reprogram astrocytes into neurons and oligodendrocytes (Li et al., 2016, 2017). Many of the discussed advancements in local delivery of therapeutic factors are directly applicable to local and controlled delivery of reprogramming molecules.

The ability of neurons to be stimulated by electrical fields has been explored as a novel strategy to promote both cell migration and differentiation. Stimulating cell migration takes advantage of the galvanotaxis demonstrated by NSPCs (Babona-Pilipos et al., 2011), whereby neurons migrate in response to an applied electric field. This approach has been proposed for *in vivo* use through externally applied electric fields to increase and direct the migration of endogenous NSPCs, though it could also be used to direct the migration of transplanted stem cells to prevent their clustering (Iwasa et al., 2017). Recent advances in electrically conductive materials may aid in scaling this approach to larger human brains where sufficient electrical fields may be difficult to generate or more spatially defined electrical fields may be desired (Zhou et al., 2017).

In addition to influencing cell migration, electrical stimulation of ESCs can bias their fate toward neuronal differentiation *via* changes in calcium influx (Yamada et al., 2007; Pires et al., 2015). Graphene is a biocompatible material with good electrical conductivity that allows electrical cues to be introduced to the cells to promote differentiation and connectivity (Gardin et al., 2016). Various forms of graphene can be used for neural cell culture, increasing differentiation of NSCs into neurons or oligodendrocytes (Menaa et al., 2015), and it can be utilized to differentiate cells *in vitro* prior to transplantation (Heo et al., 2011). An interesting study combined graphene in the form of single-walled carbon nanotubes with laminin to culture NSCs, which were then stimulated by an electrical current, generating action potentials and forming a neural network (Chao et al., 2009). Graphene has shown promise *in vitro* but the *in vivo* biocompatibility and tolerance remains unknown. Implantation of electrically preconditioned cells was recently demonstrated using a conductive polymer scaffold where Human neural progenitor cells (hNPCs) cultured on a polypyrrole scaffold and exposed to electrical stimulation upregulated genes in the VEGF-A pathway (George et al., 2017). When cells on these scaffolds were stimulated and transplanted onto the cortical surface of stroke-injured rats they elicited functional improvement in multiple behavioral tasks and increased the peri-infarct vasculature in a VEGF-dependent manner compared to unconditioned cells; however, no surviving cells were detected at two weeks posttransplantation. Future work combining electrical stimulation and cell delivery may lead to further advances in the *in vivo* control of stem cell fate.

Improving Clinical Translation

Advances in biomaterials and tissue engineering improve therapies that aim to protect and repair the brain, serving as vehicles for drug and cell delivery, and scaffolds for tissue regeneration that integrate with the host tissue. However, it remains a nascent field and successful clinical translation will require learning from the failures of previous neuroprotective efforts (O'Collins et al., 2006). Many preclinical studies with biomaterials have demonstrated a limited number of tissue-specific outcomes without providing evidence for behavioral recovery. Though the lack of behavioral recovery does not undermine the value of a study, landmark studies will require robust demonstration of functional outcomes in multiple tests. Another major hurdle is the lack of a consistent set of clinically relevant goals and study designs. Most preclinical studies limit testing to a single stroke model in young animals with homogeneous etiologies, yet the majority of clinical cases occur in an older population with heterogeneous etiologies (Savitz et al., 2011). Thus, conclusions drawn from preclinical studies using a single model may not be robust enough for the heterogeneous etiologies seen clinically, and studies exclusively on young animals are not reflective of the stroke demographic. As one set of studies demonstrated, aged animals have a less-robust capacity for plasticity and require modifications to their treatment to achieve the same outcome found in young animals (Clarkson et al., 2015). Future studies should also incorporate the guidelines set forward by Stroke Therapy Academic Industry Round Table (STAiRS) for preclinical studies in order to build a knowledge base for the field that has practical translation aspects [Stroke Therapy Academic Industry Roundtable (STAIR), 1999; Saver et al., 2009]. Along with appropriate study design, the choice of biomaterial and any chemical modifications should be carefully considered. In addition to the basic requirements discussed herein, the biomaterial must be easily sterilized and manufactured, and any chemistry involved in manufacturing the material should be reproducible, scalable and cost-effective.

Biomaterial delivery can be improved by combining it with *in vivo* imaging. One often overlooked fact is that while human strokes vary in their size and location, preclinical studies often assume a fixed infarct volume and use a fixed volume of hydrogel. To address this, the Modo group used magnetic resonance imaging (MRI) to measure the individual infarct volume in each animal, in order to adjust the volume of hydrogel delivered and to guide injections to the precise site of injury (Massensini et al., 2015). The group also employed a drainage catheter to remove any fluid buildup in the cavity, displacing it for the injected hydrogel to provide better hydrogel retention and reduce backflow. MRI can also be used to track the biomaterial implant over time, ensuring accurate material implantation, sufficient stability, and adequate degradation for newly formed tissue (Cook et al., 2017). These strategies can improve the delivery and tracking of biomaterials in the brain, increasing both the success of the treatment and its relevance to clinical applications.

Brain repair is a multifaceted process; achieving functional repair with biomaterial-based therapies may require combination with other treatment modalities, such as rehabilitation or transcranial magnetic stimulation (TMS), in order to target multiple repair pathways (Wieloch and Nikolich, 2006). Regenerated or reestablished neural circuitry, if not directed by an appropriate stimulus, can result in uncontrolled plasticity and/or aberrant connections (Murphy and Corbett, 2009). Rehabilitation may enhance functional integration and wiring of newly generated or transplanted neurons (Winstein et al., 2016). Targeting the desired neural pathways with specific rehabilitative tasks simultaneously with delivered cells or drugs may stimulate the reestablishment of appropriate functional connections and discourage the formation of aberrant ones; this was demonstrated with the use of ChABC to produce task-specific recovery (Soleman et al., 2012). Furthermore, recovery of fine motor skills appears to be dependent on receiving the proper type of training; animals that received training in gross locomotor skills performed worse in fine motor tasks than those which received no treatment

(García-Alías et al., 2009). Thus, functional outcomes with reparative therapies may require appropriate rehabilitation to guide plasticity and rewiring. The reduced plasticity exhibited in chronic injuries and aged patients may make functional integration difficult, even if combined with rehabilitation. Direct brain stimulation with TMS has been used to stimulate brain regions for stroke recovery (Takeuchi et al., 2005; Khedr et al., 2010) and enhance BDNF-mediated plasticity (Wang et al., 2011a). TMS has also been shown to increase the proliferation of resident adult NSCs in the SVZ though the miR-25/p57 pathway (Guo et al., 2014a). While TMS may be combined with delivery of cells or stimulation of endogenous cells, research has shown that the intensity of TMS must be finely tuned or it can negatively impact cell survival (Beom et al., 2015; Kremer et al., 2016), suggesting that more work needs to be done before this strategy can be combined successfully. Nonetheless, using a combinatorial therapy of biomaterials, drug and/or cells, and rehabilitation or TMS, may provide the synergistic approach required to achieve recovery in chronic injuries and aged patients.

Conclusion

Stroke is a devastating event that manifests as a complex, multicellular injury with limited ability for self-repair. By combining drug and cell delivery strategies with biomaterial solutions, we can enhance the efficacy of treatments to promote regeneration. Although the architecture and morphology of the brain impose a unique set of constraints on biomaterial design, innovative research provides superior drug and cell delivery to the brain with a wide-range of materials, from controlled release of multiple drugs to promote endogenous regeneration, to increased survival and differentiation of delivered cells. While the field has enjoyed preclinical success, several hurdles must be overcome for clinical translation. Some of these can be addressed with the use of consistent guidelines for material design, as well as methodological improvements to the delivery of the biomaterial. The use of a combinatorial strategy—combining the delivery with cells or other factors, or drugs/cells with other interventions such as rehabilitation—may provide the multipronged approach needed for regeneration and recovery. Previously failed preclinical strategies may be resurrected through combination with biomaterials, especially if the reason for failure was off-target effects or inability to cross the BBB. Future biomaterial development should be tailored to advancements in preclinical and clinical knowledge of stroke repair treatment modalities.

AUTHOR CONTRIBUTIONS

AT, SP, and MS contributed to the writing and editing of this manuscript.

FUNDING

We are grateful to funding from the Natural Sciences and Engineering Research Council, the Canadian Institutes of Health Research, and the Canada First Research Excellence Fund to Medicine by Design. We thank members of the Shoichet lab for thoughtful discussion and input.

REFERENCES

Abeysinghe, H. C. S., Bokhari, L., Quigley, A., Choolani, M., Chan, J., Dusting, G. J., et al. (2015). Pre-differentiation of human neural stem cells into GABAergic neurons prior to transplant results in greater repopulation of the damaged brain and accelerates functional recovery after transient ischemic stroke. *Stem Cell Res Ther.* 6, 1–19. doi:10.1186/s13287-015-0175-1

Addington, C. P., Dharmawaj, S., Heffernan, J. M., Sirianni, R. W., and Stabenfeldt, S. E. (2017). Hyaluronic acid-laminin hydrogels increase neural stem cell transplant retention and migratory response to SDF-1α. *Matrix Biol.* 6, 206–216. doi:10.1016/j.matbio.2016.09.007

Addington, C. P., Heffernan, J. M., Millar-Haskell, C. S., Tucker, E. W., Sirianni, R. W., and Stabenfeldt, S. E. (2015). Enhancing neural stem cell response to SDF-1α gradients through hyaluronic acid-laminin hydrogels. *Biomaterials* 72, 11–19. doi:10.1016/j.biomaterials.2015.08.041

Adil, M. M., Vazin, T., Ananthanarayanan, B., Rodrigues, G. M. C., Rao, A. T., Kulkarni, R. U., et al. (2017). Engineered hydrogels increase the post-transplantation survival of encapsulated hESC-derived midbrain dopaminergic neurons. *Biomaterials* 136, 1–11. doi:10.1016/j.biomaterials.2017.05.008

Agnihotri, S. A., Mallikarjuna, N. N., and Aminabhavi, T. M. (2004). Recent advances on chitosan-based micro- and nanoparticles in drug delivery. *J. Control Release* 100, 5–28. doi:10.1016/j.jconrel.2004.08.010

Aguado, B. A., Mulyasasmita, W., Su, J., Lampe, K. J., and Heilshorn, S. C. (2011). Improving viability of stem cells during syringe needle flow through the design of hydrogel cell carriers. *Tissue Eng. A* 18, 806–815. doi:10.1089/ten.tea.2011.0391

Amer, M. H., White, L. J., and Shakesheff, K. M. (2015). The effect of injection using narrow-bore needles on mammalian cells: administration and formulation considerations for cell therapies. *J. Pharm. Pharmacol.* 67, 640–650. doi:10.1111/jphp.12362

Arvidsson, A., Collin, T., Kirik, D., Kokaia, Z., and Lindvall, O. (2002). Neuronal replacement from endogenous precursors in the adult brain after stroke. *Nat. Med.* 8, 963–970. doi:10.1038/nm747

Austin, J. W., Kang, C. E., Baumann, M. D., DiDiodato, L., Satkunendrarajah, K., Wilson, J. R., et al. (2012). The effects of intrathecal injection of a hyaluronan-based hydrogel on inflammation, scarring and neurobehavioural outcomes in a rat model of severe spinal cord injury associated with arachnoiditis. *Biomaterials* 33, 4555–4564. doi:10.1016/j.biomaterials.2012.03.022

Babona-Pilipos, R., Droujinine, I. A., Popovic, M. R., and Morshead, C. M. (2011). Adult subependymal neural precursors, but not differentiated cells, undergo rapid cathodal migration in the presence of direct current electric fields. *PLoS ONE* 6:e23808. doi:10.1371/journal.pone.0023808

Baeten, K. M., and Akassoglou, K. (2011). Extracellular matrix and matrix receptors in blood-brain barrier formation and stroke. *Dev. Neurobiol.* 71, 1018–1039. doi:10.1002/dneu.20954

Baiguera, S., Del Gaudio, C., Lucatelli, E., Kuevda, E., Boieri, M., Mazzanti, B., et al. (2014). Electrospun gelatin scaffolds incorporating rat decellularized brain extracellular matrix for neural tissue engineering. *Biomaterials* 35, 1205–1214. doi:10.1016/j.biomaterials.2013.10.060

Ballabh, P. P., Braun, A. A., and Nedergaard, M. M. (2004). The blood-brain barrier: an overview – structure, regulation, and clinical implications. *Neurobiol. Dis.* 16, 13–13. doi:10.1016/j.nbd.2003.12.016

Ballios, B. G., Cooke, M. J., Donaldson, L., Coles, B. L. K., Morshead, C. M., van der Kooy, D., et al. (2015). A Hyaluronan-based injectable hydrogel improves the survival and integration of stem cell progeny following transplantation. *Stem Cell Reports* 4, 1031–1045. doi:10.1016/j.stemcr.2015.04.008

Banerjee, A., Arha, M., Choudhary, S., Ashton, R. S., Bhatia, S. R., Schaffer, D. V., et al. (2009). The influence of hydrogel modulus on the proliferation and differentiation of encapsulated neural stem cells. *Biomaterials* 30, 4695–4699. doi:10.1016/j.biomaterials.2009.05.050

Barkho, B. Z., Munoz, A. E., Li, X., Li, L., Cunningham, L. A., and Zhao, X. (2008). Endogenous matrix metalloproteinase (MMP)-3 and MMP-9 promote the differentiation and migration of adult neural progenitor cells in response to chemokines. *Stem Cells* 26, 3139–3149. doi:10.1634/stemcells.2008-0519

Barkho, B. Z., and Zhao, X. (2011). Adult neural stem cells: response to stroke injury and potential for therapeutic applications. *Curr. Stem Cell Res. Ther.* 6, 327–338. doi:10.2174/157488811797904362

Barreto, G. E., Gonzalez, J., Torres, Y., and Morales, L. (2011). Astrocytic-neuronal crosstalk: implications for neuroprotection from brain injury. *Neurosci. Res.* 71, 107–113. doi:10.1016/j.neures.2011.06.004

Bedard, A., and Parent, A. (2004). Evidence of newly generated neurons in the human olfactory bulb. *Brain Res. Dev. Brain Res.* 151, 159–168. doi:10.1016/j.devbrainres.2004.03.021

Béduer, A., Vieu, C., Arnauduc, F., Sol, J.-C., Loubinoux, I., and Vaysse, L. (2012). Engineering of adult human neural stem cells differentiation through surface micropatterning. *Biomaterials* 33, 504–514. doi:10.1016/j.biomaterials.2011.09.073

Belayev, L., Khoutorova, L., Zhao, K. L., Davidoff, A. W., Moore, A. F., and Cramer, S. C. (2009). A novel neurotrophic therapeutic strategy for experimental stroke. *Brain Res.* 1280, 117–123. doi:10.1016/j.brainres.2009.05.030

Beom, J., Kim, W., Han, T. R., Seo, K.-S., and Oh, B.-M. (2015). Concurrent use of granulocyte-colony stimulating factor with repetitive transcranial magnetic stimulation did not enhance recovery of function in the early subacute stroke in rats. *Neurol. Sci.* 36, 771–777. doi:10.1007/s10072-014-2046-4

Bergström, T., Holmqvist, K., Tararuk, T., Johansson, S., and Forsberg-Nilsson, K. (2014). Developmentally regulated collagen/integrin interactions confer adhesive properties to early postnatal neural stem cells. *Biochim. Biophys. Acta* 1840, 2526–2532. doi:10.1016/j.bbagen.2014.01.021

Besancon, E., Guo, S., Lok, J., Tymianski, M., and Lo, E. H. (2008). Beyond NMDA and AMPA glutamate receptors: emerging mechanisms for ionic imbalance and cell death in stroke. *Trends Pharmacol. Sci.* 29, 268–275. doi:10.1016/j.tips.2008.02.003

Bhattarai, N., Gunn, J., and Zhang, M. (2010). Chitosan-based hydrogels for controlled, localized drug delivery. *Adv. Drug Deliv. Rev.* 62, 83–99. doi:10.1016/j.addr.2009.07.019

Bible, E., Chau, D. Y., Alexander, M. R., Price, J., Shakesheff, K. M., and Modo, M. (2009). The support of neural stem cells transplanted into stroke-induced brain cavities by PLGA particles. *Biomaterials* 30, 2985–2994. doi:10.1016/j.biomaterials.2009.02.012

Bible, E., Qutachi, O., Chau, D. Y. S., Alexander, M. R., Shakesheff, K. M., and Modo, M. (2012). Neo-vascularization of the stroke cavity by implantation of human neural stem cells on VEGF-releasing PLGA microparticles. *Biomaterials* 33, 7435–7446. doi:10.1016/j.biomaterials.2012.06.085

Biran, R., Martin, D. C., and Tresco, P. A. (2005). Neuronal cell loss accompanies the brain tissue response to chronically implanted silicon microelectrode arrays. *Exp. Neurol.* 195, 115–126. doi:10.1016/j.expneurol.2005.04.020

Bithell, A., and Williams, B. P. (2005). Neural stem cells and cell replacement therapy: making the right cells. *Clin. Sci.* 108, 13–22. doi:10.1042/CS20040276

Bjugstad, K. B., Redmond, D. E. Jr., Lampe, K. J., Kern, D. S., Sladek, J. R. Jr., and Mahoney, M. J. (2008). Biocompatibility of PEG-based hydrogels in primate brain. *Cell Transplant.* 17, 409–415. doi:10.3727/096368908784423292

Bliss, T. M., Andres, R. H., and Steinberg, G. K. (2010). Optimizing the success of cell transplantation therapy for stroke. *Neurobiol. Dis.* 37, 275–283. doi:10.1016/j.nbd.2009.10.003

Bosworth, L. A., Turner, L.-A., and Cartmell, S. H. (2013). State of the art composites comprising electrospun fibres coupled with hydrogels: a review. *Nanomedicine* 9, 322–335. doi:10.1016/j.nano.2012.10.008

Brouns, R., and De Deyn, P. P. (2009). The complexity of neurobiological processes in acute ischemic stroke. *Clin. Neurol. Neurosurg.* 111, 483–495. doi:10.1016/j.clineuro.2009.04.001

Brown, C. E., Aminoltejari, K., Erb, H., Winship, I. R., and Murphy, T. H. (2009). In vivo voltage-sensitive dye imaging in adult mice reveals that somatosensory maps lost to stroke are replaced over weeks by new structural and functional circuits with prolonged modes of activation within both the Peri-infarct zone and distant sites. *J. Neurosci.* 29, 1719–1734. doi:10.1523/JNEUROSCI.4249-08.2009

Brudno, Y., Ennett-Shepard, A. B., Chen, R. R., Aizenberg, M., and Mooney, D. J. (2013). Enhancing microvascular formation and vessel maturation through temporal control over multiple pro-angiogenic and pro-maturation factors. *Biomaterials* 34, 9201–9209. doi:10.1016/j.biomaterials.2013.08.007

Buchli, A. D., and Schwab, M. E. (2005). Inhibition of Nogo: a key strategy to increase regeneration, plasticity and functional recovery of the lesioned central nervous system. *Ann. Med.* 37, 556–567. doi:10.1080/07853890500407520

Cai, L., Dewi, R. E., and Heilshorn, S. C. (2015). Injectable hydrogels with in situ double network formation enhance retention of transplanted stem cells. *Adv. Funct. Mater.* 25, 1344–1351. doi:10.1002/adfm.201570060

Caicco, M. J., Cooke, M. J., Wang, Y., Tuladhar, A., Morshead, C. M., and Shoichet, M. S. (2013). A hydrogel composite system for sustained epi-cortical delivery of Cyclosporin A to the brain for treatment of stroke. *J. Control Release* 166, 197–202. doi:10.1016/j.jconrel.2013.01.002

Capila, I., and Linhardt, R. J. (2002). Heparin-protein interactions. *Angew. Chem. Int. Ed. Engl.* 41, 391–412. doi:10.1002/1521-3773(20020201)41:3<390::AID-ANIE390>3.0.CO;2-B

Carlson, A. L., Bennett, N. K., Francis, N. L., Halikere, A., Clarke, S., Moore, J. C., et al. (2016). Generation and transplantation of reprogrammed human neurons in the brain using 3D microtopographic scaffolds. *Nat. Commun.* 7, 10862. doi:10.1038/ncomms10862

Carmichael, S. T., Archibeque, I., Luke, L., Nolan, T., Momiy, J., and Li, S. (2005). Growth-associated gene expression after stroke: evidence for a growth-promoting region in peri-infarct cortex. *Exp. Neurol.* 193, 291–311. doi:10.1016/j.expneurol.2005.01.004

Chao, T. I., Xiang, S., Chen, C.-S., Chin, W.-C., Nelson, A. J., Wang, C., et al. (2009). Carbon nanotubes promote neuron differentiation from human embryonic stem cells. *Biochem. Biophys. Res. Commun.* 384, 426–430. doi:10.1016/j.bbrc.2009.04.157

Chen, J., Li, Y., Katakowski, M., Chen, X., Wang, L., Lu, D., et al. (2003). Intravenous bone marrow stronal cell therapy reduces apoptosis and promotes endogenous cell proliferation after stroke in female rat. *J. Neurosci. Res.* 73, 778–786. doi:10.1002/jnr.10691

Chen, K.-L., Eberli, D., Yoo, J. J., and Atala, A. (2010a). Bioengineered corporal tissue for structural and functional restoration of the penis. *Proc. Natl. Acad. Sci. U.S.A.* 107, 3346–3350. doi:10.1073/pnas.0909367106

Chen, T. T., Luque, A., Lee, S., Anderson, S. M., Segura, T., and Iruela-Arispe, M. L. (2010b). Anchorage of VEGF to the extracellular matrix conveys differential signaling responses to endothelial cells. *J. Cell Biol.* 188, 595–609. doi:10.1083/jcb.200906044

Chen, Q., Zhou, L., and Shine, H. D. (2006). Expression of neurotrophin-3 promotes axonal plasticity in the acute but not chronic injured spinal cord. *J. Neurotrauma* 23, 1254–1260. doi:10.1089/neu.2006.23.1254

Cheng, T.-Y., Chen, M.-H., Chang, W.-H., Huang, M.-Y., and Wang, T.-W. (2013). Neural stem cells encapsulated in a functionalized self-assembling peptide hydrogel for brain tissue engineering. *Biomaterials* 34, 2005–2016. doi:10.1016/j.biomaterials.2012.11.043

Cheng, Y., Xi, G., Jin, H., Keep, R. F., Feng, J., and Hua, Y. (2014). Thrombin-induced cerebral hemorrhage: role of protease-activated receptor-1. *Transl Stroke Res.* 5, 472–475. doi:10.1007/s12975-013-0288-8

Chiasson, B. J., Tropepe, V., Morshead, C. M., and van der Kooy, D. (1999). Adult mammalian forebrain ependymal and subependymal cells demonstrate proliferative potential, but only subependymal cells have neural stem cell characteristics. *J. Neurosci.* 19, 4462–4471.

Christ, A. F., Franze, K., Gautier, H., Moshayedi, P., Fawcett, J., Franklin, R. J. M., et al. (2010). Mechanical difference between white and gray matter in the rat cerebellum measured by scanning force microscopy. *J. Biomech.* 43, 2986–2992. doi:10.1016/j.jbiomech.2010.07.002

Christopherson, G. T., Song, H., and Mao, H.-Q. (2009). The influence of fiber diameter of electrospun substrates on neural stem cell differentiation and proliferation. *Biomaterials* 30, 556–564. doi:10.1016/j.biomaterials.2008.10.004

Clarkson, A. N., Overman, J. J., Zhong, S., Mueller, R., Lynch, G., and Carmichael, S. T. (2011). AMPA receptor-induced local brain-derived neurotrophic factor signaling mediates motor recovery after stroke. *J. Neurosci.* 31, 3766–3775. doi:10.1523/JNEUROSCI.5780-10.2011

Clarkson, A. N., Parker, K., Nilsson, M., Walker, F. R., and Gowing, E. K. (2015). Combined ampakine and BDNF treatments enhance poststroke functional recovery in aged mice via AKT-CREB signaling. *J. Cereb. Blood Flow Metab.* 35, 1272–1279. doi:10.1038/jcbfm.2015.33

Clegg, L. W., and Mac Gabhann, F. (2015). Site-specific phosphorylation of VEGFR2 is mediated by receptor trafficking: insights from a computational model. *PLoS Comput. Biol.* 11:e1004158. doi:10.1371/journal.pcbi.1004158

Cohen-Sela, E., Teitlboim, S., Chorny, M., Koroukhov, N., Danenberg, H. D., Gao, J., et al. (2009). Single and double emulsion manufacturing techniques of an amphiphilic drug in PLGA nanoparticles: formulations of mithramycin and bioactivity. *J. Pharm. Sci.* 98, 1452–1462. doi:10.1002/jps.21527

Cook, D. J., Nguyen, C., Chun, H. N., Llorente, L., Chiu, I., Machnicki, A. S., et al. (2017). Hydrogel-delivered brain-derived neurotrophic factor promotes tissue repair and recovery after stroke. *J. Cereb. Blood Flow Metab.* 37, 1030–1045. doi:10.1177/0271678X16649964

Cooke, M. J., Wang, Y., Morshead, C. M., and Shoichet, M. S. (2011). Controlled epi-cortical delivery of epidermal growth factor for the stimulation of endogenous neural stem cell proliferation in stroke-injured brain. *Biomaterials* 32, 5688–5697. doi:10.1016/j.biomaterials.2011.04.032

Cooke, M. J., Zahir, T., Phillips, S. R., Shah, D. S. H., Athey, D., Lakey, J. H., et al. (2010). Neural differentiation regulated by biomimetic surfaces presenting motifs of extracellular matrix proteins. *J. Biomed. Mater. Res.* 93A, 824–832. doi:10.1002/jbm.a.32585

Cooper, C. A., Brown, K. K., Meletis, C. D., and Zabriskie, N. (2008). Inflammation and hyaluronic acid. *Alter. Complementary Ther.* 14, 78–84. doi:10.1089/act.2008.14201

Cramer, S. C., Fitzpatrick, C., Warren, M., Hill, M. D., Brown, D., Whitaker, L., et al. (2010). The beta-hCG plus erythropoietin in acute stroke (BETAS) study A 3-center, single-dose, open-label, noncontrolled, phase IIa safety trial. *Stroke* 41, 927–931. doi:10.1161/STROKEAHA.109.574343

Dailey, T., Eve, D. J., Tajiri, N., Lau, T., Mosley, Y., Loveren, H., et al. (2013). "Different sources of stem cells for transplantation therapy in stroke," in *Cell-Based Therapies in Stroke*, eds J. Jolkkonen and P. Walczak (Vienna: Springer), 29–46.

Dancause, N., Barbay, S., Frost, S. B., Plautz, E. J., Chen, D. F., Zoubina, E. V., et al. (2005). Extensive cortical rewiring after brain injury. *J. Neurosci.* 25, 10167–10179. doi:10.1523/JNEUROSCI.3256-05.2005

Davoust, C., Plas, B., Béduer, A., Demain, B., Salabert, A.-S., Sol, J.-C., et al. (2017). Regenerative potential of primary adult human neural stem cells on micropatterned bioimplants boosts motor recovery. *Curr. Stem Cell Res. Ther.* 8, 38. doi:10.1186/s13287-017-0702-3

de Los Ríos la Rosa, F., Khoury, J., Kissela, B. M., Flaherty, M. L., Alwell, K., Moomaw, C. J., et al. (2012). Eligibility for intravenous recombinant tissue-type plasminogen activator within a population the effect of the european cooperative acute stroke study (ECASS) III trial. *Stroke* 43, 1591–1595. doi:10.1161/STROKEAHA.111.645986

De Waele, J., Reekmans, K., Daans, J., Goossens, H., Berneman, Z., and Ponsaerts, P. (2015). 3D culture of murine neural stem cells on decellularized mouse brain sections. *Biomaterials* 41, 122–131. doi:10.1016/j.biomaterials.2014.11.025

Delplace, V., Obermeyer, J., and Shoichet, M. S. (2016). Local affinity release. *ACS Nano* 10, 6433–6436. doi:10.1021/acsnano.6b04308

Dimyan, M. A., and Cohen, L. G. (2011). Neuroplasticity in the context of motor rehabilitation after stroke. *Nat. Rev. Neurol.* 7, 76–85. doi:10.1038/nrneurol.2010.200

Doyle, K. P., Simon, R. P., and Stenzel-Poore, M. P. (2008). Mechanisms of ischemic brain damage. *Neuropharmacology* 55, 310–318. doi:10.1016/j.neuropharm.2008.01.005

Drury, J. L., and Mooney, D. J. (2003). Hydrogels for tissue engineering: scaffold design variables and applications. *Biomaterials* 24, 4337–4351. doi:10.1016/S0142-9612(03)00340-5

Duggan, P. S., Siegel, A. W., Blass, D. M., Bok, H., Coyle, J. T., Faden, R., et al. (2009). Unintended changes in cognition, mood, and behavior arising from cell-based interventions for neurological conditions: ethical challenges. *Am. J. Bioeth.* 9, 31–36. doi:10.1080/15265160902788645

Duricki, D. A., Hutson, T. H., Kathe, C., Soleman, S., Gonzalez-Carter, D., Petruska, J. C., et al. (2016). Delayed intramuscular human neurotrophin-3 improves recovery in adult and elderly rats after stroke. *Brain* 139, 259–275. doi:10.1093/brain/awv341

Dziewczapolski, G., Lie, D. C., Ray, J., Gage, F. H., and Shults, C. W. (2003). Survival and differentiation of adult rat-derived neural progenitor cells transplanted to the striatum of hemiparkinsonian rats. *Exp. Neurol.* 183, 653–664. doi:10.1016/S0014-4886(03)00212-7

Ehrbar, M., Rizzi, S. C., Hlushchuk, R., Djonov, V., Zisch, A. H., Hubbell, J. A., et al. (2007). Enzymatic formation of modular cell-instructive fibrin analogs for tissue engineering. *Biomaterials* 28, 3856–3866. doi:10.1016/j.biomaterials.2007.03.027

Elkin, B. S., Azeloglu, E. U., Costa, K. D., and Morrison, B. I. (2007). Mechanical heterogeneity of the rat hippocampus measured by atomic force microscope indentation. *J. Neurotrauma* 24, 812–822. doi:10.1089/neu.2006.0169

Elliott Donaghue, I., Tator, C. H., and Shoichet, M. S. (2015). Sustained delivery of bioactive neurotrophin-3 to the injured spinal cord. *Biomater. Sci.* 3, 65–72. doi:10.1039/c4bm00311j

Elliott Donaghue, I., Tator, C. H., and Shoichet, M. S. (2016). Local delivery of neurotrophin-3 and anti-NogoA promotes repair after spinal cord injury. *Tissue Eng. A* 22, 733–741. doi:10.1089/ten.TEA.2015.0471

Emerich, D. F., Silva, E., Ali, O., Mooney, D., Bell, W., Yu, S.-J., et al. (2010). Injectable VEGF hydrogels produce near complete neurological and anatomical protection following cerebral ischemia in rats. *Cell Transplant.* 19, 1063–1071. doi:10.3727/096368910X498278

Erlandsson, A., Lin, C.-H. A., Yu, F., and Morshead, C. M. (2011). Immunosuppression promotes endogenous neural stem and progenitor cell migration and tissue regeneration after ischemic injury. *Exp. Neurol.* 230, 48–57. doi:10.1016/j.expneurol.2010.05.018

Fawcett, J. W., and Asher, R. A. (1999). The glial scar and central nervous system repair. *Brain Res. Bull.* 49, 377–391. doi:10.1016/S0361-9230(99)00072-6

Fischl, B., and Dale, A. M. (2000). Measuring the thickness of the human cerebral cortex from magnetic resonance images. *Proc. Natl. Acad. Sci. U.S.A.* 97, 11050–11055. doi:10.1073/pnas.200033797

Fisher, S. A., Anandakumaran, P. N., Owen, S. C., and Shoichet, M. S. (2015). Tuning the microenvironment: click-crosslinked hyaluronic acid-based hydrogels provide a platform for studying breast cancer cell invasion. *Adv. Funct. Mater.* 25, 7163–7172. doi:10.1002/adfm.201502778

Fon, D., Zhou, K., Ercole, F., Fehr, F., Marchesan, S., Minter, M. R., et al. (2014). Nanofibrous scaffolds releasing a small molecule BDNF-mimetic for the re-direction of endogenous neuroblast migration in the brain. *Biomaterials* 35, 2692–2712. doi:10.1016/j.biomaterials.2013.12.016

Forrester, J. V., and Wilkinson, P. C. (1981). Inhibition of leukocyte locomotion by hyaluronic acid. *J. Cell. Sci.* 48, 315–331.

Freudenberg, U., Hermann, A., Welzel, P. B., Stirl, K., Schwarz, S. C., Grimmer, M., et al. (2009). A star-PEG–heparin hydrogel platform to aid cell replacement therapies for neurodegenerative diseases. *Biomaterials* 30, 5049–5060. doi:10.1016/j.biomaterials.2009.06.002

Fricker-Gates, R. A., Shin, J. J., Tai, C. C., Catapano, L. A., and Macklis, J. D. (2002). Late-stage immature neocortical neurons reconstruct interhemispheric connections and form synaptic contacts with increased efficiency in adult mouse cortex undergoing targeted neurodegeneration. *J. Neurosci.* 22, 4045–4056.

Führmann, T., Tam, R. Y., Ballarin, B., Coles, B., Elliott Donaghue, I., van der Kooy, D., et al. (2016). Injectable hydrogel promotes early survival of induced pluripotent stem cell-derived oligodendrocytes and attenuates longterm teratoma formation in a spinal cord injury model. *Biomaterials* 83, 23–36. doi:10.1016/j.biomaterials.2015.12.032

García-Alías, G., Barkhuysen, S., Buckle, M., and Fawcett, J. W. (2009). Chondroitinase ABC treatment opens a window of opportunity for task-specific rehabilitation. *Nat. Neurosci.* 12, 1145–1151. doi:10.1038/nn.2377

Gardin, C., Piattelli, A., and Zavan, B. (2016). Graphene in regenerative medicine: focus on stem cells and neuronal differentiation. *Trends Biotechnol.* 34, 435–437. doi:10.1016/j.tibtech.2016.01.006

George, P. M., Bliss, T. M., Hua, T., Lee, A., Oh, B., Levinson, A., et al. (2017). Electrical preconditioning of stem cells with a conductive polymer scaffold enhances stroke recovery. *Biomaterials* 142, 31–40. doi:10.1016/j.biomaterials.2017.07.020

Ghuman, H., Massensini, A. R., Donnelly, J., Kim, S.-M., Medberry, C. J., Badylak, S. F., et al. (2016). ECM hydrogel for the treatment of stroke: characterization of the host cell infiltrate. *Biomaterials* 91, 166–181. doi:10.1016/j.biomaterials.2016.03.014

Gomi, M., Takagi, Y., Morizane, A., Doi, D., Nishimura, M., Miyamoto, S., et al. (2012). Functional ecovery of the murine brain ischemia model using human induced pluripotent stem cell-derived telecephalic progenitors. *Brain Res.* 1459, 52–60. doi:10.1016/j.brainres.2012.03.049

Guan, J., Tong, W., Ding, W., Du, S., Xiao, Z., Han, Q., et al. (2012). Neuronal regeneration and protection by collagen-binding BDNF in the rat middle cerebral artery occlusion model. *Biomaterials* 33, 1386–1395. doi:10.1016/j.biomaterials.2011.10.073

Guerra-Crespo, M., De la Herran-Arita, A. K., Boronat-Garcia, A., Maya-Espinosa, G., Garcia-Montes, J. R., Fallon, J. H., et al. (2012). "Neural stem cells: exogenous and endogenous promising therapies for stroke," in *Neural Stem Cells and Therapy*, (London: InTech), 297–342.

Guo, F., Han, X., Zhang, J., Zhao, X., Lou, J., Chen, H., et al. (2014a). Repetitive transcranial magnetic stimulation promotes neural stem cell proliferation via the regulation of MiR-25 in a rat model of focal cerebral ischemia. *PLoS ONE* 9, e109267. doi:10.1371/journal.pone.0109267.g004

Guo, Z., Zhang, L., Wu, Z., Chen, Y., Wang, F., and Chen, G. (2014b). In vivo direct reprogramming of reactive glial cells into functional neurons after brain injury and in an Alzheimer's disease model. *Cell Stem Cell* 14, 188–202. doi:10.1016/j.stem.2013.12.001

Han, F. Y., Thurecht, K. J., Whittaker, A. K., and Smith, M. T. (2016). Bioerodable PLGA-based microparticles for producing sustained-release drug formulations and strategies for improving drug loading. *Front. Pharmacol.* 7:185. doi:10.3389/fphar.2016.00185

Heiss, W.-D. (2012). The ischemic penumbra: how does tissue injury evolve? *Ann. N. Y. Acad. Sci.* 1268, 26–34. doi:10.1111/j.1749-6632.2012.06668.x

Heng, B. C., Hsu, S. H., Cowan, C. M., Liu, A., Tai, J., Chan, Y., et al. (2009). Transcatheter injection-induced changes in human bone marrow-derived mesenchymal stem cells. *Cell Transplant.* 18, 1111–1121. doi:10.3727/096368909X12483162197006

Heo, C., Yoo, J., Lee, S., Jo, A., Jung, S., Yoo, H., et al. (2011). The control of neural cell-to-cell interactions through non-contact electrical field stimulation using graphene electrodes. *Biomaterials* 32, 19–27. doi:10.1016/j.biomaterials.2010.08.095

Hersel, U., Dahmen, C., and Kessler, H. (2003). RGD modified polymers: biomaterials for stimulated cell adhesion and beyond. *Biomaterials* 24, 4385–4415. doi:10.1016/S0142-9612(03)00343-0

Hettiaratchi, M. H., Miller, T., Temenoff, J. S., Guldberg, R. E., and McDevitt, T. C. (2014). Heparin microparticle effects on presentation and bioactivity of bone morphogenetic protein-2. *Biomaterials* 35, 7228–7238. doi:10.1016/j.biomaterials.2014.05.011

Hicks, A. U., Lappalainen, R. S., Narkilahti, S., Suuronen, R., Corbett, D., Sivenius, J., et al. (2009). Transplantation of human embryonic stem cell-derived neural precursor cells and enriched environment after cortical stroke in rats: cell survival and functional recovery. *Eur. J. Neurosci.* 29, 562–574. doi:10.1111/j.1460-9568.2008.06599.x

Hiscox, L. V., Johnson, C. L., Barnhill, E., McGarry, M. D. J., Huston, J., van Beek, E. J. R., et al. (2016). Magnetic resonance elastography (MRE) of the human brain: technique, findings and clinical applications. *Phys. Med. Biol.* 61, R401–R437. doi:10.1088/0031-9155/61/24/R401

Hoffman, A. S. (2012). Hydrogels for biomedical applications. *Adv. Drug Deliv. Rev.* 64(Suppl.), 18–23. doi:10.1016/j.addr.2012.09.010

Horie, N., Pereira, M. P., Niizuma, K., Sun, G., Keren-Gill, H., Encarnacion, A., et al. (2011). Transplanted stem cell-secreted vascular endothelial growth factor effects poststroke recovery, inflammation, and vascular repair. *Stem Cells* 29, 274–285. doi:10.1002/stem.584

Horne, M. K., Nisbet, D. R., Forsythe, J. S., and Parish, C. L. (2010). Three-dimensional nanofibrous scaffolds incorporating immobilized BDNF promote proliferation and differentiation of cortical neural stem cells. *Stem Cells Dev.* 19, 843–852. doi:10.1089/scd.2009.0158

Hossmann, K.-A. (2012). The two pathophysiologies of focal brain ischemia: implications for translational stroke research. *J. Cereb. Blood. Flow. Metab.* 32, 1310–1316. doi:10.1038/jcbfm.2011.186

Hou, S., Xu, Q., Tian, W., Cui, F., Cai, Q., Ma, J., et al. (2005). The repair of brain lesion by implantation of hyaluronic acid hydrogels modified with laminin. *J. Neurosci. Methods* 148, 60–70. doi:10.1016/j.jneumeth.2005.04.016

Hu, W., Qiu, B., Guan, W., Wang, Q., Wang, M., Li, W., et al. (2015). Direct conversion of normal and Alzheimer's disease human fibroblasts into neuronal cells by small molecules. *Cell Stem Cell* 17, 204–212. doi:10.1016/j.stem.2015.07.006

Hunt, J., Cheng, A., Hoyles, A., Jervis, E., and Morshead, C. M. (2010). Cyclosporin A has direct effects on adult neural precursor cells. *J. Neurosci.* 30, 2888–2896. doi:10.1523/JNEUROSCI.5991-09.2010

Hunt, J., and Morshead, C. (2010). Cyclosporin A enhances cell survival in neural precursor populations in the adult central nervous system. *Mol. Cell. Pharmacol.* 2, 81–88. doi:10.4255/mcpharmacol.10.11

Ikeda, T., Iwai, M., Hayashi, T. K., Nagano, I., Shogi, M., Ikenoue, T., et al. (2005). Limited differentiation to neurons and astroglia from neural stem cells in the cortex and triatum after ischemia/hypoxia in the neonatal rat brain. *Am. J. Obstet. Gynecol.* 193, 849–856. doi:10.1016/j.ajog.2005.01.029

Ishibashi, S., Sakaguchi, M., Kuroiwa, T., Yamasaki, M., Kanemura, Y., Shizuko, I., et al. (2004). Human neural stem/progenitor cells, expanded in long-term neurosphere culture, promote functional recovery after focal ischemia in *Mongolian gerbils*. *J. Neurosci. Res.* 78, 215–223. doi:10.1002/jnr.20246

Iwasa, S. N., Babona-Pilipos, R., and Morshead, C. M. (2017). Environmental factors that influence stem cell migration: an "electric field". *Stem Cells Int.* 2017, 4276927. doi:10.1155/2017/4276927

Jen, A. C., Wake, M. C., and Mikos, A. G. (1996). Hydrogels for cell immobilization. *Biotechnol. Bioeng.* 50, 357–364. doi:10.1002/(SICI)1097-0290(19960520)50:4<357::AID-BIT2>3.0.CO;2-K

Jin, K., Mao, X., Xie, L., Galvan, V., Lai, B., Wang, Y., et al. (2010). Transplantation of human neural precursor cells in Matrigel scaffolding improves outcome from focal cerebral ischemia after delayed postischemic treatment in rats. *J. Cereb. Blood Flow Metab.* 30, 534–544. doi:10.1038/jcbfm.2009.219

Jin, K., Sun, Y., Xie, L., Mao, X. O., Childs, J., Peel, A., et al. (2005). Comparison of ischemia-directed migration of neural precursor cells after intrastriatal, intraventricular, or intravenous transplantation in the rat. *Neurobiol. Dis.* 18, 366–374. doi:10.1016/j.nbd.2004.10.010

Jin, K., Xie, L., Mao, X., Greenberg, M. B., Moore, A., Peng, B., et al. (2011a). Effect of human neural precursor cell transplantation on endogenous neurogenesis after focal cerebral ischemia in the rat. *Brain Res.* 1374, 56–62. doi:10.1016/j.brainres.2010.12.037

Jin, Y.-C., Kim, S.-W., Cheng, F., Shin, J.-H., Park, J.-K., Lee, S., et al. (2011b). The effect of biodegradable gelatin microspheres on the neuroprotective effects of high mobility group box 1 A box in the postischemic brain. *Biomaterials* 32, 899–908. doi:10.1016/j.biomaterials.2010.09.054

Jongpaiboonkit, L., King, W. J., and Murphy, W. L. (2008). Screening for 3D environments that support human mesenchymal stem cell viability using hydrogel arrays. *Tissue Eng. Part A* 15, 343–353. doi:10.1089/ten.tea.2008.0096

Ju, R., Wen, Y., Gou, R., Wang, Y., and Xu, Q. (2014). The experimental therapy on brain ischemia by improvement of local angiogenesis with tissue engineering in the mouse. *Cell Transplant.* 23(Suppl. 1), S83–S95. doi:10.3727/096368914X684998

Kandalam, S., Sindji, L., Delcroix, G. J. R., Violet, F., Garric, X., André, E. M., et al. (2017). Pharmacologically active microcarriers delivering BDNF within a hydrogel: novel strategy for human bone marrow-derived stem cells neural/neuronal differentiation guidance and therapeutic secretome enhancement. *Acta Biomater.* 49, 167–180. doi:10.1016/j.actbio.2016.11.030

Kanekar, S. G., Zacharia, T., and Roller, R. (2012). Imaging of stroke: part 2, pathophysiology at the molecular and cellular levels and corresponding imaging changes. *AJR Am. J. Roentgenol.* 198, 63–74. doi:10.2214/AJR.10.7312

Kawai, H., Yamashita, T., Oha, Y., Deguchi, K., Nagotani, S., Zhang, X., et al. (2010). Tridermal tumorigenesis of induced pluripotent stem cells transplanted in ischemic brain. *J. Cereb. Blood Flow Metab.* 30, 1487–1493. doi:10.1038/jcbfm.2010.32

Kelly, S., Bliss, T. M., Shah, A. K., Sun, G. H., Ma, M., Foo, W. C., et al. (2004). Transplanted human fetal neural stem cells survive, migrate, and differentiate in ischemic rat cerebral cortex. *Proc. Natl. Acad. Sci. U.S.A.* 101, 11839–11844. doi:10.1073/pnas.0404474101

Kernie, S. G., and Parent, J. M. (2010). Forebrain neurogenesis after focal Ischemic and traumatic brain injury. *Neurobiol. Dis.* 37, 267–274. doi:10.1016/j.nbd.2009.11.002

Khaing, Z. Z., and Seidlits, S. K. (2015). Hyaluronic acid and neural stem cells: implications for biomaterial design. *J. Mater. Chem. B* 3, 7850–7866. doi:10.1039/C5TB00974J

Khedr, E. M., Etraby, A. E., Hemeda, M., Nasef, A. M., and Razek, A. A. E. (2010). Long-term effect of repetitive transcranial magnetic stimulation on motor function recovery after acute ischemic stroke. *Acta Neurol. Scand.* 121, 30–37. doi:10.1111/j.1600-0404.2009.01195.x

Kolb, B., Morshead, C., Gonzalez, C., Kim, M., Gregg, C., Shingo, T., et al. (2007). Growth factor-stimulated generation of new cortical tissue and functional recovery after stroke damage to the motor cortex of rats. *J. Cereb. Blood Flow Metab.* 27, 983–997. doi:10.1038/sj.jcbfm.9600402

Koshy, S. T., Zhang, D. K. Y., Grolman, J. M., Stafford, A. G., and Mooney, D. J. (2018). Injectable nanocomposite cryogels for versatile protein drug delivery. *Acta Biomater.* 65, 36–43. doi:10.1016/j.actbio.2017.11.024

Kremer, K. L., Smith, A. E., Sandeman, L., Inglis, J. M., Ridding, M. C., and Koblar, S. A. (2016). Transcranial magnetic stimulation of human adult stem cells in the mammalian brain. *Front. Neural Circuits* 10:17. doi:10.3389/fncir.2016.00017

Krueger, M., Haertig, W., Reichenbach, A., Bechmann, I., and Michalski, D. (2013). Blood-brain barrier breakdown after embolic stroke in rats occurs without ultrastructural evidence for disrupting tight junctions. *PLoS ONE* 8:e56419. doi:10.1371/journal.pone.0056419

Kruse, S. A., Rose, G. H., Glaser, K. J., Manduca, A., Felmlee, J. P., Jack, C. R. J., et al. (2008). Magnetic resonance elastography of the brain. *Neuroimage* 39, 231–237. doi:10.1016/j.neuroimage.2007.08.030

Kumar, M. N. V. R., Bakowsky, U., and Lehr, C. M. (2004). Preparation and characterization of cationic PLGA nanospheres as DNA carriers. *Biomaterials* 25, 1771–1777. doi:10.1016/j.biomaterials.2003.08.069

Kumar, N., Langer, R. S., and Domb, A. J. (2002). Polyanhydrides: an overview. *Adv. Drug Deliv. Rev.* 54, 889–910. doi:10.1016/S0169-409X(02)00050-9

Kuroiwa, T., Ting, P., Martinez, H., and Klatzo, I. (1985). The biphasic opening of the blood-brain-barrier to proteins following temporary middle cerebral-artery occlusion. *Acta Neuropathol.* 68, 122–129. doi:10.1007/BF00688633

Lam, J., Carmichael, S. T., Lowry, W. E., and Segura, T. (2015). Hydrogel design of experiments methodology to optimize hydrogel for iPSC-NPC culture. *Adv. Healthc. Mater.* 4, 534–539. doi:10.1002/adhm.201400410

Lam, J., Lowry, W. E., Carmichael, S. T., and Segura, T. (2014). Delivery of iPS-NPCs to the stroke cavity within a hyaluronic acid matrix promotes the differentiation of transplanted cells. *Adv. Funct. Mater.* 24, 7053–7062. doi:10.1002/adfm.201401483

Lampe, K. J., Kern, D. S., Mahoney, M. J., and Bjugstad, K. B. (2011). The administration of BDNF and GDNF to the brain via PLGA microparticles patterned within a degradable PEG-based hydrogel: protein distribution and the glial response. *J. Biomed. Mater. Res.* 96, 595–607. doi:10.1002/jbm.a.33011

Langer, R. (1990). New methods of drug delivery. *Science* 249, 1527–1533. doi:10.1126/science.2218494

Lau, L. W., Cua, R., Keough, M. B., Haylock-Jacobs, S., and Yong, V. W. (2013). Pathophysiology of the brain extracellular matrix: a new target for remyelination. *Nat. Rev. Neurosci.* 14, 722–729. doi:10.1038/nrn3550

Lee, I.-H., Huang, S.-S., Chuang, C.-Y., Liao, K.-H., Chang, L.-H., Chuang, C.-C., et al. (2017). Delayed epidural transplantation of human induced pluripotent stem cell-derived neural progenitors enhances functional recovery after stroke. *Sci. Rep.* 7, 1943. doi:10.1038/s41598-017-02137-w

Lee, K. Y., and Mooney, D. J. (2001). Hydrogels for tissue engineering. *Chem. Rev.* 101, 1869–1879. doi:10.1021/cr000108x

Li, L., Harms, K. M., Ventura, P. B., Lagace, D. C., Eisch, A. J., and Cunningham, L. A. (2010). Focal cerebral ischemia induces a multi lineage cytogenic response from adult subventricular zone that is predominantly gliogenic. *Glia* 58, 1610–1619. doi:10.1002/glia.21033

Li, X., Kozielski, K., Cheng, Y.-H., Liu, H., Zamboni, C. G., Green, J., et al. (2016). Nanoparticle-mediated conversion of primary human astrocytes into neurons and oligodendrocytes. *Biomater. Sci.* 4, 1100–1112. doi:10.1039/c6bm00140h

Li, X., Tzeng, S. Y., Zamboni, C. G., Koliatsos, V. E., Ming, G.-L., Green, J. J., et al. (2017). Enhancing oligodendrocyte differentiation by transient transcription activation via DNA nanoparticle-mediated transfection. *Acta Biomater.* 54, 249–258. doi:10.1016/j.actbio.2017.03.032

Li, X., Zuo, X., Jing, J., Ma, Y., Wang, J., Liu, D., et al. (2015). Small-molecule-driven direct reprogramming of mouse fibroblasts into functional neurons. *Cell Stem Cell* 17, 195–203. doi:10.1016/j.stem.2015.06.003

Li, Y., Liu, M., Yan, Y., and Yang, S.-T. (2014). Neural differentiation from pluripotent stem cells: the role of natural and synthetic extracellular matrix. *World J. Stem Cells* 6, 11–23. doi:10.4252/wjsc.v6.i1.11

Lin, Y.-H., Chang, C.-H., Wu, Y.-S., Hsu, Y.-M., Chiou, S.-F., and Chen, Y.-J. (2009). Development of pH-responsive chitosan/heparin nanoparticles for stomach-specific anti-*Helicobacter pylori* therapy. *Biomaterials* 30, 3332–3342. doi:10.1016/j.biomaterials.2009.02.036

Lindvall, O., and Kokaia, Z. (2010). Stem cells in human neurodegenerative disorders – time for clinical translation? *J. Clin. Invest.* 120, 29–40. doi:10.1172/JCI40543

Lindvall, O., and Kokaia, Z. (2011). Stem cell research in stroke: how far from the clinic? *Stroke* 42, 2369–2375. doi:10.1161/STROKEAHA.110.599654

Liu, B. P., Cafferty, W. B. J., Budel, S. O., and Strittmatter, S. M. (2006). Extracellular regulators of axonal growth in the adult central nervous system. *Philos. Trans. R Soc. Lond. B Biol. Sci.* 361, 1593–1610. doi:10.1098/rstb.2006.1891

Liu, Z., Li, Y., Cui, Y., Roberts, C., Lu, M., Wilhelmsson, U., et al. (2014). Beneficial effects of gfap/vimentin reactive astrocytes for axonal remodeling and motor behavioral recovery in mice after stroke. *Glia* 62, 2022–2033. doi:10.1002/glia.22723

Lu, A., Tang, Y., Ran, R., Clark, J. F., Aronow, B. J., and Sharp, F. R. (2003). Genomics of the periinfarction cortex after focal cerebral ischemia. *J. Cereb. Blood Flow Metab.* 23, 786–810. doi:10.1097/01.WCB.0000062340.80057.06

Luft, A. R., Waller, S., Forrester, L., Smith, G. V., Whitall, J., Macko, R. F., et al. (2004). Lesion location alters brain activation in chronically impaired stroke survivors. *Neuroimage* 21, 924–935. doi:10.1016/j.neuroimage.2003.10.026

Ma, J., Tian, W.-M., Hou, S.-P., Xu, Q. Y., Spector, M., and Cui, F. Z. (2007). An experimental test of stroke recovery by implanting a hyaluronic acid hydrogel carrying a Nogo receptor antibody in a rat model. *Biomed. Mater.* 2, 233–240. doi:10.1088/1748-6041/2/4/005

Ma, W., Fitzgerald, W., Liu, Q.-Y., O'shaughnessy, T. J., Maric, D., Lin, H. J., et al. (2004). CNS stem and progenitor cell differentiation into functional neuronal circuits in three-dimensional collagen gels. *Exp. Neurol.* 190, 276–288. doi:10.1016/j.expneurol.2003.10.016

Ma, W., Tavakoli, T., Derby, E., Serebryakova, Y., Rao, M. S., and Mattson, M. P. (2008). Cell-extracellular matrix interactions regulate neural differentiation of human embryonic stem cells. *BMC Dev. Biol.* 8:90. doi:10.1186/1471-213X-8-90

Mahoney, M. J., and Anseth, K. S. (2007). Contrasting effects of collagen and bFGF-2 on neural cell function in degradable synthetic PEG hydrogels. *J. Biomed. Mater. Res.* 81A, 269–278. doi:10.1002/jbm.a.30970

Massensini, A. R., Ghuman, H., Saldin, L. T., Medberry, C. J., Keane, T. J., Nicholls, F. J., et al. (2015). Concentration-dependent rheological properties of ECM hydrogel for intracerebral delivery to a stroke cavity. *Acta Biomater.* 27, 116–130. doi:10.1016/j.actbio.2015.08.040

Massey, J. M., Hubscher, C. H., Wagoner, M. R., Decker, J. A., Amps, J., Silver, J., et al. (2006). Chondroitinase ABC digestion of the perineuronal net promotes functional collateral sprouting in the cuneate nucleus after cervical spinal cord injury. *J. Neurosci.* 26, 4406–4414. doi:10.1523/JNEUROSCI.5467-05.2006

Mead, P. A., Safdieh, J. E., Nizza, P., Tuma, S., and Sepkowitz, K. A. (2014). Ommaya reservoir infections: a 16-year retrospective analysis. *J. Infect.* 68, 225–230. doi:10.1016/j.jinf.2013.11.014

Medberry, C. J., Crapo, P. M., Siu, B. F., Carruthers, C. A., Wolf, M. T., Nagarkar, S. P., et al. (2013). Hydrogels derived from central nervous system extracellular matrix. *Biomaterials* 34, 1033–1040. doi:10.1016/j.biomaterials.2012.10.062

Mehta, A. M., Sonabend, A. M., and Bruce, J. N. (2017). Convection-enhanced delivery. *Neurotherapeutics* 14, 358–371. doi:10.1007/s13311-017-0520-4

Menaa, F., Abdelghani, A., and Menaa, B. (2015). Graphene nanomaterials as biocompatible and conductive scaffolds for stem cells: impact for tissue engineering and regenerative medicine. *J. Tissue Eng. Regen. Med.* 9, 1321–1338. doi:10.1002/term.1910

Meretoja, A., Keshtkaran, M., Tatlisumak, T., Donnan, G. A., and Churilov, L. (2017). Endovascular therapy for ischemic stroke: save a minute-save a week. *Neurology* 88, 2123–2127. doi:10.1212/WNL.0000000000003981

Milner, R., and Campbell, I. L. (2002). The integrin family of cell adhesion molecules has multiple functions within the CNS. *J. Neurosci. Res.* 69, 286–291. doi:10.1002/jnr.10321

Minger, S. L., Ekonomou, A., Carta, E. M., Chinoy, A., Perry, R. H., and Ballard, C. G. (2007). Endogenous neurogenesis in the human brain following cerebral infarction. *Regen. Med.* 2, 69–74. doi:10.2217/17460751.2.1.69

Minnerup, J., Sutherland, B. A., BUCHAN, A. M., and Kleinschnitz, C. (2012). Neuroprotection for stroke: current status and future perspectives. *Int. J. Mol. Sci.* 13, 11753–11772. doi:10.3390/ijms130911753

Misra, A., Ganesh, S., Shahiwala, A., and Shah, S. P. (2003). Drug delivery to the central nervous system: a review. *J. Pharm. Pharm. Sci.* 6, 252–273.

Mo, L., Yang, Z., Zhang, A., and Li, X. (2010). The repair of the injured adult rat hippocampus with NT-3-chitosan carriers. *Biomaterials* 31, 2184–2192. doi:10.1016/j.biomaterials.2009.11.078

Modo, M., Stroemer, R. P., Tang, E., Patel, S., and Hodges, H. (2002). Effects of implantation site of stem cell grafts on behavioral recovery from stroke damage. *Stroke* 33, 2270–2278. doi:10.1161/01.STR.0000027693.50675.C5

Moeendarbary, E., Weber, I. P., Sheridan, G. K., Koser, D. E., Soleman, S., Haenzi, B., et al. (2017). The soft mechanical signature of glial scars in the central nervous system. *Nat. Commun.* 8, 14787. doi:10.1038/ncomms14787

Mohammadi-Samani, S., and Taghipour, B. (2015). PLGA micro and nanoparticles in delivery of peptides and proteins; problems and approaches. *Pharm. Dev. Technol.* 20, 385–393. doi:10.3109/10837450.2014.882940

Morshead, C. M., Reynolds, B. A., Craig, C. G., McBurney, M. W., Staines, W. A., Morassutti, D., et al. (1994). Neural stem cells in the adult mammalian forebrain: a relatively quiescent subpopulation of subependymal cells. *Neuron* 13, 1071–1082. doi:10.1016/0896-6273(94)90046-9

Moshayedi, P., Nih, L. R., Llorente, I. L., Berg, A. R., Cinkornpumin, J., Lowry, W. E., et al. (2016). Systematic optimization of an engineered hydrogel allows for

selective control of human neural stem cell survival and differentiation after transplantation in the stroke brain. *Biomaterials* 105, 145–155. doi:10.1016/j.biomaterials.2016.07.028

Mozaffarian, D., Benjamin, E. J., Go, A. S., Arnett, D. K., Blaha, M. J., Cushman, M., et al. (2016). Heart disease and stroke statistics-2016 update: a report from the American Heart Association. *Circulation* 133, e38–e360. doi:10.1161/CIR.0000000000000366

Müller, H. D., Hanumanthiah, K. M., Diederich, K., Schwab, S., Schäbitz, W.-R., and Sommer, C. (2008). Brain-derived neurotrophic factor but not forced arm use improves long-term outcome after photothrombotic stroke and transiently upregulates binding densities of excitatory glutamate receptors in the rat brain. *Stroke* 39, 1012–1021. doi:10.1161/STROKEAHA.107.495069

Murphy, T. H., and Corbett, D. (2009). Plasticity during stroke recovery: from synapse to behaviour. *Nat. Rev. Neurosci.* 10, 861–872. doi:10.1038/nrn2735

Nair, L. S., and Laurencin, C. T. (2007). Biodegradable polymers as biomaterials. *Prog. Polym. Sci.* 32, 762–798. doi:10.1016/j.progpolymsci.2007.05.017

Nakagomi, N., Nakagomi, T., Kubo, S., Nakano-Doi, A., Saino, O., Takata, M., et al. (2009). Endothelial cells support survival, proliferation, and neuonal differentiation of transplanted adult ischemia-induced neural stem/progenitor cells after cerebral infarction. *Stem Cells* 27, 2185–2195. doi:10.1002/stem.161

Nakaguchi, K., Jinnou, H., Kaneko, N., Sawada, M., Hikita, T., Saitoh, S., et al. (2012). Growth factors released from gelatin hydrogel microspheres increase new neurons in the adult mouse brain. *Stem Cells Int.* 2012, 915160. doi:10.1155/2012/915160

Nakatomi, H., Kuriu, T., Okabe, S., Yamamoto, S.-I., Hatano, O., Kawahara, N., et al. (2002). Regeneration of hippocampal pyramidal neurons after ischemic brain injury by recruitment of endogenous neural progenitors. *Cell* 110, 429–441. doi:10.1016/S0092-8674(02)00862-0

Niclis, J. C., Turner, C., Durnall, J., McDougal, S., Kauhausen, J. A., Leaw, B., et al. (2017). Long-distance axonal growth and protracted functional maturation of neurons derived from human induced pluripotent stem cells after intracerebral transplantation. *Stem Cells Transl. Med.* 6, 1547–1556. doi:10.1002/sctm.16-0198

Nih, L. R., Carmichael, S. T., and Segura, T. (2016). Hydrogels for brain repair after stroke: an emerging treatment option. *Curr. Opin. Biotechnol.* 40, 155–163. doi:10.1016/j.copbio.2016.04.021

Nih, L. R., Sideris, E., Carmichael, S. T., and Segura, T. (2017). Injection of microporous annealing particle (MAP) hydrogels in the stroke cavity reduces gliosis and inflammation and promotes NPC migration to the lesion. *Adv. Mater. Weinheim* 29. doi:10.1002/adma.201606471

Nimmo, C. M., and Shoichet, M. S. (2011). Regenerative biomaterials that "Click": simple, aqueous-based protocols for hydrogel synthesis, surface immobilization, and 3D patterning. *Bioconjug. Chem.* 22, 2199–2209. doi:10.1021/bc200281k

Nisbet, D. R., Rodda, A. E., Horne, M. K., Forsythe, J. S., and Finkelstein, D. I. (2009). Neurite infiltration and cellular response to electrospun polycaprolactone scaffolds implanted into the brain. *Biomaterials* 30, 4573–4580. doi:10.1016/j.biomaterials.2009.05.011

Niu, W., Zang, T., Zou, Y., Fang, S., Smith, D. K., Bachoo, R., et al. (2013). In vivo reprogramming of astrocytes to neuroblasts in the adult brain. *Nat. Cell Biol.* 15, 1164–1175. doi:10.1038/ncb2843

Nudo, R. J., Wise, B. M., SiFuentes, F., and Milliken, G. W. (1996). Neural substrates for the effects of rehabilitative training on motor recovery after ischemic infarct. *Science* 272, 1791–1794. doi:10.1126/science.272.5269.1791

O'Collins, V. E., Macleod, M. R., Donnan, G. A., Horky, L. L., van der Worp, B. H., and Howells, D. W. (2006). 1,026 experimental treatments in acute stroke. *Ann. Neurol.* 59, 467–477. doi:10.1002/ana.20741

Oki, K., Tatarishvili, J., Wood, J., Koch, P., Wattananit, S., Mine, Y., et al. (2012). Human-induced pluripotent stem cells form functional neurons and improve recovery after grafting in stroke-damaged brain. *Stem Cells* 30, 1120–1133. doi:10.1002/stem.1104

Pakulska, M. M., Donaghue, I. E., Obermeyer, J. M., Tuladhar, A., McLaughlin, C. K., Shendruk, T. N., et al. (2016a). Encapsulation-free controlled release: electrostatic adsorption eliminates the need for protein encapsulation in PLGA nanoparticles. *Sci. Adv.* 2, e1600519–e1600519. doi:10.1126/sciadv.1600519

Pakulska, M. M., Miersch, S., and Shoichet, M. S. (2016b). Designer protein delivery: from natural to engineered affinity-controlled release systems. *Science* 351, aac4750. doi:10.1126/science.aac4750

Pakulska, M. M., Tator, C. H., and Shoichet, M. S. (2017). Local delivery of chondroitinase ABC with or without stromal cell-derived factor 1α promotes functional repair in the injured rat spinal cord. *Biomaterials* 134, 13–21. doi:10.1016/j.biomaterials.2017.04.016

Pakulska, M. M., Vulic, K., and Shoichet, M. S. (2013). Affinity-based release of chondroitinase ABC from a modified methylcellulose hydrogel. *J. Control. Release* 171, 11–16. doi:10.1016/j.jconrel.2013.06.029

Pan, L., North, H. A., Sahni, V., Jeong, S. J., McGuire, T. L., Berns, E. J., et al. (2014). β1-integrin and integrin linked kinase regulate astrocytic differentiation of neural stem cells. *PLoS ONE* 9:e104335. doi:10.1371/journal.pone.0104335

Pardridge, W. M. (2003). Blood-brain barrier drug targeting: the future of brain drug development. *Mol. Interv.* 3, 90–105–51. doi:10.1124/mi.3.2.90

Pardridge, W. M. (2011). Drug transport in brain via the cerebrospinal fluid. *Fluids Barriers CNS* 8, 7. doi:10.1186/2045-8118-8-7

Pardridge, W. M. (2012). Drug transport across the blood-brain barrier. *J. Cereb. Blood Flow Metab.* 32, 1959–1972. doi:10.1038/jcbfm.2012.126

Parent, J. M., Vexler, Z. S., Gong, C., Derugin, N., and Ferriero, D. M. (2002). Rat forebrain neurogenesis and striatal neuron replacement after focal stroke. *Ann. Neurol.* 52, 802–813. doi:10.1002/ana.10393

Park, K. I., Teng, Y. D., and Snyder, E. Y. (2002). The injured brain itneracts reciprocally with neural stem cells supported by scaffolds to reconstitute lost tissue. *Nat. Biotechnol.* 20, 1111–1117. doi:10.1038/nbt751

Patel, T. D., Kramer, I., Kucera, J., Niederkofler, V., Jessell, T. M., Arber, S., et al. (2003). Peripheral NT3 signaling is required for ETS protein expression and central patterning of proprioceptive sensory afferents. *Neuron* 38, 403–416. doi:10.1016/S0896-6273(03)00261-7

Payne, S. L., Anandakumaran, P. N., Varga, B. V., Morshead, C. M., Nagy, A., and Shoichet, M. S. (2018). In vitro maturation of human iPSC-derived neuroepithelial cells influences transplant survival in the stroke-injured rat brain. *Tissue Eng. Part A* 24, 351–360. doi:10.1089/ten.tea.2016.0515

Pekarek, K. J. K., Jacob, J. S. J., and Mathiowitz, E. E. (1994). Double-walled polymer microspheres for controlled drug release. *Nature* 367, 258–260. doi:10.1038/367258a0

Pencea, V., Bingaman, K. D., Freedman, L. J., and Luskin, M. B. (2001). Neurogenesis in the subventricular zone and rostral migratory stream of the neonatal and adult primate forebrain. *Exp. Neurol.* 172, 1–16. doi:10.1006/exnr.2001.7768

Pires, F., Ferreira, Q., Rodrigues, C. A. V., Morgado, J., and Ferreira, F. C. (2015). Neural stem cell differentiation by electrical stimulation using a cross-linked PEDOT substrate: expanding the use of biocompatible conjugated conductive polymers for neural tissue engineering. *Biochim. Biophys. Acta* 1850, 1158–1168. doi:10.1016/j.bbagen.2015.01.020

Ploughman, M., Windle, V., MacLellan, C. L., White, N., Doré, J. J., and Corbett, D. (2009). Brain-derived neurotrophic factor contributes to recovery of skilled reaching after focal ischemia in rats. *Stroke* 40, 1490–1495. doi:10.1161/STROKEAHA.108.531806

Pollauf, E. J., Kim, K. K., and Pack, D. W. (2005). Small-molecule release from poly(D,L-lactide)/poly(D,L-lactide-co-glycolide) composite microparticles. *J. Pharm. Sci.* 94, 2013–2022. doi:10.1002/jps.20408

Purcell, B. P., Lobb, D., Charati, M. B., Dorsey, S. M., Wade, R. J., Zellars, K. N., et al. (2014). Injectable and bioresponsive hydrogels for on-demand matrix metalloproteinase inhibition. *Nat. Mater.* 13, 653–661. doi:10.1038/nmat3922

Quittet, M.-S., Touzani, O., Sindji, L., Cayon, J., Fillesoye, F., Toutain, J., et al. (2015). Effects of mesenchymal stem cell therapy, in association with pharmacologically active microcarriers releasing VEGF, in an ischaemic stroke model in the rat. *Acta Biomater.* 15, 77–88. doi:10.1016/j.actbio.2014.12.017

Rajah, G. B., and Ding, Y. (2017). Experimental neuroprotection in ischemic stroke: a concise review. *Neurosurg. Focus* 42, E2. doi:10.3171/2017.1.FOCUS16497

Richardson, T. P., Peters, M. C., Ennett, A. B., and Mooney, D. J. (2001). Polymeric system for dual growth factor delivery. *Nat. Biotechnol.* 19, 1029–1034. doi:10.1038/nbt1101-1029

Rosenblum, S., Smith, T. N., Wang, N., Chua, J. Y., Westbroek, E., Wang, K., et al. (2015). BDNF pretreatment of human embryonic-derived neural stem cells improves cell survival and functional recovery after transplantation in hypoxic-ischemic stroke. *Cell Transplant.* 24, 2449–2461. doi:10.3727/096368914X679354

Rossetti, T., Nicholls, F., and Modo, M. (2016). Intracerebral cell implantation: preparation and characterization of cell suspensions. *Cell Transplant.* 25, 645–664. doi:10.3727/096368915X690350

Ruhrberg, C., Gerhardt, H., Golding, M., Watson, R., Ioannidou, S., Fujisawa, H., et al. (2002). Spatially restricted patterning cues provided by heparin-binding

VEGF-A control blood vessel branching morphogenesis. *Genes Dev.* 16, 2684–2698. doi:10.1101/gad.242002

Rundhaug, J. E. (2005). Matrix metalloproteinases and angiogenesis. *J. Cell. Mol. Med.* 9, 267–285. doi:10.1111/j.1582-4934.2005.tb00355.x

Sachewsky, N., Hunt, J., Cooke, M. J., Azimi, A., Zarin, T., Miu, C., et al. (2014). Cyclosporin A enhances neural precursor cell survival in mice through a calcineurin-independent pathway. *Dis. Model Mech.* 7, 953–961. doi:10.1242/dmm.014480

Sakiyama-Elbert, S. E. (2014). Incorporation of heparin into biomaterials. *Acta Biomater.* 10, 1581–1587. doi:10.1016/j.actbio.2013.08.045

Saver, J. L., Albers, G. W., Dunn, B., Johnston, K. C., Fisher, M., and Consortium, S. V. (2009). Stroke therapy academic industry roundtable (STAIR) recommendations for extended window acute stroke therapy trials. *Stroke* 40, 2594–2600. doi:10.1161/STROKEAHA.109.552554

Savitz, S. I., Chopp, M., Deans, R., Carmichael, S. T., Phinney, D., and Wechsler, L. (2011). Stem cell therapy as an emerging paradigm for stroke (STEPS) II. *Stroke* 42, 825–829. doi:10.1161/STROKEAHA.110.601914

Saxena, S., and Caroni, P. (2011). Selective neuronal vulnerability in neurodegenerative diseases: from stressor thresholds to degeneration. *Neuron* 71, 35–48. doi:10.1016/j.neuron.2011.06.031

Schabitz, W. R., Schwab, S., Spranger, M., and Hacke, W. (1997). Intraventricular brain-derived neurotrophic factor reduces infarct size after focal cerebral ischemia in rats. *J. Cereb. Blood Flow Metab.* 17, 500–506. doi:10.1097/00004647-199705000-00003

Schnell, E., Klinkhammer, K., Balzer, S., Brook, G., Klee, D., Dalton, P., et al. (2007). Guidance of glial cell migration and axonal growth on electrospun nanofibers of poly-epsilon-caprolactone and a collagen/poly-epsilon-caprolactone blend. *Biomaterials* 28, 3012–3025. doi:10.1016/j.biomaterials.2007.03.009

Schwab, M. E., and Strittmatter, S. M. (2014). Nogo limits neural plasticity and recovery from injury. *Curr. Opin. Neurobiol.* 27, 53–60. doi:10.1016/j.conb.2014.02.011

Seghier, M. L., Ramsden, S., Lim, L., Leff, A. P., and Price, C. J. (2014). Gradual lesion expansion and brain shrinkage years after stroke. *Stroke* 45, 877–879. doi:10.1161/STROKEAHA.113.003587

Seidlits, S. K., Gower, R. M., Shepard, J. A., and Shea, L. D. (2013). Hydrogels for lentiviral gene delivery. *Expert Opin. Drug Deliv.* 10, 499–509. doi:10.1517/17425247.2013.764864

Seidlits, S. K., Khaing, Z. Z., Petersen, R. R., Nickels, J. D., Vanscoy, J. E., Shear, J. B., et al. (2010). The effects of hyaluronic acid hydrogels with tunable mechanical properties on neural progenitor cell differentiation. *Biomaterials* 31, 3930–3940. doi:10.1016/j.biomaterials.2010.01.125

Shin, S., and Shea, L. D. (2010). Lentivirus immobilization to nanoparticles for enhanced and localized delivery from hydrogels. *Mol. Ther.* 18, 700–706. doi:10.1038/mt.2009.300

Smith, E. J., Stroemer, R. P., Gorenkova, N., Nakajima, M., Crum, W. R., Tang, E., et al. (2012). Implantation site and lesion topology determine efficacy of a human neural stem cell line in a rat model of chronic stroke. *Stem Cells* 30, 785–796. doi:10.1002/stem.1024

Soleman, S., Yip, P. K., Duricki, D. A., and Moon, L. D. F. (2012). Delayed treatment with chondroitinase ABC promotes sensorimotor recovery and plasticity after stroke in aged rats. *Brain* 135, 1210–1223. doi:10.1093/brain/aws027

Somaa, F. A., Wang, T.-Y., Niclis, J. C., Bruggeman, K. F., Kauhausen, J. A., Guo, H., et al. (2017). Peptide-based scaffolds support human cortical progenitor graft integration to reduce atrophy and promote functional repair in a model of stroke. *Cell Rep.* 20, 1964–1977. doi:10.1016/j.celrep.2017.07.069

Soppimath, K. S., Aminabhavi, T. M., Kulkarni, A. R., and Rudzinski, W. E. (2001). Biodegradable polymeric nanoparticles as drug delivery devices. *J. Control Release* 70, 1–20. doi:10.1016/S0168-3659(00)00339-4

Spencer, K. C., Sy, J. C., Ramadi, K. B., Graybiel, A. M., Langer, R., and Cima, M. J. (2017). Characterization of mechanically matched hydrogel coatings to improve the biocompatibility of neural implants. *Sci. Rep.* 7, 1952. doi:10.1038/s41598-017-02107-2

Stabenfeldt, S. E., García, A. J., and LaPlaca, M. C. (2006). Thermoreversible laminin-functionalized hydrogel for neural tissue engineering. *J. Biomed. Mater. Res.* 77, 718–725. doi:10.1002/jbm.a.30638

Stabenfeldt, S. E., Gautam, M., Garcia, A. J., and LaPlaca, M. C. (2010). Biomimetic microenvironment modumales neural stem cell survival, migration, and differentiation. *Tissue Eng. A* 16, 3747–3758. doi:10.1089/ten.tea.2009.0837

Stemer, A., and Lyden, P. (2010). Evolution of the thrombolytic treatment window for acute ischemic stroke. *Curr. Neurol. Neurosci. Rep.* 10, 29–33. doi:10.1007/s11910-009-0076-8

Stroke Therapy Academic Industry Roundtable (STAIR). (1999). Recommendations for standards regarding preclinical neuroprotective and restorative drug development. *Stroke* 30, 2752–2758. doi:10.1161/01.STR.30.12.2752

Struzyna, L. A., Wolf, J. A., Mietus, C. J., Adewole, D. O., Chen, H. I., Smith, D. H., et al. (2015). Rebuilding brain circuitry with living micro-tissue engineered neural networks. *Tissue Eng. Part A* 21, 2744–2756. doi:10.1089/ten.TEA.2014.0557

Sutherland, B. A., Minnerup, J., Balami, J. S., Arba, F., Buchan, A. M., and Kleinschnitz, C. (2012). Neuroprotection for ischaemic stroke: translation from the bench to the bedside. *Int. J. Stroke* 7, 407–418. doi:10.1111/j.1747-4949.2012.00770.x

Syková, E., and Nicholson, C. (2008). Diffusion in brain extracellular space. *Physiol. Rev.* 88, 1277–1340. doi:10.1152/physrev.00027.2007

Takeuchi, N., Chuma, T., Matsuo, Y., Watanabe, I., and Ikoma, K. (2005). Repetitive transcranial magnetic stimulation of contralesional primary motor cortex improves hand function after stroke. *Stroke* 36, 2681–2686. doi:10.1161/01.STR.0000189658.51972.34

Taluja, A., Youn, Y. S., and Bae, Y. H. (2007). Novel approaches in microparticulate PLGA delivery systems encapsulating proteins. *J. Mater. Chem.* 17, 4002–4017. doi:10.1039/b706939a

Tam, R. Y., Cooke, M. J., and Shoichet, M. (2012). Covalently modified hydrogel blend of hyaluronan-methyl cellulose with peptides and growth factors influences neural stem/progenitor cell fate. *J. Mater. Chem.* 22, 19402–19411. doi:10.1039/c2jm33680d

Tarus, D., Hamard, L., Caraguel, F., Wion, D., Szarpak-Jankowska, A., van der Sanden, B., et al. (2016). Design of hyaluronic acid hydrogels to promote neurite outgrowth in three dimensions. *ACS Appl. Mater. Interfaces* 8, 25051–25059. doi:10.1021/acsami.6b06446

Tate, C. C., Shear, D. A., Tate, M. C., Archer, D. R., Stein, D. G., and LaPlaca, M. C. (2009). Laminin and fibronectin scaffolds enhance neural stem cell transplantation into the injured brain. *J. Tissue Eng. Regen. Med.* 3, 208–217. doi:10.1002/term.154

Thoenen, H. (1995). Neurotrophins and neuronal plasticity. *Science* 270, 593–598. doi:10.1126/science.270.5236.593

Thorne, R. G., Lakkaraju, A., Rodriguez-Boulan, E., and Nicholson, C. (2008). In vivo diffusion of lactoferrin in brain extracellular space is regulated by interactions with heparan sulfate. *Proc. Natl. Acad. Sci. U.S.A.* 105, 8416–8421. doi:10.1073/pnas.0711345105

Tombari, D., Loubinoux, I., Pariente, J., Gerdelat, A., Albucher, J.-F., Tardy, J., et al. (2004). A longitudinal fMRI study: in recovering and then in clinically stable sub-cortical stroke patients. *Neuroimage* 23, 827–839. doi:10.1016/j.neuroimage.2004.07.058

Tornero, D., Tsupykov, O., Granmo, M., Rodriguez, C., Grønning-Hansen, M., Thelin, J., et al. (2017). Synaptic inputs from stroke-injured brain to grafted human stem cell-derived neurons activated by sensory stimuli. *Brain* 140, 692–706. doi:10.1093/brain/aww347

Tornero, D., Wattananit, S., Grønning Madsen, M., Koch, P., Wood, J., Tatarishvili, J., et al. (2013). Human induced pluripotent stem cell-derived cortical neurons integrate in stroke-injured cortex and improve functional recovery. *Brain* 136, 3561–3577. doi:10.1093/brain/awt278

Touzani, O., Roussel, S., and MacKenzie, E. T. (2001). The ischaemic penumbra. *Curr. Opin. Neurol.* 14, 83–88. doi:10.1097/00019052-200102000-00013

Tuladhar, A., Morshead, C. M., and Shoichet, M. S. (2015). Circumventing the blood-brain barrier: local delivery of cyclosporin A stimulates stem cells in stroke-injured rat brain. *J. Control Release* 215, 1–11. doi:10.1016/j.jconrel.2015.07.023

Tyler, W. J. (2012). The mechanobiology of brain function. *Nat. Rev. Neurosci.* 13, 867–878. doi:10.1038/nrn3383

Uemura, M., Refaat, M. M., Shinoyama, M., Hayashi, H., Hashimoto, N., and Takahashi, J. (2010). Matrigel supports survival and neuronal differentiation of grafted embryonic stem cell-derived neural precursor cells. *J. Neurosci. Res.* 88, 542–551. doi:10.1002/jnr.22223

Vasilevich, A. S., Carlier, A., de Boer, J., and Singh, S. (2017). How not to drown in data: a guide for biomaterial engineers. *Trends Biotechnol.* 35, 743–755. doi:10.1016/j.tibtech.2017.05.007

Vaysse, L., Beduer, A., Sol, J. C., Vieu, C., and Loubinoux, I. (2015). Micropatterned bioimplant with guided neuronal cells to promote tissue reconstruction and

improve functional recovery after primary motor cortex insult. *Biomaterials* 58, 46–53. doi:10.1016/j.biomaterials.2015.04.019

Velier, J. J., Ellison, J. A., Kikly, K. K., Spera, P. A., Barone, F. C., and Feuerstein, G. Z. (1999). Caspase-8 and caspase-3 are expressed by different populations of cortical neurons undergoing delayed cell death after focal stroke in the rat. *J. Neurosci.* 19, 5932–5941.

Vulic, K., and Shoichet, M. S. (2014). Affinity-based drug delivery systems for tissue repair and regeneration. *Biomacromolecules* 15, 3867–3880. doi:10.1021/bm501084u

Vulic, K. K., and Shoichet, M. S. M. (2012). Tunable growth factor delivery from injectable hydrogels for tissue engineering. *J. Am. Chem. Soc.* 134, 882–885. doi:10.1021/ja210638x

Vykhodtseva, N., McDannold, N., and Hynynen, K. (2008). Progress and problems in the application of focused ultrasound for blood-brain barrier disruption. *Ultrasonics* 48, 279–296. doi:10.1016/j.ultras.2008.04.004

Wang, C., Poon, S., Murali, S., Koo, C.-Y., Bell, T. J., Hinkley, S. F., et al. (2014). Engineering a vascular endothelial growth factor 165-binding heparan sulfate for vascular therapy. *Biomaterials* 35, 6776–6786. doi:10.1016/j.biomaterials.2014.04.084

Wang, D., and Fawcett, J. (2012). The perineuronal net and the control of CNS plasticity. *Cell Tissue Res.* 349, 147–160. doi:10.1007/s00441-012-1375-y

Wang, H.-Y., Crupi, D., Liu, J., Stucky, A., Cruciata, G., Di Rocco, A., et al. (2011a). Repetitive transcranial magnetic stimulation enhances BDNF-TrkB signaling in both brain and lymphocyte. *J. Neurosci.* 31, 11044–11054. doi:10.1523/JNEUROSCI.2125-11.2011

Wang, Y., Cooke, M. J., Lapitsky, Y., Wylie, R. G., Sachewsky, N., Corbett, D., et al. (2011b). Transport of epidermal growth factor in the stroke-injured brain. *J. Control Release* 149, 225–235. doi:10.1016/j.jconrel.2010.10.022

Wang, J., Gallagher, D., DeVito, L. M., Cancino, G. I., Tsui, D., He, L., et al. (2012a). Metformin activates an atypical PKC-CBP pathway to promote neurogenesis-sand enhance spatial memory formation. *Stem Cell* 11, 23–35. doi:10.1016/j.stem.2012.03.016

Wang, Y., Cooke, M. J., Morshead, C. M., and Shoichet, M. S. (2012b). Hydrogel delivery of erythropoietin to the brain for endogenous stem cell stimulation after stroke injury. *Biomaterials* 33, 2681–2692. doi:10.1016/j.biomaterials.2011.12.031

Wang, Y., Cooke, M. J., Sachewsky, N., Morshead, C. M., and Shoichet, M. S. (2013). Bioengineered sequential growth factor delivery stimulates brain tissue regeneration after stroke. *J. Control Release* 172, 1–11. doi:10.1016/j.jconrel.2013.07.032

Wei, Y. T., Tian, W. M., Yu, X., Cui, F. Z., Hou, S. P., Xu, Q. Y., et al. (2007). Hyaluronic acid hydrogels with IKVAV peptides for tissue repair and axonal regeneration in an injured rat brain. *Biomed. Mater.* 2, S142. doi:10.1088/1748-6041/2/3/S11

Wernig, M., Benninger, F., Schmandt, T., Rade, M., Tucker, K. L., Bussow, H., et al. (2004). Functional integration of embryonic stem cell-derived neurons in vivo. *J. Neurosci.* 24, 5258–5268. doi:10.1523/JNEUROSCI.0428-04.200

Wieloch, T., and Nikolich, K. (2006). Mechanisms of neural plasticity following brain injury. *Curr. Opin. Neurobiol.* 16, 258–264. doi:10.1016/j.conb.2006.05.011

Willing, A., and Shahaduzzaman, M. (2013). "Delivery routes for cell therapy in stroke," in *Cell-Based Therapies in Stroke*, eds J. Jolkkonen and P. Walczak (Vienna: Springer), 15–28.

Wiltrout, C., Lang, B., Yan, Y., Dempsey, R. J., and Vemuganti, R. (2007). Repairing brain after stroke: a review on post-ischemic neurogenesis. *Neurochem. Int.* 50, 1028–1041. doi:10.1016/j.neuint.2007.04.011

Winhuisen, L., Thiel, A., Schumacher, B., Kessler, J., Rudolf, J., Haupt, W. F., et al. (2005). Role of the contralateral inferior frontal gyrus in recovery of language function in poststroke aphasia – a combined repetitive transcranial magnetic stimulation and positron emission tomography study. *Stroke* 36, 1759–1763. doi:10.1161/01.STR.0000174487.81126.ef

Winship, I. R., and Murphy, T. H. (2008). In vivo calcium imaging reveals functional rewiring of single somatosensory neurons after stroke. *J. Neurosci.* 28, 6592–6606. doi:10.1523/JNEUROSCI.0622-08.2008

Winstein, C. J., Stein, J., Arena, R., Bates, B., Cherney, L. R., Cramer, S. C., et al. (2016). Guidelines for adult stroke rehabilitation and recovery: a guideline for healthcare professionals from the American Heart Association/American Stroke Association. *Stroke* 47, E98–E169. doi:10.1161/STR.0000000000000098

Winter, C. C., Katiyar, K. S., Hernandez, N. S., Song, Y. J., Struzyna, L. A., Harris, J. P., et al. (2016). Transplantable living scaffolds comprised of micro-tissue engineered aligned astrocyte networks to facilitate central nervous system regeneration. *Acta Biomater.* 38, 44–58. doi:10.1016/j.actbio.2016.04.021

Wojcik-Stanaszek, L., Gregor, A., and Zalewska, T. (2011). Regulation of neurogenesis by extracellular matrix and integrins. *Acta Neurobiol. Exp.* 71, 103–112.

Xing, C., Arai, K., Lo, E. H., and Hommel, M. (2012). Pathophysiologic cascades in ischemic stroke. *Int. J. Stroke* 7, 378–385. doi:10.1111/j.1747-4949.2012.00839.x

Yamada, M., Tanemura, K., Okada, S., Iwanami, A., Nakamura, M., Mizuno, H., et al. (2007). Electrical stimulation modulates fate determination of differentiating embryonic stem cells. *Stem Cells* 25, 562–570. doi:10.1634/stemcells.2006-0011

Yamashita, T., Kawai, H., Tian, F., Ohta, Y., and Abe, K. (2011). Tumorigenic development of induced pluripotent stem cells in ischemic mouse brain. *Cell Transplant.* 20, 883–891. doi:10.3727/096368910X539092

Yamashita, T., Liu, W., Matsumura, Y., Miyagi, R., Zhai, Y., Kusaki, M., et al. (2017). Novel therapeutic transplantation of induced neural stem cells for stroke. *Cell Transplant.* 26, 461–467. doi:10.3727/096368916X692988

Yamashita, T., Ninomiya, M., Hernández Acosta, P., García-Verdugo, J. M., Sunabori, T., Sakaguchi, M., et al. (2006). Subventricular zone-derived neuroblasts migrate and differentiate into mature neurons in the post-stroke adult striatum. *J. Neurosci.* 26, 6627–6636. doi:10.1523/JNEUROSCI.0149-06.2006

Yasuda, Y., Tateishi, N., Shimoda, T., Satoh, S., Ogitani, E., and Fujita, S. (2004). Relationship between S100 beta and GFAP expression in astrocytes during infarction and glial scar formation after mild transient ischemia. *Brain Res.* 1021, 20–31. doi:10.1016/j.brainres.2004.06.015

Zhang, H., Hayashi, T., Tsuru, K., Deguchi, K., Nagahara, M., Hayakawa, S., et al. (2007). Vascular endothelial growth factor promotes brain tissue regeneration with a novel biomaterial polydimethylsiloxane-tetraethoxysilane. *Brain Res.* 1132, 29–35. doi:10.1016/j.brainres.2006.09.117

Zhang, L., Yin, J.-C., Yeh, H., Ma, N.-X., Lee, G., Chen, X. A., et al. (2015). Small molecules efficiently reprogram human astroglial cells into functional neurons. *Cell Stem Cell* 17, 735–747. doi:10.1016/j.stem.2015.09.012

Zhang, P., Li, J., Liu, Y., Chen, X., Lu, H., Kang, Q., et al. (2011). Human embryonic neural stem cell transplantation increases subventricular zone cell proliferation and promotes peri-infarct angiogenesis after focal cerebral ischemia. *Neuropathology* 31, 384–391. doi:10.1111/j.1440-1789.2010.01182.x

Zhang, Z. G., and Chopp, M. (2009). Neurorestorative therapies for stroke: underlying mechanisms and translation to the clinic. *Lancet Neurol.* 8, 491–500. doi:10.1016/S1474-4422(09)70061-4

Zhong, J., Chan, A., Morad, L., Kornblum, H. I., Guoping, F., and Carmichael, S. T. (2010). Hydrogel matrix to support stem cell survival after brain transplantation in stroke. *Neurorehabil. Neural Repair* 24, 636–644. doi:10.1177/1545968310361958

Zhou, T., Hong, G., Fu, T.-M., Yang, X., Schuhmann, T. G., Viveros, R. D., et al. (2017). Syringe-injectable mesh electronics integrate seamlessly with minimal chronic immune response in the brain. *Proc. Natl. Acad. Sci. U.S.A.* 114, 5894–5899. doi:10.1073/pnas.1705509114

Conflict of Interest Statement: The authors declare that the research was conducted in the absence of any commercial or financial relationships that could be construed as a potential conflict of interest.

frontiers in Materials

REVIEW
published: 23 March 2018
doi: 10.3389/fmats.2018.00015

Stroke Repair *via* Biomimicry of the Subventricular Zone

*Rita Matta and Anjelica L. Gonzalez**

Department of Biomedical Engineering, Yale University, New Haven, CT, United States

Stroke is among the leading causes of death and disability worldwide, 85% of which are ischemic. Current stroke therapies are limited by a narrow effective therapeutic time and fail to effectively complete the recovery of the damaged area. Magnetic resonance imaging of the subventricular zone (SVZ) following infarct/stroke has allowed visualization of new axonal connections and projections being formed, while new immature neurons migrate from the SVZ to the peri-infarct area. Such studies suggest that the SVZ is a primary source of regenerative cells for the repair and regeneration of stroke-damaged neurons and tissue. Therefore, the development of tissue engineered scaffolds that serve as a bioreplicative SVZ niche would support the survival of multiple cell types that reside in the SVZ. Essential to replication of the human SVZ microenvironment is the establishment of microvasculature that regulates both the healthy and stroke-injured blood–brain barrier, which is dysregulated poststroke. In order to reproduce this niche, understanding how cells interact in this environment is critical, in particular neural stem cells, endothelial cells, pericytes, ependymal cells, and microglia. Remodeling and repair of the matrix-rich SVZ niche by endogenous reparative mechanisms may then support functional recovery when enhanced by an artificial niche that supports the survival and proliferation of migrating vascular and neuronal cells. Critical considerations to mimic this area include an understanding of resident cell types, delivery method, and the use of biocompatible materials. Controlling stem cell survival, differentiation, and migration are key factors to consider when transplanting stem cells. Here, we discuss the role of the SVZ architecture and resident cells in the promotion and enhancement of endogenous repair mechanisms. We elucidate the interplay between the extracellular matrix composition and cell interactions prior to and following stroke. Finally, we review current cell and neuronal niche biomimetic materials that allow for a tissue-engineered approach in order to promote structural and functional restoration of neural circuitry. By creating an artificial mimetic SVZ, tissue engineers can strive to facilitate tissue regeneration and functional recovery.

Keywords: stem cell transplantation, cell therapy, tissue engineering, extracellular matrix, pericytes, endothelial cells

OPEN ACCESS

Edited by:
Brendan Harley, University of Illinois at Urbana–Champaign, United States

Reviewed by:
Rachael Weiss Sirianni, St. Joseph's Hospital and Medical Center, United States
Stephanie Michelle Willerth, University of Victoria, Canada
Justin Lee Brown, Pennsylvania State University, United States
Silviya Petrova Zustiak, Saint Louis University, United States

***Correspondence:**
Anjelica L. Gonzalez
anjelica.gonzalez@yale.edu

Specialty section:
This article was submitted to Biomaterials, a section of the journal Frontiers in Materials

Received: *07 December 2017*
Accepted: *05 March 2018*
Published: *23 March 2018*

Citation:
Matta R and Gonzalez AL (2018) Stroke Repair via Biomimicry of the Subventricular Zone. Front. Mater. 5:15. doi: 10.3389/fmats.2018.00015

STROKE: IMPACT AND BACKGROUND

Stroke is among the most prominent public health issues in the world, ranking among the top five leading causes of death and disability and impacting 1 in 6 people worldwide (Marlier et al., 2015). In the US alone, someone suffers a stroke every 4 s (Mozaffarian et al., 2016). Both the incidence and prevalence of stroke have been correlated to an aging population as well as socioeconomic burden (Boisserand et al., 2016), causing trends in incidence and severity of stroke outcomes to vary

significantly between states and countries. Regardless of age or socioeconomic variables, most stroke patients present impaired motor and sensory function and output, though the severity of impairment may differ. The only current therapy for ischemic stroke being administration of recombinant tissue plasminogen activator (rtPA). While the treatment of rtPA therapy can be beneficial, it is currently constrained to just 2–5% of stroke patients, as rtPA is only effective if administered 4.5 h following symptom onset (Ruan et al., 2015). For patients who are unable to meet the criteria for rtPA therapy, intracranial hemorrhage often causes permanent neurological functional deficits (Ruan et al., 2015). A need for therapies that can be administered beyond a short therapeutic window remains, in addition to those that have the potential to restore the damaged tissue cavity that is formed by hypoxic conditions following stroke.

Responsible for approximately 85% of strokes (Boisserand et al., 2016), ischemia occurs when there is a blockade of a cerebral artery by a foreign clot or mass. This prevents sufficient blood flow through macrovessels and the invested microvasculature, thereby limiting oxygen exchange into the surrounding tissue. Reduction of blood supply under 15–20% of baseline levels contributes to tissue necrosis and irreversible damage (Sommer, 2017). Tissue necrosis and apoptosis can also be caused by ischemia-induced complications, including calcium overload, oxidative stress, and ATP dependence (Moskowitz et al., 2010). Vascular occlusion disrupts the cells and proteins that maintain the tightly regulated barrier at the vascular–tissue interface, known as the blood–brain barrier (BBB). The BBB contains endothelial cells (ECs), pericytes (PCs), a basement membrane, and astrocytic feet. Damage to one or all of these components causes increased permeability and subsequent edema and neuroinflammation. Furthermore, soluble factors including tumor necrosis factor alpha (TNF-α), thrombin, hemoglobin, and iron sulfate can be released into the local area through diffusion of soluble blood and blood plasma constituents, which may cause cytotoxic effects to the milieu (Nour et al., 2013). The volume of necrotic lesion core resulting from cellular and tissue damage is directly correlated to the extent of motor impairment experienced by the patient. The final infarct size, or area of dead tissue due to hypoxia, varies from patient to patient, contributing to the heterogeneity and complexity of this disorder (Alexander et al., 2010).

In an effort to achieve neurological function after stroke, neurogenesis creates new neurons (neuroblasts) in two germinal regions in the adult mammalian brain: the subventricular zone (SVZ) of the lateral ventricles (LV) and the subgranular zone (SGZ) in the hippocampus (Alvarez-Buylla and García-Verdugo, 2002). Under normal conditions, the adult brain inhibits new axonal sprouting. Recent studies have demonstrated that existing neurons may sprout new connections after the occurrence of ischemic stroke, as seen in **Figure 1** (Carmichael, 2006). Axonal sprouting in peri-infarct tissue, or tissue surrounding the lesion core, results in remapping of connections adjacent to the infarct area, allowing for new connections to form up to several millimeters away from the infarct area (Carmichael, 2006). The degree of axonal sprouting depends on the carefully regulated induction of growth-promoting and inhibitory genes (Carmichael et al., 2001, 2005). Proteins involved in axonal growth including growth-associated protein 43, have been well studied, characterizing the precise network of molecules required for the growth cone phosphorylation cascade and initiation of axonal sprouting (Ng et al., 1988). The "trigger phase" inducing axonal sprouting occurs 1–3 days after stroke (Carmichael and Chesselet, 2002) and is followed by cytoskeletal rearrangement and gene transcription (Carmichael, 2006).

In addition to neurogenesis, the process of angiogenesis, or development of new blood vessels, is necessary to achieve functional neurological recovery following stroke (Ruan et al., 2015). The peri-infarct area is hypoxic, triggering angiogenesis through upregulation of EC-secreted vascular endothelial growth factor (VEGF) within 6–24 h following occlusion. Angiogenesis is followed by a coordinated upregulation of the VEGF-receptor after 48 h (Marti et al., 2000). Due to this signaling cascade, EC proliferation and sprouting contribute to early and necessary microvessel formation, as the number of new vessels formed in the ischemic penumbra is associated with longer survival for ischemic stroke patients (Krupinski et al., 1994). Many factors beyond VEGF, such as fibroblast growth factor (FGF) and brain-derived neurotrophic factor (BDNF) regulate angiogenesis. These function to promote vasodilation and increase circulation and

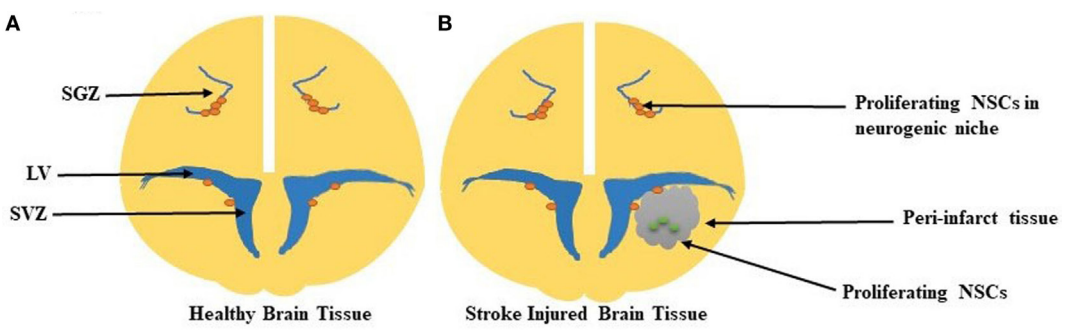

FIGURE 1 | **(A)** Healthy brain tissue with proliferating neural stem cells (NSCs) in the neurogenic niches of both the subgranular zone (SGZ) and subventricular zone (SVZ). The SVZ lines the lateral wall of the lateral ventricle (LV). **(B)** In the stroke-injured brain, the peri-infarct tissue, which contains the ischemic core, contains proliferating NSCs in this damaged parenchyma.

tissue oxygenation as initial steps for repair following ischemic damage (Ruan et al., 2015).

Angiogenesis and neurogenesis are coupled processes critical for functional and structural recovery of the brain infarct region following stroke. Neural stem cells (NSCs), cells with the capacity to differentiate into cells of all glial and neuronal lineages, are able to populate central nervous system (CNS) regions. NSCs are natively resident in the SVZ niche and secrete growth factors and chemokines that promote proliferation and expansion of the NSC pool. Regenerative capacity is maintained by switching from asymmetric division, a process allowing stem cells to self-renew, to symmetric division, a process enabling cells to expand in number after injury. Following NSC proliferation, neuroblasts (cells differentiated from NSCs that are committed to neuronal fate) migrate to the ischemic region and boundary of the infract region. This migration is characterized by cellular interactions between immature neuroblasts and blood vessels, suggesting that angiogenesis and neurogenesis are time-dependent and codependent upon one another (Ruan et al., 2015).

Goal of Tissue Engineering Strategies

In order to improve behavioral recovery following stroke, the goal of regenerative medicine is to successfully transplant stem or progenitor cells that have the ability to differentiate into neurons and integrate with the host microenvironment, improving both neurological and behavioral outcomes. Ideally, the act of transplantation and cell survival would enhance the endogenous repair processes, including axonal sprouting, neurogenesis, brain plasticity, and motor remapping. Integrated neural progenitor cells have the potential to replace and re-build impacted circuitry and reduce lesion size, in conjunction with the fine-coordinated events of angiogenesis and neurogenesis. This repair includes recruitment of vascular cells for increased neovascularization and vascular stabilization (Bliss et al., 2007; Vishwakarma et al., 2014).

Neural stem cells enact cell proliferation and recruitment through the production and secretion of growth factors that are correlated with recovery following ischemia, including endothelial growth factor (EGF) and FGF-2 (Greenberg and Jin, 2006; Vishwakarma et al., 2014). Some growth factors such as VEGF have a short-term impact, having demonstrated an increase in vascularity of infarcted tissue following stroke (Greenberg and Jin, 2006), and presenting upregulation in rat middle cerebral artery occlusion (MCAO) models after 3 h (Marti et al., 2000). Both insulin-growth factor-1 (IGF-1) and BDNF have also demonstrated promising results as acute therapies, beginning administration after 30 and 15 min post MCAO, respectively, and primarily attributed to reduction in infarct volume (Greenberg and Jin, 2006). Growth factor presentation in various forms is integral to promoting repair and functional recovery following stroke.

Tissue engineering constructs for the goal of neural regeneration and repair of the stroke region require that cell survival and activity be sustained and, often, enhanced for appropriate integration of exogenous transplanted cells into the host tissue. The successful use of biomaterials that recreate the SVZ native niche should support cell survival, proliferation, growth factor production, and protein secretion as necessary for appropriate cellular delivery and engraftment into the damaged area. Combining tissue engineering and cell transplantation advances can directly influence the differentiation and survival of neural progenitor and stem cells *in vitro* and *in vivo* (Ghuman and Modo, 2016).

Objective of Review

While we have come to understand many of the cellular and structural interactions that occur during stroke recovery, we remain unable to harness this knowledge to enhance therapeutic recovery. To date, there remains no effective treatment to foster recovery following ischemic stroke, though cell therapy has emerged as a promising approach to encourage functional replacement of the damaged neurons. As a therapeutic approach, transplanted NSCs have the potential to differentiate into numerous phenotypes required for neurogenesis in response to biological cues, and may integrate with the host environment to recover the effects of neurodegeneration. By incorporating factors that enhance both neurogenesis and angiogenesis through cell therapy, a neurorestorative therapy can be created to promote re-growth in the neurogenic niche (Delcroix et al., 2010).

Here, we discuss attributes to an effective cell-based therapy, focusing on the resident SVZ niche cell types that are critical for both tissue homeostasis and response to injury. We elucidate many of the microenvironmental factors defined by the cytoarchitecture and extracellular matrix (ECM) that can influence the success of tissue engineered constructs for neural progenitor cell transplantation. Assessing how the SVZ is damaged post-stroke, we consider the use of natural and synthetic biomaterials in facilitating recovery of the damaged ischemic core by creating a biomimetic microenvironment.

SVZ STRUCTURE AND BIOLOGY

Cytoarchitecture

The SVZ is one of the two niches in the adult brain where neurons can regenerate, the other being the SGZ of the hippocampus (Alvarez-Buylla and García-Verdugo, 2002). This highly organized microenvironment begins to form during embryonic development with the generation of excitatory neurons. New excitatory neurons are generated in the ventricular zone that faces the LV, an area adjacent to the SVZ. Upon migration toward the brain surface during the developmental period, neurons that are born earlier are in deeper layers while neurons born later remain superficial (Tabata et al., 2012). The SVZ is highly vascularized and NSCs are in close contact with the rich vascular system, as evidenced by close interactions between NSCs (type-B), ependymal cells, and ECs. Direct contact between each of these cells and NSCs promote NSC self-renewal and neurogenesis in the SVZ, seen in **Figure 2** (Doetsch, 2003).

The microvasculature of the SVZ contains a more expansive vascular network than other areas of the brain, including non-neurogenic niches and the SGZ. While the microvasculature of the SVZ maintains vascular integrity to support the BBB, there are regions of the SVZ blood vessels where contact with astrocytic

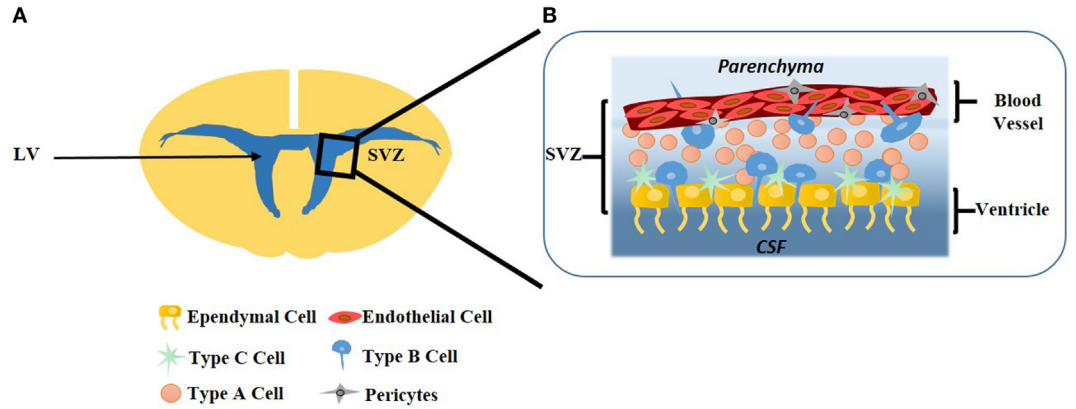

FIGURE 2 | **(A)** The subventricular (SVZ) area is most prominent on the lateral wall of the lateral ventricle (LV). **(B)** Lining the ventricle is a layer of ependymal cells which form a single-cell layer. Type-C neural stem cells (NSCs) are transit-amplifying cells lining the ependymal cells. Type-B NSCs interact with the ependymal cells as well as the endothelial cells (ECs), where ECs form the vasculature of the blood–brain barrier. Type-A NSCs, known as neuroblasts, have the ability to migrate to the olfactory bulb. Pericytes surround ECs of the capillaries which facilitates communication with the surrounding microenvironment.

endfeet and microvasculature support cells, particularly PCs, is absent. The intermittent absence of astrocytic and PC contact with the vessel allows for transit-amplifying NSCs to directly contact the endothelium, enabling rapid signaling, and molecular exchange between the two cells (Girouard and Iadecola, 2006). The unique SVZ microvasculature suggests that a modified BBB in this niche exists (Goldberg and Hirschi, 2009).

Extrinsic factors that directly influence cells of the SVZ originate from blood vessels (Shen et al., 2008), the ependymal layer (Lim et al., 2000), and cerebrospinal fluid (CSF). In particular, the CSF is a major supplier of both proteins and small molecules responsible for signaling this niche (Falcão et al., 2012). The choroid plexus determines the composition of CSF in order to directly delivery these proteins and molecules to the SVZ and impact the behavior of neural progenitor cells (Lim et al., 2000; Shen et al., 2008). Secreted CSF is important in maintaining normal brain function as well as response to neuropathological conditions, where changes in CSF to the SVZ may alter the brain parenchyma metabolism.

The interactions between both ECs and PCs with NSCs, as well as with each other, are critical for maintaining vessel integrity and niche cell maintenance. The connection between type-B cells and ECs is characterized by short, thick processes extended from the body of NSCs in the ventricular zone. These processes allow cells to anchor to the basement membrane and migrate rapidly along the vessel length, enabling interactions critical for both NSC self-renewal and cell differentiation (Gonzalez-Cano et al., 2016). Clustering progenitor cells in close contact with cerebral ECs are supported in their proliferation and response to ischemia, though the process by which EC mediate this support has yet to be elucidated (Stolp and Molnár, 2015). Like ECs, PCs also intricately interact with type-B cells, where NSCs both project and ensheath PCs of the SVZ capillaries (Lacar et al., 2012). While abundant in large numbers within the SVZ, PC distribution along the length of brain microvessels varies, which is not surprising since the vascular endothelial tissue is extremely heterogeneous. Type-B cells control capillary tone in the SVZ due to the contractile nature of PCs (Goldberg and Hirschi, 2009). As a result, the interactions between vascular cells and NSCs are critical to the SVZ functioning as a neurogenic network.

Cell Types

Stem Cells

The goal of stem cell-based therapy is to replace dying and dead cells in the brain in order to restore damaged neural circuitry. There is a broad pool of stem cells with the potential to be used as therapeutic agents with the goal of *de novo* neuron and glial cell generation in following stroke-induced neurodegeneration (Lindvall and Kokaia, 2010). The use of NSCs, mesenchymal stem cells (MSCs), embryonic stem cells (ESCs), and induced pluripotent stem cells (IPSCs) are summarized in **Table 1**.

Neural Stem Cells

In the adult brain, NSCs can be subdivided into 3 types: (1) type-B quiescent stem cells, (2) type-C cells, which are transit-amplifying progenitors derived from activated type-B cells, and (3) type-A neuroblasts, which are formed from amplifying type-C cells that ultimately migrate to the olfactory bulb where they differentiate into interneurons (Ottone et al., 2014). Type-B cells, commonly referred to as SVZ astrocytes, are in close proximity to the vasculature and interact with ECs directly. Type-B cells are characterized both by their distinct morphology of long projections with specialized endfeet, as well as their expression of glial-fibrillary acidic protein (GFAP) (Kriegstein and Alvarez-Buylla, 2009). Because the interactions between quiescent type-B NSCs and ECs are key to the stability and remodeling of the SVZ, their relationship remains a highly active area of investigation (Alvarez-Buylla and García-Verdugo, 2002; Ottone et al., 2014).

Neural stem cells are able to generate neural tissue that possesses some capacity for self-renewal, as well as the ability to undergo asymmetric cell division to produce cells other than

TABLE 1 | A summary of neural stem cell (NSC), mesenchymal stem cell (MSC), embryonic stem cell (ESC), and induced pluripotent stem cell (IPSC) isolation sources, advantages, and limitations.

	Source	Features	Limitations	References
NSC	Skin/blood	Multipotent Standard isolation Control over cellular fate High survival rate in controlled culture condition Ability to generate tissue Some capacity to self-renew Ability to differentiate to specified lineage	Differentiation state variable Inconsistency in cell isolation	Gage (2000); Alvarez-Buylla and García-Verdugo (2002); Hermann et al. (2006); Kriegstein and Alvarez-Buylla (2009); Ottone et al. (2014)
MSC	Bone marrow Iliac crest	Multipotent Ease of isolation and expansion No ethical issues Impact resident cell survival Ability to survive, migrate, and differentiate	Poor differentiation into functional maturel neuronal cells Control of properties	Delcroix et al. (2010); Chen et al. (2001); Wakabayashi et al. (2010); Ruan et al. (2013); Kalladka and Muir (2014)
ESC	Inner cell mass of blastocyst	Pluripotent Ability to differentiate to specified lineage Ease of expansion	Ethical issues Tumorigenic Oncogenic	Thomson et al. (1998); Arvidsson et al. (2002); Buhnemann et al. (2006); Reyes et al. (2008); Ben-David and Benvenisty (2011); Kalladka and Muir (2014)
IPSC	Adult tissue Human somatic cells Human fibroblasts	Similar to ESCs in properties High reproductive capacity High degree of pluripotency No ethical issues	Limited yield Oncogenic transcription factor genes Tumorigenic	Jensen et al. (2013); Kalladka and Muir (2014)

themselves, including neurons or glial cells (Gage, 2000). They can give rise to neurons, astrocytes, and oligodendrocytes *in vitro* and *in vivo* and have been positively correlated with replacement or repair to damaged brain tissue in animal models of stroke. NSCs in the adult brain are consistently present in the SVZ and the hippocampus (Hermann et al., 2006). NSC isolation for use *in vitro* requires excision of these regions of the brain and agitation of the tissue to dissociate cells (Gage, 2000). *In vitro*, cellular fate has been determined through staining with antibodies specific for neuron-specific class III B-tubulin (TUJ1), a marker specific for identification of NSC derived neurons. GFAP has been used for identification of astrocytes, and galactosylceramide is a marker used to identify oligodendrocytes. *In vitro* and *in vivo* observation of NSC differentiation suggests that cell fate to a specific lineage can be induced by withdrawing mitogens or by exposing cells to factors, such as FGF-2, to permit neurogenesis (Gage, 2000; Kriegstein and Alvarez-Buylla, 2009).

Neural stem cells are located within close proximity to the abundant vasculature of the SVZ. More than 50% of NSC nuclei within the murine SVZ are located within 20 μm of blood vessels. Additionally, NSC proliferation occurs close to blood vessels, suggesting that neurogenesis is dependent upon direct and indirect interaction with the vasculature. Endothelial signaling, specifically ephrin-B/EphB, regulates NSC proliferation and niche cell plasticity, while Notch signaling regulates NSC maintenance (Imayoshi et al., 2010; Nomura et al., 2010). These signaling pathways facilitate EC inhibition of NSC differentiation and limit NSC proliferation. ECs of the SVZ vasculature are functionally important for the NSCs lineage by regulating these cell processes (Shen et al., 2008).

To date, the consistency of data acquired from the use of NSCs has been limited, primarily due to inconsistent protocols in cell culture. As one example, mitogens EGF and FGF-2 are inconsistently used between laboratories to expand primitive cells. Many experimental protocols call for the individual use of such growth factors, where others suggest that most effective manipulation requires the combined use of growth factors. In addition, methods of cell isolation vary due to differences in dissection methods, donor age, and cell density within each neural region (Gage, 2000). The variability in NSC cultural protocol and isolation creates an undefined depiction of how to harvest NSCs, ultimately making utility studies and outcomes inconsistent.

Mesenchymal Stem Cells

Mesenchymal stem cells, multipotent adult stem cells, are isolated from the iliac crest or bone marrow and are easily expanded *in vitro* (Delcroix et al., 2010). MSCs can impact resident cell survival, including astrocytes, by upregulating kinase pathways. MSCs can then migrate to ischemic boundaries in several animal models with temporary or permanent MCAO. However, it remains unclear whether MSCs that differentiate along neuronal lines in culture are intrinsically similar to NSCs, as specific characterization of MSCs over time has resulted which makes comparability and consistency between studies difficult (Kalladka and Muir, 2014).

Mesenchymal stem cells have been utilized in animal models with stroke, demonstrating positive results in terms of repair. Transplantation of rat bone marrow-derived MSCs into a rat MCAO model has resulted in a reduction of infarct size. In this context, MSCs can survive, migrate, differentiate, and support significant recovery in motor and somatosensory behavioral tests in rats with transplanted MSCs upon activation with nerve growth factor (Chen et al., 2001). In fact, even xenotransplantation of human MSCs isolated from bone marrow has enhanced functional recovery of mice following induction of stroke (Ruan et al., 2013). Beyond MCAO injections, MSCs are delivered through various routes. For example, bone marrow MSCs delivered *via* intraventricular transplantation, carotid artery transplantation,

and internal jugular vein injection have migrated to the brain injury area and cortex, surviving in the infarct area following middle MCAO in rats (Ruan et al., 2013). Rats receiving MSC transplantation demonstrated reduction in infarct volume at 7 and 14 days, as well as expression of neurotrophic factors VEGF, EGF, and FGF within 7 days (Wakabayashi et al., 2010). It appears that there is wide potential for MSC delivery to promote functional recovery through activation of endogenous restorative responses in the brain (Wakabayashi et al., 2010).

Embryonic Stem Cells

Embryonic stem cells are pluripotent cells derived from the first stage of embryonic development, containing the potential to replace tissues lost by injury (Reyes et al., 2008; Kalladka and Muir, 2014). However, due to their isolation source, the usage of ESCs presents ethical issues in medical research and as a potential therapeutic strategy (Kalladka and Muir, 2014). Despite these issues, ESCs have demonstrated major advantages for therapeutic uses and are studied intensely for *in vitro* generation of neuronal cell lines. The use of ESCs in xenotransplantation into the necrotic area of adult rats subjected to stroke demonstrates that murine ESCs improved functional outcome. In these studies, engrafted cells were able to survive within the infarct area up to 12 weeks following transplantation (Arvidsson et al., 2002). The support pluripotent ESCs provide to resident cells make them an attractive candidate for improving functional recovery poststroke.

In addition to promoting survival, ESCs can differentiate into specific neuronal populations, including glial cells, neurons, and astrocytes (Arvidsson et al., 2002). Transplanted and engrafted cells exhibit characteristics of functional neurons and astrocytes, including neuron-specific nuclear protein (NeuN) + and GFAP + expression, respectively. They also resemble mature glial cells with enhanced green fluorescent protein + expression (Buhnemann et al., 2006). Differentiation is successfully controlled through the use of specific media and culture conditions. For example, the use of media containing fetal bovine serum and ESC supplement coincides with upregulation of TUJ1, suggesting the differentiation of ESCs to neuronal cells (Reyes et al., 2008). By tightly controlling experimental parameters and timing in conjunction with growth and inhibitory factors in media and culture conditions, ESCs can be preferentially driven toward specific cell phenotypes (Arvidsson et al., 2002).

The expanded and immediate translation of ESCs to clinical application is somewhat limited because ESCs display tumorigenic properties *in vivo* and *in vitro*. For example, ESCs have formed teratomas when injected into immunodeficient mice (Ben-David and Benvenisty, 2011). ESCs also display a high level of telomerase activity, which is directly related to immortality in human cell lines (Thomson et al., 1998). Nonetheless, ESCs have shown positive results when transplanted to the diseased brain or spinal cord, directly or after pre-differentiation or genetic modification in culture. Experimentation utilizing ESC based clinical trials have been targeted for macular degeneration, Parkinson's disease, and spinal cord injury (Trounson and McDonald, 2015). While it appears that there is potential for the use of ESCs in neural regeneration and repair, additional studies are needed to understand how tumorigenic characteristics of ESCs can be controlled before being considered for therapeutic applications.

Induced Pluripotent Stem Cells

Induced pluripotent stem cells can be reprogramed to an embryonic-like state, subsequently performing similarly to ESCs. IPSCs can be isolated from adult tissue, such as human somatic cells and fibroblasts and have both a high reproductive capacity while maintaining a high degree of pluripotency (Kalladka and Muir, 2014). However, there is a low yield achieved during induced reprogramming in addition to the expression of oncogenic transcription factors (Kalladka and Muir, 2014). Transplanted IPSCs have formed teratomas in rat MCAO models, and unlike ESCs, have demonstrated little effect in terms of functional recovery. Although some studies report improvement in function and reduced infarct volume, as well as differentiated neuronal cells following intracerebral implantation of human fibroblast derived IPSCs, there is limited functional improvement to be reported using stereotactic injections to the brain (Jensen et al., 2013; Kalladka and Muir, 2014). In order to improve the use of IPSCs, parameters such as the optimal timing following stroke, dose of cells, source, culture protocol of cells, and maturation time must be optimized (Jensen et al., 2013).

Endothelial Cells

Endothelial cells comprise the lumen of the brain microvasculature and are critical for regulating tissue homeostasis and facilitating information transfer between neurons and glial cells. During ischemic stroke, microvascular ECs are damaged by oxygen and nutrient deprivation, which results in degradation of tight junctions that produces an increase in BBB permeability. Following stroke, disturbance of the EC framework and local cytokine levels poses danger to the milieu due to ECs' role in maintaining the BBB integrity when responding to injury (Girouard and Iadecola, 2006).

As previously discussed, angiogenesis and neurogenesis are interdependent processes that intrinsically rely upon each other. In the BBB, the vascular framework is formed through tight junctions, which are responsible for regulating vascular permeability and stabilizing the vessel wall. As the BBB is notably impermeable to large, polar molecules, true biomimetic *in vitro* models must maintain endothelial specific markers that facilitate vascular integrity and restrict permeability. Experimental use of the immortalized mouse brain EC line, bEnd3 is common because these cells retain the expression of mRNA and proteins that are required for the formation of tight junction proteins. These include zonal occludins-1 and -2 (ZO-1 and ZO-2), and claudin-5 (Fanning et al., 1998; Brown et al., 2007). Although immortalized brain ECs are utilized heavily *in vitro*, utilizing primary ECs can more closely mimic brain microvasculature. In order to prepare a pure culture, for example from a mouse, a standard protocol typically includes an enzyme-based tissue disruption, selective adhesion to collagen I, a culture in EC medium, and selective survival over non-ECs when cultured with a protein synthesis inhibitor (Welser-Alves et al., 2014). Utilizing brain ECs through benchtop work allows researchers to re-create complex 3-D environments and contribute to our understanding on how

they contribute to vascular remodeling and BBB breakdown. In addition to controlling differentiation and promoting quiescence, ECs are critical for healing the neuronal niche following ischemic damage. Specifically, ECs promote NSCs survival through Notch signaling regulated growth factor secretion. Growth factors, including VEGF, can stimulate neurogenesis, demonstrating that the NSCs lie directly adjacent to the vasculature in an interdependent manner, ultimately promoting NSC homeostasis and survival (Shen et al., 2008).

Pericytes

Pericytes are microvascular mural cells that are instrumental to vasculogenesis, the process of new blood vessel formation during embryonic development, and vascular stability. PCs enact their roles in neurovasculature development and integrity maintenance through direct contact with microvascular EC and exchange of soluble factors between the two cells, where the highest density of PCs (EC:PC ratio 1:1) is in neural tissues (Korn et al., 2002; Geevarghese and Herman, 2014). PCs are capable of expressing proteoglycans, specifically chondroitin-sulfate proteoglycan-4, and other ECM proteins. They are known to support the structure of the microvasculature and provide signals necessary for the differentiation of plastic cells within the SVZ (Korn et al., 2002). There is no universal marker to identify PCs, rather they are typically recognized by their coexpression of multiple markers and absence of EC, fibroblast, leukocyte, and smooth muscle cell specific markers. Positive identifying markers for PC include chondroitin-sulfate proteoglycan neuron-glial antigen 2 NG2, platelet-derived growth factor-beta (PDGFβ) receptor, and CD13—a type II membrane metalloprotease (MMP) that is specific for brain PCs (Armulik et al., 2011). PC markers may be downregulated during various stages of development and location within organs, suggesting a heterogeneity among PCs. PC heterogeneity is correlated with specialized function required for vascular homeostasis in specific microenvironments (Girouard and Iadecola, 2006; Armulik et al., 2011).

Pericytes respond to EC-secreted PDGFβ, where PDGFβ receptor is functionally involved in PC recruitment during angiogenesis (Daneman et al., 2010; Armulik et al., 2011). PCs promote neurovasculature maturation and are influenced by transforming growth factor-beta (TGF-β) to regulate cell proliferation, differentiation, and survival. Secretion of TGF-β by ECs is elevated following ischemic stroke, indicating that the injured brain may induce mural cell expansion in order to promote neovascularization and repair (Rustenhoven et al., 2016). Primary rat brain PCs in coculture with mouse brain capillary ECs have exhibited both induction and upregulation of microvascular integrity. This was demonstrated by a decrease in permeability to sodium fluorescein, where the enhancement of integrity was inhibited when TGF-β activity was neutralized *via* antibody binding. This suggests that brain PCs contribute to BBB maintenance through TGF-β production (Dohgu et al., 2005).

Although PCs are present in the SVZ niche, their role is poorly understood. The contractile nature of PCs is known to regulate blood flow in *ex vivo* cerebellar brain slices and retina preparations; however, the mechanisms driving regulation of capillary tone and blood flow in the SVZ remain unknown (Armulik et al., 2011). Recent work in mouse models suggests that type-B NSCs send projections that ensheath PCs on SVZ capillaries may indirectly regulating capillary blood by activating purinergic receptors on PCs. Despite their ambiguous role, PCs are known regulators of oxygen and glucose, directly impacting niche cell proliferation and metabolic changes within the environment (Lacar et al., 2012). Continued studies investigating the signaling mechanisms involved in PC regulated blood flow are critical for a better understanding of the neuronal niche.

Ependymal Cells

Ependymal cells are multi-nucleated cells that intricately interact with the apical NSC layer and LV. Ependymal cells have microvilli and motile cilia, wherein cilia create a current of CSF along the LV walls. Malfunction of these cells is correlated with disturbance of CSF flow (Spassky et al., 2005). Ependymal cells are identified through their presentation of surface and intracellular proteins, including β-catenin, *N*-cadherin, Vimentin, and α-tubulin, in addition to their close proximity, within 5 μm, to vessels (Shen et al., 2008). Ependymal cells, like ECs, secrete soluble factor pigment epithelium-derived factor (PEDF) which potentially promotes NSC self-renewal and plays a role in NSC maintenance in the murine SVZ (Ramirez-Castillejo et al., 2006). The pathways associated with PEDF activation can present a therapeutic advantage by promoting self-renewal of NSCs in many neurodegenerative diseases.

In the SVZ, ependymal cells differ from ECs and NSCs in their role and behavior. For one, ependymal cells are not connected to one another nor their articulating cells *via* tight junctions (unlike ECs). This enables large molecules to penetrate the ependymal layer through the gap junctions that connect ependymal cells and astrocytes (Shen et al., 2008; Nomura et al., 2010). Ependymal cells exist in a postmitotic state and do not divide after differentiation, unlike NSCs (Spassky et al., 2005). Stroke injury is disruptive to the quiescent state of ependymal cells enforced by canonical Notch signaling, a signaling pathway that is necessary to conserve stem cell maintenance. In turn, neurogenesis is promoted through inhibition of Notch signaling following stroke, allowing ependymal cells to lose ependymal cell features, enter the cell cycle, and give rise to astrocytes and neuroblasts. The ependymal cells lack self-renewal capacity and do not maintain their population after stroke, unlike ECs and NSCs, suggesting their role as a reservoir recruited following injury (Carlen et al., 2009).

Ependymal cells play an important role in maintaining a neurogenic niche. These cells produce bone morphogenic protein (BMP) antagonist, Noggin, where Noggin antagonizes type-B cell BMP signaling and promotes neurogenesis in the SVZ. Type-B cell BMP signaling blocks the neurogenic pathway, instead promoting gliogenesis. Thereby, ependymal cells contribute to the promotion and enhancement of neurogenesis in the SVZ, which is critical to re-building damaged tissue (Lim et al., 2000).

Microglia

Microglia are resident immune cells known to maintain brain homeostasis. These cells monitor the microenvironment by

responding to injury through the secretion of cytokines and phagocytosing cellular debris at the site (Weinstein et al., 2010; Ghuman and Modo, 2016). Within minutes following stroke, the brain tissue surrounding the core contains activated microglia that accumulate within the lesioned cavity (Patel et al., 2013). Microglia are detected using Iba-1 and Mac-2, markers for cells of myeloid origin and activated/proliferating resident microglia, respectively. Flow cytometry provides the ability to distinguish between residential and infiltrating microglia and myeloid cells, defined by low and high expression of cell-surface marker CD45, respectively. However, the stability of this marker during pathological state is in question (Lalancette-Hebert et al., 2007).

Microglial activation is triggered by ischemic stroke, where endogenous neuronal–glial interactions are disrupted, leading to upregulation of pro-inflammatory cytokines. CD200, a transmembrane glycoprotein expressed on neurons, and its receptor expressed on myeloid cells, modulate microglial activation under homeostasis, promoting quiescence until the occurrence of injury. Following stroke, CD200 gene transcription in the ischemic hemisphere is decreased (Patel et al., 2013), facilitating alternative activation of microglia. In addition, following injury the quiescence of microglia is also disrupted through a decrease in neurons secreting the cytokine fractalkine (CX3CL1). ATP release from dying neurons, as well as monocyte chemotactic protein-1 secretion from surrounding brain cells, induces chemotaxis and migration of microglia to the ischemic area (Patel et al., 2013).

Following tissue damage, changes in microglia migration patterns, cell-surface protein expressions and functions are observed. Motility of microglia toward injury site is seen within minutes. Microglial polarization promotes the development of two phenotypes; M1 or M2. M1 is a classical pro-inflammatory activation phenotype, increasing pro-inflammatory mediators including TNF-α, IL-6, IL-1, nitric oxide, and proteolytic enzymes including MMP-3 and MMP-9. M2, an alternative activation, releases anti-inflammatory mediators, including IGF-1, TGF-B, IL-10, IL-4, and IL-13 (Patel et al., 2013). The fine-tuned balance of M1 and M2 are offset by stroke. Identifying microglia of each subpopulation can contribute understanding of functional changes poststroke (Patel et al., 2013).

The pro-inflammatory mediators associated with the M1 phenotype can be detrimental to injured brain tissue. MMPs breakdown the ECM and BBB poststroke. This adverse effect is diminished using an MMP knock out mouse model, demonstrating less neuronal injury post ischemia. In addition, TNF-α is rapidly upregulated in the brain following injury within 1 h after induction of ischemia (Lambertsen et al., 2005) and inhibition of this pleiotropic cytokine has been displayed in studies to be neuroprotective (Barone et al., 1997). Microglia thereby plays a detrimental role in the acute phase by exacerbating the inflammatory phase.

Recent evidence suggests that activated microglia may actually provide benefits to the SVZ following stroke by orchestrating brain tissue repair. Following cerebral ischemia in transgenic mice, a resident proliferating microglia population presents an endogenous pool of neurotrophic molecules, including IGF-1, where activated microglial proliferation peaks 48–72 h post injury (Lalancette-Hebert et al., 2007). At 72 h postischemic injury, resident microglia undergo proliferative expansion and neutrophil infiltration is diminished, suggesting that microglia are resolving the acute inflammatory phase of repair and promoting reparative environmental remodeling (Denes et al., 2007). Stimulating microglial proliferation can thereby be explored as a therapeutic tool in order to assess the neuroprotective properties of these resident immune cells.

ROLE OF THE ECM

ECM Composition and Proteins

The ECM compromises 20% of the brain tissue volume and presents structural and functional proteins that are necessary for cellular function (Sobel, 1998). Brain-specific ECM varies in density and composition, as well as association with specific neuron types within different areas of the brain. Areas with mature synaptic activity show densely packed areas, known as perineuronal nets, directly impacting neuronal activity in this tight network (Bikbaev et al., 2015). The ECM comprises the basement membranes that support epithelia and vascular ECs. The BBB contains an endothelium basement membrane in addition to a parenchymal basement membrane. Under normal conditions, these two basement membranes are closely in contact. The parenchymal basement membrane is formed by astrocytes and creates a barrier for leukocyte migration into the brain parenchyma. The anatomical location between ECs and astrocytes regulates barrier function, provides physical support and anchoring for cells, and contains ligands that regulate cell processes and signaling through integrin and ECM receptor interactions.

There is a bidirectional relationship between cells and ECM proteins, where ECM proteins, once secreted, interact with cells to both induce and maintain the regulatory properties of this barrier system (Baeten and Akassoglou, 2011). These proteins include collagen, fibronectin, laminin, tenascin, and proteoglycans, interacting closely with ECs, astrocytes, PCs, and microglial, which secrete these proteins poststroke. Many tissue engineering strategies aim to expose cells to an environment within a scaffold that possesses biological ECM-derived molecules to drive cellular function (Delcroix et al., 2010).

The general structure of the ECM includes a variety of macromolecules including proteoglycans and fibrous proteins, each of which are expressed to different degrees in tissues throughout the body. For example, more than 20 distinct collagens have been identified which are expressed differentially in specific tissues based on mechanical requirements of the area. Laminins demonstrate multiple isoforms, synthesized by a variety of cells in a tissue specific manner, expressing explicit α, β, and γ chains. The effect of laminin on adjacent cells is exerted through integrins that recognize laminins, heightening the role of laminin mediating cell–ECM interactions. Laminin 2, specifically, promotes neurite outgrowth from neural cells, where laminin 5 and 10 are seem predominantly in the vascular basement membrane to mediate adhesion of platelets, leukocytes, and ECs. The tenascin family, a group of glycoproteins with strikingly diverse expression

patterns, possesses complex domain structures, implying the molecule can interact with multiple ECM proteins. Tenascins are not expressed in normal adult tissues, however, under pathological conditions, including injury induced neovascularization, tenascin-c is expressed. Proteoglycans, heavily glycosylated proteins consisting of a core protein with covalently attached glycosaminoglycan chains, are grouped into several families, characterized by their composition. For example, decorin, a key member of a leucine-rich repeat proteoglycan family, is involved in signal transduction *via* EGF receptor. It is involved in modulation and differentiation of epithelial and ECs, and also interacts with TGF-β. The heparin sulfate proteoglycans have high affinity bonding to a range of cytokines and growth factors, including FGF and VEGF, implying an important role in pathological processes including the modulation of cell migration, proliferation, and differentiation. MMPs, the main ECM enzymes with proteolytic degradation potential, are responsible for the constant ECM remodeling, facilitating the synthesis and deposition of new ECM proteins and thereby plays an essential role in tissue repair and cell metastasis. At homeostasis, the adult brain has very little MMP expression and activity, though is the microenvironment is rapidly altered when activated by cytokines and growth factors that trigger tissue remodeling (Bosman and Stamenkovic, 2003). Overall, this intrinsically complex ECM system is essential for normal development as well as response to disease and injury, consequently there is an intricate interplay between resident cells and this matrix.

ECM–Stem Cell Interactions

Extracellular matrix components supply a microenvironment that promotes the maintenance of stem cell homeostasis, dictated by signals derived by both ECM–cell interactions and soluble factors. Integrins, a family of heterodimeric transmembrane receptors connecting extracellular environments to intracellular cytoskeletons, are key receptors that facilitate cellular processes including migration and differentiation. Integrins and cell presented matrix receptors mediate a number of interactions by activating downstream signaling. As an example, integrins directly activate downstream signaling through focal adhesion kinase and phosphoinositide 3-kinase, thereby regulating self-renewal and proliferation of cells including hematopoietic stem and progenitor cells. Epithelial cells in the brain express high levels of α6 and/or β1 integrins, which heterodimerize in order to generate a laminin receptor (Marthiens et al., 2010). In particular, α6β1 integrin facilitates cell binding to laminin and is required for NSC adhesion to SVZ blood vessels, where adult SVZ progenitor cells express α6β1 receptor. Blocking this receptor inhibits adhesion to ECs, negatively impacting SVZ progenitor cell proliferation *in vivo*, and highlights the importance of these integrin mediated interactions (Shen et al., 2008). In addition, integrins can bind directly to laminin, collagen, and fibronectin, and to cell-surface adhesion molecules including intercellular adhesion molecule-1 and vascular cell adhesion molecule-1, both present in the stem cell niche.

In addition to integrins, cadherin molecules mediate both cell–cell adhesions and interactions with cytoskeleton-associated proteins. Scaffold proteins β-catenin and α-catenin can interact with intracellular domains of cadherins, thereby connecting cadherins to the cytoskeletal network and forming stable adherns junctions by clustering cadherin molecules. E-cadherin, expressed by ependymal cells in the SVZ, forms adherns junctions between ependymal cells and NSCs. When eliminating E-cadherin *in vitro*, NSC self-renewal is reduced as seen *in vivo* by disrupting E-cadherin through mutations in areas where NSCs specifically reside (Karpowicz et al., 2009). NSCs use both cadherin and integrin to interact with the niche and exploiting the necessity of these adhesion molecules can aid transplantation approaches (Chen et al., 2013).

The ECM can regulate stem cell activity by non-canonical growth factor presentation. It both avidly binds growth factors, regulating their local availability, and functions as a reservoir, making growth factors unavailable and insoluble. By capturing FGF-2 from the milieu, the ECM of the NSC niche in the SVZ promotes growth factor activity in the niche and regulates the neurogenic niche. Thereby, the ECM is extremely dynamic in its response to regulating stem cell maintenance and activity by providing and controlling access to growth factors in the milieu (Gattazzo et al., 2014).

Due to the important role of ECM proteins in cell survival and function, many ECM moieties have been incorporated into engineered scaffolds as a strategy for creating microenvironments that promote neuronal regeneration (Lemons and Condic, 2008). Within biomimetic polymer scaffolds, presentation of laminin, collagen, or fibronectin to MSC in culture demonstrates that laminin, in contrast to fibronectin or collagen, is a strong promoter of neuronal differentiation. Laminin also positively impacts neurite length and the formation of a growth cone, the structure that drives axon extension, through integrin-dependent signaling. Laminin-211 can both increase and decrease neurite extension due to the affinity of integrin binding, demonstrating its ability to drive precise and complex integrin mediated pathways (Qian and Saltzman, 2004; Delcroix et al., 2010). While the entirety of the laminin protein has been used in investigation matrix derived cell function, isolated laminin derived peptides are responsible for specific cell function. Laminin derived peptides, including and Tyr–Ile–Gly–Ser–Arg (YIGSR) and Ile–Lys–Val–Ala–Val (IKVAV) sequences, are responsible for outgrowth of dorsal root ganglion neurons and are widely utilized in a variety of polymeric based scaffolds (Delcroix et al., 2010). The use of a scaffold to guide cell survival and differentiation *in vivo* includes incorporation of ECM components or derived peptides. As one example, the inclusion of fibronectin derived Arg–Gly–Asp (RGD) to poly-(ethylene glycol) (PEG) hydrogel systems illustrates improved human MSCs cell survival *in vitro* (Salinas and Anseth, 2008). Human plasma fibronectin and human plasma fibrinogen demonstrate enhanced survival of cells and increased cell metabolic activity *in vitro* when encapsulating human MSCs in fibronectin or fibrinogen containing hydrogel capsules, most likely due to integrin clustering and activation of extracellular signaling cascades such as the mitogen activated protein kinase cascade (Karoubi et al., 2009). Thereby, the use of ECM proteins can enhance therapeutic cell survival *in vivo* by triggering native cell pathways.

ECM Following Stroke

Following stroke, basement membranes of the BBB are degraded. New ECM proteins are deposited, either by secretion of ECM proteins, or leakage of plasma proteins into the CNS. Degradation of basement membranes after stroke demonstrates notable changes at later time points after injury, for instance, 12–18 h after MCAO in a rat model, although changes in cell presented matrix receptors occur within a few hours. Degradation occurs through proteolysis, mainly by MMPs and plasmin, where these are upregulated and activated following pathological conditions such as stroke (Baeten and Akassoglou, 2011). MMP-9, synthesized by both macrophages as well as ECs, is present within and at the periphery of infarct within 24 h, thereby creating a significant disturbance to BBB integrity following stroke. These degradation pathways are correlated with increased BBB disruption, as well as secondary inflammation and edema and the promotion of vascular permeability (Romanic et al., 1998).

As an inherent method of tissue repair following stroke, ECM proteins are deposited or penetrate the CNS to recover the structure of the microenvironment. In particular, osteopontin (OPN), a secreted glycosylated phosphoprotein, binds receptors that act on several cell types and is expressed in neurons, macrophages, and astrocytes. Following stroke, OPN is upregulated around the infarct zone, and appears to be beneficial after ischemic insult. In rat pups, OPN injections are correlated with reduction in infarct volume and improvement in functional recovery following ischemia (Baeten and Akassoglou, 2011). Fibrinogen, a major plasma protein involved in blood coagulation, cannot normally penetrate the CNS parenchyma due to the BBB. In stroke, however, fibrinogen can occlude blood vessels and leak in the brain, forming deposits and potentially increasing inflammation. In order to remove fibrin to reestablish blood flow, enzymatic degradation by plasmin as well as MMP-2/9 activity is mechanistically helpful (Baeten and Akassoglou, 2011). Considering the alteration of the ECM composition in response to BBB disruption and the direct impact on neurologic disease are functionally important when considering ECM functions in physiology and disease pathology.

CELL-BASED THERAPIES

Cell Delivery Technologies

Cell therapies have demonstrated some ability to induce spontaneous recovery following stroke and can promote endogenous neurogenesis (Kalladka and Muir, 2014). Current methods of cell therapy include exogenous, autologous, and allogenic cell delivery into experimental stroke models, each presenting their own set of advantages and drawbacks. Exogenous cell therapy, in which cells are derived from a source external to the stroke, has demonstrated impact on cell migration, survival, and differentiation which subsequently promote functional recovery in animal models. However, these transplanted cells may induce an immunogenic response. An alternative to exogenous cell therapy is the use of autologous cells, which avoids the risk of rejection. This therapy presents its own challenges, though, as limited access to these cells often requires *in vitro* expansion, which may delay treatment. Allogenic cell therapy, or transplanting stem cells from a genetically similar donor, is potentially the most successful method of cell transplantation. The use of allogenic cells presents advantages of reduced immunogenicity, in addition to being readily available. Of note, ongoing research is still required in order to improve patient selection regarding eligibility for allogenic based therapy (Kalladka and Muir, 2014). Stereotaxic implantation, a minimally invasive surgical method relying on exact 3-D coordinate anatomical systems, is challenging due to time constraints, where lesion size varies greatly over time and from patient to patient. Intravenous (IV) delivery, a non-invasive delivery route, can overcome this set back, though there is a lack of a direct pathway of cells to the ischemic area. Although intra-arterial (IA) delivery can deliver cells to the peri-infarct area directly, occlusion of the target artery that persists can create a blockade for a route of delivery while also compromising survival of delivered cells (Kalladka and Muir, 2014). Interestingly, there is a lack of evidence that IA delivery is superior to IV when delivering bone derived MSCs to a mouse stroke model. With no difference in functional or structural outcomes detected (Yang et al., 2013), the ideal route of administration to optimize the effect of cell therapy, in particular that of stem cells, remains a matter of debate.

Stem cells can be used in stroke therapies to dynamically respond to a stroke-damaged tissue, in which stem cells have phenotypic properties that allow direct interaction with the host environment. Engrafted stem cells, unlike terminally differentiated cells, can respond dynamically to temporal and spatial changes of the environment that follow ischemic injury (Kim, 2004; Kalladka and Muir, 2014; Duncan et al., 2015). Delivery of stem cells to a brain-injury site has effectively reduced lesion size and host cell death. Additionally, successfully delivered stem cells have the potential to replace lost circuitry by forming new synaptic contacts. Even the use of stem cell xenografts in animal models has been shown to decrease infarct area, promote expression of the neuronal proteins such as synaptic proteins, and restore synaptic activity. In fact, stem cells can also strengthen existing synapses (Ishibashi et al., 2004; Bliss et al., 2007), promoting enhanced signaling among uninjured neurons. Further, an induction of host brain plasticity has been observed following exogenous cell engraftment. In this context, increased levels of factors (i.e., FGF and BDNF) that induce angiogenesis resulted in successful integration of transplanted cells with the host circuitry, as well as increased neovascularization and recruitment of endogenous progenitors (Bliss et al., 2007; Lindvall and Kokaia, 2010).

The use of cell therapy requires collaboration between neurologists and engineers to create new and effective delivery methods. Cellular behavior manipulation and induction are explored to enhance cell state prior to and after delivery (Lindvall and Kokaia, 2010). The approaches utilized for cell transplantation, including the control of differentiation and proliferation, are necessary to provide insight for *ex vivo* models that address relevant biological questions regarding SVZ cell interactions. Fundamental considerations include the cell type, cell number, and delivery vehicle and route. Here, we consider the key cell types native to the SVZ and their potential use as cell therapy: stem cells, ECs, ependymal cells, PCs, and microglia, summarized in **Table 2**.

TABLE 2 | Resident cell types of the subventricular zone (SVZ) niche, including endothelial cells, ependymal cells, pericytes (PCs), and microglia, with their respective cellular markers, secreted factors, and impact to other cells present in the niche.

Cell type	Markers	Secreted factors	Impact	Reference
Endothelial cells	Tight junction markers (ZO-1, ZO-2, and claudin-5) NCAM Laminin	PDGFβ Pigment epithelium-derived factor (PEDF) Betacellulin NT3 Vascular endothelial growth factor (VEGF) FGF-2 Endothelial growth factor Bone morphogenic protein (BMP) TGF-β Laminin Prolactin Collagen IV Angiopoietin	Influence PCs function Impact neural stem cell (NSC) self-renewal, proliferation, survival, and quiescence Proliferate in response to stroke Undergo angiogenesis in per-infarct regions Promote neuroblast recruitment	Ramirez-Castillejo et al. (2006); Goldberg and Hirschi (2009); Daneman et al. (2010); Young et al. (2011); Codega et al. (2014); Delgado et al. (2014); Ottone et al. (2014)
Ependymal cells	BMP β-Catenin N-Cadherin Vimentin α-Tubulin	PEDF Noggin	Generate cerebrospinal fluid flow Promote NSC self-renewal and maintenance Proliferate and give rise to neuroblasts and astrocytes Regulate SVZ through Noggin	Lim et al. (2000); Ramirez-Castillejo et al. (2006); Colak et al. (2008); Shen et al. (2008); Young et al. (2011)
Pericytes	αSMA PDGFβ-receptor NG2 CD13	TGF-β IGF-2	Induce and upregulate blood–brain barrier function Impact neurogenesis to be explored Exhibit contractile properties	Dohgu et al. (2005); Yemisci et al. (2009); Armulik et al. (2011); Lehtinen et al. (2011); Sharma et al. (2012)
Microglia	Iba-1 Mac-2	Tumor necrosis factor alpha-α IL-1 Cytokines: pro and anti-inflammatory VEGF Osteopontin	Monitor brain microenvironment Phagocytose foreign substances Inhibit or induce deleterious effects	Barone et al. (1997); Lambertsen et al. (2005); Denes et al. (2007); Lalancette-Hebert et al. (2007); Weinstein et al. (2010); Patel et al. (2013); Ghuman and Modo (2016)

Limitations to Successful Cell Therapy

The major restriction to successful transplantation of neural cells into the stroke-damaged area has been the survival of exogenous cells, which ranges from 1 to 32% (Zhang et al., 2001). Cell survival is compromised by delivery mechanisms that increase distorting force during syringe needle flow such as pressure drop, shearing, and stretching forces (Aguado et al., 2012). Viscosity and composition of delivery fluid contribute to cell distribution in solution and shear forces applied to cells during delivery. Additionally, sedimentation in carrier fluid becomes a limiting factor in successful cell delivery, causing the first partial injection volume to contain more cells than those delivered later. In order to achieve precise cell suspensions and cells with minimal damage, cellular delivery methods are the focus of innovation and optimization in stroke recovery therapeutics (Aguado et al., 2012; Potts et al., 2013).

The BBB and CSF barrier pose limitations to delivering therapeutics to the brain. Established delivery methods can be invasive, causing further damage to the ischemic area. Although systemic, intravenous delivery methods can be non-invasive, they often lead to an accumulation of cells in clearing organs, including kidney and spleen, rather than the brain. Targeted intracerebral cell injection can be applied directly to the peri-infarct region; however, the multiple injections required to deliver adequate numbers of cells can cause further damage to the already injured tissue (Ghuman and Modo, 2016). With minimal damage to an already fragile environment, invasive approaches are unfavorable due to the threat of further disruption of tissue and the BBB. Recent advances take these limitations in current therapeutic strategies into account, focusing on development of minimally invasive and non-damaging injections or delivery routes.

Biomimetic strategies face obstacles when considering clinical translation due to the fact the optimal cell type for transplantation therapy has not been determined. The use of stem cells in particular is impacted by ethical issues, where fetal and embryonic derived cells can create controversy. Generating an abundance of cells that maintain and recapitulate stemness is a challenge that limits the use of other cell types. Just as it has been seen with direct implantation and delivery of stem cells, many restrictions impact the success of these new therapies. First, the stroke-injured brain may compartmentalize areas of damaged tissue, creating a physical barrier to therapeutic deliveries. Stroke-injured brains also contain varying degrees of necrotic, avascular tissue, limiting access to systemic delivery of materials and cells through the vasculature. The variation in injury observed from person to person in each stroke occurrence causes significant difficulty in normalization of therapeutic methods. Due to the high variability of tissue damage and resultant function between patients, there

is a lack of a standardized way to quantify both the severity and recovery of the disease. In order to form an effective therapy, these ambiguities must be addressed to formulate a common language that can measure functional outcomes in stroke trials.

BIOMATERIAL-BASED BIOMIMICRY

We have detailed the importance of native and remodeled microenvironments in the SVZ and their role in driving cell function. The resident cell types have been described in addition to the ways these cells interact and impact one another. Both direct and indirect interactions with ECM molecules impact cell behavior, providing biomimetic scaffolds the opportunity to regulate cell behavior by modifying scaffolds to provide cues that cells in the host environment would have (Delcroix et al., 2010). Together, knowledge of SVZ cells, exogenous cells, and the ECM molecules that control cell fate and maintain the SVZ niche, tissue engineers can create biomaterials to produce a bioreplicative system that may improve experimental and therapeutic approaches.

Ideally, direct implantation of a biomaterial into the stroke-damaged area would promote cell adhesion and survival, cellular cues for healthy tissue development, and induce the recovery of the damaged ischemic core. Here, we discuss critical scaffold attributes required to facilitate poststroke healing in the brain, and two classes of biomaterials that have been demonstrated advantageous for brain repair: synthetic and natural materials.

Considerations for Development of an Ideal Scaffold

The ultimate goal of a biomimetic scaffold is to facilitate neural tissue regeneration and functional recovery following stroke. A scaffold must promote survival and proliferation of transplanted cells within the damage site, engage healthy interaction with endogenous cells, and promote the recovery of damaged neural circuitry. The mechanical and physical properties of a biomaterial impact the administration of the scaffold, the target injection site, and endogenous/exogenous cell response. In particular, solid scaffolds must present a compressive moduli allowing for cell survival rather than promoting tissue stress and damage upon implantation. A decrease in NSC proliferation in 3-D alginate scaffolds is correlated with an increase in the material modulus, where the greatest differentiation expression was attributed to the softest hydrogels. These soft hydrogels possess an elastic modulus comparable to brain tissue (100–1,000 Pa) (Banerjee et al., 2009). In addition to mechanical constraints, the initiation of the cellular and molecular cascade following transplantation must be considered. A biocompatible material is one that can coexist with living tissues without eliciting a local and systemic immune response in host tissue. Biocompatible materials do not promote a foreign body response, do not produce cytotoxic effects to the milieu, and limit the inflammatory and immune reaction in the brain (Boisserand et al., 2016). Byproducts from biomaterial degradation can be bioactive, influencing the surrounding environment and affecting both host and transplanted cells, thereby producing detrimental effects. Photopolymerization processes, which are cross-linking reactions that occur with light exposure, are often used for hydrogel production; however, these reactions can lead to the formation of free-radicals that compromise cell survival. Polymers that can polymerize at physiological conditions, dependent on temperature or pH, avoid these potential toxic effects (Ghuman and Modo, 2016). Consideration of how biomaterials will interact with host tissue is critical to contribute to functional recovery of both the infarct area and surrounding tissues.

Scaffold degradation over time to create or restore neural circuitry in stroke-damaged tissue. Degradation allows for integration of transplanted cells into the cavity. There is a fine balance between supporting cells during transplantation and controlling the rate of degradation. Injectable biomaterials, including hydrogels, are attractive candidates for stroke injury lesion cavities, which vary in size and morphology between patients. Hydrogels that structurally fill the cavity space and induce repopulation of cell depleted tissue space can be advantageous, as long as the mechanical properties are controlled in a manner that avoids further damage to the lesion cavity caused by increased intracerebral pressure with large volume of hydrogel injection. In fact, Modo et al. observed that microglia and astrocytes were able to infiltrate an ECM hydrogel where cell infiltration allows for a repopulation of host cells and ECM remodeling (Ghuman et al., 2016). While bulk hydrogel implantation into infarcted and lesional cavities has demonstrated some benefit, implantation of microencapsulated biological moieties has also demonstrated promise in the area of stroke recovery and repair. Microencapsulation techniques in which cells are encapsulated in approximately 95 microsphere diameter polymeric hydrogel spheres can be used to control the microenvironment an implanted cell is initially exposed to, thereby maintaining proper function of the cell type. In particular, is the maintenance of cell function is applicable to the SVZ niche where the cytoarchitecture organization is important to maintaining cellular and biochemical cues (Franco et al., 2011). Growth factor incorporation into biomaterials can contribute to creating biomimetic microenvironments. As one example, growth factors, including IGF-1, that are encapsulated into gelatin microspheres, promoted increased endogenous neurogenesis in the SVZ of adult mice. Hepatocyte growth factor containing microspheres also increased neuroblast migration from the SVZ to the stroke-injured tissue in the same model (Nakaguchi et al., 2012). FGF-2 in heparin–chitosan scaffolds demonstrates sustained survival and growth of NSC, where these multifunctional, biocompatible microspheres are optimized for NSC grafting (Struzyna et al., 2014). The use of stem cells and growth factors in conjunction with biocompatible and degradable scaffolds shows high potential to create a microenvironment that promotes functional recovery following injury. The use of 2-D polymer scaffolds has been advantageous as a means of exploring conditions for optimal cell growth and survival, for probing cell-surface interactions, and for trialing manipulations of the microenvironment that are impactful to cell response. In fact, such models that have been used to deconstruct the SVZ niche include the presentation of FGF covalently attached to a network of polyamide nanofibers. The scaffold maintained biological efficacy of FGF-2, strongly activating FGF receptors (Nur et al., 2008). In addition, EGF tethered to poly(methyl methacrylate)-graft-poly(ethylene oxide) promotes

MSC spreading and survival around the biomaterial (Fan et al., 2007). These advantageous promote the use of 2-D polymeric substrates as bioreplicative constructs is a method of optimizing conditions for cell culture prior to advancement to 3-D replicates of the SVZ niche. In a 2-D model, cell–cell adhesions are confined to a horizontal plane, while a 3-D model allows for adhesions on all sides. A 3-D environment constrains cells to an artificial niche, enabling dynamic variation or continuous remodeling, which are not capable in a 2-D monolayer model.

Elastic, polymeric scaffolds make an ideal candidate for neurosurgical techniques to deliver scaffolds to the SVZ. While the goal is to fill the stroke cavity with a pliable and tunable scaffold which resembles mechanical properties of the native environment that will temporarily replace lost tissue, the material must also promote the infiltration of new and healthy cells. Rat-derived NSCs vary their cellular fate depending on the hydrogel stiffness, stressing the importance of biomaterial mechanical properties on differentiation potential (Leipzig and Shoichet, 2009). Stiffness and diffusion capacity must be carefully assessed prior to scaffold delivery in order to avoid detrimental effects to surrounding tissues in addition to differentiation to undesired cellular fates.

Synthetic Polymeric Materials

Synthetic biomaterials enable direct control of key properties, including degradation rate, material stiffness, and protein incorporation. Cell incorporation in combination with these materials calls for careful observation of cell–scaffold interactions, consequently allowing for control of cell processes, such as differentiation, morphological formation, and extension, to ultimately enhance connectivity in the ischemia area (Ghuman and Modo, 2016).

Poly-(Ethylene Glycol)

Poly-(ethylene glycol) is a biologically inert, non-toxic polymeric material, presenting excellent biocompatibility and resistance of protein adsorption. The mechanical properties of PEG depend on its molecular weight, as increasing the chain length of PEG increases stiffness and viscosity (Parlato et al., 2014). PEG can be chemically modified by tethering peptides or proteins through cross-linking reactions. Due to its inert nature, the incorporation of biologically active peptides cell-adhesive peptides, such as RGD and YIGSR, promotes cell attachment to the material (Gonzalez et al., 2004). PEGylation, the process of attaching PEG polymer chains to molecules and macrostructures, changes the chemical and physical properties of the material (Roudsari et al., 2016), making PEG a highly used polymer in a broad spectrum of tissue engineering applications. PEG-based microspheres modified by adhesive sequence RGD and metalloproteinase sensitive sequence have been utilized to encapsulate murine NSCs and brain ECs, demonstrating 60–80% cell viability, cell spreading, and migration through the scaffold (Franco et al., 2011).

In order to observe PEG as a candidate for neural repair and recovery, degradation characteristics as well as delivery of both cells, and growth factors are under investigation. As one example, varying mass profiles of PEG were examined. The astrocyte response varied with degradation rate, where slowly degrading/non-degrading gels display a prolonged astrocytic response. Astrocytes extended their processes into the hydrogel, where microglia infiltrated the hydrogel and facilitated the enzymatic process. Hydrogels decreased acute microglial response during the week following implantation, suggesting PEG-based materials are beneficial for CNS delivery for both drugs and cells (Bjugstad et al., 2010). In addition, PEG-based hydrogels with increased lactic acid content and encapsulated neural cells, including postmiotic neurons and multipotent precursor cells, demonstrate an increase in cell proliferation and survival, establishing an advantage of rendering PEG materials as degradable in order to be relevant to neural cells delivered to the stroke-injured brain (Lampe et al., 2010). Delivery of EGF using modified PEG hydrogels demonstrates a significant increase in tissue penetration as well as endogenous NSCs and progenitor cells in the SVZ when delivered to the ventricles of the brain. PEG modification in this way decreased EGF degradation by proteases, allowing for a greater protein accumulation in surrounding tissues, penetrating deeply into the tissues, seen in both the healthy and stroke-injured mice brain (Cooke et al., 2011). Thereby, these studies provide support for the use of PEG as a highly adaptable and tunable scaffold to be utilized for delivery of both cells and growth factors in stroke repair applications.

Polylactide Acid (PLA), Polyglycolide Acid (PGA), and Poly(Lactic-Co-Glycolic Acid) (PLGA)

Utilizing PLA and PGA alone or as the copolymer PLGA renders a bioactive polymer with the ability to closely control material properties, specifically degradation (Ghuman and Modo, 2016). PGA, a hydrophilic polymer, can rapidly degrade over a course of 2–4 weeks *in vivo*, while hydrophobic PLA degrades slower. Incorporation of these materials, PLGA in particular, can produce a variety of biomaterials, including nano and microparticles, which present high biocompatibility, low immunogenic response, and high structural support for NSCs to enhance brain repair (Boisserand et al., 2016).

Polyglycolide acid scaffolds have been effective for encapsulating NSCs, illustrating vascular formation and access to nutrients *via* diffusion (Park et al., 2002). In addition, a copolymer of PLGA-PEG nanoparticles loaded with thyroid hormone, which has a neuroprotective role in ischemia damage and is permeable across the BBB, demonstrates a decrease in tissue infarction and brain edema when delivered to a MCAO mouse model (Mdzinarishvili et al., 2013). PLGA based microspheres can bypass the inflammatory cascade and reduce host immune response, where these microspheres produce an inflammatory response similar to that of just a needle tract, presenting a peak in astrocyte activation 1-week post injection in rat brain models (Emerich et al., 1999). Another study shows human derived NSCs seeded on VEGF-releasing PLGA microparticles delivered to a MCAO rat model exhibiting a burst and sustained VEGF release, promoting attraction to ECs from the host, and facilitating the re-establishment of neovasculature through the cell and growth factor delivery (Bible et al., 2012). These results suggest that PLGA, due to its controlled degradation rates and high biocompatibility, has potential for a stroke therapeutic delivery system of drugs, cells, or reparative and regenerative factors.

Polypyrrole

Electric fields *in vivo* play a crucial role in control of cell potential and neuronal field potential. Electrical stimulation of stem cells is known to facilitate stem cell and progenitor cell fate. Experimentation using electrical properties may be beneficial to differentiate stem cells and re-build neural circuitry. The use of conductive scaffolds makes plausible the manipulation of stem cells, in particular, the use of Polypyrrole (PPy) (George et al., 2017). Following the seeding of cells, ion channel density and neurite outgrowth are manipulated by signaling intrinsic electrical cues. PPy generates a minimal inflammatory response, supports cell growth, and guides stem cells toward differentiation (Stewart et al., 2015). By applying electrical stimulation to NSCs seeded on laminin-coated PPy films in a timely manner demonstrates neuron differentiation (Stewart et al., 2015). A study preconditioning human neural progenitor cells in a cell chamber system seeded on a PPy scaffold presents an improvement in neurologic function in a rat stroke model (George et al., 2017). The VEGF-A pathway gene expression was altered following electrical stimulation, correlated with endogenous vasculature remodeling (George et al., 2017). This suggests that electrically preconditioning stem cells can be beneficial to enhance stroke recovery.

Natural Materials

Chitosan

Chitosan is a biodegradable, inexpensive material with low toxicity that can be modified through incorporation of ECM proteins to the surface, including laminin and fibronectin that regulate cell functions (Haipeng et al., 2000; Cheng et al., 2007; Yang et al., 2010). Accordingly, due to its ability to be modified, chitosan carriers have demonstrated NSC survival, proliferation, and cell differentiation into desired phenotypes (Yang et al., 2010). In terms of neural repair, chitosan use is advantageous as the material undergoes alkaline hydrolysis, directly controlling the amine content and ultimately impacting cell adhesion and neurite extension (Cheng et al., 2007). In addition, oxygen plasma treatment preserves the chitosan microstructure in nerve conduit models, confirming improvement in behavior and functional recovery (Cheng et al., 2007). Chitosan nanoparticles loaded with acetyl-11-keto-β-boswellic acid, a resin extract which may control inflammatory responses, demonstrate a neuroprotective effect in a MCAO rat model, reducing infarct volume and cell death (Ding et al., 2016). In addition, the encapsulation of ESC derived ECs into a chitosan-based hydrogel loaded with VEGF microtubes presents minimal cytotoxicity *in vivo* and high cell survival, inducing neovascularization in hind limb ischemia mouse models (Lee et al., 2015). Chitosan-based biomaterials continue to be explored for the use in nerve repair for brain injury due to the lack of immune response post injection.

Hyaluronic Acid (HA)

Hyaluronic acid is a linear-chain polysaccharide that has demonstrated a positive role in nerve regeneration as well as neuronal development. HA is biocompatible and ubiquitous in the body. HA plays a role in CNS development and has been utilized in conjunction with neuronal progenitor cells in various applications, including the use of photocrosslinkable hydrogels varying in stiffness, presenting differences in differentiation potential (Seidlits et al., 2010; Khaing et al., 2014). The mechanical properties of HA hydrogels can be manipulated, promoting the potential to direct neural progenitor differentiation (Seidlits et al., 2010) in addition to reducing scar formation following neurolysis (Ikeda et al., 2003). These hydrogel systems express mechanical properties similar to that of brain tissue and can be altered through photo cross-linking systems, testing a variety of compressive moduli. In normal tissue, hyaluronan has a range of molecular weights that play critical rolls in controlling cell motility, cell growth, and angiogenesis (Back et al., 2005). Engrafting transplanted mouse, human progenitor, and human glial-restricted precursor cells in HA-PEG gels demonstrates prolonged survival in the xenograft, despite the induction of a mild inflammatory response after 2 weeks (Liang et al., 2013). The optimization of HA based scaffolds is under exploration for neural repair therapy as this polysaccharide plays a key role in stabilizing the ECM and regulating cell processes such as adhesion, motility, proliferation, and differentiation.

Hyaluronan–Methylcellulose (HAMC)

In HAMC systems, fine tuning of material properties is obtained by altering both the composition and molar mass of HA and methylcellulose (MC). While hyaluronan and MC are both biocompatible, hyaluronan is beneficial due to its non-immunogenic and anti-inflammatory properties (Vercruysse and Prestwich, 1998), and MC is a non-cell-adhesive material with the ability to fill brain lesions (Wells et al., 1997; Tate et al., 2001). The combination of these two materials is an ideal option for many neural therapies. HAMC polymers are fast-gelling and can be made into an injectable material. The gelation mechanisms, degradation, and cell adhesion of these materials can be varied and are well characterized (Tate et al., 2001; Gupta et al., 2006; Shoichet et al., 2007). Future uses of HAMC models rely upon their non-immunogenic nature, which is advantageous for injection therapies due to the reduced risk of infection at the injection site.

Fibrin

Fibrin has been used extensively as a scaffold for nerve regeneration, allowing for axonal regeneration and cell migration in gap nerve injuries (Williams et al., 1983; Taylor et al., 2004). Since fibrin is susceptible to enzymatic degradation, neurites are able to degrade these gels *via* plasmin activity (Herbert et al., 1996). Fibrin-based drug delivery systems have been used to release neurotrophins, a family of proteins that positively impact survival and development of neurons. Fibrin gel systems have been used to promote cell migration, neural fiber extension, and growth factor delivery (Taylor et al., 2004). In addition, fibrin matrices have been used in conjunction with glial-derived neurotrophic factor to enhance neurite extension (Wood et al., 2009), further demonstrating the advantages of this material for re-building nerve connectivity. IPSCs mixed with a fibrin glue injected to an MCAO rat model resulted in a reduction in infarct volume, improvement in behavior, a reduction in pro-inflammatory cytokines, and an increase of anti-inflammatory cytokines (Chen et al., 2010).

Collagen

Collagen, one of the most abundant proteins, is a biocompatible and immunogenic material that promotes cell adhesion and growth (Cross et al., 2010). Collagen can be remodeled by cells and is readily accessible for research and therapeutic use, as it can be obtained commercially or through established extraction protocols. However, due to the weak bulk mechanical strength of collagen, collagen-based materials must be altered to mimic the ECM and facilitate native cell interactions and biophysical cues (Knapp et al., 1997). The modulus or tensile strength of collagen can be increased through the addition of molecules, such as glycosaminoglycans (Lee et al., 2001).

Due to the biocompatibility and tunable mechanical strength of collagen, studies using collagen hydrogels have demonstrated the ability to encapsulate NSCs to increase cell survival when compared to injection of cells alone into the lesion cavity. NSCs assemble into the pores of the collagen matrix, where cells survive, differentiate, and re-build neural synapses in the MCAO rat model, displaying the start of collagen degradation after 6 days. Degradation processes facilitate the recovery of neural tissue post ischemia and allow for NSC integration to the host network (Yu et al., 2010). The incorporation of hyaluronan, heparin, and collagen into a hydrogel loaded with NSCs into a photo thrombotic stroke mouse model exhibits survival of the neural cells transplanted into the infarct cavity, a decrease in activated microglia and macrophage cells around the scaffold, and an increase in cell survival (Zhong et al., 2010). Due to the remodeling potential of a collagen scaffold, in addition to its use for observing dynamic cell processes, collagen is an attractive biomaterial for improving angiogenesis and vasculogenesis in stroke models.

PERSPECTIVE AND FUTURE DIRECTIONS

Biomaterial platforms have great potential to mimic the native interactions of the SVZ. Nevertheless, these materials must induce resident cell function and limit further damage to the stroke-injured tissue, presenting significant challenges for researchers and engineers. Ideally, a biomaterial must be biocompatible and degradable. This promotes cell interactions including molecular and biological signaling and cues, which mimic the native transplantation niche. Intracranial delivery systems must be optimized, beginning from rodent models in order to enhance knowledge of SVZ maintenance and dynamic response following brain trauma. This expanding pool of knowledge will ultimately translate to human trials. The translation to human models, however, poses its own challenges, as the human SVZ differs from that of the rodent in cellular architecture. In addition, large-scale efficacy and randomized controlled trials must be conducted to ultimately test the efficiency and safety of stroke therapeutics.

In order to produce a biomimetic scaffold that takes into account the many requirements and considerations discussed here, intense collaboration between neurologists, neural cell biologists, tissue engineers, and imaging experts is required. More profound knowledge of stem cell therapy is necessary to determine whether stem cells take on the function of the cells they replace, or if the cells integrate and need training by surrounding cells to function. Such discoveries would also aid in the understanding of these cells' impact on endogenous neurogenesis. The implications of these discoveries would contribute to neurological diseases that compromise brain homeostasis not limited to stroke, including Parkinson's disease and Huntington's disease. Using the ability of NSCs to differentiate and self-renew, these cells have great potential for cell replacement and gene therapy for a broad category of neurological disease (Kim, 2004). The observation of molecular pathways between the critical cell types discussed above will guide development of scaffolds that promote both neurogenesis and angiogenesis.

As survival of transplanted cells remains a major limitation of successful cell therapy, a tissue engineered strategy must focus on transplantation methods that do not compromise cell viability. In addition, therapies must be tunable by nature, thereby addressing patient heterogeneity. Patients show variety in lesion size, location, and neuroanatomy postischemic stroke. The availability of stem cells to incorporate into biomimetic scaffolds must further be explored to ensure that these cell sources, in addition to resident cells, will limit the inflammatory cascade from occurring. It is important that research further examine how immune cells can be neuroprotective or damaging or if their role is solely dependent on the microenvironment, in order to achieve both positive and negative impacts.

Imaging techniques will require advanced technology to monitor stem cell activity, biomarker expression, structural changes, and the integrity of the infarct area. Using fluorescent microscopy, distribution of transplanted cells and material can be observed over time, where migration of stem cells to the lesion site is desirable. In this way, temporal dynamics of migration can be observed in addition to histological analysis of transplanted cells to the lesion area. Cell tracking is made feasible through bioluminescent optical imaging at a low cost, however, limited by the low penetration of light. In order to track cells deeper in tissue, positron emission tomography, single-photon emission computed tomography, and magnetic resonance imaging (MRI) can penetrate deeper within a subject utilizing a radioactive isotope (Gavins and Smith, 2015). MRI allows for imaging modalities to assess pathophysiological changes, outcomes of cerebral ischemia, vascular lesions, and blood flow. By observing parenchyma changes through this tool, ischemic lesions and the advancing ischemia can be observed, as well as the direct consequences of the injury (Nour and Liebeskind, 2014). Computed tomographic scans of the brain allow monitoring of hemorrhaging, an observation required before intravenous rtPA can be administered (Menon et al., 2015). Customized imaging can give insight into the area of infarction over the course of therapy, where this enhanced detail is crucial when considering translation to human trial.

In summary, there is strong potential in our ability to produce and optimize biomaterials that mimic the SVZ, during homeostasis and following stroke. By incorporating multiple cell types, important matrix proteins and moieties, and appropriate biochemical and biomechanical cues native to the SVZ niche, promotion and enhancement of neurogenesis and angiogenesis

can be attained. Once accomplished, this can revolutionize the limitations of stroke therapies, where there is currently no effective treatment for full recovery following ischemia. Future therapies must mimic the SVZ niche to maintain stem cells in a quiescent, undifferentiated state with controlled differentiation potential, in addition to the direct cell to cell interactions that regulate homeostasis and promote repair following injury. As a result, integrating neuroanatomy and biomaterials can be an advantageous collaboration to confront a pressing clinical need to produce a therapy with fine-tuned control over a biomaterial's properties. Through the manipulation of engineered scaffolds, the ultimate goal of treating degenerative activity in the SVZ to allow for functional recovery and neural circuitry post-trauma can be achieved.

AUTHOR CONTRIBUTIONS

RM and AG contributed to the writing and editing of this manuscript.

ACKNOWLEDGMENTS

The authors would like to acknowledge Amanda Pellowe for review and comments in the writing of this manuscript.

FUNDING

This work was supported by the National Institutes of Health 5R01EB016629-03.

REFERENCES

Aguado, B. A., Mulyasasmita, W., Su, J., Lampe, K. J., and Heilshorn, S. C. (2012). Improving viability of stem cells during syringe needle flow through the design of hydrogel cell carriers. *Tissue Eng. Part A* 18, 806–815. doi:10.1089/ten.TEA.2011.0391

Alexander, L. D., Black, S. E., Gao, F., Szilagyi, G., Danells, C. J., and Mcilroy, W. E. (2010). Correlating lesion size and location to deficits after ischemic stroke: the influence of accounting for altered peri-necrotic tissue and incidental silent infarcts. *Behav. Brain Funct.* 6, 6–6. doi:10.1186/1744-9081-6-6

Alvarez-Buylla, A., and García-Verdugo, J. M. (2002). Neurogenesis in adult subventricular zone. *J. Neurosci.* 22, 629–634.

Armulik, A., Genové, G., and Betsholtz, C. (2011). Pericytes: developmental, physiological, and pathological perspectives, problems, and promises. *Dev. Cell* 21, 193–215. doi:10.1016/j.devcel.2011.07.001

Arvidsson, A., Collin, T., Kirik, D., Kokaia, Z., and Lindvall, O. (2002). Neuronal replacement from endogenous precursors in the adult brain after stroke. *Nat. Med.* 8, 963–970. doi:10.1038/nm747

Back, S. A., Tuohy, T. M. F., Chen, H., Wallingford, N., Craig, A., Struve, J., et al. (2005). Hyaluronan accumulates in demyelinated lesions and inhibits oligodendrocyte progenitor maturation. *Nat. Med.* 11, 966–972. doi:10.1038/nm1279

Baeten, K. M., and Akassoglou, K. (2011). Extracellular matrix and matrix receptors in blood-brain barrier formation and stroke. *Dev. Neurobiol.* 71, 1018–1039. doi:10.1002/dneu.20954

Banerjee, A., Arha, M., Choudhary, S., Ashton, R. S., Bhatia, S. R., Schaffer, D. V., et al. (2009). The influence of hydrogel modulus on the proliferation and differentiation of encapsulated neural stem cells. *Biomaterials* 30, 4695–4699. doi:10.1016/j.biomaterials.2009.05.050

Barone, F. C., Arvin, B., White, R. F., Miller, A., Webb, C. L., Willette, R. N., et al. (1997). Tumor necrosis factor-alpha. A mediator of focal ischemic brain injury. *Stroke* 28, 1233–1244. doi:10.1161/01.STR.28.6.1233

Ben-David, U., and Benvenisty, N. (2011). The tumorigenicity of human embryonic and induced pluripotent stem cells. *Nat. Rev. Cancer* 11, 268–277. doi:10.1038/nrc3034

Bible, E., Qutachi, O., Chau, D. Y. S., Alexander, M. R., Shakesheff, K. M., and Modo, M. (2012). Neo-vascularization of the stroke cavity by implantation of human neural stem cells on VEGF-releasing PLGA microparticles. *Biomaterials* 33, 7435–7446. doi:10.1016/j.biomaterials.2012.06.085

Bikbaev, A., Frischknecht, R., and Heine, M. (2015). Brain extracellular matrix retains connectivity in neuronal networks. *Nature* 5, 14527. doi:10.1038/srep14527

Bjugstad, K. B., Lampe, K., Kern, D. S., and Mahoney, M. (2010). Biocompatibility of poly(ethylene glycol)-based hydrogels in the brain: an analysis of the glial response across space and time. *J. Biomed. Mater. Res. A.* 95, 79–91. doi:10.1002/jbm.a.32809

Bliss, T., Guzman, R., Daadi, M., and Steinberg, G. K. (2007). Cell transplantation therapy for stroke. *Stroke* 38, 817–826. doi:10.1161/01.STR.0000247888.25985.62

Boisserand, L. S. B., Kodama, T., Papassin, J., Auzely, R., Moisan, A., Rome, C., et al. (2016). Biomaterial applications in cell-based therapy in experimental stroke. *Stem Cells Int.* 2016, 6810562. doi:10.1155/2016/6810562

Bosman, F. T., and Stamenkovic, I. (2003). Functional structure and composition of the extracellular matrix. *J. Pathol.* 200, 423–428. doi:10.1002/path.1437

Brown, R. C., Morris, A. P., and O'Neil, R. G. (2007). Tight junction protein expression and barrier properties of immortalized mouse brain microvessel endothelial cells. *Brain Res.* 1130, 17–30. doi:10.1016/j.brainres.2006.10.083

Buhnemann, C., Scholz, A., Bernreuther, C., Malik, C. Y., Braun, H., Schachner, M., et al. (2006). Neuronal differentiation of transplanted embryonic stem cell-derived precursors in stroke lesions of adult rats. *Brain* 129, 3238–3248. doi:10.1093/brain/awl261

Carlen, M., Meletis, K., Goritz, C., Darsalia, V., Evergren, E., Tanigaki, K., et al. (2009). Forebrain ependymal cells are notch-dependent and generate neuroblasts and astrocytes after stroke. *Nat. Neurosci.* 12, 259–267. doi:10.1038/nn.2268

Carmichael, S. T. (2006). Cellular and molecular mechanisms of neural repair after stroke: making waves. *Ann. Neurol.* 59, 735–742. doi:10.1002/ana.20845

Carmichael, S. T., Archibeque, I., Luke, L., Nolan, T., Momiy, J., and Li, S. (2005). Growth-associated gene expression after stroke: evidence for a growth-promoting region in peri-infarct cortex. *Exp. Neurol.* 193, 291–311. doi:10.1016/j.expneurol.2005.01.004

Carmichael, S. T., and Chesselet, M. F. (2002). Synchronous neuronal activity is a signal for axonal sprouting after cortical lesions in the adult. *J. Neurosci.* 22, 6062–6070.

Carmichael, S. T., Wei, L., Rovainen, C. M., and Woolsey, T. A. (2001). New patterns of intracortical projections after focal cortical stroke. *Neurobiol. Dis.* 8, 910–922. doi:10.1006/nbdi.2001.0425

Chen, J., Li, Y., Wang, L., Lu, M., Zhang, X., and Chopp, M. (2001). Therapeutic benefit of intracerebral transplantation of bone marrow stromal cells after cerebral ischemia in rats. *J. Neurol. Sci.* 189, 49–57. doi:10.1016/S0022-510X(01)00557-3

Chen, S., Lewallen, M., and Xie, T. (2013). Adhesion in the stem cell niche: biological roles and regulation. *Development* 140, 255–265. doi:10.1242/dev.083139

Chen, S. J., Chang, C. M., Tsai, S. K., Chang, Y. L., Chou, S. J., Huang, S. S., et al. (2010). Functional improvement of focal cerebral ischemia injury by subdural transplantation of induced pluripotent stem cells with fibrin glue. *Stem Cells Dev.* 19, 1757–1767. doi:10.1089/scd.2009.0452

Cheng, H., Huang, Y.-C., Chang, P.-T., and Huang, Y.-Y. (2007). Laminin-incorporated nerve conduits made by plasma treatment for repairing spinal cord injury. *Biochem. Biophys. Res. Commun.* 357, 938–944. doi:10.1016/j.bbrc.2007.04.049

Codega, P., Silva-Vargas, V., Paul, A., Maldonado-Soto, A. R., Deleo, A. M., Pastrana, E., et al. (2014). Prospective identification and purification of quiescent adult neural stem cells from their in vivo niche. *Neuron* 82, 545–559. doi:10.1016/j.neuron.2014.02.039

Colak, D., Mori, T., Brill, M. S., Pfeifer, A., Falk, S., Deng, C., et al. (2008). Adult neurogenesis requires Smad4-mediated bone morphogenic protein signaling in stem cells. *J. Neurosci.* 28, 434–446. doi:10.1523/JNEUROSCI.4374-07.2008

Cooke, M. J., Wang, Y., Morshead, C. M., and Shoichet, M. S. (2011). Controlled epi-cortical delivery of epidermal growth factor for the stimulation of endogenous neural stem cell proliferation in stroke-injured brain. *Biomaterials* 32, 5688–5697. doi:10.1016/j.biomaterials.2011.04.032

Cross, V. L., Zheng, Y., Won Choi, N., Verbridge, S. S., Sutermaster, B. A., Bonassar, L. J., et al. (2010). Dense type I collagen matrices that support cellular remodeling and microfabrication for studies of tumor angiogenesis and vasculogenesis in vitro. *Biomaterials* 31, 8596–8607. doi:10.1016/j.biomaterials.2010.07.072

Daneman, R., Zhou, L., Kebede, A. A., and Barres, B. A. (2010). Pericytes are required for blood-brain barrier integrity during embryogenesis. *Nature* 468, 562–566. doi:10.1038/nature09513

Delcroix, G. J. R., Schiller, P. C., Benoit, J.-P., and Montero-Menei, C. N. (2010). Adult cell therapy for brain neuronal damages and the role of tissue engineering. *Biomaterials* 31, 2105–2120. doi:10.1016/j.biomaterials.2009.11.084

Delgado, A. C., Ferron, S. R., Vicente, D., Porlan, E., Perez-Villalba, A., Trujillo, C. M., et al. (2014). Endothelial NT-3 delivered by vasculature and CSF promotes quiescence of subependymal neural stem cells through nitric oxide induction. *Neuron* 83, 572–585. doi:10.1016/j.neuron.2014.06.015

Denes, A., Vidyasagar, R., Feng, J., Narvainen, J., Mccoll, B. W., Kauppinen, R. A., et al. (2007). Proliferating resident microglia after focal cerebral ischaemia in mice. *J. Cereb. Blood Flow Metab.* 27, 1941–1953. doi:10.1038/sj.jcbfm.9600495

Ding, Y., Qiao, Y., Wang, M., Zhang, H., Li, L., Zhang, Y., et al. (2016). Enhanced neuroprotection of acetyl-11-keto-β-boswellic acid (AKBA)-loaded O-carboxymethyl chitosan nanoparticles through antioxidant and anti-inflammatory pathways. *Mol. Neurobiol.* 53, 3842–3853. doi:10.1007/s12035-015-9333-9

Doetsch, F. (2003). A niche for adult neural stem cells. *Curr. Opin. Genet. Dev.* 13, 543–550. doi:10.1016/j.gde.2003.08.012

Dohgu, S., Takata, F., Yamauchi, A., Nakagawa, S., Egawa, T., Naito, M., et al. (2005). Brain pericytes contribute to the induction and up-regulation of blood-brain barrier functions through transforming growth factor-beta production. *Brain Res.* 1038, 208–215. doi:10.1016/j.brainres.2005.01.027

Duncan, K., Gonzales-Portillo, G. S., Acosta, S. A., Kaneko, Y., Borlongan, C. V., and Tajiri, N. (2015). Stem cell-paved biobridges facilitate stem transplant and host brain cell interactions for stroke therapy. *Brain Res.* 1623, 160–165. doi:10.1016/j.brainres.2015.03.007

Emerich, D. F., Tracy, M. A., Ward, K. L., Figueiredo, M., Qian, R., Henschel, C., et al. (1999). Biocompatibility of poly (DL-lactide-co-glycolide) microspheres implanted into the brain. *Cell Transplant.* 8, 47–58. doi:10.1177/096368979900800114

Falcão, A. M., Marques, F., Novais, A., Sousa, N., Palha, J. A., and Sousa, J. C. (2012). The path from the choroid plexus to the subventricular zone: go with the flow! *Front. Cell. Neurosci.* 6:34. doi:10.3389/fncel.2012.00034

Fan, V. H., Tamama, K., Au, A., Littrell, R., Richardson, L. B., Wright, J. W., et al. (2007). Tethered epidermal growth factor provides a survival advantage to mesenchymal stem cells. *Stem Cells* 25, 1241–1251. doi:10.1634/stemcells.2006-0320

Fanning, A. S., Jameson, B. J., Jesaitis, L. A., and Anderson, J. M. (1998). The tight junction protein ZO-1 establishes a link between the transmembrane protein occludin and the actin cytoskeleton. *J Biol Chem* 273, 29745–29753. doi:10.1074/jbc.273.45.29745

Franco, C. L., Price, J., and West, J. L. (2011). Development and optimization of a dual-photoinitiator, emulsion-based technique for rapid generation of cell-laden hydrogel microspheres. *Acta Biomater.* 7, 3267–3276. doi:10.1016/j.actbio.2011.06.011

Gage, F. H. (2000). Mammalian neural stem cells. *Science* 287, 1433–1438. doi:10.1126/science.287.5457.1433

Gattazzo, F., Urciuolo, A., and Bonaldo, P. (2014). Extracellular matrix: a dynamic microenvironment for stem cell niche(). *Biochim. Biophys. Acta* 1840, 2506–2519. doi:10.1016/j.bbagen.2014.01.010

Gavins, F. N. E., and Smith, H. K. (2015). Cell tracking technologies for acute ischemic brain injury. *J Cereb Blood Flow Metab* 35, 1090–1099. doi:10.1038/jcbfm.2015.93

Geevarghese, A., and Herman, I. M. (2014). Pericyte-endothelial cross-talk: implications and opportunities for advanced cellular therapies. *Transl. Res.* 163, 296–306. doi:10.1016/j.trsl.2014.01.011

George, P. M., Bliss, T. M., Hua, T., Lee, A., Oh, B., Levinson, A., et al. (2017). Electrical preconditioning of stem cells with a conductive polymer scaffold enhances stroke recovery. *Biomaterials* 142, 31–40. doi:10.1016/j.biomaterials.2017.07.020

Ghuman, H., Massensini, A. R., Donnelly, J., Kim, S.-M., Medberry, C. J., Badylak, S. F., et al. (2016). ECM hydrogel for the treatment of stroke: characterization of the host cell infiltrate. *Biomaterials* 91, 166–181. doi:10.1016/j.biomaterials.2016.03.014

Ghuman, H., and Modo, M. (2016). Biomaterial applications in neural therapy and repair. *Chin Neurosurg J* 2, 34. doi:10.1186/s41016-016-0057-0

Girouard, H., and Iadecola, C. (2006). Neurovascular coupling in the normal brain and in hypertension, stroke, and Alzheimer disease. *J. Appl. Physiol.* 100, 328–335. doi:10.1152/japplphysiol.00966.2005

Goldberg, J. S., and Hirschi, K. K. (2009). Diverse roles of the vasculature within the neural stem cell niche. *Regen. Med.* 4, 879–897. doi:10.2217/rme.09.61

Gonzalez, A. L., Gobin, A. S., West, J. L., Mcintire, L. V., and Smith, C. W. (2004). Integrin interactions with immobilized peptides in polyethylene glycol diacrylate hydrogels. *Tissue Eng.* 10, 1775–1786. doi:10.1089/ten.2004.10.1775

Gonzalez-Cano, L., Fuertes-Alvarez, S., Robledinos-Anton, N., Bizy, A., Villena-Cortes, A., Fariñas, I., et al. (2016). p73 is required for ependymal cell maturation and neurogenic SVZ cytoarchitecture. *Dev. Neurobiol.* 76, 730–747. doi:10.1002/dneu.22356

Greenberg, D. A., and Jin, K. (2006). Growth factors and stroke. *NeuroRx* 3, 458–465. doi:10.1016/j.nurx.2006.08.003

Gupta, D., Tator, C. H., and Shoichet, M. S. (2006). Fast-gelling injectable blend of hyaluronan and methylcellulose for intrathecal, localized delivery to the injured spinal cord. *Biomaterials* 27, 2370–2379. doi:10.1016/j.biomaterials.2005.11.015

Haipeng, G., Yinghui, Z., Jianchun, L., Yandao, G., Nanming, Z., and Xiufang, Z. (2000). Studies on nerve cell affinity of Chitosan-derived materials. *J. Biomed. Mater. Res.* 52, 285–295. doi:10.1002/1097-4636(200011)52:2%3C285::AID-JBM7%3E3.0.CO;2-G

Herbert, C. B., Bittner, G. D., and Hubbell, J. A. (1996). Effects of fibinolysis on neurite growth from dorsal root ganglia cultured in two- and three-dimensional fibrin gels. *J. Comp. Neurol.* 365, 380–391. doi:10.1002/(SICI)1096-9861(19960212)365:3%3C380::AID-CNE4%3E3.0.CO;2-0

Hermann, A., Maisel, M., and Storch, A. (2006). Epigenetic conversion of human adult bone mesodermal stromal cells into neuroectodermal cell types for replacement therapy of neurodegenerative disorders. *Expert Opin. Biol. Ther.* 6, 653–670. doi:10.1517/14712598.6.7.653

Ikeda, K., Yamauchi, D., Osamura, N., Hagiwara, N., and Tomita, K. (2003). Hyaluronic acid prevents peripheral nerve adhesion. *Br. J. Plast. Surg.* 56, 342–347. doi:10.1016/S0007-1226(03)00197-8

Imayoshi, I., Sakamoto, M., Yamaguchi, M., Mori, K., and Kageyama, R. (2010). Essential roles of notch signaling in maintenance of neural stem cells in developing and adult brains. *J Neurosci* 30, 3489–3498. doi:10.1523/JNEUROSCI.4987-09.2010

Ishibashi, S., Sakaguchi, M., Kuroiwa, T., Yamasaki, M., Kanemura, Y., Shizuko, I., et al. (2004). Human neural stem/progenitor cells, expanded in long-term neurosphere culture, promote functional recovery after focal ischemia in Mongolian gerbils. *J. Neurosci. Res.* 78, 215–223. doi:10.1002/jnr.20246

Jensen, M. B., Yan, H., Krishnaney-Davison, R., Al Sawaf, A., and Zhang, S.-C. (2013). Survival and differentiation of transplanted neural stem cells derived from human induced pluripotent stem cells in a rat stroke model. *J Stroke Cerebrovasc Dis* 22, 304–308. doi:10.1016/j.jstrokecerebrovasdis.2011.09.008

Kalladka, D., and Muir, K. W. (2014). Brain repair: cell therapy in stroke. *Stem Cells Cloning* 7, 31–44. doi:10.2147/SCCAA.S38003

Karoubi, G., Ormiston, M. L., Stewart, D. J., and Courtman, D. W. (2009). Single-cell hydrogel encapsulation for enhanced survival of human marrow stromal cells. *Biomaterials* 30, 5445–5455. doi:10.1016/j.biomaterials.2009.06.035

Karpowicz, P., Willaime-Morawek, S., Balenci, L., Deveale, B., Inoue, T., and Van Der Kooy, D. (2009). E-cadherin regulates neural stem cell self-renewal. *J Neurosci* 29, 3885–3896. doi:10.1523/JNEUROSCI.0037-09.2009

Khaing, Z. Z., Thomas, R. C., Geissler, S. A., and Schmidt, C. E. (2014). Advanced biomaterials for repairing the nervous system: what can hydrogels do for the brain? *Mater. Today* 17, 332–340. doi:10.1016/j.mattod.2014.05.011

Kim, S. U. (2004). Human neural stem cells genetically modified for brain repair in neurological disorders. *Neuropathology* 24, 159–171. doi:10.1111/j.1440-1789.2004.00552.x

Knapp, D. M., Barocas, V. H., Moon, A. G., Yoo, K., Petzold, L. R., and Tranquillo, R. T. (1997). Rheology of reconstituted type I collagen gel in confined compression. *J Rheol* 41, 971–993. doi:10.1122/1.550817

Korn, J., Christ, B., and Kurz, H. (2002). Neuroectodermal origin of brain pericytes and vascular smooth muscle cells. *J. Comp. Neurol.* 442, 78–88. doi:10.1002/cne.1423

Kriegstein, A., and Alvarez-Buylla, A. (2009). The glial nature of embryonic and adult neural stem cells. *Annu. Rev. Neurosci.* 32, 149–184. doi:10.1146/annurev.neuro.051508.135600

Krupinski, J., Kaluza, J., Kumar, P., Kumar, S., and Wang, J. M. (1994). Role of angiogenesis in patients with cerebral ischemic stroke. *Stroke* 25, 1794–1798. doi:10.1161/01.STR.25.9.1794

Lacar, B., Herman, P., Platel, J.-C., Kubera, C., Hyder, F., and Bordey, A. (2012). Neural progenitor cells regulate capillary blood flow in the postnatal subventricular zone. *J. Neurosci.* 32, 16435–16448. doi:10.1523/JNEUROSCI.1457-12.2012

Lalancette-Hebert, M., Gowing, G., Simard, A., Weng, Y. C., and Kriz, J. (2007). Selective ablation of proliferating microglial cells exacerbates ischemic injury in the brain. *J. Neurosci.* 27, 2596–2605. doi:10.1523/JNEUROSCI.5360-06.2007

Lambertsen, K. L., Meldgaard, M., Ladeby, R., and Finsen, B. (2005). A quantitative study of microglial-macrophage synthesis of tumor necrosis factor during acute and late focal cerebral ischemia in mice. *J. Cereb. Blood Flow Metab.* 25, 119–135. doi:10.1038/sj.jcbfm.9600014

Lampe, K. J., Bjugstad, K. B., and Mahoney, M. J. (2010). Impact of degradable macromer content in a poly(ethylene glycol) hydrogel on neural cell metabolic activity, redox state, proliferation, and differentiation. *Tissue Eng. Part A* 16, 1857–1866. doi:10.1089/ten.tea.2009.0509

Lee, C. R., Grodzinsky, A. J., and Spector, M. (2001). The effects of cross-linking of collagen-glycosaminoglycan scaffolds on compressive stiffness, chondrocyte-mediated contraction, proliferation and biosynthesis. *Biomaterials* 22, 3145–3154. doi:10.1016/S0142-9612(01)00067-9

Lee, S., Valmikinathan, C. M., Byun, J., Kim, S., Lee, G., Mokarram, N., et al. (2015). Enhanced therapeutic neovascularization by CD31-expressing cells and embryonic stem cell-derived endothelial cells engineered with chitosan hydrogel containing VEGF-releasing microtubes. *Biomaterials* 63, 158–167. doi:10.1016/j.biomaterials.2015.06.009

Lehtinen, M. K., Zappaterra, M. W., Chen, X., Yang, Y. J., Hill, A. D., Lun, M., et al. (2011). The cerebrospinal fluid provides a proliferative niche for neural progenitor cells. *Neuron* 69, 893–905. doi:10.1016/j.neuron.2011.01.023

Leipzig, N. D., and Shoichet, M. S. (2009). The effect of substrate stiffness on adult neural stem cell behavior. *Biomaterials* 30, 6867–6878. doi:10.1016/j.biomaterials.2009.09.002

Lemons, M. L., and Condic, M. L. (2008). Integrin signaling is integral to regeneration. *Exp. Neurol.* 209, 343–352. doi:10.1016/j.expneurol.2007.05.027

Liang, Y., Walczak, P., and Bulte, J. W. M. (2013). The survival of engrafted neural stem cells within hyaluronic acid hydrogels. *Biomaterials* 34, 5521–5529. doi:10.1016/j.biomaterials.2013.03.095

Lim, D. A., Tramontin, A. D., Trevejo, J. M., Herrera, D. G., Garcia-Verdugo, J. M., and Alvarez-Buylla, A. (2000). Noggin antagonizes BMP signaling to create a niche for adult neurogenesis. *Neuron* 28, 713–726. doi:10.1016/S0896-6273(00)00148-3

Lindvall, O., and Kokaia, Z. (2010). Stem cells in human neurodegenerative disorders – time for clinical translation? *J. Clin. Invest.* 120, 29–40. doi:10.1172/JCI40543

Marlier, Q., Verteneuil, S., Vandenbosch, R., and Malgrange, B. (2015). Mechanisms and functional significance of stroke-induced neurogenesis. *Front. Neurosci.* 9:458. doi:10.3389/fnins.2015.00458

Marthiens, V., Kazanis, I., Moss, L., Long, K., and Ffrench-Constant, C. (2010). Adhesion molecules in the stem cell niche – more than just staying in shape? *J. Cell. Sci.* 123, 1613–1622. doi:10.1242/jcs.054312

Marti, H. J. H., Bernaudin, M., Bellail, A., Schoch, H., Euler, M., Petit, E., et al. (2000). Hypoxia-induced vascular endothelial growth factor expression precedes neovascularization after cerebral ischemia. *Am. J. Pathol.* 156, 965–976. doi:10.1016/S0002-9440(10)64964-4

Mdzinarishvili, A., Sutariya, V., Talasila, P. K., Geldenhuys, W. J., and Sadana, P. (2013). Engineering triiodothyronine (T3) nanoparticle for use in ischemic brain stroke. *Drug Deliv Transl Res* 3, 309–317. doi:10.1007/s13346-012-0117-8

Menon, B. K., Campbell, B. C. V., Levi, C., and Goyal, M. (2015). Role of imaging in current acute ischemic stroke workflow for endovascular therapy. *Stroke* 46, 1453–1461. doi:10.1161/STROKEAHA.115.009160

Moskowitz, M. A., Lo, E. H., and Iadecola, C. (2010). The science of stroke: mechanisms in search of treatments. *Neuron* 67, 181–198. doi:10.1016/j.neuron.2010.07.002

Mozaffarian, D., Benjamin, E. J., Go, A. S., Arnett, D. K., Blaha, M. J., Cushman, M., et al. (2016). Executive summary: heart disease and stroke statistics – 2016 update: a report from the American Heart Association. *Circulation* 133, 447–454. doi:10.1161/CIR.0000000000000366

Nakaguchi, K., Jinnou, H., Kaneko, N., Sawada, M., Hikita, T., Saitoh, S., et al. (2012). Growth factors released from gelatin hydrogel microspheres increase new neurons in the adult mouse brain. *Stem Cells Int.* 2012, 7. doi:10.1155/2012/915160

Ng, S.-C., De La Monte, S. M., Conboy, G. L., Karns, L. R., and Fishman, M. C. (1988). Cloning of human GAP 43: growth association and ischemic resurgence. *Neuron* 1, 133–139. doi:10.1016/0896-6273(88)90197-3

Nomura, T., Göritz, C., Catchpole, T., Henkemeyer, M., and Frisén, J. (2010). EphB signaling controls lineage plasticity of adult neural stem cell niche cells. *Cell Stem Cell* 7, 730–743. doi:10.1016/j.stem.2010.11.009

Nour, M., and Liebeskind, D. S. (2014). Imaging of cerebral ischemia: from acute stroke to chronic disorders. *Neurol. Clin.* 32, 193–209. doi:10.1016/j.ncl.2013.1007.1005

Nour, M., Scalzo, F., and Liebeskind, D. S. (2013). Ischemia-reperfusion injury in stroke. *Interv Neurol* 1, 185–199. doi:10.1159/000353125

Nur, E. K. A., Ahmed, I., Kamal, J., Babu, A. N., Schindler, M., and Meiners, S. (2008). Covalently attached FGF-2 to three-dimensional polyamide nanofibrillar surfaces demonstrates enhanced biological stability and activity. *Mol. Cell. Biochem.* 309, 157–166. doi:10.1007/s11010-007-9654-8

Ottone, C., Krusche, B., Whitby, A., Clements, M., Quadrato, G., Pitulescu, M. E., et al. (2014). Direct cell–cell contact with the vascular niche maintains quiescent neural stem cells. *Nat. Cell Biol.* 16, 1045–1056. doi:10.1038/ncb3045

Park, K. I., Teng, Y. D., and Snyder, E. Y. (2002). The injured brain interacts reciprocally with neural stem cells supported by scaffolds to reconstitute lost tissue. *Nat Biotechnol* 20, 1111–1117. doi:10.1038/nbt751

Parlato, M., Reichert, S., Barney, N., and Murphy, W. L. (2014). Poly(ethylene glycol) hydrogels with adaptable mechanical and degradation properties for use in biomedical applications(). *Macromol. Biosci.* 14, 687–698. doi:10.1002/mabi.201300418

Patel, A. R., Ritzel, R., Mccullough, L. D., and Liu, F. (2013). Microglia and ischemic stroke: a double-edged sword. *Int. J. Physiol. Pathophysiol. Pharmacol.* 5, 73–90.

Potts, M. B., Silvestrini, M. T., and Lim, D. A. (2013). Devices for cell transplantation into the central nervous system: design considerations and emerging technologies. *Surg. Neurol. Int.* 4, S22–S30. doi:10.4103/2152-7806.109190

Qian, L., and Saltzman, W. M. (2004). Improving the expansion and neuronal differentiation of mesenchymal stem cells through culture surface modification. *Biomaterials* 25, 1331–1337. doi:10.1016/j.biomaterials.2003.08.013

Ramirez-Castillejo, C., Sanchez-Sanchez, F., Andreu-Agullo, C., Ferron, S. R., Aroca-Aguilar, J. D., Sanchez, P., et al. (2006). Pigment epithelium-derived factor is a niche signal for neural stem cell renewal. *Nat. Neurosci.* 9, 331–339. doi:10.1038/nn1657

Reyes, J. H., O'Shea, K. S., Wys, N. L., Velkey, J. M., Prieskorn, D. M., Wesolowski, K., et al. (2008). Glutamatergic neuronal differentiation of mouse embryonic stem cells following transient expression of neurogenin 1 and treatment with BDNF and GDNF: in vitro and in vivo studies. *J. Neurosci.* 28, 12622–12631. doi:10.1523/JNEUROSCI.0563-08.2008

Romanic, A. M., White, R. F., Arleth, A. J., Ohlstein, E. H., and Barone, F. C. (1998). Matrix metalloproteinase expression increases after cerebral focal ischemia in rats: inhibition of matrix metalloproteinase-9 reduces infarct size. *Stroke* 29, 1020–1030. doi:10.1161/01.STR.29.5.1020

Roudsari, L. C., Jeffs, S. E., Witt, A. S., Gill, B. J., and West, J. L. (2016). A 3D poly(ethylene glycol)-based tumor angiogenesis model to study the influence of vascular cells on lung tumor cell behavior. *Sci. Rep.* 6, 32726. doi:10.1038/srep32726

Ruan, G. P., Han, Y. B., Wang, T. H., Xing, Z. G., Zhu, X. B., Yao, X., et al. (2013). Comparative study among three different methods of bone marrow mesenchymal stem cell transplantation following cerebral infarction in rats. *Neurol. Res.* 35, 212–220. doi:10.1179/1743132812Y.0000000152

Ruan, L., Wang, B., Zhuge, Q., and Jin, K. (2015). Coupling of neurogenesis and angiogenesis after ischemic stroke. *Brain Res.* 1623, 166–173. doi:10.1016/j.brainres.2015.02.042

Rustenhoven, J., Aalderink, M., Scotter, E. L., Oldfield, R. L., Bergin, P. S., Mee, E. W., et al. (2016). TGF-beta1 regulates human brain pericyte inflammatory processes involved in neurovasculature function. *J. Neuroinflammation* 13, 37. doi:10.1186/s12974-016-0503-0

Salinas, C. N., and Anseth, K. S. (2008). The influence of the RGD peptide motif and its contextual presentation in PEG gels on human mesenchymal stem cell viability. *J. Tissue Eng. Regen. Med.* 2, 296–304. doi:10.1002/term.95

Seidlits, S. K., Khaing, Z. Z., Petersen, R. R., Nickels, J. D., Vanscoy, J. E., Shear, J. B., et al. (2010). The effects of hyaluronic acid hydrogels with tunable mechanical

properties on neural progenitor cell differentiation. *Biomaterials* 31, 3930–3940. doi:10.1016/j.biomaterials.2010.01.125

Sharma, V., Ling, T. W., Rewell, S. S., Hare, D. L., Howells, D. W., Kourakis, A., et al. (2012). A novel population of α-smooth muscle actin-positive cells activated in a rat model of stroke: an analysis of the spatio-temporal distribution in response to ischemia. *J Cereb Blood Flow Metab* 32, 2055–2065. doi:10.1038/jcbfm.2012.107

Shen, Q., Wang, Y., Kokovay, E., Lin, G., Chuang, S.-M., Goderie, S. K., et al. (2008). Adult SVZ stem cells lie in a vascular niche: a quantitative analysis of niche cell-cell interactions. *Cell Stem Cell* 3, 289–300. doi:10.1016/j.stem.2008.07.026

Shoichet, M. S., Tator, C. H., Poon, P., Kang, C., and Douglas Baumann, M. (2007). Intrathecal drug delivery strategy is safe and efficacious for localized delivery to the spinal cord. *Prog. Brain Res.* 161, 385–392. doi:10.1016/S0079-6123(06)61027-3

Sobel, R. A. (1998). The extracellular matrix in multiple sclerosis lesions. *J. Neuropathol. Exp. Neurol.* 57, 205–217. doi:10.1097/00005072-199803000-00001

Sommer, C. J. (2017). Ischemic stroke: experimental models and reality. *Acta Neuropathol.* 133, 245–261. doi:10.1007/s00401-017-1667-0

Spassky, N., Merkle, F. T., Flames, N., Tramontin, A. D., Garcia-Verdugo, J. M., and Alvarez-Buylla, A. (2005). Adult ependymal cells are postmitotic and are derived from radial glial cells during embryogenesis. *J. Neurosci.* 25, 10–18. doi:10.1523/JNEUROSCI.1108-04.2005

Stewart, E., Kobayashi, N. R., Higgins, M. J., Quigley, A. F., Jamali, S., Moulton, S. E., et al. (2015). Electrical stimulation using conductive polymer polypyrrole promotes differentiation of human neural stem cells: a biocompatible platform for translational neural tissue engineering. *Tissue Eng. Part C Methods* 21, 385–393. doi:10.1089/ten.TEC.2014.0338

Stolp, H. B., and Molnár, Z. (2015). Neurogenic niches in the brain: help and hindrance of the barrier systems. *Front. Neurosci.* 9:20. doi:10.3389/fnins.2015.00020

Struzyna, L. A., Katiyar, K., and Cullen, D. K. (2014). Living scaffolds for neuroregeneration. *Curr Opin Solid State Mater Sci* 18, 308–318. doi:10.1016/j.cossms.2014.07.004

Tabata, H., Yoshinaga, S., and Nakajima, K. (2012). Cytoarchitecture of mouse and human subventricular zone in developing cerebral neocortex. *Exp Brain Res* 216, 161–168. doi:10.1007/s00221-011-2933-3

Tate, M. C., Shear, D. A., Hoffman, S. W., Stein, D. G., and Laplaca, M. C. (2001). Biocompatibility of methylcellulose-based constructs designed for intracerebral gelation following experimental traumatic brain injury. *Biomaterials* 22, 1113–1123. doi:10.1016/S0142-9612(00)00348-3

Taylor, S. J., Mcdonald, J. W., and Sakiyama-Elbert, S. E. (2004). Controlled release of neurotrophin-3 from fibrin gels for spinal cord injury. *J Control Release* 98, 281–294. doi:10.1016/j.jconrel.2004.05.003

Thomson, J. A., Itskovitz-Eldor, J., Shapiro, S. S., Waknitz, M. A., Swiergiel, J. J., Marshall, V. S., et al. (1998). Embryonic stem cell lines derived from human blastocysts. *Science* 282, 1145–1147. doi:10.1126/science.282.5391.1145

Trounson, A., and McDonald, C. (2015). Stem cell therapies in clinical trials: progress and challenges. *Cell Stem Cell* 17, 11–22. doi:10.1016/j.stem.2015.06.007

Vercruysse, K. P., and Prestwich, G. D. (1998). Hyaluronate derivatives in drug delivery. *Crit. Rev. Ther. Drug Carrier Syst.* 15, 513–555. doi:10.1615/CritRevTherDrugCarrierSyst.v15.i5.30

Vishwakarma, S. K., Bardia, A., Tiwari, S. K., Paspala, S. A. B., and Khan, A. A. (2014). Current concept in neural regeneration research: NSCs isolation, characterization and transplantation in various neurodegenerative diseases and stroke: a review. *J. Adv. Res.* 5, 277–294. doi:10.1016/j.jare.2013.04.005

Wakabayashi, K., Nagai, A., Sheikh, A. M., Shiota, Y., Narantuya, D., Watanabe, T., et al. (2010). Transplantation of human mesenchymal stem cells promotes functional improvement and increased expression of neurotrophic factors in a rat focal cerebral ischemia model. *J. Neurosci. Res.* 88, 1017–1025. doi:10.1002/jnr.22279

Weinstein, J. R., Koerner, I. P., and Möller, T. (2010). Microglia in ischemic brain injury. *Future Neurol.* 5, 227–246. doi:10.2217/fnl.10.1

Wells, M. R., Kraus, K., Batter, D. K., Blunt, D. G., Weremowitz, J., Lynch, S. E., et al. (1997). Gel matrix vehicles for growth factor application in nerve gap injuries repaired with tubes: a comparison of biomatrix, collagen, and methylcellulose. *Exp. Neurol.* 146, 395–402. doi:10.1006/exnr.1997.6543

Welser-Alves, J. V., Boroujerdi, A., and Milner, R. (2014). Isolation and culture of primary mouse brain endothelial cells. *Methods Mol. Biol.* 1135, 345–356. doi:10.1007/978-1-4939-0320-7_28

Williams, L. R., Longo, F. M., Powell, H. C., Lundborg, G., and Varon, S. (1983). Spatial-temporal progress of peripheral nerve regeneration within a silicone chamber: parameters for a bioassay. *J. Comp. Neurol.* 218, 460–470. doi:10.1002/cne.902180409

Wood, M. D., Borschel, G. H., and Sakiyama-Elbert, S. E. (2009). Controlled release of glial-derived neurotrophic factor from fibrin matrices containing an affinity-based delivery system. *J. Biomed. Mater. Res. A.* 89A, 909–918. doi:10.1002/jbm.a.32043

Yang, B., Migliati, E., Parsha, K., Schaar, K., Xi, X., Aronowski, J., et al. (2013). Intra-arterial delivery is not superior to intravenous delivery of autologous bone marrow mononuclear cells in acute ischemic stroke. *Stroke* 44, 3463–3472. doi:10.1161/STROKEAHA.111.000821

Yang, Z., Duan, H., Mo, L., Qiao, H., and Li, X. (2010). The effect of the dosage of NT-3/chitosan carriers on the proliferation and differentiation of neural stem cells. *Biomaterials* 31, 4846–4854. doi:10.1016/j.biomaterials.2010.02.015

Yemisci, M., Gursoy-Ozdemir, Y., Vural, A., Can, A., Topalkara, K., and Dalkara, T. (2009). Pericyte contraction induced by oxidative-nitrative stress impairs capillary reflow despite successful opening of an occluded cerebral artery. *Nat. Med.* 15, 1031–1037. doi:10.1038/nm.2022

Young, C. C., Brooks, K. J., Buchan, A. M., and Szele, F. G. (2011). Cellular and molecular determinants of stroke-induced changes in subventricular zone cell migration. *Antioxid. Redox Signal.* 14, 1877–1888. doi:10.1089/ars.2010.3435

Yu, H., Cao, B., Feng, M., Zhou, Q., Sun, X., Wu, S., et al. (2010). Combinated transplantation of neural stem cells and collagen type I promote functional recovery after cerebral ischemia in rats. *Anat Rec (Hoboken)* 293, 911–917. doi:10.1002/ar.20941

Zhang, M., Methot, D., Poppa, V., Fujio, Y., Walsh, K., and Murry, C. E. (2001). Cardiomyocyte grafting for cardiac repair: graft cell death and anti-death strategies. *J. Mol. Cell. Cardiol.* 33, 907–921. doi:10.1006/jmcc.2001.1367

Zhong, J., Chan, A., Morad, L., Kornblum, H. I., Fan, G., and Carmichael, S. T. (2010). Hydrogel matrix to support stem cell survival after brain transplantation in stroke. *Neurorehabil. Neural Repair* 24, 636–644. doi:10.1177/1545968310361958

Conflict of Interest Statement: The authors declare that the research was conducted in the absence of any commercial or financial relationships that could be construed as a potential conflict of interest.

frontiers in Materials

PERSPECTIVE
published: 09 May 2018
doi: 10.3389/fmats.2018.00027

Perspective on Translating Biomaterials Into Glioma Therapy: Lessons From *in Vitro* Models

*R. Chase Cornelison and Jennifer M. Munson**

Department of Biomedical Engineering and Mechanics, Virginia Polytechnic Institute and State University, Blacksburg, VA, United States

Glioblastoma (GBM) is the most common and malignant form of brain cancer. Even with aggressive standard of care, GBM almost always recurs because its diffuse, infiltrative nature makes these tumors difficult to treat. The use of biomaterials is one strategy that has been, and is being, employed to study and overcome recurrence. Biomaterials have been used in GBM in two ways: *in vitro* as mediums in which to model the tumor microenvironment, and *in vivo* to sustain release of cytotoxic therapeutics. *In vitro* systems are a useful platform for studying the effects of drugs and tissue-level effectors on tumor cells in a physiologically relevant context. These systems have aided examination of how glioma cells respond to a variety of natural, synthetic, and semi-synthetic biomaterials with varying substrate properties, biochemical factor presentations, and non-malignant parenchymal cell compositions in both 2D and 3D environments. The current *in vivo* paradigm is completely different, however. Polymeric implants are simply used to line the post-surgical resection cavities and deliver secondary therapies, offering moderate impacts on survival. Instead, perhaps we can use the data generated from *in vitro* systems to design novel biomaterial-based treatments for GBM akin to a tissue engineering approach. Here we offer our perspective on the topic, summarizing how biomaterials have been used to identify facets of glioma biology *in vitro* and discussing the elements that show promise for translating these systems *in vivo* as new therapies for GBM.

Keywords: glioblastoma, biomaterial, hydrogel, regenerative medicine, tissue engineering, brain, tumor microenvironment

OPEN ACCESS

Edited by:
Sara Pedron, University of Illinois at Urbana-Champaign, United States

Reviewed by:
Pilnam Kim, Korea Advanced Institute of Science & Technology (KAIST), South Korea
Alexander Birbrair, Universidade Federal de Minas Gerais, Brazil

****Correspondence:***
Jennifer M. Munson
munsonj@vt.edu

Specialty section:
This article was submitted to Biomaterials, a section of the journal Frontiers in Materials

Received: *01 February 2018*
Accepted: *19 April 2018*
Published: *09 May 2018*

Citation:
Cornelison RC and Munson JM (2018) Perspective on Translating Biomaterials Into Glioma Therapy: Lessons From in Vitro Models. Front. Mater. 5:27. doi: 10.3389/fmats.2018.00027

INTRODUCTION

Glioblastoma (GBM) is a high-grade brain cancer that almost always recurs (Cuddapah et al., 2014). Many *in vitro* and *in vivo* models of GBM have been developed in an effort to uncover new therapeutic strategies. Biomaterials are often primary components of *in vitro* models to chemically, mechanically, and/or topographically recreate the physiological tumor environment, as recently reviewed by Xiao et al. (2017), Gu and Mooney (2015), Pradhan et al. (2016), Cha and Kim (2017), and Heffernan and Sirianni (2018).

While GBM models are useful for studying glioma biology, the field is far from accurately predicting clinical success of a new therapy. It was recently suggested that all models, including gold-standard mouse xenografts, inherently cannot preserve the genetic landscape of patient-derived tumor cells (Ben-David et al., 2017). Where does this study (and others

like it) leave the field? Glioma is a tissue, with complex heterogeneity in tissue geometry, composition, biophysical properties, etc. Even if researchers can create sophisticated models of the tumor, these models cannot logistically account for every element of the *in vivo* environment. Therefore, a tissue-level approach may enhance our ability to treat this deadly disease.

In vitro biomaterial research has revealed crucial information about material-GBM cell interactions. And yet, implementation of biomaterials *in vivo* for treating GBM has been limited to anti-tumor drug delivery, such as BCNU-releasing Gliadel wafers (Wait et al., 2015). These wafers, made of a poly(lactic-co-glycolic) polymer backbone, have been used to line resection cavities in patients receiving surgical removal of primary tumors and offer a modest, yet significant, increase in survival. However, these systems are simply a conduit for therapy and thus in no way leverage glioma-biomaterial interactions as part of the therapy.

Many diseases are now being viewed from a regenerative medicine lens, using factors within the patient's own body to promote healing. Cancer is often described as a wound that does not heal and may similarly benefit from this approach. The fluid-filled cavity remaining after resection is a prime space in which to examine biomaterial-based therapies, analogous to experimental treatments for stroke or traumatic brain injury. In current literature, treating the post-resection cavity has primarily involved hydrogel biomaterials as passive vehicles for drug therapy (Bagó et al., 2016; Bastiancich et al., 2017). It is possible that translating collective knowledge from myriad *in vitro* models could instead transition biomaterials to an active avenue for cancer remediation. Below, we summarize current understanding of how glioma outcomes can be altered *in vitro* and offer perspectives for using this data to design biomaterials for promoting anti-tumor responses, tumor targeting, and treatment against glioblastoma.

TUNING THE EXTRACELLULAR MATRIX

Matrix Composition

While earlier experiments with glioma cells used 2D plastic, it is now understood that the underlying matrix plays an important role in glioma phenotype (Eke and Cordes, 2011; Florczyk et al., 2013; Heffernan et al., 2015). The composition of the brain matrix is different from most tissues, primarily comprising the polysaccharide hyaluronic acid (HA) and HA-binding proteoglycans, but few fibrillar proteins. Many engineered *in vitro* systems for GBM therefore employ HA-based matrices. These models have elucidated that HA increases stem cell maintenance, glioma cell adhesion and migration, and markers of malignancy (Pedron et al., 2013; Kim and Kumar, 2014; Tilghman et al., 2014; Cha et al., 2016). Other brain components, such as certain chondroitin sulfate proteoglycans (CSPGs), have also been shown to increase glioma invasion (Logun et al., 2016). However, CSPGs have also been suggested to inhibit glioma cell invasion (Silver et al., 2013), therefore the specific response may depend on CSPG sulfation pattern (Silver and Silver, 2014).

Several *in vitro* models have been developed with components not ubiquitous in the brain, like collagen I and laminin-rich basement membrane extract (Matrigel). While mixing these components with HA can recreate the invasive phenotypes observed in pure HA hydrogels (Munson et al., 2013; Gritsenko et al., 2017), collagen and Matrigel hydrogels alone comparatively limit glioma cell invasion. Some non-native components nonetheless increase invasion: The extracellular matrix (ECM) secreted by glioma cells is itself dissimilar to the native brain and is rich in aberrant proteoglycans, tenascin-c, and an overabundance of HA (Cuddapah et al., 2014; Xia et al., 2016). For example, glioma cells secrete a truncated form of the proteoglycan brevican which binds to fibronectin and promotes invasion (Hu et al., 2008). Incorporation of RGDS, the adhesive ligand found in fibronectin, similarly induced cell dissemination in poly(ethylene) glycol hydrogels (Beck et al., 2013). Further, glioma cells adhere more strongly in HA matrices that contain RGDS, potentially due to augmented integrin-mediated mechanotransduction in HA (Chopra et al., 2014; Kim and Kumar, 2014).

Topographical Cues

Topographical cues present within the tissue can also enhance migration. While the brain is relatively non-fibrous and amorphous, basement membrane-rich blood vessels are a prime substrate on which glioma cells migrate within perivascular spaces (Cuddapah et al., 2014). Herrera-Perez et al. (2015) showed that pseudovessels of Matrigel-coated collagen-oligomer fibrils increased the speed of glioma cell migration across a 3D collagen-HA matrix. White matter tracts in the brain are also a frequent route of migration. Using core-shell electrospun nanofibers to mimic white matter tracts, Rao et al. (2013) found that glioma cell morphology, migration speed, and focal adhesion kinase expression were all sensitive to fiber mechanics and composition. Altering the design parameters of fibrous biomaterials can therefore offer precise control over glioma migration.

Mechanical Forces

A major driving force for using biomaterials in cell culture platforms is the ability to control biomechanical forces, often independently from the chemical composition. The mechanical properties of a scaffold influence a wide range of cellular behaviors, including proliferation, migration, and stem cell fate (Engler et al., 2006; Ulrich et al., 2009; Seidlits et al., 2010). It is well described that many tumors outside the brain are stiffer than the surrounding tissue. In glioma, tissue mechanics appear to be extremely heterogeneous, but the tumor is likely stiffer than normal brain, which has a Young's modulus around 1.4 kPa (Miroshnikova et al., 2016). While the exact physiological properties are controversial, stiffer matrices promote glioma dissemination. Increasing the stiffness of PEG hydrogels decreased proliferation of U87 cells and increased the number of cell protrusions (Wang et al., 2014). Similar results were found using fibronectin-based matrices on which tumor cell spread and speed of migration increased with modulus while proliferation rate decreased compared to softer substrates (Ulrich et al., 2009).

Fluid flow and shear stress are also felt by glioma cells in the tumor microenvironment (Munson and Shieh, 2014). These forces have been recreated *in vitro* using HA matrices (Polacheck et al., 2011; Qazi et al., 2011; Munson et al., 2013). Interstitial flow on the order of 0.1–1 μm/s generally increased glioma cell invasion, although patient-derived glioma stem cells showed variable responses (Kingsmore et al., 2016). Manipulation of the matrix to reduce glycocalyx assembly (Qazi et al., 2013) or CD44-binding (Kingsmore et al., 2016) attenuated these effects, indicating a link between flow and the surrounding 3D matrix.

Implications for Therapeutic Translation

Biomaterials often promote cell recruitment into an implantation site after neural injury (Ghuman et al., 2016; Nih et al., 2017). A similar approach may be beneficial for promoting glioma migration into an implanted material following resection. The properties of the implanted matrix should overcome the malignancy-enhancing properties of HA in the brain, either by disrupting binding or providing effective competition. Using a low molecular weight version of HA instead of high molecular weight may promote local anti-tumor inflammation and disrupt growth factor signaling (Fuchs et al., 2013; Rayahin et al., 2015). Incorporation of components such as fibronectin or RGDS could also preferentially promote stronger binding between invaded cells and the material vs. the parenchyma (Kim and Kumar, 2014). Fibrous materials would likely increase glioma invasion into the cavity. In fact, inducing migration through topography has already proved feasible and beneficial for GBM therapy (Jain et al., 2014). Additionally, the implanted matrix should be relatively stiffer than the brain to promote durotaxis, or migration up a stiffness gradient, of glioma cells and stem-like cells but deter migration of neural cells, which prefer softer substrates (Flanagan et al., 2002; Hadden et al., 2017). The caveat is that mechanical mismatch can promote potentially detrimental astrogliosis (Prodanov and Delbeke, 2016). Matrices that are initially stiffer and gradually soften over time may have a defined niche, in this case.

CONTROLLING BIOCHEMICAL CUE PRESENTATION

Cytokine and Growth Factor Gradients

Cytokines and growth factors originating from both glioma and parenchymal cells are associated with the progression of glioma and response to therapy, as previously reviewed (Iwami et al., 2011; Zhu et al., 2012). *In vivo*, natural heterogeneity is formed as tumor and parenchymal cells secrete biological molecules, which then differentially bind to the surrounding matrix and form gradients, sources, and sinks within the tissue. Recreating gradients *in vitro* using combinations of microfluidics, biomaterials, and various cells has been a focus of models for the study of both cancer (Keenan and Folch, 2008; Pedron et al., 2015) and regenerative medicine (Khang, 2015). Microfluidic devices and tissue culture insert models have both been used to show that *in situ* gradients of CXCL12 within 3D hydrogels directly promote glioma migration up the chemokine gradient (Munson et al., 2013; Addington et al., 2015; Kingsmore et al., 2016).

Cytokines are also implicated in the maintenance of glioma stem cells, a potential driver of glioma recurrence. Glial cells and recruited endothelial cells secrete factors such as bFGF that promote stem cell maintenance (Fessler et al., 2015). Blocking the effect of these cytokines offers potential to slow or halt proliferation of glioma cells. Affinity binding peptides have been incorporated into biomaterials for controlling release of bFGF, but these materials could inversely act as effective cytokine sinks (Lin and Anseth, 2009). A similar approach using an RNA aptamer to block PDGFRβ was shown effective at slowing glioma growth (Camorani et al., 2014). Designing materials to promote cell differentiation, as is common in regenerative medicine, may be equally applicable to treating glioma (Benoit et al., 2008).

Oxygen

Aberrant vasculature and unchecked tumor growth produce hypoxic or low oxygen-containing regions within the tumor and invading tumor clusters (called pseudopalisades; Rong et al., 2006). Hypoxia is implicated in increasing angiogenesis, stem cell maintenance, immunosuppression, and cancer cell therapeutic resistance (Colwell et al., 2017). Thus, incorporation of oxygen gradients within *in vitro* systems has been used to study a major effector of glioma outcomes. Use of 3D systems or spheroid culture naturally introduce regions of hypoxia based on thickness and permeability of the materials used. Recently, an *in vitro* PEG-based system showed that immobilization of the O_2-consuming enzymes glucose oxidase and catalase effectively induced hypoxia and upregulated genes known to contribute to cancer metastasis (Dawes et al., 2017). The opposite would therefore be useful for glioma therapy: generating oxygen gradients and preventing hypoxia. Validating this approach, a paper-based PET mesh layering system showing that linear gradients of oxygen in culture functioned as a primary chemoattractant and increased invasion of lung adenocarcinoma cells (Mosadegh et al., 2015). Oxygen-creating biomaterials have been tested in regenerative medicine, showing sustain oxygen release for weeks and reducing hypoxia until angiogenesis can occur (Pedraza et al., 2012).

Implications for Therapeutic Translation

The ability to control spatiotemporal chemical gradients within the post-resection cavity has far-reaching implications for glioma therapy. An ideal biomaterial would trigger glioma cell egress from the brain parenchyma into the material through establishing chemical gradients of chemotactic factors such as oxygen or CXCL12. Alternatively, the material could eliminate or disrupt pro-malignant cytokine signaling through either release of receptor blockers or sequestration of factors that aid glioma stem cell proliferation and maintenance. Dual-release or multi-functional biomaterials would likely be optimal. Materials that enable temporally-regulated release and/or capture dynamics, similar to those used in regenerative medicine (Spiller et al., 2015), are particularly promising since they may simultaneously promote parenchyma egress, glioma stem cell differentiation, and loss of acquired drug resistance.

REMODELING THE CELLULAR MICROENVIRONMENT

Angiogenesis

One hallmark of cancer is the ability to induce aberrant angiogenesis (Hanahan and Weinberg, 2011). Multiple models of angiogenesis have been engineered and used *in vitro* (Kimlin et al., 2013), although few have been described for co-culture of glioma cells and endothelial cells (Nguyen et al., 2016). Glioma cells secrete high levels of pro-angiogenic vascular endothelial growth factor (VEGF)-A which promotes blood vessel sprouting (Folkins et al., 2009). The ECM can act to sequester or locally retain VEGF-A, thereby amplifying resultant uncontrolled angiogenesis (Belair et al., 2016). Additionally, glioma cells *in vivo* physically displace astrocytic endfeet from the surface of blood vessels, disrupting the blood-brain barrier (BBB) and astrocytic control of vascular tone (Cuddapah et al., 2014; Watkins et al., 2014). While anti-angiogenesis strategies were initially promising for limiting glioma progression, the VEGF-specific antibody bevacizumab (Avastin) completely ablated tumor blood vessels and actually enhanced tumor growth by upregulating hypoxia-inducible pathways (Conley et al., 2012). A more apt approach may be to control availability of pro-angiogenic factors to promote vascular normalization.

Immune Cell Modulation

Another hallmark of cancer is the promotion of pro-tumor inflammation (Hanahan and Weinberg, 2011). Monocyte-derived cells can account for nearly 60% of the tumor bulk (Yuan et al., 2014). Initial studies proposed that glioma-associated macrophages were conditioned toward alternative, M2 activation, but recent evidence suggests this characterization requires refinement (Mantovani et al., 2002; Szulzewsky et al., 2015; Gabrusiewicz et al., 2016). Early in tumor development, anti-inflammatory cytokines enable tumor cells to evade the host immune response (Zitvogel et al., 2006; Razavi et al., 2016). Later, immunotolerance can occur due to secretion of tolerogenic cytokines and ligands such as TGFβ, IL-10, and PD-L1 (Razavi et al., 2016). Glioma-derived ECM molecules also alter immune cell phenotype, with periostin acting to recruit and train monocytes toward pro-tumor phenotypes and tenascin-c protecting tumor cells from immune surveillance by arresting T-cell activation (Jachetti et al., 2015; Zhou et al., 2015).

While early biomaterials aimed to reduce the immune response (Bryers et al., 2012), more recent advances have resulted in development of immunomodulatory biomaterials (Hubbell et al., 2009) and immunotherapeutic biomaterials (Swartz et al., 2012). Biomaterial-based regulation of macrophage polarization was recently reviewed elsewhere (Sridharan et al., 2015). Although regenerative approaches typically focus on promoting anti-inflammatory immune cell phenotypes, the opposite is also conceivable. These approaches could easily be tailored toward anti-cancer immunotherapy, as well. T cell modulation is a rapidly growing and promising field, with several strategies currently being tested: checkpoint inhibitor targeting of programmed cell death protein (PD)-1, chimeric antigen receptor (CAR) T cell therapy, and dendritic cell therapy (Tumeh et al., 2014; Garg et al., 2017; O'Rourke et al., 2017).

Glial Cell Modulation

The glioma tumor microenvironment uniquely contains a brain-specific class of cells known collectively as glia, in part comprising astrocytes and microglia. Astrocytes provide trophic and functional support for neurons, and microglia are the resident immune cells of the central nervous system. Glioma-associated factors such as CCL21 and the proteoglycan versican promote a pro-tumor phenotype in microglia (Vinnakota et al., 2013; Hu et al., 2015). Glioma cells communicate with astrocytes via connexin-43 gap junctions to promotes glioma invasion, potentially through exchange of double stranded DNA, as was observed with metastatic breast cancer cells (Chen et al., 2016; Sin et al., 2016).

There is limited knowledge on the effects of combining glial cells in 3D culture with glioma cells. Recent histological evidence revealed that the balance between reactive astrocytes and microglia correlated with GBM patient prognosis; therefore, it will be important to investigate the combination of these cell types in the future (Yuan et al., 2016). It also remains unclear if tumor-associated astrocytes are functionally different than other reactive astrocytes, particularly after the mechanical stress of surgical resection. Nonetheless, material interventions for tissue regeneration often target astrocytic "glial scarring." A mixture of collagen, hyaluronic acid, and Matrigel maintained astrocytes in a quiescent state *in vitro* (Placone et al., 2015). Additionally, a laminin-inspired self-assembling peptide hydrogel attenuated glial scarring following a stab injury (Maclean et al., 2017).

Implications for Therapeutic Translation

Biomaterials are routinely used to target the cellular microenvironment to promote healing. A similar approach may prove useful for limiting glioma recurrence. Implanting a material with immobilized pro-angiogenic factors may help constructively direct angiogenesis within the resection cavity to promote BBB formation and oxygen normalization while restricting vessel development in the parenchyma (Li et al., 2017). A matrix that irreversibly sequesters VEGF-A from the surrounding tumor microenvironment may have similar effects. The adaptive immune system can be redirected using biomaterial-based vaccines to elicit potent, antigen-specific T cell responses, including in glioma (Ali et al., 2011; Purwada et al., 2014; Cheung et al., 2018). Reversing pro-tumor polarization in innate immune cells and glia will likely require a nuanced balance between pro- and anti-inflammatory phenotypes. In this case, it would be useful to temporally control release and/or presentation of different factors (Spiller et al., 2015). Enzyme-releasing materials could assist in mitigating the effects of glioma-derived ECM molecules (Qu et al., 2013). Additionally, astrocytes may be specifically targeted using therapeutic connectosomes to override cell-cell communication with glioma (Gadok et al., 2016). The foremost objective must remain eliminating the cancer cells, therefore fibrous materials may again be preferred given it proves desirable to promote pro-healing phenotypes in the long run (Sridharan et al., 2015).

CONCLUSIONS

Although we use the *in vivo* environment to educate development of defined *in vitro* models, we rarely do the inverse in cancer. The complexity of glioblastoma has thus far proven difficult to capture *in vitro*, and unfortunately no current model can accurately predict the translational success of a therapy. Here, we proposed synthesizing the collective knowledge from *in vitro* models to inform tissue-level interventions through rational design of therapeutic biomaterials. Several strategies may be particularly relevant: Controlling angiogenesis by presentation of VEGF-A and FGF to enable better drug delivery to tumor remnants; induction of immunogenic response through growth factor and chemokine presentation to induce immune infiltration and anti-tumor differentiation; or increased stiffness coupled with topography and/or chemokines such as CXCL12 to encourage tumor cell migration away from healthy tissue. Regardless, using biomaterials as a tissue engineering approach to treat glioblastoma is an unexplored possibility. Because a plethora of *in vitro* models have used a host of different biomaterials and approaches, there may already be a strategy hidden within these studies that could assist in the fight against this deadly disease.

AUTHOR CONTRIBUTIONS

All authors developed the presented conceptual ideas, conducted literature review, drafted the manuscript, and approved it for publication.

FUNDING

The authors would like to acknowledge support by the National Institutes of Health (1R01CA222563-01).

REFERENCES

Addington, C. P., Heffernan, J. M., Millar-Haskell, C. S., Tucker, E. W., Sirianni, R. W., and Stabenfeldt, S. E. (2015). Enhancing neural stem cell response to SDF-1α gradients through hyaluronic acid-laminin hydrogels. *Biomaterials* 72, 11–19. doi: 10.1016/j.biomaterials.2015.08.041

Ali, O. A., Doherty, E., Bell, W. J., Fradet, T., Hudak, J., Laliberte, M. T., et al. (2011). Biomaterial-based vaccine induces regression of established intracranial glioma in rats. *Pharm. Res.* 28, 1074–1080. doi: 10.1007/s11095-010-0361-x

Bagó, J. R., Pegna, G. J., Okolie, O., and Hingtgen, S. D. (2016). Fibrin matrices enhance the transplant and efficacy of cytotoxic stem cell therapy for post-surgical cancer. *Biomaterials* 84, 42–53. doi: 10.1016/j.biomaterials.2016.01.007

Bastiancich, C., Bianco, J., Vanvarenberg, K., Ucakar, B., Joudiou, N., Gallez, B., et al. (2017). Injectable nanomedicine hydrogel for local chemotherapy of glioblastoma after surgical resection. *J. Control. Release* 264, 45–54. doi: 10.1016/j.jconrel.2017.08.019

Beck, J. N., Singh, A., Rothenberg, A. R., Elisseeff, J. H., and Ewald, A. J. (2013). The independent roles of mechanical, structural and adhesion characteristics of 3D hydrogels on the regulation of cancer invasion and dissemination. *Biomaterials* 34, 9486–9495. doi: 10.1016/j.biomaterials.2013.08.077

Belair, D. G., Miller, M. J., Wang, S., Darjatmoko, S. R., Binder, B. Y. K., Sheibani, N., et al. (2016). Differential regulation of angiogenesis using degradable VEGF-binding microspheres. *Biomaterials* 93, 27–37. doi: 10.1016/j.biomaterials.2016.03.021

Ben-David, U., Ha, G., Tseng, Y. Y., Greenwald, N. F., Oh, C., Shih, J., McFarland, J. M., et al. (2017). Patient-derived xenografts undergo mouse-specific tumor evolution. *Nat. Genet.* 49, 1567–1575. doi: 10.1038/ng.3967

Benoit, D. S., Schwartz, M. P., Durney, A. R., and Anseth, K. S. (2008). Small functional groups for controlled differentiation of hydrogel-encapsulated human mesenchymal stem cells. *Nat. Mater.* 7, 816–823. doi: 10.1038/nmat2269

Bryers, J. D., Giachelli, C. M., and Ratner, B. D. (2012). Engineering biomaterials to integrate and heal: the biocompatibility paradigm shifts. *Biotechnol. Bioeng.* 109, 1898–1911. doi: 10.1002/bit.24559

Camorani, S., Esposito, C. L., Rienzo, A., Catuogno, S., Iaboni, M., Condorelli, G., et al. (2014). Inhibition of receptor signaling and of glioblastoma-derived tumor growth by a novel PDGFRβ aptamer. *Mol. Ther.* 22, 828–841. doi: 10.1038/mt.2013.300

Cha, J., Kang, S. G., and Kim, P. (2016). Strategies of mesenchymal invasion of patient-derived brain tumors: microenvironmental adaptation. *Sci. Rep.* 6:24912. doi: 10.1038/srep24912

Cha, J., and Kim, P. (2017). Biomimetic strategies for the glioblastoma microenvironment. *Front. Mater.* 4:45. doi: 10.3389/fmats.2017.00045

Chen, Q., Boire, A., Jin, X., Valiente, M., Emrah Er, E., Lopez-Soto, A., et al. (2016). Carcinoma-astrocyte gap junctions promote brain metastasis by cGAMP transfer. *Nature* 533, 493–498. doi: 10.1038/nature18268

Cheung, A. S., Zhang, D. K. Y., Koshy, S. T., and Mooney, D. J. (2018). Scaffolds that mimic antigen-presenting cells enable *ex vivo* expansion of primary T cells. *Nat. Biotechnol.* 36, 160–169. doi: 10.1038/nbt.4047

Chopra, A., Murray, M. E., Byfield, F. J., Mendez, M. G., Halleluyan, R., Restle, D. J., et al. (2014). Augmentation of integrin-mediated mechanotransduction by hyaluronic acid. *Biomaterials* 35, 71–82. doi: 10.1016/j.biomaterials.2013.09.066

Colwell, N., Larion, M., Giles, A. J., Seldomridge, A. N., Sizdahkhani, S., Gilbert, M. R., et al. (2017). Hypoxia in the glioblastoma microenviornment: shaping the phenotype of cancer stem-like cells. *Neurooncology* 19, 887–896. doi: 10.1093/neuonc/now258

Conley, S. J., Gheordunescu, E., Kakarala, P., Newman, B., Korkaya, H., Heath, A. N., et al. (2012). Antiangiogenic agents increase breast cancer stem cells via the generation of tumor hypoxia. *Proc. Natl. Acad. Sci. U.S.A.* 109, 2784–2789. doi: 10.1073/pnas.1018866109

Cuddapah, V. A., Robel, S., Watkins, S., and Sontheimer, H. (2014). A neurocentric perspective on glioma invasion. *Nat. Rev. Neurosci.* 15, 455–465. doi: 10.1038/nrn3765

Dawes, C. S., Konig, H., and Lin, C. C. (2017). Enzyme-immobilized hydrogels to create hypoxia for *in vitro* cancer cell culture. *J. Biotechnol.* 248, 25–34. doi: 10.1016/j.jbiotec.2017.03.007

Eke, I., and Cordes, N. (2011). Radiobiology goes 3D: how ECM and cell morphology impact on cell survival after irradiation. *Radiother. Oncol.* 99, 271–278. doi: 10.1016/j.radonc.2011.06.007

Engler, A. J., Sen, S., Sweeney, H. L., and Discher, D. E. (2006). Matrix elasticity directs stem cell lineage specification. *Cell* 126, 677–689. doi: 10.1016/j.cell.2006.06.044

Fessler, E., Borovski, T., and Medema, J. P. (2015). Endothelial cells induce cancer stem cell features in differentiated glioblastoma cells via bFGF. *Mol. Cancer* 14:157. doi: 10.1186/s12943-015-0420-3

Flanagan, L. A., Ju, Y. E., Marg, B., Osterfield, M., and Janmey, P. A. (2002). Neurite branching on deformable substrates. *Neuroreport* 13, 2411–2415. doi: 10.1097/00001756-200212200-00007

Florczyk, S. J., Wang, K., Jana, S., Wood, D. L., Sytsma, S. K., Sham, J., et al. (2013). Porous chitosan-hyaluronic acid scaffolds as a mimic of glioblastoma microenvironment ECM. *Biomaterials* 34, 10143–10150. doi: 10.1016/J.BIOMATERIALS.2013.09.034

Folkins, C., Shaked, Y., Man, S., Tang, T., Lee, C. R., Zhu, Z., et al. (2009). Glioma tumor stem-like cells promote tumor angiogenesis and vasculogenesis via vascular endothelial growth factor and stromal-derived factor 1. *Cancer Res.* 69, 7243–7251. doi: 10.1158/0008-5472.CAN-09-0167

Fuchs, K., Hippe, A., Schmaus, A., Homey, B., Sleeman, J. P., and Orian-Rousseau, V. (2013). Opposing effects of high- and low-molecular weight hyaluronan on CXCL12-Induced CXCR4 signaling depend on CD44. *Cell Death Dis.* 4, e819–e819. doi: 10.1038/cddis.2013.364

Gabrusiewicz, K., Rodriguez, B., Wei, J., Hashimoto, Y., Healy, L. M., Maiti, S. N., et al. (2016). Glioblastoma-infiltrated innate immune cells resemble M0 macrophage phenotype. *JCI Insight* 1:e85841. doi: 10.1172/jci.insight.85841

Gadok, A. K., Busch, D. J., Ferrati, S., Li, B., Smyth, H. D., and Stachowiak, J. C. (2016). Connectosomes for direct molecular delivery to the cellular cytoplasm. *J. Am. Chem. Soc.* 138, 12833–12840. doi: 10.1021/jacs.6b05191

Garg, A. D., Coulie, P. G., Van den Eynde, B. J., and Agostinis, P. (2017). Integrating next-generation dendritic cell vaccines into the current cancer immunotherapy landscape. *Trends Immunol.* 38, 577–593. doi: 10.1016/j.it.2017.05.006

Ghuman, H., Massensini, A. R., Donnelly, J., Kim, S. M., Medberry, C. J., Badylak, S. F., et al. (2016). ECM hydrogel for the treatment of stroke: characterization of the host cell infiltrate. *Biomaterials* 91, 166–181. doi: 10.1016/j.biomaterials.2016.03.014

Gritsenko, P., Leenders, W., and Friedl, P. (2017). Recapitulating in vivo-like plasticity of glioma cell invasion along blood vessels and in astrocyte-rich stroma. *Histochem. Cell Biol.* 148, 395–406. doi: 10.1007/s00418-017-1604-2

Gu, L., and Mooney, D. J. (2015). Biomaterials and emerging anticancer therapeutics: engineering the microenvironment. *Nat. Rev. Cancer* 16, 56–66. doi: 10.1038/nrc.2015.3

Hadden, W. J., Young, J. L., Holle, A. W., McFetridge, M. L., Kim, D. Y., Wijesinghe, P., et al. (2017). Stem cell migration and mechanotransduction on linear stiffness gradient hydrogels. *Proc. Natl. Acad. Sci. U.S.A.* 114, 5647–5652. doi: 10.1073/pnas.1618239114

Hanahan, D., and Weinberg, R. A. (2011). Hallmarks of cancer: the next generation. *Cell* 144, 646–674. doi: 10.1016/j.cell.2011.02.013

Heffernan, J. M., Overstreet, D. J., Le, L. D., Vernon, B. L., and Sirianni, R. W. (2015). Bioengineered scaffolds for 3D analysis of glioblastoma proliferation and invasion. *Ann. Biomed. Eng.* 43, 1965–1977. doi: 10.1007/s10439-014-1223-1

Heffernan, J. M., and Sirianni, R. W. (2018). Modeling microenvironmental regulation of glioblastoma stem cells: a biomaterials perspective. *Front. Mater.* 5:7. doi: 10.3389/fmats.2018.00007

Herrera-Perez, M., Voytik-Harbin, S. L., and Rickus, J. L. (2015). "Extracellular matrix properties regulate the migratory response of glioblastoma stem cells in three-dimensional culture," in *Tissue Engineering Part A 21 (19–20)* (New Rochelle, NY: Mary Ann Liebert, Inc.), 2572–2582.

Hu, F., a Dzaye, O. D., Hahn, A., Yu, Y., Scavetta, R. J., Dittmar, G., et al. (2015). Glioma-derived versican promotes tumor expansion via glioma-associated microglial/macrophages Toll-like receptor 2 signaling. *Neuro Oncol.* 17, 200–210. doi: 10.1093/neuonc/nou324

Hu, B., Kong, L. L., Matthews, R. T., and Viapiano, M. S. (2008). The Proteoglycan brevican binds to fibronectin after proteolytic cleavage and promotes glioma cell motility. *J. Biol. Chem.* 283, 24848–24859. doi: 10.1074/jbc.M801433200

Hubbell, J. A., Thomas, S. N., and Swartz, M. A. (2009). Materials engineering for immunomodulation. *Nature* 462, 449–460. doi: 10.1038/nature08604

Iwami, K., Natsume, A., and Wakabayashi, T. (2011). Cytokine networks in glioma. *Neurosurg. Rev.* 34, 253–264. doi: 10.1007/s10143-011-0320-y

Jachetti, E., Caputo, S., Mazzoleni, S., Brambillasca, C. S., Parigi, S. M., Grioni, M., et al. (2015). Tenascin-C protects cancer stem-like cells from immune surveillance by arresting T-cell activation. *Cancer Res.* 75, 2095–2108. doi: 10.1158/0008-5472.CAN-14-2346

Jain, A., Betancur, M., Patel, G. D., Valmikinathan, C. M., Mukhatyar, V. J., Vakharia, A., et al. (2014). Guiding intracortical brain tumour cells to an extracortical cytotoxic hydrogel using aligned polymeric nanofibres. *Nat. Mater.* 13, 308–316. doi: 10.1038/nmat3878

Keenan, T. M., and Folch, A. (2008). Biomolecular gradients in cell culture systems. *Lab. Chip* 8, 34–57. doi: 10.1039/b711887b

Khang, G. (2015). Evolution of gradient concept for the application of regenerative medicine. *Biosurface Biotribol.* 1, 202–213. doi: 10.1016/j.bsbt.2015.08.004

Kim, Y., and Kumar, S. (2014). CD44-mediated adhesion to hyaluronic acid contributes to mechanosensing and invasive motility. *Mol. Cancer Res.* 12, 1416–1429. doi: 10.1158/1541-7786.MCR-13-0629

Kimlin, L. C., Casagrande, G., and Virador, V. M. (2013). *In vitro* three-dimensional (3D) models in cancer research: an update. *Mol. Carcinog.* 52, 167–182. doi: 10.1002/mc.21844

Kingsmore, K. M., Logsdon, D. K., Floyd, D. H., Peirce, S. M., Purow, B. W., and Munson, J. M. (2016). Interstitial flow differentially increases patient-derived glioblastoma stem cell invasion via CXCR4, CXCL12, and CD44-mediated mechanisms. *Integr. Biol.* 8, 1246–1260. doi: 10.1039/C6IB00167J

Li, S., Nih, L. R., Bachman, H., Fei, P., Li, Y., Nam, E., et al. (2017). Hydrogels with precisely controlled integrin activation dictate vascular patterning and permeability. *Nat. Mater.* 16, 953–961. doi: 10.1038/nmat4954

Lin, C. C., and Anseth, K. S. (2009). Controlling affinity binding with peptide-functionalized poly(ethylene Glycol) hydrogels. *Adv. Funct. Mater.* 19, 2325–2331. doi: 10.1002/adfm.200900107

Logun, M. T., Bisel, N. S., Tanasse, E. A., Zhao, W., Gunasekera, B., Mao, L., et al. (2016). Glioma cell invasion is significantly enhanced in composite hydrogel matrices composed of chondroitin 4- and 4,6-sulfated glycosaminoglycans. *J. Mater. Chem. B* 4, 6052–6064. doi: 10.1039/C6TB01083K

Maclean, F. L., Lau, C. L., Ozergun, S., O'Shea, R. D., Cederfur, C., Wang, J., et al. (2017). Galactose-functionalised PCL nanofibre scaffolds to attenuate inflammatory action of astrocytes *in vitro* and *in vivo*. *J. Mater. Chem. B* 5, 4073–4083. doi: 10.1039/C7TB00651A

Mantovani, A., Sozzani, S., Locati, M., Allavena, P., and Sica, A. (2002). Macrophage polarization: tumor-associated macrophages as a paradigm for polarized M2 mononuclear phagocytes. *Trends Immunol.* 23, 549–555. doi: 10.1016/S1471-4906(02)02302-5

Miroshnikova, Y. A., Mouw, J. K., Barnes, J. M., Pickup, M. W., Lakins, J. N., Kim, Y., et al. (2016). Tissue mechanics promote IDH1-Dependent HIF1α-tenascin C feedback to regulate glioblastoma aggression. *Nat. Cell Biol.* 18, 1336–1345. doi: 10.1038/ncb3429

Mosadegh, B., Lockett, M. R., Thu, K., Simon, K. A., Gilbert, K., Hillier, S., et al. (2015). Biomaterials a paper-based invasion assay : assessing chemotaxis of cancer cells in gradients of oxygen 52, 262–271. doi: 10.1016/j.biomaterials.2015.02.012

Munson, J. M., Bellamkonda, R. V., and Swartz, M. A. (2013). Interstitial flow in a 3d microenvironment increases glioma invasion by a cxcr4-dependent mechanism. *Cancer Res.* 73, 1536–1546. doi: 10.1158/0008-5472.CAN-12-2838

Munson, J. M., and Shieh, A. C. (2014). Interstitial fluid flow in cancer: implications for disease progression and treatment. *Cancer Manag. Res.* 6, 317–328. doi: 10.2147/CMAR.S65444

Nguyen, D. T., Fan, Y., Akay, Y. M., and Akay, M. (2016). Investigating glioblastoma angiogenesis using a 3D *in vitro* GelMA microwell platform. *IEEE Trans. Nanobiosci.* 15, 289–293. doi: 10.1109/TNB.2016.2528170

Nih, L. R., Sideris, E., Carmichael, S. T., and Segura, T. (2017). Injection of Microporous Annealing Particle (MAP) hydrogels in the stroke cavity reduces gliosis and inflammation and promotes NPC migration to the lesion. *Adv. Mater.* 29:1606471. doi: 10.1002/adma.201606471

O'Rourke, D. M., Nasrallah, M. P., Desai, A., Melenhorst, J. J., Mansfield, K., Morrissette, J. J. D., Martinez-Lage, M., et al. (2017). A single dose of peripherally infused EGFRvIII-directed CAR T cells mediates antigen loss and induces adaptive resistance in patients with recurrent glioblastoma. *Sci. Transl. Med.* 9:eaaa0984. doi: 10.1126/scitranslmed.aaa0984

Pedraza, E., Coronel, M. M., Fraker, C. A., Ricordi, C., and Stabler, C. L. (2012). Preventing hypoxia-induced cell death in beta cells and islets via hydrolytically activated, oxygen-generating biomaterials *Proc. Natl. Acad. Sci. U.S.A.* 109, 4245–4250. doi: 10.1073/pnas.1113560109

Pedron, S., Becka, E., and Harley, B. A. (2013). Regulation of glioma cell phenotype in 3D matrices by hyaluronic acid. *Biomaterials* 34, 7408–7417. doi: 10.1016/J.BIOMATERIALS.2013.06.024

Pedron, S., Becka, E., and Harley, B. A. (2015). Spatially gradated hydrogel platform as a 3D engineered tumor microenvironment. *Adv. Mater.* 27, 1567–1572. doi: 10.1002/adma.201404896

Placone, A. L., McGuiggan, P. M., Bergles, D. E., Guerrero-Cazares, H., Quiñones-Hinojosa, A., and Searson, P. C. (2015). Human astrocytes develop physiological morphology and remain quiescent in a novel 3D matrix. *Biomaterials* 42, 134–143. doi: 10.1016/j.biomaterials.2014.11.046

Polacheck, W. J., Charest, J. L., and Kamm, R. D. (2011). Interstitial flow influences direction of tumor cell migration through competing mechanisms. *Proc. Natl. Acad. Sci. U.S.A.* 108, 11115–11120. doi: 10.1073/pnas.1103581108

Pradhan, S., Hassani, I., Clary, J. M., and Lipke, E. A. (2016). Polymeric biomaterials for *in vitro* cancer tissue engineering and drug testing applications. *Tissue Eng. B Rev.* 22, 470–484. doi: 10.1089/ten.teb.2015.0567

Prodanov, D., and Delbeke, J. (2016). Mechanical and biological interactions of implants with the brain and their impact on implant design. *Front. Neurosci.* 10:11. doi: 10.3389/fnins.2016.00011

Purwada, A., Roy, K., and Singh, A. (2014). Engineering vaccines and niches for immune modulation. *Acta Biomater.* 10, 1728–1740. doi: 10.1016/j.actbio.2013.12.036

Qazi, H., Palomino, R., Shi, Z.-D., Munn, L. L., and Tarbell, J. M. (2013). Cancer cell glycocalyx mediates mechanotransduction and flow-regulated invasion. *Integr. Biol.* 5, 1334–1343. doi: 10.1039/c3ib40057c

Qazi, H., Shi, Z. D., and Tarbell, J. M. (2011). Fluid shear stress regulates the invasive potential of glioma cells via modulation of migratory activity and matrix metalloproteinase expression. *PLoS ONE* 6:e20348. doi: 10.1371/journal.pone.0020348

Qu, F., Lin, J. M., Esterhai, J. L., Fisher, M. B., and Mauck, R. L. (2013). Biomaterial-mediated delivery of degradative enzymes to improve meniscus integration and repair. *Acta Biomater.* 9, 6393–6402. doi: 10.1016/j.actbio.2013.01.016

Rao, S. S., Nelson, M. T., Xue, R., DeJesus, J. K., Viapiano, M. S., Lannutti, J. J., et al. (2013). Mimicking white matter tract topography using core–shell electrospun nanofibers to examine migration of malignant brain tumors. *Biomaterials* 34, 5181–5190. doi: 10.1016/j.biomaterials.2013.03.069

Rayahin, J. E., Buhrman, J. S., Zhang, Y., Koh, T. J., and Gemeinhart, R. A. (2015). High and low molecular weight hyaluronic acid differentially influence macrophage activation. *ACS Biomater. Sci. Eng.* 1, 481–93. doi: 10.1021/acsbiomaterials.5b00181

Razavi, S. M., Lee, K. E., Jin, B. E., Aujla, P. S., Gholamin, S., and Li, G. (2016). Immune evasion strategies of glioblastoma. *Front. Surg.* 3:11. doi: 10.3389/fsurg.2016.00011

Rong, Y., Durden, D. L., Van Meir, E. G., and Brat, D. J. (2006). 'Pseudopalisading' necrosis in glioblastoma: a familiar morphologic feature that links vascular pathology, hypoxia, and angiogenesis. *J. Neuropathol. Exp. Neurol.* 65, 529–539. doi: 10.1097/00005072-200606000-00001

Seidlits, S. K., Khaing, Z. Z., Petersen, R. R., Nickels, J. D., Vanscoy, J. E., Shear, J. B., et al. (2010). The effects of hyaluronic acid hydrogels with tunable mechanical properties on neural progenitor cell differentiation. *Biomaterials* 31, 3930–3940. doi: 10.1016/j.biomaterials.2010.01.125

Silver, D. J., Siebzehnrubl, F. A., Schildts, M. J., Yachnis, A. T., Smith, G. M., Smith, A. A., et al. (2013). Chondroitin sulfate proteoglycans potently inhibit invasion and serve as a central organizer of the brain tumor microenvironment. *J. Neurosci.* 33, 15603–15617. doi: 10.1523/JNEUROSCI.3004-12.2013

Silver, D. J., and Silver, J. (2014). Contributions of chondroitin sulfate proteoglycans to neurodevelopment, injury, and cancer. *Curr. Opin. Neurobiol.* 27, 171–178. doi: 10.1016/J.CONB.2014.03.016

Sin, W. C., Aftab, Q., Bechberger, J. F., Leung, J. H., Chen, H., and Naus, C. C. (2016). Astrocytes promote glioma invasion via the gap junction protein connexin43. *Oncogene* 35, 1504–1516. doi: 10.1038/onc.2015.210

Spiller, K. L., Nassiri, S., Witherel, C. E., Anfang, R. R., Ng, J., Nakazawa, K. R., et al. (2015). sequential delivery of immunomodulatory cytokines to facilitate the M1-to-M2 transition of macrophages and enhance vascularization of bone scaffolds. *Biomaterials* 37, 194–207. doi: 10.1016/j.biomaterials.2014.10.017

Sridharan, R., Cameron, A. R., Kelly, D. J., Kearney, C. J., and O'Brien, F. J. (2015). Biomaterial based modulation of macrophage polarization: a review and suggested design principles. *Mater. Today.* 18, 313–325. doi: 10.1016/j.mattod.2015.01.019

Swartz, M. A., Hirosue, S., and Hubbell, J. A. (2012). Engineering approaches to immunotherapy. *Sci. Transl. Med.* 4:148rv9. doi: 10.1126/scitranslmed.3003763

Szulzewsky, F., Pelz, A., Feng, X., Synowitz, M., Markovic, D., Langmann, T., et al. (2015). Glioma-associated microglia/macrophages display an expression profile different from m1 and m2 polarization and highly express gpnmb and spp1. *PLOS ONE* 10:e0116644. doi: 10.1371/journal.pone.0116644

Tilghman, J., Wu, H., Sang, Y., Shi, X., Guerrero-Cazares, H., Quinones-Hinojosa, A., et al. (2014). HMMR maintains the stemness and tumorigenicity of glioblastoma stem-like cells. *Cancer Res.* 74, 3168–3179. doi: 10.1158/0008-5472.CAN-13-2103

Tumeh, P. C., Harview, C. L., Yearley, J. H., Peter Shintaku, I., Taylor, E. J. M., Robert, L., et al. (2014). PD-1 blockade induces responses by inhibiting adaptive immune resistance. *Nature* 515, 568–571. doi: 10.1038/nature13954

Ulrich, T. A.,de Juan Pardo, E. M., and Kumar, S. (2009). The mechanical rigidity of the extracellular matrix regulates the structure, motility, and proliferation of glioma cells. *Cancer Res.* 69, 4167–4174. doi: 10.1158/0008-5472.CAN-08-4859

Vinnakota, K., Hu, F., Ku, M. C., Georgieva, P. B., Szulzewsky, F., Pohlmann, A., et al. (2013). Toll-like receptor 2 mediates microglia/brain macrophage MT1-MMP expression and glioma expansion. *Neurooncology* 15, 1457–1468. doi: 10.1093/neuonc/not115

Wait, S. D., Prabhu, R. S., Burri, S. H., Atkins, T. G., and Asher, A. L. (2015). Polymeric drug delivery for the treatment of glioblastoma. *Neuro Oncol.* 17 (Suppl. 2), ii9–ii23. doi: 10.1093/neuonc/nou360

Wang, C., Tong, X., and Yang, F. (2014). Bioengineered 3D brain tumor model to elucidate the effects of matrix stiffness on glioblastoma cell behavior using peg-based hydrogels. *Mol. Pharmaceut.* 11, 2115–2125. doi: 10.1021/mp5000828

Watkins, S., Robel, S., Kimbrough, I. F., Robert, S. M., Ellis-Davies, G., and Sontheimer, H. (2014). Disruption of astrocyte-vascular coupling and the blood-brain barrier by invading glioma cells. *Nature Commun* 5:4196. doi: 10.1038/ncomms5196

Xia, S., Lal, B., Tung, B., Wang, S., Goodwin, C. R., and Laterra, J. (2016). Tumor microenvironment tenascin-C promotes glioblastoma invasion and negatively regulates tumor proliferation. *Neuro Oncol.* 18, 507–517. doi: 10.1093/neuonc/nov171

Xiao, W., Sohrabi, A., Seidlits, S., and Seidlits. (2017). Integrating the glioblastoma microenvironment into engineered experimental models. *Future Science.* 3, FSO18. doi: 10.4155/fsoa-2016-0094

Yuan, J. X., Bafakih, F. F., Mandell, J. W., Horton, B. J., and Munson, J. M. (2016). Quantitative analysis of the cellular microenvironment of glioblastoma to develop predictive statistical models of overall survival. *J. Neuropathol. Exp. Neurol.* 75, 1110–1123. doi: 10.1093/jnen/nlw090

Yuan, Z., Mehta, H. J., Mohammed, K., Nasreen, N., Roman, R., Brantly, M., et al. (2014). TREM-1 Is induced in tumor associated macrophages by Cyclo-oxygenase pathway in human non-small cell lung cancer. *PLoS ONE* 9:e94241. doi: 10.1371/journal.pone.0094241

Zhou, W., Ke, S. Q., Huang, Z., Flavahan, W., Fang, X., Paul, J., et al. (2015). Periostin secreted by glioblastoma stem cells recruits M2 tumour-associated macrophages and promotes malignant growth. *Nat. Cell Biol.* 17, 170–182. doi: 10.1038/ncb3090

Zhu, V. F., Yang, J., Lebrun, D. G., and Li, M. (2012). Understanding the role of cytokines in glioblastoma multiforme pathogenesis. *Cancer Lett.* 316, 139–150. doi: 10.1016/j.canlet.2011.11.001

Zitvogel, L., Tesniere, A., and Kroemer, G. (2006). Cancer despite Immunosurveillance: immunoselection and Immunosubversion. *Nat. Rev. Immunol.* 6, 715–727. doi: 10.1038/nri1936

Conflict of Interest Statement: The authors declare that the research was conducted in the absence of any commercial or financial relationships that could be construed as a potential conflict of interest.

frontiers in Materials

REVIEW
published: 19 February 2018
doi: 10.3389/fmats.2018.00007

Modeling Microenvironmental Regulation of Glioblastoma Stem Cells: A Biomaterials Perspective

*John M. Heffernan[1,2] and Rachael W. Sirianni[1,2]**

[1] *Laboratory for Nanomedicine, Barrow Brain Tumor Research Center, Barrow Neurological Institute (BNI), Phoenix, AZ, United States,* [2] *School of Biological and Health Systems Engineering, Arizona State University, Tempe, AZ, United States*

Following diagnosis of a glioblastoma (GBM) brain tumor, surgical resection, chemotherapy, and radiation together yield a median patient survival of only 15 months. Importantly, standard treatments fail to address the dynamic regulation of the brain tumor microenvironment that actively supports tumor progression and treatment resistance. It is becoming increasingly recognized that specialized niches within the tumor microenvironment maintain a population of highly malignant glioblastoma stem-like cells (GSCs). GSCs are resistant to traditional chemotherapy and radiation therapy, suggesting that they may be responsible for the near universal rates of tumor recurrence and associated morbidity in GBM. Thus, disrupting microenvironmental support for GSCs could be critical to developing more effective GBM therapies. Three-dimensional culture models of the tumor microenvironment are powerful tools for identifying key biochemical and biophysical inputs that impact malignant behaviors. Such systems have been used effectively to identify conditions that regulate GSC proliferation, invasion, stem-specific phenotypes, and treatment resistance. Considering the significant role that GSC microenvironments play in regulating this tumorigenic subpopulation, these models may be essential for uncovering mechanisms that limit GSCs malignancy.

Keywords: tumor microenvironment, niche microenvironments, brain tumor stem cells, cancer stem cells, scaffolds, hydrogels, three-dimensional cell culture

OPEN ACCESS

Edited by:
Sara Pedron, University of Illinois at Urbana–Champaign, United States

Reviewed by:
Ece Ozturk, Columbia University, United States
Joseph Chen, University of California, Berkeley, United States
Nor Eddine Sounni, University of Liège, Belgium

****Correspondence:***
Rachael W. Sirianni
rachael.sirianni@dignityhealth.org

Specialty section:
This article was submitted to Biomaterials, a section of the journal Frontiers in Materials

Received: *27 October 2017*
Accepted: *26 January 2018*
Published: *19 February 2018*

Citation:
Heffernan JM and Sirianni RW (2018) Modeling Microenvironmental Regulation of Glioblastoma Stem Cells: A Biomaterials Perspective. Front. Mater. 5:7. doi: 10.3389/fmats.2018.00007

GLIOBLASTOMA (GBM)

Glioblastoma is the most common and deadly pathological classification of malignant primary brain tumors. Epidemiological data collected for the United States between 2009 and 2013 indicate that GBM represents 46.6% of these diagnoses and 14.9% of all malignant and non-malignant primary brain tumor diagnoses (Ostrom et al., 2016). Overall age adjusted incidence rates are 3.2 per 100,000, with a median age of diagnosis of 64.0 years; risk rises with age (Ostrom et al., 2016). Symptoms of a GBM vary widely depending on tumor location and size but may include severe headaches, seizures, vision and speech impairment, or loss of cognitive and motor functions. Standard treatment modalities include removal of the bulk tumor *via* surgical resection, followed by radiotherapy and concomitant chemotherapy. However, treatment is rarely curative, and the prognosis is poor. Median survival remains stagnated at only 15 months (Stupp et al., 2009), and the 5-year survival rate is reported between 4.7 and 5.5% (Omuro and DeAngelis, 2013; Ostrom et al., 2016).

Barriers to Treatment

From a clinical perspective, successful treatment of GBM remains challenging due to several factors. Complete surgical resection, while the best treatment for GBM, is often impossible as a result of tumor location, as well as the potential for irreparable damage to healthy brain tissue during surgery (Sanai et al., 2011). Radiation treatment can often be targeted to areas of the brain that would be otherwise difficult to access surgically. Although radiation is an effective means for killing remaining tumor cells, simultaneous damage incurred on surrounding healthy tissue limits tolerability and may worsen patient outcome. Treatment of GBM with chemotherapeutics is inhibited by the blood–brain barrier, which segregates the brain from systemic circulation and prevents the vast majority of drugs from effectively reaching malignant cells in the brain. The primary chemotherapeutic currently used in GBM treatment is the DNA alkylating agent temozolomide, which is administered orally, is brain available and generally well tolerated, but imparts only a modest improvement in patient outcome (Stupp et al., 2009). Overall, current treatment options remain inadequate.

One of the key biological features of GBM is that, unlike other tumor types tumors, it does not metastasize through the blood to peripheral organs; instead, individual cells invade healthy brain, preferentially migrating along white matter tracts and perivascular spaces (Giese and Westphal, 1996; Giese et al., 2003). These cells are responsible for initiating secondary tumors that most often arise within centimeters of the original tumor (Petrecca et al., 2012) but may manifest even on the contralateral side of the brain (Matsukado et al., 1961; Giese and Westphal, 1996). Invasive cells are undetectable by current imaging methods, and almost impossible to remove *via* surgical resection without damaging healthy brain. Radiation and chemotherapy fail to address invasive cells that are shielded by radiosensitive healthy tissue and an intact blood–brain barrier. Thus, the invasive nature of GBM drives near universal rates of tumor recurrence as secondary tumors arise from seemingly healthy brain (Petrecca et al., 2012; Omuro and DeAngelis, 2013).

A factor that further complicates the treatment landscape is that GBM tumors display a high degree of genetic, epigenetic, and cellular diversity. Presently, GBM is classified into four distinct subtypes: Proneural, Neural, Classical, and Mesenchymal; each of which corresponds to a common set of neoplastic genetic alterations (Verhaak et al., 2010). However, individual subtype classifications may not be relevant to all cells found in a single tumor, as intratumoral heterogeneity is also a common feature of GBM (Sottoriva et al., 2013). This heterogeneity is a primary source of treatment resistance, whereby one tumor region that is sensitive to treatment is sustained or replaced by another region that is tolerant (Bonavia et al., 2011). Tumor heterogeneity is therefore an adaptive growth pattern that is challenging to address through monotherapy, even when targeted.

GBM TUMOR MICROENVIRONMENT

The GBM tumor microenvironment is a complex regulatory structure composed of cellular and non-cellular components that collectively contribute to disease progression. The tumor microenvironment significantly influences many important aspects of GBM biology; the specific functions of the GBM tumor microenvironment have been reviewed extensively by others (Bonavia et al., 2011; Charles et al., 2011; Wiranowska and Rojiani, 2011; Xiao et al., 2017); here, we provide an overview to introduce key features of this relationship that are important for modeling this unique microenvironment.

Unlike other tissues in the body, the brain extracellular matrix (ECM) does not contain high concentrations of fibrous proteins (Bellail et al., 2004). Instead, the dense tumor microenvironment ECM is primarily composed of the glycosaminoglycan hyaluronic acid (HA), and to a lesser degree, tenascin-C, collagen IV and V, fibronectin, laminin, and vitronectin, which are generally associated with blood vessels (Delpech et al., 1993; Giese and Westphal, 1996; Bellail et al., 2004; Wiranowska and Rojiani, 2011; Rape et al., 2014). GBM cells interact with HA *via* the cell surface receptors CD44 and RHAMM, which are often overexpressed on GBM cells, and promote invasive phenotypes (Merzak et al., 1994; Ariza et al., 1995; Koochekpour et al., 1995; Akiyama et al., 2001). The proteoglycan tenascin-C has been described to promote GBM invasion (Giese and Westphal, 1996; Sarkar et al., 2006) and to stimulate angiogenesis, which leads to tumor progression (Bellail et al., 2004; Rape et al., 2014). Other vascular-associated ECM constituents (collagen, fibronectin, laminin, and vitronectin) both promote and guide GBM invasion into healthy brain tissue (Mahesparan et al., 2003; Kawataki et al., 2007; Rape et al., 2014). Moreover, these molecules also enable integrin-mediated focal adhesions, which play a significant role in GBM progression, and have been proposed as a biomarker target for treatment (Kawataki et al., 2007; Lathia et al., 2010; Ruiz-Ontañon et al., 2013; Paolillo et al., 2016; Haas et al., 2017). Furthermore, in addition to affecting invasion, various isoforms of laminin proteins have been shown to potentiate glioblastoma stem-like cell (GSC) phenotypes *via* integrin interactions (Pollard et al., 2009; Lathia et al., 2010, 2012; Haas et al., 2017).

The concentration of ECM in the tumor microenvironment is increased compared with healthy brain, as its constituents are manufactured by GBM cells to support tumor progression (Delpech et al., 1993; Giese and Westphal, 1996; Akiyama et al., 2001; Wiranowska and Rojiani, 2011; Lathia et al., 2012). The dense ECM and the high cellularity of the tumor contribute to increased mechanical stiffness. GBM cells sense microenvironmental stiffness primarily through integrins and focal adhesion complexes *via* mechanosensation (Rape et al., 2014). While the biochemical and biophysical effects of matrix composition appear to be complementary or even synergistic in promoting malignancy, they are not easily isolated *in vivo*. *In vitro* studies have identified stiffness as a strong regulator of GBM proliferation and invasion (Ananthanarayanan et al., 2011; Wiranowska and Rojiani, 2011; Pathak and Kumar, 2012; Pedron and Harley, 2013; Heffernan et al., 2014; Kim and Kumar, 2014; Rape et al., 2014; Umesh et al., 2014). Moreover, blood vessels provide the greatest stiffness in the brain and are preferential routes for GBM invasion (Giese and Westphal, 1996; Giese et al., 2003). Therefore, it is likely that the stiffness of these and other structures instructs malignant behaviors *in vivo*.

The tumor-associated cells within the tumor microenvironment are key regulators of GBM growth and tumor vascularization. Cells that commonly provide support to GBM include tumor-associated endothelial cells, pericytes, astrocytes, fibroblasts, and infiltrating immune cells such as macrophages and microglia (Charles et al., 2011). One of the primary modes of support from tumor and tumor-associated cells is secretion of soluble signaling factors that stimulate malignant phenotypes, i.e., proliferation (EGF, FGF, IGF, and HGF), angiogenesis [vascular endothelial growth factor (VEGF)], and invasion (IGF, HGF, and TGF-β) (Wiranowska and Plaas, 2008). These secreted signaling factors may be sequestered within the dense network of ECM and serve as a depot for GBM cells (Wiranowska and Plaas, 2008; Wiranowska and Rojiani, 2011). Tumor vascularization is achieved in part by recruitment of vascular-associated endothelial cells, pericytes, and astrocytes, to meet the nutrient demands of a growing tumor (Wiranowska and Plaas, 2008; Charles et al., 2011; Soda et al., 2013). Specifically, endothelial cells are stimulated to proliferate and migrate toward tumor regions with poor oxygenation as a result of VEGF productions by hypoxic tumor cells (Soda et al., 2013). However, the resulting tumor-associated neovasculature is significantly different from healthy vessels as it forms a dense and disordered network of leaky vessels with necrosis developing in regions of severe chronic hypoxia (<1% O_2) (Holmquist-Mengelbier et al., 2006; Soda et al., 2013).

GLIOBLASTOMA STEM-LIKE CELLS

Before 2003, GBM, like most solid tumors, was widely believed to be driven by a stochastic model of clonal evolution in which tumors were initiated *via* neoplastic transformation of glia. The identification and characterization of tumorigenic GSCs within human brain tumors have since reshaped conventional wisdom over the architecture of GBM biology (Ignatova et al., 2002; Singh et al., 2003, 2004; Galli et al., 2004). This discovery supports the hypothesis that cells within a tumor display a hierarchical order of tumorigenic potential that is maintained by cancer stem cells (Tan et al., 2006; Venere et al., 2011). It is now widely recognized that within GBM tumors, GSCs are essential to tumor maintenance, drivers of heterogeneity, and also may represent the cell of origin (Sanai et al., 2005; Venere et al., 2011).

GSC Characteristics

Glioblastoma stem-like cells display many biological similarities to neural stem cells (NSCs); they are capable of indefinite self-renewal and multipotent differentiation, and they express genes that promote NSC phenotypes such as NESTIN, SOX2, and OLIG2 (Ignatova et al., 2002; Singh et al., 2003, 2004; Galli et al., 2004; Sanai et al., 2005; Lee et al., 2006; Ligon et al., 2007). Identification and enrichment of GSCs can be achieved by sorting tumor cells that express validated cell surface biomarkers [CD133 (Singh et al., 2003), SSEA-1 (Son et al., 2009), and Integrin α6 (Lathia et al., 2010)] followed by functional analysis of stem behaviors (Lathia et al., 2015). Of the stem behaviors, none is more important to GSC tumorigenicity than self-renewal. This was demonstrated when GSCs were first isolated and were observed to form orthotopic xenograft tumors from as few as 100 cells. In comparison, non-stem GBM cells (NGSCs) from the same tumor sample were incapable of forming tumors from injections of 100,000 cells (Singh et al., 2004). GSCs also display a capacity for multipotent differentiation into non-tumorigenic cancer-associated cells, such as vascular cells, that provide critical support for tumor growth (Ricci-Vitiani et al., 2010; Wang et al., 2010a; Lathia et al., 2011; Cheng et al., 2013a). Multipotency contributes to cellular heterogeneity observed in primary GBM; this behavior has been recapitulated in experimental orthotopic xenograft tumor models (Singh et al., 2004).

Ex vivo purification of GSCs requires a multistep process that tests self-renewal, multipotency, and stem-marker expression. Failure to test all three components often results in false positive identification (Lathia et al., 2015). Another method for identifying GSCs has been through the use of label retaining assays to identify quiescent or slow-cycling cells (Deleyrolle et al., 2011; Zeng et al., 2016). Using robust verification, long-term established GBM cell lines are found to lack fully functional GSCs, even in NSC culture conditions (Lee et al., 2006; Lathia et al., 2015). Thus to properly research GSC behaviors, experiments should ideally be performed on low-passage patient-derived cells that have been validated as a stem population.

GSC Response to Treatment

Glioblastoma stem-like cells are highly treatment resistant, which is facilitated by their propensity to invade healthy brain (Cheng et al., 2011), potential quiescence (Chen et al., 2012), and activation of molecular machinery that is protective against radiation (Bao et al., 2006a) and cytotoxic insult (Liu et al., 2006). Many of the invasive mechanisms utilized by GSCs mimic NSC motility along white matter tracts and blood vessels (Sanai et al., 2005). Thus, GBM tumors characteristically display an infiltrative leading edge that disseminates into healthy tissue. GSC derived orthotopic xenograft tumors recapitulate this invasive behavior with GSCs concentrated at the tumor edge (Strojnik et al., 2007), whereas NGSCs from the same patient tumor sample are minimally invasive (Cheng et al., 2011). Resistance to both radiation (Bao et al., 2006a) as well as many conventional chemotherapeutics, including temozolomide (Liu et al., 2006; Chen et al., 2012), has been reported in the GSC population. This resistance is ascribed to increased activation of DNA damage checkpoint and repair proteins (Bao et al., 2006a), as well as increased expression of ATP-binding cassette drug transporters, which contribute to increased drug efflux and chemoresistance (Bleau et al., 2009). Recurrent tumors are also enriched for GSCs compared with the primary tumor suggesting that GSCs evade conventional therapy and play a prominent role in the high rates of GBM relapse (Liu et al., 2006).

GSC NICHE MICROENVIRONMENTS

Similar to NSCs, which are primarily found in the subventricular zone and hippocampus of the adult brain, GSCs are also concentrated in niche microenvironments (**Figure 1**) (Sanai et al., 2005). One notable difference is that GSC niche microenvironments appear to be mitogenic, encouraging growth, while NSCs are generally sustained in quiescence (Lathia et al., 2011). These

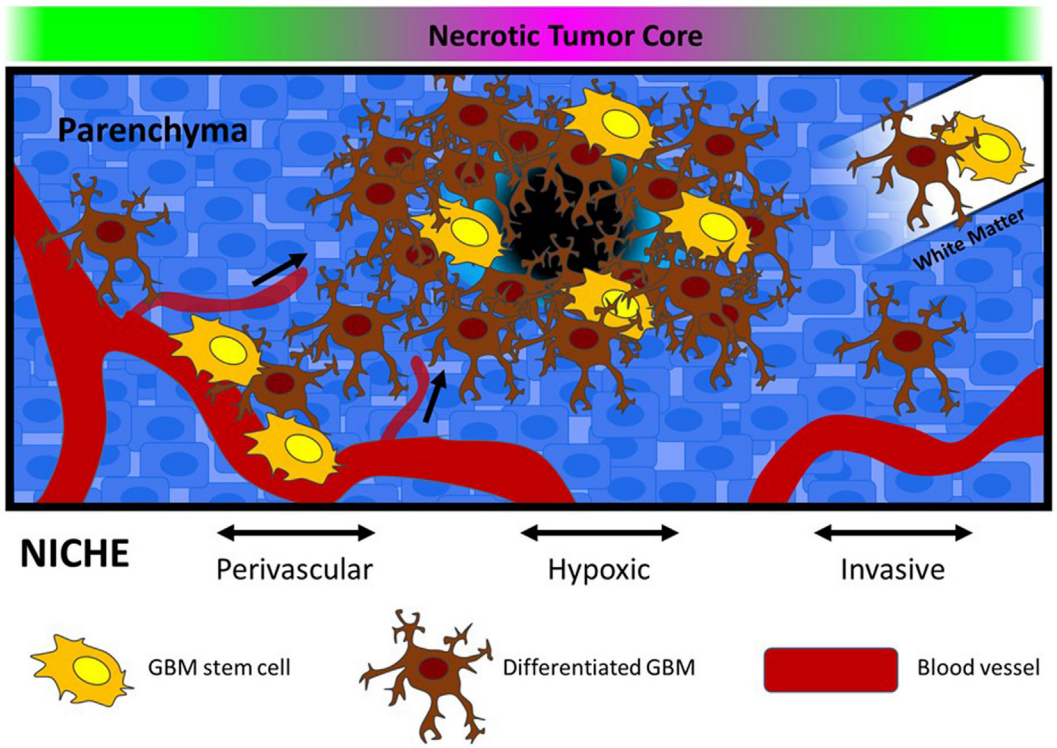

FIGURE 1 | Glioblastoma stem-like cells are located in defined microenvironments within the brain, including perivascular, hypoxic, and invasive niches. Each niche varies in terms of biophysical features (stiffness and porosity), extracellular matrix composition, and oxygen availability. In the graphic, vessel co-option is depicted within the perivascular niche, and movement along white matter tracts is depicted in the invasive niche. Within the hypoxic niche, necrosis and altered metabolism is expected to drive alterations in pH, as well as recruitment of new blood vessels.

physical regions within the larger tumor microenvironment include a range of microenvironmental features that sustain and regulate GSC phenotypes through hypoxia, growth factor signaling, and adhesion to the ECM. It is thus unsurprising that the microenvironment plays a role in provoking treatment resistance (Gilbertson and Rich, 2007; Rich, 2007; Jamal et al., 2010, 2012; Mannino and Chalmers, 2011; Lathia et al., 2012).

Perivascular Niche

A niche microenvironment has been identified in regions directly adjacent to blood vessels known as the vascular or perivascular niche (Calabrese et al., 2007; Gilbertson and Rich, 2007). Tumor vascularization is a requisite process to provide GBM tumors with adequate oxygen and nutrients that sustain rapid growth. Bao et al. determined that GSCs initiate neovascularization by stimulating endothelial cell proliferation, migration, and tube formation through secretion of VEGF and stromal-derived factor 1 (Bao et al., 2006b; Folkins et al., 2009). In parallel, vascular endothelial cells promote GSC self-renewal and proliferation, through secretion of soluble signaling factors such as nitric oxide, as well as *via* activation of NOTCH signaling (Calabrese et al., 2007; Charles et al., 2010; Hovinga et al., 2010; Galan-Moya et al., 2011). This support appears to be unique to endothelial cells. For example, Calabrese et al. (2007) determined that neither NGSCs, astrocytes, nor fibroblasts were able to produce comparable enrichment of GSCs *in vitro*. Importantly, GSCs are also capable of transdifferentiation into tumor-derived vascular cells. In experimental tumor models, GSCs have been observed to differentiate into pericytes and endothelial cells that participate in the formation and maintenance of neovasculature (Ricci-Vitiani et al., 2010; Wang et al., 2010a; Lathia et al., 2011; Cheng et al., 2013a; Schonberg et al., 2014). Therefore, interactions between endothelial cells and GSCs in the perivascular niche may create a self-sustaining paracrine signaling cycle that is critical for tumor maintenance and progression (Schonberg et al., 2014).

Hypoxic Niche

In juxtaposition to the nutrient-rich perivascular niche, GSCs are also found concentrated surrounding tumor regions that have limited access to blood vessels and are often necrotic (Li et al., 2009). The disorganized vasculature of GBM tumors leads to regional oxygen concentration gradients that have significant effects on GSC phenotypes. The primary molecular response to oxygen deprivation involves activation of the hypoxia inducible factor (HIF) family of transcription factors whose canonical downstream targets are proangiogenic (Heddleston et al., 2010). As a result, the hypoxic niche may in some cases exist as a transitional microenvironment in which GSCs use proangiogenic factors such as VEGF to recruit blood vessels and establish a perivascular niche (Venere et al., 2011).

Hypoxia inducible factor activation has also been found to be a potent regulator of various GSC behaviors. HIF1α and HIF2α exhibit overlapping functions in both vasculogenesis and enriching stem phenotypes (Heddleston et al., 2009, 2010; Li et al., 2009; Soeda et al., 2009; Bar et al., 2010; Seidel et al., 2010). However, unique downstream target genes have also been identified particularly for HIF2α, which include stem markers Oct4, c-Myc, and Nanog (Heddleston et al., 2009; Li et al., 2009; Keith et al., 2011). Importantly, Li et al. (2009) reported that while HIF1α is expressed in both NSC and GSC populations, HIF2α expression is restricted to GSCs and is required for GSC tumorigenicity *in vivo*. HIF2α induction also promotes stem plasticity in the pool of NGSCs, which may be particularly important for repopulating the GSC pool in response to treatment (Heddleston et al., 2009). HIF expression also appears to be regulated by distinct components of the microenvironment. HIF1α expressing cells are enriched in regions of chronic hypoxia (>1% O_2), while HIF2α expression is more sporadically identified in both hypoxic and normoxic regions surrounding blood vessels (Holmquist-Mengelbier et al., 2006; Li et al., 2009). In addition, tumor acidity, a byproduct of overactive glycolytic energy production, increases HIF2α stabilization independent of oxygen concentration and also promotes stem plasticity (Hjelmeland et al., 2011). Thus, the hypoxic niche regulates GSC phenotypes primarily through HIF activity, which is essential to stem maintenance and tumorigenicity.

Invasive Niche

Glioblastoma stem-like cell populations have been identified at the leading edge of GBM tumors suggesting that this invasive front also contributes to GSC maintenance (Lee et al., 2006; Kitai et al., 2010; Cheng et al., 2011; Ishiwata et al., 2011; Lathia et al., 2011; Ortensi et al., 2013). Orthotopic GSC tumors recapitulate the invasive profile observed in patient tumors compared with NGSCs, which generally form noninvasive tumors (Cheng et al., 2011). Furthermore, recurrent tumors are enriched with GSCs indicating that these cells are likely responsible for infiltrative growth that is characteristic of GBM (Liu et al., 2006). Therefore, while an invasive niche has yet to be definitively established, microenvironmental interactions, particularly with the ECM protein laminin, have been identified that regulate both invasive behaviors and stem phenotypes. For example, laminin receptor integrins α6 and α7 have been proposed as biomarkers for functional GSCs (Lathia et al., 2010; Haas et al., 2017), while GSC regulation has also been described through interactions with the laminin subunit α2 (Lathia et al., 2012). In healthy brain, laminin is primarily located on the outside of blood vessels, which are primary routes of GBM invasion (Giese and Westphal, 1996). Expression of laminin (Ljubimova et al., 2006) and localization of laminin within the perivascular niche (Lathia et al., 2012) relate to poor patient prognosis; the integrin family of laminin receptor proteins are overexpressed in CD133 + GSCs, which have been demonstrated to promote invasion (Nakada et al., 2013), proliferation (Lathia et al., 2012), and resistance to apoptosis (Huang et al., 2012). These integrin-mediated phenotypic shifts are significant at the level of disease progression and may be related to active microenvironmental regulation (Paolillo et al., 2016). For example, Ljubimova et al. (2006) observed a switch in laminin isoform expression during tumor progression that was associated with both invasion and angiogenesis, suggesting that laminin is a dynamic partner in the development of tumor malignancy. The interaction of tumor cells with vascular-associated laminins has been shown to be an important factor for GSC regulation in the perivascular niche (Lathia et al., 2012). In addition, certain isoforms of laminin sustain GSC phenotypes during *in vitro* stem cell cultures (Pollard et al., 2009), and conversely, may also be used to promote GSC differentiation to NGSCs in serum-supplemented conditions (Ignatova et al., 2002). These relationships warrant further study to understand the complexities of GBM–laminin interactions, and to determine how they may contribute to treatment resistance and/or tumor recurrence.

Therapeutic Challenges and Opportunities

Along with regulatory inputs, niche microenvironments provide GSCs with protection from cytotoxic treatments (Gilbertson and Rich, 2007). The perivascular niche has been described as radioprotective for medulloblastoma tumors (Hambardzumyan et al., 2008). This resistance was initiated by signaling through the oncogenic PI3K/Akt pathway, which is a downstream target of the epidermal growth factor receptor (EGFR). In relation to GBM biology, EGFR is one of the most important biomarkers for malignancy (Verhaak et al., 2010) and is critical to the maintenance of stem phenotypes *in vitro* (Lee et al., 2006). Moreover, inhibiting EGFR has been observed to sensitize otherwise radioresistant GSCs to treatment (Kang et al., 2012). Therefore, activation of this receptor in the nutrient-rich perivascular niche would conceivably negatively impact the efficacy of radiotherapy on GSCs. VEGF signaling, which is critical for tumor vascularization and establishment of the perivascular niche, has also been shown to enhance resistance to radiation (Knizetova et al., 2008). Similarly, Notch signaling, which functions through direct cell–cell contact of transmembrane proteins, also supports radioresistant behaviors in GSCs and is an integral signaling pathway in the vascular niche (Wang et al., 2010b).

The hypoxic niche provides some of the best direct evidence of niche protection from chemotherapy and radiation. For both treatments, a common mode of action is through the generation of reactive oxygen species (ROS), which induces double strand breaks in DNA (Harrison and Blackwell, 2004). However, due to the relative lack of oxygen, ROS generation is attenuated thereby limiting this mechanism. In addition, hypoxia is capable of promoting downstream activation of numerous survival pathways that may further limit treatment efficacy (Harrison and Blackwell, 2004; Bhatt et al., 2008; Bertout et al., 2009). For example, GSCs identified in hypoxia have been observed to highly express MGMT, which functions to repair DNA and promotes resistance to TMZ (Pistollato et al., 2010).

Targeting niche microenvironments may provide an opportunity to disrupt GSC regulation and increase GBM treatment efficacy. Recently, inhibition of vascular niche formation initially appeared to be a promising direction for the development of new treatments; in experimental tumors, GSCs were depleted and tumor growth retarded by the antiangiogenic therapy bevacizumab, which is a VEGF function blocking antibody (Bao et al., 2006b; Calabrese et al., 2007). However, bevacizumab was

subsequently found to effect an increase invasion of GBM cells in response to increased hypoxia resulting from the inhibition of blood vessel formation (Pàez-Ribes et al., 2009; Keunen et al., 2011). In a phase III clinical trial, this treatment failed as a first-line therapy but remains an approved and viable option as a salvage treatment for increasing progression free survival in recurrent GBM (Kreisl et al., 2008). Bevacizumab fails as a GBM treatment primarily as a result of the strong hypoxia response of these tumors, and thus any approach seeking to inhibit blood supply to GBM must consider molecular responses of cells to hypoxic environments. For example, HIF2α may present a potential co-therapeutic target due to its specificity for GSCs, prominent role in GSC tumorigenicity, and regulation of responses to oxygen (Li et al., 2009; Hjelmeland et al., 2011).

Glioblastoma stem-like cell niches are complex and diverse microenvironments that provide adaptive regulation of stem functions along with protective support against GBM treatments. The striking capacity of these cells to survive insults decreases the likelihood that any monotherapy will be significantly effective. Therefore, although clinical results have thus far been disappointing, targeting and disrupting microenvironmental mechanisms of GSC regulation should remain a focus of novel treatment designs.

GBM RESEARCH MODELS

Cell Lines and *In Vitro* Culture

In vitro cell culture models have been fundamental to GBM research since the first tumor cell lines were isolated and immortalized in the 1960s (Ponten and Macintyre, 1968). Various immortalized cell lines are now widely available for research and provide a platform for disease research that ideally enables reproducible testing. Propagation *in vitro* is performed using a simplified two-dimensional (2D) isotropic plate [often poly(styrene)] that is treated to present a negative charge, or coated with poly-D-lysine, or ECM proteins to promote anchorage dependent cell growth. This 2D design is optimized for cells to experience consistency in their access to adhesion sites, nutrients, soluble signaling factors, and oxygen in culture (Woolard and Fine, 2009). These cultures enable biologically instructive assays that measure behaviors such as proliferation, migration, stem cell status, and drug sensitivity under various discrete conditions (Giese et al., 1995; Pollard et al., 2009).

Although immortalized GBM cell lines have provided invaluable understanding of aspects of the disease process in GBM, their utility in generating new therapies for clinical application is limited. *In vitro*, cells are polarized and attach to the stiff culture substrate in a single plane that provides little to no resistance to proliferation or migration. In response, cells converge on a singular phenotype through a rapid loss of cellular heterogeneity, which is a fundamental feature of GBM (Li et al., 2008). Immortalized cell lines show significant differences in their molecular signature compared with primary GBM tissue, which is a direct result of prolonged propagation and genetic instability (Li et al., 2008). Another prominent issue with long-term cell lines is the potential for contamination with other cell lines that replace the original population. As an example, one of the most widely used and first established *in vitro* models of GBM, the U87 MG cell line, was originally isolated from a 44-year-old female patient (Ponten and Macintyre, 1968). Recently, the genome of this line was compared with the original tumor sample and was determined to be a GBM of male origin (Allen et al., 2016). These problems, among others, illustrate that more representative disease models are necessary to overcome challenges in studying GBM biology.

The use of low-passage primary cells derived from patient tissue provides an improvement in the biological relevance of *in vitro* models. These are established by mechanical and enzymatic digestion of tumor tissue, whereby the resulting heterogeneous cell mix is cultured *in vitro* using standard culture conditions. GSC lines may also be established from primary tissue through culture in serum-free NSC optimized media with the mitogenic growth factors EGF and FGF (Venugopal et al., 2012). These conditions maintain the GSC population such that cells preserve genotypic and phenotypic features of the original tumor, whereas serum-supplemented cultures promote selection of differentiated GBM phenotypes and the GSC pool is subsequently depleted (Zhang et al., 2013; Lathia et al., 2015).

Standard 2D cultures may also be modified to produce models that better represent native GBM biology. For example, GBM has been cocultured with a secondary cell type such as astrocytes (Rath et al., 2013, 2015) or endothelial cells (Galan-Moya et al., 2011) to promote malignant phenotypes. The most common method for establishing cocultures is through a transwell or Boyden chamber system. In these cultures, cells are separated by a semi-permeable membrane that allows access to signaling factors secreted by the otherwise physically separated cell populations. Coculture studies have indicated that supporting cells are well capable of directing the behavior of tumor cells, including provocation of invasion and treatment resistance (Galan-Moya et al., 2011; Rath et al., 2013, 2015).

Similar to coculture methods, three-dimensional (3D) cell cultures model aspects of the tumor microenvironment to elicit interactions that are generally absent from 2D cultures. Techniques such as hanging drop culture or culture on soft agar gels generate multicellular GBM spheroids that exhibit proliferation and invasion that better recapitulates *in vivo* scenarios (Del Duca et al., 2004; Pampaloni et al., 2007; Heffernan et al., 2014). Suspension culture, in which non-adherent cells are free-floating in media, is most often used to propagate GSCs where, similar to NSCs, stem-like cells form multicellular neurospheres (also called tumorspheres) (Ignatova et al., 2002; Singh et al., 2003; Galli et al., 2004; Lee et al., 2006; Fael Al-Mayhani et al., 2009; Venugopal et al., 2012). Spheroid cultures can also be initiated as cocultures in which GBM cells are combined with endothelial or glial cells and incorporated into spheroid structures (Chen et al., 2009). Brain slice cultures further improve the relevance of the *in vitro* culture by enabling GBM cells to be analyzed in live brain tissue *ex vivo*. Here, viable brain slices are cultured and inoculated with tumor cells to enable tracking of GBM proliferation and invasion within a complete brain microenvironment. The primary drawbacks to brain slice culture include technical challenges with maintaining the tissue, reproducibility, and rapid cell death and/or alterations in the tissue during cultures (Rao et al.,

2014; Jensen et al., 2016). Taken in sum, each of these approaches to culturing GBM have been valuable to isolate specific cellular responses under defined experimental conditions, although the degree to which neurosphere or hanging drop cultures can be engineered to capture essential aspects of the niche remain limited.

Preclinical *In Vivo* Models

In vivo models of GBM are the gold standard for analyzing tumor growth and response to therapy within a physiologically relevant system. *In vivo* models are either syngeneic or xenograft. Syngeneic murine GBM models have been established *via* development of native GBM cell lines (e.g., through chemical insult) or genetic engineering that induces spontaneous and reproducible tumor formation (Huszthy et al., 2012). Primary advantages of syngeneic models include the ability to analyze tumors in the context of a fully functional immune system, and in genetic models, alterations in signaling pathways that are known to drive GBM malignancy (EGFR, PDGFR, Rb, Ras, and Akt) (Jacobs et al., 2011; Huszthy et al., 2012). Alternatively, xenograft models are established by the transplantation of human derived cell lines into an immunocompromised mouse host. The primary advantage of xenograft models is that they enable study of human GBM progression within a functional albeit immunodeficient brain.

Human xenograft models may be established from long-term cell lines or from freshly isolated patient-derived GBM tissue. Tumors can be induced in either the flank or directly in the brain. Flank models enable rapid confirmation of tumorigenicity and rapid growth of tumor within an easy to access physical compartment, while also providing a more permissive paradigm for treatment studies due to the lack of a blood–brain barrier protecting the tumor. Orthotopic models, on the other hand, are best suited for studying GBM behaviors in the context of the native brain tumor microenvironment. Various immortalized cell lines (U87, U118, etc.) have been used to produce aggressive orthotopic tumors with reproducible cellular architecture (Jacobs et al., 2011; Huszthy et al., 2012). However, tumors generated through orthotopic transplant of immortalized cells often present significant genetic and histological variations from patient tumors thereby limiting their translational relevance (Lee et al., 2006; Jacobs et al., 2011). For example, U87 tumors are highly vascularized, possess a relatively leaky blood–brain barrier, and do not exhibit the infiltrative behavior that is characteristic of patient GBM tissue (Jacobs et al., 2011). The generation of noninvasive tumors is one of the primary drawbacks common to using immortalized cells in preclinical models. Conversely, low-passage patient-derived xenografts, particularly those established in serum-free culture or *via* direct *in vivo* inoculation, are characterized by their maintenance of parental tumor genotypes, an invasive leading edge, and minimal disruption of the blood–brain barrier (Galli et al., 2004; Singh et al., 2004; Sanai et al., 2005; Lee et al., 2006; Fael Al-Mayhani et al., 2009). Thus, patient-derived xenografts are presently considered the most biologically relevant research model of the human disease (Huszthy et al., 2012).

ENGINEERING THE GBM TUMOR MICROENVIRONMENT

The reduction of microenvironmental complexity in 2D cell culture limits analysis of disease biology because the 3D ECM regulates numerous essential cellular phenotypes (Pampaloni et al., 2007). Tissue engineering strategies address this gap in understanding by providing methods to model key components of the 3D tumor microenvironment such as insoluble ECM components, stiffness, matrix degradability, and soluble signaling factors. These tools are not a direct surrogate for the complex, anisotropic, and heterogeneous *in vivo* scenario; instead, they enable characterization of contributions from individual microenvironmental factors. Here, we review how these approaches have been utilized to understand important features of GBM and GSC biology.

Biomaterials in GBM Research

Both natural and synthetic polymers have been used to study GBM response to the microenvironment (relevant studies are summarized in **Table 1**). Natural materials are bioactive, degradable by enzymatic or hydrolytic mechanisms, and cells interact with them directly through specific and established biochemical pathways. Due to their specific bioactivity, some of the most important and commonly used in GBM research are HA, collagen, and Matrigel® (**Table 1**). One potential challenge with using ECM biomaterials derived from live hosts or cell cultures, such as Matrigel®, is a lack of experimental reproducibility. These multicomponent materials exhibit variation in composition across batches (e.g., growth factor content and ECM protein concentration), which may adversely impact the interpretation of results due to changes in the constituent materials (Pampaloni et al., 2007). Juxtaposed to natural materials, synthetic biomaterials used in GBM cultures are derived from organic sources, which enables a high degree of control over their physical and chemical properties. Of these, poly(ethylene glycol) (PEG) is by far the most common. Its hydrophilicity and chemical structure enable cell encapsulation and functionalization reactions that can be performed *in situ*. Synthetic biomaterials can be either degradable or non-degradable, and in general, are expected to possess lower intrinsic bioactivity than natural materials, since they do not possess cellular adhesion sites that would be expected to elicit biological responses. Cells are capable of interfacing with a purely synthetic polymer either through surface adsorbed proteins (vitronectin, laminin, etc.) or through non-specific charge interactions (Hubbell, 1995). Grafting synthetic polymers with bioactive proteins or peptides (e.g., RGD) is a common approach to enable cellular adhesion or biodegradation (**Table 1**). This method of combining natural and/or synthetic components into a composite biomaterial is useful for leveraging advantages of both classifications.

The majority of natural, synthetic, and composite scaffolds applied in GBM studies are hydrophilic hydrogels, which, like tissue, are composed of a high fraction of water and swell considerably in aqueous solution. However, in some instances hydrophobic polymers are also incorporated, often coated with

TABLE 1 | Biomaterial models of the glioblastoma (GBM) microenvironment enable analysis of malignant behaviors *in vitro*.

	Reference
SCAFFOLD COMPONENTS	
Hyaluronic acid	Tamaki et al. (1997), Jin et al. (2009), Ananthanarayanan et al. (2011), Florczyk et al. (2013), Pedron et al. (2013, 2015, 2017), Rao et al. (2013a,b), Fernandez-Fuente et al. (2014), Heffernan et al. (2014), Jiguet Jiglaire et al. (2014), Kim and Kumar (2014), Rape and Kumar (2014), Wang et al. (2014, 2016), Herrera-Perez et al. (2015), Rape et al. (2015), Cha et al. (2016), Kievit et al. (2016), Chen et al. (2017), and Ngo and Harley (2017)
Collagen	Tamaki et al. (1997), Sarkar et al. (2006), Kim et al. (2008), Ulrich et al. (2010), Yang et al. (2010, 2014), Eke et al. (2012), Florczyk et al. (2013), Pedron and Harley (2013), Pedron et al. (2013, 2015, 2017), Rao et al. (2013a,b), Ruiz-Ontañon et al. (2013), Fernandez-Fuente et al. (2014), Heffernan et al. (2014), Jain et al. (2014), Jiguet Jiglaire et al. (2014), Herrera-Perez et al. (2015), Wong et al. (2015), Cha et al. (2016), Chen et al. (2017), Chonan et al. (2017), and Ngo and Harley (2017)
Matrigel	Cordes et al. (2003), Jin et al. (2009), Kievit et al. (2010), Cheng et al. (2011), Rao et al. (2013a), Ruiz-Ontañon et al. (2013), Herrera-Perez et al. (2015), Grundy et al. (2016), Hubert et al. (2016), and Chonan et al. (2017)
Poly(ethylene glycol)	Pedron and Harley (2013), Pedron et al. (2013), Heffernan et al. (2014), Jiguet Jiglaire et al. (2014), Wang et al. (2014), Fan et al. (2016), Li et al. (2016), Oh et al. (2016), and Ngo and Harley (2017)
Chitosan	Kievit et al. (2010, 2014, 2016), Florczyk et al. (2013, 2016), and Wang et al. (2016)
Alginate	Kievit et al. (2010, 2014, 2016), Florczyk et al. (2016), and Oh et al. (2016)
Poly(*N*-isopropylacrylamide)	Heffernan et al. (2016, 2017), and Li et al. (2016)
Polyacrylamide	Ulrich et al. (2009), Pathak and Kumar (2012), Ruiz-Ontañon et al. (2013), Fernandez-Fuente et al. (2014), Rape and Kumar (2014), Umesh et al. (2014), Wong et al. (2015), and Grundy et al. (2016)
Polycaprolactone	Rao et al. (2013a), Jain et al. (2014), Kievit et al. (2014, 2016), and Cha et al. (2016)
Polystyrene	Kievit et al. (2014) and Ma et al. (2016a)
Poly(lactic acid)	Ma et al. (2012)
Bioactive peptide/protein	Tamaki et al. (1997), Cordes et al. (2003), Sarkar et al. (2006), Ulrich et al. (2009), Ananthanarayanan et al. (2011), Pathak and Kumar (2012), Ruiz-Ontañon et al. (2013), Jain et al. (2014), Kim and Kumar (2014), Rape and Kumar (2014), Umesh et al. (2014), Wang et al. (2014), Rape et al. (2015), Wong et al. (2015), Heffernan et al. (2016), Ma et al. (2016a), and Ngo and Harley (2017)
Complex three-dimensional (3D) models	Ma et al. (2012), Pathak and Kumar (2012), Rao et al. (2013a), Jain et al. (2014), Herrera-Perez et al. (2015), Pedron et al. (2015), Rape et al. (2015), Cha et al. (2016), Fan et al. (2016), Li et al. (2016), and Chonan et al. (2017)
BIOPHYSICAL PROPERTIES	
Stiffness	Kim et al. (2008), Ulrich et al. (2009, 2010), Yang et al. (2010), Ananthanarayanan et al. (2011), Pathak and Kumar (2012), Florczyk et al. (2013, 2016), Pedron and Harley (2013), Pedron et al. (2013, 2015), Rao et al. (2013a,b), Fernandez-Fuente et al. (2014), Heffernan et al. (2014, 2016, 2017), Kim and Kumar (2014), Rape and Kumar (2014), Umesh et al. (2014), Wang et al. (2014), Herrera-Perez et al. (2015), Rape et al. (2015), Wong et al. (2015), Cha et al. (2016), Grundy et al. (2016), Chen et al. (2017), and Ngo and Harley (2017)
Porosity	Kim et al. (2008), Yang et al. (2010, 2014), Ananthanarayanan et al. (2011), Ma et al. (2012, 2016a), Pathak and Kumar (2012), Florczyk et al. (2013, 2016), Pedron and Harley (2013), Rao et al. (2013a,b), Kievit et al. (2014, 2016), Wang et al. (2014, 2016), Herrera-Perez et al. (2015), Cha et al. (2016), Fan et al. (2016), and Oh et al. (2016)
Microchannels	Pathak and Kumar (2012), Pedron et al. (2015), Fan et al. (2016), and Chonan et al. (2017)
Fibers/alignment	Kim et al. (2008), Ulrich et al. (2010), Yang et al. (2010), Rao et al. (2013a,b), Jain et al. (2014), Herrera-Perez et al. (2015), Cha et al. (2016), and Ma et al. (2016a)
GBM CELL LINES	
U87	Kim et al. (2008), Jin et al. (2009), Ulrich et al. (2009), Kievit et al. (2010, 2014, 2016), Ananthanarayanan et al. (2011), Eke et al. (2012), Pedron and Harley (2013), Pedron et al. (2013, 2015), Fernandez-Fuente et al. (2014), Heffernan et al. (2014), Jain et al. (2014), Jiguet Jiglaire et al. (2014), Kim and Kumar (2014), Rape and Kumar (2014), Umesh et al. (2014), Wang et al. (2014), Fan et al. (2016), Florczyk et al. (2016), and Ngo and Harley (2017)
U373	Jin et al. (2009), Ulrich et al. (2009, 2010), Ananthanarayanan et al. (2011), Pathak and Kumar (2012), Kim and Kumar (2014), Rape and Kumar (2014), Umesh et al. (2014), Rape et al. (2015), and Wong et al. (2015)
U251	Sarkar et al. (2006), Jin et al. (2009), Ulrich et al. (2009), Ma et al. (2016a), and Chen et al. (2017)
U118	Kievit et al. (2010, 2014), Florczyk et al. (2013), and Heffernan et al. (2014, 2016)
U138	Cordes et al. (2003) and Eke et al. (2012)
A172	Cordes et al. (2003), Eke et al. (2012), and Fernandez-Fuente et al. (2014)
U343	Jin et al. (2009)
U178	Sarkar et al. (2006)
T98	Fernandez-Fuente et al. (2014)

(*Continued*)

TABLE 1 | Continued

	Reference
LN229	Cordes et al. (2003) and Eke et al. (2012)
LN18	Cordes et al. (2003)
SNB19	Ulrich et al. (2009)
M059K	Ma et al. (2012)
Genetically modified GBM	Pedron et al. (2013, 2015), Heffernan et al. (2014), and Kim and Kumar (2014)
Coculture	Ma et al. (2012), Ruiz-Ontañon et al. (2013), Kievit et al. (2016), Chonan et al. (2017), and Ngo and Harley (2017)
Murine model	Tamaki et al. (1997), Ulrich et al. (2009), Kievit et al. (2010), Yang et al. (2010), Jiguet Jiglaire et al. (2014), Hubert et al. (2016), and Chonan et al. (2017)
Patient derived	Eke et al. (2012), Rao et al. (2013a,b), Ruiz-Ontañon et al. (2013), Fernandez-Fuente et al. (2014), Jiguet Jiglaire et al. (2014), Yang et al. (2014), Herrera-Perez et al. (2015), Wong et al. (2015), Cha et al. (2016), Grundy et al. (2016), Hubert et al. (2016), Li et al. (2016), Oh et al. (2016), Wang et al. (2016), Heffernan et al. (2017), and Pedron et al. (2017)
BIOLOGICAL BEHAVIORS	
Two-dimensional migration	Kim et al. (2008), Jin et al. (2009), Ulrich et al. (2009), Ananthanarayanan et al. (2011), Eke et al. (2012), Pathak and Kumar (2012), Rao et al. (2013a), Ruiz-Ontañon et al. (2013), Fernandez-Fuente et al. (2014), Kim and Kumar (2014), Rape and Kumar (2014), Wong et al. (2015), Grundy et al. (2016), and Chonan et al. (2017)
3D invasion	Tamaki et al. (1997), Cordes et al. (2003), Sarkar et al. (2006), Kim et al. (2008), Jin et al. (2009), Ulrich et al. (2010), Yang et al. (2010), Ananthanarayanan et al. (2011), Cheng et al. (2011), Eke et al. (2012), Pathak and Kumar (2012), Florczyk et al. (2013), Rao et al. (2013b), Ruiz-Ontañon et al. (2013), Heffernan et al. (2014, 2016), Jain et al. (2014), Kim and Kumar (2014), Rape and Kumar (2014), Herrera-Perez et al. (2015), Wong et al. (2015), Cha et al. (2016), Grundy et al. (2016), Chen et al. (2017), and Chonan et al. (2017)
Proliferation	Tamaki et al. (1997), Ulrich et al. (2009), Kievit et al. (2010, 2014, 2016), Yang et al. (2010, 2014), Ananthanarayanan et al. (2011), Eke et al. (2012), Ma et al. (2012, 2016a), Florczyk et al. (2013, 2016), Pedron and Harley (2013), Pedron et al. (2013, 2015, 2017), Ruiz-Ontañon et al. (2013), Heffernan et al. (2014, 2016, 2017), Jain et al. (2014), Jiguet Jiglaire et al. (2014), Umesh et al. (2014), Wang et al. (2014, 2016), Wong et al. (2015), Cha et al. (2016), Hubert et al. (2016), Li et al. (2016), and Chen et al. (2017)
Malignancy markers	Cordes et al. (2003), Sarkar et al. (2006), Kim et al. (2008), Jin et al. (2009), Kievit et al. (2010, 2014, 2016), Cheng et al. (2011), Eke et al. (2012), Florczyk et al. (2013, 2016), Pedron and Harley (2013), Pedron et al. (2013, 2015, 2017), Rao et al. (2013a), Ruiz-Ontañon et al. (2013), Fernandez-Fuente et al. (2014), Jiguet Jiglaire et al. (2014), Kim and Kumar (2014), Umesh et al. (2014), Wang et al. (2014, 2016), Yang et al. (2014), Herrera-Perez et al. (2015), Rape et al. (2015), Wong et al. (2015), Cha et al. (2016), Hubert et al. (2016), Li et al. (2016), Ma et al. (2016a), Chen et al. (2017), Chonan et al. (2017), and Heffernan et al. (2017)
Stem phenotypes	Cheng et al. (2011), Florczyk et al. (2013, 2016), Ruiz-Ontañon et al. (2013), Fernandez-Fuente et al. (2014), Kievit et al. (2014, 2016), Yang et al. (2014), Herrera-Perez et al. (2015), Wong et al. (2015), Cha et al. (2016), Grundy et al. (2016), Hubert et al. (2016), Li et al. (2016), Ma et al. (2016a), Wang et al. (2016), Chonan et al. (2017), Heffernan et al. (2017), and Pedron et al. (2017)
In vivo characteristics	Kievit et al. (2010, 2014), Cheng et al. (2011), Ruiz-Ontañon et al. (2013), Jain et al. (2014), Jiguet Jiglaire et al. (2014), Yang et al. (2014), Wong et al. (2015), Florczyk et al. (2016), Hubert et al. (2016), Li et al. (2016), and Pedron et al. (2017)
TREATMENT RESPONSE	
Chemotherapy	Kim et al. (2008), Ulrich et al. (2009), Eke et al. (2012), Ma et al. (2012), Pathak and Kumar (2012), Florczyk et al. (2013), Fernandez-Fuente et al. (2014), Jain et al. (2014), Jiguet Jiglaire et al. (2014), Rape and Kumar (2014), Umesh et al. (2014), Yang et al. (2014), Cha et al. (2016), Fan et al. (2016), Wang et al. (2016), and Pedron et al. (2017)
Radiation	Cordes et al. (2003), Eke et al. (2012), Jiguet Jiglaire et al. (2014), Hubert et al. (2016), and Heffernan et al. (2017)

hydrophilic ECM proteins (Rao et al., 2013a; Cha et al., 2016; Ma et al., 2016a). Scaffolds of either classification can be further designed as porous, fibrous, anisotropic, or some combination, each with varying degrees of control of these physical properties dependent on the constituents. These properties enable modeling of a wide variety of topographies to mimic the physiological microenvironment. Chemical and physical cross-linking reactions are often necessary to increase the molecular weight of a biomaterial such that it forms an insoluble physical structure in aqueous solution. Strategies that do not negatively impact cell viability are particularly desirable. For chemically cross-linked biomaterials, click chemistry, such as Michael addition (Ananthanarayanan et al., 2011; Heffernan et al., 2014; Jiguet Jiglaire et al., 2014; Kim and Kumar, 2014; Rape and Kumar, 2014; Rape et al., 2015), describes stepwise reactions that proceed efficiently at neutral pH, do not require biologically damaging solvents or reaction conditions, and do not produce any cytotoxic byproducts (Hoyle et al., 2010). Another common example of chemical cross-linking is UV free radical polymerization, which, unlike most free radical reactions, may utilize an aqueous compatible initiator that is photoreactive (e.g., Irgacure 2959). This method enables polymerization of reactive monomers such as terminal olefins (e.g., acrylates)

(Pedron and Harley, 2013; Pedron et al., 2013, 2015, 2017; Chen et al., 2017; Ngo and Harley, 2017). Alternatively, physical cross-linking proceeds without a chemical reaction; alterations in pH or temperature produce electrostatic interactions that result in polymerization and/or precipitation (El-Sherbiny and Yacoub, 2013); typical examples include collagen (pH stimulus) or poly(*N*-isopropylacrylamide) (temperature stimulus). It is well known that the degree of cross-linking (chemical or physical) for any given material will affect the porosity, density, and stiffness of the scaffold, which are each independently important considerations in GBM tissue engineering.

3D Culture Methods

Biomaterial cultures are performed with cells or spheroids either seeded on the scaffold surface or encapsulated within the scaffold during cross-linking. Surface cultures enable measurement of cellular behaviors (motility, invasion, proliferation, viability, etc.) in response to the biophysical and biochemical material properties. They also provide a set initial location for cells and do not necessarily require biodegradation of the material to allow for cell proliferation or motility, since cells are capable of moving across the surface. Encapsulation cultures offer a more physiologically relevant scenario but require biocompatible cross-linking and matrix degradation for cell growth and motility. Both scenarios are regularly used to measure invasive capacity, which cannot be fully recapitulated in 2D *in vitro* systems.

For both surface and encapsulation cultures, biological assays must be either performed *in situ* (e.g., immunofluorescence and cell tracking) or alternatively, on cells recovered from the scaffold (e.g., western blot, polymerase chain reaction, and fluorescence activated cell sorting). Both culture approaches pose various technical challenges to performing these assays that are specific to the biomaterial system; a significant consideration in designing a 3D culture format. For example, chemically cross-linked materials may require degradation or cell dissociation conditions that adversely affect cell viability or the presentation of surface proteins. Physical scaffolds, on the other hand, may offer reversible formation in response to mild environmental changes and thereby enable easy cell recovery for post-culture analysis.

Biophysical and Biochemical Regulation of GBM Behaviors

The *in vivo* tumor microenvironment provides critical regulatory functions for GBM tumors. As a result, there are many reports investigating how the physical microarchitecture and biochemical features of 3D biomaterials regulate or elicit specific GBM behaviors *in vitro* (summarized in detail in **Table 1**). These studies have been reviewed in great detail elsewhere (Rao et al., 2014; Rape et al., 2014; Xiao et al., 2017). One well-established observation is that matrix stiffness and topography (porosity, fiber content, geometry) can alter cellular phenotype to elicit malignant behaviors, including proliferation, migration, and invasion. Mechanosensation, or the ability for cells to sense mechanical forces and stiffness, is a key component of GBM biology that mediates tumor growth and cell motility (Rape et al., 2014). This was demonstrated *in vitro* by Ulrich et al. (2009) who described that GBM cell lines displayed both higher motility and proliferation on high stiffness substrates and also identified that the motile responses were governed at least in part by non-muscle myosin II. Furthermore, one of the more intriguing developments in understanding biophysical regulation has been the discovery that biomaterial fibers mimicking the structure of blood vessels are capable of encouraging and guiding GBM invasion (Rao et al., 2013a; Jain et al., 2014; Herrera-Perez et al., 2015; Cha et al., 2016). The primary method for changing the biophysical properties of 3D models is *via* altering the concentration of the constituent biomaterials. While effective, this often also coupled with changing the density of bioactive components. Isolating the impact of different biophysical cues on cellular behavior is almost impossible *in vivo*, but biomaterial platforms offer an opportunity to independently manipulate these variables, which will be important to deepening understanding of the disease (Wang et al., 2014).

In considering the biochemical influence of the microenvironment on GBM biology, various different scaffold components have been explored (complete list in **Table 1**); one of the most common materials utilized for this purpose is HA. Given that HA, discussed earlier, has many essential functions in GBM (Giese and Westphal, 1996), it is unsurprising that HA hydrogels have been shown to regulate a wide variety of behaviors including proliferation (Pedron et al., 2013), invasion (Heffernan et al., 2014), stem phenotypes (Cha et al., 2016), and treatment resistance (Jiguet Jiglaire et al., 2014). HA does not provide cellular adhesion sites, and as a result is regularly modified with cell adhesion peptides or combined with other biomaterials, such as collagen, to enable cell attachment (Ananthanarayanan et al., 2011; Pedron et al., 2013; Heffernan et al., 2014; Jiguet Jiglaire et al., 2014). While relatively insignificant components of the native brain ECM, collagen and Matrigel® are also prominent biomaterials in GBM research primarily because of their high density of focal adhesion sites, their history of use in other cancer models (e.g., breast cancer), and the ease with which they can be experimentally implemented. Both models have been used to investigate the role of matrix signaling in promoting focal adhesion mediated GBM invasion (Herrera-Perez et al., 2015; Heffernan et al., 2016). Alternatively, PEG-based biomaterials offer a tunable synthetic platform with the potential for easy chemical modification. PEG gels have been designed to be enzymatically degradable (Wang et al., 2014), hydrolytically stable or degradable (Heffernan et al., 2014), or modified with cell instructive peptides (Ananthanarayanan et al., 2011), each of which have been shown to modify malignant GBM behaviors. Moreover, complex multicomponent biomaterial models have also been reported for developing high-throughput studies of GBM behaviors across a range of different microenvironmental conditions (Pedron et al., 2015), or alternatively, through cocultures with microenvironmental support cells within a single 3D *in vitro* system (Ngo and Harley, 2017). Together, the current body of work (**Table 1**) illustrates the breadth of understanding that has developed in response to implementing *in vitro* biomaterial cultures.

BIOMATERIALS FOR PROBING GSC BIOLOGY

Engineering the Stem Cell Microenvironment

Engineering GSC instructive *in vitro* microenvironments is a relatively new approach derived from well-established tissue engineering research. Stem cells are widely regarded for their potential to regenerate and establish functional tissues. Neural tissue engineering, which is most closely related to methods for modeling the GBM microenvironment, primarily focuses on developing novel techniques for directing NSC behaviors. In this field, biomaterials have been utilized to elucidate various stem cell behaviors with a focus on understanding how biophysical and biochemical factors in 2D and 3D environments affect NSC maintenance, self-renewal, and differentiation mechanisms (Teixeira et al., 2007). Through these studies, the mechanical stiffness of culture substrates and matrices has been identified as a potent regulator of NSC fate. Saha et al. (2008) reported that NSC differentiation could be directed with soft substrates (100–500 Pa) to promote neurogenesis and stiff (>1,000 Pa) matrices to promote gliogenesis. In addition to matrix stiffness, Soen et al. (2006) and Nakajima et al. (2007) demonstrated that specific ECM components and growth factors were also capable of controlling stem cell fate and differentiation in culture. Other cellular components of the NSC microenvironment have been investigated as regulators of stem cell fate *in vitro*. For example, Shen et al. (2004) determined that endothelial cells secrete soluble factors that promote and maintain stem phenotypes in NSC populations.

The regenerative capacity of NSCs has also been investigated in 3D microenvironment models with both matrix composition and stiffness again identified as key regulatory components. Here, Saha et al. (2008) described that very soft substrates (<100 Pa) promoted quiescent NSC phenotypes, while stiffening these substrates (≥100 Pa) promoted expansion of the NSC pool. The structure of the ECM is also important to NSC neural regenerative properties, as Yang et al. (2005) described scaffolds composed of aligned poly(L-lactic acid) nanofibers promoted neuronal phenotypes and neurite outgrowth along the fibers. More biomimetic approaches have also been tested using ECM components of the *in vivo* NSC niche as well. To this end, Cheng et al. (2013b) described that a laminin-derived IKVAV peptide-based hydrogel supported NSC neuronal differentiation and improved tissue regeneration *in vivo* following a traumatic brain injury. In addition, we reported that an HA–laminin composite hydrogels increase the migratory response of NSCs a result of increased sensitivity to stromal cell-derived factor 1α both *in vitro* and *in vivo* (Addington et al., 2015, 2017).

Similar regulatory mechanisms govern both GSC and NSC biology (Sanai et al., 2005), and as such, these examples have direct relevance to understanding and predicting how model microenvironments may affect malignant GSC phenotypes. In applying these same tissue engineering approaches to GSCs, conditions under which these cells acquire or enhance stem phenotypes, prefer to initiate invasive mechanisms, or exhibit treatment resistance have been identified. These results provide better understanding of the underlying mechanisms that drive microenvironmental support for GSC populations.

GBM Stem Plasticity in 3D Culture

Glioblastoma stem-like cells and NGSCs are believed to exist in a regulated state of plasticity where induction of differentiation is a bidirectional process regulated by the microenvironment, epigenetics, and response to treatment (Heddleston et al., 2009; Dahan et al., 2014; Safa et al., 2015). This stem plasticity has been investigated using immortalized GBM cell lines as a model of NGSCs. Although, as previously described, these cell lines do not offer a complete and accurate depiction of GBM biology, and the mechanisms that are employed to acquire stem phenotypes may mimic GSC plasticity (Jacobs et al., 2011; Zhang et al., 2013).

Stem plasticity has been studied in GBM cell lines cultured in chitosan-based scaffolds; for example, Florczyk et al. (2013) developed a chitosan–HA composite scaffold that elucidated stem-like characteristics in U118 cells. The authors reported that these scaffolds promoted sphere formation, expression of stem markers (Nestin, Musashi-1, and CD44), and increased invasive capacity compared with traditional 2D cultures. In addition, scaffold-cultured cells displayed increased resistance to both TMZ and doxorubicin, coupled with increased expression of the ABCG2 drug efflux pump, suggesting a phenotypic switch toward a more GSC-like state (Florczyk et al., 2013). In a follow-up study, Kievit et al. (2014) used a chitosan–alginate scaffold to also examine stem plasticity. Using these models, U118 and U87 GBM cells again displayed increased stem protein and gene expression (CD133, Nestin, CD44, Notch, among others) in scaffold environments, which was again a function of scaffold composition. Functionally, scaffold grown cells also exhibited increased tumorigenicity in a flank tumor model. Kievit et al. (2016) further optimized this approach by coating chitosan–alginate scaffolds with HA and establishing a 3D coculture model of U87 and endothelial cells. These conditions also increased expression of CD133, ID1, and CD44 but interestingly slowed the growth of spheroids. Outside of GBM, Florczyk et al. (2016) employed this platform to enrich CD133 expression in prostate, breast, and liver cancer cells.

Chitosan-based scaffolds are also not the only biomaterial platform that has been reported to drive stem plasticity, as Ma et al. (2016a) also identified stem-specific responses to 3D electrospun polystyrene scaffolds coated with a library of seven different isoforms of laminin. The resulting behavior of U251 cells was, similar to the chitosan studies, contingent both on 3D context and matrix chemistry. Specifically, 3D scaffolds presenting the laminin isoforms 411, 421, 511, and 521 promoted an increase in expression of the GSC markers (including, for example, integrin α6, SOX2, and OLIG2) that coincided with an increase in clonogenicity of these cells (Ma et al., 2016a).

Together, these works emphasize the significance of using engineered microenvironments to drive relevant GSC behaviors in culture. The use of immortalized cell lines provides some insight into how GBM cells exhibit plasticity in a shift from differentiated phenotypes to more stem-like behaviors.

Biomaterials Promoting GSC Expansion and Enrichment

Engineered tumor microenvironments have also been designed to assay conditions under which patient-derived GSCs may be enriched *in vitro*. GSCs are typically maintained in non-adherent neurosphere conditions (Singh et al., 2003) or in adherent cultures on laminin (Pollard et al., 2009), with the desired condition often selected based on cellular affinity. In general, neurosphere conditions are most common as sphere forming capacity is regularly accompanied by a broader array of GSC specific phenotypes (self-renewal, multipotency, and stem-marker expression) (Venugopal et al., 2012). However, neurosphere culture has well-characterized drawbacks. Specifically, as spheres increase in size, the constituent cells experience differential access to oxygen and soluble signaling factors as a result of diffusion limitations (Woolard and Fine, 2009). This problem is amplified by variations in rates of cell proliferation and fusion of adjacent spheres. As a result, a single neurosphere may contain a heterogeneous mixture of clonogenic, differentiated, apoptotic, and necrotic cells (Bez et al., 2003; Beier et al., 2008; Pollard et al., 2009; Woolard and Fine, 2009).

A number of biomaterials have been described as useful tools for addressing problems associated with neurosphere aggregation. For example, Yang et al. (2014) reported that gelatin foam scaffolds maintained GSC protein expression, while also increasing HIF1α and VEGF signaling to provide a GSC supportive microenvironment. As stated previously (see Therapeutic Challenges and Opportunities), hypoxia signaling, including HIFs and VEGF, has been proposed as a potential mechanism for sensitizing GSCs to treatment. Thus, this platform may be relevant for testing these hypotheses. In a separate study, Oh et al. (2016) reported that GSCs encapsulated in an alginate–PEG hydrogel formed neurospheres with relative uniformity in size, which may improve nutrient and oxygen access. Li et al. (2016) used a similar approach to expand patient-derived GSCs in a temperature-responsive PNIPAAm-based scaffold. In this context, cells were capable of high density culture without aggregating, thus overcoming a key drawback to traditional neurosphere cultures. This system subsequently enabled improved cellular yield from GSC cultures while maintaining multipotency and stem-marker expression.

Beyond GSC expansion, conditions under which GSC phenotypes are actively enriched have also been explored in 3D culture. Chitosan–HA scaffolds were recently applied to patient-derived GSCs by Wang et al. (2016) and were found to increase stem gene expression (SOX2, and TAZ, NANOG), invasion gene expression (TWIST1, TWIST2, SNAIL1, SNAIL2, and ZEB2), and expression of genes that drive drug resistance (MGMT, HIF1A, and SOD1) compared with cells cultured as a 2D monolayer. GSCs cultured in these scaffolds also exhibited higher tolerance to the chemotherapeutics TMZ, carmustin (BCNU), and lomustine (CCNU). Similarly, we recently reported another set of 3D culture conditions that promote GSC enrichment utilizing temperature-responsive PNIPAAm-co-Jeffamine (PNJ) scaffolds (Heffernan et al., 2017). This culture platform increased self-renewal capacity, expression of the stem marker Nestin, and EGFR expression while maintaining cellular multipotency in two genetically distinct models of GBM. In addition, we observed that PNJ cultured cells also exhibited increased resistance to clinical dosages of radiation following 3D culture. EGFR signaling has been shown to be an important mediator of medulloblastoma radioresistance, and this platform may help to elucidate whether this mechanism is applicable to GSCs (Hambardzumyan et al., 2008).

In total, these studies suggest that there are a diverse set of biomaterials capable of maintaining GSCs cultures, and a subset of these materials are useful for actively enriching GSC specific phenotypes. Considering the differences in scaffold composition, it is also likely that GSCs are regulated *via* distinct mechanisms in the described culture systems.

In Vitro Models of GSC Invasion

Invasion of neoplastic cells into healthy brain tissue has and continues to be considered the most clinically significant issue inhibiting effective GBM treatment (Berens and Giese, 1999). Considering the role, GSCs play in tumor recurrence and invasion, understanding how these cells respond to specific microenvironmental cues to promote invasive behaviors is of particular importance. In the seminal work of Cheng et al. (2011), GSCs were determined to exhibit a heightened propensity for invasion. This characteristic was first identified *in vitro*, using a 3D Matrigel-transwell invasion assay, and was subsequently confirmed *in vivo* when compared with NGSCs from a matched tumor sample (Cheng et al., 2011). This description provided a foundation for employing *in vitro* microenvironments to determine how the biochemical, biophysical, and cellular components of the tumor microenvironment affect GSC invasion.

Biochemical input signals from the tumor microenvironment ECM influence GSC propensity for invasion, and this hypothesis has been supported in various different *in vitro* paradigms. Using a library of Matrigel, collagen, and HA–collagen matrices, Herrera-Perez et al. (2015) determined that modes of GSC invasion were directly dependent on ECM chemistry. These matrices accurately modeled the stiffness of healthy brain tissue, and different preparations of collagen were used to separate the effects of matrix stiffness and collagen concentration. As a result, this study identified an interplay between matrix stiffness and chemistry that influenced invasion distance and velocity. Interestingly, soluble HA (non-immobilized) decreased GSC invasion in HA–collagen matrices, and Matrigel coated microfibers, mimicking the structure of blood vessels, encouraged directional strand motility reminiscent of white matter tract invasion tendencies *in vivo* (Herrera-Perez et al., 2015).

Identification of biochemical pathways that promote or inhibit GSC invasion is necessary for complete characterization of these behaviors but is often underreported; a limitation of many 3D culture studies. As an example, Cha et al. (2016) explored a similar paradigm to Herrera-Perez et al. by measuring GSC invasion through collagen matrices that included soluble HA and PCL fibers to model blood vessels. Yet, in apparent contrast to the prior study, Cha et al. (2016) reported that soluble HA increased GSC invasion in collagen matrices, while also exhibiting increased expression of CD44, and HA synthase. In addition, treatment with an HA synthase inhibitor decreased invasion and

effected an increase in FAK and MMP2 expression (Cha et al., 2016). While the functional results of these studies (i.e., invasion) appear contradictory, it is important to recognize differences in methodology which include the source of patient-derived cells, and the concentrations of collagen and HA in the model systems. Therefore, molecular level descriptions may improve cross-study comparisons and allow for more robust descriptions of GSC invasive mechanisms.

From analysis of the *in vivo* tumor microenvironment, it is clear that non-GBM cells, such as endothelial cells, are capable of regulating GSC phenotypes and promoting invasion. This behavior was studied by Chonan et al. (2017) in which a 3D collagen gel was applied to separate a murine GSC line from endothelial cells in an engineered microfluidic invasion model. Here, endothelial cells stimulated increased invasion of Nestin expressing cells through the 3D microenvironment. These GSCs also exhibited increased expression of integrin α2 and β3 in response to coculture, suggesting a potential mechanistic role for endothelial cells in promoting motility of GSCs in this model. Meanwhile, cells expressing the neuronal differentiation marker tubulin β3 were less invasive, which agrees with prior reports of increased GSC invasive capacity vs. NGSCs (Cheng et al., 2011).

As previously stated, microenvironmental stiffness regulates the invasive capacity of GBM cell lines *via* mechanosensation mechanisms (Ulrich et al., 2009; Ananthanarayanan et al., 2011; Pedron and Harley, 2013; Heffernan et al., 2014; Kim and Kumar, 2014). While the stiffness of healthy brain is generally characterized between 100 and 1,000 Pa, GBM tumors can present significantly increased stiffness due to their high cellularity and dense ECM (Netti et al., 2000; Georges et al., 2006; Saha et al., 2008; Buxboim et al., 2010). At present, reports investigating the effects of matrix stiffness on GSC motility in both 2D and 3D paradigms describe a complex relationship (Ruiz-Ontañon et al., 2013; Herrera-Perez et al., 2015; Wong et al., 2015; Grundy et al., 2016). Ruiz-Ontañon et al. (2013) reported that GSCs harvested from different tumor regions (peritumoral vs. bulk tumor) display invasive tendencies and sensitivity to microenvironmental stiffness that was a function of their regional origin. Unsurprisingly, peritumoral GSCs were observed to have a heightened invasive capacity. These behaviors were modeled on 2D laminin functionalized polyacrylamide matrices, within 3D Matrigel and collagen I hydrogels, as well as in chicken embryo and mouse xenografts. Moreover, peritumoral invasion was insensitive to stiffness as a result of Rac and RhoA signaling activation, and integrin αVβ3, an RGD peptide binding integrin, was identified as a key regulator of GSC invasion and potential target for therapy (Ruiz-Ontañon et al., 2013). Similarly, Wong et al. (2015) also reported that GSCs exhibited an insensitivity to matrix stiffness on 2D laminin coated polyacrylamide matrices. Here, matrix stiffness ranging from 80 Pa to 119 kPa produced no effect on cellular migration. However, in contrast to the previous study, activation of myosin II signaling *via* genetic constitutive activation of RhoA, ROCK, or MLCK sensitized cells to matrix stiffness and effected a decrease in motility on soft matrices.

Together, these studies suggest that GSCs employ diverse invasion strategies that may be cell-type specific. This hypothesis was supported by Grundy et al. (2016) who suggested that a GSC subtype-specific relationship exists between invasive behavior and sensitivity to microenvironmental stiffness. In this study, migration and invasion were measured on 2D Matrigel coated polyacrylamide matrices with varying stiffness (200 Pa–50 kPa) and also within soft (~400 Pa) 3D Matrigel hydrogels. With this platform, the invasive behavior of neural subtype GSCs was observed to be insensitive to stiffness, while mesenchymal subtype GSCs exhibited stiffness dependent motility. The authors surmise that the cell of origin (neural GSCs—neuronal lineage; mesenchymal GSCs—astrocytic lineage) may be a primary factor influencing GSC motility in response to microenvironmental stiffness (Grundy et al., 2016). This hypothesis also draws relevance back to the NSC paradigm, in which neuronal phenotypes manifest on soft matrices while astrocytic phenotypes dominate on stiff substrates (Saha et al., 2008).

These 3D invasion studies provide unique opportunities to isolate specific microenvironmental features (chemistry, stiffness, architecture, cellular support, etc.) and may be instrumental in identifying targets for therapy to address GSC invasion at the clinical level. However, the wide range of reported results indicate that a more comprehensive picture of subtype-specific and context-specific molecular mechanisms of invasion may be necessary to develop predictive hypotheses.

Modeling Treatment Resistance and the Influence of Tumor Heterogeneity

Tumors generated through orthotopic transplant of human GSCs display treatment resistance that is supported by the tumor microenvironment (Mannino and Chalmers, 2011). Yet, similar to challenges faced in studying GBM invasion, direct identification of specific resistance promoting factors remains challenging *in vivo*; the mechanisms underlying microenvironmental contributions to treatment resistance can be efficiently modeled *in vitro*. For example, Fernandez-Fuente et al. (2014) proposed that resistance to sunitinib induced receptor tyrosine kinase (RTK) inhibition is mediated by interactions specific to a 3D microenvironment. Using a number of different GSC, NGSC, and established GBM cell lines, the authors determined that GSCs were comparatively insensitive to RTK inhibition in 3D collagen gels vs. standard 2D conditions and 2D collagen coated polyacrylamide. The observed resistance was abrogated *via* chemical inhibition of the PI3K/Akt and MEK/ERK signaling pathways leading the authors to hypothesize that focal adhesions in 3D were responsible for promoting RTK resistance. Notably, changes in collagen content, stiffness (2D and 3D), and soluble HA inclusion in 3D collagen gels did not produce a measurable effect on drug sensitivity.

The biochemical response to matrix bound HA has also been identified as a regulator of GSC resistance to chemotherapy in 3D culture. In a recent study by Pedron et al. (2017), the EGFR inhibitor erlotinib produced little GSC cytotoxicity in gelatin hydrogels, and its effects were predictably dependent on basal EGFR status ($EGFR^{wt}$, $EGFR^{+}$, and the GBM specific constitutively active form $EGFR^{VIII}$). In addition, incorporation of HA within the gelatin hydrogels increased erlotinib resistance in $EGFR^{VIII}$ cells, while

inhibition of EGFR and CD44 increased cytotoxic effects in $EGFR^{wt}$ and $EGFR^{+}$ cells. This study provides evidence for EGFR–CD44 signaling interactions that promote GSC resistance to RTK inhibition dependent on the microenvironment and molecular profile of the GBM cells. Considering the clinical importance of EGFR in GBM, this mechanism may be highly relevant designing novel inhibition strategies for GSCs. Moreover, measuring divergent responses as a function of EGFR signaling provides an example of how tumor heterogeneity may negatively impact treatment.

The development of tumor heterogeneity diminishes sensitivity to treatment as a result of divergent phenotypes (proliferative vs. quiescent, invasive vs. stationary, protein expression, etc.). Hubert et al. (2016) modeled this process by culturing GSCs in Matrigel coupled with continuous mechanical agitation. This model generated large GBM organoids with hypoxic cores that were composed of populations of GSCs and NGSCs. GSCs were primarily located at the organoid rim but were also sporadically identified in regions of hypoxia. Moreover, the GSC populations within the organoids displayed resistance to apoptosis following radiation treatment, while NGSCs were observed to be sensitive to treatment. This test demonstrates a prevailing GSC theory that conventional modes of treatment may effectively target NGSCs but leave GSCs relatively unharmed. Finally, organoid cultures were orthotopically implanted and formed tumor architecture and single-cell invasive patterns that were a better representation of the parent tumor than matched cells in neurosphere culture (Hubert et al., 2016). Thus, developing models that can recapitulate tumor heterogeneity may provide avenues for determining patient-specific drug responses *via* personalized medicine.

CRITICAL PERSPECTIVE AND FUTURE DIRECTIONS

Biomaterial models of the GBM tumor microenvironment have been useful to interrogate aspects of GSC biology that could not be studied easily under standard 2D culture conditions or with *in vivo* tumor models. While this has undoubtedly leads to progress in GBM research, there remain opportunities for improving the overall impact of these studies. Primarily, the choice of cell line remains one of the most important variables to the biological relevance of model microenvironments. Immortalized cell lines simply do not provide accurate representation of the disease in this area and should be restricted to proof of concept use if possible. Ultimately, biomaterial models are designed to identify biological features that are important to the *in vivo* scenario. Therefore, low-passage patient-derived cell sources that have been validated to retain genotypic and phenotypic features of the parent tumor, such as GSCs, should be prioritized. The impact of these studies will be further increased by providing detailed characterization data on both the cell lines and biomaterial system employed. Incomplete descriptions often omit key information needed to replicate studies or draw broader conclusions about GBM behaviors. One important consideration in utilizing patient-derived cells is that the heterogeneity of GBM tumors makes it unlikely that cells from different sources will behave identically. However, understanding these differences will be essential to making progress in the treatment of human disease. By classifying GSC lines into the clinically accepted subtypes, providing gene and/or protein expression data, and reporting comprehensive behavioral analyses, the field can gain a more comprehensive understanding intra- and interpatient heterogeneity. We further propose that the definition of a GSC should be considered carefully and well defined for the purpose of each study: cell behaviors should be characterized in more than one context, and standard characterization should include features such as self-renewal capacity, expression of stem related genes or proteins, their ability to differentiate into multiple lineages, and the behavior of cells transplanted *in vivo*. Similarly, microenvironmental variables should be tightly controlled, with consideration given to the potential interdependence of different scaffold properties. Given the role that both biochemical and biophysical signaling play in GSC regulation, decoupling these responses concepts may be key to truly isolating these biological relationships.

Looking forward, modeling GSC behaviors in engineered microenvironments provides significant opportunities for the advancement of GBM research and eventual translation of new therapies to target this population. The primary motivator is to identify treatable mechanisms or biochemical pathways that are critical for GSC persistence, invasion, or tumorigenesis. To this end, efforts focused developing heterogeneity *via* microenvironmental cues are particularly impactful, as heterogeneity limits the capacity for non-personalized therapies to be successful. However, if heterogeneity in recurrent tumors develops as a result of interactions with the microenvironment, there may be models that could identify key mechanisms in this process that would enable prevention. Alternatively, models designed to enable long-term maintenance of parental tumor features would also be a welcome innovation. Following resection, patient-derived cell line models lose their heterogeneity, converge on a dominant phenotype, and experience genetic drift over time. Thus, models that are able to maintain and enrich GSCs with minimal plastic culture, or even straight from the patient, would be enable analysis on samples that represent the original tumor. Microenvironmental modeling may also better our understanding of the role of GSCs in driving angiogenesis. We understand that GSCs respond to hypoxic microenvironments by recruiting endothelial cells, and in some cases differentiating into vascular support cells to vascularize the tumor. However, these behaviors have not been fully demonstrated *in vitro*. Employing a hypoxic microenvironment model in combination with cocultured endothelial cells and microenvironmental components designed to encourage vessel formation (laminin proteins, VEGF, etc.) may enable elucidation of these processes and their mechanisms. Finally, personalized medicine options remain a long-standing goal of tumor microenvironment models. Considering again the heterogeneity of GBM, platforms that enable high-throughput testing of patient-derived tumor samples could allow for therapies to be tailored for different individuals. Such models could focus on treating tumorigenesis, invasion, or GSC maintenance.

CONCLUSION

Although GBM is aggressively treated, conventional radiation and chemotherapy are relatively ineffective, and tumor recurrence is nearly inevitable. The GBM microenvironment is broadly protective to various tumor and tumor-associated cells; specialized niches therein provide critical functions for maintaining a population of treatment resistant GSCs that fuel tumor recurrence. Importantly, a growing body of evidence suggests that these microenvironments directly support treatment resistance and induction of stem plasticity through a diverse set of dynamic interactions. *In vitro* studies utilizing 3D scaffolds are proven tools for identifying and isolating microenvironmental mechanisms that regulate GBM and GSC behaviors. Therefore, we propose that further development of these models may facilitate better understanding of the mechanisms that maintain GSCs in the microenvironment and may precede the development of new methods for disrupting niche regulation.

AUTHOR CONTRIBUTIONS

JMH and RWS were equally involved in conceptualizing, writing, and editing this manuscript.

FUNDING

The authors gratefully acknowledge funding support for this work provided by the Rick Oehme Foundation and the Barrow Neurological Foundation.

REFERENCES

Addington, C. P., Dharmawaj, S., Heffernan, J. M., Sirianni, R. W., and Stabenfeldt, S. E. (2017). Hyaluronic acid-laminin hydrogels increase neural stem cell transplant retention and migratory response to SDF-1α. *Matrix Biol.* 60-61, 206–216. doi:10.1016/j.matbio.2016.09.007

Addington, C. P., Heffernan, J. M., Millar-Haskell, C. S., Tucker, E. W., Sirianni, R. W., and Stabenfeldt, S. E. (2015). Enhancing neural stem cell response to SDF-1α gradients through hyaluronic acid-laminin hydrogels. *Biomaterials* 72, 11–19. doi:10.1016/j.biomaterials.2015.08.041

Akiyama, Y., Jung, S., Salhia, B., Lee, S., Hubbard, S., Taylor, M., et al. (2001). Hyaluronate receptors mediating glioma cell migration and proliferation. *J. Neurooncol.* 53, 115–127. doi:10.1023/A:1012297132047

Allen, M., Bjerke, M., Edlund, H., Nelander, S., and Westermark, B. (2016). Origin of the U87MG glioma cell line: good news and bad news. *Sci. Transl. Med.* 8, 354re3. doi:10.1126/scitranslmed.aaf6853

Ananthanarayanan, B., Kim, Y., and Kumar, S. (2011). Elucidating the mechanobiology of malignant brain tumors using a brain matrix-mimetic hyaluronic acid hydrogel platform. *Biomaterials* 32, 7913–7923. doi:10.1016/j.biomaterials.2011.07.005

Ariza, A., López, D., Mate, J. L., Isamat, M., Musulen, E., Pujol, M., et al. (1995). Role of CD44 in the invasiveness of glioblastoma multiforme and the noninvasiveness of meningioma: an immunohistochemistry study. *Hum. Pathol.* 26, 1144–1147. doi:10.1016/0046-8177(95)90278-3

Bao, S., Wu, Q., McLendon, R. E., Hao, Y., Shi, Q., Hjelmeland, A. B., et al. (2006a). Glioma stem cells promote radioresistance by preferential activation of the DNA damage response. *Nature* 444, 756–760. doi:10.1038/nature05236

Bao, S., Wu, Q., Sathornsumetee, S., Hao, Y., Li, Z., Hjelmeland, A. B., et al. (2006b). Stem cell-like glioma cells promote tumor angiogenesis through vascular endothelial growth factor. *Cancer Res.* 66, 7843–7848. doi:10.1158/0008-5472.CAN-06-1010

Bar, E. E., Lin, A., Mahairaki, V., Matsui, W., and Eberhart, C. G. (2010). Hypoxia increases the expression of stem-cell markers and promotes clonogenicity in glioblastoma neurospheres. *Am. J. Pathol.* 177, 1491–1502. doi:10.2353/ajpath.2010.091021

Beier, D., Wischhusen, J., Dietmaier, W., Hau, P., Proescholdt, M., Brawanski, A., et al. (2008). CD133 expression and cancer stem cells predict prognosis in high-grade oligodendroglial tumors. *Brain Pathol.* 18, 370–377. doi:10.1111/j.1750-3639.2008.00130.x

Bellail, A. C., Hunter, S. B., Brat, D. J., Tan, C., and Van Meir, E. G. (2004). Microregional extracellular matrix heterogeneity in brain modulates glioma cell invasion. *Int. J. Biochem. Cell Biol.* 36, 1046–1069. doi:10.1016/j.biocel.2004.01.013

Berens, M. E., and Giese, A. (1999). "…those left behind." Biology and oncology of invasive glioma cells. *Neoplasia* 1, 208–219. doi:10.1038/sj.neo.7900034

Bertout, J. A., Majmundar, A. J., Gordan, J. D., Lam, J. C., Ditsworth, D., Keith, B., et al. (2009). HIF2α inhibition promotes p53 pathway activity, tumor cell death, and radiation responses. *Proc. Natl. Acad. Sci. U.S.A.* 106, 14391–14396. doi:10.1073/pnas.0907357106

Bez, A., Corsini, E., Curti, D., Biggiogera, M., Colombo, A., Nicosia, R. F., et al. (2003). Neurosphere and neurosphere-forming cells: morphological and ultrastructural characterization. *Brain Res.* 993, 18–29. doi:10.1016/j.brainres.2003.08.061

Bhatt, R. S., Landis, D. M., Zimmer, M., Torregrossa, J., Chen, S., Sukhatme, V. P., et al. (2008). Hypoxia-inducible factor-2α: effect on radiation sensitivity and differential regulation by an mTOR inhibitor. *BJU Int.* 102, 358–363. doi:10.1111/j.1464-410X.2008.07558.x

Bleau, A.-M., Hambardzumyan, D., Ozawa, T., Fomchenko, E. I., Huse, J. T., Brennan, C. W., et al. (2009). PTEN/PI3K/Akt pathway regulates the side population phenotype and ABCG2 activity in glioma tumor stem-like cells. *Cell Stem Cell* 4, 226–235. doi:10.1016/j.stem.2009.01.007

Bonavia, R., Inda, M.-M., Cavenee, W. K., and Furnari, F. B. (2011). Heterogeneity maintenance in glioblastoma: a social network. *Cancer Res.* 71, 4055–4060. doi:10.1158/0008-5472.CAN-11-0153

Buxboim, A., Rajagopal, K., Brown, A. E. X., and Discher, D. E. (2010). How deeply cells feel: methods for thin gels. *J. Phys. Condens. Matter* 22, 194116. doi:10.1088/0953-8984/22/19/194116

Calabrese, C., Poppleton, H., Kocak, M., Hogg, T. L., Fuller, C., Hamner, B., et al. (2007). A perivascular niche for brain tumor stem cells. *Cancer Cell* 11, 69–82. doi:10.1016/j.ccr.2006.11.020

Cha, J., Kang, S.-G., and Kim, P. (2016). Strategies of mesenchymal invasion of patient-derived brain tumors: microenvironmental adaptation. *Sci. Rep.* 6, 24912. doi:10.1038/srep24912

Charles, N., Ozawa, T., Squatrito, M., Bleau, A.-M., Brennan, C. W., Hambardzumyan, D., et al. (2010). Perivascular nitric oxide activates notch signaling and promotes stem-like character in PDGF-induced glioma cells. *Cell Stem Cell* 6, 141–152. doi:10.1016/j.stem.2010.01.001

Charles, N. A., Holland, E. C., Gilbertson, R., Glass, R., and Kettenmann, H. (2011). The brain tumor microenvironment. *Glia* 59, 1169–1180. doi:10.1002/glia.21136

Chen, J., Li, Y., Yu, T.-S., McKay, R. M., Burns, D. K., Kernie, S. G., et al. (2012). A restricted cell population propagates glioblastoma growth after chemotherapy. *Nature* 488, 522–526. doi:10.1038/nature11287

Chen, J.-W. E., Pedron, S., and Harley, B. A. C. (2017). The combined influence of hydrogel stiffness and matrix-bound hyaluronic acid content on glioblastoma invasion. *Macromol. Biosci.* 17. doi:10.1002/mabi.201700018

Chen, Z., Htay, A., Santos, W. D., Gillies, G. T., Fillmore, H. L., Sholley, M. M., et al. (2009). In vitro angiogenesis by human umbilical vein endothelial cells (HUVEC) induced by three-dimensional co-culture with glioblastoma cells. *J. Neurooncol.* 92, 121–128. doi:10.1007/s11060-008-9742-y

Cheng, L., Huang, Z., Zhou, W., Wu, Q., Donnola, S., Liu, J. K., et al. (2013a). Glioblastoma stem cells generate vascular pericytes to support vessel function and tumor growth. *Cell* 153, 139–152. doi:10.1016/j.cell.2013.02.021

Cheng, T.-Y., Chen, M.-H., Chang, W.-H., Huang, M.-Y., and Wang, T.-W. (2013b). Neural stem cells encapsulated in a functionalized self-assembling peptide hydrogel for brain tissue engineering. *Biomaterials* 34, 2005–2016. doi:10.1016/j.biomaterials.2012.11.043

Cheng, L., Wu, Q., Guryanova, O. A., Huang, Z., Huang, Q., Rich, J. N., et al. (2011). Elevated invasive potential of glioblastoma stem cells. *Biochem. Biophys. Res. Commun.* 406, 643–648. doi:10.1016/j.bbrc.2011.02.123

Chonan, Y., Taki, S., Sampetrean, O., Saya, H., and Sudo, R. (2017). Endothelium-induced three-dimensional invasion of heterogeneous glioma initiating cells in a microfluidic coculture platform. *Integr. Biol.* 9, 762–773. doi:10.1039/C7IB00091J

Cordes, N., Hansmeier, B., Beinke, C., Meineke, V., and van Beuningen, D. (2003). Irradiation differentially affects substratum-dependent survival, adhesion, and invasion of glioblastoma cell lines. *Br. J. Cancer* 89, 2122–2132. doi:10.1038/sj.bjc.6601429

Dahan, P., Martinez Gala, J., Delmas, C., Monferran, S., Malric, L., Zentkowski, D., et al. (2014). Ionizing radiations sustain glioblastoma cell dedifferentiation to a stem-like phenotype through survivin: possible involvement in radioresistance. *Cell Death Dis.* 5, e1543. doi:10.1038/cddis.2014.509

Del Duca, D., Werbowetski, T., and Del Maestro, R. F. (2004). Spheroid preparation from hanging drops: characterization of a model of brain tumor invasion. *J. Neurooncol.* 67, 295–303. doi:10.1023/B:NEON.0000024220.07063.70

Deleyrolle, L. P., Harding, A., Cato, K., Siebzehnrubl, F. A., Rahman, M., Azari, H., et al. (2011). Evidence for label-retaining tumour-initiating cells in human glioblastoma. *Brain* 134, 1331–1343. doi:10.1093/brain/awr081

Delpech, B., Maingonnat, C., Girard, N., Chauzy, C., Olivier, A., Maunoury, R., et al. (1993). Hyaluronan and hyaluronectin in the extracellular matrix of human brain tumour stroma. *Eur. J. Cancer* 29, 1012–1017. doi:10.1016/S0959-8049(05)80214-X

Eke, I., Storch, K., Kästner, I., Vehlow, A., Faethe, C., Mueller-Klieser, W., et al. (2012). Three-dimensional invasion of human glioblastoma cells remains unchanged by x-ray and carbon ion irradiation in vitro. *Int. J. Radiat. Oncol.* 84, e515–e523. doi:10.1016/j.ijrobp.2012.06.012

El-Sherbiny, I. M., and Yacoub, M. H. (2013). Hydrogel scaffolds for tissue engineering: progress and challenges. *Glob. Cardiol. Sci. Pract.* 2013, 316–342. doi:10.5339/gcsp.2013.38

Fael Al-Mayhani, T. M., Ball, S. L. R., Zhao, J.-W., Fawcett, J., Ichimura, K., Collins, P. V., et al. (2009). An efficient method for derivation and propagation of glioblastoma cell lines that conserves the molecular profile of their original tumours. *J. Neurosci. Methods* 176, 192–199. doi:10.1016/j.jneumeth.2008.07.022

Fan, Y., Nguyen, D. T., Akay, Y., Xu, F., and Akay, M. (2016). Engineering a brain cancer chip for high-throughput drug screening. *Sci. Rep.* 6, 25062. doi:10.1038/srep25062

Fernandez-Fuente, G., Mollinedo, P., Grande, L., Vazquez-Barquero, A., and Fernandez-Luna, J. L. (2014). Culture dimensionality influences the resistance of glioblastoma stem-like cells to multikinase inhibitors. *Mol. Cancer Ther.* 13, 1664–1672. doi:10.1158/1535-7163.MCT-13-0854

Florczyk, S. J., Kievit, F. M., Wang, K., Erickson, A. E., Ellenbogen, R. G., and Zhang, M. (2016). 3D porous chitosan–alginate scaffolds promote proliferation and enrichment of cancer stem-like cells. *J. Mater. Chem. B.* 4, 6326–6334. doi:10.1039/C6TB01713D

Florczyk, S. J., Wang, K., Jana, S., Wood, D. L., Sytsma, S. K., Sham, J. G., et al. (2013). Porous chitosan-hyaluronic acid scaffolds as a mimic of glioblastoma microenvironment ECM. *Biomaterials* 34, 10143–10150. doi:10.1016/j.biomaterials.2013.09.034

Folkins, C., Shaked, Y., Man, S., Tang, T., Lee, C. R., Zhu, Z., et al. (2009). Glioma tumor stem-like cells promote tumor angiogenesis and vasculogenesis via vascular endothelial growth factor and stromal-derived factor 1. *Cancer Res.* 69, 7243–7251. doi:10.1158/0008-5472.CAN-09-0167

Galan-Moya, E. M., Le Guelte, A., Lima Fernandes, E., Thirant, C., Dwyer, J., Bidere, N., et al. (2011). Secreted factors from brain endothelial cells maintain glioblastoma stem-like cell expansion through the mTOR pathway. *EMBO Rep.* 12, 470–476. doi:10.1038/embor.2011.39

Galli, R., Binda, E., Orfanelli, U., Cipelletti, B., Gritti, A., Vitis, S. D., et al. (2004). Isolation and characterization of tumorigenic, stem-like neural precursors from human glioblastoma. *Cancer Res.* 64, 7011–7021. doi:10.1158/0008-5472.CAN-04-1364

Georges, P. C., Miller, W. J., Meaney, D. F., Sawyer, E. S., and Janmey, P. A. (2006). Matrices with compliance comparable to that of brain tissue select neuronal over glial growth in mixed cortical cultures. *Biophys. J.* 90, 3012–3018. doi:10.1529/biophysj.105.073114

Giese, A., Berens, M. E., and Westphal, M. (2003). Cost of migration: invasion of malignant gliomas and implications for treatment. *J. Clin. Oncol.* 21, 1624–1636. doi:10.1200/JCO.2003.05.063

Giese, A., Loo, M. A., Rief, M. D., Tran, N., and Berens, M. E. (1995). Substrates for astrocytoma invasion. *Neurosurgery* 37, 294–301. doi:10.1227/00006123-199508000-00015

Giese, A., and Westphal, M. (1996). Glioma invasion in the central nervous system. *Neurosurgery* 39, 235–252. doi:10.1097/00006123-199608000-00001

Gilbertson, R. J., and Rich, J. N. (2007). Making a tumour's bed: glioblastoma stem cells and the vascular niche. *Nat. Rev. Cancer* 7, 733–736. doi:10.1038/nrc2246

Grundy, T. J., De Leon, E., Griffin, K. R., Stringer, B. W., Day, B. W., Fabry, B., et al. (2016). Differential response of patient-derived primary glioblastoma cells to environmental stiffness. *Sci. Rep.* 6, 23353. doi:10.1038/srep23353

Haas, T. L., Sciuto, M. R., Brunetto, L., Valvo, C., Signore, M., Fiori, M. E., et al. (2017). Integrin α7 is a functional marker and potential therapeutic target in glioblastoma. *Cell Stem Cell* 21, 35–50.e9. doi:10.1016/j.stem.2017.04.009

Hambardzumyan, D., Becher, O. J., Rosenblum, M. K., Pandolfi, P. P., Manova-Todorova, K., and Holland, E. C. (2008). PI3K pathway regulates survival of cancer stem cells residing in the perivascular niche following radiation in medulloblastoma in vivo. *Genes Dev.* 22, 436–448. doi:10.1101/gad.1627008

Harrison, L., and Blackwell, K. (2004). Hypoxia and anemia: factors in decreased sensitivity to radiation therapy and chemotherapy? *Oncologist* 9, 31–40. doi:10.1634/theoncologist.9-90005-31

Heddleston, J. M., Li, Z., Lathia, J. D., Bao, S., Hjelmeland, A. B., and Rich, J. N. (2010). Hypoxia inducible factors in cancer stem cells. *Br. J. Cancer* 102, 789–795. doi:10.1038/sj.bjc.6605551

Heddleston, J. M., Li, Z., McLendon, R. E., Hjelmeland, A. B., and Rich, J. N. (2009). The hypoxic microenvironment maintains glioblastoma stem cells and promotes reprogramming towards a cancer stem cell phenotype. *Cell Cycle* 8, 3274–3284. doi:10.4161/cc.8.20.9701

Heffernan, J., Overstreet, D., Le, L., Vernon, B., and Sirianni, R. (2014). Bioengineered scaffolds for 3D analysis of glioblastoma proliferation and invasion. *Ann. Biomed. Eng.* 43, 1965–1977. doi:10.1007/s10439-014-1223-1

Heffernan, J. M., McNamara, J. B., Borwege, S., Vernon, B. L., Sanai, N., Mehta, S., et al. (2017). PNIPAAm-co-Jeffamine® (PNJ) scaffolds as in vitro models for niche enrichment of glioblastoma stem-like cells. *Biomaterials* 143, 149–158. doi:10.1016/j.biomaterials.2017.05.007

Heffernan, J. M., Overstreet, D. J., Srinivasan, S., Le, L. D., Vernon, B. L., and Sirianni, R. W. (2016). Temperature responsive hydrogels enable transient three-dimensional tumor cultures via rapid cell recovery. *J. Biomed. Mater. Res. A.* 104, 17–25. doi:10.1002/jbm.a.35534

Herrera-Perez, M., Voytik-Harbin, S. L., and Rickus, J. L. (2015). Extracellular matrix properties regulate the migratory response of glioblastoma stem cells in three-dimensional culture. *Tissue Eng. Part A* 21, 2572–2582. doi:10.1089/ten.tea.2014.0504

Hjelmeland, A. B., Wu, Q., Heddleston, J. M., Choudhary, G. S., MacSwords, J., Lathia, J. D., et al. (2011). Acidic stress promotes a glioma stem cell phenotype. *Cell Death Differ.* 18, 829–840. doi:10.1038/cdd.2010.150

Holmquist-Mengelbier, L., Fredlund, E., Löfstedt, T., Noguera, R., Navarro, S., Nilsson, H., et al. (2006). Recruitment of HIF-1α and HIF-2α to common target genes is differentially regulated in neuroblastoma: HIF-2α promotes an aggressive phenotype. *Cancer Cell* 10, 413–423. doi:10.1016/j.ccr.2006.08.026

Hovinga, K. E., Shimizu, F., Wang, R., Panagiotakos, G., Van Der Heijden, M., Moayedpardazi, H., et al. (2010). Inhibition of notch signaling in glioblastoma targets cancer stem cells via an endothelial cell intermediate. *Stem Cells* 28, 1019–1029. doi:10.1002/stem.429

Hoyle, C. E., Lowe, A. B., and Bowman, C. N. (2010). Thiolclick chemistry: a multifaceted toolbox for small molecule and polymer synthesis. *Chem. Soc. Rev.* 39, 1355–1387. doi:10.1039/B901979K

Huang, P., Rani, M. R. S., Ahluwalia, M. S., Bae, E., Prayson, R. A., Weil, R. J., et al. (2012). Endothelial expression of TNF receptor-1 generates a proapoptotic signal inhibited by integrin α6β1 in glioblastoma. *Cancer Res.* 72, 1428–1437. doi:10.1158/0008-5472.CAN-11-2621

Hubbell, J. A. (1995). Biomaterials in tissue engineering. *Nat. Biotech.* 13, 565–576. doi:10.1038/nbt0695-565

Hubert, C. G., Rivera, M., Spangler, L. C., Wu, Q., Mack, S. C., Prager, B. C., et al. (2016). Culture system derived from human glioblastomas recapitulates the hypoxic gradients and cancer stem cell heterogeneity of tumors found in vivo. *Cancer Res.* 76, 2465–2477. doi:10.1158/0008-5472.CAN-15-2402

Huszthy, P. C., Daphu, I., Niclou, S. P., Stieber, D., Nigro, J. M., Sakariassen, P. O., et al. (2012). In vivo models of primary brain tumors: pitfalls and perspectives. *Neuro Oncol.* 14, 979–993. doi:10.1093/neuonc/nos135

Ignatova, T. N., Kukekov, V. G., Laywell, E. D., Suslov, O. N., Vrionis, F. D., and Steindler, D. A. (2002). Human cortical glial tumors contain neural stem-like cells expressing astroglial and neuronal markers in vitro. *Glia* 39, 193–206. doi:10.1002/glia.10094

Ishiwata, T., Teduka, K., Yamamoto, T., Kawahara, K., Matsuda, Y., and Naito, Z. (2011). Neuroepithelial stem cell marker nestin regulates the migration, invasion and growth of human gliomas. *Oncol. Rep.* 26, 91–99. doi:10.3892/or.2011.1267

Jacobs, V. L., Valdes, P. A., Hickey, W. F., and De Leo, J. A. (2011). Current review of in vivo GBM rodent models: emphasis on the CNS-1 tumour model. *ASN Neuro* 3, 171–181. doi:10.1042/AN20110014

Jain, A., Betancur, M., Patel, G. D., Valmikinathan, C. M., Mukhatyar, V. J., Vakharia, A., et al. (2014). Guiding intracortical brain tumour cells to an extracortical cytotoxic hydrogel using aligned polymeric nanofibres. *Nat. Mater.* 13, 308–316. doi:10.1038/nmat3878

Jamal, M., Rath, B. H., Tsang, P. S., Camphausen, K., and Tofilon, P. J. (2012). The brain microenvironment preferentially enhances the radioresistance of CD133+ glioblastoma stem-like cells. *Neoplasia N. Y. N.* 14, 150. doi:10.1593/neo.111794

Jamal, M., Rath, B. H., Williams, E. S., Camphausen, K., and Tofilon, P. J. (2010). Microenvironmental regulation of glioblastoma radioresponse. *Clin. Cancer Res.* 16, 6049–6059. doi:10.1158/1078-0432.CCR-10-2435

Jensen, S. S., Meyer, M., Petterson, S. A., Halle, B., Rosager, A. M., Aaberg-Jessen, C., et al. (2016). Establishment and characterization of a tumor stem cell-based glioblastoma invasion model. *PLoS ONE* 11:e0159746. doi:10.1371/journal.pone.0159746

Jiguet Jiglaire, C., Baeza-Kallee, N., Denicolaï, E., Barets, D., Metellus, P., Padovani, L., et al. (2014). Ex vivo cultures of glioblastoma in three-dimensional hydrogel maintain the original tumor growth behavior and are suitable for preclinical drug and radiation sensitivity screening. *Exp. Cell Res.* 321, 99–108. doi:10.1016/j.yexcr.2013.12.010

Jin, S. G., Jeong, Y. I., Jung, S., Ryu, H. H., Jin, Y. H., and Kim, I. Y. (2009). The effect of hyaluronic acid on the invasiveness of malignant glioma cells: comparison of invasion potential at hyaluronic acid hydrogel and matrigel. *J. Korean Neurosurg. Soc.* 46, 472–478. doi:10.3340/jkns.2009.46.5.472

Kang, K. B., Zhu, C., Wong, Y. L., Gao, Q., Ty, A., and Wong, M. C. (2012). Gefitinib radiosensitizes stem-like glioma cells: inhibition of epidermal growth factor receptor-Akt-DNA-PK signaling, accompanied by inhibition of DNA double-strand break repair. *Int. J. Radiat. Oncol. Biol. Phys.* 83, e43–e52. doi:10.1016/j.ijrobp.2011.11.037

Kawataki, T., Yamane, T., Naganuma, H., Rousselle, P., Andurén, I., Tryggvason, K., et al. (2007). Laminin isoforms and their integrin receptors in glioma cell migration and invasiveness: evidence for a role of α5-laminin(s) and α3β1 integrin. *Exp. Cell Res.* 313, 3819–3831. doi:10.1016/j.yexcr.2007.07.038

Keith, B., Johnson, R. S., and Simon, M. C. (2011). HIF1α and HIF2α: sibling rivalry in hypoxic tumor growth and progression. *Nat. Rev. Cancer* 12, 9–22. doi:10.1038/nrc3183

Keunen, O., Johansson, M., Oudin, A., Sanzey, M., Rahim, S. A. A., Fack, F., et al. (2011). Anti-VEGF treatment reduces blood supply and increases tumor cell invasion in glioblastoma. *Proc. Natl. Acad. Sci. U.S.A.* 108, 3749–3754. doi:10.1073/pnas.1014480108

Kievit, F. M., Florczyk, S. J., Leung, M. C., Veiseh, O., Park, J. O., Disis, M. L., et al. (2010). Chitosan–alginate 3D scaffolds as a mimic of the glioma tumor microenvironment. *Biomaterials* 31, 5903–5910. doi:10.1016/j.biomaterials.2010.03.062

Kievit, F. M., Florczyk, S. J., Leung, M. C., Wang, K., Wu, J. D., Silber, J. R., et al. (2014). Proliferation and enrichment of CD133+ glioblastoma cancer stem cells on 3D chitosan-alginate scaffolds. *Biomaterials* 35, 9137–9143. doi:10.1016/j.biomaterials.2014.07.037

Kievit, F. M., Wang, K., Erickson, A. E., Lan Levengood, S. K., Ellenbogen, R. G., and Zhang, M. (2016). Modeling the tumor microenvironment using chitosan-alginate scaffolds to control the stem-like state of glioblastoma cells. *Biomater. Sci.* 4, 610–613. doi:10.1039/C5BM00514K

Kim, H.-D., Guo, T. W., Wu, A. P., Wells, A., Gertler, F. B., and Lauffenburger, D. A. (2008). Epidermal growth factor-induced enhancement of glioblastoma cell migration in 3D arises from an intrinsic increase in speed but an extrinsic matrix- and proteolysis-dependent increase in persistence. *Mol. Biol. Cell* 19, 4249–4259. doi:10.1091/mbc.E08-05-0501

Kim, Y., and Kumar, S. (2014). CD44-mediated adhesion to hyaluronic acid contributes to mechanosensing and invasive motility. *Mol. Cancer Res.* 12, 1416–1429. doi:10.1158/1541-7786.MCR-13-0629

Kitai, R., Horita, R., Sato, K., Yoshida, K., Arishima, H., Higashino, Y., et al. (2010). Nestin expression in astrocytic tumors delineates tumor infiltration. *Brain Tumor Pathol.* 27, 17–21. doi:10.1007/s10014-009-0261-0

Knizetova, P., Ehrmann, J., Hlobilkova, A., Vancova, I., Kalita, O., Kolar, Z., et al. (2008). Autocrine regulation of glioblastoma cell cycle progression, viability and radioresistance through the VEGF-VEGFR2 (KDR) interplay. *Cell Cycle Georget. Tex.* 7, 2553–2561. doi:10.4161/cc.7.16.6442

Koochekpour, S., Pilkington, G. J., and Merzak, A. (1995). Hyaluronic acid/CD44H interaction induces cell detachment and stimulates migration and invasion of human glioma cells in vitro. *Int. J. Cancer* 63, 450–454. doi:10.1002/ijc.2910630325

Kreisl, T. N., Kim, L., Moore, K., Duic, P., Royce, C., Stroud, I., et al. (2008). Fine, phase II trial of single-agent bevacizumab followed by bevacizumab plus irinotecan at tumor progression in recurrent glioblastoma. *J. Clin. Oncol.* 27, 740–745. doi:10.1200/JCO.2008.16.3055

Lathia, J. D., Gallagher, J., Heddleston, J. M., Wang, J., Eyler, C. E., MacSwords, J., et al. (2010). Integrin alpha 6 regulates glioblastoma stem cells. *Cell Stem Cell* 6, 421–432. doi:10.1016/j.stem.2010.02.018

Lathia, J. D., Heddleston, J. M., Venere, M., and Rich, J. N. (2011). Deadly teamwork: neural cancer stem cells and the tumor microenvironment. *Cell Stem Cell* 8, 482–485. doi:10.1016/j.stem.2011.04.013

Lathia, J. D., Li, M., Hall, P. E., Gallagher, J., Hale, J. S., Wu, Q., et al. (2012). Laminin alpha 2 enables glioblastoma stem cell growth. *Ann. Neurol.* 72, 766–778. doi:10.1002/ana.23674

Lathia, J. D., Mack, S. C., Mulkearns-Hubert, E. E., Valentim, C. L. L., and Rich, J. N. (2015). Cancer stem cells in glioblastoma. *Genes Dev.* 29, 1203–1217. doi:10.1101/gad.261982.115

Lee, J., Kotliarova, S., Kotliarov, Y., Li, A., Su, Q., Donin, N. M., et al. (2006). Tumor stem cells derived from glioblastomas cultured in bFGF and EGF more closely mirror the phenotype and genotype of primary tumors than do serum-cultured cell lines. *Cancer Cell* 9, 391–403. doi:10.1016/j.ccr.2006.03.030

Li, A., Walling, J., Kotliarov, Y., Center, A., Steed, M. E., Ahn, S. J., et al. (2008). Genomic changes and gene expression profiles reveal that established glioma cell lines are poorly representative of primary human gliomas. *Mol. Cancer Res.* 6, 21–30. doi:10.1158/1541-7786.MCR-07-0280

Li, Q., Lin, H., Wang, O., Qiu, X., Kidambi, S., Deleyrolle, L. P., et al. (2016). Scalable production of glioblastoma tumor-initiating cells in 3 dimension thermoreversible hydrogels. *Sci. Rep.* 6, 31915. doi:10.1038/srep31915

Li, Z., Bao, S., Wu, Q., Wang, H., Eyler, C., Sathornsumetee, S., et al. (2009). Hypoxia-inducible factors regulate tumorigenic capacity of glioma stem cells. *Cancer Cell* 15, 501–513. doi:10.1016/j.ccr.2009.03.018

Ligon, K. L., Huillard, E., Mehta, S., Kesari, S., Liu, H., Alberta, J. A., et al. (2007). Olig2-regulated lineage-restricted pathway controls replication competence in neural stem cells and malignant glioma. *Neuron* 53, 503–517. doi:10.1016/j.neuron.2007.01.009

Liu, G., Yuan, X., Zeng, Z., Tunici, P., Ng, H., Abdulkadir, I. R., et al. (2006). Analysis of gene expression and chemoresistance of CD133+ cancer stem cells in glioblastoma. *Mol. Cancer* 5, 67. doi:10.1186/1476-4598-5-67

Ljubimova, J. Y., Fujita, M., Khazenzon, N. M., Ljubimov, A. V., and Black, K. L. (2006). Changes in laminin isoforms associated with brain tumor invasion and angiogenesis. *Front. Biosci. J. Virtual Libr.* 11:81–88. doi:10.2741/1781

Ma, L., Barker, J., Zhou, C., Li, W., Zhang, J., Lin, B., et al. (2012). Towards personalized medicine with a three-dimensional micro-scale perfusion-based two-chamber tissue model system. *Biomaterials* 33, 4353–4361. doi:10.1016/j.biomaterials.2012.02.054

Ma, N. K. L., Lim, J. K., Leong, M. F., Sandanaraj, E., Ang, B. T., Tang, C., et al. (2016a). Collaboration of 3D context and extracellular matrix in the

development of glioma stemness in a 3D model. *Biomaterials* 78, 62–73. doi:10.1016/j.biomaterials.2015.11.031

Mahesparan, R., Read, T.-A., Lund-Johansen, M., Skaftnesmo, K., Bjerkvig, R., and Engebraaten, O. (2003). Expression of extracellular matrix components in a highly infiltrative in vivo glioma model. *Acta Neuropathol.* 105, 49–57. doi:10.1007/s00401-002-0610-0

Mannino, M., and Chalmers, A. J. (2011). Radioresistance of glioma stem cells: intrinsic characteristic or property of the 'microenvironment-stem cell unit'? *Mol. Oncol.* 5, 374–386. doi:10.1016/j.molonc.2011.05.001

Matsukado, Y., MacCarty, C. S., and Kernohan, J. W. (1961). The growth of glioblastoma multiforme (astrocytomas, grades 3 and 4) in neurosurgical practice. *J. Neurosurg.* 18, 636–644. doi:10.3171/jns.1961.18.5.0636

Merzak, A., Koocheckpour, S., and Pilkington, G. J. (1994). CD44 mediates human glioma cell adhesion and invasion in vitro. *Cancer Res.* 54, 3988–3992.

Nakada, M., Nambu, E., Furuyama, N., Yoshida, Y., Takino, T., Hayashi, Y., et al. (2013). Integrin α3 is overexpressed in glioma stem-like cells and promotes invasion. *Br. J. Cancer* 108, 2516. doi:10.1038/bjc.2013.218

Nakajima, M., Ishimuro, T., Kato, K., Ko, I.-K., Hirata, I., Arima, Y., et al. (2007). Combinatorial protein display for the cell-based screening of biomaterials that direct neural stem cell differentiation. *Biomaterials* 28, 1048–1060. doi:10.1016/j.biomaterials.2006.10.004

Netti, P. A., Berk, D. A., Swartz, M. A., Grodzinsky, A. J., and Jain, R. K. (2000). Role of extracellular matrix assembly in interstitial transport in solid tumors. *Cancer Res.* 60, 2497–2503.

Ngo, M. T., and Harley, B. A. (2017). The influence of hyaluronic acid and glioblastoma cell coculture on the formation of endothelial cell networks in gelatin hydrogels. *Adv. Healthc. Mater.* 6. doi:10.1002/adhm.201700687

Oh, Y., Cha, J., Kang, S.-G., and Kim, P. (2016). A polyethylene glycol-based hydrogel as macroporous scaffold for tumorsphere formation of glioblastoma multiforme. *J. Ind. Eng. Chem.* 39, 10–15. doi:10.1016/j.jiec.2016.05.012

Omuro, A., and DeAngelis, L. M. (2013). Glioblastoma and other malignant gliomas: a clinical review. *JAMA* 310, 1842–1850. doi:10.1001/jama.2013.280319

Ortensi, B., Setti, M., Osti, D., and Pelicci, G. (2013). Cancer stem cell contribution to glioblastoma invasiveness. *Stem Cell Res. Ther.* 4, 18. doi:10.1186/scrt166

Ostrom, Q. T., Gittleman, H., Xu, J., Kromer, C., Wolinsky, Y., Kruchko, C., et al. (2016). CBTRUS statistical report: primary brain and other central nervous system tumors diagnosed in the United States in 2009–2013. *Neuro Oncol.* 18, v1–v75. doi:10.1093/neuonc/now207

Pàez-Ribes, M., Allen, E., Hudock, J., Takeda, T., Okuyama, H., Viñals, F., et al. (2009). Antiangiogenic therapy elicits malignant progression of tumors to increased local invasion and distant metastasis. *Cancer Cell* 15, 220–231. doi:10.1016/j.ccr.2009.01.027

Pampaloni, F., Reynaud, E. G., and Stelzer, E. H. K. (2007). The third dimension bridges the gap between cell culture and live tissue. *Nat. Rev. Mol. Cell Biol.* 8, 839–845. doi:10.1038/nrm2236

Paolillo, M., Serra, M., and Schinelli, S. (2016). Integrins in glioblastoma: still an attractive target? *Pharmacol. Res.* 113, 55–61. doi:10.1016/j.phrs.2016.08.004

Pathak, A., and Kumar, S. (2012). Independent regulation of tumor cell migration by matrix stiffness and confinement. *Proc. Natl. Acad. Sci. U.S.A.* 109, 10334–10339. doi:10.1073/pnas.1118073109

Pedron, S., Becka, E., and Harley, B. A. (2015). Spatially gradated hydrogel platform as a 3D engineered tumor microenvironment. *Adv. Mater.* 27, 1567–1572. doi:10.1002/adma.201404896

Pedron, S., Becka, E., and Harley, B. A. C. (2013). Regulation of glioma cell phenotype in 3D matrices by hyaluronic acid. *Biomaterials* 34, 7408–7417. doi:10.1016/j.biomaterials.2013.06.024

Pedron, S., Hanselman, J. S., Schroeder, M. A., Sarkaria, J. N., and Harley, B. A. C. (2017). Extracellular hyaluronic acid influences the efficacy of EGFR tyrosine kinase inhibitors in a biomaterial model of glioblastoma. *Adv. Healthc. Mater.* 6. doi:10.1002/adhm.201700529

Pedron, S., and Harley, B. A. C. (2013). Impact of the biophysical features of a 3D gelatin microenvironment on glioblastoma malignancy. *J. Biomed. Mater. Res. A.* 101, 3404–3415. doi:10.1002/jbm.a.34637

Petrecca, K., Guiot, M.-C., Panet-Raymond, V., and Souhami, L. (2012). Failure pattern following complete resection plus radiotherapy and temozolomide is at the resection margin in patients with glioblastoma. *J. Neurooncol.* 111, 19–23. doi:10.1007/s11060-012-0983-4

Pistollato, F., Abbadi, S., Rampazzo, E., Persano, L., Della Puppa, A., Frasson, C., et al. (2010). Intratumoral hypoxic gradient drives stem cells distribution and MGMT expression in glioblastoma. *Stem Cells* 28, 851–862. doi:10.1002/stem.415

Pollard, S. M., Yoshikawa, K., Clarke, I. D., Danovi, D., Stricker, S., Russell, R., et al. (2009). Glioma stem cell lines expanded in adherent culture have tumor-specific phenotypes and are suitable for chemical and genetic screens. *Cell Stem Cell* 4, 568–580. doi:10.1016/j.stem.2009.03.014

Ponten, J., and Macintyre, E. (1968). Long term culture of normal and neoplastic human glia. *Acta Pathol. Microbiol. Scand.* 74, 465–486. doi:10.1111/j.1699-0463.1968.tb03502.x

Rao, S. S., Lannutti, J. J., Viapiano, M. S., Sarkar, A., and Winter, J. O. (2014). Toward 3D biomimetic models to understand the behavior of glioblastoma multiforme cells. *Tissue Eng. B Rev.* 20, 314–327. doi:10.1089/ten.teb.2013.0227

Rao, S. S., Nelson, M. T., Xue, R., DeJesus, J. K., Viapiano, M. S., Lannutti, J. J., et al. (2013a). Mimicking white matter tract topography using core–shell electrospun nanofibers to examine migration of malignant brain tumors. *Biomaterials* 34, 5181–5190. doi:10.1016/j.biomaterials.2013.03.069

Rao, S. S., DeJesus, J., Short, A. R., Otero, J. J., Sarkar, A., and Winter, J. O. (2013b). Glioblastoma behaviors in three-dimensional collagen-hyaluronan composite hydrogels. *ACS Appl. Mater. Interfaces* 5, 9276–9284. doi:10.1021/am402097j

Rape, A., Ananthanarayanan, B., and Kumar, S. (2014). Engineering strategies to mimic the glioblastoma microenvironment. *Adv. Drug Deliv. Rev.* 79-80, 172–183. doi:10.1016/j.addr.2014.08.012

Rape, A. D., and Kumar, S. (2014). A composite hydrogel platform for the dissection of tumor cell migration at tissue interfaces. *Biomaterials* 35, 8846–8853. doi:10.1016/j.biomaterials.2014.07.003

Rape, A. D., Zibinsky, M., Murthy, N., and Kumar, S. (2015). A synthetic hydrogel for the high-throughput study of cell-ECM interactions. *Nat. Commun.* 6, 8129. doi:10.1038/ncomms9129

Rath, B. H., Fair, J. M., Jamal, M., Camphausen, K., and Tofilon, P. J. (2013). Astrocytes Enhance the Invasion Potential of Glioblastoma Stem-Like Cells. *PLoS ONE* 8:e54752. doi:10.1371/journal.pone.0054752

Rath, B. H., Wahba, A., Camphausen, K., and Tofilon, P. J. (2015). Coculture with astrocytes reduces the radiosensitivity of glioblastoma stem-like cells and identifies additional targets for radiosensitization. *Cancer Med.* 4, 1705–1716. doi:10.1002/cam4.510

Ricci-Vitiani, L., Pallini, R., Biffoni, M., Todaro, M., Invernici, G., Cenci, T., et al. (2010). Tumour vascularization via endothelial differentiation of glioblastoma stem-like cells. *Nature* 468, 824–828. doi:10.1038/nature09557

Rich, J. N. (2007). Cancer stem cells in radiation resistance. *Cancer Res.* 67, 8980–8984. doi:10.1158/0008-5472.CAN-07-0895

Ruiz-Ontañon, P., Orgaz, J. L., Aldaz, B., Elosegui-Artola, A., Martino, J., Berciano, M. T., et al. (2013). Cellular plasticity confers migratory and invasive advantages to a population of glioblastoma-initiating cells that infiltrate peritumoral tissue. *Stem Cells* 31, 1075–1085. doi:10.1002/stem.1349

Safa, A. R., Saadatzadeh, M. R., Cohen-Gadol, A. A., Pollok, K. E., and Bijangi-Vishehsaraei, K. (2015). Glioblastoma stem cells (GSCs) epigenetic plasticity and interconversion between differentiated non-GSCs and GSCs. *Genes Dis.* 2, 152–163. doi:10.1016/j.gendis.2015.02.001

Saha, K., Keung, A. J., Irwin, E. F., Li, Y., Little, L., Schaffer, D. V., et al. (2008). Substrate modulus directs neural stem cell behavior. *Biophys. J.* 95, 4426–4438. doi:10.1529/biophysj.108.132217

Sanai, N., Alvarez-Buylla, A., and Berger, M. S. (2005). Neural stem cells and the origin of gliomas. *N. Engl. J. Med.* 353, 811–822. doi:10.1056/NEJMra043666

Sanai, N., Polley, M.-Y., McDermott, M. W., Parsa, A. T., and Berger, M. S. (2011). An extent of resection threshold for newly diagnosed glioblastomas. *J. Neurosurg.* 115, 3–8. doi:10.3171/2011.2.JNS10998

Sarkar, S., Nuttall, R. K., Liu, S., Edwards, D. R., and Yong, V. W. (2006). Tenascin-C stimulates glioma cell invasion through matrix metalloproteinase-12. *Cancer Res.* 66, 11771–11780. doi:10.1158/0008-5472.CAN-05-0470

Schonberg, D. L., Lubelski, D., Miller, T. E., and Rich, J. N. (2014). Brain tumor stem cells: molecular characteristics and their impact on therapy. *Mol. Aspects Med.* 39, 82–101. doi:10.1016/j.mam.2013.06.004

Seidel, S., Garvalov, B. K., Wirta, V., von Stechow, L., Schänzer, A., Meletis, K., et al. (2010). A hypoxic niche regulates glioblastoma stem cells through hypoxia inducible factor 2α. *Brain* 133, 983–995. doi:10.1093/brain/awq042

Shen, Q., Goderie, S. K., Jin, L., Karanth, N., Sun, Y., Abramova, N., et al. (2004). Endothelial cells stimulate self-renewal and expand neurogenesis of neural stem cells. *Science* 304, 1338–1340. doi:10.1126/science.1095505

Singh, S., Hawkins, C., Clarke, I. D., Squire, J. A., Bayani, J., Hide, T., et al. (2004). Identification of human brain tumour initiating cells. *Nature* 432, 393–396. doi:10.1038/nature03031

Singh, S. K., Clarke, I. D., Terasaki, M., Bonn, V. E., Hawkins, C., Squire, J., et al. (2003). Identification of a cancer stem cell in human brain tumors. *Cancer Res.* 63, 5821–5828.

Soda, Y., Myskiw, C., Rommel, A., and Verma, I. M. (2013). Mechanisms of neovascularization and resistance to anti-angiogenic therapies in glioblastoma multiforme. *J. Mol. Med. Berl. Ger.* 91, 439–448. doi:10.1007/s00109-013-1019-z

Soeda, A., Park, M., Lee, D., Mintz, A., Androutsellis-Theotokis, A., McKay, R. D., et al. (2009). Hypoxia promotes expansion of the CD133-positive glioma stem cells through activation of HIF-1α. *Oncogene* 28, 3949–3959. doi:10.1038/onc.2009.252

Soen, Y., Mori, A., Palmer, T. D., and Brown, P. O. (2006). Exploring the regulation of human neural precursor cell differentiation using arrays of signaling microenvironments. *Mol. Syst. Biol.* 2, 37. doi:10.1038/msb4100076

Son, M. J., Woolard, K., Nam, D.-H., Lee, J., and Fine, H. A. (2009). SSEA-1 is an enrichment marker for tumor-initiating cells in human glioblastoma. *Cell Stem Cell* 4, 440–452. doi:10.1016/j.stem.2009.03.003

Sottoriva, A., Spiteri, I., Piccirillo, S. G. M., Touloumis, A., Collins, V. P., Marioni, J. C., et al. (2013). Intratumor heterogeneity in human glioblastoma reflects cancer evolutionary dynamics. *Proc. Natl. Acad. Sci. U.S.A.* 110, 4009–4014. doi:10.1073/pnas.1219747110

Strojnik, T., Røsland, G. V., Sakariassen, P. O., Kavalar, R., and Lah, T. (2007). Neural stem cell markers, nestin and musashi proteins, in the progression of human glioma: correlation of nestin with prognosis of patient survival. *Surg. Neurol.* 68, 133–143. doi:10.1016/j.surneu.2006.10.050

Stupp, R., Hegi, M. E., Mason, W. P., van den Bent, M. J., Taphoorn, M. J., Janzer, R. C., et al. (2009). Effects of radiotherapy with concomitant and adjuvant temozolomide versus radiotherapy alone on survival in glioblastoma in a randomised phase III study: 5-year analysis of the EORTC-NCIC trial. *Lancet Oncol.* 10, 459–466. doi:10.1016/S1470-2045(09)70025-7

Tamaki, M., McDonald, W., Amberger, V. R., Moore, E., and Del Maestro, R. F. (1997). Implantation of C6 astrocytoma spheroid into collagen type I gels: invasive, proliferative, and enzymatic characterizations. *J. Neurosurg.* 87, 602–609. doi:10.3171/jns.1997.87.4.0602

Tan, B. T., Park, C. Y., Ailles, L. E., and Weissman, I. L. (2006). The cancer stem cell hypothesis: a work in progress. *Lab. Invest.* 86, 1203–1207. doi:10.1038/labinvest.3700488

Teixeira, A. I., Duckworth, J. K., and Hermanson, O. (2007). Getting the right stuff: controlling neural stem cell state and fate in vivo and in vitro with biomaterials. *Cell Res. Lond.* 17, 56–61. doi:10.1038/sj.cr.7310141

Ulrich, T. A., de Juan Pardo, E. M., and Kumar, S. (2009). The mechanical rigidity of the extracellular matrix regulates the structure, motility, and proliferation of glioma cells. *Cancer Res.* 69, 4167–4174. doi:10.1158/0008-5472.CAN-08-4859

Ulrich, T. A., Jain, A., Tanner, K., MacKay, J. L., and Kumar, S. (2010). Probing cellular mechanobiology in three-dimensional culture with collagen-agarose matrices. *Biomaterials* 31, 1875–1884. doi:10.1016/j.biomaterials.2009.10.047

Umesh, V., Rape, A. D., Ulrich, T. A., and Kumar, S. (2014). Microenvironmental stiffness enhances glioma cell proliferation by stimulating epidermal growth factor receptor signaling. *PLoS ONE* 9:e101771. doi:10.1371/journal.pone.0101771

Venere, M., Fine, H. A., Dirks, P. B., and Rich, J. N. (2011). Cancer stem cells in gliomas: identifying and understanding the apex cell in cancer's hierarchy. *Glia* 59, 1148–1154. doi:10.1002/glia.21185

Venugopal, C., McFarlane, N. M., Nolte, S., Manoranjan, B., and Singh, S. K. (2012). Processing of primary brain tumor tissue for stem cell assays and flow sorting. *J. Vis. Exp.* 67. doi:10.3791/4111

Verhaak, R. G. W., Hoadley, K. A., Purdom, E., Wang, V., Qi, Y., Wilkerson, M. D., et al. (2010). Integrated genomic analysis identifies clinically relevant subtypes of glioblastoma characterized by abnormalities in PDGFRA, IDH1, EGFR, and NF1. *Cancer Cell* 17, 98–110. doi:10.1016/j.ccr.2009.12.020

Wang, C., Tong, X., and Yang, F. (2014). Bioengineered 3D brain tumor model to elucidate the effects of matrix stiffness on glioblastoma cell behavior using PEG-based hydrogels. *Mol. Pharm.* 11, 2115–2125. doi:10.1021/mp5000828

Wang, K., Kievit, F. M., Erickson, A. E., Silber, J. R., Ellenbogen, R. G., and Zhang, M. (2016). Culture on 3D chitosan-hyaluronic acid scaffolds enhances stem cell marker expression and drug resistance in human glioblastoma cancer stem cells. *Adv. Healthc. Mater.* 5, 3173–3181. doi:10.1002/adhm.201600684

Wang, R., Chadalavada, K., Wilshire, J., Kowalik, U., Hovinga, K. E., Geber, A., et al. (2010a). Glioblastoma stem-like cells give rise to tumour endothelium. *Nature* 468, 829–833. doi:10.1038/nature09624

Wang, J., Wakeman, T. P., Lathia, J. D., Hjelmeland, A. B., Wang, X.-F., White, R. R., et al. (2010b). Notch promotes radioresistance of glioma stem cells. *Stem Cells* 28, 17–28. doi:10.1002/stem.261

Wiranowska, M., and Plaas, A. (2008). Cytokines and extracellular matrix remodeling in the central nervous system. *NeuroImmune Biol.* 6, 167–197. doi:10.1016/S1567-7443(07)10009-0

Wiranowska, M., and Rojiani, M. V. (2011). *Extracellular Matrix Microenvironment in Glioma Progression*. INTECH Open Access Publisher. Available at: https://cdn.intechopen.com/pdfs-wm/22475.pdf.

Wong, S. Y., Ulrich, T. A., Deleyrolle, L. P., MacKay, J. L., Lin, J.-M. G., Martuscello, R. T., et al. (2015). Constitutive activation of myosin-dependent contractility sensitizes glioma tumor-initiating cells to mechanical inputs and reduces tissue invasion. *Cancer Res.* 75, 1113–1122. doi:10.1158/0008-5472.CAN-13-3426

Woolard, K., and Fine, H. A. (2009). Glioma stem cells: better flat than round. *Cell Stem Cell* 4, 466–467. doi:10.1016/j.stem.2009.05.013

Xiao, W., Sohrabi, A., and Seidlits, S. K. (2017). Integrating the glioblastoma microenvironment into engineered experimental models. *Future Sci. OA* 3, FSO189. doi:10.4155/fsoa-2016-0094

Yang, F., Murugan, R., Wang, S., and Ramakrishna, S. (2005). Electrospinning of nano/micro scale poly(l-lactic acid) aligned fibers and their potential in neural tissue engineering. *Biomaterials* 26, 2603–2610. doi:10.1016/j.biomaterials.2004.06.051

Yang, M.-Y., Chiao, M.-T., Lee, H.-T., Chen, C.-M., Yang, Y.-C., Shen, C.-C., et al. (2014). An innovative three-dimensional gelatin foam culture system for improved study of glioblastoma stem cell behavior. *J. Biomed. Mater. Res. B Appl. Biomater.* 103, 618–628. doi:10.1002/jbm.b.33214

Yang, Y., Motte, S., and Kaufman, L. J. (2010). Pore size variable type I collagen gels and their interaction with glioma cells. *Biomaterials* 31, 5678–5688. doi:10.1016/j.biomaterials.2010.03.039

Zeng, L., Zhao, Y., Ouyang, T., Zhao, T., Zhang, S., Chen, J., et al. (2016). Label-retaining assay enriches tumor-initiating cells in glioblastoma spheres cultivated in serum-free medium. *Oncol. Lett.* 12, 815–824. doi:10.3892/ol.2016.4690

Zhang, S., Xie, R., Wan, F., Ye, F., Guo, D., and Lei, T. (2013). Identification of U251 glioma stem cells and their heterogeneous stem-like phenotypes. *Oncol. Lett.* 6, 1649–1655. doi:10.3892/ol.2013.1623

Conflict of Interest Statement: The authors declare that the research was conducted in the absence of any commercial or financial relationships that could be construed as a potential conflict of interest.

frontiers in Materials

ORIGINAL RESEARCH
published: 26 June 2018
doi: 10.3389/fmats.2018.00039

Influence of Hyaluronic Acid Transitions in Tumor Microenvironment on Glioblastoma Malignancy and Invasive Behavior

Jee-Wei E. Chen[1], *Sara Pedron*[2], *Peter Shyu*[3], *Yuhang Hu*[3], *Jann N. Sarkaria*[4] *and Brendan A. C. Harley*[1,2]*

[1] Department of Chemical and Biomolecular Engineering, University of Illinois at Urbana-Champaign, Urbana, IL, United States, [2] Carl R. Woese Institute for Genomic Biology, University of Illinois at Urbana-Champaign, Urbana, IL, United States, [3] Department of Mechanical Science and Engineering, University of Illinois at Urbana-Champaign, Urbana, IL, United States, [4] Department of Radiation Oncology, Mayo Clinic, Rochester, MN, United States

OPEN ACCESS

Edited by:
Paul De Vos,
University Medical Center Groningen, Netherlands

Reviewed by:
Bilikere S. Dwarakanath, Shanghai Proton and Heavy Ion Center (SPHIC), China
Banani Kundu, 3B's Research Group in Biomaterials, Biodegradables and Biomimetics, Portugal

***Correspondence:**
Brendan A. C. Harley
bharley@illinois.edu

Specialty section:
This article was submitted to Biomaterials, a section of the journal Frontiers in Materials

Received: *29 March 2018*
Accepted: *07 June 2018*
Published: *26 June 2018*

Citation:
Chen J-WE, Pedron S, Shyu P, Hu Y, Sarkaria JN and Harley BAC (2018) Influence of Hyaluronic Acid Transitions in Tumor Microenvironment on Glioblastoma Malignancy and Invasive Behavior. Front. Mater. 5:39. doi: 10.3389/fmats.2018.00039

The extracellular matrix (ECM) is critical in tumor growth and invasive potential of cancer cells. In glioblastoma tumors, some components of the native brain ECM such as hyaluronic acid (HA) have been suggested as key regulators of processes associated with poor patient outlook such as invasion and therapeutic resistance. Given the importance of cell-mediated remodeling during invasion, it is likely that the molecular weight of available HA polymer may strongly influence GBM progression. Biomaterial platforms therefore provide a unique opportunity to systematically examine the influence of the molecular weight distribution of HA on GBM cell activity. Here we report the relationship between the molecular weight of matrix-bound HA within a methacrylamide-functionalized gelatin (GelMA) hydrogel, the invasive phenotype of a patient-derived xenograft GBM population that exhibits significant *in vivo* invasivity, and the local production of soluble HA during GBM cell invasion. Hyaluronic acid of different molecular weights spanning a range associated with cell-mediated remodeling (10, 60, and 500 kDa) was photopolymerized into GelMA hydrogels, with cell activity compared to GelMA only conditions (-HA). Polymerization conditions were tuned to create a homologous series of GelMA hydrogels with conserved poroelastic properties (i.e., shear modulus, Poisson's ratio, and diffusivity). GBM migration was strongly influenced by HA molecular weight; while markers associated with active remodeling of HA (hyaluronan synthase and hyaluronidase) were found to be uninfluenced. These results provide new information regarding the importance of local hyaluronic acid content on the invasive phenotype of GBM.

Keywords: cell invasion, hyaluronic acid, hydrogels, tumor microenvironment, tumor margins, molecular weight, glioblastoma, brain tumor

INTRODUCTION

Glioblastoma (GBM), a WHO grade IV astrocytoma, is the most common and deadly form of brain cancer and accounts for more than 50% of primary brain tumors (Furnari et al., 2007; Nakada et al., 2007; Wen and Kesari, 2008). Unlike many other cancers that metastasize to a secondary site, GBM instead is known to diffusely infiltrate throughout but rarely metastasize beyond the brain, and this invasive phenotype contributes to poor patient prognosis (median survival <15 months and 5 year survival <5%) (Stupp et al., 2005; Jackson et al., 2011; Johnson and O'neill, 2012; Mehta et al., 2015). The brain extracellular matrix and GBM tumor microenvironment (TME) display striking differences to other tumors, show a large amount of spatial and temporal heterogeneity, and can differ patient-to-patient. However, while fibrillar proteins such as collagen and fibronectin are abundant in many other tissues, the brain ECM has minimal fibrillar structures and is mainly composed of hyaluronic acid (HA, also called hyaluronan, or hyaluronate) (Bonneh-Barkay and Wiley, 2009; Sivakumar et al., 2017).

The GBM TME is not homogeneous but a complicated heterogeneous environment, especially on the tumor margins, where transitions between the tumor microenvironment and surrounding brain parenchyma are characterized by transitions in structural, biomolecular, and cellular composition. The matrix compositional transition from natural brain to tumor provides a potential invasion path for GBM and, therefore, might contribute to poor patient prognosis (Syková, 2002; Quirico-Santos et al., 2010; Charles et al., 2011; Jackson et al., 2011; Wiranowska and Rojiani, 2011; Junttila and de Sauvage, 2013). Processes of GBM invasion, particularly in the perivascular niche in the tumor margins, involve exposure to not only HA but a range of fibrillar protein content and significant matrix remodeling, resulting in GBM cell exposure to not only HA but also a wide range of molecular weights of HA (Bayin et al., 2014; Lathia et al., 2015; Paw et al., 2015). In this context, the amount and molecular weight distribution of HA, associated with constant turnover from oligosaccharides to high MW HA, across the tumor microenvironment is believed as an important regulator of GBM invasion (Itano and Kimata, 2008). Hyaluronic acid, a negatively charged, nonsulfated GAG, is the main component of brain ECM. HA is naturally produced by hyaluronan synthase (HAS) family and degraded by hyaluronidase (HYAL) in mammalian animals (Misra et al., 2011). While the presence of HA has been shown to be important to tumor progression (Toole, 2004; Stern, 2008; Kim and Kumar, 2014), significant investigation is needed to explore the role of the molecular weight (MW) of HA on processes associated with GBM invasion, progression, and therapeutic response.

Remodeling of hyaluronic acid in the context of GBM cell invasion requires the combined effort of a range of degradative and biosynthetic proteins. Notably, HA biosynthesis is driven by hyaluronic synthase (HAS), which has multiple isoforms responsible for secreting different MW HA (HAS1: 200–2,000 kDa; HAS2: >2,000 kDa; HAS3: 100–1,000 kDa). Similarly, the degradation of HA by hyaluronidase (HYAL) can produce final fragments with different MW. In GBM, HYAL1 (<20 kDa) and HYAL2 (20–50 kDa) are the most abundant HYAL isoforms (Misra et al., 2011; Khaldoyanidi et al., 2014). Due to the constant synthesis and degradation of HA, a wide range of different molecular weight HA (High, >500 kDa; Medium, 50–350 kDa; Low, <30 kDa) are present in the brain and TME (Toole, 2004; Lam et al., 2014; Monslow et al., 2015). HMW HA is important for structural support and the biophysical properties in tissue, and is directly synthesized via HAS. While HMW HA can inhibit tumor growth in colon cancer (Mueller et al., 2010) it also decreases production of MMPs by suppression of MAPK and Akt pathways (Chang et al., 2012). L-MMW, generated from HYAL degradation as final products, are often associated with enhanced invasion and increased tumor growth (Monslow et al., 2015). LMW and MMW HA have been reported to enhance cancer proliferation, cell adhesion as well as secretion of MMPs for matrix remodeling (Tofuku et al., 2006). LMW HA has also been reported to be pro-inflammatory and pro-angiogenic, which may contribute to cancer invasion (West et al., 1985; Lam et al., 2014). In contrast, the effects of oligo HA have been more variable. In papillary thyroid carcinoma, oligo HA is associated with increased (Dang et al., 2013), while other studies demonstrate suppression of signaling pathways such as Ras and Erk and reduced tumor progression (Misra et al., 2006; Toole et al., 2008).

Despite the conflicting HA-cancer relations and lack of full understanding of HA MW contribution, HA clearly plays a significant role in many signaling pathways and in tumor progression. In this study, we analyze the effects of matrix-bound HA on GBM cell invasion by using an *in vitro* fully three-dimensional gelatin based hydrogel system that our lab has previously developed (Pedron et al., 2013; Chen et al., 2017). Previous efforts have used this platform to demonstrate the effect of a single MW HA immobilized within the GelMA hydrogel on the invasive phenotype of GBM cell lines as well as the gene expression signature and response to a model tyrosine kinase inhibitor (erlotinib) (Chen et al., 2017, 2018; Pedron et al., 2017a,b). Here we selectively decorate the GelMA hydrogel with a range of MW HA spanning those seen in the GBM TME (10, 60, and 500 kDa). Further, we examine the behavior of a patient-derived xenograft (PDX) GBM specimen that maintains patient specific molecular and morphologic characteristics (Sarkaria et al., 2006, 2007). We evaluate cell growth, invasion, and proteomic responses of GBM cells within our platform and demonstrate the influence HA MW on GBM invasive phenotype. The understanding of the effect of HA MW in GBM cell invasion may open up new lines of investigation to identify novel targeted therapies.

MATERIALS AND METHODS

Hydrogel Fabrication and Characterization

Fabrication of methacrylated gelatin (GelMA) and methacrylated hyaluronic acid (HAMA) precursors and hydrogels were as described in previous publications (Pedron et al., 2013; Chen et al., 2017). Briefly, gelatin powder (Type A, 300 bloom from porcine skin, Sigma-Aldrich) was dissolved in 60°C phosphate buffered saline (PBS; Lonza, Basel, Switzerland) then methacrylic anhydride (MA; Sigma-Aldrich) was added into the gelatin-PBS

solution dropwise and allowed the reaction proceed for 1 h. The GelMA solution was then dialyzed (12–14 kDa; Fisher Scientific) and lyophilized. HAMA was synthesized by adding 10 mL MA dropwise into a cold (4°C) HA sodium salt (10, 60 or 500 kDa; Lifecore Biomedical) solution (1 g HA sodium salt in 100 mL DI water). The pH was adjusted to 8 with the addition of 5N sodium hydroxide solution (NaOH; Sigma-Aldrich) and the reaction proceeded overnight at 4°C. The product was then purified by dialysis and lyophilized. The degree of MA functionalization of both GelMA and HAMA was determined by ^{1}H NMR (data not shown) (Pedron et al., 2013; Chen et al., 2017).

Hydrogels (GelMA ± HAMA) were prepared by dissolving GelMA and HAMA in PBS at a total concentration of 4 wt% with gentle heating (37°C ∼45°C) in the presence of a lithium acylphosphinate (LAP) as photoinitiator (PI, adjusted to maintain same Young's modulus). The mixture was placed into Teflon molds (0.15 mm thick, 5 mm radius) and photopolymerized under UV light (AccuCure LED 365 nm, Intensity 7.1 mW/cm^2) for 30 s (Mahadik et al., 2015). Cell-containing hydrogels were made similarly but with addition of cells (4×10^6 cells/mL hydrogel solution) to the pre-polymer solution, prior to pipetting into Teflon molds, and then photopolymerized. Details regarding the hydrogel compositions are listed in **Table 1**. All HA containing GelMA hydrogel groups were fabricated with 15% w/w HA, consistent with previous HA-decorated GelMA hydrogels described by our group (Pedron et al., 2015, 2017a,b; Chen et al., 2017, 2018).

Characterization of Hydrogels

Young's Modulus

The compressive modulus of each hydrogel variant was measured using an Instron 5943 mechanical tester. Hydrogels were tested under unconfined compression with a pre-load 0.005N at the rate of 0.1 mm/min, with their Young's modulus obtained from the linear region of the stress-strain curve (0–10% strain).

Diffusivity

The water diffusivity of each hydrogel was measured through indentation tests using atomic force microscopy (AFM, MFP-3D AFM, Asylum Research; **Figure 1**). The stiffness of the cantilever used in the measurements is 0.6 N/m. A spherical polystyrene probe of 25 μm diameter was attached to the tip (Novascan). Three separate measurements of different indentation depths were taken. After surface detection, the spherical indenter was pressed into the sample to a certain depth in the rate of 50 μm/s and was held for a period of time until the force on the indenter reaches a constant value. The force on the indenter was measured as a function of time F(t). The time-dependent response of hydrogels is due to solvent migration. The poroelastic relaxation indentation problem has been solved theoretically by Hu et al. (2010, 2011). Simple solutions have been derived for direct extraction of material properties from the relaxation indentation measurement. According to this method, the normalized force relaxation function is a function of a single variable: the normalized time $\tau = Dt/a^2$, with D being the diffusivity, t being time, and a being the contact radius that is related to the radius of the spherical probe R and indentation depth h by $a = \sqrt{Rh}$:

$$\frac{F(t) - F(\infty)}{F(0) - F(\infty)} = g\left(\frac{Dt}{a^2}\right) \quad (1)$$

This master curve has been derived numerically as

$$g(\tau) = 0.491e^{-0.908\sqrt{\tau}} + e^{-1.679\tau} \quad (2)$$

Normalizing the experimental data and fitting it with the theoretical curve (Equation 2), we can extract the single fitting parameter diffusivity D. More details can be seen in references (Hu et al., 2010, 2011).

Patient Derived Xenograft Cell Culture

Short-term explant cultures derived from the GBM39 PDX model were obtained from Mayo Clinic (Rochester, Minnesota). PDX samples were mechanically disaggregated, plated on low-growth factor Matrigel coated tissue culture flasks in in standard culture media made with Dulbecco's modified eagle medium (DMEM; Gibco) supplemented with 10% fetal bovine serum (FBS; Atlanta biologicals) and 1% penicillin/streptomycin (P/S; Lonza) at 37°C in a 5% CO_2 environment. Flasks were shipped by overnight expression and then used upon arrival after trypsinzation. For analysis of cell metabolic health and protein expression, GBM39 cells were homogeneously mixed with the GelMA ± HAMA solution at a density of 4×10^6 cells/mL. Cell-seeded hydrogels were incubated in cell culture medium at 37°C, 5% CO_2 in low adhesion well plates containing standard culture media (DMEM with 10% FBS and 1% P/S). Culture media was changed at day 3 and day 5 for all cell-containing hydrogels.

Time-Lapse Cell Invasion Assay Using Spheroids

To measure relative cell motion in the fully three-dimensional hydrogel environment, we embedded GBM spheroids into our hydrogel. A methylcellulose (MC, 12 wt% in 0.5x PBS, Sigma-Aldrich) solution was made with constant stirring at 4°C overnight, then autoclaved and kept at 4°C for storage. MC solution was then added into 96-well plate and kept at 37°C overnight to form a non-adherent MC-hydrogel layer. 10^5 GBM cells were added to each well, placed at 37°C, 5% CO_2 environment with constant horizontal-shaking (60 rpm) overnight to aid spheroid formation (Lee et al., 2011). Spheroids were then mixed with pre-polymer GelMA ± HAMA solution, photopolymerized and cultured following the same method previously described. Cell invasion into the hydrogel was traced throughout 7-day culture by taking images on days 0 (immediately after embedding), 1, 2, 3, 5, and 7 using a Leica DMI 400B florescence microscope under bright field. Analysis of cell invasion distance ($d_i = r_i - r_0$) was quantified via ImageJ using the relative radius (cell spreading shape $\sim \pi r_i^2$) compared to day 0 (r_0) using a method previously described by our group (Chen et al., 2017).

TABLE 1 | Hydrogel composition and characterization results ($n = 6$).

Hydrogel	-HA	10 K	60 K	500 K
GelMA (wt%)	4.0	3.4	3.4	3.4
HAMA (wt%)	0	0.6	0.6	0.6
HA sodium salt MW	N/A	∼10 kDa	∼60 kDa	∼500 kDa
LAP (wt%)	0.1	0.02	0.02	0.02
Young's modulus (kPa)	2.76 ± 0.24	2.97 ± 0.15	2.79 ± 0.15	2.70 ± 0.03
Diffusivity ($\mu m^2/s$)	161.04 ± 70.33	153.54 ± 34.92	169.90 ± 26.88	156.43 ± 50.18

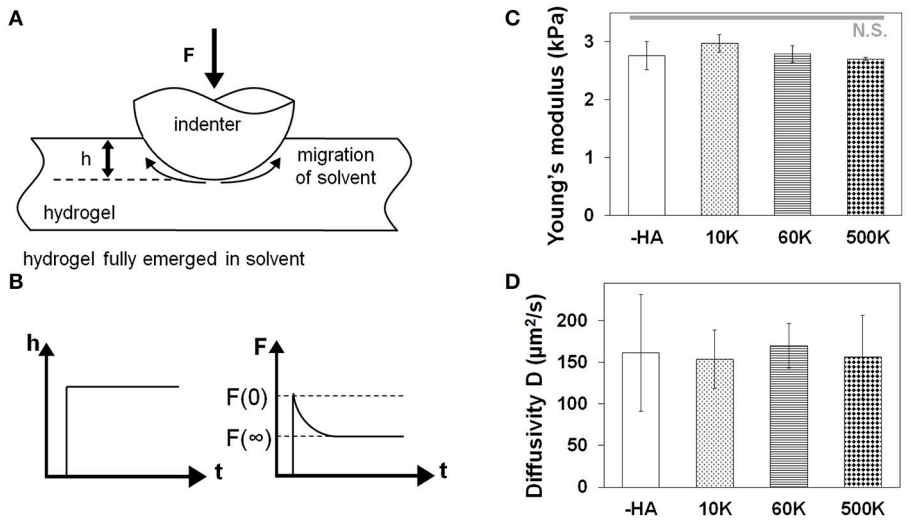

FIGURE 1 | (A) Schematic drawing of measuring hydrogel water diffusivity via AFM. **(B)** Poroelastic parameters are extracted via indentation performed to a fixed depth followed by force relaxation to a new equilibrium state. Characterization that for a homologous series of GelMA hydrogels developed for this project there was a negligible effect of the molecular weight of hyaluronic acid incorporated into the GelMA hydrogel on **(C)** hydrogel Young's modulus measured via MTS ($n = 6$) and **(D)** hydrogel diffusivity via AFM ($n = 6$).

Analysis of Cell Metabolic Activity

The total metabolic activity of cell-containing hydrogels was measured immediately after hydrogel encapsulation (day 0) and then subsequently at days 3 and 7 of hydrogel culture. Metabolic activity was analyzed using a dimethylthiazol-diphenyltetrazolium bromide assay (MTT; Molecular Probes) following manufacturer's instructions. Briefly, at each time point the culture media surrounding each hydrogel sample was replaced with MTT-containing media and incubated for 4 h, then solution was replaced with dimethyl sulfoxide (DMSO; Sigma-Aldrich) and set overnight. Metabolic activity of samples was measured via absorbance at 540 nm using a microplate reader (Synergy HT, Biotek), with data normalized to day 0 samples (immediately after seeding) as fold change.

Quantification and Size Analysis of Soluble Hyaluronic Acid Secretion

The concentration of soluble HA in the media was quantified from sample media using an enzyme-linked immunosorbent assay (ELISA, R&D systems) following the manufacturer's instructions. Sample media were collected at days 3, 5, and 7. Samples were analyzed via a microplate reader (Synergy HT, Biotek) with 450/540 nm wavelength absorbance. Soluble HA concentration within the media at each time point was calculated, with accumulated results reported as a function of all previous time point measurements.

The HA isolation from media samples and the MW distribution analysis was assessed following a protocol from Cleveland Clinic (Hyaluronan size analysis by agarose gel electrophoresis, http://pegnac.sdsc.edu/cleveland-clinic/protocols/). Briefly, after consecutive digestion–precipitation steps, HA was extracted from media samples and lyophilized. Half of the sample was completely digested with hyaluronidase to serve as a reference. The remaining sample was dissolved in formamide (Sigma-Aldrich) before loading into the electrophoresis gel. A 1% agarose (Fisher Scientific) gel in 1x TAE buffer (Invitrogen) was prepared and electrophoresis (Horizon 58; LabRepCo) was ran for 4.5 h at 80 V to remove any impurity. Each lane was then loaded with 12 μL of sample and run for 1.25 h at 100 V. The agarose gel was then equilibrated with 30% ethanol for 1 h and stained with Stains-All (Sigma-Aldrich) in the dark at room temperature overnight. The agarose

gel was then washed using ddH_2O, exposed to light for 90 min to reduce background signal, and imaged using a blue light transilluminator compatible with smartphone imaging (color).

Protein Isolation and Western Blotting

Procedures of protein isolation and Western blotting were described in previous publication (Caliari et al., 2015). Protein isolation was done by extracting proteins from cell-containing hydrogels by using cold RIPA buffer and incubating for 30 min. Total protein concentration in the lysates was determined by Pierce™ BCA Protein Assay Kit (Thermo Scientific). Lysates were then mixed with 2x Laemmli Sample Buffer (Bio-Rad) and 2-Mercaptoethanol (Sigma-Aldrich), heated to 95°C for 10 min, then loaded (3 μg protein loaded onto per lane) onto polyacrylamide gels (4–20% gradient; Bio-Rad). Gel electrophoresis was performed at 150 V. Proteins were then transferred onto nitrocellulose membrane (GE Healthcare) using Trans-Blot SD (Bio-Rad) under 300 mA for 2 h. Membranes were then cut into desired MW range and blocked in blocking buffer for 1 h followed by primary antibodies incubation at 4°C overnight. Membranes were subsequently washed with Tris Buffered Saline with Tween20 (TBST), followed by secondary antibody incubation for 2 h at room temperature. Imaging signal was visualized using imaging kits (SuperSignal™ West Pico PLUS Chemiluminescent Substrate or SuperSignal™ West Femto Maximum Sensitivity Substrate, Sigma-Aldrich) via an Image Quant LAS 4010 chemiluminescence imager (GE Healthcare). Band intensities were quantified using ImageJ and normalized to β-actin expression. Buffers and antibodies used in each condition are listed (Table S1).

Statistics

All statistical analysis was performed using one-way analysis of variance (ANOVA) followed by Tukey's test. A minimum sample number of $n = 3$ (MTT, ELISA, Western), $n = 6$ (Young's modulus, diffusivity, invasion) samples were used for all assays. Statistical significance was set at $p < 0.05$. Error is reported as the standard error of the mean.

RESULTS

GelMA hydrogels lacking matrix-bound HA will be denoted as "-HA" while hydrogels containing 15 w/w% HAMA will be denoted as "10 K", "60 K", or "500 K" to denote the molecular weight of the incorporated HA sodium.

Molecular Weight of Matrix-Bound HA Does Not Impact Young's Moduli or Diffusive Properties of the Family of Gelatin Hydrogels

The biophysical properties of the homologous series of GelMA hydrogel (-HA, 10, 60, and 500 K) were assessed via unconfined compression and AFM indentation. The Young's moduli of all hydrogels did not vary as a result of inclusion of matrix-bound HA regardless of the HA MW. Critically, the Young's modulus of these hydrogels (-HA: 2.76 ± 0.24 kPa; 10 K: 2.97 ± 0.15 kPa; 60 K: 2.79 ± 0.15 kPa; 500 K: 2.70 ± 0.03 kPa) are within physio-relevant range (10^0-10^1 kPa) for the GBM TME. Similarly, the diffusivity of all hydrogel variants was not significantly influenced by the presence or absence of matrix immobilized HA (-HA: 161.04 ± 70.33 $\mu m^2/s$; 10 K: 153.54 ± 34.92 $\mu m^2/s$; 60 K: 169.90 ± 26.88; 500 K: 156.43 ± 50.18 $\mu m^2/s$; **Figure 1**).

Metabolic Activity of GBM39 PDX Cells Cultured in GelMA Hydrogels Is Sensitive to the Molecular Weight of Matrix Bound HA

The metabolic activity of GBM39 PDX cells encapsulated within the homologous series of GelMA hydrogels (-HA, 10, 60, and 500 K) was traced through 7 days in culture, with results normalized to day 0 values for each group. The groups with matrix-bound HA (10, 60, and 500 K) showed a significantly higher metabolic activity compared to -HA group ($p < 0.05$), with the 60 K HA group showing the highest metabolic activity amongst all groups (**Figure 2**).

The Molecular Weight of Matrix-Bound HA Significantly Affects Invasion

The invasion of GBM39 PDX cells into the surrounding hydrogel matrix was measured via a previously reported spheroid assay through 7-days in culture. GBM39 invasion was strongly influenced by hydrogel HA content. The highest level of invasion was observed for GelMA hydrogels either lacking matrix bound HA (-HA), or those containing mid-range (60 K) molecular weight matrix-immobilized HA (**Figure 3**). At early-to-mid time points (up to day 5), GBM cell invasion was significantly depressed in the low molecular weight 10 K group, but GBM invasion increased steeply at later time points (day

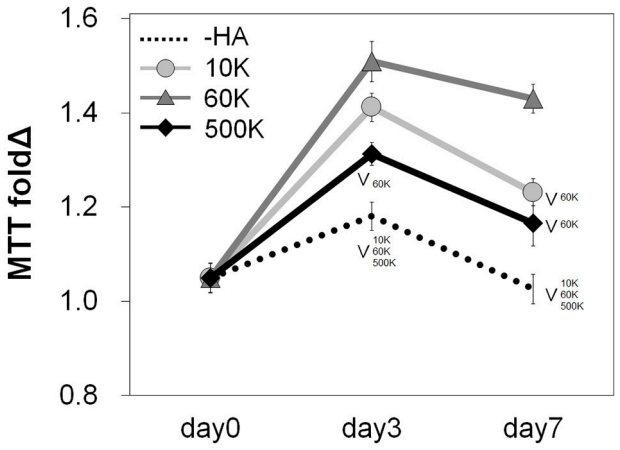

FIGURE 2 | Overall metabolic activities ($n = 3$) of GBM seeded GelMA hydrogels as a function of incorporated hyaluronic acid molecular weight. Results are provided throughout the 7-day culture and are normalized to the metabolic activity of each group at day 0. Samples containing matrix-bound HA showed an overall higher metabolic activity compared to GelMA only (–HA) hydrogels. The greatest metabolic activity was observed for GelMA hydrogels containing 60 kDa (60 K) HA. $^{\vee}p < 0.05$ significant decrease between groups.

7), matching the highest invasion groups. GelMA hydrogels containing the largest molecular weight HA (500 K) showed significantly reduced invasion compared to all other hydrogel groups (-HA, 10, and 60 K) throughout the entire period studied.

The Accumulation of Soluble HA in Media Reflects Matrix-Composition

ELISA was performed to measure the concentration of soluble HA in the culture media over the course of the invasion experiment. An increase in soluble HA concentration was observed in the hydrogels lacking matrix bound HA (-HA) compared to all groups containing matrix-bound HA. Interestingly, the presence of soluble HA for hydrogel groups containing matrix-immobilized HA was found to be strongly associated with the molecular weight of immobilized HA, with 500 K group showing significantly upregulated secretion compared to GBM cells in 10 and 60 K HA hydrogels as early as day 3. Significant increases were observed in soluble HA production in 60 vs. 10 K hydrogels appeared by day 7 of culture (**Figure 4A**). Moreover, the molecular weight distribution of soluble HA in the culture media showed that the 500 K group produced higher MW HA, as compared to the rest of the groups with matrix bound-HA, suggesting an association between smaller MW HA and increased mobility. On the other hand, -HA samples showed very weak signals (at all time points), that may be explained by high concentration of very low MW HA that escaped the electrophoresis gel.

Protein Expression of Hyaluronic Acid Remodeling Associated Proteins Were Not Strongly Influenced by Hydrogel HA Content

The expression of protein families, biosynthetic hyaluronan synthase (HAS1, HAS2, HAS3) and degradative hyaluronidase (HYAL1, HYAL2), associated with HA remodeling were subsequently quantified via Western blot analyses (**Figure 5**, Figure S1, S2). No significant differences were observed in expression levels within each group as a function of immobilized HA molecular weight. However, GBM cells in the highest molecular weight HA hydrogels (500 K) showed generalized increases in both HAS and HYAL (significant for HYAL2) compared to all other hydrogel conditions.

DISCUSSION

The heterogeneity of GBM tumor microenvironment complicates its study both *in vivo* and *in vitro*. Within that high diversity, the extracellular HA has been widely associated with cancer invasion and response to treatment (Park et al., 2008; Rankin and Frankel, 2016; Zhao et al., 2017). Naturally, HA is synthesized and deposited in the extracellular space by HAS family and degraded into different size fragments by HYAL enzyme family. The alteration of the levels of these enzymes are associated with various types of diseases. LMW HA (<30 kDa) has been associated mainly with increased tumor growth, cell migration and angiogenesis, while HMW (250 to >1,000 kDa) is commonly believed to lead to greater structural stability with reduced tumor growth, migration, and angiogenesis (Monslow et al., 2015). However, despite their relevance in GBM microenvironment, the influence of HA MW has been largely neglected in regard to the construction of *ex vivo* biomaterial platforms to examine GBM cell activity. This project seeks to understand the effect of HA molecular weight, both matrix bound and cell secreted, on the invasive phenotype of a patient-derive GBM specimen. We developed and characterized a homologous series of HA-decorated gelatin-based hydrogels to evaluate the effect of HA MW on GBM invasiveness and phenotypic responses.

A family of hydrogels with no matrix-bound HA or with increasing MW HA (10, 60, and 500 kDa) was fabricated using a method previously described (Pedron et al., 2013; Chen et al., 2017). Studies demonstrate that substrate stiffness and diffusion can deeply influence the migration capacity of GBM cells in HA containing hydrogels (Rape et al., 2014; Umesh et al., 2014; Wang et al., 2014; Chen et al., 2017). However, we have previously described a framework to adjust the relative ratio of GelMA to HA content as well as manipulating the crosslinking conditions to generate a series of GelMA hydrogels containing increasing wt% of a single MW HA (Pedron et al., 2013). We therefore adapted this approach to create the homologous series of hydrogels described in this study, that contained a conserved wt% of HA but that varied the MW of matrix-immobilized HA. We then employed a series of biophysical and biochemical characterization protocols to describe poroelastic features of these hydrogels. Crosslinking density can be preserved by adjusting the photoinitiator concentration in the pre-polymer solution (**Table 1**), and therefore maintaining the Young's modulus between different hydrogels. Moreover, the deformation of the gel in contact with the AFM tip results from two simultaneous molecular processes: the conformational change of the network, and the migration of the solvent molecules (Hu et al., 2010). In this case, the poroelasticity of the hydrogels, characterized by the diffusivity (**Figure 1D**), stays unchanged for all samples used. Both Young's modulus and diffusivity showed no significant difference among all groups suggesting these hydrogels were able to provide similar culture conditions for cells while providing the opportunity to adjust the molecular weight of bound HA.

We subsequently measured the metabolic activity of GBM39 PDX cells as a function of matrix bound HA MW. The presence of matrix-bound HA aided GBM metabolic response compared to the -HA group. In general, all cells remained viable within the hydrogel up to 7 days, without showing apoptosis or cell death. Further, we performed a spheroid-based invasion assay to investigate the effects of matrix-bound HA MW on invasion at different time points, including early (1 and 2 days), mid (3 and 5 days) and longer (7 day) time points. Consistent with earlier observations described by our group using GBM cell lines (Chen et al., 2017, 2018), we found GBM invasion in GelMA hydrogels lacking matrix bound HA was greatest. However, invasion was strongly influenced by the MW of immobilized HA with GBM cell invasion in hydrogels containing 60 kDa

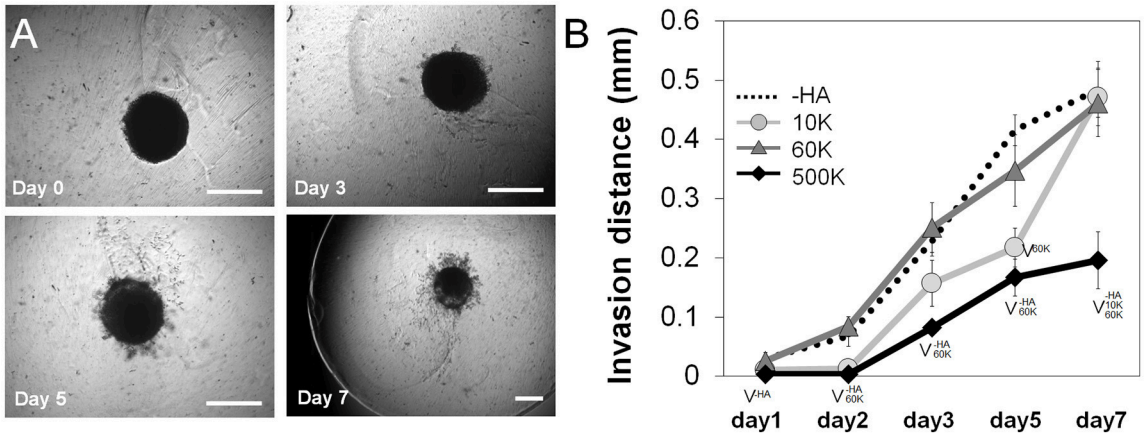

FIGURE 3 | (A) PDX invasion ($n = 6$) into the surrounding hydrogel was quantified via a spheroid assay throughout the 7-day culture period. Representative images of spheroid invasion throughout the 7 day culture, showing GBM cells progressively leave the spheroid and invade the hydrogel. Scale bar 0.5 mm. **(B)** Quantification of GBM cell invasion into the GelMA hydrogel as a function of the molecular weight of matrix immobilized HA. GelMA only (–HA) and GelMA hydrogels containing 60 kDa (60 K) HA showed the greatest levels of invasion, with no significant difference between those groups across the culture period. Interestingly, GelMA hydrogels containing high molecular weight HA (500 K) showed significantly reduced invasion. $^{\vee}p < 0.05$ significant decrease between groups.

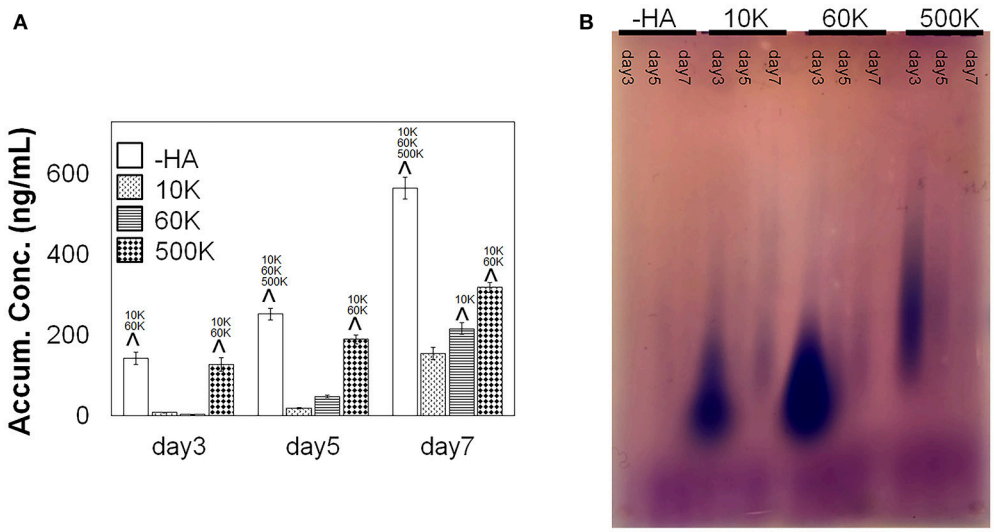

FIGURE 4 | (A) Accumulative of soluble HA in the media over the course of GBM culture in GelMA hydrogels, measured via ELISA ($n = 3$). GBM cells in GelMA hydrogels lacking any matrix immobilized HA (-HA) showed secreted significantly higher amount of soluble HA compare to GBM cells cultured within GelMA hydrogels containing matrix-bound HA. Production of soluble HA by GBM cells in GelMA hydrogels containing matrix-immobilized HA were strongly sensitive to the molecular weight of the matrix immobilized HA. Notably, soluble HA secretion increased with the MW of immobilized HA, with the 500 K group secreting significantly higher amount of soluble HA compare to 60 and 10 K. $^{\wedge}p < 0.05$ significant increase between different groups. **(B)** Agarose gel showing the molecular weight distribution of HA in culture media (blue). Low molecular weight chondroitin sulfate appears in purple. The most intense signals are samples at day 3 for 10, 60, and 500 K hydrogels.

being equivalent to hydrogels lacking matrix bound HA. Further, this invasive potential of GBM39 cells within –HA and +HA hydrogels is not associated to their metabolic activity profiles (**Figure 2**). Although migration and proliferation are considered to be circumscribed phenotypes that do not co-occur with each other in GBM, the complex microenvironment of PDX suggests that both can coexist. Moreover, GBM cells adapt to the different phenotypes by using regulatory signaling from the local microenvironment (Xie et al., 2014). Interestingly, while invasion was initially significantly reduced in low MW HA hydrogels (10 K), GBM invasion increased significantly at later time points. However, GBM invasions was strongly reduced in GelMA hydrogels containing high molecular weight HA (500 K) throughout the entirety of the study, suggesting more mature HA matrices will inhibit GBM invasion. While recent studies have begun to examine the design of implants to reduce GBM invasion (Jain et al., 2014), these findings potentially pave the way for the design of new bioactive hydrogels with potential

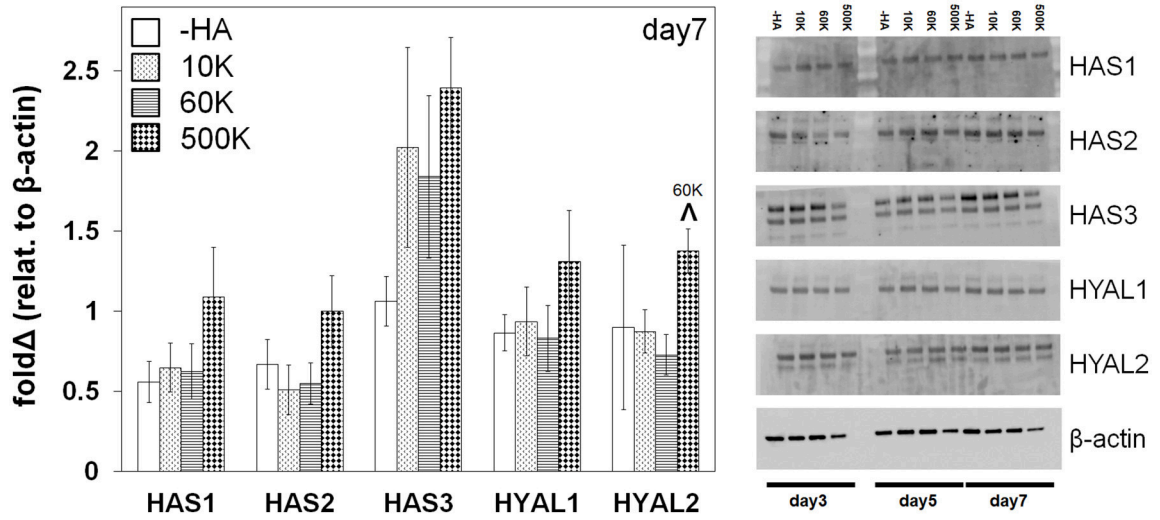

FIGURE 5 | Hyaluronan synthase (HAS) and hyaluronidase (HYAL) protein expression of GBM cells in gelatin hydrogels as a function of matrix immobilized HA molecular weight, analyzed via Western Blot at day 7 ($n = 3$). β-actin is used as loading control. $\wedge p < 0.05$ significant increase between different groups.

to reduce invasive spreading upon post-resection incorporation in the tumor margins. Regardless, the presence of both fibrillar and HA associated features of the TME in these HA decorated GelMA hydrogels may be particularly useful in the context of GBM invasion in perivascular niches that contain such matrix diversity (Ngo and Harley, 2018).

Studies have shown that HMW HA could inhibit tumor invasion by inhibiting MMPs production and down-regulating invasion related pathways such as MAPK and Akt (Chang et al., 2012), while LMW HA may promote these invasion related pathways (West et al., 1985; Lam et al., 2014). We hypothesize that the significant decrease of motility in PDX cells in 500 kDa hydrogels is due to the down-regulation of invasion related pathways, induced by the local extracellular microenvironment. We observed endogenous HA production was significantly elevated without the presence of matrix-bound HA (-HA) (**Figure 4A**), consistent with previous studies reported by our group using immortalized cell lines that demonstrated soluble HA production was associated with increased GBM cell invasion (Chen et al., 2017). More interestingly, soluble HA production across the homologous series of hydrogels tested in this study (-HA, 10, 60, and 500 K) showed greatest endogenous HA production in hydrogels lacking matrix immobilized HA. However, endogenous production of HA was also sensitive to the molecular weight of matrix bound HA, with greater endogenous HA production seen with increasing molecular weight of bound HA. This trend of increasing soluble HA production with increasing molecular weight of matrix-bound HA may be associated to an adaptation required to mobilize matrix bound HA for invasion. The local microenvironment is constantly remodeled, with HA present in culture media suggesting a combination of cell secreted HA in addition to the products of degradation of matrix-bound HA as cells evolve into the hydrogel. The distribution of molecular weights suggests a higher concentration of low molecular weight HA in 10 and 60 K matrices may be associated to increased motility (**Figure 4B**).

Many studies have shown that the levels of HAS correlate with breast and colon cancer malignancy and patient prognosis (Bullard et al., 2003; Auvinen et al., 2014). Inhibition of HAS has been used as an alternative therapeutic strategy using mRNA silencing HAS or HAS-targeting drugs (e.g., 4-Methylubelliferone) (Nakamura et al., 1997; Li et al., 2007; Nagy et al., 2015). While some studies suggest addition of HYAL into chemotherapy efficiently improves the patient prognosis (Baumgartner et al., 1998; Klocker et al., 1998; Stern, 2008), others show HYAL levels are correlated with cancer malignancy and invasiveness in breast, prostate and bladder cancers (Lokeshwar et al., 1996, 2005; Madan et al., 1999; Stern, 2008). While we observe no significant across-the-board trends in HAS and HYAL proteins levels as a function of matrix immobilized HA, GBM cells in hydrogels containing the highest molecular weight HA (500 kDa) show overall a higher expression of all HAS and HYAL families compared to the rest. However, these results did not directly correlate with the GBM invasiveness as for what we observed. While HAS and HYAL both play a key role in tumor progression and invasiveness, the dynamic balance might be more crucial instead of one over the other, suggesting opportunities for future studies using an expanded library of patient-derived GBM specimens using this homologous series of GelMA hydrogels.

High production of HA is normally associated with tumor progression, although overly high levels of hyaluronic acid secretion may lead to an opposite behavior (Itano et al., 2004). Moreover, in gliomas, this HA associated tumor progression only occurs if hyaluronan is expressed simultaneously with HAS (Enegd et al., 2002). Therefore, studies suggest that HA turnover is required for the increase of HA associated GBM

tumor malignancy. Additionally, the relative contribution of matrix-bonded and cell produced HA increases this complexity. Therefore, a feedback mechanism between stromal and produced HA has been drafted for epithelial cancers (Koyama et al., 2007) but is still unexplored in glioblastoma. In this study, using an *ex vivo* biomaterial model, we show how the dynamic interplay between extracellular matrix associated and cell produced HA affects GBM cell behavior. Further ongoing research may allow identification of alternative antitumor treatments in the context of the GBM microenvironment.

CONCLUSION

There are numerous reports that cover the importance of HA molecular weight on a variety of diseases, including cancer. However, discerning between matrix-bound and cell secreted HA signaling still needs to be elucidated. Here, we highlight the impact of matrix-bound HA MW on GBM cell malignancy. Cells cultured in hydrogels containing 500 kDa matrix-immobilized HA, with controlled physical properties, showed less invasive potential than those in hydrogels containing matrix immobilized 10 or 60 kDa HA. This increased malignancy seems to be related to different interrelated factors: cell secreted HA, matrix degradation and cell-matrix signaling. Going forward, these results pave the way for a deeper analysis of HA molecular weight as a therapeutic target for controlling tumor progression.

AUTHOR CONTRIBUTIONS

J-WC, SP, and BH designed experiments, performed cell experiments, data analysis, results interpretation, and wrote the manuscript. PS and YH performed AFM experiments and assisted with manuscript writing. JS assisted with experiment design, results interpretation, and manuscript writing. BH is the principal investigator.

ACKNOWLEDGMENTS

Hydrogel diffusivity measurements were carried out in part in the Frederick Seitz Materials Research Laboratory Central Research Facilities, University of Illinois at Urbana-Champaign. We acknowledge Jan Lumibao and Dr. Rex Gaskins for assistance in performing agarose gel electrophoresis. We acknowledge the protocol from Cleveland Clinic: Hyaluronan size analysis by agarose gel electrophoresis (Award number PO1HL107147). Research reported in this publication was supported by the National Cancer Institute, National Institute of Diabetes and Digestive and Kidney Diseases, and the National Institute of Biomedical Imaging and Bioengineering of the National Institutes of Health under Award Numbers R01CA197488 (BH), R01 DK099528 (BH), and T32EB019944 (J-WC). The content is solely the responsibility of the authors and does not necessarily represent the official views of the National Institutes of Health. The authors are also grateful for additional funding provided by the Department of Chemical & Biomolecular Engineering (BH) and the Carl R. Woese Institute for Genomic Biology (BH) at the University of Illinois at Urbana-Champaign. Development and maintenance of the GBM PDX models was supported by Mayo Clinic, the Mayo SPORE in Brain Cancer (CA108961), and the Mayo Clinic Brain Tumor Patient-Derived Xenograft National Resource (NS092940).

SUPPLEMENTARY MATERIAL

The Supplementary Material for this article can be found online at: https://www.frontiersin.org/articles/10.3389/fmats.2018.00039/full#supplementary-material

REFERENCES

Auvinen, P., Rilla, K., Tumelius, R., Tammi, M., Sironen, R., Soini, Y., et al. (2014). Hyaluronan synthases (HAS1-3) in stromal and malignant cells correlate with breast cancer grade and predict patient survival. *Breast Cancer Res. Treat.* 143, 277–286. doi: 10.1007/s10549-013-2804-7

Baumgartner, G., Gomar-Hoss, C., Sakr, L., Ulsperger, E., and Wogritsch, C. (1998). The impact of extracellular matrix on the chemoresistance of solid tumors–experimental and clinical results of hyaluronidase as additive to cytostatic chemotherapy. *Cancer Lett.* 131, 85–99. doi: 10.1016/S0304-3835(98)00204-3

Bayin, N. S., Modrek, A. S., and Placantonakis, D. G. (2014). Glioblastoma stem cells: molecular characteristics and therapeutic implications. *World J. Stem Cells* 6, 230–238. doi: 10.4252/wjsc.v6.i2.230

Bonneh-Barkay, D., and Wiley, C. A. (2009). Brain extracellular matrix in neurodegeneration. *Brain Pathol.* 19, 573–585. doi: 10.1111/j.1750-3639.2008.00195.x

Bullard, K. M., Kim, H. R., Wheeler, M. A., Wilson, C. M., Neudauer, C. L., Simpson, M. A., et al. (2003). Hyaluronan synthase-3 is upregulated in metastatic colon carcinoma cells and manipulation of expression alters matrix retention and cellular growth. *Int. J. Cancer* 107, 739–746. doi: 10.1002/ijc.11475

Caliari, S. R., Weisgerber, D. W., Grier, W. K., Mahmassani, Z., Boppart, M. D., and Harley, B. A. (2015). Collagen scaffolds incorporating coincident gradations of instructive structural and biochemical cues for osteotendinous junction engineering. *Adv. Healthc. Mater.* 4, 831–837. doi: 10.1002/adhm.201400809

Chang, C. C., Hsieh, M. S., Liao, S. T., Chen, Y. H., Cheng, C. W., Huang, P. T., et al. (2012). Hyaluronan regulates PPARγ and inflammatory responses in IL-1β-stimulated human chondrosarcoma cells, a model for osteoarthritis. *Carbohydr. Polym.* 90, 1168–1175. doi: 10.1016/j.carbpol.2012.06.071

Charles, N. A., Holland, E. C., Gilbertson, R., Glass, R., and Kettenmann, H. (2011). The brain tumor microenvironment. *Glia* 59, 1169–1180. doi: 10.1002/glia.21136

Chen, J. W., Blazek, A., Lumibao, J., Gaskins, H. R., and Harley, B. (2018). Hypoxia activates enhanced invasive potential and endogenous hyaluronic acid production by glioblastoma cells. *Biomater. Sci.* 6, 854–862. doi: 10.1039/C7BM01195D

Chen, J. W., Pedron, S., and Harley, B. A. C. (2017). The combined influence of hydrogel stiffness and matrix-bound hyaluronic acid content on glioblastoma invasion. *Macromol. Biosci.* 17:1700018. doi: 10.1002/mabi.201700018

Dang, S., Peng, Y., Ye, L., Wang, Y., Qian, Z., Chen, Y., et al. (2013). Stimulation of TLR4 by LMW-HA induces metastasis in human papillary thyroid carcinoma through CXCR7. *Clin. Dev. Immunol.* 2013:712561. doi: 10.1155/2013/712561

Enegd, B., King, J. A., Stylli, S., Paradiso, L., Kaye, A. H., and Novak, U. (2002). Overexpression of hyaluronan synthase-2 reduces the tumorigenic potential of glioma cells lacking hyaluronidase activity. *Neurosurgery* 50, 1311–1318. doi: 10.1097/00006123-200206000-00023

Furnari, F. B., Fenton, T., Bachoo, R. M., Mukasa, A., Stommel, J. M., Stegh, A., et al. (2007). Malignant astrocytic glioma: genetics, biology, and paths to treatment. *Genes Dev.* 21, 2683–2710. doi: 10.1101/gad.1596707

Hu, Y., Chen, X., Whitesides, G. M., Vlassak, J. J., and Suo, Z. (2011). Indentation of polydimethylsiloxane submerged in organic solvents. *J. Mater. Res.* 26, 785–795. doi: 10.1557/jmr.2010.35

Hu, Y., Zhao, X., Vlassak, J. J., and Suo, Z. (2010). Using indentation to characterize the poroelasticity of gels. *Appl. Phys. Lett.* 96, 121904. doi: 10.1063/1.3370354

Itano, N., and Kimata, K. (2008). Altered hyaluronan biosynthesis in cancer progression. *Semin. Cancer Biol.* 18, 268–274. doi: 10.1016/j.semcancer.2008.03.006

Itano, N., Sawai, T., Atsumi, F., Miyaishi, O., Taniguchi, S. I., Kannagi, R., et al. (2004). Selective expression and functional characteristics of three mammalian hyaluronan synthases in oncogenic malignant transformation. *J. Biol. Chem.* 279, 18679–18687. doi: 10.1074/jbc.M313178200

Jackson, C., Ruzevick, J., Phallen, J., Belcaid, Z., and Lim, M. (2011). Challenges in immunotherapy presented by the glioblastoma multiforme microenvironment. *Clin. Dev. Immunol.* 2011:732413. doi: 10.1155/2011/732413

Jain, A., Betancur, M., Patel, G. D., Valmikinathan, C. M., Mukhatyar, V. J., Vakharia, A., et al. (2014). Guiding intracortical brain tumour cells to an extracortical cytotoxic hydrogel using aligned polymeric nanofibres. *Nat. Mater.* 13, 308–316. doi: 10.1038/nmat3878

Johnson, D. R., and O'neill, B. P. (2012). Glioblastoma survival in the United States before and during the temozolomide era. *J. Neurooncol.* 107, 359–364. doi: 10.1007/s11060-011-0749-4

Junttila, M. R., and de Sauvage, F. J. (2013). Influence of tumour microenvironment heterogeneity on therapeutic response. *Nature* 501, 346–354. doi: 10.1038/nature12626

Khaldoyanidi, S. K., Goncharova, V., Mueller, B., and Schraufstatter, I. U. (2014). Hyaluronan in the healthy and malignant hematopoietic microenvironment. *Adv. Cancer Res.* 123, 149–189. doi: 10.1016/B978-0-12-800092-2.00006-X

Kim, Y., and Kumar, S. (2014). "The Role of Hyaluronic Acid and its Receptors in the Growth and Invasion of Brain Tumors," in *Tumors of the Central Nervous System, Vol. 13, Types of Tumors, Diagnosis, Ultrasonography, Surgery, Brain Metastasis, and General CNS Diseases,* ed M. A. Hayat (Dordrecht: Springer), 253–266.

Klocker, J., Sabitzer, H., Raunik, W., Wieser, S., and Schumer, J. (1998). Hyaluronidase as additive to induction chemotherapy in advanced squamous cell carcinoma of the head and neck. *Cancer Lett.* 131, 113–115. doi: 10.1016/S0304-3835(98)00207-9

Koyama, H., Hibi, T., Isogai, Z., Yoneda, M., Fujimori, M., Amano, J., et al. (2007). Hyperproduction of hyaluronan in neu-induced mammary tumor accelerates angiogenesis through stromal cell recruitment: possible involvement of versican/pg-m. *Am. J. Pathol.* 170, 1086–1099. doi: 10.2353/ajpath.2007.060793

Lam, J., Truong, N. F., and Segura, T. (2014). Design of cell-matrix interactions in hyaluronic acid hydrogel scaffolds. *Acta Biomater.* 10, 1571–1580. doi: 10.1016/j.actbio.2013.07.025

Lathia, J. D., Mack, S. C., Mulkearns-Hubert, E. E., Valentim, C. L., and Rich, J. N. (2015). Cancer stem cells in glioblastoma. *Genes Dev.* 29, 1203–1217. doi: 10.1101/gad.261982.115

Lee, W. Y., Tsai, H. W., Chiang, J. H., Hwang, S. M., Chen, D. Y., Hsu, L. W., et al. (2011). Core–shell cell bodies composed of human cbMSCs and HUVECs for functional vasculogenesis. *Biomaterials* 32, 8446–8455. doi: 10.1016/j.biomaterials.2011.07.061

Li, Y., Li, L., Brown, T. J., and Heldin, P. (2007). Silencing of hyaluronan synthase 2 suppresses the malignant phenotype of invasive breast cancer cells. *Int. J. Cancer* 120, 2557–2567. doi: 10.1002/ijc.22550

Lokeshwar, V. B., Cerwinka, W. H., and Lokeshwar, B. L. (2005). HYAL1 hyaluronidase: a molecular determinant of bladder tumor growth and invasion. *Cancer Res.* 65, 2243–2250. doi: 10.1158/0008-5472.CAN-04-2805

Lokeshwar, V. B., Lokeshwar, B. L., Pham, H. T., and Block, N. L. (1996). Association of elevated levels of hyaluronidase, a matrix-degrading enzyme, with prostate cancer progression. *Cancer Res.* 56, 651–657.

Madan, A. K., Yu, K., Dhurandhar, N., Cullinane, C., Pang, Y., and Beech, D. J. (1999). Association of hyaluronidase and breast adenocarcinoma invasiveness. *Oncol. Rep.* 6, 607–609. doi: 10.3892/or.6.3.607

Mahadik, B. P., Pedron Haba, S., Skertich, L. J., and Harley, B. A. (2015). The use of covalently immobilized stem cell factor to selectively affect hematopoietic stem cell activity within a gelatin hydrogel. *Biomaterials* 67, 297–307. doi: 10.1016/j.biomaterials.2015.07.042

Mehta, A. I., Linninger, A., Lesniak, M. S., and Engelhard, H. H. (2015). Current status of intratumoral therapy for glioblastoma. *J. Neurooncol.* 125, 1–7. doi: 10.1007/s11060-015-1875-1

Misra, S., Heldin, P., Hascall, V. C., Karamanos, N. K., Skandalis, S. S., Markwald, R. R., et al. (2011). Hyaluronan-CD44 interactions as potential targets for cancer therapy. *FEBS J.* 278, 1429–1443. doi: 10.1111/j.1742-4658.2011.08071.x

Misra, S., Toole, B. P., and Ghatak, S. (2006). Hyaluronan constitutively regulates activation of multiple receptor tyrosine kinases in epithelial and carcinoma cells. *J. Biol. Chem.* 281, 34936–34941. doi: 10.1074/jbc.C600138200

Monslow, J., Govindaraju, P., and Puré, E. (2015). Hyaluronan – a functional and structural sweet spot in the tissue microenvironment. *Front. Immunol.* 6:231. doi: 10.3389/fimmu.2015.00231

Mueller, B. M., Schraufstatter, I. U., Goncharova, V., Povaliy, T., Discipio, R., and Khaldoyanidi, S. K. (2010). Hyaluronan inhibits postchemotherapy tumor regrowth in a colon carcinoma xenograft model. *Mol. Cancer Ther.* 9, 3024–3032. doi: 10.1158/1535-7163.MCT-10-0529

Nagy, N., Kuipers, H. F., Frymoyer, A. R., Ishak, H. D., Bollyky, J. B., Wight, T. N., et al. (2015). 4-Methylumbelliferone treatment and hyaluronan inhibition as a therapeutic strategy in inflammation, autoimmunity, and cancer. *Front. Immunol.* 6:123. doi: 10.3389/fimmu.2015.00123

Nakada, M., Nakada, S., Demuth, T., Tran, N. L., Hoelzinger, D. B., and Berens, M. E. (2007). Molecular targets of glioma invasion. *Cell. Mol. Life Sci.* 64, 458–478. doi: 10.1007/s00018-007-6342-5

Nakamura, T., Funahashi, M., Takagaki, K., Munakata, H., Tanaka, K., Saito, Y., et al. (1997). Effect of 4-methylumbelliferone on cell-free synthesis of hyaluronic acid. *Biochem. Mol. Biol. Int.* 43, 263–268. doi: 10.1080/15216549700204041

Ngo, M., and Harley, B. (2018). Perivascular signals alter global genomic profile of glioblastoma and response to temozolomide in a gelatin hydrogel. *bioRxiv*. doi: 10.1101/273763

Park, J. B., Kwak, H. J., and Lee, S. H. (2008). Role of hyaluronan in glioma invasion. *Cell Adh. Migr.* 2, 202–207. doi: 10.4161/cam.2.3.6320

Paw, I., Carpenter, R. C., Watabe, K., Debinski, W., and Lo, H. W. (2015). Mechanisms regulating glioma invasion. *Cancer Lett.* 362, 1–7. doi: 10.1016/j.canlet.2015.03.015

Pedron, S., Becka, E., and Harley, B. A. (2015). Spatially-gradated hydrogel platform as a three-dimensional engineered tumor microenvironment. *Adv. Mater.* 27, 1567–1572. doi: 10.1002/adma.201404896

Pedron, S., Becka, E., and Harley, B. A. (2013). Regulation of glioma cell phenotype in 3D matrices by hyaluronic acid. *Biomaterials* 34, 7408–7417. doi: 10.1016/j.biomaterials.2013.06.024

Pedron, S., Hanselman, J. S., Schroeder, M. A., Sarkaria, J. N., and Harley, B. A. (2017a). Extracellular hyaluronic acid influences the efficacy of EGFR tyrosine kinase inhibitors in a biomaterial model of glioblastoma. *Adv. Healthc. Mater.* 6:1700529. doi: 10.1002/adhm.201700529

Pedron, S., Polishetty, H., Pritchard, A. M., Mahadik, B. P., Sarkaria, J. N., and Harley, B. A. (2017b). Spatially-graded hydrogels for preclinical testing of glioblastoma anticancer therapeutics. *MRS Commun* 7, 442–449. doi: 10.1557/mrc.2017.85

Quirico-Santos, T., Fonseca, C. O., and Lagrota-Candido, J. (2010). Brain sweet brain: importance of sugars for the cerebral microenvironment and tumor development. *Arq. Neuropsiquiatr.* 68, 799–803. doi: 10.1590/S0004-282X2010000500024

Rankin, K. S., and Frankel, D. (2016). Hyaluronan in cancer-from the naked mole rat to nanoparticle therapy. *Soft Matter* 12, 3841–3848. doi: 10.1039/C6SM00513F

Rape, A., Ananthanarayanan, B., and Kumar, S. (2014). Engineering strategies to mimic the glioblastoma microenvironment. *Adv. Drug Deliv. Rev.* 79–80, 172–183. doi: 10.1016/j.addr.2014.08.012

Sarkaria, J. N., Carlson, B. L., Schroeder, M. A., Grogan, P., Brown, P. D., Giannini, C., et al. (2006). Use of an orthotopic xenograft model for assessing the effect of epidermal growth factor receptor amplification on glioblastoma radiation response. *Clin. Cancer Res.* 12, 2264–2271. doi: 10.1158/1078-0432.CCR-05-2510

Sarkaria, J. N., Yang, L., Grogan, P. T., Kitange, G. J., Carlson, B. L., Schroeder, M. A., et al. (2007). Identification of molecular characteristics

correlated with glioblastoma sensitivity to EGFR kinase inhibition through use of an intracranial xenograft test panel. *Mol. Cancer Ther.* 6, 1167–1174. doi: 10.1158/1535-7163.MCT-06-0691

Sivakumar, H., Strowd, R., and Skardal, A. (2017). Exploration of dynamic elastic modulus changes on glioblastoma cell populations with aberrant egfr expression as a potential therapeutic intervention using a tunable hyaluronic acid hydrogel platform. *Gels* 3:28. doi: 10.3390/gels3030028

Stern, R. (2008). Hyaluronidases in cancer biology. *Semin. Cancer Biol.* 18, 275–280. doi: 10.1016/j.semcancer.2008.03.017

Stupp, R., Mason, W. P., Van Den Bent, M. J., Weller, M., Fisher, B., Taphoorn, M. J. B., et al. (2005). Radiotherapy plus concomitant and adjuvant temozolomide for glioblastoma. *New Engl. J. Med.* 352, 987–996. doi: 10.1056/NEJMoa043330

Syková, E. (2002). "Plasticity of Extracellular Space," in *The Neuronal Environment: Brain Homeostasis in Health and Disease*, ed W. Walz (Totowa, NJ: Humana Press), 57–81.

Tofuku, K., Yokouchi, M., Murayama, T., Minami, S., and Komiya, S. (2006). HAS3-related hyaluronan enhances biological activities necessary for metastasis of osteosarcoma cells. *Int. J. Oncol.* 29, 175–183. doi: 10.3892/ijo.29.1.175

Toole, B. P. (2004). Hyaluronan: from extracellular glue to pericellular cue. *Nat. Rev. Cancer* 4, 528–539. doi: 10.1038/nrc1391

Toole, B. P., Ghatak, S., and Misra, S. (2008). Hyaluronan oligosaccharides as a potential anticancer therapeutic. *Curr. Pharm. Biotechnol.* 9, 249–252. doi: 10.2174/138920108785161569

Umesh, V., Rape, A. D., Ulrich, T. A., and Kumar, S. (2014). Microenvironmental stiffness enhances glioma cell proliferation by stimulating epidermal growth factor receptor signaling. *PLoS ONE* 9:e101771. doi: 10.1371/journal.pone.0101771

Wang, C., Tong, X., and Yang, F. (2014). Bioengineered 3D brain tumor model to elucidate the effects of matrix stiffness on glioblastoma cell behavior using peg-based hydrogels. *Mol. Pharm.* 11, 2115–2125. doi: 10.1021/mp5000828

Wen, P. Y., and Kesari, S. (2008). Malignant gliomas in adults. *N. Engl. J. Med.* 359, 492–507. doi: 10.1056/NEJMra0708126

West, D. C., Hampson, I. N., Arnold, F., and Kumar, S. (1985). Angiogenesis induced by degradation products of hyaluronic acid. *Science* 228, 1324–1326. doi: 10.1126/science.2408340

Wiranowska, M. R., and Rojiani, M. V. (2011). *Extracellular Matrix Microenvironment in Glioma Progression.* INTECH Open Access Publisher

Xie, Q., Mittal, S., and Berens, M. E. (2014). Targeting adaptive glioblastoma: an overview of proliferation and invasion. *Neuro-oncology* 16, 1575–1584. doi: 10.1093/neuonc/nou147

Zhao, Y. F., Qiao, S. P., Shi, S. L., Yao, L. F., Hou, X. L., Li, C. F., et al. (2017). Modulating three-dimensional microenvironment with hyaluronan of different molecular weights alters breast cancer cell invasion behavior. *ACS Appl. Mater. Interfaces* 9, 9327–9338. doi: 10.1021/acsami.6b15187

Conflict of Interest Statement: The authors declare that the research was conducted in the absence of any commercial or financial relationships that could be construed as a potential conflict of interest.

frontiers in Bioengineering and Biotechnology

PERSPECTIVE
published: 11 July 2018
doi: 10.3389/fbioe.2018.00092

Characterizing Glioblastoma Heterogeneity via Single-Cell Receptor Quantification

Si Chen[1], *Thien Le*[2], *Brendan A. C. Harley*[3,4] *and P. I. Imoukhuede*[1,4,5]*

[1] Department of Bioengineering, University of Illinois at Urbana–Champaign, Champaign, IL, United States, [2] Department of Mathematics and Department of Computer Science, University of Illinois at Urbana–Champaign, Champaign, IL, United States, [3] Department of Chemical and Biomolecular Engineering, University of Illinois at Urbana–Champaign, Urbana, IL, United States, [4] Carl R. Woese Institute for Genomic Biology, University of Illinois at Urbana Champaign, Urbana, IL, United States, [5] Department of Biomedical Engineering, Washington University, St. Louis, MO, United States

Dysregulation of tyrosine kinase receptor (RTK) signaling pathways play important roles in glioblastoma (GBM). However, therapies targeting these signaling pathways have not been successful, partially because of drug resistance. Increasing evidence suggests that tumor heterogeneity, more specifically, GBM-associated stem and endothelial cell heterogeneity, may contribute to drug resistance. In this perspective article, we introduce a high-throughput, quantitative approach to profile plasma membrane RTKs on single cells. First, we review the roles of RTKs in cancer. Then, we discuss the sources of cell heterogeneity in GBM, providing context to the key cells directing resistance to drugs. Finally, we present our provisionally patented qFlow cytometry approach, and report results of a "proof of concept" patient-derived xenograft GBM study.

Keywords: single-cell, glioblastoma, RTK, heterogeneity, VEGFR, EGFR, IGFR, stem cell

OPEN ACCESS

Edited by:
Paul De Vos,
University Medical Center Groningen, Netherlands

Reviewed by:
Alessandro Poggi,
Dipartimento delle Terapie Oncologiche Integrate, Ospedale Policlinico San Martino, Italy
Cristiana Tanase,
Victor Babes National Institute of Pathology, Romania

***Correspondence:**
P. I. Imoukhuede
pimoukhuede@wustl.edu

Specialty section:
This article was submitted to Biomaterials, a section of the journal Frontiers in Bioengineering and Biotechnology

Received: *13 March 2018*
Accepted: *21 June 2018*
Published: *11 July 2018*

Citation:
Chen S, Le T, Harley BAC and Imoukhuede PI (2018) Characterizing Glioblastoma Heterogeneity via Single-Cell Receptor Quantification. Front. Bioeng. Biotechnol. 6:92. doi: 10.3389/fbioe.2018.00092

INTRODUCTION

GBMs are the most frequent and lethal malignant primary adult brain tumor (Yadav et al., 2018), which presents a critical need to develop new therapeutics. Addressing the dysregulation of RTK signaling pathways offers promise in overcoming GBM lethality (Hawkins-Daarud et al., 2013; Cloughesy et al., 2014; Smith et al., 2016; Massey et al., 2018). RTK dysfunction has been observed in GBM, where these pathways are correlated with tumor cell proliferation (Johnson et al., 2012; Furnari et al., 2015), angiogenesis (Plate et al., 1994; Kuczynski et al., 2011), tumor invasiveness (Giannini et al., 2005; Sangar et al., 2014), and resistance to therapy (Murat et al., 2008; Lu and Bergers, 2013; Popescu et al., 2015). Moreover, these pathways are popular targets for small-molecule inhibitors (Rich and Bigner, 2004; Candolfi et al., 2011). Unfortunately, the clinical benefit of these targeted therapies is limited by drug resistance (De Witt Hamer, 2010; Szopa et al., 2017).

Increasing evidence suggests that drug resistance may be attributed to tumor heterogeneity (variations within an individual tumor) (Saunders et al., 2012; Furnari et al., 2015; Qazi et al., 2017). For example, a landmark study identified tumor subpopulations resistant to therapy prior to treatment by sequencing 4,645 single cells from 19 melanoma patients. This thorough analysis was enabled by single-cell technology, and may have been overlooked with ensemble sequencing (Tirosh et al., 2016). Additionally, a single-cell analysis of patient-derived xenografts (PDXs) of GBM39 also found higher heterogeneity in resistant tumors than in responsive tumors (Shi et al., 2012). In line with these single-cell measurements, we previously discovered, measured,

and statistically described heterogeneity in breast cancer xenografts by quantifying vascular endothelial growth factor plasma membrane receptor (VEGFR) concentrations at the single-cell level (Imoukhuede and Popel, 2014). When we combined this quantitative analysis with computational modeling, we arrived at the prediction that tumors having "high" concentrations of plasma membrane VEGFR1 could be resistant to anti-VEGF drugs (angiogenesis inhibitors) (Weddell and Imoukhuede, 2014). Clinical work supports this prediction for colorectal cancer (Weickhardt et al., 2015), and application of this quantification and prediction should offer a new paradigm for biomarker discovery in cancer medicine.

To address the need for quantitative, single-cell analysis of GBM heterogeneity, we apply our optimized and provisionally patented VEGFR quantitative flow (qFlow) cytometry approach to GBM (Imoukhuede and Popel, 2011, 2014; Imoukhuede et al., 2013; Weddell and Imoukhuede, 2014; Chen et al., 2015, 2017; Imoukhuede and Chen, 2018). We describe expanded measurement to several RTKs critical to tumor development. To provide further context we, briefly, review the roles of RTKs in cancer and present connections between RTK heterogeneity and drug resistance. We then present our approach, qFlow cytometry, and report promising findings of a "proof of concept" PDX GBM study.

ROLES OF RTKS IN CANCER

RTKs are widely expressed transmembrane proteins (Cadena and Gill, 1992; Ferrara et al., 2003). Upon ligand binding, they are activated via canonical (Mac Gabhann and Popel, 2007; Sarabipour and Hristova, 2016) and non-canonical (Steinkamp et al., 2014; Chen et al., 2015; Pennock et al., 2016; Mamer et al., 2017) ligand-induced dimerization and tyrosine phosphorylation mechanisms. Importantly, unligated receptors can dimerize (Ruch et al., 2007; Chung et al., 2010; Low-Nam et al., 2011; Lin et al., 2012; Comps-Agrar et al., 2015; King et al., 2016; Sarabipour and Hristova, 2016; Sarabipour et al., 2016) and signal (Wu et al., 2010; Sarabipour et al., 2016; Kazlauskas, 2017), although ligand binding stabilizes the dimeric receptor structure. These receptor-initiated signaling events regulate cell survival, proliferation, differentiation, and motility (Hubbard and Miller, 2007; Volinsky and Kholodenko, 2013).

VEGFRs are upregulated in many cancers (Ferrara, 2002; Kut et al., 2007; Mac Gabhann and Popel, 2008). Signals through endothelial VEGFRs and the neuropilin (NRP) co-receptors (Imoukhuede and Popel, 2011, 2012, 2014; Imoukhuede et al., 2013; Gelfand et al., 2014) induce the sprouting angiogenic hallmarks of cell proliferation and cell migration (Simons et al., 2016). These sprouting angiogenesis hallmarks also sustain tumor growth and enable tumor metastasis (Hanahan and Weinberg, 2011; Shibuya, 2014). VEGF and other pro-angiogenic factors, may also regulate vascular growth and regression in tumors that co-opt pre-existing blood vessels (Holash et al., 1999; Jayson et al., 2016; Kuczynski et al., 2016).

In addition to these canonical pathways, cross-family signaling may also affect tumor vascularization. In this paradigm, ligands from one growth factor family bind to and signal through receptor(s) of another family. For instance, we have shown VEGF-mediated downregulation of PDGFRs (Chen et al., 2015), and discovered that both VEGF–PDGFR binding and PDGF–VEGFR binding is high affinity (Mamer et al., 2017). Other cross-family studies have identified VEGF–PDGFR binding and signaling (Ball et al., 2007; Pennock et al., 2016) and VEGFR–PDGFR dimerization in tumor associated pericytes (Greenberg et al., 2008). Altogether, these canonical and cross-family RTK mechanisms suggest several possible receptor activation landscapes that can contribute to tumor growth and drug resistance.

GBM-ASSOCIATED CELL HETEROGENEITY: STEM AND ENDOTHELIAL

An accepted origin of tumor heterogeneity involves clonal evolution; an reiterative process of genetic mutation, clonal selection, and expansion, which drives the growth of single cancer cells into heterogeneous tumor masses (Greaves and Maley, 2012; Greaves, 2015; McGranahan and Swanton, 2017). In addition to cancer cells, other cell types within the tumor may also differentiate or transition as tumor develops. Some such cells include: tumor-associated fibroblasts, macrophages/monocytes, endothelial cells (ECs), and stem cells (Saunders et al., 2012). Here, we describe glioblastoma stem cells (GSCs) and ECs, which we focus on in our pilot study.

GSCs are an important tumor cell component, because despite their small number (∼0.5–10%) (Pallini et al., 2011), GSCs are more resistant to radiotherapy and chemotherapy than other cancer cells (Schonberg et al., 2014; Seymour et al., 2015). Furthermore, their resistance can amplify tumor heterogeneity, because they have self-renewing and tumor-initiating capabilities (Lathia et al., 2015). GSCs are often identified by CD133 (Mak et al., 2011), which is associated with poor prognosis in a number of tumor types. There is controversy surrounding the usage of CD133 as a GSC marker (Golebiewska et al., 2013; Seymour et al., 2015; Bradshaw et al., 2016). Early studies showed a subpopulation of GBM cells expressing CD133 were able to form tumors (Singh et al., 2004) and further studies showed subpopulations of $CD133^-$ cells were also able to form tumors *in vivo* (Beier et al., 2007). While these studies do not negate the possible role of CD133 in identifying GSCs, they do highlight the importance of heterogeneity and the need for additional markers. Therefore, establishing a "barcode" of RTK plasma membrane concentrations on GSCs may help to identify novel markers, aiding in the isolation and understanding of these stem cells.

ECs, the primary structural unit of the vasculature, are an important contributor to GBM development. Unlike normal vessels, tumor vasculature is leaky, tortuous, and dilated (Jain, 2005; Aird, 2009). In addition to typical tumor vascular pathological features, brain tumor vasculature exhibits the loss of the important blood-brain-barrier feature of tight EC-EC junctions when tumor size grows beyond 1–2 mm in diameter

(Jain et al., 2007). The close interaction between tumors and tumor vessels, and the observation of extensive EC heterogeneity supports the need for profiling tumor-associated ECs.

A PARADIGM SHIFT IN SINGLE-CELL TECHNOLOGIES: FROM GENE-CENTRIC TO PROTEOMICS

Studies characterizing GBM heterogeneity primarily focus on genetic and transcriptomic profiling (Verhaak et al., 2010; Snuderl et al., 2011; Dunn et al., 2012; Szerlip et al., 2012; Brennan et al., 2013; Patel et al., 2014; Ellis et al., 2015), which does not always correlate with functional changes (Simonson and Schnitzer, 2007; Feng et al., 2009; Taniguchi et al., 2010). Moreover, multiple studies show discordance between sequence data and protein expression in GBM, particularly with regards to epidermal growth factor receptor (EGFR) (Brennan et al., 2009) and PDGFR (Hermanson et al., 1992) gene vs. protein expression. Because proteins are the effectors of signaling toward functional response (Grecco et al., 2011; Imoukhuede et al., 2013; Chen et al., 2017), there is a need for increased protein-based, functional measurements.

qFlow cytometry offers a powerful tool for protein-based, single-cell measurements. It applies fluorescent calibration to traditional flow cytometry, converting signal to absolute protein concentrations (Lyer et al., 1997; Lee-Montiel and Imoukhuede, 2013; Chen et al., 2017). Absolute protein quantification allows detection of variations in proteins across published studies, tissues, replicates, and instrument settings (Wheeless et al., 1989; Rocha-Martins et al., 2012; Baumgartner et al., 2013; Nguyen et al., 2013; Vigelsø et al., 2015). Moreover, qFlow cytometry advances systems biology, providing the quantitative data needed for computational studies (Chen et al., 2014; Weddell and Imoukhuede, 2018). For example, using qFlow cytometry coupled with systems biology, we predicted that anti-VEGF efficacy depends on tumor endothelial VEGFR1 plasma membrane concentrations (Weddell and Imoukhuede, 2014). Furthermore, a receptor-internalization computational model recently predicted that small increases in plasma membrane RTK concentrations (<1,000 receptors/cell) may double nuclear-based RTK signaling (Weddell and Imoukhuede, 2017), which further implicates RTK concentrations as a determinant of signal transduction. These predictions were only possible with the accurate experimental data offered by qFlow cytometry.

A NEW APPROACH FOR EXAMINING GBM HETEROGENEITY

We performed a "proof of concept" qFlow cytometry study on a PDX, GBM39 (**Figure 1**). GBM39 is known for $EGFR^{vIII}$ and low invasiveness, *in vivo* (Johnson et al., 2012; Wei et al., 2016). The xenograft was established with tumor tissue from patients undergoing surgical treatment at Mayo Clinic, Rochester, MN. Multiple studies characterize these PDX models and report maintenance of patient morphologic and molecular characteristics including EGFR amplification as well as tumor invasiveness (Giannini et al., 2005; Sarkaria et al., 2007).

Following dissociation, PDX cells were stained with Sytox Blue (a live/dead cell stain), CD45 (Patenaude et al., 2010), CD34 (Soares et al., 2007; Moghadam et al., 2015), and CD133 (Singh et al., 2004; Calabrese et al., 2007; Molina et al., 2014; Naujokat, 2014; Soeda et al., 2015) fluorophore-conjugated antibodies that target EC-like cells and GSCs, respectively (**Figure 1**). This labeling scheme excludes both dead cells and hematopoietic cells and enables identification of human tumor EC-like cells ($hCD34^+$), mouse tumor EC-like cells ($mCD34^+$), and GSCs ($hCD133^+$) from the live $CD45^-$ pool (**Figure 2A**). To obtain reliable data, we obtained fluorescence signals from 2 to 3 samples/RTK with 10,000–35,000 live single cells collected per sample. As expected, the bulk GBM39 PDX sample was primarily non-EC, non-GSC cells (62.46%). In addition, we found 6-fold higher mouse tumor EC-like cells than human tumor EC-like cells (**Figure 2B**). This quantification aligned with prior studies of GBM xenograft showing ∼7.1% EC population ($CD45^-CD31^+CD34^+$). Consistent with our quantification of GSCs, a primary human study of 37 patients reported a range of 0.5–10% (Pallini et al., 2011), when identifying GSCs using the CD133 marker.

We labeled and screened 9 plasma membrane RTKs on these cells, which included two established GBM biomarkers, EGFR and insulin-like growth factor receptor (IGFR) (Sangar et al., 2014), and angiogenic signaling biomarkers: VEGFRs, PDGFRs, NRP1, and Tie2 (Carmeliet and Jain, 2000, 2011; Ferrara, 2002; Ferrara and Kerbel, 2005; Dudley, 2012). Using qFlow cytometry and statistical models, we quantitatively characterized GBM39 PDX via four patented metrics (**Figure 1**): cell composition, ensemble RTK concentration, cell-by-cell analysis with Gaussian mixture modeling, and heterogeneity analysis (Imoukhuede and Chen, 2018).

Percentage of gated cell populations were exported using FlowJo software (TreeStar). Ensemble RTK concentrations and cell-by-cell analysis were performed as previously described (Chen et al., 2015, 2017). We then applied Gaussian mixture modeling to identify log-normal sub-populations within each distribution, described by its mean, standard deviation, and density. We reduced the chance of overfitting the subpopulations by using Bayesian Information Criterion (BIC) (Raftery, 1995; Huedo-Medina et al., 2006). A detailed description of heterogeneity quantification is provided in section Quantification of Cell-RTK Heterogeneity.

Human Tumor EC-Like Cells Have High EGFR and IGFR on Plasma Membrane

EGFR and IGFR are expressed on tumor cells and contribute to tumor progression. Interestingly, the human tumor EC-like population had high plasma membrane EGFR and IGFR concentrations (∼21,000/cell and ∼20,000/cell, respectively) (**Figure 2C**), consistent with qualitative findings of higher EGFR on breast carcinoma-derived ECs compared to normal ECs (Amin et al., 2006). Our results of high EGFR on human tumor

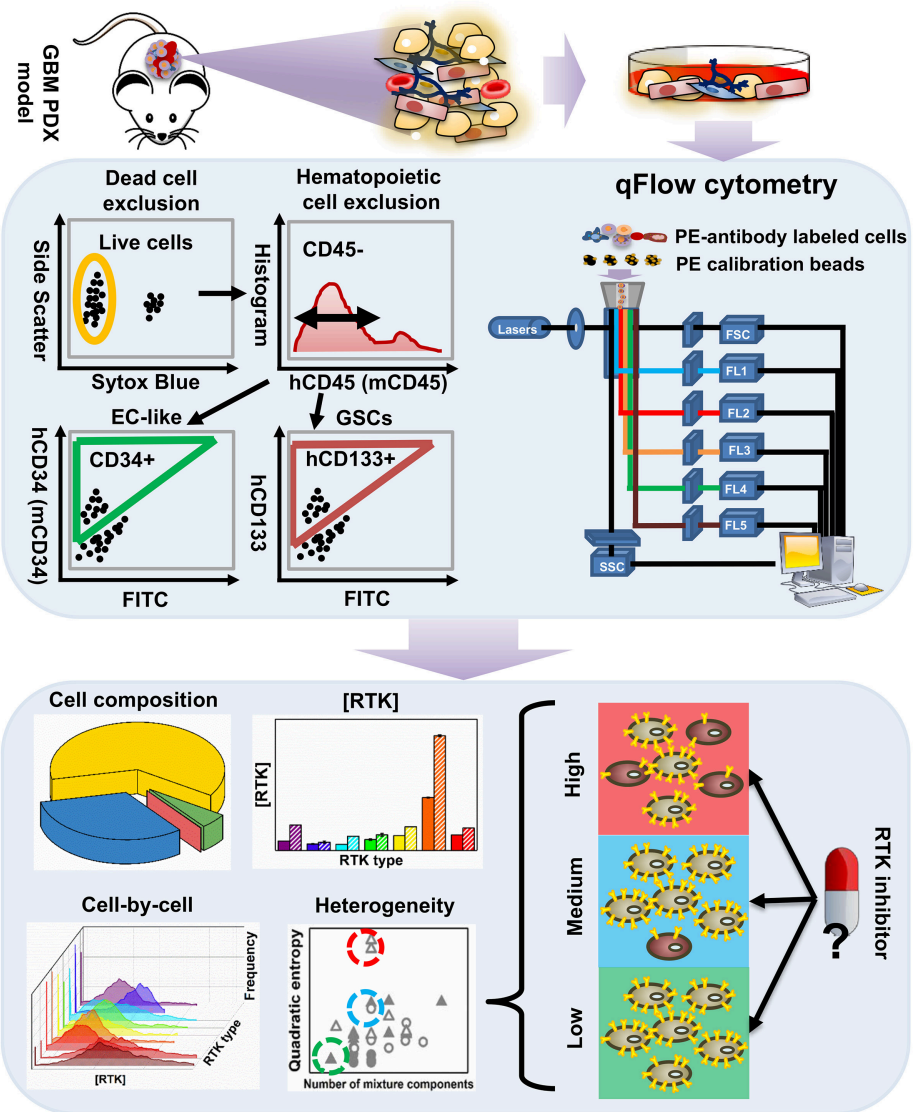

FIGURE 1 | An overview of the workflow for characterizing tumor heterogeneity in GBM39 PDX samples. The GBM39 PDX is established with tumor tissue from patients at Mayo Clinic, Rochester, MN. Following dissociation, multi-channel flow cytometer is used to characterize PDX cells. Briefly, dead cells are excluded using a live/dead cell stain, and hematopoietic cells are excluded using the CD45 antigen, then the endothelial marker CD34 and CD133 can be used to identify EC-like cells and GSCs respectively from the $CD45^{-}$ pool. Percentage of GSCs, EC-like cells and other PDX cells within all live cells can be exported from the flow cytometer. Cells are also stained with phycoerythrin (PE)-conjugated antibodies targeting one of the 9 plasma membrane RTKs: established GBM biomarkers, EGFR and IGFR, and those within the angiogenic signaling networks, VEGFRs, PDGFRs, NRP1, and Tie2. qFlow cytometry is performed as described previously, and ensemble averaged plasma membrane RTK concentrations and cell-by-cell RTK distributions can be obtained (Imoukhuede and Popel, 2011; Chen et al., 2015, 2017). We use two parameters to quantify RTK heterogeneity across EC-like and non EC-like cells: number of mixture components and Quadratic entropy of the cell-by-cell RTK distribution. Bayesian Information Criterion (BIC)-guided Gaussian mixture modeling is used to select the best number of mixture components existed in a larger cell population based on their RTK concentration. Alternatively, Quadratic entropy sums the weighted differences of the means between two bins from 500 equally distributed bins from each cell-by-cell distribution. We envision that characterizing RTK heterogeneity may help understand why RTK inhibitors have not been efficient in treating GBMs.

EC-like cells from GBM39 is also consistent with results of clinical GBM samples (Soda et al., 2011).

The mixture modeling revealed that 8% of human tumor EC-like subpopulations had a ~12-fold higher membrane localization of EGFRs than average. We found a similar pattern for IGFRs in human tumor EC-like subpopulations. Together, the ensemble-averaged data and the mixture modeling indicated significant plasma membrane localization of EGFR and IGFR on human tumor EC-like cells. High concentrations of EGFR and IGFR suggest an opportunity for targeted inhibition, which could be a mechanism for disrupting tumor vessels on GBMs with a similar profile.

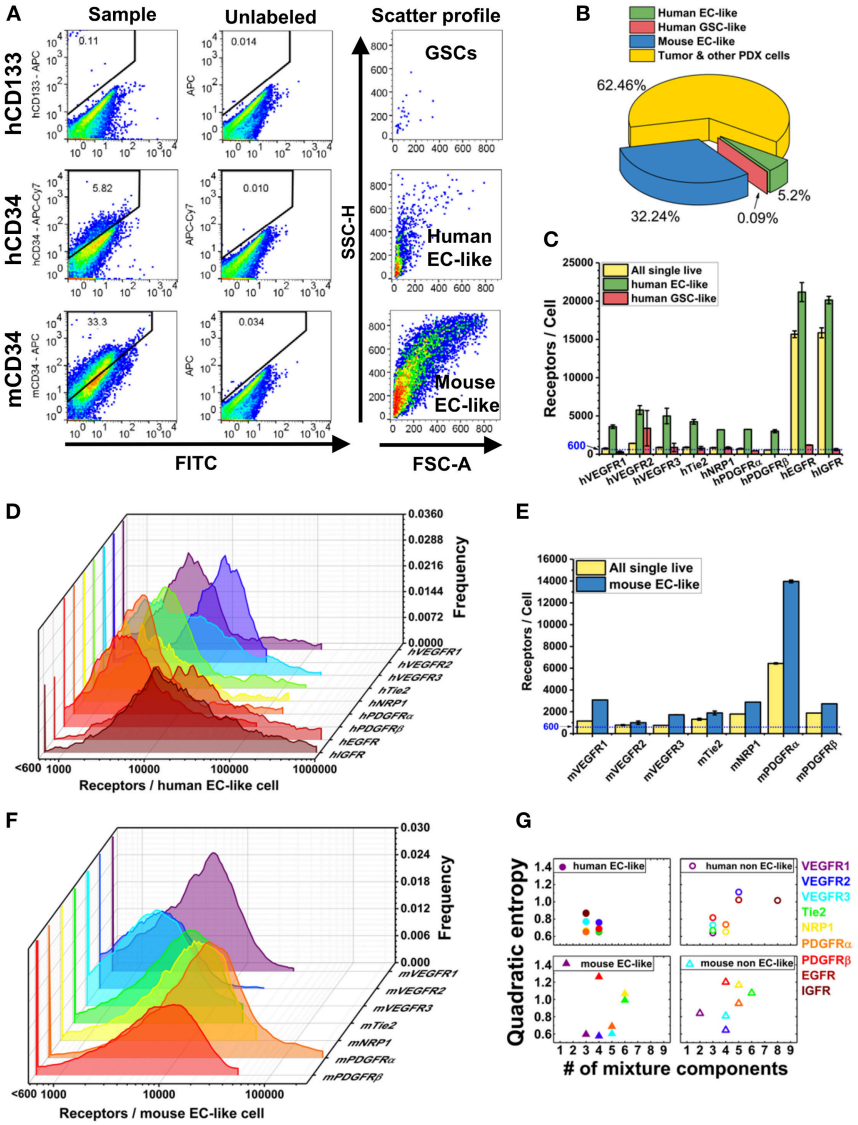

FIGURE 2 | Characterization of plasma membrane RTK concentrations and tumor heterogeneity in GBM39 PDX sample using a LSR Fortessa flow cytometer (BD). We obtain fluorescence signal from 2 to 3 sample tubes for each RTK with 10,000–35,000 live single cells per sample tube. BD FACSDIVA software was used for data acquisition, and FlowJo (TreeStar) software was used for data analysis. **(A)** Representative flow cytometry plots for gating GSCs (hCD45-hCD133+), human EC-like cells (hCD45-hCD34+), and mouse EC-like cells (mCD45-mCD34+) from live cell population. **(B)** Percentage of GSCs, human EC-like, mouse EC-like, and tumor & other PDX cells in the GBM39 PDX sample. **(C)** Ensemble-averaged concentrations and **(D)** cell-by-cell distributions of plasma membrane VEGFRs, Tie2, NRP1, PDGFRs, EGFR, and IGFR on human EC-like cells. **(E)** Ensemble-averaged concentrations and **(F)** cell-by-cell distributions of plasma membrane VEGFRs, Tie2, NRP1, and PDGFRs on mouse EC-like cells. **(G)** Heterogeneity analysis of RTKs in EC-like and non EC-like cell populations. Number of mixture components estimates how many cell subpopulations there are having different plasma membrane RTK concentrations. Quadratic entropy represents the diversity of RTK concentrations within EC-like and non EC-like populations.

Mouse Tumor EC-Like Cells Have Similar Plasma Membrane VEGFR Concentrations as Healthy Mouse ECs From Skeletal Muscle

VEGFRs are key regulators of tumor angiogenesis, so their quantification can offer insight into the tumor vasculature. Furthermore, as biomarkers of vasculature, these receptors have been proposed as diagnostic biomarkers of anti-angiogenic drug efficacy (Lambrechts et al., 2013; Wehland et al., 2013) with computational (Weddell and Imoukhuede, 2014) and clinical (Weickhardt et al., 2015) support to their use. We found that VEGFR1 and VEGFR2 had similar concentrations and ratios on mouse tumor EC-like cells (∼3,100 VEGFR1/cell and ∼1,000 VEGFR2/cell) as on healthy ECs obtained from mouse skeletal muscle (Imoukhuede and Popel, 2012) (**Figure 2E**). This finding of a low VEGFR2:VEGFR1 ratio aligns with a previous study on breast cancer xenografts (Imoukhuede and Popel, 2014);

however, the receptor abundance we report here is much lower. These findings of EC-like cells from GBM39 having VEGFRs at levels similar to normal mouse skeletal muscle ECs suggests a need for further quantification of normal brain ECs VEGFR concentrations to establish tissue standards. Similarly, it suggests a need to examine other GBM specimens to identify whether this is a property of co-opted vessels or specific to this GBM strain.

We analyzed the human tumor EC-like population (5.20% of the population, **Figure 2B**), which should reflect the original tumor vessels from the patient (**Figure 2C**). We found similar plasma membrane VEGFR1 and VEGFR2 ratios (∼3,600 VEGFR1/cell & ∼5,800 VEGFR2/cell) as previous reports *in vitro* (Imoukhuede and Popel, 2011; Chen et al., 2015). However, these data show that not all tumors have the same concentrations or ratios of plasma membrane VEGFRs on their endothelium. Importantly, tumor EC-like cells display much greater heterogeneity than normal ECs with subpopulations that have high concentrations of VEGFRs. Indeed, cell-by-cell analysis and mixture modeling of human tumor EC-like cells reveals the existence of a high-VEGFR1 subpopulation (∼10%) with ∼41,000 VEGFR1/cell, while the highest VEGFR2 subpopulation is ∼18,500 VEGFR2/cell, comprising ∼35% of the total human tumor EC-like population (**Figures 2D,G**). The difference in VEGFR2:VEGFR1 ratio and receptor concentrations between human and mouse tumor EC-like population shows a significant level of endothelial heterogeneity. Such data may enable correlations between these tumor vessel regulators and anti-angiogenic drug efficacy.

Plasma Membrane PDGFRs Localize on Tumor EC-Like Cells

PDGFRs serve important roles in supporting vasculature in tumor microenvironments (Andrae et al., 2008). We observed lower levels of PDGFRs on human tumor EC-like cell membranes than on mouse (**Figures 2C,E**). The cell-by-cell analysis and mixture modeling suggests that this ensemble average does not capture the subpopulations having high-PDGFR plasma membrane localization: 66 and 16% of mouse tumor EC-like cell membrane had ∼23,400 PDGFRα and ∼19,800 PDGFRβ, respectively (**Figure 2F**). This significant heterogeneity may be attributed to the use of the CD34 marker to designate EC-like cells, because it is also found on stem cells/precursors, mast cells, and neurons (Nielsen and McNagny, 2008; Imoukhuede and Popel, 2014; AbuSamra et al., 2017). PDGFRα is also considered an important mesenchymal stem cell marker (Farahani and Xaymardan, 2015). So, the co-labeling of PDGFRα and CD34 suggests these cells may be mesenchymal stem cells (Aguirre et al., 2010).

If these $CD34^{+}PDGFR^{+}$ cells are endothelial, then our data correlates with studies finding PDGFRs on tumor ECs (Hermansson et al., 1988; Werner et al., 1990; Plate et al., 1992). PDGFR localization on ECs is controversial, because it is characteristic of mural cells and not of ECs (Heldin et al., 1981; Bowen-Pope and Ross, 1982; Kazlauskas and DiCorleto, 1985; Raines et al., 1991; Battegay et al., 1994; Marx et al., 1994). However, they have been observed on monolayer microvascular ECs, *in vitro* (Bar et al., 1989; Marx et al., 1994) and on angiogenic ECs that formed sprout and tubes *in vitro* (Battegay et al., 1994). If we subscribe to the canonical PDGFR localization understanding, then these tumor vessels induce "non-conventional" PDGFR localization patterns.

GSCs Have Little-To-No Surface EGFR or IGFR

Multiple studies suggest that a higher degree of GSC "stemness" is associated with *EGFR* amplification (Mazzoleni et al., 2010; Liffers et al., 2015); however, we observed ∼13-fold lower EGFRs on GSC plasma membranes compared to the bulk PDX cells (**Figure 2C**). This trend was also seen with IGFR (**Figure 2C**). The low membrane EGFR concentrations on GSCs is concerning, given reports that EGFR signaling is necessary for GSC proliferation and tumor-sphere formation (Soeda et al., 2008; Griffero et al., 2009). Yet, this may explain the lower percentage of GSCs in the PDX sample (∼0.9%) compared to the expected stem cell fraction (0.5–10%; Pallini et al., 2011). A possible explanation is that serially transplanted tumors can lose their EGFR overexpression, even *in vivo* (Liffers et al., 2015). Clearly, further investigation of both gene expression and protein quantification on other GBM PDX GSCs is necessary to understand their contribution to heterogeneity and drug-resistance.

Quantification of Cell-RTK Heterogeneity

To quantify heterogeneity of each cell subpopulation, we used two parameters: number of mixture components and Quadratic Entropy (QE). To quantitatively assess the number of subpopulations within each cell population, we fit each cell-by-cell RTK distribution with mixture models consisting of 1–9 log-normal Gaussian sub-distributions (mixture components); we then applied BIC as the criterion to select the mixture model with the lowest BIC. The number of mixture components is determined by how many log-normal Gaussian sub-distributions are in the mixture model. The number of mixture components, thus, is a measurement of cell heterogeneity. Generally, 1–2 mixture components are considered low heterogeneity (Chen et al., 2017), while more than two components is considered highly heterogeneous (Imoukhuede and Popel, 2014; Weddell and Imoukhuede, 2014).

Alternatively, QE requires equally spaced bins, here we chose 500 bins, from each cell-by-cell distribution (**Figures 2D,F**). QE then sums the weighted differences of the means between two bins (Rao, 1982; Pavoine and Dolédec, 2005; Zoltán, 2005). Thus, QE is a measurement of the increase in random variation in the cellular response. Because healthy ECs and human fibroblasts *in vitro* have shown QE within 0.2–0.7 (Chen et al., 2015), we describe QE < 0.7 as low heterogeneity and QE > 0.7 as high heterogeneity. QE provides a quantitative measure of the diversity of cellular phenotypes in cancer tissue sections for diagnostic applications (Potts et al., 2012) and drug discovery (Gough et al., 2014). Interestingly, human tumor EC-like cells showed lower QE and number of mixture components when compared to mouse tumor EC-like cells (**Figure 2G**). We suspect that the likely loss of human tumor-associated cells over time in

a PDX model (Chao et al., 2017) may be the reason why human tumor EC-like cells present a more homogenous state than the mouse tumor EC-like cells.

Clinical Implications of GBM Heterogeneity

We envision that RTK quantification can identify ideal receptor targets across the bulk tumor specimen and on specific cell populations in the tumor. First, the ideal receptor target would be highly available (Rich and Bigner, 2004; Weis and Cheresh, 2011; Cloughesy et al., 2014): it would have high concentrations on a high percentage of bulk cells or specific cells. Next, the target RTK would exhibit low heterogeneity: it would have low QE in bulk cells or on the specific cell subpopulation (Jain et al., 2009; Heath et al., 2016). An ideal receptor target would also be highly specific to the tumor, which would manifest as higher receptor concentrations in the tumor vs. healthy tissue (Rich and Bigner, 2004).

Based on these guidelines, we offer possible targets on GBM39. If the goal is targeting tumor vessels, then VEGFR2 and PDGFRα are highly targetable: >70% target cells have > 6,000 VEGFR2 or PDGFRα/cell plasma membrane with QE = 0.20 or 0.32, respectively. Furthermore, they are likely targets, because they are more highly expressed in GBM specimens than health tissue (Chen et al., 2015): ∼5-fold higher VEGFR2 and ∼4-fold higher PDGFRα. Therefore, targeting VEGFR2 and PDGFRα should preferentially target the tumor.

Our work suggests that targeting EGFR and IGFR on tumors like GBM39 may not be effective by itself. Although, they have high concentrations on ∼70–90% EC-like and non-EC-like GBM cells, their high GBM heterogeneity (QE = ∼1.0) and high concentration on healthy tissue (2–2,000 × 10^3 EGFR/fibroblast or epithelial cell; 2.5 × 10^4 IGFR/NIH 3T3 mouse fibroblasts (Sorkin and Duex, 2010; Brennan et al., 2013; Weddell and Imoukhuede, 2017) may lower their targeting specificity, resulting in lower drug efficacy (Wheeler et al., 2010). Better drug delivery to the tumor site will likely improve targeting specificity without disrupting healthy tissue. An alternative strategy is to develop dual-inhibitors targeting both EGFR/IGFR and VEGFR2 to increase their specificity for tumor EC-like cells.

We believe our method can also identify cellular and molecular mechanisms underlying reduced response to drugs. For example, upregulation of alternative signaling pathways has been implicated in anti-VEGF drug resistance (Bergers and Hanahan, 2008; Shojaei and Ferrara, 2008). This mechanism of drug resistance is often accompanied by significant tumor heterogeneity (Snuderl et al., 2011; Szerlip et al., 2012; Lu and Bergers, 2013). Therefore, these alternative pathways may be overlooked in bulk studies if they are only present on small cell subpopulations. From this study, we suggest targeting RTKs that are localized on plasma membrane at high concentrations on small cell populations (<10%) for combination therapy. For example, VEGFR1 and Tie2 on tumor ECs may become "alternative" RTKs for anti-VEGF treatment, because we found ∼10% human tumor EC-like cell subpopulations had 41,000 VEGFR1 and ∼8% had 65,700 Tie2 on the plasma membrane. Identifying alternative RTK pathways that contribute to resistance can provide tumor-specific drug targets for combination therapy.

FUTURE DIRECTION IN CHARACTERIZING GBM HETEROGENEITY

Our study of the GBM39 PDX model, arrived at 4 key findings and 2 recommendations: (1) tumor EC-like subpopulations have high concentrations of plasma membrane VEGFR1 and VEGFR2; (2) human vs. mouse tumor EC-like cells have inverted VEGFR2:VEGFR1 ratios; (3) tumor EC-like subpopulations have high plasma membrane EGFR, IGFR, and PDGFR concentrations; and (4) GSCs compose a low percentage of cells in the tumor and have little-to-no EGFRs and IGFRs on their plasma membranes.

Based on findings in this study and our RTK-targeting criteria, VEGFR2 or PDGFRα would be likely drug targets for GBM39. In addition, VEGFR1 and Tie2 are likely drug targets for combination therapy. The next step would be to test these targets in a GBM PDX model.

The results of this "proof of concept" study should be interpreted as such: it offers an approach for continued measurement of tumor samples, broadly, and GBM samples, specifically, with the GBM39 PDX sample as a first example. We present the novel method, qFlow cytometry, and show its application in characterizing GBM heterogeneity. Larger and well-powered samples are warranted to expand the current preliminary results, and to discover ideal drug targets and mechanisms underlying drug resistance.

Future opportunities for expanding this research lies in establishing protein concentration ranges on additional samples and continued development of biomimetic tumor models. Firstly, additional measurements of protein concentration on normal ECs and other cells would provide the baselines needed to compare to tumor. In establishing EC baselines, isolation of a pure EC population may be a challenge. Previous qFlow studies have identified ECs using both the CD34 and CD31 markers (Imoukhuede and Popel, 2012, 2014; Imoukhuede et al., 2013). However, it is important to note, that using multiple markers can bias cell collection: CD34 is a progenitor marker, so its use biases selection from more mature cells. Whereas, CD31 is a mature cell marker that is found on ECs, platelets, natural killer cells, monocytes, macrophages, and among other cells (Liu and Shi, 2012), so its use can lead to sample impurity. Here, we chose to bias toward progenitor-like ECs; however, expanded studies may determine if protein concentrations correlate with marker presentation (e.g., identifying whether progenitor-like cells having higher or lower protein concentrations).

Another opportunity for advancement lies in our quantitative single-cell RTK mapping, moving toward multiplexed measurement of RTKs. Toward multiplexed quantification, Lee-Montiel et al., developed a quantum dot method for receptor labeling and calibration (Lee-Montiel and Imoukhuede, 2013; Lee-Montiel et al., 2015) that can be translated to qFlow cytometry. Another approach could be to adapt receptor quantification to mass cytometry (CyTOF) (Spitzer and Nolan,

2016). Such advancements would provide multi-RTK, multi-cell insight into tumor heterogeneity.

In conclusion, cancer research is experiencing a paradigm shift from ensemble analysis to cell-to-cell variability (Niepel et al., 2009; Hoppe et al., 2014; Dar and Weiss, 2018) because of the increasing evidence correlating drug resistance with tumor heterogeneity. The perspective and work that we present here offers sensitive methods for heterogeneity characterization in tumors that should enable improved treatment. We believe that continued quantification of single-cell receptor heterogeneity is a new frontier that will offer significant clinical impact.

AUTHOR CONTRIBUTIONS

SC and PI designed the study. BH provided samples and contributed critical insight into GBM and discussion on the studies. SC performed the experiments and quantified RTK plasma membrane concentrations. SC, TL, and PI conducted and discussed data analysis. SC, TL, and PI prepared the manuscript.

ACKNOWLEDGMENTS

This work was supported by grants from the National Science Foundation (1512598 and 1653925), and the American Heart Association (16SDG26940002). Research reported in this publication was also supported by the National Cancer Institute of the National Institutes of Health under Award Number R01 CA197488 (BACH). The content is solely the responsibility of the authors and does not necessarily represent the official views of the NIH. We would like to thank members of BH's lab, Dr. Sara Pedron and Jee-Wei Emily Chen at University of Illinois at Urbana-Champaign, and Dr. Jann Sarkaria at Mayo Clinic (Rochester, MN) for the generous supply of GBM PDX samples.

REFERENCES

AbuSamra, D. B., Fajr, A. A., Asma, S. A., Heba, M. J. A., Chee, J. C., Ayman, F. A., et al. (2017). Not just a marker: cd34 on human hematopoietic stem/progenitor cells dominates vascular selectin binding along with CD44. *Blood Adv.* 1, 2799–2816. doi: 10.1182/bloodadvances.2017004317

Aguirre, A., Planell, J. A., and Engel, E. (2010). Dynamics of bone marrow-derived endothelial progenitor cell/mesenchymal stem cell interaction in co-culture and its implications in angiogenesis. *Biochem. Biophys. Res, Commun.* 400, 284–291. doi: 10.1016/j.bbrc.2010.08.073

Aird, W. C. (2009). Molecular heterogeneity of tumor endothelium. *Cell Tissue Res.* 335, 271–281. doi: 10.1007/s00441-008-0672-y

Amin, D. N., Hida, K., Bielenberg, D. R., and Klagsbrun, M. (2006). Tumor endothelial cells express epidermal growth factor receptor (EGFR) but not ErbB3 and are responsive to EGF and to EGFR |. *Cancer Res.* 66, 2173–2180. doi: 10.1158/0008-5472.CAN-05-3387

Andrae, J., Gallini, R., and Betsholtz, C. (2008). Role of platelet-derived growth factors in physiology and medicine. *Genes Dev.* 22, 1276–1312. doi: 10.1101/gad.1653708

Ball, S. G., Shuttleworth, C. A., and Kielty, C. M. (2007). Vascular endothelial growth factor can signal through platelet-derived growth factor receptors. *J. Cell Biol.* 177, 489–500. doi: 10.1083/jcb.200608093

Bar, R. S., Boes, M., Booth, B. A., Dake, B. L., Henley, S., and Hart, M. N. (1989). The effects of platelet-derived growth factor in cultured microvessel endothelial cells. *Endocrinology* 124, 1841–1848. doi: 10.1210/endo-124-4-1841

Battegay, E. J., Rupp, J., Iruela-Arispe, L., Sage, E. H., and Pech, M. (1994). PDGF-BB modulates endothelial proliferation and angiogenesis *in vitro* via PDGF beta-receptors. *J. Cell Biol.* 125, 917–928. doi: 10.1083/jcb.125.4.917

Baumgartner, R., Umlauf, E., Veitinger, M., Guterres, S., Rappold, E., Babeluk, R., et al. (2013). Identification and validation of platelet low biological variation proteins, superior to GAPDH, actin and tubulin, as tools in clinical proteomics. *J. Proteomics* 94, 540–551. doi: 10.1016/j.jprot.2013.10.015

Beier, D., Hau, P., Proescholdt, M., Lohmeier, A., Wischhusen, J., Oefner, P. J., et al. (2007). CD133(+) and CD133(-) glioblastoma-derived cancer stem cells show differential growth characteristics and molecular profiles. *Cancer Res.* 67, 4010–4015. doi: 10.1158/0008-5472.CAN-06-4180

Bergers, G., and Hanahan, D. (2008). Modes of resistance to anti-angiogenic therapy. *Nat. Rev. Cancer* 8, 592–603. doi: 10.1038/nrc2442

Bowen-Pope, D. F., and Ross, R. (1982). Platelet-derived growth factor. II. Specific binding to cultured cells. *J. Biol. Chem.* 257, 5161–5171.

Bradshaw, A., Wickremsekera, A., Tan, S. T., Peng, L., Davis, P. F., and Itinteang, T. (2016). Cancer stem cell hierarchy in glioblastoma multiforme. *Front. Surg.* 3:21. doi: 10.3389/fsurg.2016.00021

Brennan, C. W., Verhaak, R. G. W., McKenna, A., Campos, B., Noushmehr, H., Salama, S. R., Zheng, S., et al. (2013). The somatic genomic landscape of glioblastoma. *Cell* 155, 462–477. doi: 10.1016/j.cell.2013.09.034

Brennan, C., Momota, H., Hambardzumyan, D., Ozawa, T., Tandon, A., Pedraza, A., et al. (2009). Glioblastoma subclasses can be defined by activity among signal transduction pathways and associated genomic alterations. *PLoS ONE* 4:e7752. doi: 10.1371/journal.pone.0007752

Cadena, D. L., and Gill, G. N. (1992). Receptor tyrosine kinases. *FASEB J.* 6, 2332–2337. doi: 10.1096/fasebj.6.6.1312047

Calabrese, C., Poppleton, H., Kocak, M., Hogg, T. L., Fuller, C., Hamner, B., Oh, E. Y., et al. (2007). A perivascular niche for brain tumor stem cells. *Cancer Cell* 11, 69–82. doi: 10.1016/j.ccr.2006.11.020

Candolfi, M., Kroeger, K. M., Xiong, W., Liu, C., Puntel, M., Yagiz, K., Muhammad, A. G., et al. (2011). Targeted toxins for glioblastoma multiforme: pre-clinical studies and clinical implementation. *Anticancer. Agents Med. Chem.* 11, 729–738. doi: 10.2174/187152011797378689

Carmeliet, P., and Jain, R. K. (2000). Angiogenesis in cancer and other diseases. *J. Nat.* 407, 249–257. doi: 10.1038/35025220

Carmeliet, P., and Jain, R. K. (2011). Molecular mechanisms and clinical applications of angiogenesis. *Nature* 473, 298–307. doi: 10.1038/nature10144

Chao, C., Widen, S. G., Wood, T. G., Zatarain, J. R., Johnson, P., Gajjar, A., Gomez, G., et al. (2017). Patient-derived xenografts from colorectal carcinoma: a temporal and hierarchical study of murine stromal cell replacement. *Anticancer Res.* 37, 3405–3412. doi: 10.21873/anticanres.11707

Chen, S., Ansari, A., Sterrett, W., Hurley, K., Kemball, J., Weddell, J. C., et al. (2014). Current state-of-the-art and future directions in systems biology. *Progr. Commun. Sci.* 1, 12–26.

Chen, S., Guo, X., Imarenezor, O., and Imoukhuede, P. I. (2015). Quantification of VEGFRs, NRP1, and PDGFRs on endothelial cells and fibroblasts reveals serum, intra-family ligand, and cross-family ligand regulation. *Cell. Mol. Bioeng.* 8, 383–403. doi: 10.1007/s12195-015-0411-x

Chen, S., Weddell, J. C., Gupta, P., Conard, G., Parkin, J., and Imoukhuede, P. I. (2017). qFlow cytometry-based receptoromic screening: a high-throughput quantification approach informing biomarker selection and nanosensor development. *Methods Mol. Biol.* 1570, 117–138. doi: 10.1007/978-1-4939-6840-4_8

Chung, I., Akita, R., Vandlen, R., Toomre, D., Schlessinger, J., and Mellman, I. (2010). Spatial control of EGF receptor activation by reversible dimerization on living cells. *Nature* 464, 783–787. doi: 10.1038/nature08827

Cloughesy, T. F., Cavenee, W. K., and Mischel, P. S. (2014). Glioblastoma: from molecular pathology to targeted treatment. *Ann. Rev. Pathol. Mech. Dis.* 9, 1–25. doi: 10.1146/annurev-pathol-011110-130324

Comps-Agrar, L., Dunshee, D. R., Eaton, D. L., and Sonoda, J. (2015). Unliganded fibroblast growth factor receptor 1 forms density-independent dimers. *J. Biol. Chem.* 290, 24166–24177. doi: 10.1074/jbc.M115.681395

Dar, R. D., and Weiss, R. (2018). Perspective: engineering noise in biological systems towards predictive stochastic design. *APL Bioeng.* 2:020901. doi: 10.1063/1.5025033

De Witt Hamer, P. C. (2010). Small molecule kinase inhibitors in glioblastoma: a systematic review of clinical studies. *Neurooncology* 12, 304–316. doi: 10.1093/neuonc/nop068

Dudley, A. C. (2012). Tumor endothelial cells. *Cold Spring Harb. Perspect. Med.* 2:a006536. doi: 10.1101/cshperspect.a006536

Dunn, G. P., Rinne, M. L., Wykosky, J., Genovese, G., Quayle, S. N., Dunn, I. F., Agarwalla, P. K., et al. (2012). Emerging insights into the molecular and cellular basis of glioblastoma. *Genes Dev.* 26, 756–784. doi: 10.1101/gad.187922.112

Ellis, H. P., Greenslade, M., Powell, B., Spiteri, I., Sottoriva, A., and Kurian, K. M. (2015). Current challenges in glioblastoma: intratumour heterogeneity, residual disease, and models to predict disease recurrence. *Front. Oncol.* 5:251. doi: 10.3389/fonc.2015.00251

Farahani, R. M., and Xaymardan, M. (2015). Platelet-derived growth factor receptor alpha as a marker of mesenchymal stem cells in development and stem cell biology. *Stem Cells Int.* 2015:362753. doi: 10.1155/2015/362753

Feng, Y., Mitchison, T. J., Bender, A., Young, D. W., and Tallarico, J. A. (2009). Multi-parameter phenotypic profiling: using cellular effects to characterize small-molecule compounds. *Nat. Rev. Drug Discov.* 8, 567–578. doi: 10.1038/nrd2876

Ferrara, N. (2002). VEGF and the quest for tumour angiogenesis factors. *Nat. Rev. Cancer* 2, 795–803. doi: 10.1038/nrc909

Ferrara, N., and Kerbel, R. S. (2005). Angiogenesis as a therapeutic target. *Nature* 438, 967–974. doi: 10.1038/nature04483

Ferrara, N., Gerber, H., and LeCouter, J. (2003). The biology of VEGF and its receptors. *Nat. Med.* 9, 669–676. doi: 10.1038/nm0603-669

Furnari, F. B., Cloughesy, T. F., Cavenee, W. K., and Mischel, P. S. (2015). Heterogeneity of epidermal growth factor receptor signalling networks in glioblastoma. *Nat. Rev. Cancer* 15, 302–310. doi: 10.1038/nrc3918

Gelfand, M. V., Hagan, N., Tata, A., Oh, W., Lacoste, B., Kang, K., et al. (2014). Neuropilin-1 functions as a VEGFR2 co-receptor to guide developmental angiogenesis independent of ligand binding. *ELife* 3:e03720. doi: 10.7554/eLife.03720

Giannini, C., Sarkaria, J. N., Saito, A., Uhm, J. H., Galanis, E., Carlson, B. L., et al. (2005). Patient tumor EGFR and PDGFRA gene amplifications retained in an invasive intracranial xenograft model of glioblastoma multiforme. *Neurooncology* 7, 164–176. doi: 10.1215/S1152851704000821

Golebiewska, A., Bougnaud, S., Stieber, D., Brons, N. H. C., Vallar, L., Hertel, F., et al. (2013). Side population in human glioblastoma is non-tumorigenic and characterizes brain endothelial cells. *Brain* 136 (Pt 5), 1462–1475. doi: 10.1093/brain/awt025

Gough, A. H., Chen, N., Shun, T. Y., Lezon, T. R., Boltz, R. C., Reese, C. E., Wagner, J., et al. (2014). Identifying and quantifying heterogeneity in high content analysis: application of heterogeneity indices to drug discovery. *PLoS ONE* 9:e102678. doi: 10.1371/journal.pone.0102678

Greaves, M. (2015). Evolutionary determinants of cancer. *Cancer Discov.* 5, 806–820. doi: 10.1158/2159-8290.CD-15-0439

Greaves, M., and Maley, C. C. (2012). Clonal evolution in cancer. *Nature* 481, 306–313. doi: 10.1038/nature10762

Grecco, H. E., Schmick, M., and Bastiaens, P. I. H. (2011). Signaling from the living plasma membrane. *Cell* 144, 897–909. doi: 10.1016/j.cell.2011.01.029

Greenberg, J. I., Shields, D. J., Barillas, S. G., Acevedo, L. M., Murphy, E., Huang, J., Scheppke, L., et al. (2008). A Role for VEGF as a negative regulator of pericyte function and vessel maturation. *Nature* 456, 809–813. doi: 10.1038/nature07424

Griffero, F., Daga, A., Marubbi, D., Capra, M. C., Melotti, A., Pattarozzi, A., Gatti, M., et al. (2009). Different response of human glioma tumor-initiating cells to epidermal growth factor receptor kinase inhibitors. *J. Biol. Chem.* 284, 7138–7148. doi: 10.1074/jbc.M807111200

Hanahan, D., and Weinberg, R. A. (2011). Hallmarks of cancer: the next generation. *Cell* 144, 646–674. doi: 10.1016/j.cell.2011.02.013

Hawkins-Daarud, A., Rockne, R. C., Anderson, A. R. A., and Swanson, K. R. (2013). Modeling tumor-associated edema in gliomas during anti-angiogenic therapy and its impact on imageable tumor. *Front. Oncol.* 3:66. doi: 10.3389/fonc.2013.00066

Heath, J. R., Ribas, A., and Mischel, P. S. (2016). Single-cell analysis tools for drug discovery and development. *Nat. Rev. Drug Discov.* 15, 204–216. doi: 10.1038/nrd.2015.16

Heldin, C. H., Westermark, B., and Wasteson, A. (1981). Specific receptors for platelet-derived growth factor on cells derived from connective tissue and glia. *Proc. Natl. Acad. Sci. U.S.A.* 78, 3664–3668. doi: 10.1073/pnas.78.6.3664

Hermanson, M., Funa, K., Hartman, M., Claesson-Welsh, L., Heldin, C. H., Westermark, B., et al. (1992). Platelet-derived growth factor and its receptors in human glioma tissue: expression of messenger RNA and protein suggests the presence of autocrine and paracrine loops. *Cancer Res.* 52, 3213–3219.

Hermansson, M., Nistér, M., Betsholtz, C., Heldin, C. H., Westermark, B., and Funa, K. (1988). Endothelial cell hyperplasia in human glioblastoma: coexpression of mRNA for platelet-derived growth factor (PDGF) B chain and PDGF receptor suggests autocrine growth stimulation. *Proc. Natl. Acad. Sci. U.S.A.* 85, 7748–7752. doi: 10.1073/pnas.85.20.7748

Holash, J., Maisonpierre, P. C., Compton, D., Boland, P., Alexander, C. R., Zagzag, D., et al. (1999). Vessel cooption, regression, and growth in tumors mediated by angiopoietins and VEGF. *Science* 284, 1994–1998. doi: 10.1126/science.284.5422.1994

Hoppe, P. S., Coutu, D. L., and Schroeder, T. (2014). Single-cell technologies sharpen up mammalian stem cell research. *Nat. Cell Biol.* 16, 919–927. doi: 10.1038/ncb3042

Hubbard, S. R., and Miller, W. T. (2007). Receptor tyrosine kinases: mechanisms of activation and signaling. *Curr. Opin. Cell Biol.* 19, 117–123. doi: 10.1016/j.ceb.2007.02.010

Huedo-Medina, T. B., Sánchez-Meca, J., Marín-Martínez, F., and Botella, J. (2006). Assessing heterogeneity in meta-analysis: Q statistic or I^2 index? *Psychol. Methods* 11, 193–206. doi: 10.1037/1082-989X.11.2.193

Imoukhuede, P. I., and Chen, S. (2018). *Characterizing Heterogeneity via Single-Cell Receptor Quantification*. UIUC2018-032-01(PRO).

Imoukhuede, P. I., and Popel, A. S. (2011). Quantification and cell-to-cell variation of vascular endothelial growth factor receptors. *Exp. Cell Res.* 317, 955–965. doi: 10.1016/j.yexcr.2010.12.014

Imoukhuede, P. I., and Popel, A. S. (2012). Expression of VEGF receptors on endothelial cells in mouse skeletal muscle. *PLoS ONE* 7:e44791. doi: 10.1371/journal.pone.0044791

Imoukhuede, P. I., and Popel, A. S. (2014). Quantitative fluorescent profiling of VEGFRs reveals tumor cell and endothelial cell heterogeneity in breast cancer xenografts. *Cancer Med.* 3, 225–244. doi: 10.1002/cam4.188

Imoukhuede, P. I., Dokun, A. O., Annex, B. H., and Popel, A. S. (2013). Endothelial cell-by-cell profiling reveals the temporal dynamics of VEGFR1 and VEGFR2 membrane localization after murine hindlimb ischemia. *Am. J. Physiol. Heart Circ. Physiol.* 304, H1085–H1093. doi: 10.1152/ajpheart.00514.2012

Jain, R. K. (2005). Normalization of tumor vasculature: an emerging concept in antiangiogenic therapy. *Science* 307, 58–62. doi: 10.1126/science.1104819

Jain, R. K., Duda, D. G., Willett, C. G., Sahani, D. V., Zhu, A. X., Loeffler, J. S., et al. (2009). Biomarkers of response and resistance to antiangiogenic therapy. *Nat. Rev. Clin. Oncol.* 6, 327–338. doi: 10.1038/nrclinonc.2009.63

Jain, R. K., Tomaso, E. D., Duda, D. G., Loeffler, J. S., Sorensen, A. G., and Batchelor, T. T. (2007). Angiogenesis in brain tumours. *Nat. Rev. Neurosci.* 8, 610–622. doi: 10.1038/nrn2175

Jayson, G. C., Kerbel, R., Ellis, L. M., and Harris, A. L. (2016). Antiangiogenic therapy in oncology: current status and future directions. *Lancet* 388, 518–529. doi: 10.1016/S0140-6736(15)01088-0

Johnson, H., Rosario, A. M. D., Bryson, B. D., Schroeder, M. A., Sarkaria, J. N., and White, F. M. (2012). Molecular characterization of EGFR and EGFRvIII signaling networks in human glioblastoma tumor xenografts. *Mol. Cell. Proteomics* 11, 1724–1740. doi: 10.1074/mcp.M112.019984

Kazlauskas, A. (2017). PDGFs and their receptors. *Gene* 614, 1–7. doi: 10.1016/j.gene.2017.03.003

Kazlauskas, A., and DiCorleto, P. E. (1985). Cultured endothelial cells do not respond to a platelet-derived growth-factor-like protein in an autocrine manner. *Biochim. Biophys. Acta* 846, 405–412. doi: 10.1016/0167-4889(85)90013-8

King, C., Stoneman, M., Raicu, V., and Hristova, K. (2016). Fully quantified spectral imaging reveals *in vivo* membrane protein interactions. *Integr. Biol.* 8, 216–229. doi: 10.1039/C5IB00202H

Kuczynski, E. A., Patten, S. G., and Coomber, B. L. (2011). VEGFR2 expression and TGF-β signaling in initial and recurrent high-grade human glioma. *Oncology* 81, 126–134. doi: 10.1159/000332849

Kuczynski, E. A., Yin, M., Bar-Zion, A., Lee, C. R., Butz, H., Man, S., Daley, F., et al. (2016). Co-option of liver vessels and not sprouting angiogenesis drives acquired sorafenib resistance in hepatocellular carcinoma. *J. Natl. Cancer Inst.* 108:djw030. doi: 10.1093/jnci/djw030

Kut, C., Gabhann, F. M., and Popel, A. S. (2007). Where is VEGF in the body? A meta-analysis of VEGF distribution in cancer. *Brit. J. Cancer* 97, 978–985. doi: 10.1038/sj.bjc.6603923

Lambrechts, D., Lenz, H., Haas, S., Carmeliet, P., and Scherer, S. J. (2013). Markers of response for the antiangiogenic agent bevacizumab. *J. Clin. Oncol.* 31, 1219–1230. doi: 10.1200/JCO.2012.46.2762

Lathia, J. D., Mack, S. C., Mulkearns-Hubert, E. E., Valentim, C. L. L., and Rich, J. N. (2015). Cancer stem cells in glioblastoma. *Genes Dev.* 29, 1203–1217. doi: 10.1101/gad.261982.115

Lee-Montiel, F. T., and Imoukhuede, P. I. (2013). Engineering quantum dot calibration standards for quantitative fluorescent profiling. *J. Mater. Chem. B* 1, 6434. doi: 10.1039/c3tb20904k

Lee-Montiel, F. T., Li, P., and Imoukhuede, P. I. (2015). Quantum dot multiplexing for the profiling of cellular receptors. *Nanoscale* 7, 18504–18514. doi: 10.1039/C5NR01455G

Liffers, K., Lamszus, K., and Schulte, A. (2015). EGFR amplification and glioblastoma stem-like cells. *Stem Cells Int.* 2015:427518. doi: 10.1155/2015/427518

Lin, C. C., Melo, F. A., Ghosh, R., Suen, K. M., Stagg, L. J., Kirkpatrick, J., et al. (2012). Inhibition of basal FGF receptor signaling by dimeric Grb2. *Cell* 149, 1514–1524. doi: 10.1016/j.cell.2012.04.033

Liu, L., and Shi, G. P. (2012). CD31: beyond a marker for endothelial cells. *Cardiovasc. Res.* 94, 3–5. doi: 10.1093/cvr/cvs108

Low-Nam, S. T., Lidke, K. A., Cutler, P. J., Roovers, R. C., Henegouwen, P. M. B. P., Wilson, B. S., et al. (2011). ErbB1 dimerization is promoted by domain co-confinement and stabilized by ligand binding. *Nat. Struct. Mol. Biol.* 18, 1244–1249. doi: 10.1038/nsmb.2135

Lu, K. V., and Bergers, G. (2013). Mechanisms of evasive resistance to anti-VEGF therapy in glioblastoma. *CNS Oncol.* 2, 49–65. doi: 10.2217/cns.12.36

Lyer, S., Bishop, J., Abrams, B., Maino, V., Ward, A., Christian, T., et al. (1997). *QuantiBRITE: A New Standard for PE Flourescence Quantitation*. San Jose, CA: Becton Dickinson Immunocytometry Systems.

Mac Gabhann, F., and Popel, A. S. (2007). Dimerization of VEGF receptors and implications for signal transduction: a computational study. *Biophys. Chem.* 128, 125–139. doi: 10.1016/j.bpc.2007.03.010

Mac Gabhann, F. and Popel, A. S. (2008). Systems biology of vascular endothelial growth factors. *Microcirculation*. 15, 715–738. doi: 10.1080/10739680802095964

Mak, A. B., Blakely, K. M., Williams, R. A., Penttilä, P., Shukalyuk, A. I., Osman, K. T., et al. (2011). CD133 protein *N*-glycosylation processing contributes to cell surface recognition of the primitive cell marker AC133 epitope. *J. Biol. Chem.* 286, 41046–41056. doi: 10.1074/jbc.M111.261545

Mamer, S. B., Chen, S., Weddell, J. C., Palasz, A., Wittenkeller, A., Kumar, M., et al. (2017). Discovery of high-affinity PDGF-VEGFR interactions: redefining RTK dynamics. *Sci. Rep.* 7:16439. doi: 10.1038/s41598-017-16610-z

Marx, M., Perlmutter, R. A., and Madri, J. A. (1994). Modulation of platelet-derived growth factor receptor expression in microvascular endothelial cells during *in vitro* angiogenesis. *J. Clin. Invest.* 93, 131–139. doi: 10.1172/JCI116936

Massey, S. C., Rockne, R. C., Hawkins-Daarud, A., Gallaher, J., Anderson, A. R. A., Canoll, P., et al. (2018). Simulating PDGF-driven glioma growth and invasion in an anatomically accurate brain domain. *Bull. Math. Biol.* 80, 1292–1309. doi: 10.1007/s11538-017-0312-3

Mazzoleni, S., Politi, L. S., Pala, M., Cominelli, M., Franzin, A., Sergi, L. S., Falini, A., et al. (2010). Epidermal growth factor receptor expression identifies functionally and molecularly distinct tumor-initiating cells in human glioblastoma multiforme and is required for gliomagenesis. *Cancer Res.* 70, 7500–7513. doi: 10.1158/0008-5472.CAN-10-2353

McGranahan, N., and Swanton, C. (2017). Clonal heterogeneity and tumor evolution: past, present, and the future. *Cell* 168, 613–628. doi: 10.1016/j.cell.2017.01.018

Moghadam, S. A., Abadi, A. M., and Mokhtari, S. (2015). Immunohistochemical analysis of CD34 expression in salivary gland tumors. *J. Oral Maxillofac. Pathol.* 19, 30–33. doi: 10.4103/0973-029X.157197

Molina, E. S., Pillat, M. M., Moura-Neto, V., Lah, T. T., and Ulrich, H. (2014). Glioblastoma stem-like cells: approaches for isolation and characterization. *J. Cancer Stem Cell Res.* 1:1. doi: 10.14343/JCSCR.2014.2e1007

Murat, A., Migliavacca, E., Gorlia, T., Lambiv, W. L., Shay, T., Hamou, M., Tribolet, N., et al. (2008). Stem cell–related 'self-renewal' signature and high epidermal growth factor receptor expression associated with resistance to concomitant chemoradiotherapy in glioblastoma. *J. Clin. Oncol.* 26, 3015–3024. doi: 10.1200/JCO.2007.15.7164

Naujokat, C. (2014). Monoclonal antibodies against human cancer stem cells. *Immunotherapy* 6, 290–308. doi: 10.2217/imt.14.4

Nguyen, R., Perfetto, S., Mahnke, Y. D., Chattopadhyay, P., and Roederer, M. (2013). Quantifying spillover spreading for comparing instrument performance and aiding in multicolor panel design. *Cytometry* 83, 306–15. doi: 10.1002/cyto.a.22251

Nielsen, J. S., and McNagny, K. M. (2008). Novel functions of the CD34 family. *J. Cell Sci.* 121, 3683–3692. doi: 10.1242/jcs.037507

Niepel, M., Spencer, S. L., and Sorger, P. K. (2009). Non-genetic cell-to-cell variability and the consequences for pharmacology. *Curr. Opin. Chem. Biol.* 13, 556–561. doi: 10.1016/j.cbpa.2009.09.015

Pallini, R., Ricci-Vitiani, L., Montano, N., Mollinari, C., Biffoni, M., Cenci, T., et al. (2011). Expression of the stem cell marker CD133 in recurrent glioblastoma and its value for prognosis. *Cancer* 117, 162–174. doi: 10.1002/cncr.25581

Patel, A. P.,Tirosh, I., Trombetta, J. J., Shalek, A. K., Gillespie, S. M., Wakimoto, H., Cahill, D. P., et al. (2014). Single-cell RNA-Seq highlights intratumoral heterogeneity in primary glioblastoma. *Science* 344, 1396–1401. doi: 10.1126/science.1254257

Patenaude, A., Parker, J., and Karsan, A. (2010). Involvement of endothelial progenitor cells in tumor vascularization. *Microvasc. Res.* 79, 217–223. doi: 10.1016/j.mvr.2010.01.007

Pavoine, S., and Dolédec, S. (2005). The apportionment of quadratic entropy: a useful alternative for partitioning diversity in ecological data. *Environ. Ecol. Stat.* 12, 125–138. doi: 10.1007/s10651-005-1037-2

Pennock, S., Kim, L. A., and Kazlauskas., A. (2016). Vascular endothelial cell growth factor A acts via platelet-derived growth factor receptor α to promote viability of cells enduring hypoxia. *Mol. Cell. Biol.* 36, 2314–2327. doi: 10.1128/MCB.01019-15

Plate, K. H., Breier, G., Farrell, C. L., and Risau, W. (1992). Platelet-derived growth factor receptor-beta is induced during tumor development and upregulated during tumor progression in endothelial cells in human gliomas. *Lab. Invest.* 67, 529–534.

Plate, K. H., Breier, G., Weich, H. A., Mennel, H. D., and Risau, W. (1994). Vascular endothelial growth factor and glioma angiogenesis: coordinate induction of VEGF receptors, distribution of vegf protein and possible *in vivo* regulatory mechanisms. *Int. J. Cancer.* 59, 520–529. doi: 10.1002/ijc.2910590415

Popescu, A. M., Alexandru, O., Brindusa, C., Purcaru, S. O., Tache, D. E., Tataranu, L. G., et al. (2015). Targeting the VEGF and PDGF signaling pathway in glioblastoma treatment. *Int. J. Clin. Exp. Pathol.* 8, 7825–7837.

Potts, S. J., Krueger, J. S., Landis, N. D., Eberhard, D. A., Young, G. D., Schmechel, S. C., et al. (2012). Evaluating tumor heterogeneity in immunohistochemistry-stained breast cancer tissue. *Lab. Invest.* 92, 1342–1357. doi: 10.1038/labinvest.2012.91

Qazi, M. A., Vora, P., Venugopal, C., Sidhu, S. S., Moffat, J., Swanton, C., et al. (2017). Intratumoral heterogeneity: pathways to treatment resistance and relapse in human glioblastoma. *Ann. Oncol.* 28, 1448–1456. doi: 10.1093/annonc/mdx169

Raftery, A. E. (1995). Bayesian model selection in social research. *Sociol. Methodol.* 25, 111. doi: 10.2307/271063

Raines, E. W., Bowen-Pope, D. F., and Ross, R. (1991). "Platelet-derived growth factor," in *Peptide Growth Factors and Their Receptors I*, eds M. B. Sporn and A. B. Roberts (New York, NY: Springer), 173–262.

Rao, C. R. (1982). Diversity and dissimilarity coefficients: a unified approach. *Theor. Popul. Biol.* 21, 24–43.

Rich, J. N., and Bigner, D. D. (2004). Development of novel targeted therapies in the treatment of malignant glioma. *Nat. Rev. Drug Discov.* 3, 430–446. doi: 10.1038/nrd1380

Rocha-Martins, M., Njaine, B., and Silveira, M. S. (2012). Avoiding pitfalls of internal controls: validation of reference genes for analysis by QRT-PCR and western blot throughout rat retinal development. *PLoS ONE* 7:e43028. doi: 10.1371/journal.pone.0043028

Ruch, C., Skiniotis, G., Steinmetz, M. O., Walz, T., and Ballmer-Hofer, K. (2007). Structure of a VEGF–VEGF receptor complex determined by electron microscopy. *Nat. Struct. Mol. Biol.* 14, 249–250. doi: 10.1038/nsmb1202

Sangar, V., Funk, C. C., Kusebauch, U., Campbell, D. S., Moritz, R. L., and Price, N. D. (2014). Quantitative proteomic analysis reveals effects of epidermal growth factor receptor (EGFR) on invasion-promoting proteins secreted by glioblastoma cells. *Mol. Cell. Proteomics* 13, 2618–2631. doi: 10.1074/mcp.M114.040428

Sarabipour, S., and Hristova, K. (2016). Mechanism of FGF receptor dimerization and activation. *Nat. Commun.* 7:10262. doi: 10.1038/ncomms10262

Sarabipour, S., Ballmer-Hofer, K., and Hristova, K. (2016). VEGFR-2 conformational switch in response to ligand binding. *Elife* 5:e13876. doi: 10.7554/eLife.13876

Sarkaria, J. N., Yang, L., Grogan, P. T., Kitange, G. J., Carlson, B. L., Schroeder, M. A., Galanis, E., et al. (2007). Identification of molecular characteristics correlated with glioblastoma sensitivity to EGFR Kinase inhibition through use of an intracranial xenograft test panel. *Mol. Cancer Ther.* 6, 1167–1174. doi: 10.1158/1535-7163.MCT-06-0691

Saunders, N. A., Simpson, F., Thompson, E. W., Hill, M. M., Endo-Munoz, L., Leggatt, G., et al. (2012). Role of intratumoural heterogeneity in cancer drug resistance: molecular and clinical perspectives. *EMBO Mol. Med.* 4, 675–684. doi: 10.1002/emmm.201101131

Schonberg, D. L., Lubelski, D., Miller, T. E., and Rich, J. N. (2014). Brain tumor stem cells: molecular characteristics and their impact on therapy. *Mol. Aspects Med.* 39, 82–101. doi: 10.1016/j.mam.2013.06.004

Seymour, T., Nowak, A., and Kakulas, F. (2015). Targeting aggressive cancer stem cells in glioblastoma. *Front. Oncol.* 5:159. doi: 10.3389/fonc.2015.00159

Shi, Q., Qin, L., Wei, W., Geng, F., Fan, R., Shin, Y. S., et al. (2012). Single-cell proteomic chip for profiling intracellular signaling pathways in single tumor cells. *Proc. Natl. Acad. Sci. U.S.A.* 109, 419–424. doi: 10.1073/pnas.1110865109

Shibuya, M. (2014). VEGF-VEGFR signals in health and disease. *Biomol. Ther.* 22, 1–9. doi: 10.4062/biomolther.2013.113

Shojaei, F., and Ferrara, N. (2008). Role of the microenvironment in tumor growth and in refractoriness/resistance to anti-angiogenic therapies. *Drug Resist. Updates* 11, 219–230. doi: 10.1016/j.drup.2008.09.001

Simons, M., Gordon, E., and Claesson-Welsh, L. (2016). Mechanisms and regulation of endothelial VEGF receptor signalling. *Nat. Rev. Mol. Cell Biol.* 17, 611–625. doi: 10.1038/nrm.2016.87

Simonson, A. B., and Schnitzer, J. E. (2007). Vascular proteomic mapping *in vivo*. *J. Thromb. Haemostasis* 5, 183–187. doi: 10.1111/j.1538-7836.2007.02551.x

Singh, S. K., Hawkins, C., Clarke, I. D., Squire, J. A., Bayani, J., Hide, T., et al. (2004). Identification of human brain tumour initiating cells. *Nature* 432, 396–401. doi: 10.1038/nature03128

Smith, C. L., Kilic, O., Schiapparelli, P., Guerrero-Cazares, H., Kim, D., Sedora-Roman, N. I., et al. (2016). Migration phenotype of brain-cancer cells predicts patient outcomes. *Cell Rep.* 15, 2616–2624. doi: 10.1016/j.celrep.2016.05.042

Snuderl, M., Fazlollahi, L., Le, L. P., Nitta, M., Zhelyazkova, B. H., Davidson, C. J., Akhavanfard, S., et al. (2011). Mosaic amplification of multiple receptor tyrosine kinase genes in glioblastoma. *Cancer Cell* 20, 810–817. doi: 10.1016/j.ccr.2011.11.005

Soares, A. B., Juliano, P. B., Araujo, V. C., Metze, K., and Altemani, A. (2007). Angiogenic switch during tumor progression of carcinoma ex-pleomorphic adenoma. *Virchows Arch.* 451, 65–71. doi: 10.1007/s00428-007-0438-z

Soda, Y., Marumoto, T., Friedmann-Morvinski, D., Soda, M., Liu, F., Michiue, H., Pastorino, S., et al. (2011). Transdifferentiation of glioblastoma cells into vascular endothelial cells. *Proc. Natl. Acad. Sci. U.S.A.* 108, 4274–4280. doi: 10.1073/pnas.1016030108

Soeda, A., Hara, A., Kunisada, T., Yoshimura, S., Iwama, T., and Park., D. M. (2015). The evidence of glioblastoma heterogeneity. *Sci. Rep.* 5:7979. doi: 10.1038/srep07979

Soeda, A., Inagaki, A., Oka, N., Ikegame, Y., Aoki, H., Yoshimura, S., et al. (2008). Epidermal growth factor plays a crucial role in mitogenic regulation of human brain tumor stem cells. *J. Biol. Chem.* 283, 10958–10966. doi: 10.1074/jbc.M704205200

Sorkin, A., and Duex, J. E. (2010). Quantitative analysis of endocytosis and turnover of epidermal growth factor (EGF) and EGF receptor. *Curr. Protoc. Cell Biol.* Chapter 15:Unit 15.14. doi: 10.1002/0471143030.cb1514s46

Spitzer, M. H., and Nolan, G. P. (2016). Mass cytometry: single cells, many features. *Cell* 165, 780–791. doi: 10.1016/j.cell.2016.04.019

Steinkamp, M. P., Low-Nam, S. T., Yang, S., Lidke, K. A., Lidke, D. S., and Wilson, B. S. (2014). ErbB3 is an active tyrosine kinase capable of homo- and heterointeractions. *Mol. Cell. Biol.* 34, 965–977. doi: 10.1128/MCB.01605-13

Szerlip, N. J., Pedraza, A., Chakravarty, D., Azim, M., McGuire, J., Fang, Y., Ozawa, T., et al. (2012). Intratumoral heterogeneity of receptor tyrosine kinases EGFR and PDGFRA amplification in glioblastoma defines subpopulations with distinct growth factor response. *Proc. Natl. Acad. Sci. U.S.A.* 109, 3041–3046. doi: 10.1073/pnas.1114033109

Szopa, W., Burley, T. A., Kramer-Marek, G., and Kaspera, W. (2017). Diagnostic and therapeutic biomarkers in glioblastoma: current status and future perspectives. *Biomed. Res. Int.* 2017:8013575. doi: 10.1155/2017/8013575

Taniguchi, Y., Choi, P. J., Li, G., Chen, H., Babu, M., Hearn, J., et al. (2010). Quantifying *E. coli* proteome and transcriptome with single-molecule sensitivity in single cells. *Science* 329, 533–538. doi: 10.1126/science.1188308

Tirosh, I., Izar, B., Prakadan, S. M., Wadsworth, M. H., Treacy, D., Trombetta, J. J., Rotem, A., et al. (2016). Dissecting the multicellular ecosystem of metastatic melanoma by single-cell RNA-seq. *Science* 352, 189–196. doi: 10.1126/science.aad0501

Verhaak, R. G., Hoadley, K. A., Purdom, E., Wang, V., Qi, Y., Wilkerson, M. D., Miller, C. R., et al. (2010). Integrated genomic analysis identifies clinically relevant subtypes of glioblastoma characterized by abnormalities in PDGFRA, IDH1, EGFR, and NF1. *Cancer Cell* 17, 98–110. doi: 10.1016/j.ccr.2009.12.020

Vigelsø, A., Dybboe, R., Hansen, C. N., Dela, F., Helge, J. W., and Grau, A. G. (2015). GAPDH and β-actin protein decreases with aging, making stain-free technology a superior loading control in western blotting of human skeletal muscle. *J. Appl. Physiol.* 118, 386–394. doi: 10.1152/japplphysiol.00840.2014

Volinsky, N., and Kholodenko, B. N. (2013). Complexity of receptor tyrosine kinase signal processing. *Cold Spring Harb. Perspect. Biol.* 5:a009043. doi: 10.1101/cshperspect.a009043

Weddell, J. C., and Imoukhuede, P. I. (2014). Quantitative characterization of cellular membrane-receptor heterogeneity through statistical and computational modeling. *PLoS ONE* 9:e97271. doi: 10.1371/journal.pone.0097271

Weddell, J. C., and Imoukhuede, P. I. (2017). Integrative meta-modeling identifies endocytic vesicles, late endosome and the nucleus as the cellular compartments primarily directing RTK signaling. *Integr. Biol.* 9, 464–484. doi: 10.1039/C7IB00011A

Weddell, J. C., and Imoukhuede, P. I. (2018). Computational systems biology for the VEGF family in angiogenesis. *Encycloped. Cardiovasc. Res. Med.* 659–676. doi: 10.1016/B978-0-12-809657-4.99548-6

Wehland, M., Bauer, J., Magnusson, N. E., Infanger, M., and Grimm, D. (2013). Biomarkers for anti-angiogenic therapy in cancer. *Int. J. Mol. Sci.* 14, 9338–9364. doi: 10.3390/ijms14059338

Wei, W., Shin, Y. S., Xue, M., Matsutani, T., Masui, K., Yang, H., Ikegami, S., et al. (2016). Single-cell phosphoproteomics resolves adaptive signaling dynamics and informs targeted combination therapy in glioblastoma. *Cancer Cell* 29, 563–573. doi: 10.1016/j.ccell.2016.03.012

Weickhardt, A. J., Williams, D. S., Lee, C. K., Chionh, F., Simes, J., Murone, C., Wilson, K., et al. (2015). Vascular endothelial growth factor D expression is a potential biomarker of bevacizumab benefit in colorectal cancer. *Br. J. Cancer* 113, 37–45. doi: 10.1038/bjc.2015.209

Weis, S. M., and Cheresh, D. A. (2011). Tumor angiogenesis: molecular pathways and therapeutic targets. *Nat. Med.* 17, 1359–1370. doi: 10.1038/nm.2537

Werner, S., Hofschneider, P. H., Heldin, C. H., Ostman, A., and Roth, W. K. (1990). Cultured kaposi's sarcoma-derived cells express functional PDGF A-type and B-type receptors. *Exp. Cell Res.* 187, 98–103.

Wheeler, D. L., Dunn, E. F., and Harari, P. M. (2010). Understanding resistance to EGFR inhibitors[mdash]impact on future treatment strategies. *Nat. Rev. Clin. Oncol.* 7, 493–507. doi: 10.1038/nrclinonc.2010.97

Wheeless, L. L., Coon, J. S., Cox, C., Deitch, A. J., White, R. W. D., Koss, L. G., Melamed, M., et al. (1989). Measurement variability in DNA flow cytometry of replicate samples. *Cytometry* 10, 731–738. doi: 10.1002/cyto.990100610

Wu, F. T. H., Stefanini, M. O., Gabhann, F. M., Kontos, C. D., Annex, B. H., and Popel, A. S. (2010). A systems biology perspective on SVEGFR1: its biological function, pathogenic role and therapeutic use. *J. Cell. Mol. Med.* 14, 528–552. doi: 10.1111/j.1582-4934.2009.00941.x

Yadav, V. N., Altshuler, D., Kadiyala, P., Zamler, D., Comba, A., Appelman, H., et al. (2018). Molecular ablation of tumor blood vessels inhibits therapeutic effects of radiation and bevacizumab. *Neuro-Oncology, April.* doi: 10.1093/neuonc/noy055

Zoltán, B. (2005). Rao's quadratic entropy as a measure of functional diversity based on multiple traits. *J. Veg. Sci.* 16, 533–540. doi: 10.1111/j.1654-1103.2005.tb02393.x

Conflict of Interest Statement: The authors declare that the research was conducted in the absence of any commercial or financial relationships that could be construed as a potential conflict of interest.

frontiers in Materials

MINI REVIEW
published: 19 December 2017
doi: 10.3389/fmats.2017.00045

Biomimetic Strategies for the Glioblastoma Microenvironment

*Junghwa Cha and Pilnam Kim**

Department of Bio and Brain Engineering, Korea Advanced Institute of Science and Technology, Daejeon, South Korea

Glioblastoma multiforme (GBM) is a devastating type of tumor with high mortality, caused by extensive infiltration into adjacent tissue and rapid recurrence. Most therapies for GBM have focused on the cytotoxicity and have not targeted GBM spread. However, there have been numerous attempts to improve therapy by addressing GBM invasion, through understanding and mimicking its behavior using three-dimensional (3D) experimental models. Compared with two-dimensional models and *in vivo* animal models, 3D GBM models can capture the invasive motility of glioma cells within a 3D environment comprising many cellular and non-cellular components. Based on tissue engineering techniques, GBM invasion has been investigated within a biologically relevant environment, from biophysical and biochemical perspectives, to clarify the pro-invasive factors of GBM. This review discusses the recent progress in techniques for modeling the microenvironments of GBM tissue and suggests future directions with respect to recreating the GBM microenvironment and preclinical applications.

Keywords: glioblastoma, invasion, *in vitro* three-dimensional model, microenvironment, biomimetic scaffolds

OPEN ACCESS

Edited by:
Sara Pedron,
University of Illinois at Urbana–Champaign, United States

Reviewed by:
Triantafyllos Stylianopoulos,
University of Cyprus, Cyprus
Julien Georges Didier Barthès,
Protip Medical, France

***Correspondence:**
Pilnam Kim
pkim@kaist.ac.kr

Specialty section:
This article was submitted to Biomaterials, a section of the journal Frontiers in Materials

Received: *29 October 2017*
Accepted: *06 December 2017*
Published: *19 December 2017*

Citation:
Cha J and Kim P (2017) Biomimetic Strategies for the Glioblastoma Microenvironment. Front. Mater. 4:45. doi: 10.3389/fmats.2017.00045

INTRODUCTION

Malignant glioma, which is the most common primary brain tumor in adults, arises from star-shaped glial cells or their precursors within the central nervous system (Louis, 2006). Clinically, the World Health Organization grading system classifies gliomas into four stages. Of these, the most aggressive grade IV astrocytoma, glioblastoma multiforme (GBM); this tumor is the most devastating to health and cannot be cured (Louis et al., 2016). One of the main reasons why GBMs are incurable is that they spread widely within intracranial spaces, resulting in an indistinct tumor margin that prevents complete resection (Stummer et al., 2006). Unlike other systemic tumors, GBM rarely metastasizes beyond the central nervous system (Holland, 2000). GBM usually arises from the cerebrum and is prone to micrometastasis, i.e., infiltration at a single-cell level throughout the brain parenchyma, as well as across the corpus callosum from one hemisphere to the other, thus producing a bilateral butterfly like glioma (Dziurzynski et al., 2012). Although GBM invasion is confined within the intracranial spaces, the prognosis of the patients with GBM is still bleak.

The standard therapy for GBM is a surgical resection followed by a combination of radiotherapy and chemotherapy. Typically, postoperative radiotherapy is given along with the alkylating agent temozolomide (Stupp et al., 2005). Unfortunately, GBM cells are very resistant to these conventional therapies, and most patients with GBM end up developing recurrent tumors (Yip et al., 2009). Targeted therapy to overcome the low efficacy and high toxicity of postsurgical adjuvant therapies mostly focuses on treating proliferative cells, not invading cells (Wang et al., 2015). To achieve greater therapeutic efficacy, targeting the infiltration of GBM could be beneficial. Therefore, it is important to understand GBM invasion in brain tissue, to predict and evaluate tumor cell behavior; this is essential for developing new therapeutic inventions. Since GBM cells are predominantly regulated by the complex microenvironment and cause dynamic remodeling of their surroundings that facilitates

invasion (Rao, 2003), it is necessary to investigate the influence of the microenvironment of the brain to understand the unique features of GBM invasion. By reproducing both the composition and structural elements of the complex *in vivo* tumor microenvironment, the pro-invasive factors for GBM cells could be identified in pathophysiologically relevant context, which may eventually lead to novel therapeutic options for clinical trials.

This review focuses on recent research for biomimetic approaches to develop *in vitro* three-dimensional (3D) tumor models of glioblastoma cell invasion. First, the compositional and structural features of brain tumor microenvironment are introduced. Then, state-of-the-art experimental models of GBM invasion are presented and new approaches to mimic the brain microenvironment are discussed. Finally, future directions with respect to constructing *in vivo*-like tumor models for glioblastoma are suggested.

BRAIN TUMOR MICROENVIRONMENT

Brain tumor tissue comprises heterogeneous subpopulations of tumor cells intermingling with normal parenchymal cells (Hambardzumyan and Bergers, 2015). In addition to cellular components, non-cellular components such as brain extracellular matrix (ECM) and brain anatomy play crucial roles in GBM malignancy (Gritsenko et al., 2012). As pro-migratory, pro-invasive factors, these chemical and physical factors facilitate the GBM progression (**Figure 1**). By understanding the pro-invasive components within GBM microenvironment, we could recreate the *in vivo* behaviors of GBM cells.

Anatomical Features in Glioma Tissue

The unique anatomical structures in the brain include white matter tracts and capillaries, called Scherer's structures (Cuddapah

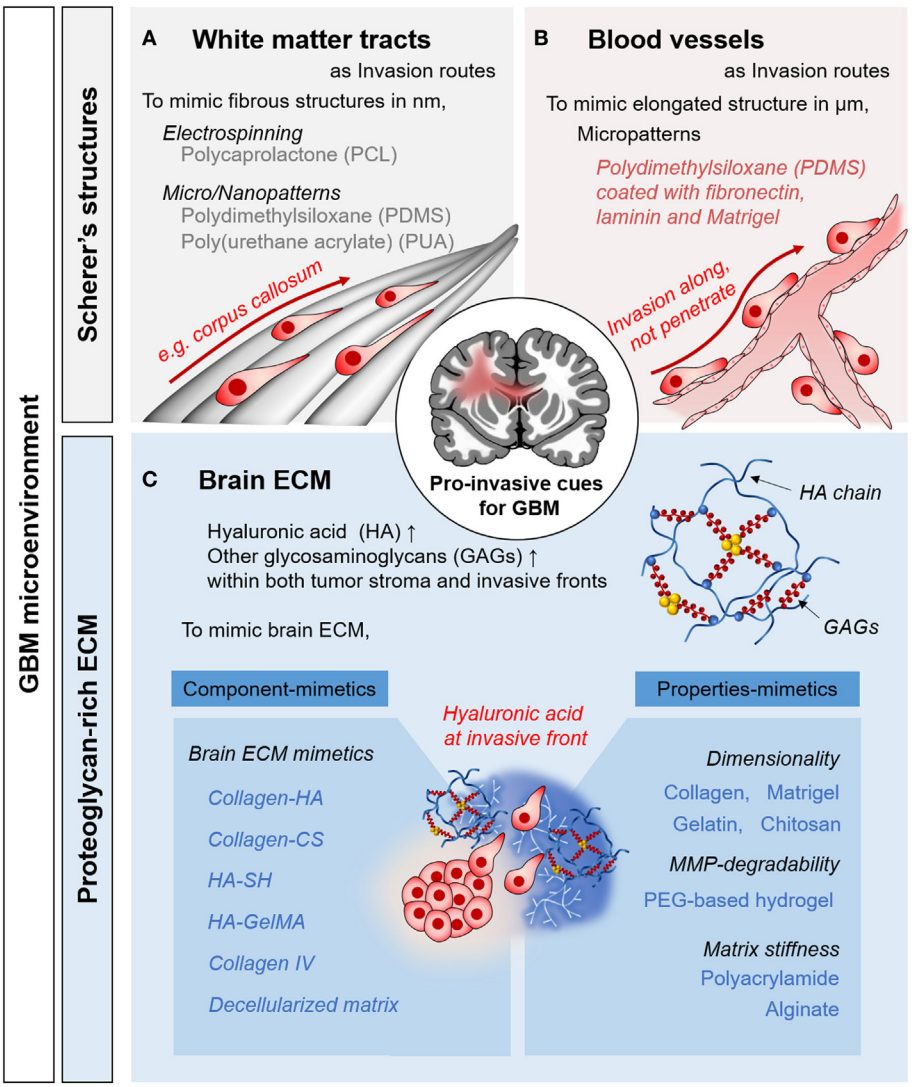

FIGURE 1 | Pro-invasive cues in glioblastoma multiforme (GBM) microenvironments and *in vitro* approaches to mimic the microenvironmental cues. Representative examples of Scherer's structures: white matter tract **(A)** and blood vessels **(B)**. **(C)** Proteoglycan-rich extracellular matrix (ECM) in tumorous brain tissue.

et al., 2014). A white matter tract is a bundle of aligned axons. These are bound manly in corpus callosum, in which fibrous structures consist of submicron-sized fibers. For pro-invasive characteristics, topography is a major mechano-physical cue derived from the ECM structure and the anatomical features or organs, which play key roles in cellular behavior and function (Friedl and Alexander, 2011). Histological observations have revealed that single GBM cells preferentially migrate to these structures (Bellail et al., 2004; Louis, 2006). As biophysical cues for pro-invasive characteristics, tumor cells interact with this existing brain anatomy, which is an important mechanism of invasion by GBM cells.

ECM in Glioma Tissue

The normal brain lacks the stiff fibrillar collagen matrix that is typical component in other organs (Bellail et al., 2004). The brain has a substantially different ECM, composed of glycosaminoglycans (GAGs), proteoglycans (PGs), and other glycoproteins (Cuddapah et al., 2014; Rao et al., 2014; Miyata and Kitagawa, 2017). The interstitial spaces in the brain parenchyma are filled with a PG-based matrix, which interacts with hyaluronic acid (HA)-binding proteins (e.g., CD44 and RHAMM) and tenascins (Gladson, 1999). By contrast, fibrous, adhesive ECM proteins, such as collagen, laminin, and fibronectins, are rarely found in the brain parenchyma, where their expression is restricted to the basement membrane of neural vasculature (Lau et al., 2013). These ECM components function as components of blood–brain barrier, which constitutes both a chemical and physical barrier, inducing the formation of tight junctions.

The composition of the ECM of glioma tissue is distinct from that of normal tissue. During cancer progression, the secretion of neural ECM molecules is increased significantly. The amorphous ECM at the invasive front of a proliferating GBM strongly expresses GAGs and PGs, especially HA (Bellail et al., 2004; Jin et al., 2009). Moreover, fibrous, adhesive ECM proteins such as collagen IV, fibronectin, and laminin are strongly upregulated (Gladson, 1999). Increased production of tumorous ECM leads to a significant increase in its volume, contributing to elevated interstitial pressure in the confined extracellular space (Munson et al., 2013). In addition to acting as a signaling molecule, tumorous ECM activates tumor-associated pathways, promoting cell survival and motility (Rape et al., 2014).

IN VITRO 3D GBM MODELS

There are several advantages of utilizing *in vitro* 3D GBM models to investigate the effects of the microenvironment on GBM invasion. Unlike two-dimensional (2D) models, *in vitro* 3D GBM models can replicate the highly complex microenvironment of *in vivo* GBM niches. Furthermore, well-defined 3D *in vitro* GBM niches are simpler and more reliable than *in vivo* animal models, which involve costly, time-consuming technical procedures (Xiao et al., 2017). Here, we presented an overview of the biomimetic approaches for reconstructing *in vitro* 3D GBM models of anatomical and matrix-related aspects of the GBM microenvironment (see also **Table 1**).

Fibrous Scaffold-Based Culture Models

Histological evidence indicates that GBM cells migrate along pre-existing brain structures and form Scherer's structures by interacting with the neural microenvironment. Brain anatomy, including the brain parenchyma, pre-existing blood vessels, white matter tracts, and the subarachnoid space below the meningeal covering of the brain, plays an important role in GBM invasion (Cuddapah et al., 2014).

To mimic these invasion routes, several synthetic polymer-based micro/nanotechnologies have been used to investigate the behavior of GBM cells. Recently, there have been reports on the effect of 2D topography on GBM invasion, replicating the *in vivo* behavior of GBM cells (Cha et al., 2015; Smith et al., 2016; Sim et al., 2017). For instance, using 2D polydimethylsiloxane (PDMS) substrates, the tapered microtract of the gradient width ranging from 3 to 100 μm was fabricated to identify the effect of topography on GBM motility (Cha et al., 2015). For microtracts smaller than 3 μm, micropatterns can induce *in vivo*-like saltatory migration, even on 2D surfaces. In addition, polyurethane acrylate-based nanotopography (Smith et al., 2016) and nanofabricated polystyrene (Zhu et al., 2004) closely mimic the fibrillar structures of brain.

Techniques to fabricate nanofibers, such as electrospinning, have been used to mimic the delicate fibrous structures of the white matter tracts (Johnson et al., 2009; Agudelo-Garcia et al., 2011; Rao et al., 2013b; Sharma et al., 2013; Beliveau et al., 2016; Cha et al., 2016). The behavior of glioma cells on nanofibers was observed to be a function of substrate topography, as GBM cells migrated much faster on aligned fibers than on random fibers (Johnson et al., 2009; Beliveau et al., 2016). This *in vivo*-like behaviors of glioma cells is associated with STAT3 signaling, a driver of malignancy during GBM progression (Agudelo-Garcia et al., 2011). Modification of both biochemical and biophysical features of nanofibers has a significant effect on GBM migration (Rao et al., 2013b; Sharma et al., 2013), emphasizing the importance of biomimetic approaches to understanding the behaviors of glioma.

Matrix Scaffold-Based Culture Models

To simulate tumorous ECM components in brain, researchers have attempted to reconstruct an HA-rich environment and GAG-based matrices. The biophysical properties of the ECM matrix have also been reported to influence GBM cell invasion; thus, numerous studies have examined the effects of matrix dimensionality, degradability, and stiffness.

Matrices to Mimic the ECM Properties

In addition to the brain anatomy, the brain ECM also has biophysical effects on GBM invasion. To provide the effects of 3D cell-ECM interaction on GBM invasion, naturally derived biomaterials, such as Matrigel (Jin et al., 2009) and collagen (Yang et al., 2010), have been used to develop a 3D ECM microenvironment for GBM. Irrelevant components of the brain ECM, such as chitosan-alginate hydrogels (Kievit et al., 2010) and collagen-agarose hydrogels (Ulrich et al., 2010), were chosen because they have a biologically inert to investigate biophysical effects of the matrices solely, resulting in a mechanosensitive

GBM invasion response. When designing matrices, their physical properties, such as degradability, stiffness, and pore sizes, are usually interconnected and thus influenced each other. Therefore, studies controlling designing parameters, such as the physical properties of matrix metalloprotease (MMP)-degradable polyethylene glycol gels (Wang et al., 2014, 2017), gelatin methacrylate (GelMA) (Pedron and Harley, 2013), and polyacrylamide (Ulrich et al., 2009; Rape and Kumar, 2014;

TABLE 1 | Representative approaches used to mimic glioblastoma multiforme (GBM) microenvironment.

		Biomaterials	Techniques	Cells	Findings	Reference
To mimic Scherer's structures						
Effects of anatomic topography		Polydimethylsiloxane (PDMS)	Soft lithography-based micropatterning	U87, U251	Effective topography to induce saltatory migration	Cha et al. (2015)
		Polyurethane acrylate	UV-assisted capillary force lithography	Patient-derived GBM cells	Mimicry of *in vivo* three-dimensional (3D) migration, PDGF-sensitive response	Smith et al. (2016)
Fibrous structure of white matter tract		Polycaprolactone (PCL)	Electrospinning	U251, X12, neurosphere glioma from biopsy	Effects of fiber directionality on glioma migration	Johnson et al. (2009)
		PCL	Electrospinning	Dissociated U87, U251, GBM-derived tumor initiating cells (G8, G9)	Involvement of STAT3 signaling in topography-induced glioma migration	Agudelo-Garcia et al. (2011)
		PCL	Electrospinning	Patient-derived GBM cells (GSC11)	Invasion preference along the fibrous structures	Cha et al. (2016)
		Polystyrene	Spinneret-based Tunable Engineered Parameters (STEP)	DBTRG-05MG	Effects of nanofibers on glioma migration and blebbing dynamics	Sharma et al. (2013)
		PCL, gelatin-PCL, PDMS-PCL, PES-PCL, PCL-collagen, PCL-HA, PCL-matrigel	Core-shell electrospinning	Patient-derived GBM cells (OSU-2)	Complex interplay of mechanics, chemistry, and topography on glioma migration	Rao et al. 2013b)
To mimic brain extracellular matrix (ECM)						
ECM properties-mimetics	Dimensional effect	Chitosan-alginate (CA) scaffolds	Ionic crosslinking of lyophilized CA mixture	C6 rat glioma, U87, U118	Higher malignancy of 3D cultured GBM than two-dimensional	Kievit et al. (2010)
		Collagen-agarose hydrogels	Physically blended mixture	U373 glioma spheroids	Mechanosensitivity to ECM-based biophysical cues	Ulrich et al. (2010)
	Matrix degradability/ stiffness/pore size	Multi-arm based polyethylene glycol with matrix metalloprotease (MMP)-cleavable peptide	UV photocrosslinking	U87	Effects of matrix stiffness on ECM deposition and remodeling through modulating HA synthases or MMPs	Wang et al. (2014, 2017)
		Gelatin methacrylate (GelMA)	UV photocrosslinking	U87	Impact of biophysical properties (matrix density, crosslinking density, and degradability) on glioma phenotype	Pedron et al. (2013)
		Polyacrylamide (PA)	Polymerization with APS, TEMED	U373, U87	Impact of microenvironmental stiffness on GBM proliferation	Ulrich et al. (2009) and Umesh et al. (2014)
		Adhesion peptide (RGD)-functionalized HA-methacrylate (Me-HA)	Control of degree of methacrylation at varying ratios of thiols	U373, U87, C6 rat glioma	Matrix stiffness-dependent cell adhesion (spreading), cell speed, cell growth, and cell invasion	Ananthanarayanan et al. (2011)
		Hyaluronic acid-methacrylate (Me-HA)	Functionalization of HA with methacrylic anhydride	U373, U87	CD44-mediated cell adhesion, motility, and invasion in stiffness-dependent manner	Kim and Kumar (2014)

(*Continued*)

TABLE 1 | Continued

	Biomaterials	Techniques	Cells	Findings	Reference
To mimic Scherer's structures					
ECM components-mimetics	Adhesion peptide (RGD)-functionalized HA-methacrylate (Me-HA)	Michael-type addition with dithiothreitol	U373, U87, C6 rat glioma	Mechanobiological regulation on brain tumor progression, elevated invasion by CD44-mediated HA	Ananthanarayanan et al. (2011) and Kim and Kumar (2014)
	Collagen I, III, or IV with thiolated HA	Interpenetrating polymer network	Patient-derived GBM cells (OSU-2)	Influence of collagen types on GBM morphology, HA-dependent GBM spreading and migration	Rao et al. (2013a)
	Collagen I-HA	Semi-interpenetrating polymer network	Patient-derived GBM cells (GSC11)	HA-induced GBM invasion and associated mechanisms	Cha et al. (2016)
	HA-MA functionalized GelMA	Photocrosslinking	U87 (+EGFR)	HA-induced GBM malignancy and effects of HA-gradated heterotypic tumor microenvironment	Pedron et al. (2013, 2015)
Hybrid scaffolds to mimic the GBM microenvironment					
Combinations					
HA matrices + fibrous structures		3D configuration of collagen-HA semi-interpenetrating polymer network on electrospun fibers	Patient-derived GBM cells (GSC11)	Microenvironmental adaptations in response to drug treatment	Cha et al. (2016)
Hydrogel stiffness + HA contents		Photocrosslinking, of GelMA + HAMA in concentration-dependent manner	U251	Coordinated effect of matrix stiffness, immobilized HA, and compensatory HA production on GBM invasion	Chen et al. (2017)
Vascular basement + HA surfaces (tissue interface)		Interfacial culture between fibronectin-coated PA and HAMA	U373, U87	Mechanochemical feedback at the tissue interfaces	Rape et al. (2014)
GBM-endothelial cell coculture (GBM perivascular niche)		Photocrosslinking, of GelMA + HAMA	U87, HUVECs, NHLF	Contribution of perivascular niche to GBM invasion	Ngo and Harley (2017)

Umesh et al., 2014), have been performed to examine the role of mechanobiological regulation in GBM invasion. For investigating mechanosensing characteristics of GBM cells, the modified forms of HA gels, such as HA-methacrylate (Me-HA) or RGD-functionalized Me-HA (Ananthanarayanan et al., 2011; Kim and Kumar, 2014), were used to control the matrix stiffness, observing the stiffness-dependent GBM features *via* CD44-mediated mechanosensing.

Matrices to Mimic the ECM Components

Hyaluronic acid, which is a major ECM component in tumorous brain, is a linear chain composed of D-glucuronic acid and *N*-acetyl-D-glucosamine, so it is hard to form cross-linked network itself. Therefore, to investigate the role of HA in GBM invasion, the HA is chemically modified so that it is cross-linked. Chemically modified forms of HA hydrogels include thiolated HA (Rao et al., 2013a), methacrylated HA (Ananthanarayanan et al., 2011; Kim and Kumar, 2014), and mixtures with GelMA (Pedron et al., 2013). GBM cells are strongly influenced by the HA concentration and show increased invasion *via* CD44-mediated HA adhesion (Kim and Kumar, 2014).

Physical blending with other cross-linkable hydrogels, such as collagen, is another means of incorporating HA components into ECM-mimetic model system. By creating interpenetrating polymer networks with HA solution and collagen gels, HA-rich matrices can be created (Yang et al., 2011; Rao et al., 2013a; Cha et al., 2016). Within this HA-rich matric, GBM develops highly proliferative, invasive phenotypes (Cha et al., 2016). These results have been confirmed using other HA-rich matrices, such as GelMA-based HA-rich matrices (Pedron et al., 2015, 2017), which have *in vivo*-like characteristics.

Various GAG-based components, such as heparin, chondroitin sulfate, and keratin sulfate, are often incorporated within the ECM of tumorous brain as the scaffolding components. Tenascin-C (Sarkar et al., 2006) and chondroitin sulfate (Yang et al., 2011; Logun et al., 2016) have been incorporated into collagen hydrogels to investigate their influence on the GBM invasion. As expected, the motility of GBM was increased by higher concentrations of both GAGs.

For advanced brain ECM-mimetic model system, decellularized matrix, obtained by isolating the ECM scaffold of an original tissue (Gilbert et al., 2006), shows utility for recreating the ECM components of GBM tissue. Using porcine brain tissue, decellularized ECM was applied to mimic the brain matrices (DeQuach et al., 2011), further indicating the potential of mimicking the tumorous ECM to investigate GBM invasion.

Hybrid Scaffolds for GBM Microenvironment

Recently, researchers have focused on integrating multiple components of GBM microenvironment to reproduce conditions corresponding more closely to *in vivo* conditions. As mentioned earlier, by controlling the various design parameters of ECM matrices, the combined effects of the chemical and mechanical properties of the ECM on GBM invasion were revealed (Chen et al., 2017). Moreover, our group developed 3D GBM models consisting of HA matrices and fibrous structures arranged in a 3D configuration. Using such integrated systems, microenvironmental adaptation was observed during GBM invasion (Cha et al., 2016); changes in the GBM invasion of the HA matrices were mediated by the focal adhesion kinase and MMP, within the fibrous structures, in response to blockade of a HA-mediated pathway of GBM invasion. Recently, other cellular components in the microenvironment were incorporated into 3D GBM models, revealing the roles of glial cells and the perivascular niche in GBM invasion (Grodecki et al., 2015; Iwadate et al., 2016; Gritsenko et al., 2017; Ngo and Harley, 2017).

FURTHER DIRECTION FOR *IN VITRO* GBM MODELS

In recent decades, the focus of cancer treatment has shifted markedly, from targeting cancer itself to understanding its microenvironment; this is because an aberrant microenvironment is pivotal to cancerous tumor progression (Joyce and Pollard, 2009). As suggested in seed-and-soil hypothesis (Fidler, 2003), a favorable environment for the metastatic cancer is crucial for enabling cells to settle down and mature. Indeed, cancers reside in complex tissue environments, including stromal cells, blood vessels, immune cells, and the ECM, which strongly influence the sustained growth, invasion, and metastasis of cancer (Gilkes et al., 2014). During tumor progression, cancer cells remodel dynamically and interact reciprocally with their microenvironment (both the cellular and non-cellular components), leading to the formation of a tumor-favorable environment (Quail and Joyce, 2013). Many recent studies have highlighted the importance of targeting tumor microenvironment to reduce tumor malignancy (Cuddapah et al., 2014; Hambardzumyan and Bergers, 2015; Xiao et al., 2017). For further progress in the development of *in vitro* GBM models, the other components of brain tumor microenvironment should be considered to better understand glioblastoma invasion.

Intratumoral Heterogeneity

Solid tumors have mass transport limitations due to their decreased surface-area-to-volume ratios and longer diffusion lengths. Owing to this limitation in diffusion, the tumor mass develops internal hypoxic areas, causing shortages of oxygen and nutrients. Tumor hypoxia is one of the key factors inducing the development of heterogeneous cell subpopulation within the tumor masses, which leads to an aggressive treatment-resistant phenotype, rapid progression, and poor prognosis (Heddleston et al., 2009; Li and Rich, 2010; Cheng et al., 2011). Recent studies have reported that these subcellular populations within the GBM mass are cancer stem cells, which exhibit increased tumorigenicity and stem cell-like capacity (Hubert et al., 2016). Histologically, GBM tissue contains a large hypoxic core, called pseudopalisading necrosis (Rong et al., 2006), which in turn contains a stem-like subpopulation (Mamun et al., 2009). Due to its greater therapeutic resistance compared with other tumor population, the roles of cancer stem cells in GBM progression should be considered.

Interaction with Surrounding Cells

Along with cancerous astrocytoma cells, GBM tissues contain other tumor-associated parenchymal cells such as glial cells, vascular cells, microglia, peripheral immune cells, and neural precursor cells. These all play crucial influencing roles in the pathology of GBM (Rape et al., 2014). For example, when activated, astrocytes in GBM tissue promote tumor progression within the GBM microenvironment (Hu et al., 2017). Moreover, the neural vasculature provides a perivascular bed not only for GBM but also for stem-like GBM cells (Bao et al., 2006; Johansson et al., 2017). In addition, microglial cells, which can comprise up to 30% of the brain tumor mass, are heavily involved in GBM invasion (Hambardzumyan et al., 2016). Therefore, by cocultivating these surrounding cells, we can investigate the supportive roles of tumor-associated cells on GBM progression.

Application: *In Vitro* GBM Models As High-Throughput Platforms

By integrating and incorporating the complex components of GBM microenvironment, the model presented herein should be used as a drug-testing tool for GBM patients. For example, by using patient-derived cells and matrices, personalized treatment plans can be constructed. Since the biomimetic approaches used to model the GBM microenvironment contribute to enhancing the similarity and reliability for *in vivo* GBM cells, anti-invasive therapies could be evaluated in a high-throughput manner.

CONCLUSION

This review offers an overview of recent development in *in vitro* GBM models in their microenvironmental context and their further perspectives. Using these biomimetic models, we can investigate and evaluate the invasive features of GBM cells, consequently providing the drug test platform to target their invasion. In the future, we thus expect that the integration of multiple components from complex microenvironment will enhance the understanding of GBM biology and further suggestion of effective therapeutics for the GBM patients.

AUTHOR CONTRIBUTIONS

JC and PK planned and wrote the manuscript of this mini review.

FUNDING

This research was supported from the National Research Foundation of Korea (NRF) (grant number: NRF-2015H1A2A1030560 and NRF-2016R1E1A1A01943393) and by a grant of the Korea

Health Technology R&D Project through the Korea Health Industry Development Institute (KHIDI), funded by the Ministry of Health & Welfare, Republic of Korea (grant number: HI14C1324). We also appreciate the financial support from the Ministry of Science ICT and Future Planning, Republic of Korea (grant number: 2016M3A9B4915823).

REFERENCES

Agudelo-Garcia, P. A., De Jesus, J. K., Williams, S. P., Nowicki, M. O., Chiocca, E. A., Liyanarachchi, S., et al. (2011). Glioma cell migration on three-dimensional nanofiber scaffolds is regulated by substrate topography and abolished by inhibition of STAT3 signaling. *Neoplasia* 13, 831–840. doi:10.1593/neo.11612

Ananthanarayanan, B., Kim, Y., and Kumar, S. (2011). Elucidating the mechanobiology of malignant brain tumors using a brain matrix-mimetic hyaluronic acid hydrogel platform. *Biomaterials* 32, 7913–7923. doi:10.1016/j.biomaterials.2011.07.005

Bao, S., Wu, Q., Sathornsumetee, S., Hao, Y., Li, Z., Hjelmeland, A. B., et al. (2006). Stem cell-like glioma cells promote tumor angiogenesis through vascular endothelial growth factor. *Cancer Res.* 66, 7843–7848. doi:10.1158/0008-5472.CAN-06-1010

Beliveau, A., Thomas, G., Gong, J., Wen, Q., and Jain, A. (2016). Aligned nanotopography promotes a migratory state in glioblastoma multiforme tumor cells. *Sci. Rep.* 6, 26143. doi:10.1038/srep26143

Bellail, A. C., Hunter, S. B., Brat, D. J., Tan, C., and Van Meir, E. G. (2004). Microregional extracellular matrix heterogeneity in brain modulates glioma cell invasion. *Int. J. Biochem. Cell Biol.* 36, 1046–1069. doi:10.1016/j.biocel.2004.01.013

Cha, J., Kang, S. G., and Kim, P. (2016). Strategies of mesenchymal invasion of patient-derived brain tumors: microenvironmental adaptation. *Sci. Rep.* 6, 24912. doi:10.1038/srep24912

Cha, J., Koh, I., Choi, Y., Lee, J., Choi, C., and Kim, P. (2015). Tapered microtract array platform for antimigratory drug screening of human glioblastoma multiforme. *Adv. Healthc. Mater.* 4, 405–411. doi:10.1002/adhm.201400384

Chen, J. E., Pedron, S., and Harley, B. A. C. (2017). The combined influence of hydrogel stiffness and matrix-bound hyaluronic acid content on glioblastoma invasion. *Macromol. Biosci.* 17. doi:10.1002/mabi.201700018

Cheng, L., Wu, Q., Guryanova, O. A., Huang, Z., Huang, Q., Rich, J. N., et al. (2011). Elevated invasive potential of glioblastoma stem cells. *Biochem. Biophys. Res. Commun.* 406, 643–648. doi:10.1016/j.bbrc.2011.02.123

Cuddapah, V. A., Robel, S., Watkins, S., and Sontheimer, H. (2014). A neurocentric perspective on glioma invasion. *Nat. Rev. Neurosci.* 15, 455–465. doi:10.1038/nrn3765

DeQuach, J. A., Yuan, S. H., Goldstein, L. S., and Christman, K. L. (2011). Decellularized porcine brain matrix for cell culture and tissue engineering scaffolds. *Tissue Eng. Part A* 17, 2583–2592. doi:10.1089/ten.TEA.2010.0724

Dziurzynski, K., Blas-Boria, D., Suki, D., Cahill, D. P., Prabhu, S. S., Puduvalli, V., et al. (2012). Butterfly glioblastomas: a retrospective review and qualitative assessment of outcomes. *J. Neurooncol.* 109, 555–563. doi:10.1007/s11060-012-0926-0

Fidler, I. J. (2003). The pathogenesis of cancer metastasis: the 'seed and soil' hypothesis revisited. *Nat. Rev. Cancer* 3, 453–458. doi:10.1038/nrc1098

Friedl, P., and Alexander, S. (2011). Cancer invasion and the microenvironment: plasticity and reciprocity. *Cell* 147, 992–1009. doi:10.1016/j.cell.2011.11.016

Gilbert, T. W., Sellaro, T. L., and Badylak, S. F. (2006). Decellularization of tissues and organs. *Biomaterials* 27, 3675–3683. doi:10.1016/j.biomaterials.2006.02.014

Gilkes, D. M., Semenza, G. L., and Wirtz, D. (2014). Hypoxia and the extracellular matrix: drivers of tumour metastasis. *Nat. Rev. Cancer* 14, 430–439. doi:10.1038/nrc3726

Gladson, C. L. (1999). The extracellular matrix of gliomas: modulation of cell function. *J. Neuropathol. Exp. Neurol.* 58, 1029–1040. doi:10.1097/00005072-199910000-00001

Gritsenko, P., Leenders, W., and Friedl, P. (2017). Recapitulating in vivo-like plasticity of glioma cell invasion along blood vessels and in astrocyte-rich stroma. *Histochem. Cell Biol.* 148, 395–406. doi:10.1007/s00418-017-1604-2

Gritsenko, P. G., Ilina, O., and Friedl, P. (2012). Interstitial guidance of cancer invasion. *J. Pathol.* 226, 185–199. doi:10.1002/path.3031

Grodecki, J., Short, A. R., Winter, J. O., Rao, S. S., Winter, J. O., Otero, J. J., et al. (2015). Glioma-astrocyte interactions on white matter tract-mimetic aligned electrospun nanofibers. *Biotechnol. Prog.* 31, 1406–1415. doi:10.1002/btpr.2123

Hambardzumyan, D., and Bergers, G. (2015). Glioblastoma: defining tumor niches. *Trends Cancer* 1, 252–265. doi:10.1016/j.trecan.2015.10.009

Hambardzumyan, D., Gutmann, D. H., and Kettenmann, H. (2016). The role of microglia and macrophages in glioma maintenance and progression. *Nat. Neurosci.* 19, 20–27. doi:10.1038/nn.4185

Heddleston, J. M., Li, Z., McLendon, R. E., Hjelmeland, A. B., and Rich, J. N. (2009). The hypoxic microenvironment maintains glioblastoma stem cells and promotes reprogramming towards a cancer stem cell phenotype. *Cell Cycle* 8, 3274–3284. doi:10.4161/cc.8.20.9701

Holland, E. C. (2000). Glioblastoma multiforme: the terminator. *Proc. Natl. Acad. Sci. U.S.A.* 97, 6242–6244. doi:10.1073/pnas.97.12.6242

Hu, B., Emdad, L., Kegelman, T. P., Shen, X. N., Das, S. K., Sarkar, D., et al. (2017). Astrocyte elevated gene-1 regulates beta-catenin signaling to maintain glioma stem-like stemness and self-renewal. *Mol. Cancer Res.* 15, 225–233. doi:10.1158/1541-7786.MCR-16-0239

Hubert, C. G., Rivera, M., Spangler, L. C., Wu, Q., Mack, S. C., Prager, B. C., et al. (2016). A three-dimensional organoid culture system derived from human glioblastomas recapitulates the hypoxic gradients and cancer stem cell heterogeneity of tumors found in vivo. *Cancer Res.* 76, 2465–2477. doi:10.1158/0008-5472.CAN-15-2402

Iwadate, Y., Fukuda, K., Matsutani, T., and Saeki, N. (2016). Intrinsic protective mechanisms of the neuron-glia network against glioma invasion. *J. Clin. Neurosci.* 26, 19–25. doi:10.1016/j.jocn.2015.07.024

Jin, S. G., Jeong, Y. I., Jung, S., Ryu, H. H., Jin, Y. H., and Kim, I. Y. (2009). The effect of hyaluronic acid on the invasiveness of malignant glioma cells: comparison of invasion potential at hyaluronic acid hydrogel and matrigel. *J. Korean Neurosurg. Soc.* 46, 472–478. doi:10.3340/jkns.2009.46.5.472

Johansson, E., Grassi, E. S., Pantazopoulou, V., Tong, B., Lindgren, D., Berg, T. J., et al. (2017). CD44 interacts with HIF-2alpha to modulate the hypoxic phenotype of perinecrotic and perivascular glioma cells. *Cell Rep.* 20, 1641–1653. doi:10.1016/j.celrep.2017.07.049

Johnson, J., Nowicki, M. O., Lee, C. H., Chiocca, E. A., Viapiano, M. S., Lawler, S. E., et al. (2009). Quantitative analysis of complex glioma cell migration on electrospun polycaprolactone using time-lapse microscopy. *Tissue Eng. Part C Methods* 15, 531–540. doi:10.1089/ten.TEC.2008.0486

Joyce, J. A., and Pollard, J. W. (2009). Microenvironmental regulation of metastasis. *Nat. Rev. Cancer* 9, 239–252. doi:10.1038/nrc2618

Kievit, F. M., Florczyk, S. J., Leung, M. C., Veiseh, O., Park, J. O., Disis, M. L., et al. (2010). Chitosan-alginate 3D scaffolds as a mimic of the glioma tumor microenvironment. *Biomaterials* 31, 5903–5910. doi:10.1016/j.biomaterials.2010.03.062

Kim, Y., and Kumar, S. (2014). CD44-mediated adhesion to hyaluronic acid contributes to mechanosensing and invasive motility. *Mol. Cancer Res.* 12, 1416–1429. doi:10.1158/1541-7786.MCR-13-0629

Lau, L. W., Cua, R., Keough, M. B., Haylock-Jacobs, S., and Yong, V. W. (2013). Pathophysiology of the brain extracellular matrix: a new target for remyelination. *Nat. Rev. Neurosci.* 14, 722–729. doi:10.1038/nrn3550

Li, Z., and Rich, J. N. (2010). Hypoxia and hypoxia inducible factors in cancer stem cell maintenance. *Curr. Top. Microbiol. Immunol.* 345, 21–30. doi:10.1007/82_2010_75

Logun, M. T., Bisel, N. S., Tanasse, E. A., Zhao, W., Gunasekera, B., Mao, L., et al. (2016). Glioma cell invasion is significantly enhanced in composite hydrogel matrices composed of chondroitin 4- and 4,6-sulfated glycosaminoglycans. *J. Mater. Chem. B Mater. Biol. Med.* 4, 6052–6064. doi:10.1039/C6TB01083K

Louis, D. N. (2006). Molecular pathology of malignant gliomas. *Annu. Rev. Pathol.* 1, 97–117. doi:10.1146/annurev.pathol.1.110304.100043

Louis, D. N., Perry, A., Reifenberger, G., von Deimling, A., Figarella-Branger, D., Cavenee, W. K., et al. (2016). The 2016 World Health Organization classification of tumors of the central nervous system: a summary. *Acta Neuropathol.* 131, 803–820. doi:10.1007/s00401-016-1545-1

Mamun, M. H., Kamitani, H., Kinoshita, Y., Tabuchi, S., Wasita, B., and Watanabe, T. (2009). Cerebral ischemia promotes rich pseudopalisading necrosis in the rat c6 glioblastoma model. *Neurol. Med. Chir. (Tokyo)* 49, 294–299. doi:10.2176/nmc.49.294

Miyata, S., and Kitagawa, H. (2017). Formation and remodeling of the brain extracellular matrix in neural plasticity: roles of chondroitin sulfate and hyaluronan. *Biochim. Biophys. Acta* 1861, 2420–2434. doi:10.1016/j.bbagen.2017.06.010

Munson, J. M., Bellamkonda, R. V., and Swartz, M. A. (2013). Interstitial flow in a 3D microenvironment increases glioma invasion by a CXCR4-dependent mechanism. *Cancer Res.* 73, 1536–1546. doi:10.1158/0008-5472.CAN-12-2838

Ngo, M. T., and Harley, B. A. (2017). The influence of hyaluronic acid and glioblastoma cell coculture on the formation of endothelial cell networks in gelatin hydrogels. *Adv. Healthc. Mater.* doi:10.1002/adhm.201700687

Pedron, S., Becka, E., and Harley, B. A. (2013). Regulation of glioma cell phenotype in 3D matrices by hyaluronic acid. *Biomaterials* 34, 7408–7417. doi:10.1016/j.biomaterials.2013.06.024

Pedron, S., Becka, E., and Harley, B. A. (2015). Spatially gradated hydrogel platform as a 3D engineered tumor microenvironment. *Adv. Mater.* 27, 1567–1572. doi:10.1002/adma.201404896

Pedron, S., Hanselman, J. S., Schroeder, M. A., Sarkaria, J. N., and Harley, B. A. C. (2017). Extracellular hyaluronic acid influences the efficacy of EGFR tyrosine kinase inhibitors in a biomaterial model of glioblastoma. *Adv. Healthc. Mater.* doi:10.1002/adhm.201700529

Pedron, S., and Harley, B. A. (2013). Impact of the biophysical features of a 3D gelatin microenvironment on glioblastoma malignancy. *J. Biomed. Mater. Res. A* 101, 3404–3415. doi:10.1002/jbm.a.34637

Quail, D. F., and Joyce, J. A. (2013). Microenvironmental regulation of tumor progression and metastasis. *Nat. Med.* 19, 1423–1437. doi:10.1038/nm.3394

Rao, J. S. (2003). Molecular mechanisms of glioma invasiveness: the role of proteases. *Nat. Rev. Cancer* 3, 489–501. doi:10.1038/nrc1121

Rao, S. S., Dejesus, J., Short, A. R., Otero, J. J., Sarkar, A., and Winter, J. O. (2013a). Glioblastoma behaviors in three-dimensional collagen-hyaluronan composite hydrogels. *ACS Appl. Mater. Interfaces* 5, 9276–9284. doi:10.1021/am402097j

Rao, S. S., Nelson, M. T., Xue, R., DeJesus, J. K., Viapiano, M. S., Lannutti, J. J., et al. (2013b). Mimicking white matter tract topography using core-shell electrospun nanofibers to examine migration of malignant brain tumors. *Biomaterials* 34, 5181–5190. doi:10.1016/j.biomaterials.2013.03.069

Rao, S. S., Lannutti, J. J., Viapiano, M. S., Sarkar, A., and Winter, J. O. (2014). Toward 3D biomimetic models to understand the behavior of glioblastoma multiforme cells. *Tissue Eng. Part B Rev.* 20, 314–327. doi:10.1089/ten.TEB.2013.0227

Rape, A., Ananthanarayanan, B., and Kumar, S. (2014). Engineering strategies to mimic the glioblastoma microenvironment. *Adv. Drug Deliv. Rev.* 7, 172–183. doi:10.1016/j.addr.2014.08.012

Rape, A. D., and Kumar, S. (2014). A composite hydrogel platform for the dissection of tumor cell migration at tissue interfaces. *Biomaterials* 35, 8846–8853. doi:10.1016/j.biomaterials.2014.07.003

Rong, Y., Durden, D. L., Van Meir, E. G., and Brat, D. J. (2006). 'Pseudopalisading' necrosis in glioblastoma: a familiar morphologic feature that links vascular pathology, hypoxia, and angiogenesis. *J. Neuropathol. Exp. Neurol.* 65, 529–539. doi:10.1097/00005072-200606000-00001

Sarkar, S., Nuttall, R. K., Liu, S., Edwards, D. R., and Yong, V. W. (2006). Tenascin-C stimulates glioma cell invasion through matrix metalloproteinase-12. *Cancer Res.* 66, 11771–11780. doi:10.1158/0008-5472.CAN-05-0470

Sharma, P., Sheets, K., Elankumaran, S., and Nain, A. S. (2013). The mechanistic influence of aligned nanofibers on cell shape, migration and blebbing dynamics of glioma cells. *Integr. Biol. (Camb.)* 5, 1036–1044. doi:10.1039/c3ib40073e

Sim, W., Cha, J., Choi, C., and Choi, K. (2017). Rapid and quantitative measurement of cell adhesion and migration activity by time-series analysis on biomimetic topography. *Biotechnol. Bioprocess Eng.* 22, 107–113. doi:10.1007/s12257-016-0625-3

Smith, C. L., Kilic, O., Schiapparelli, P., Guerrero-Cazares, H., Kim, D. H., Sedora-Roman, N. I., et al. (2016). Migration phenotype of brain-cancer cells predicts patient outcomes. *Cell Rep.* 15, 2616–2624. doi:10.1016/j.celrep.2016.05.042

Stummer, W., Pichlmeier, U., Meinel, T., Wiestler, O. D., Zanella, F., Reulen, H. J., et al. (2006). Fluorescence-guided surgery with 5-aminolevulinic acid for resection of malignant glioma: a randomised controlled multicentre phase III trial. *Lancet Oncol.* 7, 392–401. doi:10.1016/S1470-2045(06)70665-9

Stupp, R., Mason, W. P., van den Bent, M. J., Weller, M., Fisher, B., Taphoorn, M. J., et al. (2005). Radiotherapy plus concomitant and adjuvant temozolomide for glioblastoma. *N. Engl. J. Med.* 352, 987–996. doi:10.1056/NEJMoa043330

Ulrich, T. A., de Juan Pardo, E. M., and Kumar, S. (2009). The mechanical rigidity of the extracellular matrix regulates the structure, motility, and proliferation of glioma cells. *Cancer Res.* 69, 4167–4174. doi:10.1158/0008-5472.CAN-08-4859

Ulrich, T. A., Jain, A., Tanner, K., MacKay, J. L., and Kumar, S. (2010). Probing cellular mechanobiology in three-dimensional culture with collagen-agarose matrices. *Biomaterials* 31, 1875–1884. doi:10.1016/j.biomaterials.2009.10.047

Umesh, V., Rape, A. D., Ulrich, T. A., and Kumar, S. (2014). Microenvironmental stiffness enhances glioma cell proliferation by stimulating epidermal growth factor receptor signaling. *PLoS ONE* 9:e101771. doi:10.1371/journal.pone.0101771

Wang, C., Tong, X., Jiang, X., and Yang, F. (2017). Effect of matrix metalloproteinase-mediated matrix degradation on glioblastoma cell behavior in 3D PEG-based hydrogels. *J. Biomed. Mater. Res. A* 105, 770–778. doi:10.1002/jbm.a.35947

Wang, C., Tong, X., and Yang, F. (2014). Bioengineered 3D brain tumor model to elucidate the effects of matrix stiffness on glioblastoma cell behavior using PEG-based hydrogels. *Mol. Pharm.* 11, 2115–2125. doi:10.1021/mp5000828

Wang, H., Xu, T., Jiang, Y., Xu, H., Yan, Y., Fu, D., et al. (2015). The challenges and the promise of molecular targeted therapy in malignant gliomas. *Neoplasia* 17, 239–255. doi:10.1016/j.neo.2015.02.002

Xiao, W., Sohrabi, A., and Seidlits, S. K. (2017). Integrating the glioblastoma microenvironment into engineered experimental models. *Future Sci. OA* 3, FSO189. doi:10.4155/fsoa-2016-0094

Yang, Y. L., Motte, S., and Kaufman, L. J. (2010). Pore size variable type I collagen gels and their interaction with glioma cells. *Biomaterials* 31, 5678–5688. doi:10.1016/j.biomaterials.2010.03.039

Yang, Y. L., Sun, C., Wilhelm, M. E., Fox, L. J., Zhu, J., and Kaufman, L. J. (2011). Influence of chondroitin sulfate and hyaluronic acid on structure, mechanical properties, and glioma invasion of collagen I gels. *Biomaterials* 32, 7932–7940. doi:10.1016/j.biomaterials.2011.07.018

Yip, S., Miao, J., Cahill, D. P., Iafrate, A. J., Aldape, K., Nutt, C. L., et al. (2009). MSH6 mutations arise in glioblastomas during temozolomide therapy and mediate temozolomide resistance. *Clin. Cancer Res.* 15, 4622–4629. doi:10.1158/1078-0432.CCR-08-3012

Zhu, B., Zhang, Q., Lu, Q., Xu, Y., Yin, J., Hu, J., et al. (2004). Nanotopographical guidance of C6 glioma cell alignment and oriented growth. *Biomaterials* 25, 4215–4223. doi:10.1016/j.biomaterials.2003.11.020

Conflict of Interest Statement: The authors declare that the research was conducted in the absence of any commercial or financial relationships that could be construed as a potential conflict of interest.

Advantages of publishing in Frontiers

OPEN ACCESS
Articles are free to read for greatest visibility and readership

FAST PUBLICATION
Around 90 days from submission to decision

HIGH QUALITY PEER-REVIEW
Rigorous, collaborative, and constructive peer-review

TRANSPARENT PEER-REVIEW
Editors and reviewers acknowledged by name on published articles

Frontiers
Avenue du Tribunal-Fédéral 34
1005 Lausanne | Switzerland

Visit us: www.frontiersin.org
Contact us: info@frontiersin.org | +41 21 510 17 00

REPRODUCIBILITY OF RESEARCH
Support open data and methods to enhance research reproducibility

DIGITAL PUBLISHING
Articles designed for optimal readership across devices

FOLLOW US
@frontiersin

IMPACT METRICS
Advanced article metrics track visibility across digital media

EXTENSIVE PROMOTION
Marketing and promotion of impactful research

LOOP RESEARCH NETWORK
Our network increases your article's readership